

Document No 70SD4207  
11 February 1970

# EARTH RESOURCES TECHNOLOGY SATELLITE SPACECRAFT SYSTEM DESIGN STUDIES FINAL REPORT

VOLUME I

SYSTEMS STUDIES

FACILITY FORM 602

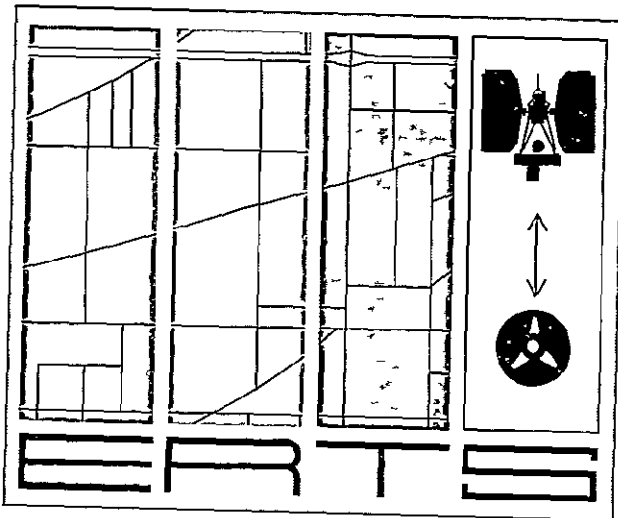
11-34454

(ACCESSION NUMBER) (THRU)

288 (PAGES)

CR-704907 (NASA CR OR TMX OR AD NUMBER)

(CODE) 31 (CATEGORY)



Prepared For  
GODDARD SPACE FLIGHT CENTER  
GREENBELT, MARYLAND 20771



DOCUMENT NO. 70SD4207  
11 FEBRUARY 1970

**EARTH RESOURCES TECHNOLOGY SATELLITE  
SPACECRAFT SYSTEM DESIGN STUDIES  
FINAL REPORT**

**VOLUME I  
SYSTEMS STUDIES**

**PREPARED FOR  
GODDARD SPACE FLIGHT CENTER  
GREENBELT, MARYLAND 20771**

**UNDER  
CONTRACT No NAS 5-11529**

**GENERAL  ELECTRIC**

**SPACE SYSTEMS ORGANIZATION  
Valley Forge Space Center  
P O Box 8555 • Philadelphia, Penna 19101**

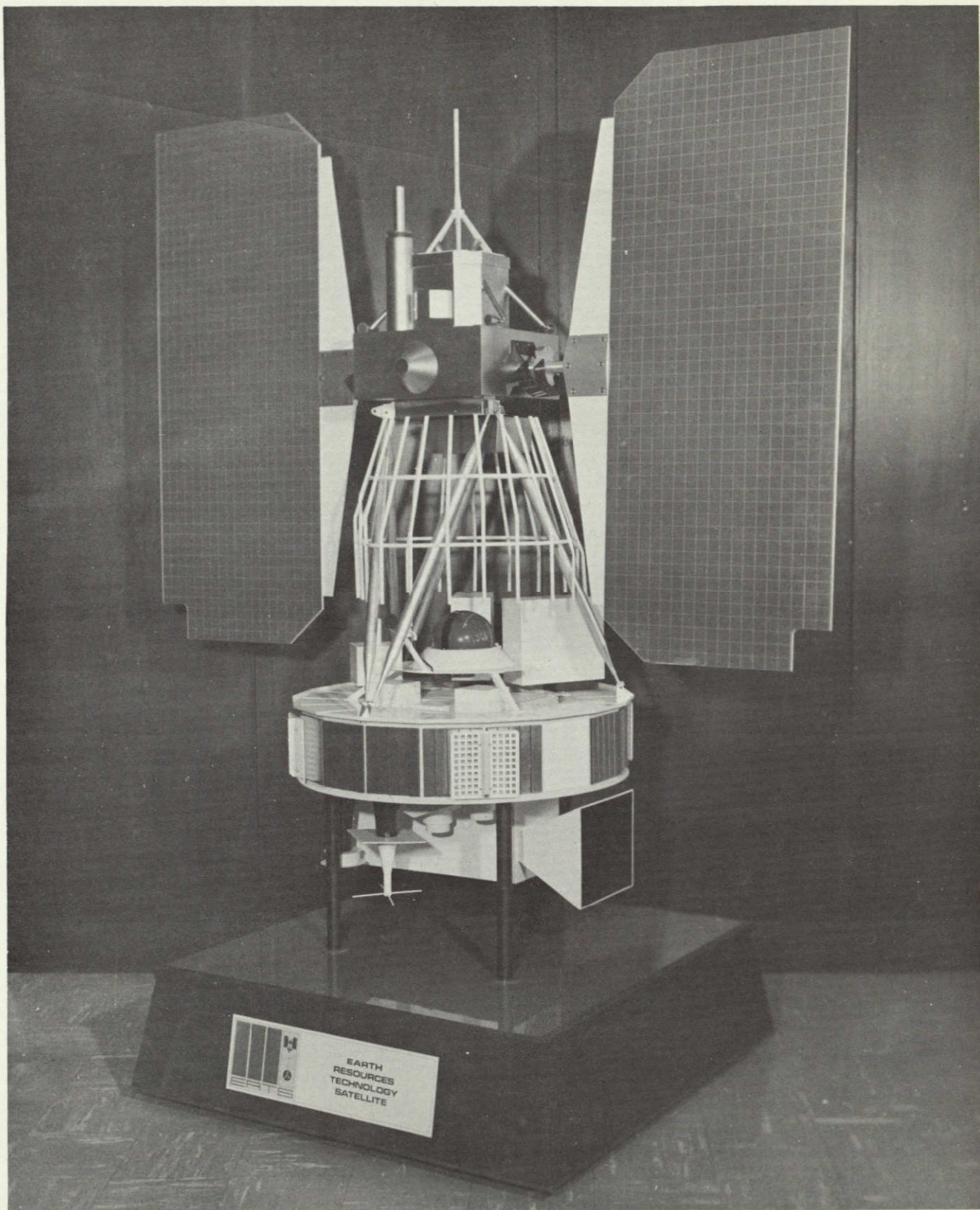


# TABLE OF CONTENTS

Section		Page
1	INTRODUCTION	
	1.1 Study Objective . . . . .	1-1
	1.2 Summary . . . . .	1-1
2	STUDY REQUIREMENTS	
	2.1 Study Tasks . . . . .	2-1
	2.2 Supplementary Study Documents . . . . .	2-1
3	BASELINE SPACECRAFT SYSTEM DESIGN	
	3.1 Introduction . . . . .	3-1
	3.2 Spacecraft System Design . . . . .	3-1
	3.2.1 System Functional Relationships . . . . .	3-1
	3.2.2 Payload Characteristics Summary . . . . .	3-6
	3.2.3 ERTS Spacecraft Configuration . . . . .	3-13
	3.2.4 Electrical and Functional Description . . . . .	3-16
	3.2.5 Subsystem Overview . . . . .	3-24
	3.3 Hardware Matrix . . . . .	3-68
	3.4 Launch Vehicle Study Result . . . . .	3-77
	3.4.1 General . . . . .	3-77
	3.4.2 ERTS/Delta Electrical Integration . . . . .	3-79
	3.5 Growth . . . . .	3-86
	3.5.1 General . . . . .	3-86
	3.5.2 Growth Missions . . . . .	3-86
	3.5.3 Spacecraft Growth . . . . .	3-92
	3.5.4 Growth Power Systems . . . . .	3-100
	3.5.5 Alternate Orbits . . . . .	3-105
4	SYSTEM STUDIES	
	4.1 ERTS System Reliability . . . . .	4-2
	4.1.1 Summary . . . . .	4-2
	4.1.2 Principles of Reliability Assessment . . . . .	4-5
	4.1.3 Source of Failure Rate Data . . . . .	4-5
	4.1.4 Subsystem Reliability Assessments . . . . .	4-6
	4.2 Orbit Analysis . . . . .	4-21
	4.2.1 Introduction . . . . .	4-21
	4.2.2 Nominal Orbit Selection . . . . .	4-22
	4.2.3 Drag Decay . . . . .	4-28
	4.2.4 Nominal Ground Track Control . . . . .	4-32
	4.2.5 Orbit Error Analysis . . . . .	4-35
	4.2.6 Operational Ground Track Control . . . . .	4-43
	4.2.7 Launch Window Analysis . . . . .	4-48

## TABLE OF CONTENTS (Continued)

Section	Page
4.3 Image Location and Coverage .....	4-75
4.3.1 General .....	4-75
4.3.2 Units .....	4-76
4.3.3 Gains .....	4-76
4.3.4 Implementation and Relative Error Effects .....	4-78
4.3.5 First -Order Error Equation, Its Solution, and Attitude Determination Sensor Requirements .....	4-79
4.3.6 Basic Coverage .....	4-82
4.3.7 Rate Requirements .....	4-86
4.3.8 Requirements Summary .....	4-91
4.4 Time Annotation .....	4-92
4.4.1 General .....	4-92
4.4.2 Approaches to Time Annotation .....	4-94
4.4.3 Discussion of Approaches .....	4-95
4.4.4 Baseline Approach .....	4-98
4.5 Mission Simulation .....	4-100
4.5.1 Simulation Problem (Introduction) .....	4-100
4.5.2 Simulation Model .....	4-100
4.5.3 Simulation Cases .....	4-104
4.5.4 Specific Study Results .....	4-109
4.6 Wideband Video Tape Recorders Management .....	4-137
4.6.1 Recorder Management .....	4-137
4.6.2 Tape Handling Requirements .....	4-140
4.6.3 Design Approach ..	4-142

## LIST OF ACRONYMS

NDPF	NASA Data Processing Facility
NTTF	NASA Tracking and Training Facility
WBVTR	Wide Band Video Tape Recorder
MSS	Multi-Spectral Scanner
RBV	Return Beam Vidicon
WB	Wide Band
RBVC	Return Beam Vidicon Camera
DCS	Data Collection System
OCC	Operations Control Center
TLM	Telemetry
NB	Narrow Band
MSFN	Manned Space Flight Network
nm	Nautical Mile
M	Meters
PCM	Pulse Code Modulated
I/O	Input/Output
STADAN	Satellite Tracking and Data Acquisition Network
AGE	Aerospace Ground Equipment (also equivalent to GSE or STE)
PMP	Premodulation Processor
CIU	Command Integration Unit
COMDEC	Command Decoder
PCM/FSK	Pulse Code Modulated/Frequency Shift Keyed
Nort	Nortronics
FHC	Fairchild-Hiller Corp
Cal Comp	California Computer Co
PCM/PSK	Pulse Code Modulated/Phase Shift Keyed
IRLS	Interrogation, Recording and Location Subsystem
ITP	Integrated Test Plan
BIT	Bench Integrated Test
T/V	Thermal Vacuum
WTR	Western Test Range
GFE	Government Furnished Equipment
C&DH	Command and Data Handling Subsystem
VIP	Versatile Information Processor
SASS	Solar Array Sun Sensor
RWS	Reaction Wheel Scanner
SAD	Solar Array Drive
ADP	Automatic Data Processing
SWR	Standing Wave Ratio
RDT	Raw Data Tape
RMP	Rate Measuring Package
YIRU	Yaw Inertial Reference Unit
LN	Lead Network
RSAD	Right Solar Array Drive
HAC	Horizon Attitude Computer
ACS	Attitude Control Subsystem
PSA	Pneumatic Subassembly

# SECTION I

## INTRODUCTION

1.1	Study Objective ..	. . . . .	1-1
1.2	Summary ..	. . . . .	1-1

SECTION 1  
INTRODUCTION

The Phase B/C study for the Earth Resources Technology Satellite, ERTS-A and -B has been successfully completed with the establishment of a spacecraft baseline design meeting the overall ERTS mission requirements.

The evolution of the design from the initial goals, requirements, analysis, conceptual design and definition of hardware to meet the criteria has culminated in a Phase D proposal being submitted with this final Phase B/C Spacecraft System Design Report.

1.1 STUDY OBJECTIVE

The primary objective of this study is to develop an observatory spacecraft capable of meeting the performance requirements of the ERTS mission. In attaining this objective, it was necessary to perform the analyses delineated in the NASA Study Specification S-701-P-3 and other analyses and design tasks as the study progressed.

1.2 SUMMARY

This final study report delineates the activities that have taken place since contract inception. A complete report of the analyses, studies, design tradeoffs and the final spacecraft baseline design is included.

This report consists of three volumes. Volume I discusses the study requirements for Phase B/C along with the specific study tasks that were performed during the spacecraft phase of the study.

The Baseline Spacecraft Design is presented in summary fashion, including the overall performance, payload characteristics, configuration of the spacecraft and an overview of each subsystem making up the spacecraft and its associated Aerospace Ground Equipment (AGE).

This baseline design includes a high percentage of space-qualified hardware including the basic structure design, attitude control subsystem, power subsystem, thermal subsystem, and electrical integration subsystem. These subsystems are basically the Nimbus design, or modifications thereof, for the ERTS application. In addition, the Orbit Adjust Subsystem was selected from those flown on other space programs and the Communications and Data Handling Subsystem components were defined to utilize, where possible, flight proven designs or modifications to space-qualified hardware. The remainder of Volume I is devoted to the following spacecraft system level study reports:

1. System Reliability - The System Reliability Study includes the analysis and subsystem reliability block diagrams for each spacecraft subsystem with the subsystem and system reliability numbers for a one-year operation.



11 February 1970

2. Orbit Analysis - The Orbit Analysis Study is an analytical treatise on the selection of the orbital parameters for the ERTS mission. The analysis resulted in establishing the requirements for controls to achieve and maintain the orbit.
3. Image Location - The analysis in this area is due to the necessity of locating a given image within 2nm in a 100 x 100 nm frame. The results of this analysis established the attitude control and attitude determination requirements for the spacecraft.
4. Time Annotation - The Time Annotation requirement is associated with the previous analysis on image location. This study included analysis on different methods of processing time information with image information aid in the location of a given image.
5. Mission Simulation - The Mission Simulation task developed the operational concepts for the ERTS mission. Mission time lines established the duty cycle for the payload and associated equipment, this in turn, established the power requirements and consequently the power subsystem performance. The same information was required to establish the thermal control performance requirements. Hence, an analysis of the coverage, ground trace, data acquisition, data transmission and payload capabilities and constraints contribute greatly to the baseline spacecraft design.

Volume II of this study report covers detailed study and analysis tasks which led to each subsystem baseline design. The introduction to Volume II includes a brief summary description of the Spacecraft System, which is presented in much more detail in Section 3 of this Volume.

Volume III is dedicated solely to the Study Performance Assurance Tasks. It includes Quality Program Plans, Parts, Materials and Processer Plans, Configuration Management Plan, Process Control, Failure Analysis and Reporting, Compliance of Existing Hardware to ERTS Requirements, and, the ERTS Reliability Program Plan. Two copies of GE SSO Quality Assurance Procedures are included with two copies of applicable specifications as other supporting documentation.

Appendices are included at the end of the section to which they apply.

The Baseline System Design Description appears in this study report and in the Phase D proposal. This was done intentionally to clearly establish and have available for the reader, the baseline designs resulting from the study on which the Phase D proposal is based. Detailed component descriptions appear only in the respective proposal volumes, thus avoiding unnecessary duplication of written material. Summaries of the subsystem

11 February 1970

analyses and studies, reported in detail in the study report, have been included in the Proposal for convenience of the reader. Subsystem descriptions are similarly detailed in the study report and either summarized or repeated in the proposal as is required for clarity.

# SECTION 2

## STUDY REQUIREMENTS

2.1	Study Tasks	..	.	.	.....	...	2-1
2 2	Supplementary Study Documents	..	.			..	2-1

## SECTION 2

## STUDY REQUIREMENTS

The Phase B&C study requirements are specified in NASA/GSFC's Design Study Specifications for the Earth Resources Technology Satellite, ERTS A and B, dated April 1, 1969, re-issued October 1969 (S-701-D-3). These requirements were analyzed in detail and specific study tasks identified as part of GE's proposal to the government for the ERTS Phase B/C Study. \* Having been awarded this study, the General Electric Company has diligently pursued these tasks, as well as many others which it considered pertinent and in the government's best interest in performing a comprehensive and complete design study.

2.1 STUDY TASKS

For convenience in locating the specific section(s) of the SSD final report in which each study task is addressed, Table 2-1 has been prepared. The task numbers (assigned by GE) use the first four digits to reference the appropriate paragraphs of the Design Study Specification and the final two digits as sequence numbers. The tasks derive from those contained in GE's proposal in two respects

1. The 14XXXX and subsequent tasks are not included since they are part of the GDHS final report to be submitted in April.
2. Additional tasks have been added that are of interest to the government, but not specifically included in the reference proposal.

2.2 SUPPLEMENTARY STUDY DOCUMENTS

During the course of the study, the government has made many advisory documents, reports, articles and memos available to the General Electric Company to supplement the information contained in the design study specification and to generally aid in performance of the study. A list of the documents received is contained in Table 2-2. In addition to the title, author and data received, a document number used for internal control is included.

---

\* MSD Proposal No. N-21611, Volume V - Revision B, 14 November 1969

TABLE 2-1. SUMMARY TASK DESCRIPTION REFERENCE

Task No.	Task Description	Location in SSD Final Report
710001	<p>Show capability of the proposed spacecraft to satisfy payload requirements.</p> <ul style="list-style-type: none"> <li>● Configuration layouts</li> <li>● Thermal analysis</li> <li>● Mechanical and structural analysis</li> <li>● Integration into a final spacecraft design which supports the payload requirements.</li> </ul>	Volume I Section 3.2.3
710002	<p>Identify specification items not compatible with existing designs. Determine where spacecraft design changes are required to achieve compatibility. Where appropriate, recommend payload changes to GSFC.</p> <ul style="list-style-type: none"> <li>● Establish whether MSPS can use an existing Nimbus D Clock signal</li> <li>● Determine modifications required to the Power Subsystem to accommodate the WBVTR's and RBV camera transients</li> <li>● Review all other payload characteristics for spacecraft compatibility. Resolve incompatibilities if they exist.</li> </ul>	Volume I Section 3.2.2
713001	<p>Review basic DCS conceptual approach, define and justify departures if required. Outline functional and operational system concept, conceptual designs and prepare preliminary specifications and optimize costs.</p> <ul style="list-style-type: none"> <li>● Review the basic conceptual approach for definition and evaluation of successful reception, platform distribution, overall system accuracy, clock accuracy, ERP, spacecraft and platform antennas, reliability and cost.</li> <li>● Recommend any departures from the concept if required.</li> <li>● Outline functional and operational systems concepts.</li> <li>● Prepare a conceptual design of the DCS</li> <li>● Prepare preliminary specifications for the DCP and the spacecraft equipment.</li> </ul>	Separate Report

TABLE 2-1. SUMMARY TASK DESCRIPTION REFERENCE (Contd.)

Task No.	Task Description	Location in SSD Final Report
714001	<p>Study an additional spacecraft configuration which excludes the WBVTR's.</p> <ul style="list-style-type: none"> <li>● Provide overall spacecraft configuration layout</li> <li>● Evaluate thermal and mechanical provisions of configuration</li> <li>● Provide mass properties</li> <li>● Revise command/telemetry functions and determine impact on these subsystems</li> <li>● Evaluate effect on overall wideband telemetry system</li> <li>● Develop alternate power profiles and evaluate effect</li> <li>● Evaluate implications to the GDHS</li> </ul>	Deleted from Study requirements
720001	<p>Investigate equipment capability for 1 year life Identify elements that might prevent achievement of 1 year life. Investigate sizing expendables, redundancy, recommend design solutions.</p> <ul style="list-style-type: none"> <li>● Identify equipment whose reliability fails to meet reliability allocation</li> <li>● Recommend design study of equipment for Phase D</li> <li>● Evaluate ability of Orbit Adjust system to meet 1 year life requirement</li> <li>● Review existing Nimbus analysis of pneumatics storage vs 1 year life requirement</li> </ul>	Volume I Section 4 1
730001	<p>Study mechanical, thermal and structural provisions for payload.</p> <ul style="list-style-type: none"> <li>● Modify component and payload arrangement layouts</li> <li>● Perform dynamic and stress analysis of primary crossbeam structural members</li> </ul>	Volume II Section 2.4.5  Section 2.4.7

TABLE 2-1. SUMMARY TASK DESCRIPTION REFERENCE (Contd.)

Task No	Task Description	Location in SSD Final Report
730002	<p>Study sensor alignment provisions and perform alignment error analysis for individual sensors.</p> <ul style="list-style-type: none"> <li>• Perform analyses and provide the mechanical design to assure required sensor alignments</li> </ul> <p>(Note Overall system performance, including effects of misalignment is included in Task 151001)</p>	Volume II Section 2.3.4
None	Demonstrate Flexibility of Spacecraft Design	Volume II Section 2
740001	Review the results of the Nimbus study "Thorad/Delta Launch Vehicle Study for Nimbus E Spacecraft" for applicability to ERTS.	Volume I Section 3.2 7
741001	<p>Study and indicate moments and products of inertia</p> <ul style="list-style-type: none"> <li>• Provide periodic Mass Properties Reports which list weight, moments and products of inertia of the spacecraft and payload</li> <li>• Determine spacecraft control system tolerance to uncompensated momentum and magnetic moment</li> </ul>	Volume II Section 2  Volume II Section 5.4.5
751001	<p>Study compatibility with Orbit Adjust system.</p> <ul style="list-style-type: none"> <li>• Compute rate and attitude errors during the orbit adjust maneuver</li> <li>• Determine what control system design changes, if any, are required to achieve a pointing accuracy compatible with the orbit adjust maneuver.</li> </ul>	Volume II Section 5.4.3

TABLE 2-1. SUMMARY TASK DESCRIPTION REFERENCE (Contd.)

Task No.	Task Description	Location in SSD Final Report
751002	<p>Study attitude determination for image location and hardware associated with meeting goals. Identify problems</p> <ul style="list-style-type: none"> <li>• Define techniques for accurately determining the attitude of the spacecraft in order to determine the location of an image in photographs taken from orbital altitude to within less than 2 nautical miles in a 100 x 100 nautical mile picture</li> <li>• Define requirements for and select attitude sensor for this purpose</li> </ul>	<p>Volume I Section 4.3</p> <p>Volume II Section 5.4.9</p>
751003	<p>Determine location of imagery using ground features, predicted satellite performance and imagery information</p> <ul style="list-style-type: none"> <li>• Investigate visibility and identifiability of control-point images on RBV and MSPS imagery</li> <li>• Evaluate time and pointing errors for manual image identification and location</li> <li>• Evaluate time and pointing errors for automatic image matching of RBV/MSPS imagery</li> <li>• Determine extent and type of positioning to be performed</li> </ul>	<p>Later (April)</p>
751004	<p>Update control system block diagram. Analyze results of computer simulations performed on Nimbus program. Select analyses applicable to ERTS to demonstrate control system performance to ERTS requirements.</p>	<p>Volume II Section 5.4.2 and 5.3</p>
751005	<p>Define yaw sun sensor control back-up mode.</p> <ul style="list-style-type: none"> <li>• Identify the components and techniques to be used to control the yaw axis in the event of failure of the rate measuring package (gyrocompass)</li> </ul>	<p>Volume II Section 5.4.4</p>

11 February 1970





TABLE 2-1. SUMMARY TASK DESCRIPTION REFERENCE (Contd.)

Task No.	Task Description	Location in SSD Final Report
None	System Design Changes to Achieve Desired Attitude Rate.	5.4.2.3.2
None	Provide Block Diagram of Control System and Demonstrate Performance.	5.3
None	Recommend Control System Provisions during Orbit Adjust.	5.4.3.3
761001	<p>Determine and recommend number and type of command functions for payload and spacecraft operation, and indicate availability of command status telemetry monitoring</p> <ul style="list-style-type: none"> <li>● Update list of command functions required for proper operation of the spacecraft and payload sensors</li> <li>● Determine requirement for telemetry</li> </ul>	<p>Volume II Section 4</p> <p>Volume II Section 4 Appendix</p>
761101	<p>Consider command storage requirements and provisions for multiple executions of stored commands and define interface requirements.</p> <ul style="list-style-type: none"> <li>● Rewrite specification reflecting any changes</li> <li>● Update definition of the command storage interface</li> <li>● Document the provisions for overriding of stored commands</li> <li>● Update the command addressing technique</li> <li>● Document the inherent reliability, flexibility, and adaptability</li> </ul>	Volume II Section 4
761201	<p>Investigate techniques for providing "Fail Safe" design to prevent non-reversible command action.</p> <ul style="list-style-type: none"> <li>● Select the optimum technique to insure that no single occurrence of an erroneous command can initiate a non-reversible command</li> </ul>	Volume II Section 4

TABLE 2-1. SUMMARY TASK DESCRIPTION REFERENCE (Contd.)

Task No.	Task Description	Location in SSD Final Report
762001	<p>Define NB telemetry system and determine capacity, sampling rate, flexibility and growth capability. Consider existing VHF or UHF transmission system.</p> <ul style="list-style-type: none"> <li>● Obtain specifications of existing spacecraft PCM systems</li> <li>● Determine their ability to handle all housekeeping data and data from the Attitude Determination System</li> <li>● Study the formatting, flexibility and growth capability of the selected PCM unit</li> <li>● Define the system capability, sampling rate available, provisions for digital words, single bit indicators, sampling flexibility, growth provisions and the total bit rate for each available format</li> <li>● Choose an existing PCM/PM transmitter which meets the requirement of a received bit error rate of 1 in <math>10^6</math> or less for real time telemetry</li> </ul>	Volume II Section 4
763101	<p>Perform W/B Telemetry RF downlink power calculations for two stated conditions.</p> <ul style="list-style-type: none"> <li>● Determine the optimum parameters of the system components</li> </ul>	Volume II Section 4
763102	<p>Prepare system design and block diagram, estimate size, weight and power input requirements and specify the transmitter to be used.</p> <ul style="list-style-type: none"> <li>● Study and verify the GSFC baseline system configuration in order to achieve the desired operational features at minimum cost, within the allowable time</li> <li>● Prepare specifications for system components</li> <li>● Refine the estimated physical characteristics of the system components</li> </ul>	Volume II Section 4

TABLE 2-1 SUMMARY TASK DESCRIPTION REFERENCE (Contd.)

Task No.	Task Description	Location in SSD Final Report
763103	Study the expected degradation of the wideband sensor data. <ul style="list-style-type: none"> <li>● Identify sources of degradation to the sensor output data</li> <li>● Select the optimum system configuration</li> </ul>	Volume II Section 4
763104	Evaluate both PCM and FM S-band transmitter designs. <ul style="list-style-type: none"> <li>● Survey vendors for transmitters meeting ERTS specified requirements</li> <li>● Select design for the ERTS program</li> </ul>	Volume II Section 4
763105	Evaluate Breadboard PCM and FM modulators. <ul style="list-style-type: none"> <li>● Provide modulator breadboards</li> <li>● Test to verify electrical specifications of wideband telemetry link</li> </ul>	Volume II Section 4
763106	Study, define, and evaluate diplexer and shaped antenna system for W/B telemetry. <ul style="list-style-type: none"> <li>● Analysis of candidate designs</li> <li>● Definition of antenna system configuration</li> </ul>	Volume II Section 4
763201	Study scanner and TV data links. Recommend cross strapping to achieve maximum redundancy <ul style="list-style-type: none"> <li>● Study switching and command functions, for interconnecting the RBV sensor, MSPS sensor, tape recorders, and wideband transmitters and antennas</li> <li>● Recommend detailed interconnection switching subsystem</li> </ul>	Volume II Section 4

TABLE 2-1. SUMMARY TASK DESCRIPTION REFERENCE (Contd.)

Task No.	Task Description	Location in SSD Final Report
763202	<p>Perform overall study of wideband communication system design including verification of selected multiplexing techniques</p> <ul style="list-style-type: none"> <li>• Determine data characteristics of object plane MSPS and RBV sensor signals</li> <li>• Perform communication system studies of Object Plane MSPS and of RBV to verify the selected multiplex techniques and parameters, recording techniques and carrier modulation techniques</li> <li>• Consider implementation factors (size, weight, power, development time and effort), and growth capacity</li> </ul>	Volume II Section 4
764001	<p>Verify mmtrack link calculations.</p> <ul style="list-style-type: none"> <li>• Perform RF downlink power calculations</li> </ul>	Volume II Section 4
765101	<p>Determine that the system design is compatible with the wideband tape recorder characteristics.</p> <ul style="list-style-type: none"> <li>• Study specification of GFE WBVTR</li> <li>• Establish requirements imposed on ERTS by WBVTR</li> <li>• Prepare report</li> </ul>	Volume II Section 4
765201	<p>Study application of existing flight proven recorders to ERTS</p> <ul style="list-style-type: none"> <li>• Study use of redundant recorders</li> <li>• Analyze suitability of Nimbus Recorders to ERTS mission</li> <li>• Conduct survey of available off the shelf recorders</li> <li>• Prepare specification</li> <li>• Prepare report</li> </ul>	Volume II Section 4

TABLE 2-1. SUMMARY TASK DESCRIPTION REFERENCE (Contd )

Task No.	Task Description	Location in SSD Final Report
766001	<p>Define the clock subsystem and determine its accuracy, stability, reliability and suitability for ERTS mission.</p> <ul style="list-style-type: none"> <li>● Identify all timing requirements of ERTS</li> <li>● Document the accuracy and tolerances with which universal time may be annotated with picture data</li> <li>● Study the provisions for resetting the clock and accelerating it through one year of time</li> <li>● Investigate methods for uniquely identifying the camera exposure time with the spacecraft clock</li> </ul>	<p>Volume II Section 4</p> <p>Volume I Section 4.4</p>
767001	<p>Study the baseline GSFC combined TT&amp;C system in order to implement the design.</p> <ul style="list-style-type: none"> <li>● Investigate techniques to integrate STADAN/VHF and MSFN/USB dual command capability</li> <li>● Determine modifications required to existing command hardware</li> <li>● Determine specifications for new command hardware required for integrated dual command capability.</li> <li>● Determine specifications for 1.024 MHz subcarrier oscillator and bi-phase modulator</li> <li>● Determine optimum modulation indices for 1.024 MHz subcarrier data and range-and-range rate signal using USB transmitter</li> <li>● Determine degradation caused by transmitting NB telemetry recorder playback on 136 MHz beacon</li> <li>● Prepare detailed specification for the subsystem components.</li> <li>● Perform link calculations to determine output power requirements for USB transmitters</li> </ul>	<p>Volume II Section 4</p>



TABLE 2-1 SUMMARY TASK DESCRIPTION REFERENCE (Contd )

Task No.	Task Description	Location in SSD Final Report
780001	<p>Consider satellite configuration on overall basis for thermal requirements.</p> <ul style="list-style-type: none"> <li>● Update existing ERTS studies</li> <li>● Identify any required design or hardware changes</li> <li>● Update heat rejection capability of Attitude Control System</li> <li>● Verify overall thermal design of the ACS</li> <li>● Determine maximum and minimum orbital temperature excursions for equipment in sensory ring and center section</li> <li>● Define the payload/spacecraft thermal interface</li> </ul>	Volume II Section 7
780002	<p>Investigate specific problems associated with payload or with proposed spacecraft configuration.</p> <ul style="list-style-type: none"> <li>● Investigate localized payload problems</li> <li>● Determine the thermal interaction between the orbit adjust engine and the spacecraft</li> <li>● Determine the effects of orbital adjust engine plume impingement on spacecraft structure, equipment and thermal coatings</li> </ul>	Volume II Section 7
791001	<p>Specify the orbit adjust system to permit attainment of the stated specification requirements.</p> <ul style="list-style-type: none"> <li>● Update the existing preliminary specifications</li> <li>● Revise the specification of total <math>\Delta V</math></li> <li>● Investigate the effects of thrust duration, pointing accuracy, impulse uncertainty and cross coupling of <math>\Delta V</math>'s</li> </ul>	Volume I Section 4. 2

TABLE 2-1. SUMMARY TASK DESCRIPTION REFERENCE (Contd.)

Task No.	Task Description	Location in SSD Final Report
791002	<p>Estimate the injection residuals after a nominal orbit adjust</p> <ul style="list-style-type: none"> <li>● Update estimates of injection residuals</li> <li>● Determine range of expected orbit adjust system residuals</li> <li>● Apportion of errors between the orbit adjust system and orbit determination capability</li> </ul>	Volume 1 Section 4.2
791003	<p>Specify the orbit adjust operational/procedural sequence necessary for removal of the injection errors.</p> <ul style="list-style-type: none"> <li>● Refine operational/procedural sequence</li> </ul>	Volume 1 Section 4.2
791004	<p>Design orbit adjust propulsion subsystem and generate subsystem and component specifications.</p> <ul style="list-style-type: none"> <li>● Consider alternate propulsion configurations</li> <li>● Relate effective thermal control to the spacecraft</li> <li>● Perform a comprehensive analysis of propulsion performance</li> <li>● Update the selection of all propulsion components</li> <li>● Prepare the subsystem specification</li> <li>● Identify long lead items</li> <li>● Write component specifications and vendor work statements</li> </ul>	Volume II Section 6
791005	<p>Verify the 496 nm, 99.04° retrograde circular orbit as optimum for ERTS coverage requirements.</p>	Volume I Section 4.2
791006	<p>Predict the variations in orbital parameters expected for a one year operation subsequent to removal of initial injection errors, and predict the need for subsequent orbit adjust maneuvers.</p> <ul style="list-style-type: none"> <li>● Update predictions based on residual errors subsequent to orbit adjust maneuvers</li> </ul>	Volume 1 Section 4.2



TABLE 2-1. SUMMARY TASK DESCRIPTION REFERENCE (Contd.)

Task No.	Task Description	Location in SSD Final Report
791007	<p>Verify the present GSFC assumption that orbit maintenance for drag decay over a 1-year lifetime is required.</p> <ul style="list-style-type: none"> <li>● Re-run digital computer programs to re-confirm conclusions as ballistic coefficients, density and residual orbit errors become more firm</li> </ul>	Volume I Section 4.2
791008	<p>Examine the effects of launch window duration and inclination errors on variations in "Beta" angle, subsatellite solar elevation angle and shadow history.</p> <ul style="list-style-type: none"> <li>● Evaluate the effect of a launch at the end of the launch window on the subsatellite's sun elevation angle, the beta angle and the shadow history</li> <li>● Evaluate the effects of inclination errors on the same three conditions (solar elevation, beta angles, and shadow history)</li> <li>● Evaluate injection inclination errors versus reduced orbit adjust system propellant requirements</li> </ul>	Volume I Section 4.2
791009	<p>Determine the optimum method for computing the required orbit adjust <math>\Delta V</math>, based on orbit determination data, and gradual accumulation of ground track errors.</p> <ul style="list-style-type: none"> <li>● Investigate alternate techniques for devising the best way of determining the actual ERTS orbit period, or ascending node longitude shift</li> <li>● Develop logic from which velocity impulse commands are ordered and monitored</li> <li>● Minimize effects of orbit determination errors</li> </ul>	Volume I Section 4.2

TABLE 2-1. SUMMARY TASK DESCRIPTION REFERENCE (Contd.)

Task No.	Task Description	Location in SSD Final Report
100001	<p>Prepare hardware availability matrix for major spacecraft assemblies</p> <ul style="list-style-type: none"> <li>● Update the matrix of ERTS major hardware</li> <li>● Determine extent of re-design to accommodate ERTS requirements</li> <li>● Overview of hardware availability</li> </ul>	Volume I Section 3.3
110001	<p>Review hardware for compliance with reliability, quality and testing requirements</p> <ul style="list-style-type: none"> <li>● Review all related hardware documents</li> <li>● Report on reliability, quality and test review ERTS hardware.</li> </ul>	Volume III Section 8
110002	<p>Develop reliability model and make numerical assessment for proposed hardware.</p> <ul style="list-style-type: none"> <li>● Report the nature of the model developed for the ERTS design</li> <li>● Discuss "weak" system links</li> </ul>	Volume I Section 7
110003	<p>Study configuration management and failure reporting procedures, and determine compliance with Goddard management instructions.</p> <ul style="list-style-type: none"> <li>● Review the existing Nimbus Configuration Management and Failure Reporting systems</li> <li>● Measure these against the requirements of existing policies specified for the Phase D proposal</li> </ul>	Volume III Section 7
110004	<p>Prepare parts and material lists, procurement specifications, and sources of supply</p> <ul style="list-style-type: none"> <li>● Update approved parts, materials and processes lists</li> </ul>	Volume III Sections 3 and 4

TABLE 2-1. SUMMARY TASK DESCRIPTION REFERENCE (Contd.)

Task No.	Task Description	Location in SSD Final Report
110005	<p>Develop the following performance assurance documentation for the ERTS-A and B Phase D Proposal.</p> <ul style="list-style-type: none"> <li>● Reliability Program Plan</li> <li>● Quality Program Plan</li> <li>● Test Monitor and Control Program Plan</li> <li>● Configuration Management Plan</li> <li>● Soldering Program Plan</li> <li>● Failure Reporting Plan</li> </ul>	<p>Volume III</p> <p>Vol. III, Sect. 9 Vol. III, Sect. 2 Vol. III, Ap. 2C Vol. III, Sect. 5 Vol. III, Sect. 6 Vol. III, Sect. 7</p>
120001	<p>Provide outline of integration, test, and launch support plan, including facility requirements. Define and justify any deviations from environmental test specifications, functions not testable during all-up test, proposed sequence, basic test philosophy.</p> <ul style="list-style-type: none"> <li>● Revise and update outlines of Phase D plans contained in Volume IV</li> <li>● Use Nimbus Test and Launch Support experience as well as existing Nimbus plans, test reports and procedures</li> </ul>	<p>Volume II Section 10</p>
130001	<p>Describe GSE, its application, and define new requirements and develop hardware matrix</p> <ul style="list-style-type: none"> <li>● Identify all GSE end items</li> <li>● Determine applicability of existing GSE hardware</li> <li>● Define design modifications</li> <li>● Establish new design items</li> <li>● Establish source and usage of all GSE end items</li> <li>● Summarize the study (Ref 767001)</li> </ul>	<p>Volume II Section 11</p>

TABLE 2-2 SUPPLEMENTARY STUDY DOCUMENT

Document/ Drawing No	Title	Author	Date Received
RM-001	General Environmental Test Specification for Spacecraft and Components	GSFC	17 November 1969
RM-002	GSFC Specification Contractor-Prepared Monthly, Periodic, Periodic, and Final Reports	GSFC	
RM-003	MSS Multiplexer/Modem Demultiplexer Final Study Report	SBRC	10 November 1969
RM-004	MSS Ground Recording And Processing Study Report	SBRC	10 November 1969
RM-005	MSS Processing Techniques Study Constraints	SBRC	5 November 1969
RM-006	Optimization of a Multispectral Scanner For ERTS	Hughes	4 November 1969
RM-007	Attachment II (Section 1 4. 5) Design Study Spec S-701-P-3	GSFC	10 November 1969
RM-008	Attachment III (Section 1. 4. 8) Design Study Spec S-701-P-3	GSFC	10 November 1969
RM-009	GSFC Specification Multispectral Scanner Sys.	GSFC	4 November 1969
RM-010	Appendix A Revision GSFC MSS Spec	GSFC	5 November 1969
RM-011	Ground Display Equipment Interface Requirements B1-Weekly Report No. 7	GSFC	10 November 1969
RM-012	Ground Display Equipment Interface Requirements B1-Weekly Report No. 8	GSFC	10 November 1969
RM-013	MSS Design Study	SBRC	10 November 1969
RM-014	First Quarterly Report on Wideband Video Recorder	RCA	10 November 1969
RM-015	Multi-Spectral Picture Registration Study	RCA	10 November 1969

TABLE 2-2. SUPPLEMENTARY STUDY DOCUMENTS (Cont'd.)

Document/ Drawing No.	Title	Author	Date Received
RM-016	U. S. Government Memorandum Meeting on Nov. 10, 1969 concerning ERTS Unified S-Band Link	Tracking and Data Systems Manager for ERTS	28 November 1969
RM-017	MSS Monthly Progress Report No. 1	Hughes	28 November 1969
RM-018	Memorandum for Record Proposed Constants and Equations For ERTS A and ERTS B Atmospheric Density Model	A Fuchs R. Strafella	1 December 1969
RM-019	Memorandum From Tracking and Data Systems Mgr.	Bradley	3 December 1969
RM-020	RBV Shutter Drive Schematic	RCA	2 December 1969
RM-021	RBV Progress Report October 1969	RCA	5 December 1969
RM-022	RBV Design Study Report AED-R-3413 Dated January 1969	RCA	25 November 1969
RM-023	USB Acquisition Techniques	GSFC	5 December 1969
RM-024	S-Band Xmtr - Design Study Report and First Quarterly Report - 16 June 1969 to 16 Sept. '69	ITT	12 December 1969
RM-025	RBVC Drawings 1976466 Camera Electronics Assy 1976467 Camera Controller Assy 1976696 Sensor Outline 2" RBV	RCA	25 November 1969
RM-026	MSS Radiometer Drawing - 24391	HAC	
RM-027	Design Study Specifications For ERTS April 1969 Revised October 1969	NASA	

TABLE 2-2. SUPPLEMENTARY STUDY DOCUMENTS (Cont'd.)

Document/ Drawing No.	Title	Author	Date Received
RM-028	Second Quarterly Report For Design, Fabrication Development and Test of 4 MHz Video Recorder/ Reproducer	RCA	4 November 1969
RM-030	Thor Delta Performance Preliminary Mission Analysis	GSFC	17 December 1969
RM-031	Preliminary Specs for Triple Line Transmitter and Receivers (1969)	RAD	18 December 1969
RM-032	Dual Line Receiver and Driver Bulletin	TI	18 December 1969
RM-033	MSS Radiometer Interface Control Drawing	SBRC	18 December 1969
RM-034	Ground Display Equipment Interface Requirements B1-Weekly Report No 9	GSFC/ Westinghouse	17 December 1969
RM-035	Ground Display Equipment Interface Requirements B1-Weekly Report No. 10	GSFC/ Westinghouse	17 December 1969
RM-036	Ground Display Equipment Interface Requirements B1-Weekly Report No. 11	GSFC	17 December 1969
RM-037	MSS December Interface Meeting (Vu-Graph)	HAC	18 December 1969
RM-038	MSS Interface Specification	HAC	18 December 1969
RM-039	RBV's Monthly Progress Report No. 1	RCA	18 December 1969
RM-040	Two inch Return Beam Vidicon Camera System	RCA	18 December 1969
RM-041	Minutes of MSS Interface Meeting Held at HAC 12/18/69	HAC	22 December 1969
RM-042	Preliminary Statement of RBV Camera Mounting and Alignment Constraints	RCA	23 December 1969

TABLE 2-2. SUPPLEMENTARY STUDY DOCUMENTS (Cont'd.)

Document/ Drawing No.	Title	Author	Date Received
RM-043	NASA Memorandum 29DEC69 Subject Manpower Phasing Plan for ERTS/6DHS M and O Type Personnel, GSFC Furnished	NASA	
RM-044	VIDEO Tape Recorder Power Profiles	GSFC	9 January 1970
RM-045	MSS Thermal Analysis	GSFC	9 January 1970
RM-046	MSS Monthly Progress Report No. 2	Hughes	9 January 1970
RM-047	RBV Interface Action Items	RCA	9 January 1970
RM-048	Data System Development Plan NASCOM Network Revision 4, Section I Revision 5, Section I Revision 5, Section II	GSFC	12 January 1970
RM-049	2" RBV Envelope Drawing - Three Sensors	RCA	9 January 1970
RM-050	MSS Spacecraft Wiring	Hughes	14 January 1970
RM-051	USB Ranging Spectra	GSFC	15 January 1970
RM-052	Management, Processing, and Discrimination of Sensory Data for ERTS	ARA	20 January 1970
RM-053	Changes to Specification S-701-P-3 Section 2.14	GSFC	16 January 1970
RM-054	MSS/ERTS Interface	GSFC/Hughes	26 January 1970
RM-055	MSS Monthly Progress Report No. 3	SBRC	26 January 1970
RM-056	RBV Monthly Progress Report No. 2	RCA	23 January 1970
RM-057	RBV Power Profiles Faceplate Temperature Control Function	RCA	30 January 1970

11 February 1970

## SECTION 3

### BASELINE SPACECRAFT SYSTEM DESIGN

3.1	Introduction . . . . .	3-1
3.2	Spacecraft System Design . . . . .	3-1
3 2.1	System Functional Relationships . . . . .	3-1
3.2.2	Payload Characteristics Summary . . . . .	3-6
3.2.3	ERTS Spacecraft Configuration . . . . .	3-13
3.2.4	Electrical and Functional Description . . . . .	3-16
3.2.5	Subsystem Overview . . . . .	3-24
3.3	Hardware Matrix . . . . .	3-68
3.4	Launch Vehicle Study Result . . . . .	3-77
3 4.1	General . . . . .	3-77
3 4.2	ERTS/Delta Electrical Integration . . . . .	3-79
3.5	Growth . . . . .	3-86
3.5 1	General . . . . .	3-86
3.5.2	Growth Missions . . . . .	3-86
3.5.3	Spacecraft Growth . . . . .	3-92
3.5.4	Growth Power Systems . . . . .	3-100
3.5.5	Alternate Orbits . . . . .	3-105



## SECTION 3

### BASELINE SPACECRAFT SYSTEM DESIGN

#### 3.1 INTRODUCTION

The basic requirements specified by NASA for the ERTS A&B Spacecraft System Design (SSD) have been studied in detail. The results of these studies are reported in this and subsequent volumes. The culmination of these studies is a proposed spacecraft design which optimally satisfies the ERTS A&B requirements. This section provides a top level summary description of the proposed ERTS A&B spacecraft design which has evolved. Detail discussion, analysis and trade studies which have led to this selection and more detailed subsystem and component descriptions are contained in subsequent sections.

A matrix of all major spacecraft components and Aerospace Ground Equipment (AGE) end items follows. This identifies all hardware, quantities, source, design status, and flight experience.

Next, the selected launch vehicle and shroud is presented.

The final section considers growth beyond ERTS A&B. Growth missions, and in particular, the oceanographic mission, are discussed briefly. Then spacecraft growth, based on logical extensions of the proposed baseline design, is considered which meet the projected needs of an ongoing Earth Resources program.

#### 3.2 SPACECRAFT SYSTEM DESIGN

This section provides a summary description of the spacecraft system design which was selected as a result of the Phase B/C study effort. Compared to the baseline design presented in General Electric's proposal of June 1969, the most significant changes have occurred in the telemetry, tracking and command equipment. These changes result from the requirement to operate compatibly with both STADAN and MSFN ground stations. Even with these changes, the basic requirements specified by NASA are met largely by existing designs or straightforward modifications of existing designs.

##### 3.2.1 SYSTEM FUNCTIONAL RELATIONSHIPS

The functional relationship between the ERTS Spacecraft subsystems is designed to provide maximum mission performance. The overall Spacecraft system is comprised of nine subsystems:

1. Structures
2. Communications and Data Handling
3. Attitude Control
4. Orbit Adjust

5. Thermal
- 6 Power
7. Electrical Integration
- 8 Aerospace Ground Equipment (AGE)
9. Payload (GFE)

The overall system is illustrated in a simplified block diagram, Figure 3.2.1-1. This figure delineates, in accessible form, the main functional elements within each subsystem. Table 3.2 1-1 summarizes the functional relationships among the subsystems

The overall configuration of the spacecraft is shown in Figure 3 2 1-2. The cross-section layouts show the ERTS B Multispectral scanner with the radiative cooler. The ERTS A configuration is identical except for the deletion of this cooler. The selection and arrangement has evolved through careful study using established guidelines which will assure successful integration of a payload consisting of several earth viewing sensors.

The high resolution payload sensors for ERTS A&B require an extremely stable, low rate, and highly accurate platform to realize their maximum capability. The attitude control system requirements compatible with these sensor requirements has been specified as less than 0.7 degrees pointing control with error rates of less and 0.04 degree per second and as a goal 0.015 degrees per second.

The Nimbus D derived ERTS attitude control subsystem has the capability to meet these requirements. This control subsystem is based on a flight proven design which has demonstrated its capability to operate for several years in orbit. Modifications to meet ERTS requirements include simple switching changes to the logic, adjustment of loop gains and the provision of a redundant yaw gyro.

In addition to the pointing requirements, a requirement exists for locating any point on a 100 by 100 nm image with an accuracy of less than 2 nm. This position location accuracy requires precise attitude knowledge which is provided by an attitude sensor. The sensor selected is a passive radiometric balance type of earth sensor which is developed and fully qualified. This sensor provides pitch and roll attitude to better than 0.1 degree. The only significant modification is the lens design which is changed to accommodate the ERTS altitude. Yaw attitude data is determined from processing of existing spacecraft telemetry.

The mission coverage requirements for precisely controlled and repeating observation by the relatively narrow field of view sensors necessitate the inclusion of an orbit adjust subsystem in the spacecraft. This system must remove initial launch vehicle injection errors to establish the precise ERTS orbital parameters and must make adjustments throughout the one year life of the mission in order to maintain the orbital parameters under disturbing influences such as aerodynamic drag. A simple monopropellant blowdown

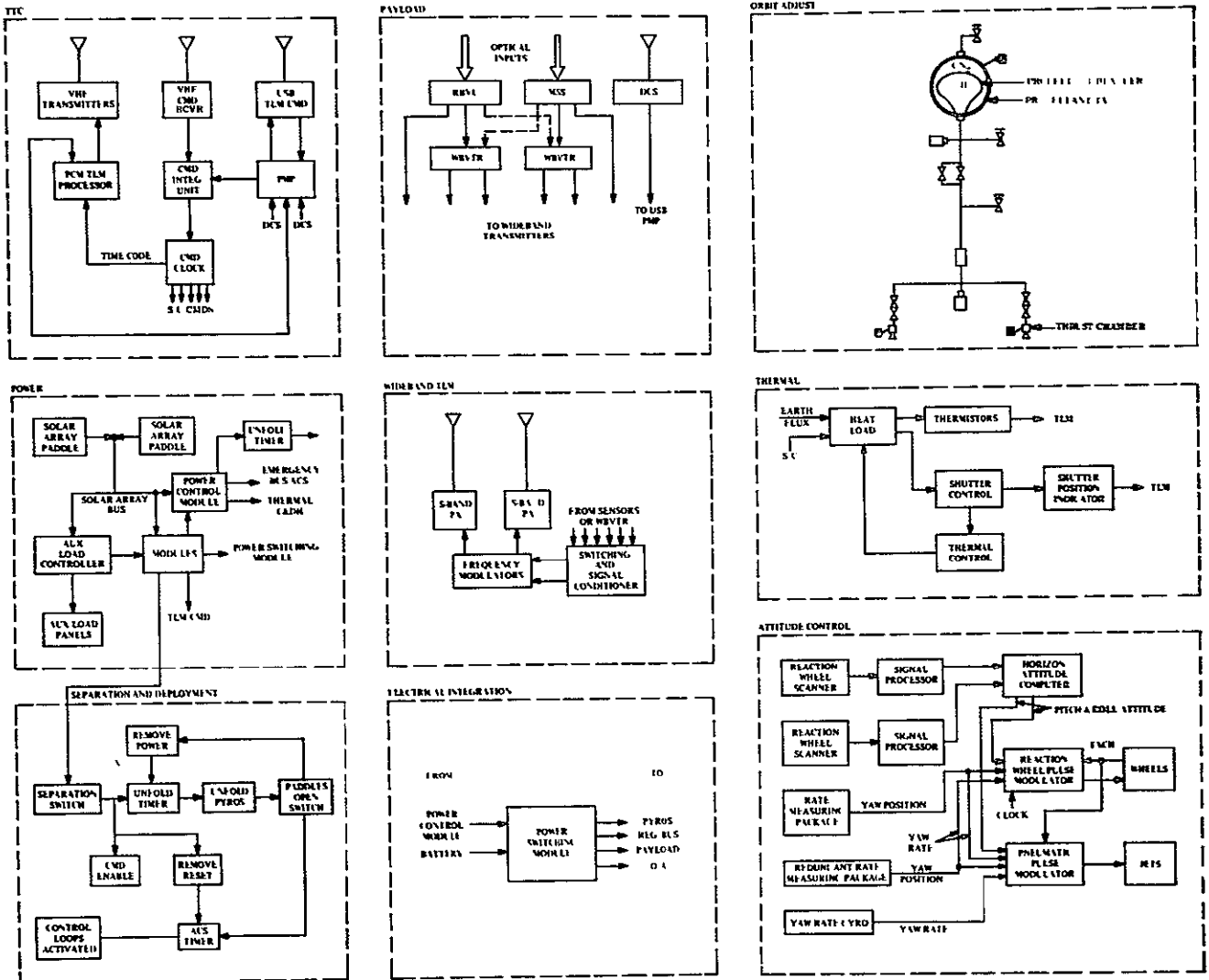


Figure 3.2.1-1. ERTS Simplified Block Diagram

Table 3.2 1-1 Functional Relationships

Requires	Subsystem	Provides
<ul style="list-style-type: none"> <li>• Power</li> <li>• Commands               <ul style="list-style-type: none"> <li>- On-Off</li> <li>- Operations Modes</li> </ul> </li> <li>• Data from Payload</li>   <li>• Status from all Subsystems</li> <li>• Power</li>   <li>• Commands</li> <li>• Power</li>   <li>• Commands</li> <li>• Power</li>   <li>• Commands for auxiliary loads</li> <li>• Commands for On-Off Control</li>   <li>• Power</li> <li>• Ground Data from (DCP)</li> <li>• Spacecraft Stability Control</li> <li>• Operational Control</li>   <li>• Structural Support</li> <li>• Commands</li>   <li>• Power</li> <li>• Temperature Status</li> </ul>	<p style="text-align: center;"><u>COMMUNICATIONS AND DATA HANDLING</u></p> <p><u>Wide-Band Telemetry</u></p> <p>The wideband telemetry provides the transmission channel for the MSS and RBV data and accepts the stored data from the WBVTR. Transmission of the PCM (MSS) data or the Video (RBV) data can be on either channel of the redundant system.</p> <p><u>Narrow Band Telemetry, Tracking and Command</u></p> <p>The Narrow Band Telemetry Tracking and Command equipment provide the means for tracking the vehicle, commanding the vehicle and its equipment and telemetering housekeeping data. Uplink and downlink is available both through MSFN and STADAN stations.</p> <p><u>ORBIT ADJUST</u></p> <p>The orbit adjust subsystem provides the means to correct for initial injection errors and to provide orbit maintenance due to drag.</p> <p><u>ATTITUDE CONTROL</u></p> <p>The attitude control subsystem acquires and maintains three axis stabilization of the spacecraft and provides a stable platform for sensor operation. Also through utilization of the Attitude sensor image location within <math>\pm 2</math> nm is achieved.</p> <p><u>POWER</u></p> <p>Primary power is generated by the solar array panels with excess power dissipated in the auxiliary loads. Battery charging is controlled by circuitry in each storage module and regulated voltages are provided by redundant pulse width modulators in the Power Control Modules. Automatic switchover is available in each Power Control Module.</p> <p><u>PAYLOAD</u></p> <p>The spacecraft payload consists of three RBV's, two WBVTR's, the DCS receiver and antenna and the MSS. These provide the data for multi-spectral analysis of the selected coverage areas.</p> <p><u>ELECTRICAL INTEGRATION</u></p> <p>The electrical integration subsystem distributes the power and signals throughout the spacecraft.</p> <p><u>THERMAL</u></p> <p>The thermal subsystem provides thermal control for the sensory ring, the ACS, the equipment mounted within, below, and above the sensory ring.</p>	<ul style="list-style-type: none"> <li>• Data link to Corpus Christi, NTTF and Alaska</li>   <li>• Implements Command functions for all subsystems</li> <li>• Communications</li> <li>• Tracking Beacon</li> <li>• MSFN/STADAN Command Compatibility</li>   <li>• <math>\Delta V</math> for orbit correction</li>   <li>• Control stability for sensors</li> <li>• Status to Telemetry</li> <li>• Data for image location</li>   <li>• Regulated and Unregulated power for all Subsystems</li>   <li>• Image data via wideband telemetry</li> <li>• DCS data via USB telemetry</li> <li>• Stored data from the WBVTR's</li>   <li>• Power switching</li> <li>• Signal switching</li> <li>• All electrical I/F's</li>   <li>• Passive control</li> <li>• Active control</li> <li>• Thermal sensing for various subsystems</li> </ul>

hydrazine system was selected which provides a thrust level of about one pound. This level allows launch vehicle injection corrections to be made in a reasonably short time, still permits the metering of relative small corrections for drag make-up, and is compatible with the ACS control torques. A modular packaging concept has been employed, allowing the complete orbit adjust subsystem to be assembled and tested as an integral unit prior to assembly to the spacecraft. Interfaces are especially simple. The selected system uses components which are all flight qualified. The total  $\Delta V$  requirement for one year has been derived and is 45 fps.

The Communications and Data Handling (C&DH) system is unique in that it must be compatible with two different NASA ground networks, STADAN and MSFN/USB, and also must routinely transmit data at the highest rate and bandwidth ever required for any previous NASA program. For the Telemetry, Tracking and Command (TT&C) portion of this subsystem, dual equipments are required. To operate with the MSFN/USB requires the use of the Apollo USB type equipment which operates at 2106.4 MHz (command uplink) and at 2287.5 MHz down for TLM. The STADAN TT&C operates at 154.2 MHz for command and at 137.86 MHz for telemetry.

The proposed TT&C system uses existing designs for the command/clock and telemetry processor (VIP). A simple harness change allows the output data rate of the VIP to be reduced from 4 (as used on Nimbus D) to 1 kbps for ERTS. The VHF transmitters are based on existing designs, however the modulation is changed from AM to PM, and two power levels are provided. In order to make the USB command compatible with the existing command clock a command integrator unit (CIU) is used. Although a new design, it incorporates the state of the art circuitry and serves to demodulate and sub-bit decode the USB uplink command signal providing a compatible output at 200 kbps to the command clock. The VHF receivers have been modified to make them fully compatible with STADAN requirements. The USB transponders and the premodulation processor are based on Apollo designs but will require re-packaging. The narrow band tape recorder designs are based on a currently qualified recorder. All antennas are existing designs currently used on NIMBUS D.

The wideband telemetry system accepts either RBV video at 3.5 MHz or MSS PCM at 15 Mbps. Switching and signal conditioning of the six possible data inputs (RBV or MSS, Realtime or Playback, WBVTR No. 1 or WBVTR No. 2) results in the selection of any two. These are processed through identical parallel modulator/power amplifier/antenna systems. Commandable 20/10 watt levels are provided in the TWT power amplifiers. Two shaped beam antennas provide a near constant earth illumination with  $> 4$  dB gain over a +60 degree cone angle.

The relatively large power demands and varying duty cycles of the payload equipment plus the housekeeping loads of the spacecraft specify the energy and conversion requirements that the power system must satisfy. These are satisfied with the existing and flight proven Nimbus power system design, consisting of independently driven solar arrays, eight individual battery modules with a total capacity of 36 ampere-hours, an auxiliary load controller and two power control modules. The use of a second Power Control Module

(PCM) is the only change from the flight proven Nimbus system. This increases the peak capacity of the system to about 1000 watts (500 from each PCM) and allows the RBV and WBVTR's to operate from an isolated regulator system.

The thermal requirements for ERTS payload equipment ( $20^{\circ} \pm 10^{\circ} \text{C}$ ) are quite similar to existing Nimbus requirements ( $25^{\circ} \pm 10^{\circ} \text{C}$ ). They can be met with existing thermal control hardware (adjusted to operate at a lower nominal temperature) and previously used thermal control techniques. Flight experience with the proposed combination of passive, semiactive and active thermal control approaches has been highly successful.

In Table 3.2 1-2, the expected performance of the proposed spacecraft design is compared with the major ERTS A&B design requirements.

### 3 2 2 PAYLOAD CHARACTERISTICS SUMMARY

The ERTS payload consists of the Return Beam Vidicon Subsystem (RBV), the Multispectral Scanner Subsystem (MSS), the Wide Band Video Tape Recorder Subsystems (2) (WBVTR) and the Data Collection Subsystem (DCS). These provide the data for multispectral analysis of the selected coverage areas.

A summary of the pertinent characteristics of these components is shown in Table 3 2.2-1. The interfaces between these components is depicted, in a "top-level" basis, in Figure 3 2.2-1. All items shown except for the DCS and switching module are Government Furnished Equipment (GFE). The payload/spacecraft interface is at the input to the switching and signal conditioning module, and, for the DCS, at the output of the limiter.

The individual subsystems with the exception of DCS terminate their outputs in the Wide Band (S-Band) Transmitters. DCS data is received via the DCS antenna and receiver operating at 402.1 MHz and transmitted through the unified S-Band equipment. RBV and MSS outputs can be either transmitted direct (real time) or recorded for delayed playback. This is accomplished by using two identical WBVTR's on either line.

As a result of this interconnection scheme for the imaging sensors (RBV and MSS) the Wide Band Telemeter input is supplied with six types of outputs, namely

- RBV Video    - Real Time Signal
- WBVTR No. 1 - Playback Signal
- WBVTR No. 2 - Playback Signal
- MSS Signal    - Real Time Signal
- WBVTR No. 1 - Playback Signal
- WBVTR No. 2 - Playback Signal

Table 3.2.1-2 ERTS Spacecraft Requirements and Performance

	Design Requirement	ERTS Performance
<u>ORBIT</u>		
Sun Synchronous		Meets
Altitude	492 35 ± nm	Capable to correct worst case
Inclination	99 085°	Injection and maintenance for
Ascending Node Time	2130	1 year 30% margin built in.
Eccentricity	0	100% margin with no redesign.
<u>PAYLOAD</u>		
Weight	450 pounds	530 pounds
Volume	12 ft <sup>3</sup>	37 ft <sup>3</sup>
Earth viewing	payload sufficient plus 25%	available
<u>ATTITUDE CONTROL</u>		
Attitude Accuracy	± 0 7° all axes	- 0 7° pitch & roll - 1 0° yaw
Attitude rate		
Requirement	0 04°/sec	Meets
Goal	0 015°/sec	0 02°/sec
Image Location	±2 NM	Meets using simple passive attitude sensor
<u>THERMAL</u>		
	20°C - 10°C	20°C - 10°C
<u>COMMUNICATIONS &amp; DATA HANDLING</u>		
<u>Command</u>		
Uplink Frequency		
STADAN	148-154 MHz	1 1 MHz
MSFN	2106 4 MHz	>106 4 MHz
Real Time Digital Commands	256	31 total 480 external
Stored Digital Commands	70	10 plus recycle
Fail Safe Design	Required	Meets
<u>Narrow Band Telemetry</u>		
Downlink Frequency		
STADAN	176 - 178 8 MHz	13 86 MHz
MSFN	2287 5 MHz	278 5 MHz
Data Accuracy	8 bits	10 bits
Real Time Data Rate	≤1 Kbs	1 Kbs
Playback Data Rate	≥20 Kbs	4 Kbs
Transmitter Power		300 MW
(Commandable)		1 Watt (emergency)
<u>Wideband Telemetry</u>		
Downlink Frequency	226 5 MHz	6 5 MHz
	2229 5 MHz	2229 5 MHz
Bandwidth (RDV)	70 MHz	0 MHz
Transmitter Power (Commandable)	20 Watt	10 Watt & 10 Watt
Operating Elevation	≥ 0	≥ 0
Receiving Antenna		
	30 foot dish	either with
	85 foot dish	1 dB degradation
Bandwidth (MSS)	20 MHz	20 MHz
<u>Tracking</u>		
Minitrack System		
Transmitter Power		300 MW
<u>Timing</u>		
Common Spacecraft Clock	Provide all necessary timing signals	Meets
<u>Power</u>		
Payload Operation	20 Min/Orbit	15 Min/Orbit
<u>Lifetime</u>		
	One year in orbit	Meets

\* Can meet 20 min per orbit by canting solar array - analysis verifies that 15 min/orbit is adequate  
Analysis shows mission requirements be met with ±1 0 yaw control Can improve to 0 7  
with subsystem modification

Table 3.2 2-1 ERTS Sensor Payload Summary

Multispectral Scanner		Return Beam Vidicon Camera Subsystem	Video Tape Recorder
	<u>Radiometer Head (1 required)</u>	<u>Camera Head (each) (3 required)</u>	<u>Tape Transport (2 required)</u>
Size (in.)	14H x 15W x 36L (ERTS-A) 14H x 15W x 48L (ERTS-B)	22L x 8 75H x 7 75W	21 5L x 14.8W x 6 5H
Weight (lb)	105 (ERTS-A) 120 (ERTS-B)	31 2	45
Power (Watts, avg )	50 (ERTS-A) 55 (ERTS-B)	30	Record 85 Standby 40 Rewind 40
	<u>MSS Signal Processor (1 required)</u>	<u>Electronics (each) (3 required)</u>	<u>Recorder Electronics (2 required)</u>
Size (in.)	Module 2/2	Module 3/3 (6x6x13 in.)	16 6L x 16W x 7 0H
Weight (lb)	10	12 0	25
Power (Watts)	15 (est)	15 (est)	30 (est)
		<u>Controller (1 required)</u>	
Size		Module 3/0 (6x6x5 in.)	
Weight (lb)		7	
Power (Watts)		10 (est)	
		<u>Video Combiner (1 required)</u>	
Size		Module 3/0 (6x6x5 in.)	
Weight (lb)		9	
Power (Watts avg )		5 (est)	
Commands Total	47	74	9 (tent )
Telemetry Points Total	50	54	24 (tent )



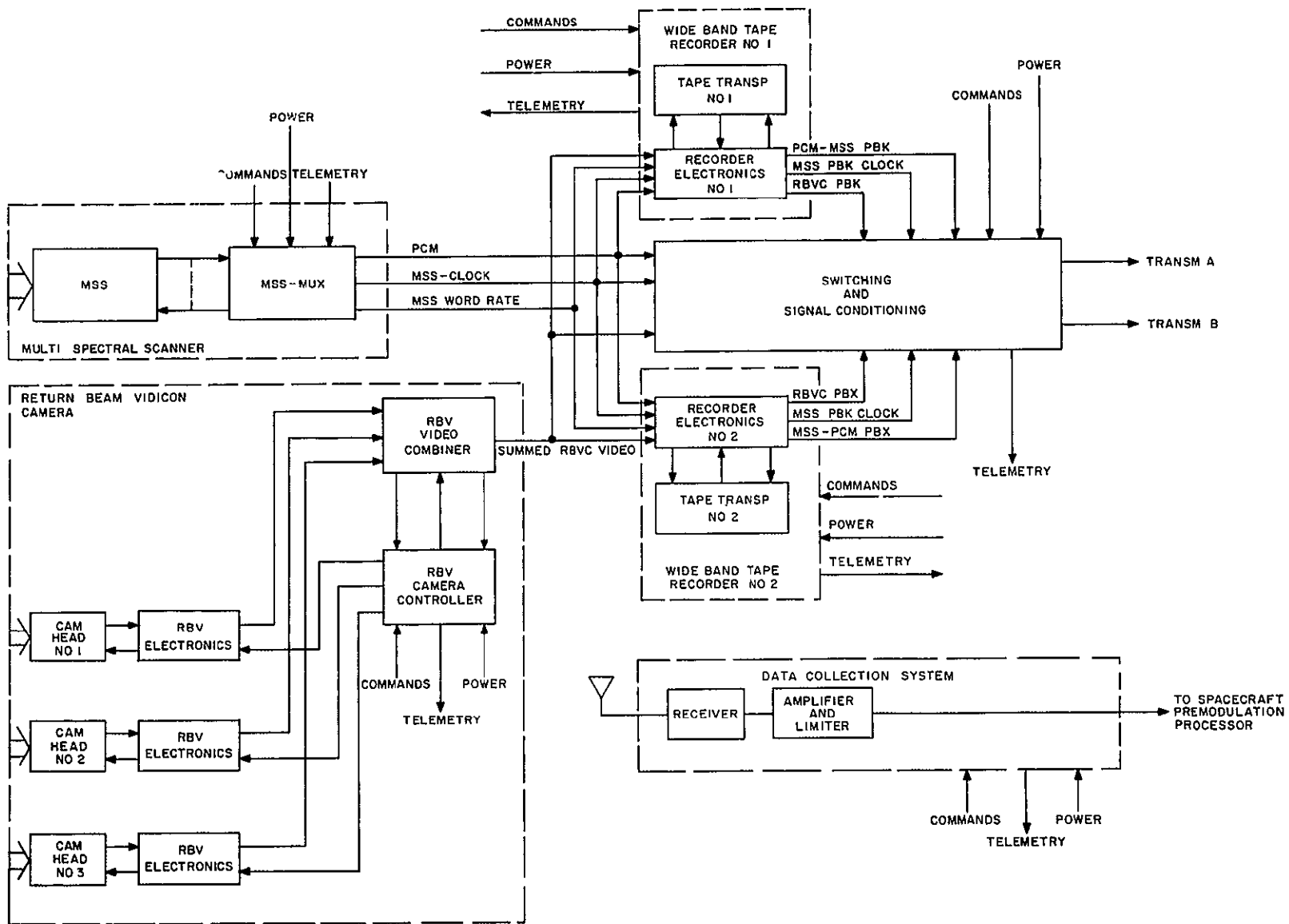


Figure 3.2 2-1. ERTS Payload Subsystems

Switching of these inputs is performed by the Wide Band Communication Subsystem and permits any two of the six inputs to be transmitted simultaneously.

### 3.2.2.1 Return Beam Vidicon Camera Subsystem

The RBV camera subsystem consists of

1. Camera Head (3 required)
2. Camera Electronics (3 required)
3. Camera Controller (1 required)
4. RBVC Video Combiner (1 required)

Except for the RBV Camera Heads all other units are in a form of standard Nimbus modules. Camera Heads are irregular in shape. The details on other RBVC modules is summarized in Table 3.2.2-1. In all other aspects, the modules conform to Nimbus D Experimenter's Handbook.

Return Beam Vidicon Camera Subsystem signal output is analog and is the result of time multiplexing the three individual camera outputs plus synchronizing signals. The baseband of this signal is from DC to about 3.5 MHz. The WBVTR subsystem accepts the RBVC signal, video, and records it in FM mode. Playback mode of RBVC video reconverts the FM tape readout back to an analog signal with less than 1 dB signal to noise degradation.

### 3.2.2.2 Multispectral Scanner Subsystem

The Multispectral Scanner Subsystem consists of only two units

1. Scanner Head (Radiometer)
2. MSS Multiplexer

The scanner head is irregular in shape and will have two possible configurations. The ERTS B configuration includes a passive radioactive cooler, required for the fifth spectral band. The ERTS A configuration excludes the fifth spectral band and associated cooler.

The MSS multiplexer is in a form of Nimbus 2/2 standard module, and its design conforms to Nimbus D Experimenter's Handbook.

Power consumption of MSS is 50 watts for ERTS A application and 55 watts for ERTS B, and includes 15 watts allotted to the MUX.

A summary of pertinent characteristics is shown in Table 3.2.2-1.

The data output after multiplexing emerge as a 15 Mbs PCM signal. In addition, two auxiliary signals are produced in the multiplexer, the 7.5 MHz MSS clock and MSS word

rate These two are needed by the WBVTR in the encoder, where PCM to 8 level FM conversion is accomplished and thus permits the use of the same recorder for both MSS and RBV data.

The playback signal from WBVTR in the MSS mode is 8 level FM and, therefore, it is reconverted back to PCM This makes the direct and playback MSS PCM signals fully identical and therefore compatible with the wideband communication subsystem The 7.5 MHz clock signal is also reconstructed so it can be used by the wideband communication subsystem if reclocking of PCM signal is desired

### 3.2.2.3 Wideband Video Tape Recorder Subsystem

The Wide Band Video Tape Recorder Subsystem is provided for the enhancement of RBVC and MSS operational flexibility

WBVTR's can be operated in either RBVC or MSS Record or Playback modes The switching is provided internally in each WBVTR by means of commands applied from the spacecraft command subsystem.

Each WBVTR has two recording tracks First track is compatible with either RBVC or MSS wideband signals. The second track is intended for auxiliary purposes, such as, telemetry, time code or other support purposes. It can be erased if desired, and also can be played back a number of times without erasing Its frequency response is DC to 5 kHz and will accept  $\pm 0.75V$  amplitudes across 600 ohms input.

In playback the WBVTR also provides a search track signal output. This signal is recovered from a prerecorded track with data prerecorded at 6 inch intervals. Its intended use is for lasting data. It may be readout during forward or rewind, fast or normal operation.

Physically, the WBVTR is subdivided into two functional units, the Tape Unit and Electronics Power dissipation of the tape unit is complex, and has quite severe transient power demands, depending on the mode of operation The electronics unit dissipates uniformly about 30 watts The summary of WBVTR parameters is provided in Table 3.2.2-1.

### 3.2.2.4 Data Collection Subsystem (DCS)

The DCS for ERTS A&B consists of three segments They are the Data Collection Platforms (DCP's), the Spacecraft Receiving Subsystem and the DCS Ground Preprocessing Equipment The DCP's are collocated with sensors throughout the continental United States and its coastal waters Each DCP accepts inputs from eight sensors The analog inputs are multiplexed using time division multiplexing. Each input is then coded using Pulse Code Modulation (PCM). A convolutional encoder then encodes the pulse train before it is passed on to the FSK modulator and transmitter The signal is transmitted to the spacecraft on a carrier at a frequency of 401.9 MHz.

The signal is received at the spacecraft through a crossed dipole antenna and passes to the DCS spacecraft receiver subsystem. The receiver is a double heterodyne receiver with a 3 dB overall noise figure, an IF bandwidth of 100 kHz and an output center frequency of

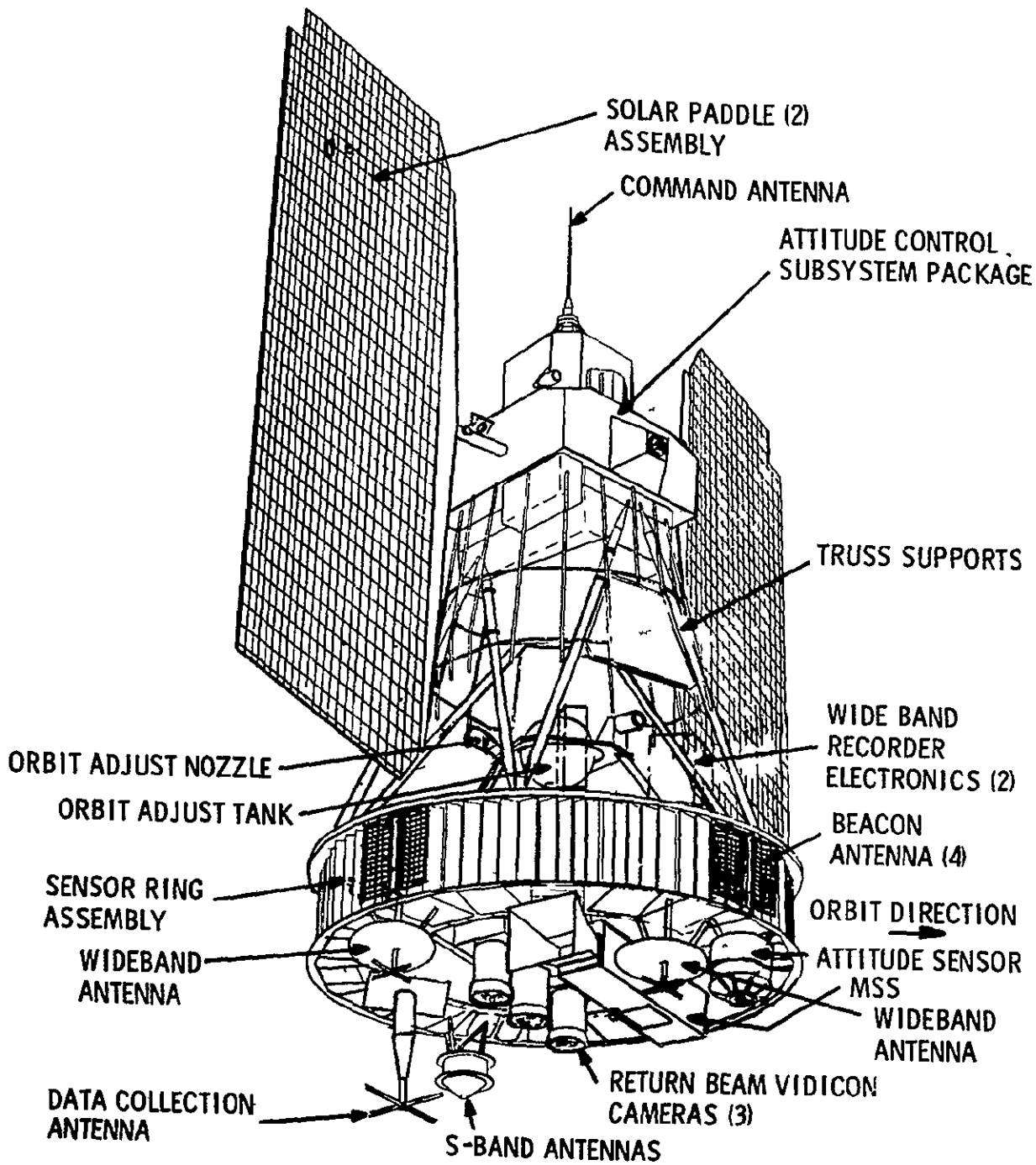


Figure 3.2.3-1. ERTS Configuration

1 024 MHz. The 1.024 MHz signal is passed to the Unified S-Band (USB) premodulation processor where it is combined with other signals for relay to the ground over the USB downlink

At the three receiving sites (Alaska, Corpus Christi, and NTTF), the USB downlink signal is received and demodulated. The DCS signal is stripped out of the composite baseband and routed to the DCS ground preprocessing equipment. In the preprocessing equipment the PCM/FSK signal is detected and demodulated and then decoded and formatted for transmission over telephone lines to the Operation Control Center (OCC) and the NASA Data Processing Facility (NDPF). At the NDPF the data is formatted and prepared for dissemination to the users.

The system provides for a 1000 DCPs with 0.95 probability of receiving interference free data from each platform every 12 hours. The coding provided will assure that the probability of errors in a message being undetected is less than 0.05.

### 3.2.3 ERTS SPACECRAFT CONFIGURATION

The ERTS spacecraft provides payload accommodations and meets payload requirements for the ERTS A&B missions. The ERTS configuration is shown in Figure 3.2.3-1 in the orbit configuration. With the exception of the equipment arrangement in the sensory ring assembly, including the accommodation of the Orbit Adjust S/S Assembly and the payload equipment, this configuration is identical with the flight proven Nimbus spacecraft. The ERTS configuration is a two body spacecraft connected by a truss (set of 6 struts). The lower body is the sensory ring assembly which houses the payload and housekeeping subsystems, and the upper body is the attitude control package and solar array to provide orientation for the spacecraft and provide power for the spacecraft.

The ERTS configuration and packaging arrangement is defined in Figure 3.2.3-2, (drawing 47J220030). This drawing identifies the major elements of the baseline configuration.

The Attitude Control Subsystem package, identified in axis Y-Y profile of Figure 3.2.3-2, provides an unobstructed exposed mounting for the solar paddle sun sensors, horizon scanners and gas nozzles. The subsystem electronics, mechanical assemblies and pneumatics are internally packaged, as are the solar array drives. The command antenna and the upper part of the ground plane are mounted on the top surface of the ACS.

The solar arrays attach to the shaft projecting from the ACS package, Figure 3.2.3-2 axis Y-Y profile. In the launch configuration, the solar arrays are folded along the longitudinal axis to fit within the Sensory Ring envelope and is secured by a latching mechanism, Figure 3.2.3-2, axis X-X profile.

The truss structure provides a tripod connection between the ACS and the Sensory Ring Assembly, allowing alignment adjustment between the ACS and the Sensory Ring. See Figure 3.2.3-2, axis X-X profile. The truss also supports the command antenna lower ground plane, the auxiliary load panel and the ERTS/ACS connector IF panel.

The Sensory Ring Assembly is a torus structure with 18 modular bays for packaging equipment. The lower surface of the sensory ring provides mounting for payload equipment and antennas. The upper surface of the sensory ring provides mounting for spacecraft equipment. The center of the sensory ring has crossbeam assemblies to mount additional payload equipment and other non-modular spacecraft equipment.

Figure 3.2.3-2 presents the baseline packaging of the equipment in the Sensory Ring Assembly. Section A-A of the figure identifies the equipment packaged in each of the 18 peripheral bays and also defines the equipment packaged on the crossbeams, including

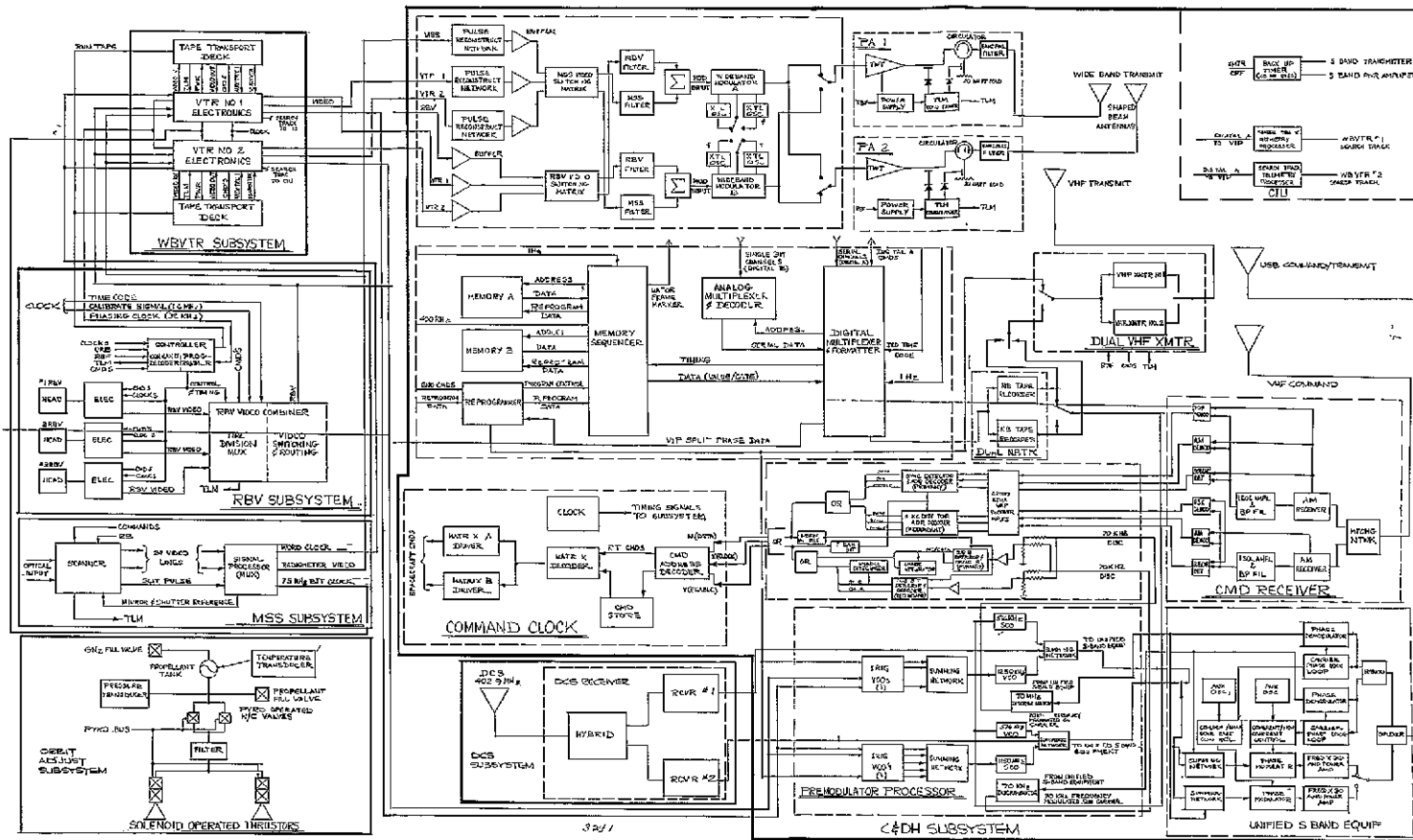
- 1 RBV Assembly (3 RBV's plus mounting plate)
2. WBVTR (2)
- 3 NBTR (2)
- 4 Power Switching Module (1)
- 5 Unfold Timer (1)
- 6 TLM Conversion Module (3)

On the top of the Sensory Ring, Section B-B of Figure 3.2.3-2, the following equipment is mounted

1. OA Subsystem Assembly
2. WBVTRE (2)
- 3 Magnetic Moment Assembly

Below the Sensory Ring, Section C-C of Figure 3.2.3-2, the following equipment is mounted

- 1 MSS
2. Wide Band WBV/PCM Antenna (2)
- 3 USB Antenna
4. DCS Antenna
5. Attitude Sensor



FOLDOUT FRAME

Figure 3 2.4-1 Electrical Block Diagram (Sheet 2 of 2)

FOLDOUT FRAME

Table 3 2 4-1 Spacecraft Regulated Power Demand  
for Various Operating Modes

<u>All Systems On</u>		
<u>Subsystem</u>	<u>Continuous</u>	<u>Peak</u>
Power	1.3	1 3
Attitude Control	35 5	99 5
Thermal Control	10 2	10 2
Command and Data Handling	55.9	102.0
Orbit Adjust Telemetry (turned on as required)	<u>negligible</u>	<u>1 8</u>
	102 9	217.8
<p>Note For end-of-life, thermal control requirements will be reduced to 1 watt System total becomes 93.7 watts for that condition.</p>		
<u>Payload-Real Time</u>		<u>Peak</u>
DCS Receiver		1 0
Attitude Sensor		1.6
RBV		155 0
MSS (ERTS B)		70 0
WB PA & MOD. (2)		<u>125 0</u>
		351 6
<u>Payload-Record</u>	<u>Peak 13 5 seconds</u>	<u>Peak 11 5 seconds</u>
DCS Receiver	1 0	1 0
Attitude Sensor	1 6	1.6
RBV	163.0 (Prepare)	145.0 (Readout)
MSS	70 0	70.0
WBVTR (2)	<u>118 0 (one on standby)</u>	<u>166 0 (both recording)</u>
	353 6	383.6
<u>Payload-Playback</u>	<u>RBV/MSS</u>	<u>MSS</u>
DCS Receiver	1.0	1.0
WBVTR	152 0	76 0
WB Power Amplifier & Modulator (2)	<u>125 0</u>	<u>45 0</u>
	278.0	122 0



Table 3 2 4-1 Spacecraft Regulated Power Demand  
for Various Operating Modes (Cont'd)

Note: If RBV and MSS record simultaneously, one recorder will only playback 46% of total operate time because the RBV picture readout time is only 11.5 seconds out of the 25 second cycle. Therefore, the RBV recorder will be on standby power for 54% of that time.

<u>Payload-Rewind</u>	<u>Watts</u>
DCS Receiver	1 0
WBVTR (2)	60 0 (1 15 minutes)
WBVTR (1)	<u>30.0 (2.5 minutes)</u>
	61 (1 15 minutes)/31 (2 5 minutes)

Minimum Satellite

<u>Service Subsystem</u>	<u>Watts</u>
Power	1.3
Attitude Control	35 5
Thermal Control	10.2
Communication and Data Handling	55.9
Compensation Heaters	36 9
Orbit Adjust Telemetry	1.8

Payload Subsystems

Attitude Sensor	0
RBV	0
MSS	0
WBVTR	0
WTMR	0
DCS Receiver	<u>0</u>
	141 6

Launch

<u>Subsystem</u>	<u>Watts</u>
Power	1.3
Attitude Control	64 8
Orbit Adjust Telemetry	1 8
Thermal Control	10.2
Compensation Heaters	0

Table 3 2 4-1 Spacecraft Regulated Power Demand  
for Various Operating Modes (Cont'd)Subsystem (Cont'd)

Communications and Data Handling	55.9
Attitude Sensor	0
RBV	0
MSS	0
WBVTR	0
WBTMR	0
DCS Receiver	<u>0</u>
	131.0 watts

Attitude Control Launch and Initial Stabilization

	<u>Launch</u>	<u>Initial Stabilization</u>
Control Logic and Signal Processors	8 8	8 8
Roll Flywheels and Scanners	1 5	30 0
Pitch Flywheel	-	15 0
Roll Flywheel	-	15.0
RMP	32 3	10.0
Initiation Timer	0.8	0.8
Solar Array Drives	13 0	24 0
Continuous Telemetry	1 7	1 7
Pneumatics	-	44.6
Yaw Axis Rate Gyro	<u>6 7</u>	<u>9.0</u>
	64 8	158.9

Regulated Power Requirements

<u>Power Subsystem</u>	<u>Orbital Average or Continuous</u>	<u>Peak</u>
Auxiliary Load Controller	0 65	0 65
Power Switching Module	0 65	0 65
Unfold Timer	<u>-</u>	<u>-</u>
	1.3 watts	1.3 watts

Table 3 2.4-1 Spacecraft Regulated Power Demand  
for Various Operating Modes (Cont'd)

Note Solar array, power control module, payload regulator module, and battery module regulated power requirements are included as internal subsystem losses. The power requirements shown above are mainly for telemetry circuits. Unfold timer pyrotechnic devices actuated off the unregulated pyro bus and the timing circuits off the regulated bus are automatically switched off when deployment is completed.

<u>Attitude Control Subsystem</u>	Orbital Average or	
	<u>Continuous</u>	<u>Peak</u>
Control Logic and Signal Processors	7.3	8.8
Roll Flywheels and Scanners	2.2	10.8
Pitch Flywheel	1.1	10.0
Yaw Flywheel	0.3	10.4
RMP	9.4	10.0
Initiation Timer	0.8	0.8
Solar Array Drives	13.8	17.6
Telemetry Conversion Module	1.7	1.7
Pneumatics	0.6	29.4 (2 axes)
	37.2 watts	99.5 watts

Note All other ACS equipment not utilized in normal orbital mode of operation

<u>Thermal Control Subsystem</u>	Orbital Average or	
	<u>Continuous</u>	<u>Peak</u>
Telemetry Conversion Modules (3)	2.25	2.25
Auxiliary Load Panels (2)	0.20	0.2
Attitude Control Subsystem	2.23	2.23
Orbit Adjust Heaters	3.00	3.0
Payload and Other	2.52	2.52
Compensation Heaters		36.9
	10.20 watts	50.1 watts

Note Continuous load of 10.2 watts is for temperature telemetry circuits. All but 1 watt will be switched off.

Table 3 2 4-1 Spacecraft Regulated Power Demand  
for Various Operating Modes (Cont'd)

Compensation heaters are cycled to maintain temperature as required. Will not normally be needed during normal full on operation. Generally only used after more than one orbit at low load conditions.

<u>Communications &amp; Data Handling</u>	<u>Orbital Average or Continuous</u>	<u>Peak</u>
VHF Transmitter	0.5	12.0 (Emergency)
*VHF Command Receiver	2.0	2.0
USB Equipment		22.2
Premodulation Processor	1.6	4.0
PCM Telemetry Processor	6.8	6.8
*Command Clock	27.0	27.0
*Command Integration Unit	3.0	3.0
Narrow Band Tape Recorder (2)	<u>10.6</u>	<u>25.0</u>
Subsystem	55.9 watts	102.0 watts

\* Also connected to Emergency Bus. Narrowband tape recorders load based on one on standby and one recording for continuous demand and one recording and one in playback for peak demand.

Attitude Sensor 1.6 watt

Data Collection System Receiver 1.0 watt

<u>Return Beam Vidicon</u>	<u>Watts</u>
Camera Head (3 @ 30 w)	90.0
Camera Electronics (3 @ 15 w)	45.0
Camera Controller	10.0
Video Combiner	<u>10.0</u>
	155.0 watts

Note Shutter solenoid power is 30 amperes/100 ms at 26 volts. Can be connected to 26 to 39 volt bus.

Table 3.2.4-1. Spacecraft Regulated Power Demand  
for Various Operating Modes (Cont'd)

Multispectral Scanner

Signal Processor	15.0	15.0
Scanner	<u>50.0</u> (ERTS A)	<u>55.0</u> (ERTS B)
	65.0 watts	70.0 watts

Wide Band Storage

Recorder Electronics (2) Each is	20.0
Video Tape Recorder (2) Each is	15.0 (Standby)
	63.0 (Record)
	56.0 (Playback)
	10.0 (Rewind)

Note Each recorder has a 250 watt transient decaying in 4 seconds to steady state standby level. Commands to turn on should have a 4 second interval between recorders.

Wide Band Telemetry

FM Modulator	5.0
S-Band Power Amplifier (2)	80.0 (RBV)
	<u>40.0</u> (MSS)
	125.0 watts

Orbit Adjust Subsystem

Telemetry Transducers (3)	1.5
Pressure Transducer	<u>0.3</u>
	1.8 watts

Note Solenoid valves, energized off unregulated pyro bus, require less than 10 watts. Pyrotechnic valves are actuated off the unregulated pyro bus. Transducers will be energized prior to launch and through removal of injection errors, then switched off until next operation.

### 3.2.5 SUBSYSTEM OVERVIEW

#### 3.2.5.1 Structures Subsystem Summary

##### 3.2.5.1.1 Structure and Spacecraft Arrangement

The ERTS spacecraft and structures subsystem meets the payload accommodation and requirements for the ERTS A and B missions. The ERTS spacecraft is shown in Figure 3.2.5-1 (isometric) and is similar to the Nimbus spacecraft. The spacecraft has four major configurational elements

1. The Attitude Control Subsystem (ACS), the upper structure that provides unobstructed exposed mounting for the solar paddle sun sensors, horizon scanners, and gas nozzles. The necessary electronics, mechanical drives and pneumatics are assembled internally, as is the drive for the solar array paddles. The command antenna and the upper part of its ground plane are mounted on the top surface.
2. The solar array paddles attach to the shaft projecting from the ACS housing. In the launch configuration, the solar array is folded along its longitudinal axis to fit within the Sensory Ring envelope and is secured to the truss structure by a latch mechanism. The spacecraft is mounted on an adapter structure, which, in turn, is bolted to the launch vehicle adapter ring.
3. A truss structure provides a tripod connection between the ACS and Sensory Ring assemblies, allowing the alignment required between the ACS and the sensors. The truss also supports the command antenna lower ground plane and the auxiliary load panel.
4. The Sensory Ring is a torus structure composed of 18 rectangular module bays, 13 inches in depth. The bays house the electronic equipment and battery modules. The lower surface of the torus provides mounting space for payload and antennas. A crossbeam structure, mounted within the center of the torus, provides support for additional payload equipment and tape recorders.
5. The Adapter (not shown) is the transition section between the spacecraft and the launch vehicle. The adapter is 24 inches high and interfaces with the spacecraft with a Marmon Band Separation device and with the launch vehicle with eight-1/2 inch diameter bolts on a 58 inch diameter bolt circle. The adapter also provides a support beam to accommodate payload sensor stimulators and antennas pickups and reradiators.

##### 3.2.5.1.2 Requirements

The structural subsystem primary functional requirements are to provide volume, strength and stiffness to

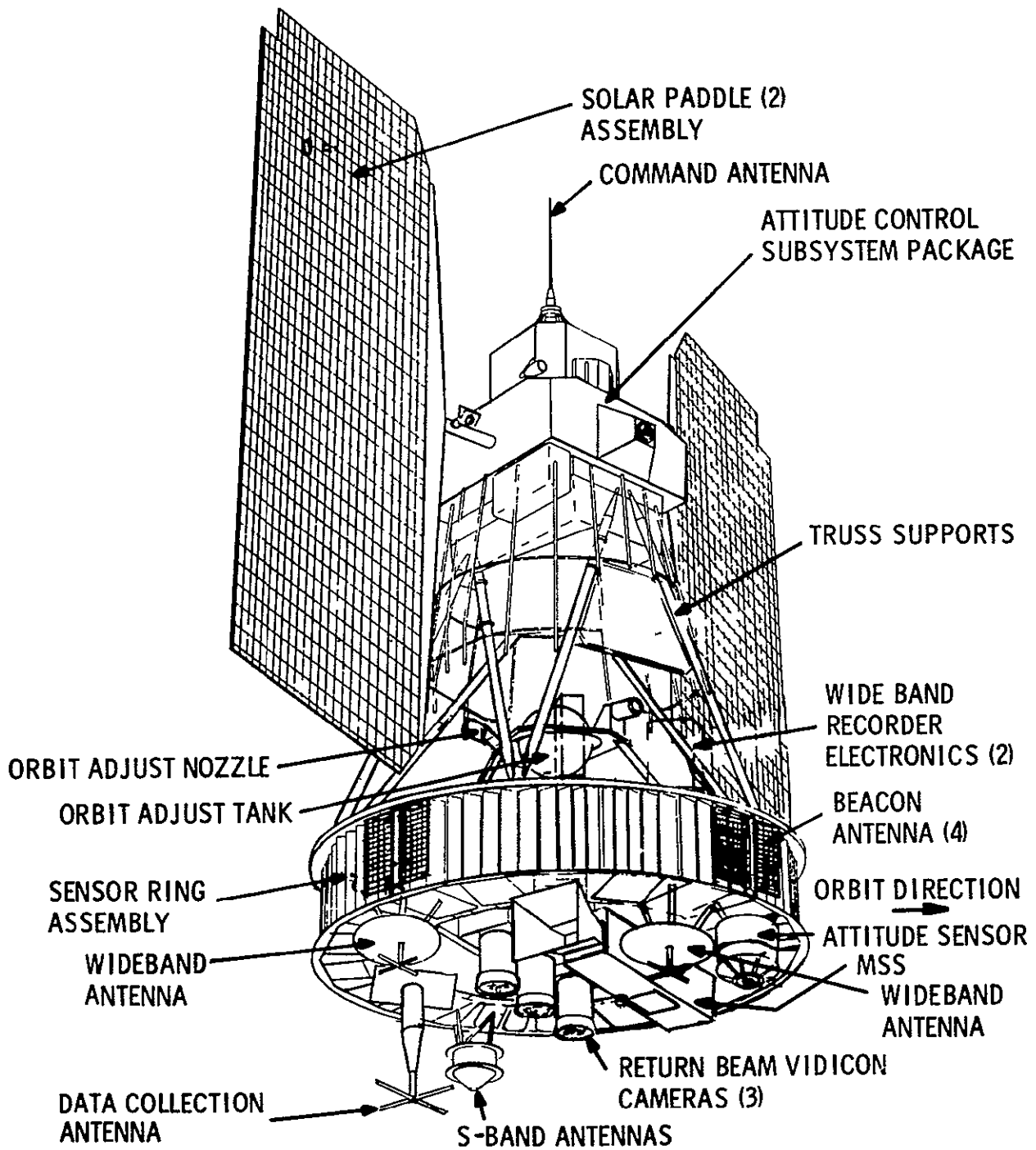


Figure 3. 2. 5-1. ERTS Spacecraft

1. Support the payload and all other subsystems throughout all phases of the mission. As well as the basic housekeeping subsystem accommodation, payload requirements are to accommodate 450 lbs and 12 cu ft of payload equipment
2. Maintain the location and alignment of components within the specified tolerances. The payload sensor and Attitude Control Subsystem Components require 0.1 degree alignment of the components with respect to the vehicle axes.
3. Be compatible with the Delta launch vehicle and SACS shroud. Spacecraft space envelope, static and dynamics, must have clearance of 0.25 inch with surrounding shroud structure during ground handling and launch through shroud separation. Spacecraft adapter must be primary load interface at 58 inch diameter bolt circle of eight bolts.
4. Withstand the environments through all mission phases. The principal requirements are to withstand launch environment of quasi-static and dynamic load requirements. All prelaunch phases will be attenuated with AGE as required.

#### 3.2.5.1.3 Structure Assemblies

The arrangement and major features of the structural assemblies and their function are provided in Figure 3-2-5-2 (Structural Isometric)

##### 3.2.5.1.3.1 Solar Paddle Assemblies

The structural subsystem interfaces with the Solar Paddle Assemblies and supports these assemblies during launch and in orbit. The in-orbit support is provided by the solar paddle to solar array drive interface which is a socket built into the paddle transition section engaged to the Solar Array Drive Shaft.

In a launch position, the solar paddle assemblies are secured by three points in a stowed position. The points are at the ends of the arrays shafts as described above and at the paddle unfold latch system which is attached to the sensory ring. In the launch configuration, the paddles are folded back along the hinge line and the paddles are connected to each other by hinge-like jaws (7) spaced along the paddle edge. The jaws are latched with pins that are connected to each other by a cable. The cable, at the lower end, has a rod anchored in the lower latch assembly and tensioned by a spring at the top. Unlatching occurs when a pyrotechnic cutter severs the anchor rod, permitting the cable to be pulled upward by the upper tension spring. This motion withdraws the pins from the jaws and each array unfolds by means of the paddle drive motor. The paddles are then latched in the full open position. Teflon lined guides are strategically located to prevent hangup of the array during deployment.

##### 3.2.5.1.3.2 Attitude Control Subsystem (ACS) Package

The structural subsystem interfaces with the ACS in order to control the interfaces of this package with the solar paddle assemblies. The truss tube support and special fittings on the ACS serve as lift lugs for the entire spacecraft.



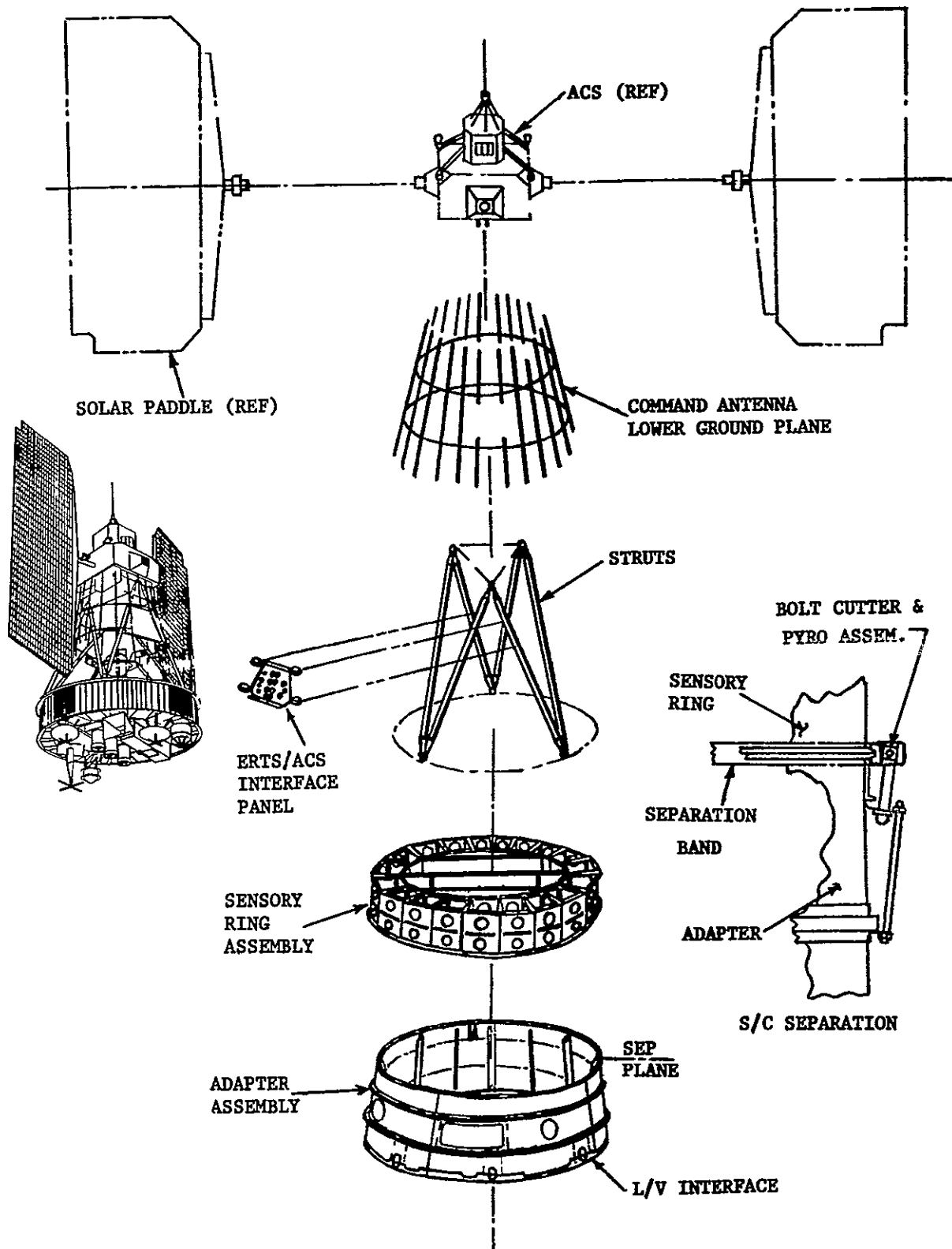


Figure 3.2.5-2. Arrangement and Major Features of the Structural Assemblies and their Function

### 3.2.5.1.3.3 Strut Support

The strut support consists of six tabular assemblies forming a stable framework to support and connect ACS package to the sensory ring assembly. The strut supports provide primary spacecraft structural continuity and provision to permit alignment adjustments of the ACS package to the vehicle axes. In the top spacecraft assembly, the following equipment is attached to the strut supports

1. Lower ground plane for VHF Receiver Antenna
2. ERTS/ACS connector interface panel
3. Electrical Power Subsystem Auxiliary Load Panels
4. ERTS/ACS Connecting Harness and Support

### 3.2.5.1.3.4 Sensory Ring Assembly

The Sensory Ring Assembly is the major element of the ERTS structural subsystem. This assembly supports and accommodates the required payload equipment and most of the supporting spacecraft subsystems.

The Sensory Ring structure will be the basic Nimbus Torus Ring. The Torus Ring structure is the basic structure which forms the 18 sided ring of the spacecraft. The Torus ring structure consists of 18 magnesium alloy separator castings, an upper ring, a lower ring, inner ring channels, and external and internal shear webs. The outboard lower ring is the separation interface with the spacecraft adapter and incorporates a Marmon Band Cross Section. Each equipment bay accepts electronic packages up to 13 inches high x 8 inches deep x 6 inches wide. Placement is achieved by means of evaluating component module size, thermal dissipation requirements and proximity of components that have inter-connecting functions.

The ERTS center cross beam structure will be the same for ERTS A and B vehicles and is unique for ERTS. The cross beam structure accommodates and supports some of the payload and spacecraft support components. One section of the cross beam structure supports the Return Beam Vidicon Cameras (3) on a common mounting. This common mounting plate is provided to achieve alignment between the RBV's of 30 secs before installation into the spacecraft. This structural plate is separate from the other cross beam structures in order to minimize induced spacecraft loads and deflections for maintaining alignment. The major section of the cross beam structure supports the following equipment

1. Wideband Video Tape Recorder (WBVTR) (2)
2. Narrow Band Tape Recorder (NBTR) (2)
3. Solar Paddle Unfold Timer (1)

4. Power Switching Module (1)
5. T/M Conversion Module (1)

The upper plane of the Sensory Ring is utilized to support and accommodate the Orbit Adjust (OA) Subsystem, the Wide Band Video Tape Recorder Electronics (WBVTRE) and the Magnetic Moment Assembly. The OA interface is a simple three point attachment of the mounting feet to pads on the upper plane of the Sensory Ring. The Structures Subsystem provides the support structure for the WBVTRE and the Magnetic Moment Assembly.

The lower plane of the Sensory Ring is utilized to support and accommodate the Multi-Spectral Scanner (MSS), Attitude Measurement Sensor (AMS), UHF-DCS Antenna, Wide Band Antenna (2), and the Unified S-Band Antenna. The support structure has stand-off configurations to provide the proper fields of view for the components. In addition, there is accommodation and interfaces for the thermal insulation for the lower surface of the Sensory Ring, the MSS and the AMS

#### 3.2.5.1.3.5 Adapter

The Adapter Structure provides structural continuity between the spacecraft and the launch vehicle during the launch phase of the mission. It also provides the separation function for the spacecraft. Additionally, the adapter supports and accommodates payload sensor stimulators (RVB and MSS), and antenna pickups and reradiators.

The Adapter is a shell structure with longitudinal stiffeners, and upper and lower closure rings that are machined from forgings to mate with the spacecraft sensory ring and the launch vehicle ring, respectively. Secondary structure is the adapter cross beams necessary to support the payload stimulators.

The separation function is provided by the following hardware

1. Two separation band halves
2. Two pyrotechnic bolt cutters and bolts
3. Marmon Band retaining cables
4. Four separation spring assemblies with guides and brackets
5. Four separation switches and brackets

The spacecraft and adapter are clamped together with the Marmon Band, which is pre-loaded by a force to prevent gapping at the separation plane. Separation springs are provided to produce a nominal zero tumble rate and specified separation velocity. Separation begins with the ignition of the pyrotechnic bolt cutters, which disconnects the Marmon

Band halves. The bands displace from the separation rings, but are retained with the adapter by the retaining cables. Four separation springs provide velocity to separate the spacecraft and the adapter. Four switches monitor the event.

3.2.5.2 Communications and Data Handling Subsystem

The Communications and Data Handling Subsystem is composed of the Wide Band Data Link, the Narrow Band Telemetry, Tracking and Command Link and the transmission link for the Data Collection System. With the exceptions of the Wide Band Equipment all equipment in this subsystem is either identical to flight proven equipment or a modification there-of.

3.2.5.2.1 Wide Band Telemetry

The Wide Band Telemetry equipment is designed to transmit the data from the Multi-Spectral Scanner, Return Beam Vidicon Camera and the Wide Band Video Tape Recorders. The characteristics and requirements for the Wide Band Telemetry equipment have been derived from the mission image resolution requirements, the sensor signal characteristics, the available ground equipment as defined in the Design Study Specification S-701-P-3 and the analysis performed during the Phase B/C study. Figure 3.2.5-3 illustrates the Wide Band Telemetry hardware. This equipment interfaces with the ERTS spacecraft payload and the ground stations. The Power, Command and Telemetry interfaces are not shown. The WBVTR Search and Auxiliary Tracks contain low rate PCM data and are routed to the Narrow Band Communications. The subsystem consists of four (4) component types a redundant Signal Conditioner, a redundant Frequency Modulator, two (2) Power Amplifiers and two (2) Shaped Beam Antennas.

3.2.5.2.1.1 Signal Conditioner

The Signal Conditioner interfaces with the payload. It accepts stored and real time signals from the MSS, the RBV, and the two (2) associated wide band video tape recorders. The unit is commanded by the spacecraft command/clock and selects pairs of input lines. The unit conditions the inputs as follows

	15 MBS <u>MSS (PCM)</u>	(3.5 MHZ) <u>RBV (Video)</u>
Impedance Matching	X	X
Digital Reconstruction	X	
Premodulation Filtering	X	X

The selected and conditioned MSS/RBV signals are routed to the Frequency Modulators.

3.2.5.2.1.2 Frequency Modulator

The Frequency Modulator consists of two identical, commandable units. Each unit is capable of operation at either center frequency (2229.5 MHz or 2265.5 MHz) and will accept either MSS or RBV signals. The modulator routes a frequency modulated signal to the two Power Amplifiers. Cross strapping switches are employed at the output lines of both units for redundancy.

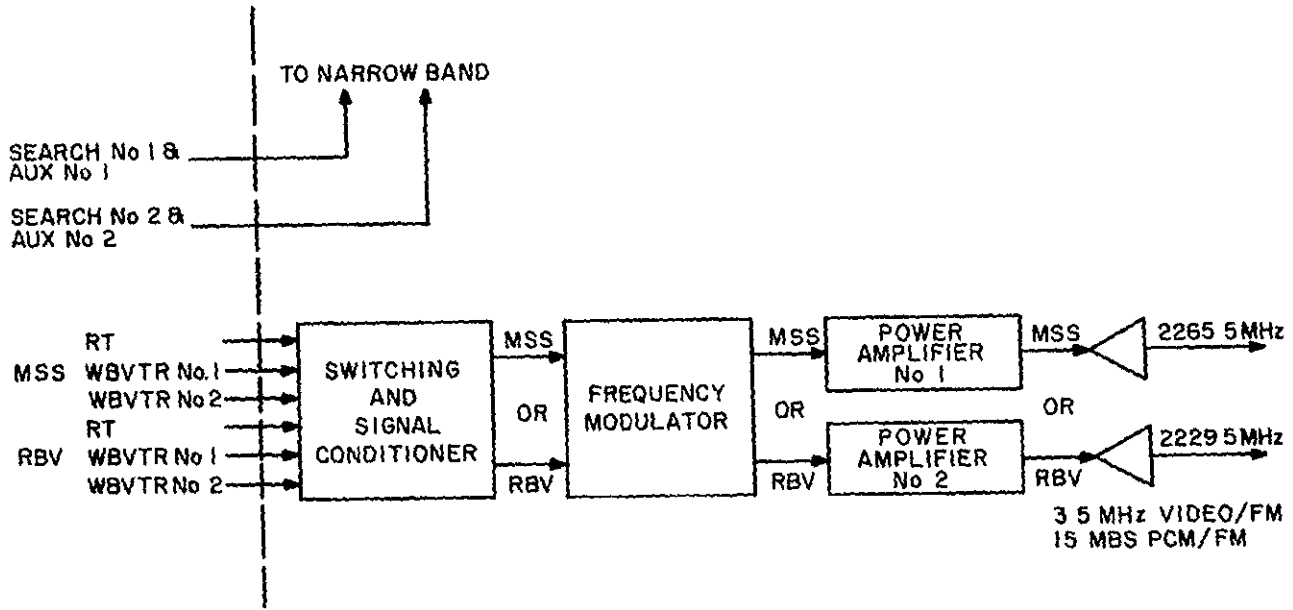


Figure 3.2.5-3. Wide Band Subsystem

### 3.2.5.2.1.3 Power Amplifier

Either of the two separate Power Amplifiers accepts the frequency modulated MSS or RBV inputs on command. The units contain TWT's with commandable (10 and 20 watt) power levels, R. F. band pass filters, a circulator for isolation and individual power supplies.

### 3.2.5.2.1.4 Shaped Beam Antennas

Two identical shaped beam antennas are located on the underside of the spacecraft. A simple, compact turnstile design is used. One antenna is dedicated to P. A. No. 1 and the other is dedicated to P. A. No. 2. Near constant earth illumination is achieved with a gain  $\geq$  4dB over a cone angle of  $\pm 60.6$  degrees.

### 3.2.5.2.2 Narrow Band Telemetry, Tracking and Command

The Narrow Band Telemetry, Tracking and Command equipment provides the means for collecting and transmitting housekeeping data from the spacecraft to the Ground Net, providing a tracking beacon for the spacecraft, receiving commands from either the MSFN or STADAN Net and implementing those commands aboard the spacecraft. In addition, it provides the link for transmitting data from the Data Collection System to the Ground Net

Figure 3 2 5-4 illustrates the Narrowband Communications hardware. This equipment interfaces with other spacecraft subsystems and the ground stations. It consists of the items shown exclusive of the DCS receiver and antenna.

#### 3.2.5.2.2.1 PCM Telemetry Processor

The PCM Telemetry Processor samples the output of all the telemetry (housekeeping) sensors on board the spacecraft, it processes the data, and inserts it into a 1 KBPS output stream to be stored on the Narrow Band Digital Tape Recorder or transmitted real time. This unit is identical to the Nimbus D PCM Telemetry Processor.

The processor handles the following inputs

1. Analog and Digital spacecraft telemetry channels.
2. A command/clock generated Clocking Signal and a PWM serial time code.

#### 3.2.5.2.2.2 VHF Transmitter

This unit contains two (2) commandable transmitters each capable of two (2) power levels (300 mw for Real Time data and 1 watt for Play Back Data). The transmitter receives real time 2-phase TLM data from the PCM TLM Processor at a 1 KBS rate or it receives stored 2-Phase TLM data from either of two commandable Narrow Band Tape Recorders. This data phase modulates a 137.86 MHz carrier in either one of the two transmitters. The transmitters interface with the VHF quadraloop antennas and supply carrier power for Minitrack.

#### 3.2.5.2.2.3 Command Clock

The Command Clock provides an accurate time base for spacecraft operations, generates time codes for transmission or storage, receives, processes and stores command infor-

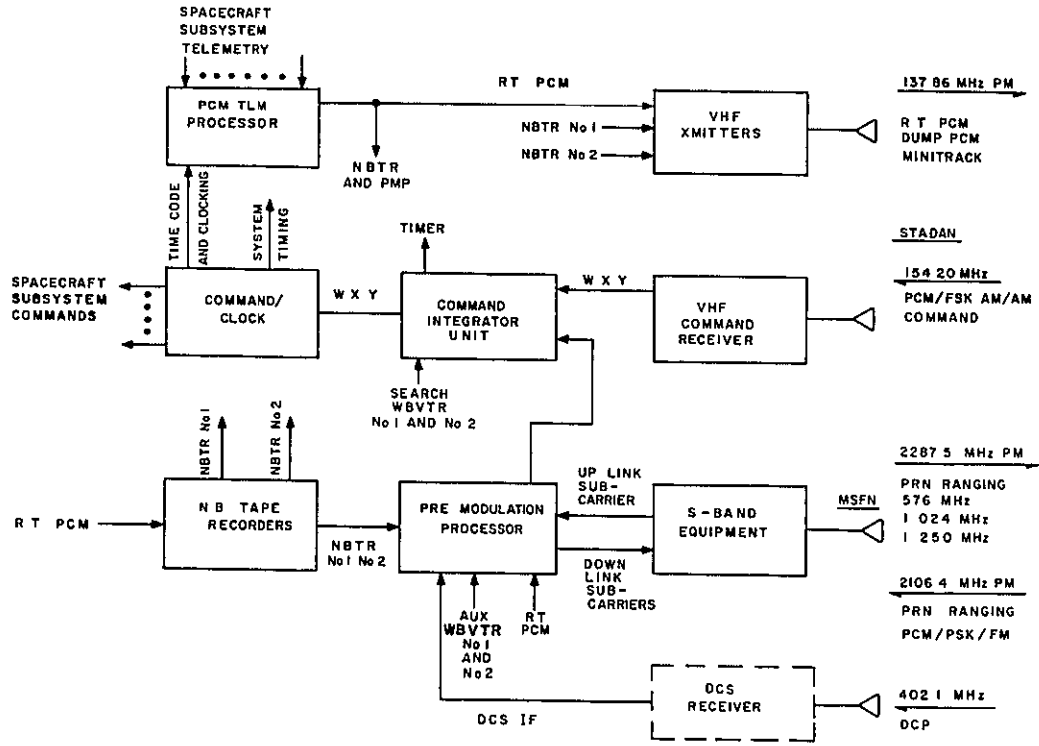


Figure 3.2.5-4. Narrow Band Communications

mation from the Command Integrator and executes these commands at predetermined times. The capability for 30 stored Commands and more than 256 real time digital commands exist within the component. The Command/Clock receives serial PCM data in a compatible format on three lines from the Command Integration unit: NRZ-L Data (w), NRZ-L Sync (x), and NRZ-L Enable (y). It also implements previously stored commands. It contains a command decoder and relay matrix drivers for command implementation. In addition, a self-contained clock generates system timing signals and a Time Code.

#### 3.2.5.2.2.4 Command Integrator Unit

The Command Integrator Unit accepts signals from the VHF Command Link at 128 bps or the USB Command Link at 1 kbps, operates on the signals and provides an acceptable input for the Command Clock. The resulting signal from the USB is sub-bit decoded to yield a 200 bps NRZ-L Data (w) plus Clock (x). An Enable (y) signal is also generated from the presence of the clock signal. This resulting signal is compatible with the clock input.

Provision is made to inhibit commands that are being transmitted from one site while commands are going in via another site. The design is also such that commands from the same site for another spacecraft will not be accepted.

In addition, the command integrator unit contains a back-up timer. This timer is initiated when the system is commanded on for payload operation and will turn off all equipment having the same duty cycle as the payload after 28 minutes. This will back-up the condition when a real time command fails to turn off the equipment after a station pass. In addition it contains a shift register for assembling the serial PCM data from the WBVTR search track.

#### 3.2.5.2.2.5 VHF Command Receiver

The receiver interfaces with the command stub antenna at a 154.20 MHz carrier frequency. The function of the receiver is to convert Commands, received at 128 bps, from the STADAN ground station into intelligence suitable for storage and/or execution. One channel remains on continuously. The receiver consists of two commandable units consisting of a Front end, AGC, and a Demodulator. The Demodulator generates, 1) an Enable (y) based on "presence of subcarrier", 2) a Clock (x) via detection of AM on the carrier, and 3) NRZ-L Data (w) via demodulation of the PCM/FM. The resultant signal (3 separate lines) is outputted to the C. I. U.

#### 3.2.5.2.2.6 Unified S-Band Equipment

The Unified S-Band Equipment consists of a diplexer, hybrid, transponder and mixing amplifiers. Commands are received from the MSFN site through the Unified S-Band Antenna at a 1 KBS rate to the diplexer, hybrid, receiver portion of the transponder. The receiver output goes into a 70 KHZ Discriminator packaged in the Premodulation Processor. Downlink information enters the equipment through a mixing amplifier, an S-Band transmitter, to a diplexer and out through the Antenna. The power output of the transmitter is 2 watts. This equipment is similar to equipment flight proven on Apollo.



### 3.2.5.2.2.7 Premodulation Processor

The PMP comprises a redundant subcarrier modulation and demodulation unit. It contains a 70 KHz FM discriminator for command demodulation and FM subcarrier modulators and pre-modulation filters to handle the following down-link TLM signals

1. Either of two (2) N. B. Tape Recorders at 24 KBS
2. One (1) D C S I F at 100 KHz B W
3. One (1) R. T. TLM Channel at 1 KBS
4. Two (2) W. B. V. T R. Aux TLM Channels at 100 bps

### 3.2.5.2.2.8 Narrow Band Tape Recorders

The Narrow Band Digital Tape Recorder accepts NRZ-L data from the PCM Telemetry Processor at a 1 KBS rate. The data is recorded directly on the tape and played back at a 32 KBS rate. The data can be played back either over the VHF transmitter link or through the USB equipment to the ground net. The unit is similar to those flown on other space programs.

### 3.2.5.2.2.9 Antennas

The Narrow Band antennas have the following characteristics

#### VHF Beacon and Telemetry

Frequency - 137.86 MHz  
Pattern Coverage - Spherical  
Minimum Gain - -10 dB with 3 dB nulls

#### VHF Command

Frequency - 154.2 MHz  
Pattern Coverage - Spherical  
Minimum Gain - 0 dB with 20 dB nulls

#### Unified S-Band

Frequency - 2100 - 2300 MHz  
Pattern Coverage - Hemi-spherical  
Gain - 0 dB for ±60 degree Cone

### 3.2.5.3 ERTS Attitude Control Subsystem (ACS)

The ERTS-ACS is a 3-axis, active control subsystem which maintains the spacecraft alignment with the local earth vertical and orbit velocity vectors. The ACS employs horizon scanners for local vertical roll and pitch attitude sensing, and rate gyros for sensing yaw rate and for use in a gyrocompassing mode to sense yaw attitude. The

11 February 1970

torquing is provided by a combination of reaction jets to provide net momentum control and large control torques when required and flywheels for fine control and residual momentum storage.

The ERTS-ACS is a flexible, long life, highly reliable system having several operational and backup modes. These modes are summarized in Figure 3.2.5-5. The summary discussion of these operational modes is presented in Section 3.2.5.3.3.

The ERTS-ACS consists of the following major elements

- Roll Reaction Wheel Scanner      -2 per ACS, provides front and rear IR scanners whose output is proportional to pitch and roll errors. Scan function provided by reaction wheels which also provide momentum exchange.
- Control Logic Box                      - contains control electronics for the ACS functions as well as mode selection and switching.
- Yaw Gyrocompass                        - 2 per ACS (redundant) serves as the primary yaw sensor providing an output proportional to yaw error and rate.
- Pitch and Yaw Reaction Wheels      - provide momentum exchange about the pitch and yaw axes respectively.
- Pneumatics                                - provides high-torque reaction and wheel unloading
- Yaw Rate Gyro                            - used only during acquisition, senses yaw rate for improved yaw damping
- Solar Array Drive                        - provides controlled motion of the solar array to maintain solar array illumination
- Magnetic Moment Assembly            - commandable magnetic dipole about pitch, roll and yaw to cancel spacecraft magnetic dipole
- Attitude Sensor                         - precise attitude measurement (0.1 degree) for use in image location

Back-up Modes  
Element Condition Shown Representative of Normal Mode

Control Loop	Control Loop Elements	Launch Mode	Acquisition Mode	Normal Mode	Orbit Adjust Mode	Gyrocompass Backup	Pitch Momentum Bias	IR Scanner Failure	MMA Unload
Pitch	IR Scanners	Off	X	X	X	X	X	Switch in Pseudo Earth Pulse in Place of Failed Scanner	X
	Control Electronics	Off	X	X	X	X	X	X	X
	Reaction Wheel Pneumatics	Off Off	X X	X X(Unload)	X X	X X(Unload)	X+1100 RPM X(Unload)	X X(Unload)	X Off
Roll	IR Scanners	Off	X	X	X	X	X	Switch OFF Failed Scanner	X
	Control Electronics	Off	X	X	X	X	X	X	X
	Reaction Wheel	Wheel Running	X	X	X	X	X	X	X
	Pneumatics	Off	X	X(Unload)	X	X(Unload)	X(Unload)	X(Unload)	Off
Yaw	Yaw Gyrocompass No. 1	On	X	X	X	Off	Off	X	X
	Yaw Gyrocompass No. 2	On	Off	Off	Off	X	Off	Off	Off
	Yaw Rate Gyro	On	X	Off	On-Output Disabled	Off	Off	Off	Off
	Control Electronics	Off	X	X	X	X	Off	X	X
	Reaction Wheel	Off	X	X	Off	X	Off	X	X
	Pneumatics	Off	X	Off	X	Off	Off	Off	Off
Solar Array Drive (2)	Sun Sensor	↑	X	X	X				
	Control Electronics		X	X	X				
	Servo Motor	Off	X	X	X				
	Potentiometer (Position Readout Only) Tachometer	↓	X X	X X	X X				
							Each Paddle Driven Independently		

FOLDOUT FRAME

FOLDOUT FRAME

Figure 3.2.5-5. ERTS - ACS  
Control Modes

The design of the ACS relies on the Nimbus designs. The components are similar to Nimbus except for the Magnetic Moment Assembly and the Attitude Sensor.

The proposed ACS is a self-contained, major spacecraft subassembly, which is assembled and thoroughly tested as a subsystem prior to mating with the spacecraft. Figure 3.2.5-6 is a photograph of the Nimbus Attitude Control Module having completed test and ready for integration into the spacecraft. The controls subsystem module has the shape of a square parallelepiped. Solar paddles for power generation are attached to shafts which emanate from opposing faces of this parallel piped, the shaft being driven by the solar array drive motors.

#### 3.2.5.3.1 Requirements - Summary

The ERTS mission requires that instrumentation aboard the spacecraft be able to measure spacecraft accuracy compatible with locating any point in a 100 x 100 nautical mile photograph to within 2 nautical miles.

- The ACS is required to maintain the alignment of the ERTS Spacecraft body axes to the local earth-vertical orbit-velocity orientation of the orbital reference axes to within 0.7 degree for each of the three body axes, with the instantaneous angular rates about the satellites body axes to be less than 0.04 degree per second, with a goal of less than 0.015 deg/sec. An analysis of these NASA requirements, in conjunction with the attitude control capabilities, led to the following attitude control performance requirements.
- Provide an Attitude Sensor with  $\pm 0.1$  degree pitch and roll measurement accuracy.
- Acquisition of the reference orientation from an initial orientation, and with angular rates of up to 2 deg/sec about each axis.
- Independent, single-axis rotation of the solar array paddles for sun-tracking to within  $\pm 10$  degrees of the pitch axis-sun line plane.
- Provide three axes stabilization during orbit adjust maneuver with accuracies of less than  $\pm 6$  degrees for pitch and roll and  $\pm 10$  degrees in yaw considering a 600 sec OA engine on-time. For longer OA engine on times, the pitch and roll accuracies remain the same, and the yaw error increases at a rate of 0.01 deg/sec.
- Reacquisition of the reference orientation from the same angular rates specified for acquisition and from any attitude should some disturbance temporarily interrupt the attitude stabilization. The ERTS-ACS shall provide this capability a minimum of four times.

#### 3.2.5.3.2 ERTS-ACS Description

The ERTS-ACS employs two infrared horizon scanners to provide pitch and roll attitude error sensing. The conical scan axes for the two scanner units are aligned parallel to the

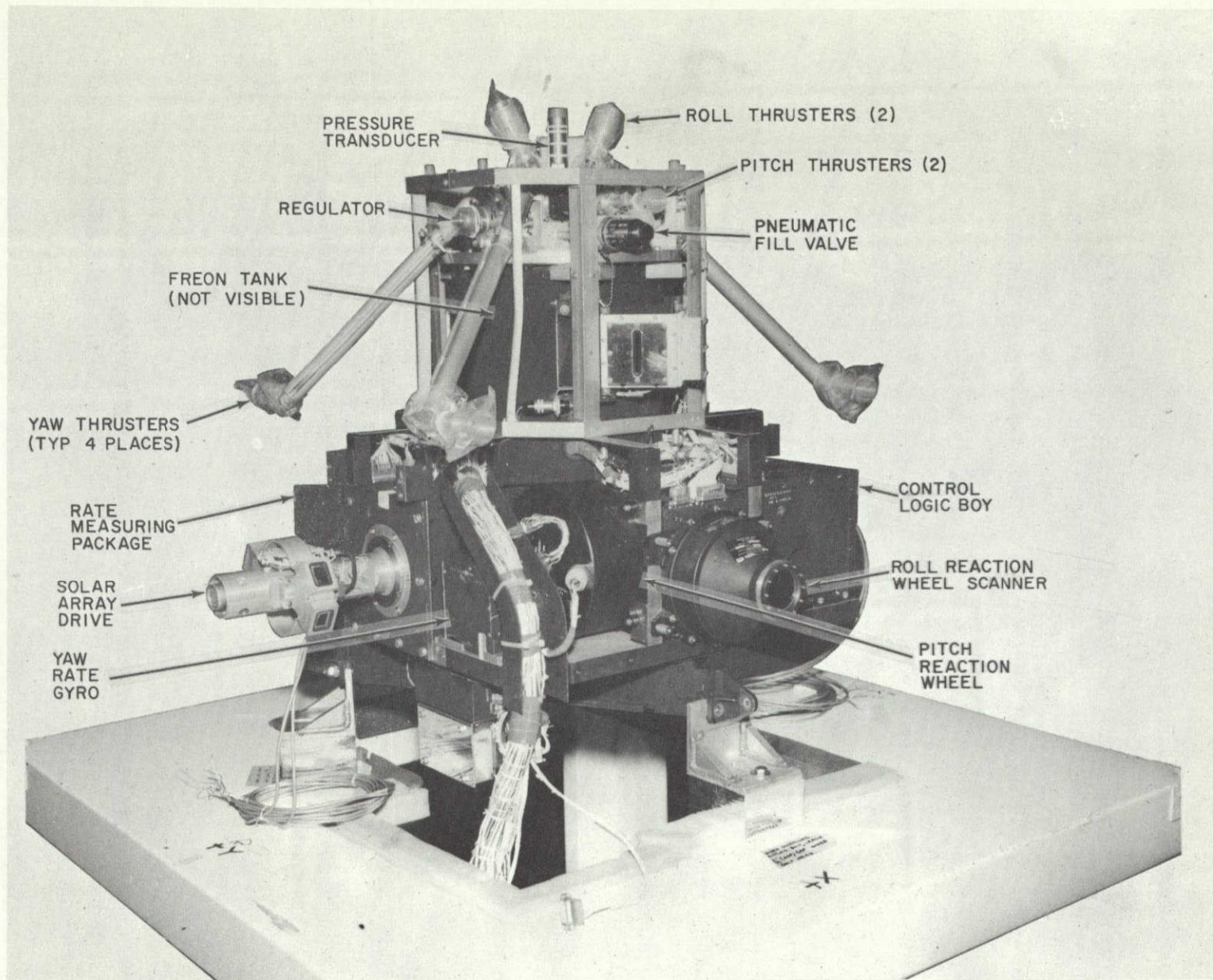


Figure 3.2.5-6. Nimbus Attitude Control Module

roll axis, one directed forward and one aft. The scanning motion is provided by the roll reaction wheels to which prisms are attached. A minimum scan speed (600 rpm) is maintained for each of the two wheels, which are rotated in opposite directions so that the net angular momentum along the roll axis is nominally zero. Roll momentum control is provided by speed variation of the wheels relative to each other. Figure 3.2.5-7 is the ACS block diagram.

The yaw channel error signals are derived from two sources, a yaw axis rate gyro or yaw gyrocompasses, determined by the commanded control mode. The various yaw control loop mechanizations provide for yaw rate damping as well as yaw attitude control.

Initial alignment of the pitch, roll and yaw spacecraft body axes to the reference orbital frame is effected by the use of the 3-axis, pneumatics-reaction wheel torquing subsystem. Acquisition about each of the three body axes occurs when the reaction wheels "capture" spacecraft control from the pneumatic jet torquers, reducing gas expenditure thereafter to periodic unloading of any momentum build-up in the reaction wheels.

The pitch and roll attitude control loop functions are identical for both the acquisition, orbit adjust, and normal orbit control modes. The yaw control loop, however, can be commanded to operate somewhat differently in the various modes, in order to achieve the required control. During the initial acquisition maneuvers, rate errors signals from the yaw axis rate gyro are fed directly to the pneumatics for corrective control action, while the yaw gyrocompass error signals are channeled to the yaw reaction wheel. The gyrocompass consists of a rate-integrating gyro, and gyro control electronics and is operated in a rate mode. It is mounted with its input axis in the roll-yaw plane tilted up 45 degrees from the positive roll axis towards the negative yaw axis. Its output signal contains components proportional to yaw attitude and rate as well as roll attitude and rate. Once the yaw reaction wheel is controlled by the gyrocompass attitude rate switching line, the yaw axis rate gyro and yaw pneumatics is disabled by command. Further yaw reaction wheel unloading is accomplished through the use of roll axis momentum unloading. During orbit adjust, the gyrocompass output is channeled directly to the yaw pneumatics in order to provide sufficient torque and rate limiting during this mode, and the yaw axis rate gyro is disabled.

The circuits used to control the pneumatic thrusters and reaction wheel drivers, provide as output, a constant amplitude pulse train whose duty cycle is proportional to the input error signal. Each circuit has a threshold, below which no output occurs, and a full on level, above which the device is saturated. No output corresponds to a zero duty cycle while saturation corresponds to a 100% duty cycle. This arrangement provides most of the benefits of proportional control while using simple on-off control elements.

### 3.2.5.3.3 ACS Control Modes - Summary

#### 3.2.5.3.3.1 Launch

During the launch and orbit injection phase, all pneumatic pulse modulators, pitch and yaw wheel pulse modulators, the fine roll error signal (that error signal being fed to the roll wheels), and the solar array drive control loop are inhibited.

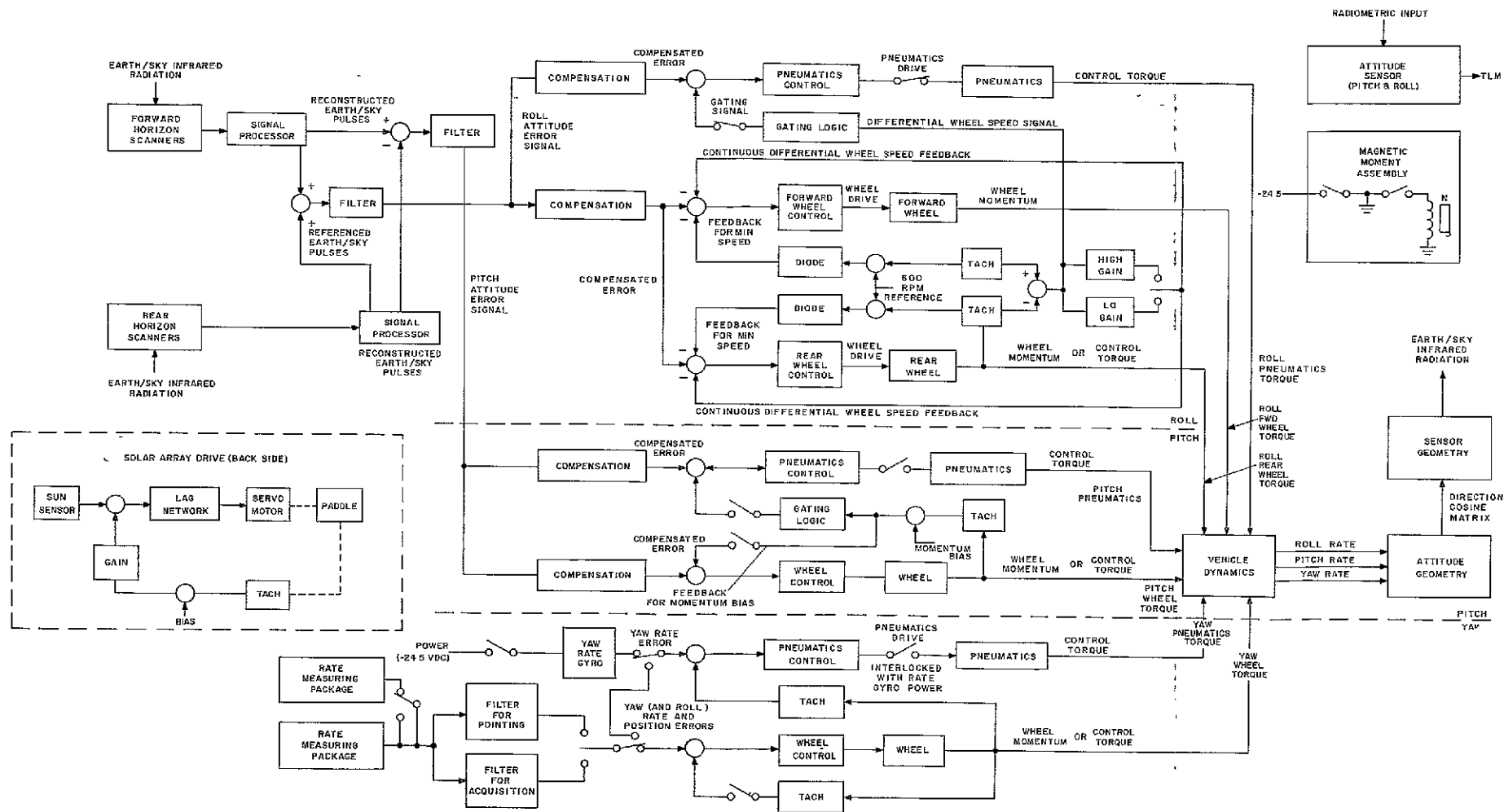


Figure 3 2.5-7 ERTS-ACS Block Diagram

FOLDOUT FRAME

FOLDOUT FRAME

The gyros are powered and the scanners are running at 600 rpm, during this phase of operation.

#### 3.2.5.3.3.2 Acquisition

Following orbit injection, the ACS is required to acquire the reference earth-vertical orbit-velocity orientation from any initial spacecraft orientation.

Following separation and time out of the 15 second timer, the inhibited elements of the ACS are enabled. Pitch and roll attitude error signals are provided by the IR horizon scanners, while yaw axis rate gyro and yaw gyrocompass provide yaw axis rate and attitude error signals.

The ACS, in this configuration, can acquire from any attitude with initial angular rates about any or all body axes up to 2 degree/sec. The presence of the yaw axis rate gyro in the yaw control loop assures that any initial yaw angular rates will be quickly reduced, since the yaw pneumatics will be activated for yaw rates greater than 0.1 degree per second.

The control laws are designed such that once the pitch, roll and yaw errors have been reduced to below the pneumatic modulator threshold levels, torquing control will gradually and smoothly be transferred to the reaction wheel system. This transfer occurs automatically and is referred to as wheel capture.

#### 3.2.5.3.3.6 Back Up Modes - Summary

The ERTS-ACS possesses several, inherent, back up modes, which enhance its high reliability and long life capability.

- The yaw gyrocompass is block redundant.
- Capability is provided to switch out either of the IR Horizon Scanners and simultaneously supply a "pseudo earth pulse" to the pitch Horizon Attitude Computer. In this mode, the ACS will continue to function within requirements.
- The Magnetic Moment Assembly can unload wheel momentum in the event of pneumatic loss.
- The system can be switched to the orbit adjust mode to compensate for a yaw wheel failure.
- The Pitch Momentum Bias mode provides for a back up of the total yaw control loop.

#### 3.2.5.3.3.3 Normal

The ACS provides automatic transition from the acquisition mode to the normal orbit operation in pitch and roll without the requirement of orbit adjust commands. The mechanization of the yaw control loop includes both an acquisition orbit adjust and a normal mode.



The normal mode control in yaw provides tighter yaw control than is possible while the ACS is subjected to acquisition constraints. Yaw momentum build up is removed by the roll pneumatics and yaw attitude and rate sensing is provided by the yaw gyrocompass, the yaw axis rate gyro and yaw pneumatics are turned off (by a single command) after wheel capture has occurred.

#### 3.2.5.3.3.4 Orbit Adjust

During this mode, disturbances to the ACS are caused as a result of mis-alignment of the orbit adjust engine thrust vector relative to the spacecraft center of mass. The pitch and roll control axes will function in their normal mode, and will go automatically to pneumatic control. The yaw axis will be commanded to the orbit adjust mode, in which the output of the yaw gyrocompass is switched (acquisition) to the yaw pneumatics, and the yaw axis rate gyro output is disabled. Upon completion of the orbit adjust, the yaw axis is commanded to the acquisition mode and then to the normal mode.

- In a low voltage condition, the pneumatic solenoid supply voltage is automatically turned off, placing the ACS in a "wheels only" operating state. This insures that spurious pneumatic operation will not occur during a low voltage condition.

#### 3.2.5.3.3.5 Solar Array Control Loop

The solar array control loops independently drive the two solar paddles which provides accurate paddle illumination and inherent redundancy. Sun sensors provide closed-loop tracking of the sun during sunlit portions of the orbit.

A geared ac servomotor is the primary drive mechanism for each solar paddle. A constant nominal rate command ( $\omega_B$ ) of 3.33 deg/min is provided at all times, subject to override by the sun sensor error signal when the sun is in view. The measured paddle rate is compared with the commanded rate, and the rate error signal is amplified by a relative angle-rate gain. The resulting equivalent angle error signal is summed with the output of the sun sensor.

#### 3.2.5.4 Orbit Adjust Subsystem Design Summary

The Orbit Adjust Subsystem is shown schematically on Figure 3.2.5-8 and in assembled form on Figure 3.2.5-9 and 3.2.5-10. It is a single module for ease of integration into the ERTS spacecraft.

The propellant and nitrogen gas pressurant are stored in a single tank, separated by a positive expulsion bladder. Two manually operated fill valves are provided for pressurant and propellant loading and unloading. Immediately downstream of the propellant fill valve are two paralleled normally closed explosively actuated valves. Operation of either of these valves arms the subsystem after launch. Just beyond this point in the propellant line is a third manually operated valve. This valve is used as a test port for functional checks of the downstream portion of the subsystem without operating the normally closed explosive valves. All three manually operated fill and test valves are capped after closing to minimize the possibility of leaks. The propellant is filtered through a 25 micron absolute filter in the manifold. In addition, there are pressurant valve inlet filters of the same 25 micron size.

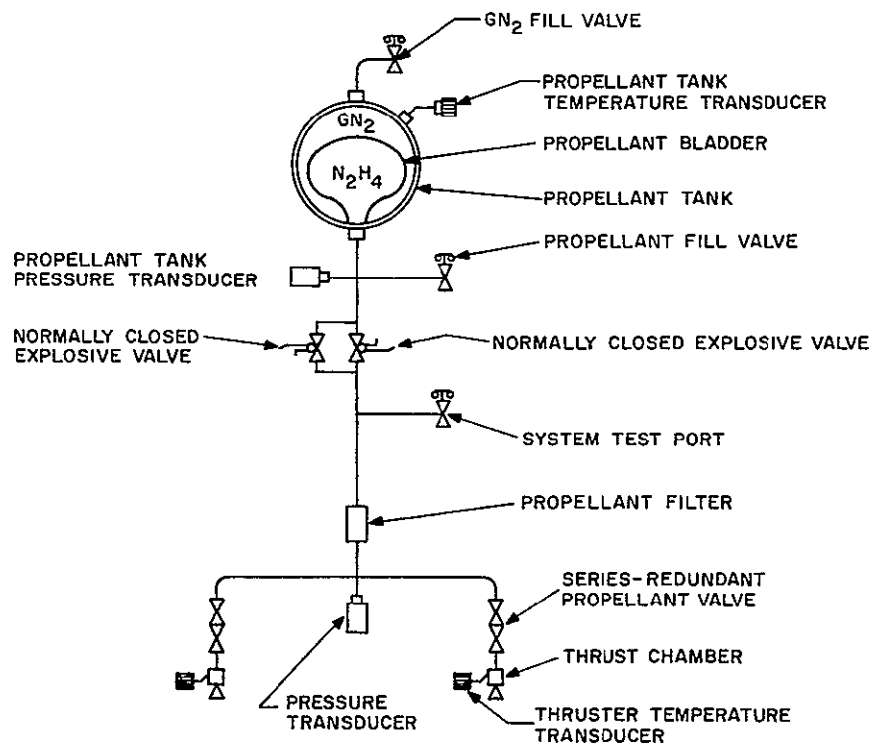


Figure 3.2.5-8. Orbit Adjust Subsystem - Schematic





These valves are solenoid operated and series redundant. They consist of two complete valves assembled in a common housing. Operation of the solenoid valves by an electrical command fires the thruster assemblies. With the temperature of the subsystem at a nominal 70°F, the initial thrust is nominally 0.870 pounds force, decaying to 0.568 pounds force as the propellant is consumed from the storage tank. Subsystem instrumentation includes two pressure transducers to monitor propellant tank pressure and propellant manifold pressure and temperature transducers mounted on the external surface of the tank and on each of the thruster catalyst chambers. A "cocoon" of insulation is used around the subsystem module to maintain acceptable temperature limits (4°C to 49°C) in the worst case orbit plus firing duty cycle conditions. This insulation covers all but the mounting feet, thrusters, and bottom of the module.

Thruster identification and spacecraft axes definition are shown on Figure 3.2.5-11. The subsystem is mounted in the spacecraft so that the thrusters are located on the -x and x roll axis. The modular design of the subsystem readily enables alignment of the thruster axis to within a 0.100 inch radius sphere about the measured CM of the spacecraft. One thruster is canted upwards at an angle of approximately 20° so that its exhaust plume will not impinge upon the spacecraft struts and the paddle latch mechanism. Because of subsystem is designed as a module, it can be readily subjected to testing prior to installation on the spacecraft. This all-brazed propellant feed system minimizes leaks and heavy connecting fittings. The total subsystem weight is 31.7 pounds fully fueled with 10.1 pounds of hydrazine. The hydrazine thrusters of the subsystem are designed for and have been tested for operational firing modes ranging from 1.0 to 0.1 pounds force thrust for pulses varying from 1 second to 8 hours. Thrusters of this design have accumulated as much as 114 hours of burn time under vacuum conditions. The operational requirements for the Orbit Adjust Subsystem at an average thrust level of 0.75 pounds force include firings for durations as long as 18 minutes. Firings for drag makeup, however, will be as short as 12 seconds.

All components of the Orbit Adjust Subsystem were selected to take advantage of previously documented experience with components which satisfy the subsystem requirements. Extensive qualification testing is not required. A component matrix is shown on Table 3.2.5-1. The propellant tank, supplied by Pressure Systems, Inc. has undergone extensive qualifications for Mariner Mars '69 flight. Some redesign of the propellant tank is required to accommodate the higher operating pressures required for the ERTS Orbit Adjust Subsystem. This redesign will be verified by additional qualification testing. In addition, the bladder material will be replaced with ethylene-propylene, although the same design, and fabrication techniques will be used. The propellant solenoid valve, manufactured by the Panther-Hannefin Corp. are of a soft seat, Belleville actuation solenoid design. The explosively actuated valves are a normally closed design wherein the squib exhaust gases push a piston which shears a tube, pushing the sheared section clear of the flow path. The propellant filter is manufactured by Vacco Valve Company. The filter is a stocked, etched disc type. The pressure transducers, manufactured by the Instrument Systems Division of the Whittaker Corporation, are a bonded strain gage type. The temperature transducer selected to monitor the subsystem temperature is also manufactured by the Whittaker Corporation and uses a platinum resistance thermometer and a central signal conditioning unit.

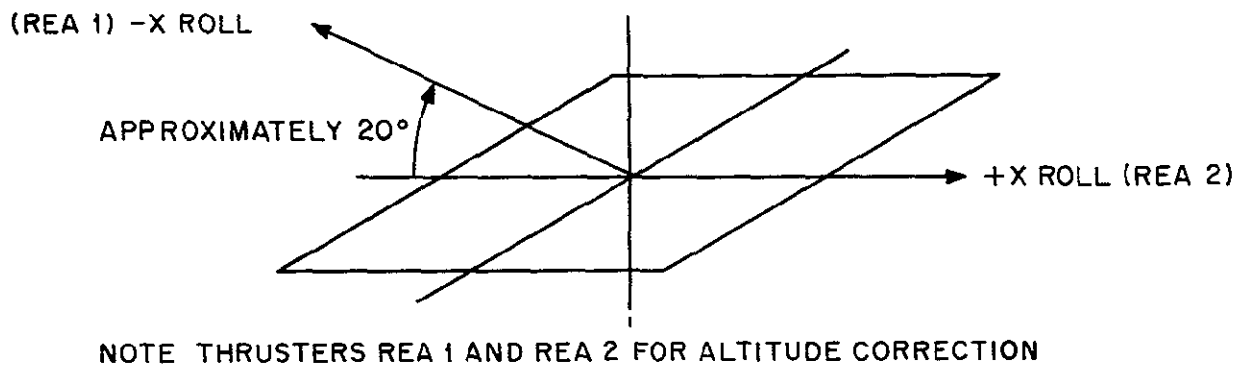
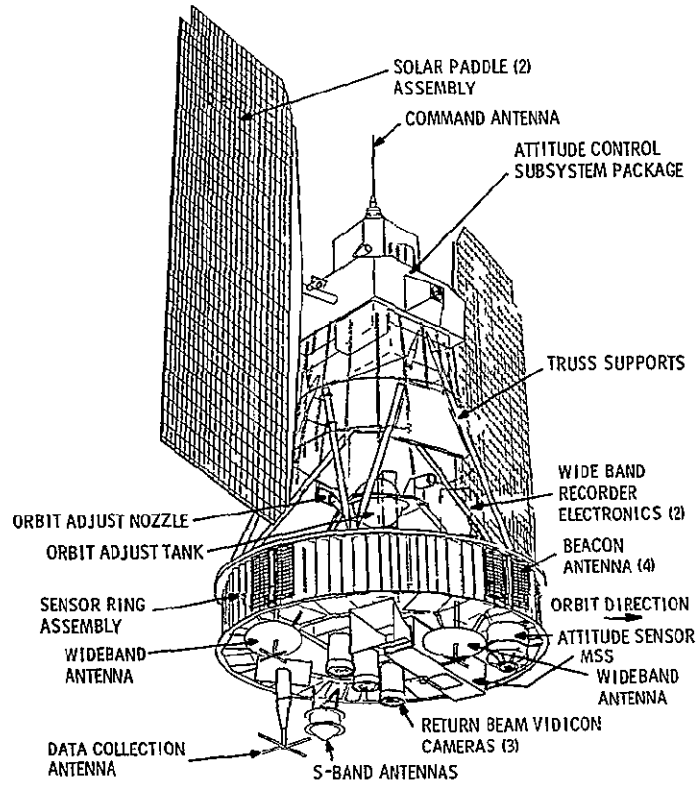


Figure 3.2.5-11. Thruster Identification and Spacecraft Axes

Table 3 2 5-1 Components Matrix

Component	Qty	Vendor	Previous Use (Qualification)
Propellant tank	1	Pressure Systems, Inc.	Mariner '64, '69
Thruster	2	Rocket Research Corp.	
NC explosive valve	2	Pyronetics, Inc.	
Fill and test valve	3	Rocket Research Corp.	
Filter	1	Vacco Valve Co.	Classified Program
Pressure transducer	1	Whittaker Corp., Instrument Systems Division	
Temperature transducer	3	Whittaker Corp., Instrument Systems Division	
Propellant valve	2	Parker - Hannecin Corp.	

In summarizing its performance capabilities, the Orbit Adjust Subsystem is designed to operate in a blowdown mode, resulting in a decreasing level of thrust during the one year spacecraft life. As orbit adjustments are performed, propellant is consumed, and the pressure drops, resulting in decreased thrust. The mission requires 2169 pound-seconds total impulse. Figure 3.2.5-12 shows that with the subsystem at 70°F, the thrust will decrease from 0.870 pounds force to 0.568 pounds force

#### 3.2.5.5 Thermal Subsystem Description Summary

The ERTS thermal control subsystem is required to maintain the temperature of the payload environment to  $20^{\circ} \pm 10^{\circ}\text{C}$ , and the temperature of the attitude control subsystem component mounting structure to  $25^{\circ} \pm 10^{\circ}\text{C}$ . Temperature control is accomplished by different means in each of the four major regions of the spacecraft, utilizing a combination of thermally actuated shutters, low duty cycle compensation electric heaters, radiator plates, thermal radiation and rigid conductor coupling, multilayer insulation, thermal coatings, and mass thermal capacity.

##### 3.2.5.5.1 Sensory Ring

Figure 3.2.5-13 shows the plan form of the sensory ring and lists the components included in its 18 equipment bays. Heat from this equipment is conducted to the periphery of the ring, where it is radiated from the spacecraft through shutters that are opened or closed according to the temperature of the bay. Multilayer insulation covers the top and bottom of the ring to isolate it from the external environment and channel the component heat to the shutter regulated radiating surfaces. These radiating surfaces are coated with white paint

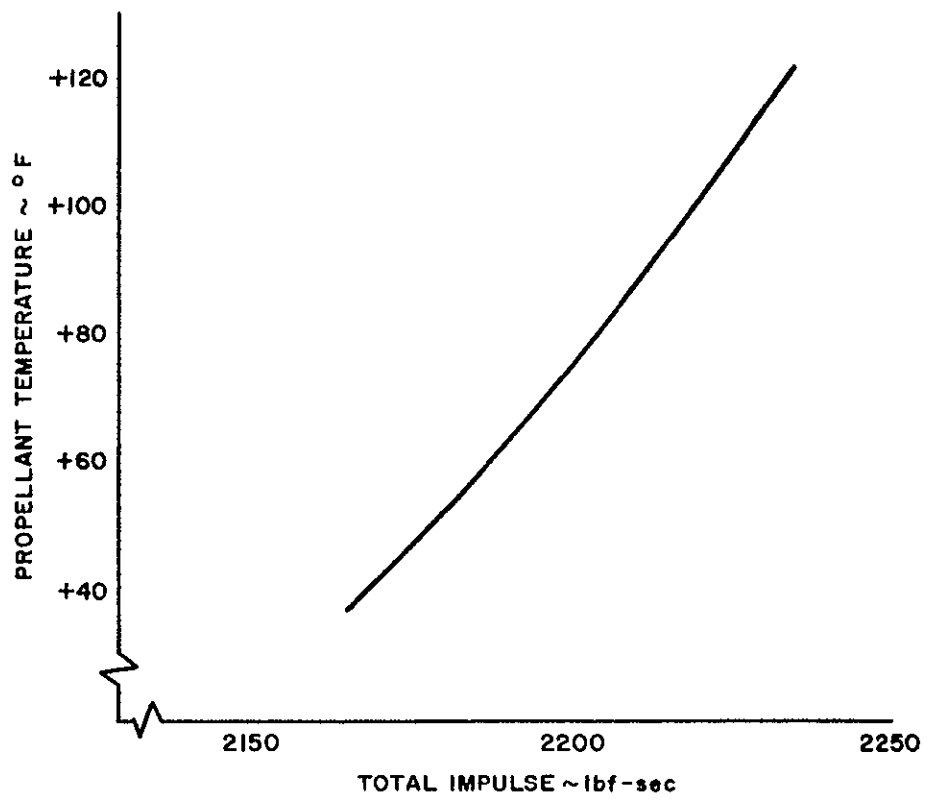


Figure 3. 2. 5-12. - System Operating Characteristics



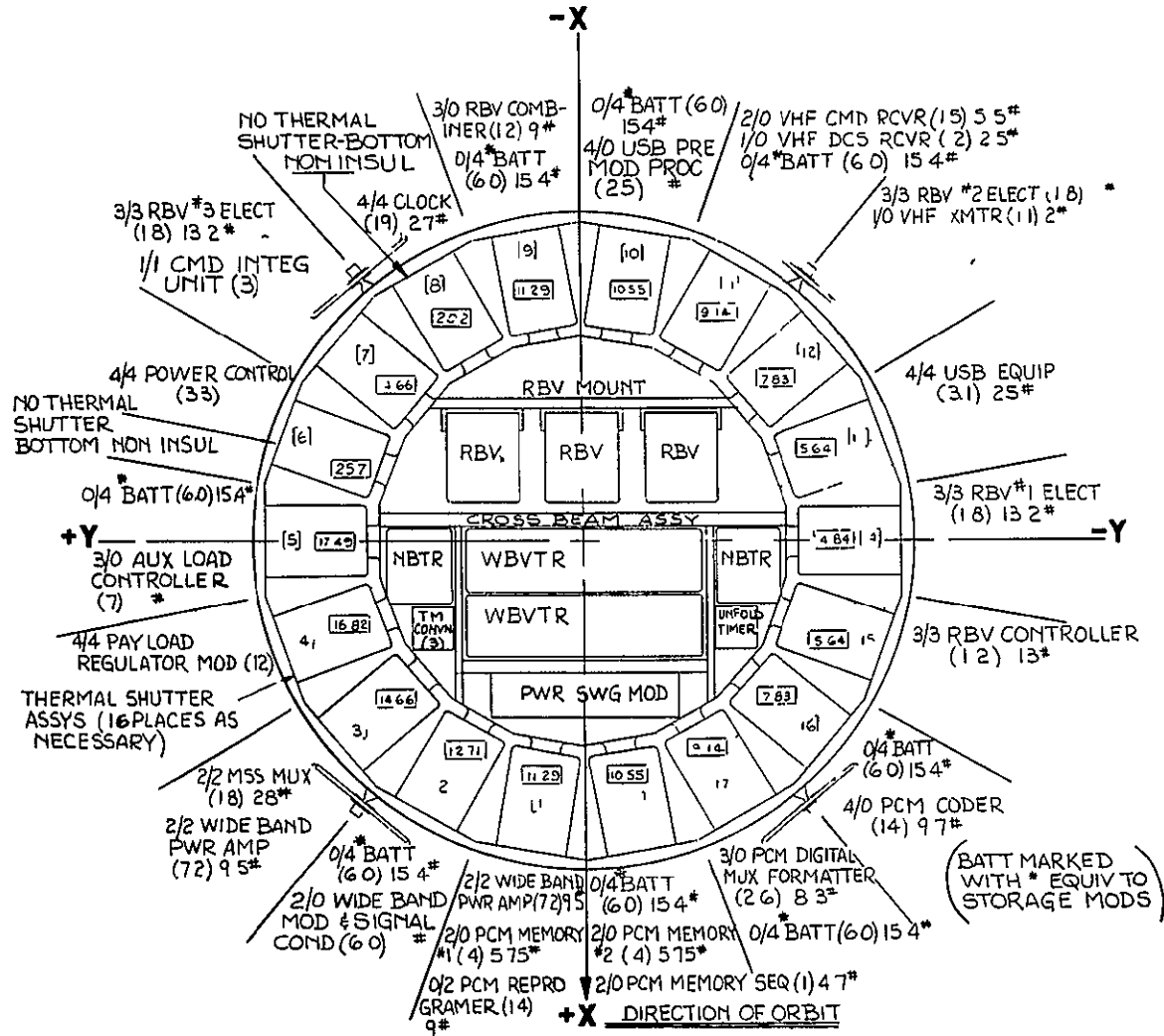


Figure 3.2.5-13. Sensory Ring

( $\alpha_s \leq 0.2$ ,  $\epsilon \geq 0.85$ ) to maximize IR heat rejection and minimize solar and albedo heat absorption. During low duty cycle periods when component heat may not be sufficient to maintain minimum temperature with closed shutters, electric heaters are activated by command to supplement the heat balance.

#### 3.2.5.5.2 Sensory Ring Center Section

Figure 3.2.5-14 shows that the Multi-Spectral Scanner and Return Beam Vidicon Cameras are mounted on the structural beams of the sensory ring center section. These beams also support the Wideband Video Tape Recorders, the Narrow Band Tape Recorders, and several other components. The heat dissipated by this equipment is radiated away, from the MSS directly, from the cavity surrounding the RBVs, from the radiator plate attached to the structure at the +X side of the MSS instrument mount, and through the insulation that covers the top of the center section. The heat dissipated by this equipment varies from an orbit average of 87.8 watts during an orbit with 25.8 minutes of payload operation, to an average of 11.2 watts during an orbit with no payload operation.

Temperature control of these center section components is accomplished by sizing the radiating areas to reject a carefully selected orbit average heat load, using insulation over the components to restrict other heat flow paths. Compensation heaters supply auxiliary heat and thereby prevent component subcooling below 10°C during those low duty cycle orbits when the component heat dissipation is below the radiation heat rejection capability. The radiating areas are chosen so that the component mounting interface temperature will not exceed 30°C for the worst case series of high duty cycle orbits, considering both radiation heat rejection and component mass heat capacity. Components mounted in the center section will be coated with black paint ( $\epsilon = 0.9$ ) to maximize radiation exchange, and the external radiator plate will be coated with white paint ( $\alpha_s = 0.2$ ,  $\epsilon = 0.85$ ) to provide high radiating capacity and minimize solar absorption. Silver filled silicone grease will be used to prevent high thermal path resistance in the vacuum environment at all attachment connections.

The orbit adjust subsystem is mounted over the center section. It is covered by the center section top insulation blanket and maintained above its minimum allowable temperature of 4.5° by radiation and conduction from the center section equipment and the sensory ring structure. The thrusters are exposed, but are raised to satisfactory pre-operation temperature by built in 1.5 watt heaters.

#### 3.2.5.5.3 Above Sensory Ring

Figure 3.2.5-15 shows the location of the wideband video tape recorder electronics boxes. These packages are insulated and radiate their heat through windows cut in the insulation blankets. The insulation on the sides of the boxes is faired into the top insulation of the sensory ring so that radiation can freely exchange between the bottom of the boxes and the ring. Black paint is used on these internal radiating surfaces, and white paint is used on the exposed box windows. The orbit average heat load can vary from 11 watts to 0. The window area is sized (40 square inches per box) so that the net heat rejection, after accounting for solar, albedo, and earth fluxes, is sufficient to prevent the box from exceeding 30°C during the worst case series of orbits, when accounting for both duty cycle timing and component mass heat capacity. 3.5 watts compensation heat per box is required to prevent these components from cooling below 10°C during orbits when the recorders are not operated.

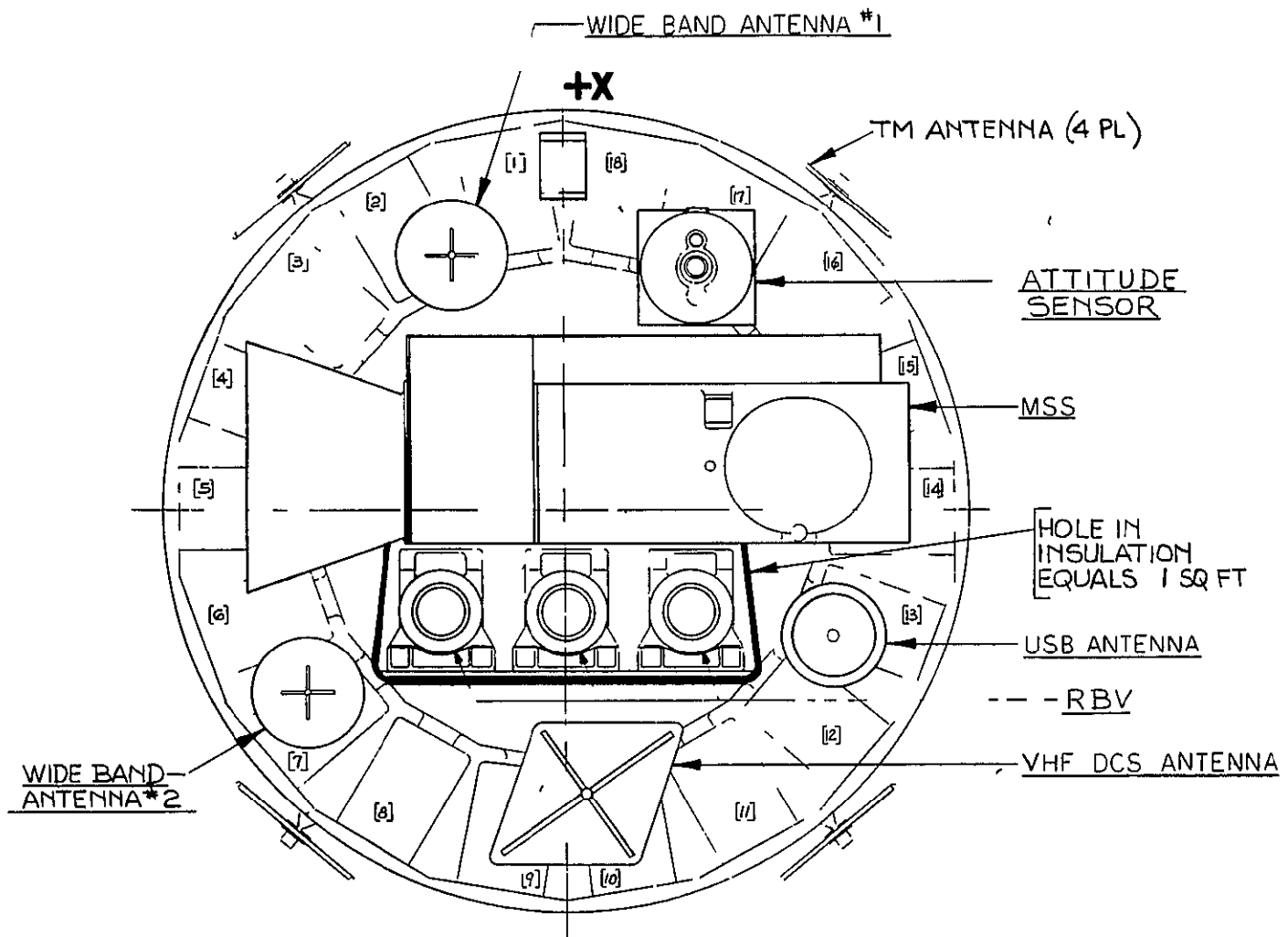


Figure 3.2 5-14. Sensory Ring Center Section

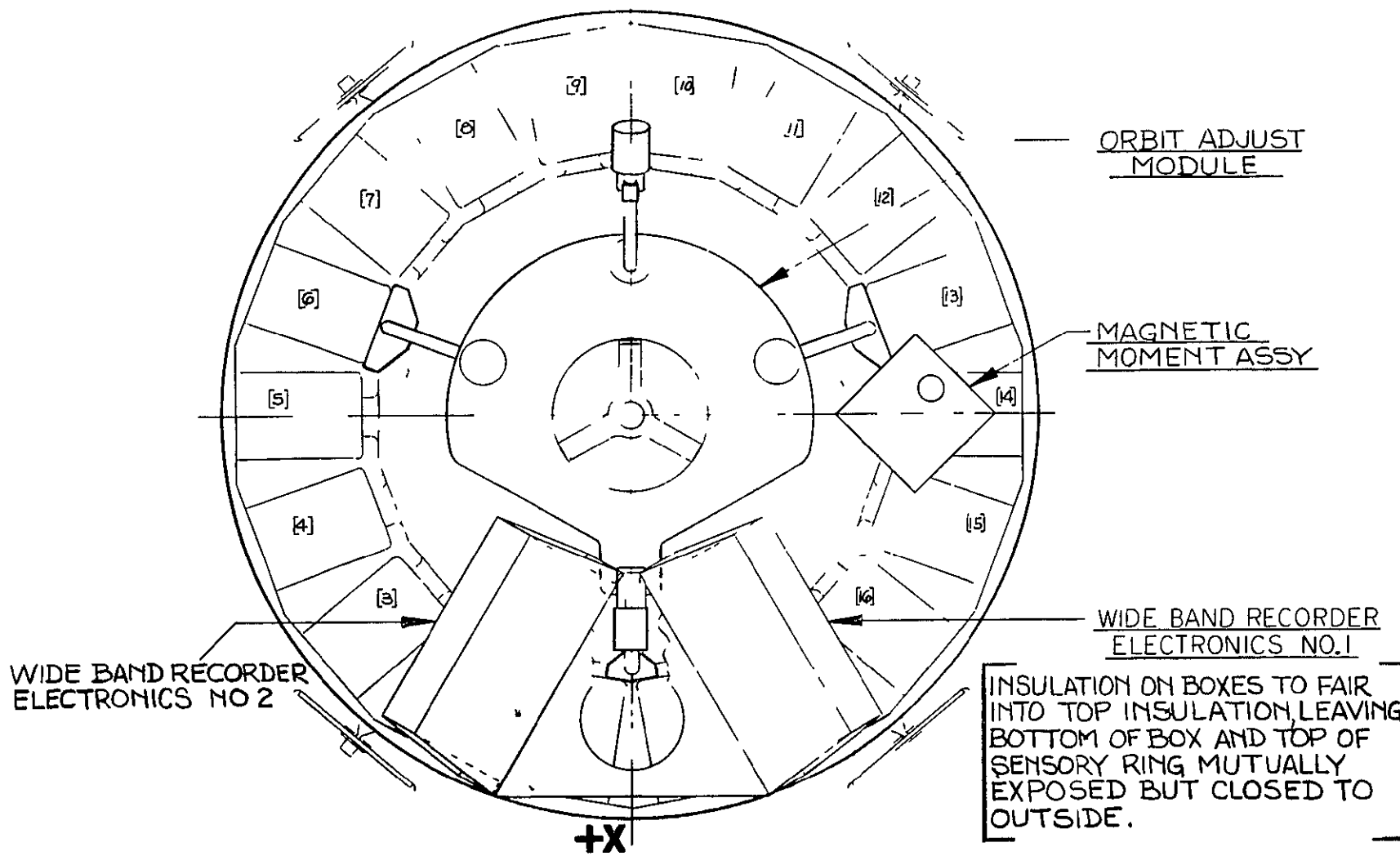


Figure 3.2.5-15. Top View, Sensory Subsystem

11 February 1970

#### 3.2.5.5.4 Attitude Control System

The attitude control system is a separate and distinct structural assembly located above the Sensory Subsystem and attached to it by six (6) structural tubes. The ACS also provides support to and actuation of the solar arrays. ACS thermal control for ERTS is the same as for Nimbus D. This system is designed to accommodate a wide range of orbit Beta ( $\beta$ ) angles. Temperature of the ACS is provided by passive and semi-passive techniques, similar to the sensory ring. A unique aspect of the ACS thermal design is the enclosed shutter assembly. The shutter assembly is located between the equipment mounting deck and a dust cover/heat sink as shown previously in Figure 3.2.5-14. This dust cover, suspended from the lower surface of the ACS, is painted black on the inside and white on the outside.

The white paint on the outside causes the dust cover to operate at low temperatures. The low temperature and black paint on the inside provide an adequate heat sink for the components mounted above, which radiate to the cover through the shutter blades.

Parametric analyses performed by the subsystem contractor and extended by GE for ERTS show that temperature control to  $25 \pm 10^\circ\text{C}$  can be maintained in the 37 degree Beta angle orbit. Average temperatures will be about  $5^\circ\text{C}$  higher (to  $26^\circ\text{C}$ ) than for the  $0^\circ\beta$  angle operation with Nimbus. This extension includes the small radiation blockage effect of the WBRE boxes mounted on top of the sensory ring.

#### 3.2.5.6 Power Subsystem

The power subsystem provides the electrical power required to operate the spacecraft and its subsystems from transfer to internal power prior to launch through the one year design point. The subsystem is comprised of the following components listed in Table 3.2.5-2.

The solar array/battery system provides power through a regulated bus to sustain orbital operations. The battery complement provides sufficient energy to support the spacecraft during launch, ascent and acquisition phases prior to deployment of the solar array. A block diagram of the subsystem is shown in Figure 3.2.5-16 and the component characteristics are summarized in Table 3.2.5-2. The deployment mechanism is included as part of the structure subsystem and the solar array drive is considered as part of the Attitude Control Subsystem. The total weight of the power subsystem, as defined above, is 254 pounds.

##### 3.2.5.6.1 Functional Description

During the launch sequence, the solar arrays are in the stowed position and the batteries deliver power to the unregulated bus through the Power Control module. Upon separation of the adapter from the spacecraft, relays are energized in the Unfold Timer which causes the paddle unfold pyros to fire at predetermined intervals. When the cables are cut the unfold motor is started, deploying the solar arrays. They then begin tracking the sun, with its acquisition, the solar array assumes the power generating function for the spacecraft.

During sunlight periods the solar array delivers power to the unregulated bus in the Power Control Module at a voltage of from about -30 to -39 volts. The lower limit is set by the battery discharge voltage as -30 volts is approached load sharing occurs and the batteries begin to discharge. A

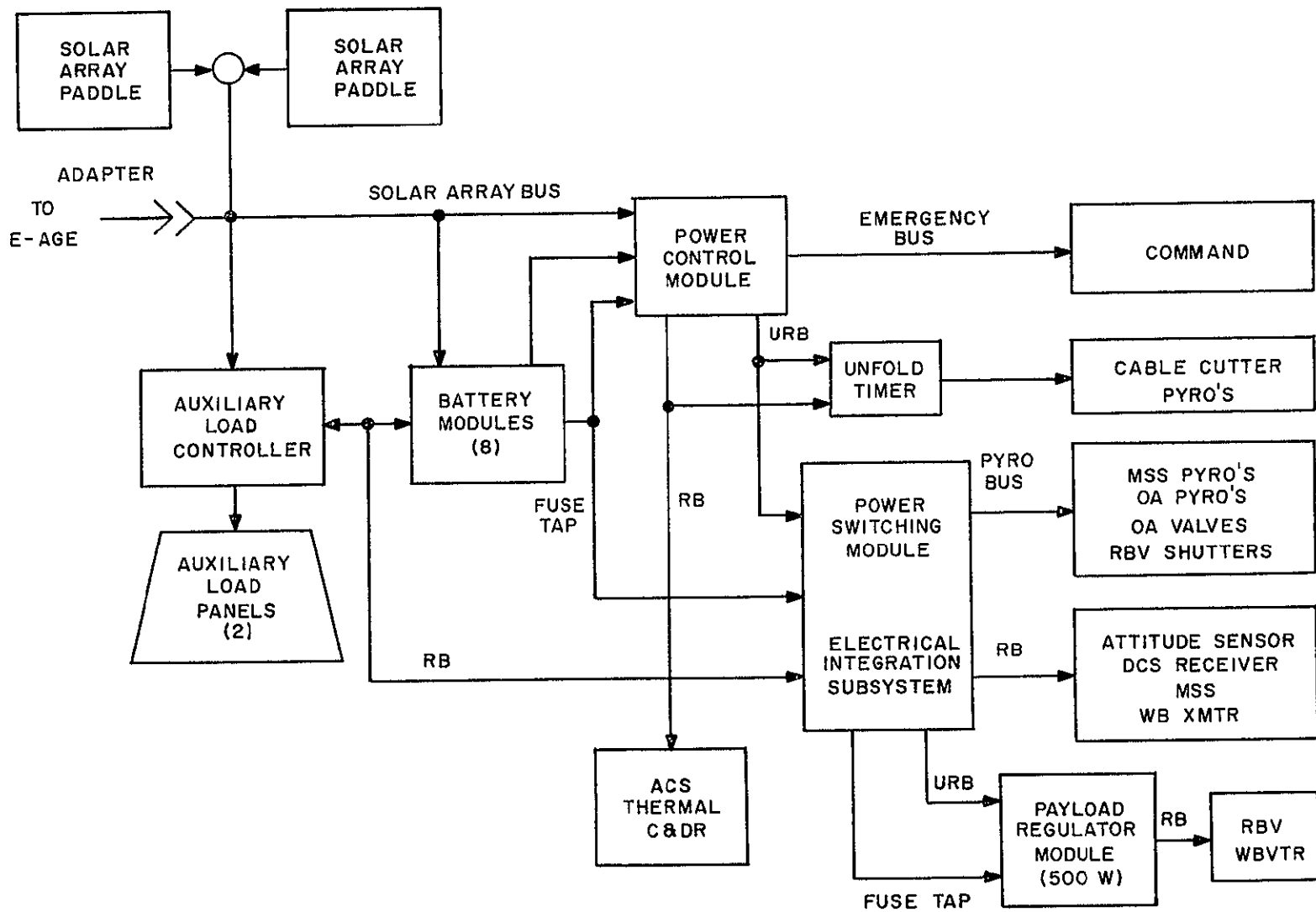


Figure 3.2.5-16. Block Diagram, ERTS Power Subsystem

Table 3 2 5-2 Power Subsystem Components

Item	Need Modification	Weight Pounds Each	Dimensions Each	Max Power Dissipated Watts	Make/buy	Comments
Solar Paddle (2)	No	36 4	38 4" X 96" (25 ft <sup>2</sup> )	-	RCA	Same as Nimbus D/E
Battery Modules (8)	No	15.5	0/4	7 6	RCA	Same as Nimbus D/E
Power Control Module (1)	No	21 3	4/4	41	RCA	Same as Nimbus D/E
Aux Load Controller (1)	No	6 0	3 0	0 6	Make	Same as Nimbus D/E
Aux Load Panel (2)	No	5 0	10" (top) X 15 X 1 3/4 16" (bottom)	200	Make	Same as Nimbus D/E
Unfold Timer (1)	No	3 5	6 3/4" X 5 1/2" X 3 1/4"	-	Make	Same as Nimbus D/E
Payload Regulator Module (1)	No	21.3	4/4	41	RCA	Same as Power Control Module
<b>Total</b>		<b>253 9</b>				

approached load sharing occurs and the batteries begin to discharge. Above -39 volts voltage limiters, located in each of the battery modules, automatically shunt excessive current from the solar array bus up to a maximum of 12 amperes. Additional power management functions are carried out by the commandable auxiliary load controller which causes power to be drained from the solar array bus to one of the auxiliary load panels. These auxiliary loads are generally required only when normal spacecraft loads are very light, solar array output is high, and it is desired to reduce the power dissipated in the battery modules through the shunt resistors.

In addition to battery cells and shunt elements the battery modules contain the charge control electronics, a battery on/off relay and a 15 cell tap for providing large surges of current directly to the regulated bus in case of emergencies.

The power control module contains two redundant pulse width modulated regulators which supply the -24.5 volt regulated bus, two redundant auxiliary regulators supplying a -23.5 volt bus, a trickle charge override switch to override the trickle charge on the battery modules, 8 battery isolation diodes, a regulated bus comparator, the shunt dissipation driver, and fuse blow inputs for the 15 cell battery tap.

The power control module feeds regulated -24.5 volt power to the ACS, thermal control, command and data handling subsystem and the power switching module. It also feeds unregulated power to the Unfold Timer and the Power Switching Module. The emergency bus, from the auxiliary regulators, is used by the command subsystem for receiver and clock operation.

The power switching module contains pyro firing circuitry and relays for control of input power to the commandable subsystems as well as the Payload Regulator Module.

The Payload Regulator Module is identical to the Power Control Module and contains redundant PWM regulators for providing -24.5 volts to the RBV cameras and wideband video tape recorders.

When the power required by the spacecraft subsystems is in excess of that which the solar array can provide, as evidenced by the array voltage dropping to the battery discharge voltage (less the drop across the isolation diodes) the batteries will discharge and load sharing will occur between batteries and solar array. Should the drain be excessive, such as might occur during a short, and the regulated bus voltage drop to less than 18 volts, the 15 cell battery fuse tap is activated and 15 cells discharge directly onto the regulated bus. This will blow the fuse or clear the short by burning it out.

During eclipse periods the batteries discharge onto the unregulated bus through the isolation diodes located in the Power Control Module to supply spacecraft loads. Batteries are recharged by voltage limited temperatures compensated charge controllers located in the individual modules. Each module also contains circuitry to reduce the charge to a trickle rate should battery temperature increase to 45°C. The trickle charge can be overridden by the trickle charge override function located in the power control module. Battery charging



occurs when the solar arrays receive solar energy. Should the charge controller not prove effective in controlling overcharge, the auxiliary load panels are activated to drain off excess power.

### 3.2.5 7 Electrical Integration

The electrical integration subsystem includes the distribution harness and the following components Preflight Disconnect, Power Switching Module. Electromagnetic interface considerations are also discussed as part of this subsystem.

The Harness provides the electrical interfaces between the payload sensors and all spacecraft components. It is a critical element in the performance of the communications subsystems and also in the minimization of interference between components. The functions of the Harness Subsystem include the following

1. Provides signal interconnections between spacecraft service subsystems and sensors
2. Distribution of regulated and unregulated power
3. Collection of telemetry data
4. Distribution of commands
5. Provides ground reference for all components

The primary design objectives established for the harness are

1. To provide accessibility to all components during test while the vehicle is in an operating mode
2. To minimize the noise radiated from and the noise picked up by the harness
3. To limit the voltage drop in the power harness to 1% of the supply voltage
4. To provide an adequate transfer function for all signals
5. To provide selective redundancy for critical vehicle functions
6. To minimize subsystem weight
7. To minimize the magnetic moment of the harness

Design features of the Harness which will attain these objectives are as follows

1. The component accessibility achieved through judicious harness routing in the component area.

2. Requirements for shielding, shield termination, and routing of harness have been specified. Critical signals are run as twisted lines or coaxial cables.
3. Wire gauge for each power line and return will be sized to limit the IR drop to less than 1%
4. Minimization of harness weight will be a key factor in the design of the Telemetry and Command Subsystem Harnesses and in the design of the Power Subsystem Harness.
5. The selection of nonmagnetic connectors and the twisting of the Power Distribution wires will minimize the contribution of the harness to the magnetic moment of the spacecraft.

Physically, the Harness divides into 1) Sensory Ring Harness, top and bottom, to include both the spacecraft and sensor subsystem segments, 2) the Attitude Controls Interface Harness, routed up the struts, and 3) the Adapter Harness.

The major portion of the Harness is located at the top of the sensory ring with interconnections to the bottom loaded sensor equipment being routed down through the cross beam area just inboard of the modules. Connector breakouts to the sensory ring modules are routed along the castings between the modules to facilitate installation and removal of modules. The Solar Array and Attitude Control Subsystem interface segments are routed and clamped external to the truss tubes.

Functionally, the harness can be engineered as follows

- Power
- Separation
- Command
- Telemetry
- Thermal
- Communication
- Sensor

Each of the functional harnesses is analyzed for signal level and frequency content to determine shielding and routing requirements to minimize electromagnetic interference. When Harness separation for EMI purposes is impractical due to physical space limitation, the harness segments will be individually shielded for maximum isolation. The functional harness segments will be segmented to facilitate fabrication, test, and installation.

Table 3.2 5-3 shows a summary of the major harness segments, including an approximation of the number of connectors. The estimated weight of the harness subsystem is 135 pounds. Major portion of the weight data is derived from actual Nimbus data thus offering more accuracy to the estimate.

Table 3 2 5-3 Harness Summary

Subsystem Power & Separation	Number of Harness* Segments	Number of Connectors**
Power	18	114
Command	8	57
PCM Telemetry	19	118
Thermal	6	6
Power Switching Mod (Switched Power and Signals)	1	20
DCS	2	4
Wideband Telemetry	12	33
Narrowband Recorder	12	33
RBV	9	27
MSS	2	6
Adapter	7	18
Total	96	436
*Includes 31 coaxial segments		
**Includes intrasubsystem interface connectors		

### 3 2 5 7 1 Power Switching Module

The power switching module is the interface between power, spacecraft loads, and command subsystems. The major functions are to provide power and signal switching, load fault protection, and to provide voltage for limiting the unregulated voltage applied to the orbit adjust solenoid valves. Telemetry circuits are necessary to indicate switch position, pyro firing events, and system bus voltages.

11 February 1970

The pyro firing relays and small signal relays are housed in separate rf compartments. Fuses and telemetry circuits are mounted on circuit boards. Power command and telemetry circuits are electrically input.

The power switching module is 13 by 13 by 3-3/4 inches, and is designed for mounting on the ERTS sensory ring cross-beam, where its central location will optimize the interconnecting harness, which interfaces with all major subsystems.

### 3 2 5 7 2 Preflight Disconnect Component

The preflight disconnect component provides for remote disconnect of power and monitor circuits (required during the pre-launch phase only) between the adapter and spacecraft prior to launch. Demating prior to launch eliminates the requirement for an umbilical quick-pull type disconnect which would be demated and operation of the shroud or adapter, in flight, thus enhancing the overall reliability of the separation sequence.

The preflight disconnect is a motor-driven plug which remains in the adapter, and the associated receptacle is spring-mounted on its base to provide movement in the event of slight misalignment during mating. The plug can be remotely mated or demated to make or break connections to externally located ground equipment.

### 3.2.5.8 AGE

Equipment under the general category of Aerospace Ground Equipment (AGE) includes all mechanical and electrical spacecraft oriented equipment required to support sub-system and system level testing, handling, transportation, checkout, servicing, stimulation and simulation, packaging and maintenance of the satellite during its complete ground mission profile including factory, remote test facility, and field operations.

The AGE required to support the ERTS Program is logically divided into two categories Mechanical AGE and Electrical AGE. There are numerous individual equipment items in each of these categories. For summary purposes, these items have been consolidated into functional groups. Table 3 2 5-4 is a tabulation of these functional equipment groups and a summary of equipment items as functions included in each group.

The AGE design approach capitalizes upon the successful AGE designs previously used for Nimbus A, C, B, and B2 and currently in use or planned for use on the Nimbus series D, E and F programs. The degree of Nimbus design and hardware utilization is shown by end item categories for Electrical and Mechanical AGE in Table 3 2 5-5, AGE Status Summary

Table 3.2.5-4 ERTS AGE Summary

Equipment Group No	Nomenclature	Function/Equipment Items
<b>Mechanical AGE</b>		
M1	Attitude Control Subsystem BTE	A group of mechanical AGE required to support test of the ACS Equipment includes RWS simulators, ACS support fixture, SPSS simulators, alignment fixture, SAD alignment targets, AC B handling sling, RCS T/V test equipment, and vibration fixture, SAD shaft dual indicator, SAD shaft drive fixture, RWS shipping containers, solar paddle transition simulator
M2	Orbit Adjust Subsystem BTE	The following items of mechanical AGE are required OA shipping container, OA alignment targets, OA handling fixture,
M3	Payload Subsystem BTE	A group of mechanical AGE including RBV handling fixture, RBV S/A alignment fixture, RWT reveal, check of calibration fixture.
M4	Spacecraft Handling and Transportation Equipment	A group of mechanical AGE including a Test and Calibration Dolly, Spacecraft Dolly and Sensory S/S Fixture, Utility Dolly, Cover Sling, Hydract, S/C Cover Mounting Ring, Sensor Ring Lift Sling, Transport Trailer, Spacecraft Spacer, S/C Humidity Covers Spacecraft Sling, Spacecraft Cover, Flight adapter handling fixture, and AGE packaging.
M5	Spacecraft Checkout Equipment	Spacecraft checkout equipment includes the following Matchmate Tool, Leak Test Equipment, Alignment Equipment, Mass Property Meas Equip, Wt and c g Separation Rate Fixture Paddle Hub Clamp RFI Sling Vibration Fixtures ambient check of calibration adapter
M6	Spacecraft Servicing Equipment	A group of mechanical AGE including Nitrogen gas, charging equipment, S/C access ladders and platforms, S/C cleaning kit S/C mechanics tool kit, S/C accountability kit, orbit adjust fuel servicing equipment
M7	Spacecraft Thermal-Vacuum Equipment	A group of special support and check of calibration equipment required for spacecraft T/V testing
<b>Electrical AGE</b>		
E1	Electrical Systems Test Set	Controls and Monitors spacecraft operation during integration and systems test. Supplies ground power performs battery charging, verifies attitude control S/S Power S/S and unfold MSS and OA EED Circuitry Controls Sun, Earth, and Attitude Sensor Simulators Provides hardwire command signals Provides special test signals and verifies responses Controls RBV and MSS-Go/NoGo targets. Provides troubleshooting capability Contains Protective circuitry to assure spacecraft electrical test safety
E2	Test Ground Station	Generates and verifies RF Commands (VHF and USB) to spacecraft. Receives, records, processes, and displays real time and stored telemetry Verifies PRN and DCS performance Receives and records RBV and MSS data. Processes RBV and MSS Data with GFE Test equipment, Provides troubleshooting, debugging evaluation and statistical analysis
E3	Auxiliary Test Equipment	A group of equipment providing RBV Collimator and MSS Target Controls Solar Array Simulation Solar Array Testing RF Test Equipment, Test Antennas RF Dummy Loads and Protection Ambient Test Cables Test Tees and Breakout Boxes and Passive Simulation of spacecraft and adapter loads
E4	Environmental Electrical Support Equipment	A group of equipments providing Thermal Vacuum Test support including Power and Control of Heater arrays, Thermal vacuum Test Cables, Temperature monitoring thermocouples, and special test modules
E5	Field Operations Equipment	A group of equipment including Blockhouse Console to power and monitor spacecraft during prelaunch and launch operation, Attitude Controls Stimulator Control Console Simulators to electrically check Launch Vehicle interfaces and special test modules.
E6	Subsystem Bench Test Equipment	Subsystem Bench Test Equipment to functionally test the following subsystems ACS Power S/S, Command S/S TLM S/S RBV S/S (GFE); MSS S/S (GFE) DCB; and Wide Band Comm. S/S.

11 February 1970

Equipment Category	Design Sources		
	Nimbus	Mod Nimbus	New
<b>Mechanical</b>			
1. ACS Bench Test Equipment	11	1	1
2. Orbit Adjust BTE	1	1	2
3. Payload Subsystem BTE	7	-	3
4. Spacecraft Handling and Transportation Equipment	13	-	-
5. Checkout Equipment	6	2	-
6. Servicing Equipment	1	4	-
7. Spacecraft Thermal Vacuum Equipment	1	1	2
<b>Electrical</b>			
1. Electrical Systems Test Set	5	5	1
2. Test Ground Station	-	-	1
3. Auxiliary Equipment	3	6	1
4. Environmental Test Support Equipment	1	2	-
5. Field Operations Equipment	1	5	-
6. Subsystem Bench	3	1	4

Table 3 2 5-5 AGE Status Summary

Utilization of the basic Nimbus D spacecraft as a bus with integrated ERTS payloads and the orbit adjust subsystem incorporated minimizes the number of new AGE designs in both the electrical and mechanical areas.

The individual payload subsystems and their associated equipment, the Communications and Data Handling subsystem and to a lesser degree, the orbit-adjust subsystem, comprise the major differences between Nimbus and the proposed ERTS spacecraft which affect AGE

Highlights of the approach to AGE for ERTS are as follows

1. Maximum utilization of the spacecraft telemetry system is made for performance monitoring and fault diagnosis. This minimizes the number of hardware test points required.
2. Fault isolation to the black box level is attained through the use of supplementary test tees and breakout boxes.
3. In the interest of cost effectiveness and the versatility achieved by direct operator control, test equipment is manual. Interlock circuitry is provided to preclude spacecraft damage through incorrect sequences of operation. The exception is that telemetry and command data is processed by computer in the Test Ground Station.
4. Wherever feasible, identical equipment supports factory, field, and prelaunch operations to produce correlatable data.
5. Sensor, payload, and critical control components are aligned at the control package and sensory ring subassembly level and these subassemblies are aligned to each other at spacecraft assembly. Following environmental tests, alignments is rechecked in the optical facility to insure that components have remained within requirements.
6. As a result of measured results closely confirming calculated results early in the Nimbus program, moments of inertia are calculated only.
7. The spacecraft is transported with the yaw axis horizontal in a transporter having passive environmental control except for humidity which is controlled by continuous purge.
8. Spacecraft payloads are stimulated and calibrated as an "all-up" system in ambient and vacuum-thermal environments during system test.
9. Hard points for handling the assembled spacecraft are provided on sensory ring.
10. Handling equipment is designed to a minimum static limit loading of 3g at yield or 4.5g at ultimate, whichever is less and is proof loaded to a static load of 2g.

11 February 1970

### 3.3 HARDWARE MATRIX

Table 3.3-1 is a compilation of the major spacecraft components that will be used for the Earth Resources Technology Satellite (ERTS). Since the Observatory design has been predicated upon an existing spacecraft which already meets many of the ERTS mission requirements, most of the ERTS hardware is identical or requires very little design modification. The table is presented in the format designated in Attachment VI (Section 1.4.16) of S-701-P-3, Design Study Specifications for the Earth Resources Technology Satellite ERTS "A" and "B"

It can be seen from the Spacecraft Hardware Table that approximately 56 percent of the line items listed will require no change from the existing design in order to be used for ERTS, and another 21 percent will require only minor design modifications. The remaining line items (23 percent) require new designs and will be procured from well established, technically competent subcontractors or produced in-house. This approach allows for maximum control of the relatively few newly designed components for the ERTS program.

Implementation of the actual hardware procurement program will follow well established and proven procedures, utilizing for the most part, the same material sources and subcontractors found to be most suitable on the Nimbus program. In-house fabrication and test functions will be performed with the same (or newly built but equivalent) equipment and facilities and by the personnel previously trained and experienced on Nimbus.



Table 3 3-1 Preliminary Availability Status Information on Potential ERTS Hardware

MAJOR SPACECRAFT ASSEMBLY NOMENCLATURE	ANTICIPATED SOURCE	NEW DESIGN REQUIRED?	USE EXISTING DESIGN WITH		QUANTITY FOR ERTS A, B, & SPARES			UNITS AVAILABLE FOR ERTS		ERTS ESTIMATED COST	FLIGHT HISTORY
			NO CHANGE	MINOR CHANGE	REQUIRED	AVAILABLE	TO BE FABRICATED	SERIAL NUMBERS	PROGRAM ACCOUNTABILITY		
<u>Structure Subsystem</u>											
• Structure	GE	No	X		2	0	2			Sec Phase D Proposal Volume III	Nimbus II III
• Sensory S/S Primary Structure		Yes		X	2	0	2				
• Sensory S/S Secondary Structure	GE	Yes		X	2	0	2		-		
• Paddle Unfold Switch	Micro Switch	No	X		3	0	3		-		Nimbus II III
• Cable Cutter & Squibs Assembly	Atlas Chemical Company	No	X		18	0	18 (14 spares)		-		Nimbus II III
• Load Cells	GE	No	X		2	0	2		-		Nimbus II III
• Paddle Latch Hardware	GE	No	X		2	0	2		-		Nimbus II III
• Bolt Cutter Assembly & Squibs	Atlas Chemical Company	No	X		4	0	4		-		Nimbus II, III
• Adapter Primary Structure	GE	No		X	2	0	2		-		Nimbus II III
• Adapter Secondary Structure	GE	No		X	2	0	2		--		Nimbus II III
• Separation Band	GE	No	X		2	0	2		-		Nimbus II, III
• Separation Springs	GE	No		X	12	0	12		-		Nimbus II, III
• Paddle Dampers	GE	No	X		4	0	4		-		Nimbus II, III
• Separation Switches	Micro Switch	No	X		14	0	14		-		Nimbus II, III
• ACS Shroud Stimulators	GE	No	X		12	0	12		-	--	Nimbus II, III
• Adapter Go/No-Go Targets	GE	Yes			2 sets	0	2 sets		--	--	Nimbus II, III
• WB Antenna Pickup & Re-radiator	GE	Yes			2	0	2		--		Nimbus II, III
• USB Antenna Pickup & Re-radiator	GE	No		X	2	0	2		--	-	Nimbus II III

Table 3.3-1. Preliminary Availability Status Information on Potential ERTS Hardware (Cont)

MAJOR SPACECRAFT ASSEMBLY NOMENCLATURE	ANTICIPATED SOURCE	NEW DESIGN REQUIRED?	USE EXISTING DESIGN WITH		QUANTITY FOR ERTS-A, -B, & SPARES			UNITS AVAILABLE FOR ERTS		ERTS ESTIMATED COST	FLIGHT HISTORY
			NO CHANGE	MINOR CHANGE	REQUIRED	AVAILABLE	TO BE FABRICATED	SERIAL NUMBERS	PROGRAM ACCOUNTABILITY		
<u>C&amp;DH Subsystem</u>											
• Command Clock	Cal Comp	No	X		2	0	2(a)	(a)	Nimbus E/F	See Phase D Proposal Volume III	Nimbus D
• VHF Command Receiver	RCA	Yes			2	0	2(b)	-	-		
• PCM Telemetry Processor	Radiation	No	X		2	0	2(a)	(e)	Nimbus E/F		Nimbus D
• N/B Tape Recorders	Leach	No		X	4	0	4(b)	-	-		
• VHF Transmitter	Radiation	No		X	2	0	2(b)	-	-		
• W/B FM Modulator	GE	Yes			2	0	2(b)	-	--		
• W/B Power Amp	Watkins Johnson	Yes			4	0	4(b)	--	-		
• Premod Processor	Motorola	Yes			2	0	2(b)	--	-		
• Unified S-Band Equip	Motorola	Yes			2	0	2(b)	--	-		
• Conditioner Box	GE	Yes			2	0	2(b)	-	-		
• Command Integrator	GE	Yes			2	0	2(b)	-	-		
• W/B Antenna	GE	Yes			4	0	4	-	-		
• Command Antenna	GE	No		X	2	0	2	-	--		
• Quadraloop Antenna	GE	No		X	8	0	8	-	--		
• USB Antenna	GE	No			2	0	2	-	-		
<u>ACS Subsystem</u>											
• ACS Structure	Fairchild	No			2	0	2	-	--		
• Thermal Control Assembly	Fairchild	No	X		2	0	2(a)	(a)	Nimbus E/F		Nimbus D
• Pitch Flywheel	Bendix	No	X		2	0	2(a)	(a)	Nimbus E/F		Nimbus II III D
• Yaw Flywheel	Bendix	No	X		2	0	2(a)	(a)	Nimbus E/F		Nimbus II III D

11 February 1970

Table 3 3-1 Preliminary Availability Status Information on Potential ERTS Hardware (Cont)

MAJOR SPACECRAFT ASSEMBLY NOMENCLATURE	ANTICIPATED SOURCE	NEW DESIGN REQUIRED?	USE EXISTING DESIGN WITH		QUANTITY FOR ERTS-A, -B, & SPARES			UNITS AVAILABLE FOR ERTS		ERTS ESTIMATED COST	FLIGHT HISTORY
			NO CHANGE	MINOR CHANGE	REQUIRED	AVAILABLE	TO BE FABRICATED	SERIAL NUMBERS	PROGRAM ACCOUNTABILITY		
<u>ACS Subsystem (Cont.)</u>											
• Pneumatics Assembly	TRW	No	X		2	0	2(a)	(f)	Nimbus E/F	See Phase D Proposal Volume III	Nimbus D
• Solar Array Drive (S&D)	TRW	No	X		5	0	5(a)	(g)	Nimbus E/F		Nimbus D
• Rate Measuring Package (RMP)	Sperry	No	X		4	0	4(a)	(a)	Nimbus E/F		Nimbus III D
• Yaw Rate Gyro	Northrup	No	X		2	0	2(a)	(a)	Nimbus E/F		Nimbus-Nimbus D
• Harness	GE	No		X	2 sets	0	2 sets	--	--		Nimbus II, III, D
• Attitude Sensor	Quantic	No		X	2	0	2(b)	-	--		
• Initiation Timer	GE	No	X		2	0	2	--	--		Nimbus D
• Magnetic Moment Assy	Ithaco	No	X		2	0	2(a)	--	-		Nimbus D
• Roll Reaction Wheel Scanner	Bendix	No	X		4	0	4(a)	(a)	Nimbus E/F		Nimbus D
• Control Logic Box	Ithaco	No		X	2	0	2(b)		--		Nimbus D
• Signal Processor	Ithaco	No	X		4	0	4(a)	(h)	--		Nimbus D
<u>Orbit Adjust Subsystem</u>											
• Propellant Tank	Rocket Research	No		X	2	0	2(b)	--	-		Classified Prog
• Thruster Assembly	Rocket Research	No	X		2	0	2(b)	--	-		Classified Prog
• Structure	Rocket Research	No	X		2	0	2(b)	--	-		Classified Prog
• Other Components	Rocket Research	No	X		2	0	2(b)		-		Classified Prog
<u>Thermal Subsystem</u>											
• Thermal Radiation Plates	GE	Yes			4	0	4	-			
• Temperature Controller Assembly	GE	No	X		36	0	36 (4 spares)	--	--		Nimbus II III, D
• Shutter Position Indicator Assembly	GE	No	X		32	0	32		-		Nimbus II III, D

11 February 1970

TABLE 3.3-1. PRELIMINARY AVAILABILITY STATUS INFORMATION  
ON POTENTIAL ERTS HARDWARE

MAJOR SPACECRAFT ASSEMBLY NOMENCLATURE	ANTICIPATED SOURCE	NEW DESIGN REQUIRED?	USE EXISTING DESIGN WITH		QUANTITY FOR ERTS-A, -B, & SPARES			UMITS AVAILABLE FOR ERTS		ERTS ESTIMATED COST	FLIGHT HISTORY
			NO CHANGE	MINOR CHANGE	REQUIRED	AVAILABLE	TO BE FABRICATED	SERIAL NUMBERS	PROGRAM ACCOUNTABILITY		
<u>Thermal Subsystem (Cont)</u>											
• Insulation	GE	Yes			3 sets	0	3 sets(c)	--	--	See Phase D Proposal Volume III	Nimbus II, III, D
• Shutter Assemblies	GE	No	X		36	0	36(4' spares)	--	-		Nimbus II, III, D
• Compensating Loads	GE	No	X		65	0	65(5 spares)	--	-		Nimbus II, III, D
• Thermal Coatings & Tapes	GE	No			As Required			--	--		Nimbus II, III, D
<u>Power Subsystem</u>											
• Solar Paddles	RCA-AED	No	X		4	0	4	--	-		Nimbus II, III, D
• Storage Modules	RCA-AED	No	X		17	0	17(a)	(d)	Nimbus E/F		Nimbus II, III, D
• Power Control Module	RCA-AED	No	X		2	0	2(a)	(a)	Nimbus E/F		Nimbus II, III, D
• P/L Regulator Module	RCA-AED	No	X	Identical To Power Control Module	2	0	2(a)	(a)	Nimbus E/F		Nimbus II, III, D
• Auxiliary Load Panel	GE	No	X		4	0	4(a)	(a)	Nimbus E/F		Nimbus II, III, D
• Auxiliary Load Controller	GE	No	X		2	0	2(a)	(a)	Nimbus E/F		Nimbus II, III, D
• Separation Unfold/Timer	GE	No	X		2	0	2(a)	(a)	Nimbus E/F		Nimbus II, III, D
<u>Electrical Integration Subsystem</u>											
• Spacecraft Harnesses	GE	Yes			2 sets	0	2 sets	--	--		Nimbus II, III, D
• Flight Adapter Harnesses	GE	Yes		X	2 sets	0	2 sets	--	--		Nimbus II, III, D
• Power Switching Module	GE	Yes			2	0	2	--	--		
• T/M Conversion Modules	GE	No	X		6	0	6	--	--		Nimbus II, III, D
• Thermistors	GE	No	X		180	0	180	--	--		Nimbus II, III, D
• Preflight Disconnect	GE	No	X		2	0	2	--	--		Nimbus II, III, D

(a) - Nimbus F and ERTS B share common backup

(b) - Qual Model Refurbished for Spares

(c) - Shells only required for Spares

(d) - ERTS Provides 1 Spare

(e) - PCM Telemetry Processor Memory

(f) - ERTS Provides Spare Regulator

(g) - ERTS Provides 1 Spare

(h) - ERTS Provides Circuit Cards For Signal Processor

### 3.4 LAUNCH VEHICLE STUDY RESULTS

#### 3.4.1 GENERAL

A study was performed under Program Directive Number 55 (Nimbus E/F) dated June 6, 1969 (NASA Contract #11570) to "Determine the impact on the Nimbus E/F spacecraft design using a Thorad/Delta launch vehicle for launching of the spacecraft with a payload as defined in GSFC Nimbus "E" configuration modified to include addition of the T&DR system and deletion of the SDR system." The study considered the mechanical and electrical interfaces, and the support equipment (AGE). In the course of the study, various "Delta" problems arose for which "Nimbus" solutions were obvious. These problems were identified and proposed solutions were recommended.

This study was reviewed to determine the applicability of the results with respect to the ERTS spacecraft and its electrical and mechanical interface requirements.

##### 3.4.1.1 Review Summary

The study was reviewed against the ERTS requirements. The conclusion reached was that while most of the potential mechanical and electrical problems identified for the Nimbus E/Delta L/V interface are extremely minor and readily solvable there is one area which was not completely resolved. This area is the inadequate clearance between the upper-paddle latch of the spacecraft and the Delta shroud.

This clearance problem is created by the method of shroud attachment to the launch vehicle. The Delta configuration has the shroud mounted directly to the forward end of the launch vehicle. The spacecraft adapter is mounted to a two-inch adapter ring (or spacer) which in turn mounts to the forward end of the Delta. Because of this ring and the manner and position of mounting the shroud, the upper end of the paddle assembly protrudes into the conical portion of the shroud, thus creating an interference problem. Figure 3-4-1 illustrates this problem. Both Nimbus "B" and Nimbus "D" were mounted to two-inch spacer rings which were mounted on top of the Agena, however, the shroud used was attached to the top of this spacer resulting in an adequate clearance for the upper paddle latch.

Several methods by which this problem can be resolved are listed as follows:

1. Use a SACS type shroud with an SACS adapter ring (spacer) which raises the shroud 2 inches and attaches to the Delta booster, which requires modifying the front end of the Delta.
2. Use the present Delta shroud configuration except mounted to a new adapter ring.
3. Increase the length of the shroud by two inches.
4. Dimple the Delta shroud around the clearance problem area.

11 February 1970

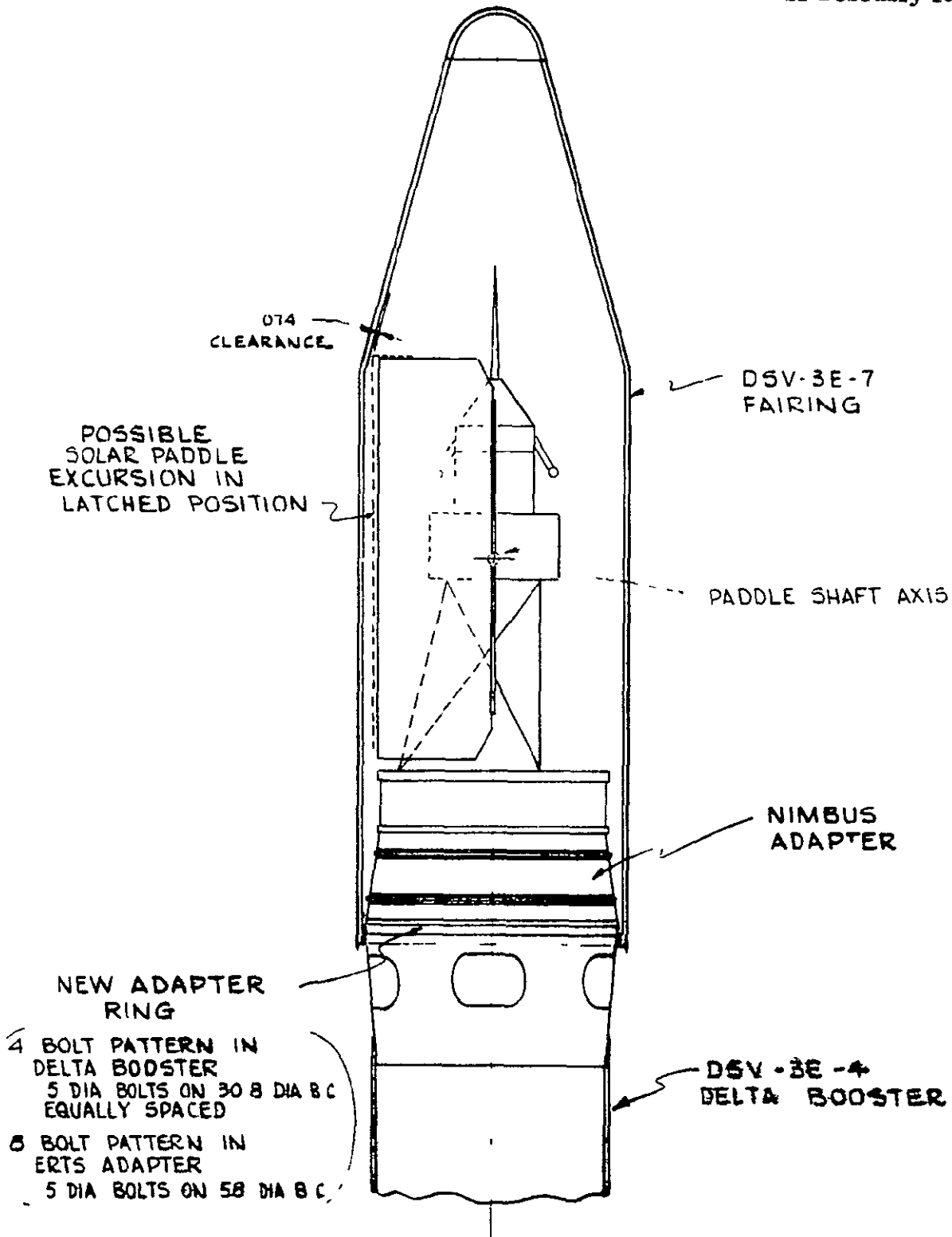


Figure 3.4-1. Paddle Assembly Protrudes into Conical Portion of Shroud

- 5 Design a new adapter to fit on top of the Delta booster, eliminating the need for an intermediate adapter ring (spacer)
6. Design a shorter adapter

### 3 4 1 2 Baseline Configuration

Figure 3.4-2 shows the recommended approach which is to modify the upper end of the Delta to accept the SACS ring, thus permitting the use of the SACS shroud. This change has been requested by the NASA/GSFC Nimbus E/F Project Office.

## 3 4 2 ERTS/DELTA ELECTRICAL INTEGRATION STUDY

### 3 4 2 1 Introduction

The Electrical Interface design of the ERTS Spacecraft and the Delta launch vehicle is presented in this section. As a result of this study, it has been determined that the ERTS Spacecraft can be made electrically compatible with the Delta Launch Vehicle if the following requirements are met by the Delta electrical system as follows:

1. Supply 24 amperes to the spacecraft separation pyros (bolt cutters) at the initiation of the separation event.
2. Accept and transmit five telemetry signals from the spacecraft flight adapter.
3. Provide the above telemetry monitors with regulated power.
4. The fairing should be RF transparent between 130 MHz through 2300 MHz in specific areas.
5. Relay contacts for the separation pyro circuitry should be "break-before-make".
6. The umbilical should be able to accommodate 47 pins + 20 percent spares for spacecraft functions.
7. RF compatibility.

### 3.4.2.2 Interface Description

An interconnection diagram of the proposed ERTS Delta Electrical Interface is shown in Figure 3.4-3. The Delta bulkhead connector functions are listed generically in Table 3.4-1.

### 3 4.2 3 Umbilical Pin Requirements

A review of the spacecraft blockhouse electrical interface requirements indicates that 47 pins plus 20 percent spares are required through the Delta umbilical.

Table 3.4-2 categorizes the functional requirements assigned to the umbilical pins.

11 February 1970

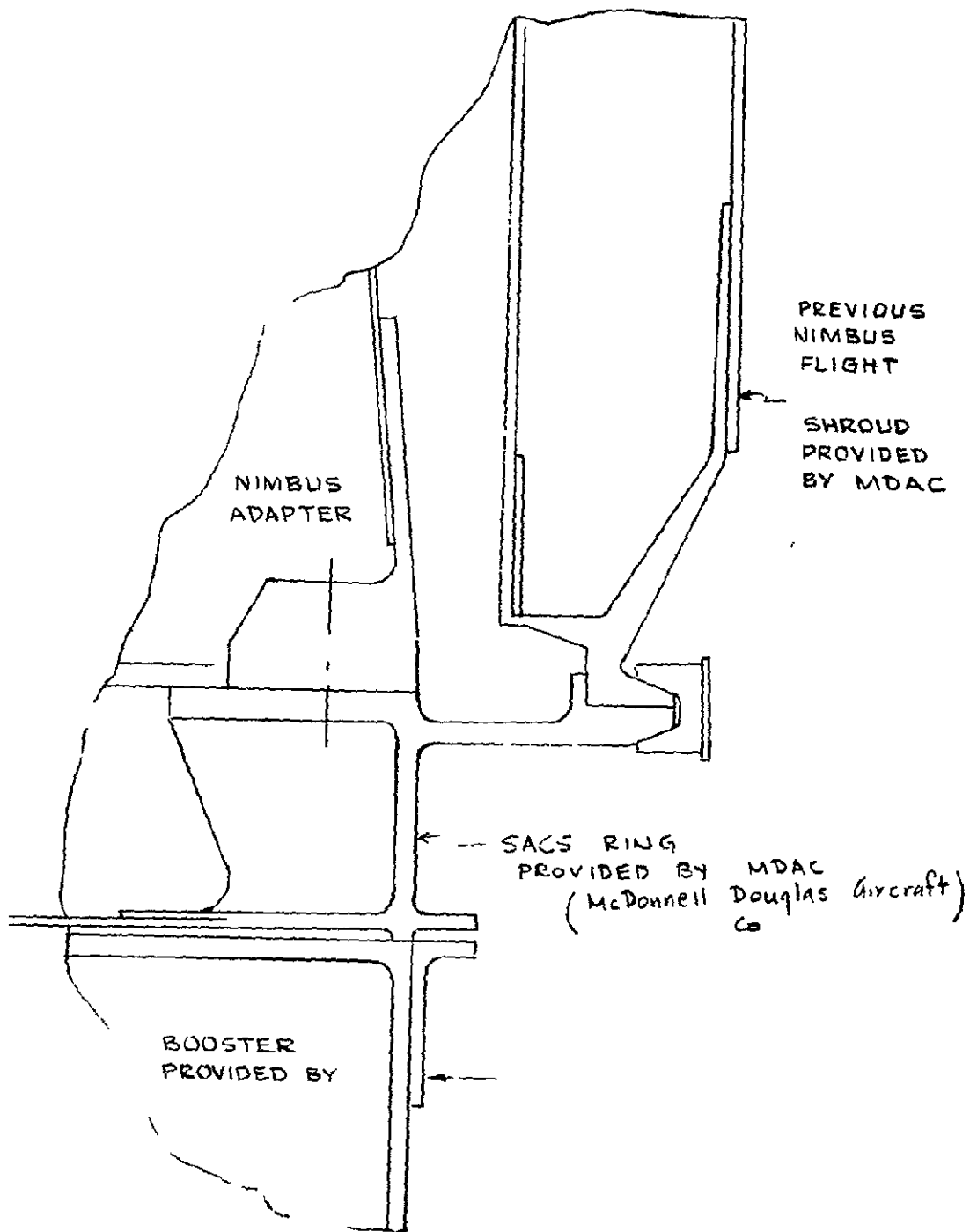


Figure 3.4-2 Delta Modified to Accept SACS Ring



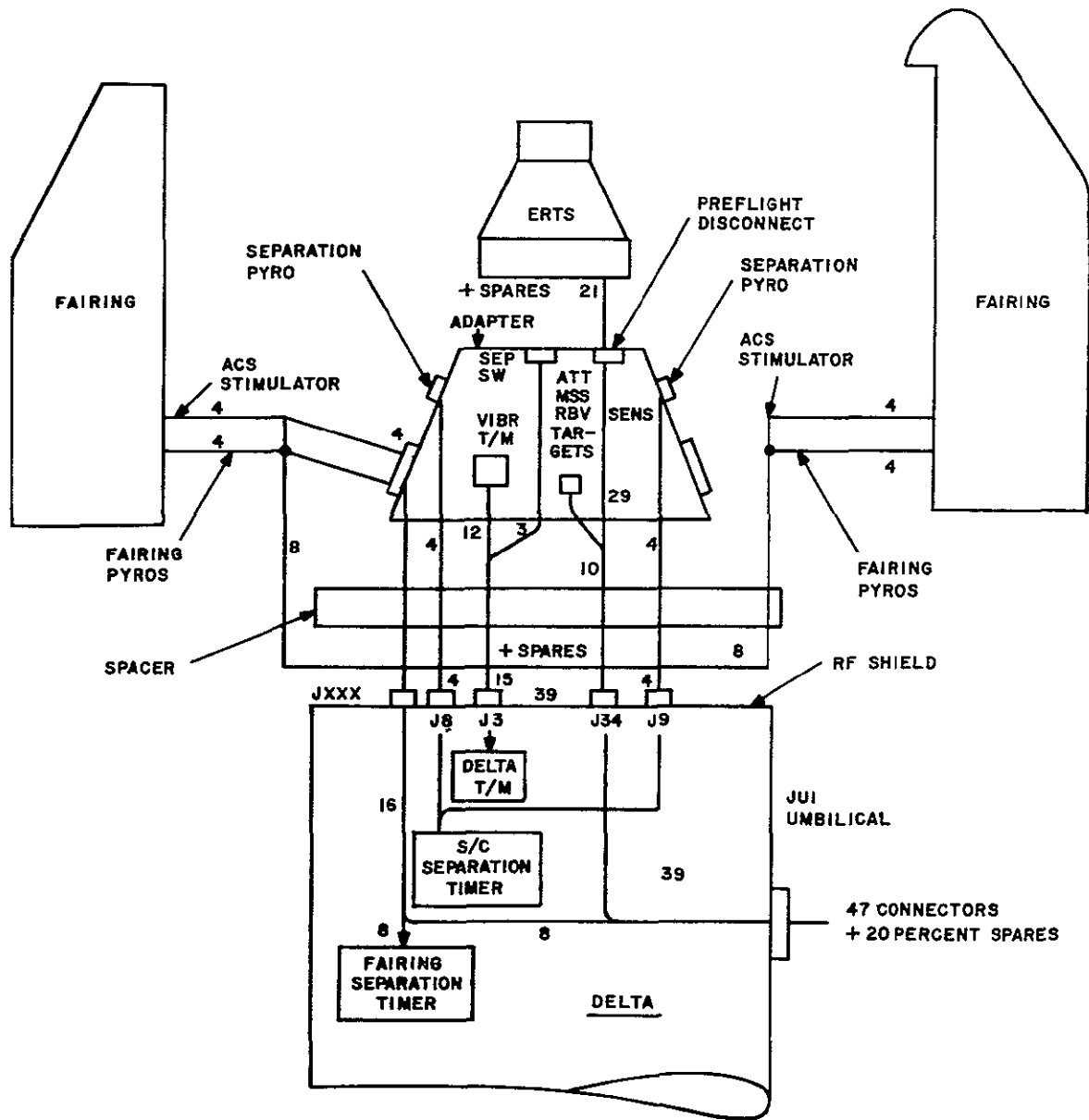


Figure 3.4-3. Interconnection Diagram Delta/ERTS Electrical Interface

Table 3 4-1 Spacecraft Adapter/Delta Connector Functions

Delta Connector Number	Minimum Number of Pins Required	Conductor Functions
J8	4	Power from Delta events timer to spacecraft separation pyros (1/2)
J9	4	Power from Delta events timer to spacecraft separation pyros (1/2)
J3	15 to 23 depending upon shield termination design	5 spacecraft telemetry monitors to Delta telemetry 3 Accelerometers 1 Vibration Sensor 1 Separation-Event Switch
J34	39 + spares	Spacecraft power, T/M & Control functions from Blockhouse & Experiment Target Power
JXXX	8 for ACS Simulators and 8 for Fairing pyros	Blockhouse Power to ACS Stimulators & Delta Events Timer to Fairing separation pyros

Table 3.4-2 Umbilical Pin Assignment Summary

Pins	Assignment
8	<u>Power</u>
	4      Spacecraft Power
	1      Gyro Heater
	2      T/M Power
	1      Unipoint Ground
10	<u>Control</u>
	3      Preflight Disconnect Control
	2      Dump ACS Pneumatics
	1      RMP Emergency OFF
	1      Umbilical Isolate Control
	1      Command Enable Control
	1      Separation Switch OFF Control
	1      All Batteries ON
18	<u>Targets</u>
	8      ACS Horizon Scanners
	2      RBV Cam 1
	2      RBV Cam 2
	2      RBV Cam 3
	2      MSS
	2      Attitude Sensor
11	<u>Telemetry</u>
	5      Preflight Disconnect Position & Voltage Monitor
	2      Spacecraft Voltage Monitor
	1      Gyro Temperature
	1      ACS Manifold Pressure
	2      ACS Tank Pressure & Temperature
47 Total + 20% spares	

11 February 1970

3.4.2.4 Electrical AGE

The electrical AGE required to support Spacecraft Delta electrical compatibility testing are listed in Table 3.4-3. This equipment is similar in all respects to that designed for Nimbus "D." No "new scope" pieces of AGE have been identified.

(Standard modifications to AGE resulting from different connector interfaces will be required.)

3.4.2.5 AGE Location at Launch Complex

Nimbus electrical AGE has historically been located in the Blockhouse and Launch PAD building in order to support launches from SLC-2E. Other than changes in cable length Blockhouse to SLC-2W vs SLC-2E and possible relocation of the Blockhouse Console within the Blockhouse, no other changes are foreseen. Since the distance from Blockhouse to SLC-2W is approximately 800 feet shorter than SLC-2E, no problem with AGE line driving capability should exist.

Table 3 4-3 Electrical AGE Required to Support L/V Compatibility Testing

Item	Function	Location
Blockhouse Console	Supply Spacecraft power & target control	In Blockhouse
Line Resistance Simulator	Simulate Blockhouse to Booster Electrical Line Resistance during equipment checkout	At PAD and Booster Facility
Boltcutter Bridgewire (GFE)	Simulate Spacecraft Separation Pyro Electrical Resistance	At PAD during vertical all systems test At Booster facility during compatibility checkout
AGE Simulator	Simulate Blockhouse Console and ACS Stimulator Control Console	At Booster Facility during compatibility checkout
ACS Stimulator Control Console	Control ACS Stimulators mounted in Faring	In Launch PAD Building
Spacecraft & Adapter Load Simulator	Simulate Spacecraft Electrical Loads and Interface	At Booster Facility during comps. checkout At PAD during Horizontal all systems test
Interconnect Harnesses	Interconnect Spacecraft & Booster Flight hardware and AGE during non-flight configuration testing	At Booster Facility At PAD

### 3 5 GROWTH

#### 3 5 1 GENERAL

Because of the exploratory nature of the ERTS program, payload growth predictions for the future ERTS mission are extremely difficult. Additional knowledge is constantly being obtained from earth resource instrumented aircraft which will provide the answers to such specific questions as what spectral bands are most useful for agricultural mapping, to provide species identification and to provide yield estimates. A scanner with 24 bands will be operated from such aircraft to provide data to aid in making this selection. Questions concerning the utility of multi-frequency, dual polarization, microwave observations for the purpose of assessing sea state hopefully will be answered by ocean overflights. Thermal IR readings versus time-of-day, for various types of soil and varying amounts of moisture are being taken by the Universities of California and Michigan to assess the methods of IR observations for hydrology applications.

Apart from the aircraft earth resources program, considerable knowledge and experience will be obtained from related application spacecraft missions such as Apollo, Nimbus, ITOS, ATS, and of course, ERTS A/B. Missions planned include radiometric sensors for IR mapping and microwave radiometry for passive mapping, as well as a variety of spectrographic and imaging sensors. Many of these sensors and payloads, though not specifically optimized for the ERTS application missions, will enable a more accurate identification of required spatial and spectral resolution, problems of communication and data handling, optimum orbital characteristics, vehicle motion and attitude rates, etc., all of which directly affect designs of future growth payloads. Factors such as these are constantly being studied by NASA, GE, user agencies, and industry. From the assessments of these combined studies the optimum growth payloads will evolve.

#### 3.5 2 GROWTH MISSIONS

The growth area discussed in this section is based on advances in technology projected for the post-ERTS A/B period and is primarily concerned with oceanography. Emphasis has been given to the oceanographic area since it is an important area that is not specifically addressed by the ERTS A/B mission. Because of the importance of oceanographic processes on the natural resources of contiguous land masses, as well as due to their importance in their own right, the ERTS/Oceanographic payload ensemble will be discussed in some detail.

##### 3.5 2 1 ERTS - Oceanographic

The understanding of large-scale oceanographic processes is expected to have a tremendous economic and scientific impact in such diverse areas as weather prediction, shipping, and fishing industries. The study performed by GE for the Marine Council supported this contention. Thus, it is anticipated that a specific ERTS satellite beyond ERTS A/B in the early nineteen-seventies, may be devoted to an oceanographic mission. An appropriate payload for such a mission could consist of an Electrically Scanning Microwave Radiometer similar to the one to be flown on Nimbus E, WISP, a scanner operating in the Thermal IR region, and a data collection system to collect data from specially equipped ships. Each of these payload subsystems, its function, and its operation is described below. A typical Oceanographic ERTS configuration is shown in Figure 3 5-1.

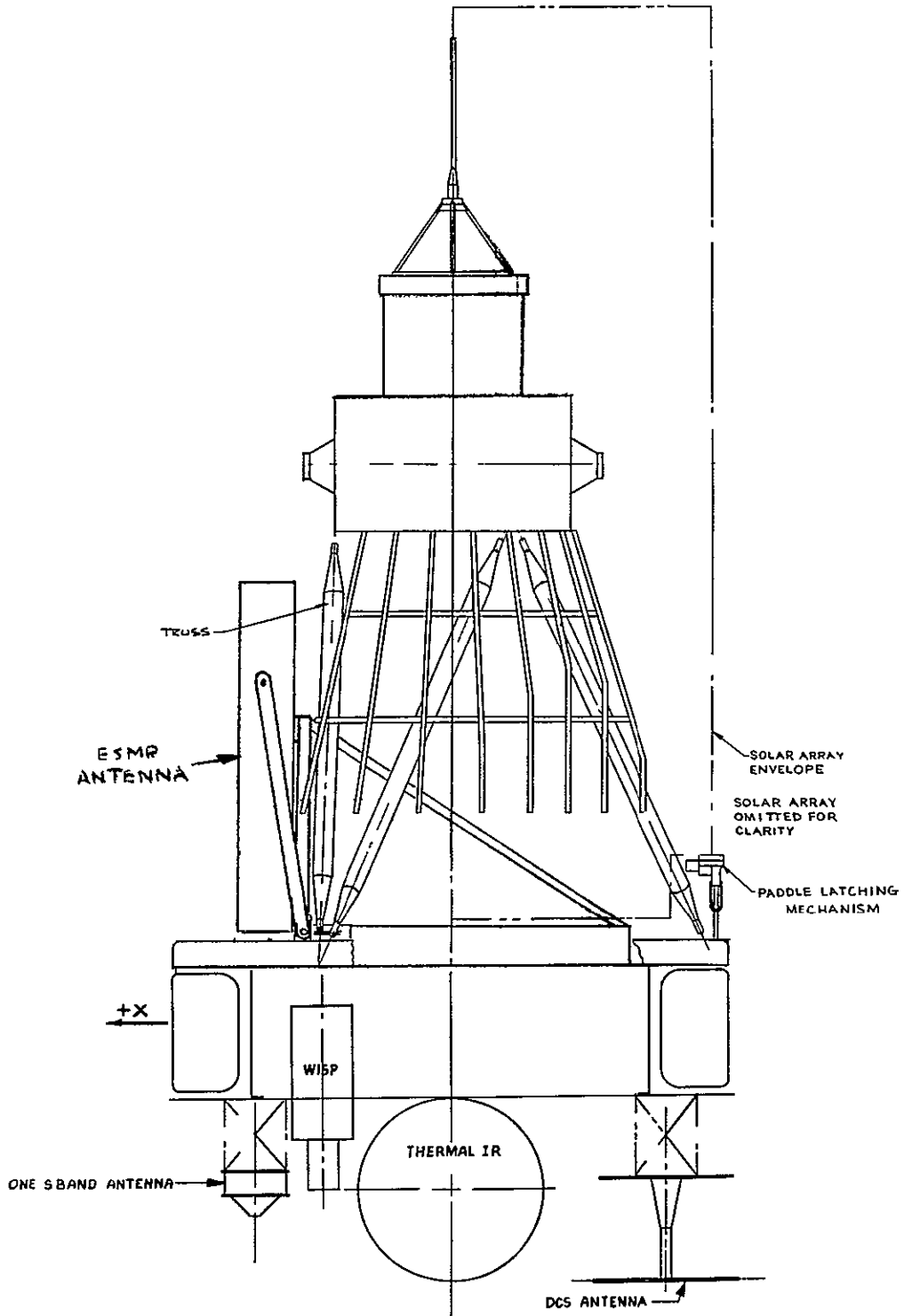


Figure 3 5-1 Oceanographic ERTS Configuration

### Wide-range Image Spectrophotometer (WISP)

The measurement of ocean color has potential applications for the fishing industries. The efficiency of fishing operations would increase considerably, if the search time for productive fishing grounds could be reduced. The forecasting of potentially productive areas hinges on deriving meaningful correlation between environmental conditions and the abundance of fish species. Such environmental conditions are sea temperatures, (as discussed below) and biological activity, which is reflected through the ocean color. Thus, synoptic observation of ocean color, with short response time data analysis, can be applied to identification of good fishing grounds. Monitoring of pollution and assimilation of waste discharged into the ocean are other possible applications.

The sensor selected for this application is WISP. WISP can operate with relatively poor angular resolution. It is this mode of operation where WISP can be a valuable ocean color sensor.

The Wide-range Image Spectrophotometer is a slit camera that has the capability of splitting the image into several regions and selectively scanning these regions.

An objective lens focuses the incident radiation on a narrow slit, which determines the field of view. The narrow dimension of the slit is oriented along the velocity vector and determines the resolution along the ground track. The long dimension is perpendicular to the direction of motion and determines the ground swath width. Radiation passing through the slit is converted into a beam of parallel rays by a collimating lens. A diffraction grating breaks up the beam according to wavelength, with different wavelength components leaving at different angles. Another lens assembly focuses these spectral components on the photosensitive surface of an imaging tube. Each component is focused in a unique location on the tube surface.

Selected regions can be electronically scanned to provide an image of the scene for each spectral band selected. The total number of bands that may be selected is fixed, that is, it is preselected by the sensor design. Selection of individual bands for data transmission may be accomplished by ground command. Thus, for spacecraft application where bandwidths are limited, only those spectral bands of current interest are used.

The overall performance of the WISP is governed largely by the characteristics of the tube selected as the detector. Both the image disector and FPS vidicon have been used to provide a relatively lightweight, low-power-consuming sensor. The sensitivity of the image disector and the spectral response of the FPS vidicon are the salient tube characteristics which limit the WISP performance. Other detectors, such as the image orthicon, could also be used, but with considerably increased weight and power requirements.

### Thermal IR - Sea Surface Temperature and Currents

Oceanographers have a strong interest in measuring the temperatures of the oceans, since the thermal structure is related to all marine processes, including the migration of marine life. Synoptic and repetitive measurement of the oceans temperatures is required and the word repetitive is to be stressed, since the large scale thermal features of the oceans change frequently.



11 February 1970

More specifically, cold upwelling regions are quite often biologically fertile areas and are good fishing grounds. Most of the time the sea current boundaries are characterized by temperature differences. Thus, mapping of ocean currents, which is important to the shipping industry, can be carried out by temperature mapping.

In the thermal IR region, the emissivity of water is very close to unity. Thus, measuring radiation temperatures using an IR scanner is tantamount to measuring actual water temperatures. However, the atmospheric moisture content affects these measurements. Thus, it is proposed to use a two-channel scanner, one with ground resolution of the order of 0.5 mm, in the window band of 10.5 to 12.5 microns, and one with much poorer resolution, measuring in the 7-micron band, the absorption band of water vapor. The concept proposed is similar to that of THIR.

The Temperature Humidity Infrared Radiometer (THIR) is a relatively low resolution scanning radiometer which measures radiation in two IR bands: the "water vapor" band of 6.5 to 7.0 microns and the "window" of 10.5 to 12.5 microns.

The water-vapor channel has a field of view of 21 milliradians, and the atmospheric window channel has a field of view of 7 milliradians. The dynamic range of these channels is 0 to 270°K and 0 to 330°K respectively.

The sensor consists of two units, the scanner and the electronics module. The scanner provides the optical scan motion to produce cross-track scanning with reference to the satellite ground path of the radiometer instantaneous field of view. The scanner consists of the scan drive power supply, motor and mirror, the optical telescope, detectors pre-amplifiers, detector power supply, scan line synchronization pulse generators and amplifiers and housekeeping thermistors.

The electronic module contains the command power switching circuits, a dc-to-dc converter to power the electronics, the logic circuits to provide the signal format, the signal amplifiers, and the thermistor biasing circuits.

#### Electrically Scanning Microwave Radiometer

Data on sea state in all kinds of weather on an ocean-wide basis is of crucial importance to the shipping industry, and also in weather forecasting, since the energy exchange processes between the sea and the atmosphere have a strong influence on the weather.

The optical techniques, such as glitter analysis, are severely limited by the vast cloud cover which is quite prevalent over the marine areas of the earth. Thus, the application of microwave techniques, with its all weather capability, has great attraction.

A variety of observations and analytical studies have demonstrated the practicality of employing microwave sensors to monitor sea state, and also to monitor ice distribution. The oceans in the near polar regions are seasonally or perennially covered with sea ice. Adequate knowledge of the properties, distribution variability and behavior of the sea ice in these areas

is presently lacking. The all-weather information on ice and icebergs, has applications for meteorological services, ice patrols and the shipping industries. Satellite data obtained with the existing meteorological satellites (TIROS, ESSA, Nimbus) are currently used, when available. Microwave radiometry has a great potential here, since the difference in brightness temperature (radiation temperature) between ice and water is very large ( $\sim 100^{\circ}\text{K}$ ). The microwave radiometer measures the radiation temperature of the surface. The electronically scanned antenna sweeps periodically in the direction transverse to the satellite forward velocity. The continuous forward overlay of such successive scans is obtained by the satellite motion.

Except for wavelength, the microwave radiometer will be a copy of that to be flown on Nimbus E. This applies especially to size, weight, configuration, structure and thermal design of the instrument. It consists of a receiver and an electrically scanning phased array antenna operating at a wavelength between 3-5cm. The following components will be contained in the flight instrument in addition to the basic antenna and receiver:

1. Beam steering network
2. Hot and cold calibration temperature sources
3. Data readout
4. Timing and control
5. Power supplies
6. Command

The antenna is perhaps the most critical component of the radiometer. Microwave radiometry of the earth from a satellite can be viewed as a radio-astronomy with one unique distinction. The earth has a roughly uniform temperature and fills nearly an entire hemisphere so that temperature differences of the order of a few degrees must be mapped with relatively high spatial resolution. This is very precise by the current standards of radioastronomy.

The antenna is capable of scanning through an angle of  $\pm 50^{\circ}$  with respect to the nadir and perpendicular to the direction of motion of the satellite. This will permit coverage of a large portion of the earth.

The most important characteristics of the proposed instrument are listed in Table 3.5-1. The 90 by 90 cm antenna requires that a system of deployment be used after satellite orbit is achieved. This system would be identical to the one used for Nimbus E.

#### Oceanographic Data Collection System

For oceanography applications, depth profile data from buoys and surface ships cannot only complement the broad coverage of surface data obtainable by remote sensing from satellites, but can also serve as ground (ocean) truth calibration marks when using satellite data.

Table 3 5-1 Specifications for ERTS Microwave Radiometer

RECEIVER	Central Frequency	10 GHz
	Bandwidth	100 MHz
	Noise Temperature	800°K
	Integration Time	75 millisecc
	$\Delta T_{rms}$	0.6°K
	Absolute Accuracy	2°K
	Dynamic Range	50-330°K
	Dimensions less Antenna	15 by 20 by 32.5 cm Nimbus Module
	Calibration	Sky horn and internal hot blackbody (reference load)
ANTENNA	Type	Two dimensional phased array containing about 55 linear arrays
	Dimensions	90 by 90 by 10 cm
	Resolution	2.7° at 3 dB points broadside
		3.5° at 3 dB points at scan angle of $\pm 50^\circ$
	Loss	1.5 dB
	Polarization	Receives component with electric field parallel to earth's surface at all scan angles
	Sidelobe Contribution	5 percent or less of total received power
	Scan Angle	$\pm 50^\circ$
	Scan Period	3.2 sec
Total Experiment Weight	25 kg	
Total Experiment Power Requirement	25 watts	
Telemetry	10 bit word read each 80 milliseconds Serial readout	

Note (Calculated for 600 km circular orbit, 90 x 90 cm antenna and a 3 cm wavelength)

1. Hydrological Measurements Remote stations will be useful in transmitting data with respect to existing water supply, the quality of ground and surface water, and the advent of flood conditions. Measurements in this category include water stage or stream level, discharge rate, water temperature, evaporation, water content of snow, and precipitation. In addition, the soil conditions of moisture, temperature, and evapotranspiration will be important.
2. Oceanography Water temperature profile, salinity, surface turbulence, etc., are considered standard candidates for the buoy. More specialized measurements include acoustical sound level at selected frequency intervals, biological content of the surface water, and depth soundings. A potentially valuable application that has gained recent interest is the monitoring of ice conditions in sea passages in the Arctic Circle, such as the Amundsen Gulf, in North Canada. Extensive oil deposits in the Arctic region depend on a real-time knowledge of the navigability of those passages for their successful exploitation and thus could benefit from a large network of remote stations.

### 3 5 3 SPACECRAFT GROWTH

#### 3 5 3.1 General

Increasing demands on the spacecraft's supporting subsystems by the various sensor configurations have led to studies in areas such as power, attitude control, structure (for more viewing area), and communications. The results of these studies will be discussed in the following paragraphs.

#### 3 5 3 2 Power

The introduction of additional sensors and the use of high power consuming data systems requires an increase in the available electrical power. Increased power may also be required because of more sustained payload operation.

The Bi-fold Advanced Solar Array considered for Nimbus by NASA/GSFC presents an approach that is directly applicable to growth ERTS spacecraft. Figure 3 5-2 shows a photograph of the engineering model of these solar-array paddles attached to a Nimbus spacecraft model.

A bi-fold solar array version of ERTS is a logical extension of the basic Nimbus configuration. The obvious modification is the array, each half of which contains an additional panel that is stowed by folding it against the main panel. Due to the extra weight of the additional panel, local structural "beef-ups" will be necessary. These include increasing the truss tube size and strengthening the latch mechanism.

An engineering model of bi-fold panels was designed, fabricated and tested by Fairchild-Hiller Corporation, with no failure. Another similar design was prepared by GE. Either version appears suitable for an ERTS growth application. The electrical power considerations were studied by RCA Corporation\* and GE.

---

\*Study of Power Supply Configurations for Advanced Nimbus Missions, RCA-AED  
Report No. R-3431, (Contract No. NAS5-11549)

11 February 1970

(This page left blank intentionally )

Figure 3 5 2

Figure 3.5-3 is a plan view of the bi-fold paddle showing a possible 94-series cell string layout on the auxiliary platform. The corresponding nominal case, beginning-of-life, bi-fold current voltage curves at three temperatures are shown in Figure 3.5-4. The bi-fold array increases the array power capacity by 84 percent

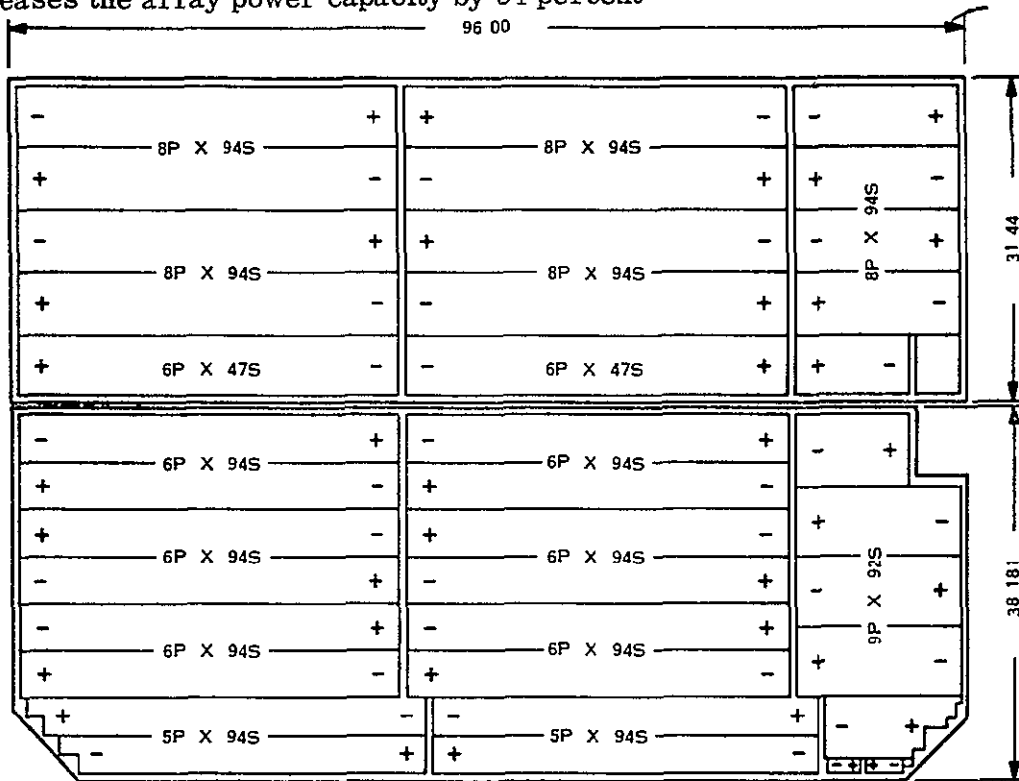


Figure 3.5-3. Typical Solar Cell Layout on Bi-Fold Paddles

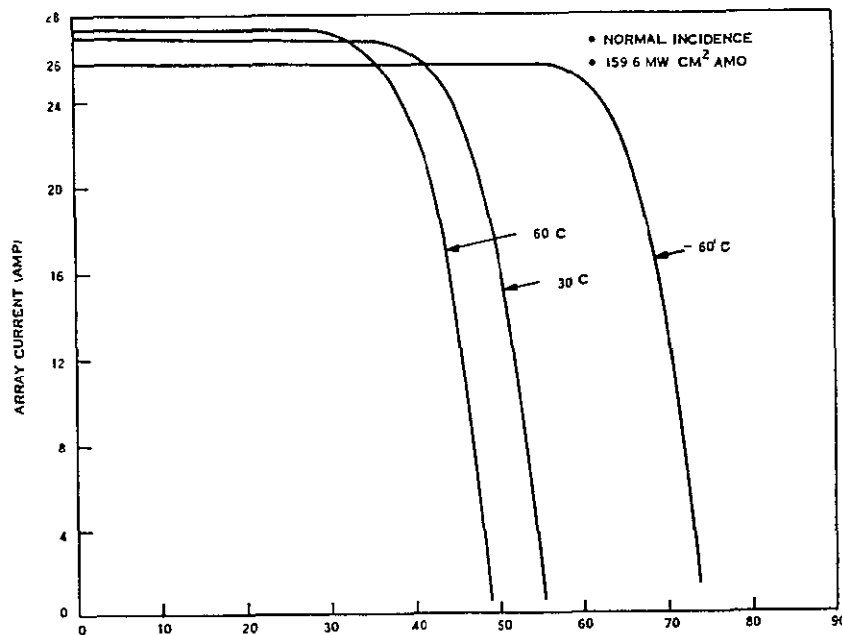


Figure 3.5-4. Solar Array I-V Curves, Nominal Case, Beginning of Life

### 3 5 3 3 Attitude Control

The ERTS attitude control system was evaluated for its ability to control a 3000 pound, 9-foot diameter advance earth resources satellite. The size and weight of this version were based on the maximum size and weight capability, of the Atlas/Centaur launch vehicle. This spacecraft was considered to have the basic ERTS orbital parameters and configuration while incorporating advanced bi-fold-solar paddles and a nine-foot diameter sensory ring.

The study results indicated that, with the exception of control of the yaw axis, the ERTS attitude control system can control a vehicle of this size to less than  $\pm 1^\circ$  in pitch and roll. Because of the increased yaw inertia of this configuration, the yaw flywheel inertia must be increased by a factor of three to avoid cyclic disturbances by the pneumatic gating threshold at a frequency which could quickly deplete the available gas supply. With this modification, the pointing error in this axis should remain below  $1^\circ$ . Another modification which is required involves the canting of the roll nozzles to avoid plume impingement on solar panels.

### 3 5 3 4 Structure/Configuration

A spacecraft configuration study was made to investigate and evaluate concepts of ring design and the ring/adapter/fairing interfaces for a nine-foot diameter ERTS spacecraft.

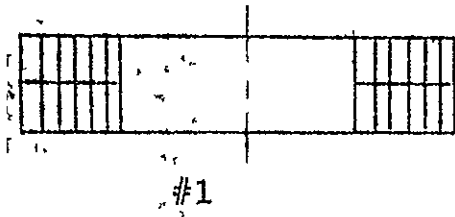
Figure 3 5-5 shows four different ring configurations studied. Table 3 5-2 lists the capacity of each of these configurations in terms of bays and total number of 1/0 type modules (i.e., 6 x 2 x 6.5 inches) the particular configuration can hold. The last column refers to the number of 1/0 modules which can be accommodated between the inner radius and the outer radius of the sensory ring, which is known as the inboard depth.

Table 3 5-2 Module Capacity

Configuration Number	Total Modules	Bays	No of Modules, Inboard Depth
Existing	144	18	4
1	324	27	6
2	360	18	4
		27	4
3	330	33	5
4	336	42	4

All of these configurations are a simple ring except Number 2 which is a "wedding cake" design using the existing ring as the top layer.

Structurally Configuration 1 is regarded as superior since the crossbeam span is less than for Configurations 3 and 4 and the truss attachment points are only a few inches inboard of



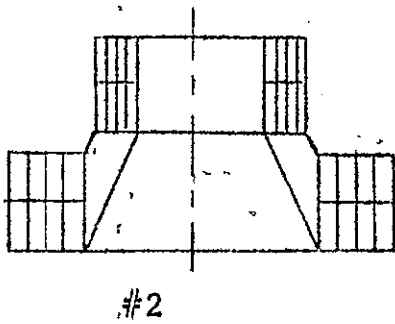
27 bays 6/6

324 total 1/0 spaces

I.R. = 30"

O.R. = 42"

} neglecting  
structure



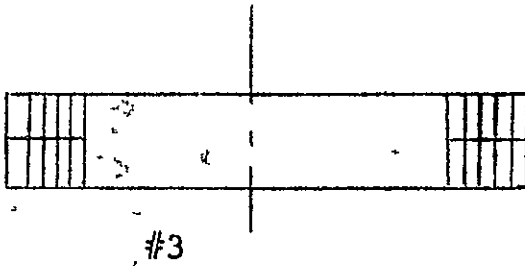
18 bays 4/4

& 27 bays 4/4

360 total 1/0 spaces

I.R. = 19.9"

O.R. = 38.0"

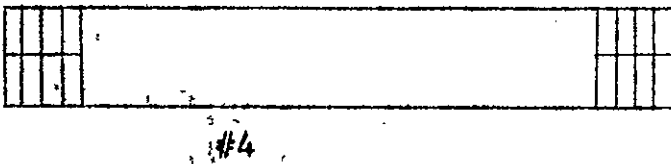


33 bays 5/5

330 total 1/0 spaces

I.R. = 36.7"

O.R. = 46.7"



42 bays 4/4

336 total 1/0 spaces

I.R. = 46.80"

O.R. = 54.80"

NOTE: I.R. = Inner Radius  
O.R. = Outer Radius

Figure 3.5-5. Conceptual Sensory Ring Configurations



the sensory ring It is structurally desirable to have as small a distance as possible from these truss attachment points to the separation flange at the lower outside edge of the sensory ring, since this is a primary load path for several major loading conditions Thermally, Configuration No 3 is the best, but No 1 can be modified to provide the needed additional thermal dissipation

Overall, Configuration No 1 was judged the best choice as a growth configuration, with No 3 rated as second choice The factors leading to this judgment are summarized in Table 3 5-3

Table 3 5-3

Configuration Number	Pro	Con
1	Simple ring adequate space for sensors-truss points close to ring lowest weight	Outboard web extensions and radiator required
2	Lowest inertias - more than adequate thermal dissipation	More complex, heavier ring crossbeam area quite crowded, sensor mounting difficult, somewhat short of sensor mounting area  More structural elements than computer can handle.
3	Simple ring best thermal match-ample space for sensors	Ring too far from truss, crossbeam more flexible
4	Simple ring - excess space for sensors	Ring furthest from truss points Crossbeam, not ring, is primary structure  Tight shroud clearance

3 5 3 5 Communications/Data Relay

The data requirements of earth observation satellites have continuously grown and, with the advent of the Earth Resources Program, will soon exceed the data capacity of existing and contemplated storage devices The gathering of such large amounts of data results in the need for either more dedicated ground stations or continuous real-time data relay to the ground via a synchronous data relay satellite system. The latter approach eases or eliminates the storage requirement In addition, the ability to have real-time command and control of the experiments and spacecraft subsystems can significantly improve the performance of the spacecraft in meeting the mission requirements

The main advantages of the use of a synchronous satellite relay link for transmission of ERTS wideband sensor signals (RBV and/or MSS) include the following

1. A continuous link is provided so that on-board recording of wideband sensor signals is not required (The WBVTR is considered the weakest link in the present wideband sensor subsystem of ERTS.)
2. Because of the continuous link, more data could be returned during a given mission life.
3. The elimination of the WBVTR should result in improved quality of the received wideband signals.

For proper viewing of the relay satellite the ERTS relay link antenna must be capable of coverage over all portions of a sphere except that portion bonded by the earth's horizon. This coverage may be stated as an elevation angle of  $120^{\circ}$  and azimuth of  $360^{\circ}$ . Elevation is measured from the yaw axis, azimuth in a plane perpendicular to this axis. The variation of these two angles during a two-day period is shown in Figure 3 5-6. Comparable angles for a pitch-roll gimbal can be calculated.

Figure 3 5-7 is a block diagram showing the elements of the ERTS to DRS link. The relay unique equipment is shown in dotted lines. The output of the wideband sensor will be sampled and encoded by the Data Encoder. The encoder output is used to drive the modulator, which, in turn, modulates the X-band TWT RF amplifier. The modulation format tentatively selected is PCM-PM for the sensors. The ERTS antenna is coarsely pointed by pre-programmed commands, and, through the use of a monopulse acquisition and tracking system, will acquire and track the DRS via the beacon signal transmitted from the DRS.

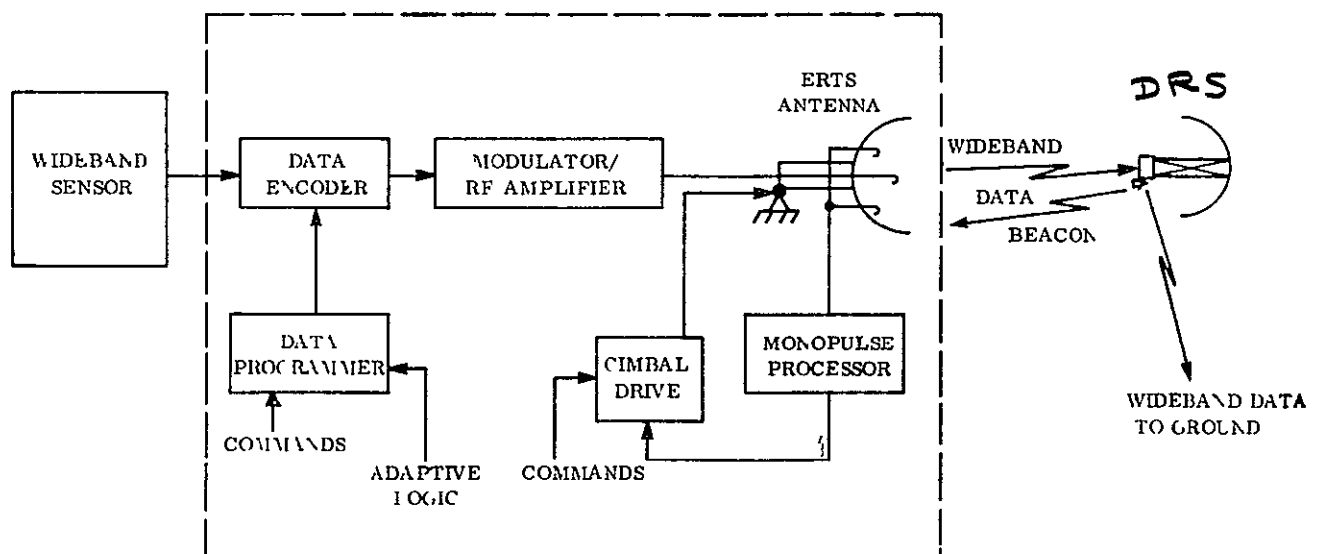


Figure 3. 5-7 System Block Diagram

Table 3.5-4 shows the link calculations for three ERTS high-gain antenna sizes 2-, 3-, and 4.5-feet in diameter. The results are plotted in Figure 3 5-8 to show the variation of  $S/N_0$ , at the ground receiver, with the ERTS antenna diameter as the variable, this was done for two values of DRS G/T. The lower curve is for a G/T of +16 dB, while the other curve is for a G/T of +20 dB, this is to show the effect the G/T of the DRS system has on the antenna size required for ERTS.

The  $C/N_0$  required for each of the two ERTS sensors considered is shown for two different error rates (1)  $P_e = 4 \times 10^{-6}$  and (2)  $P_e = 10^{-4}$ . Figure 3 5-8 shows that to transmit the MSS data during the times of mutual visibility between ERTS and DRS, an antenna with a diameter of about 2.5 to 3.0 feet (with a 20-watt transmitter) is required. To relay the RBVC data, however, requires the use of an antenna between 3.5 and 4.5 feet. This is with a G/T of +16 dB. \* Considering a G/T of +20 dB reduces the antenna sizes to 1.5 to 2.0 feet for MSS data and about 2.2 to 2.6 feet for RBVC data.

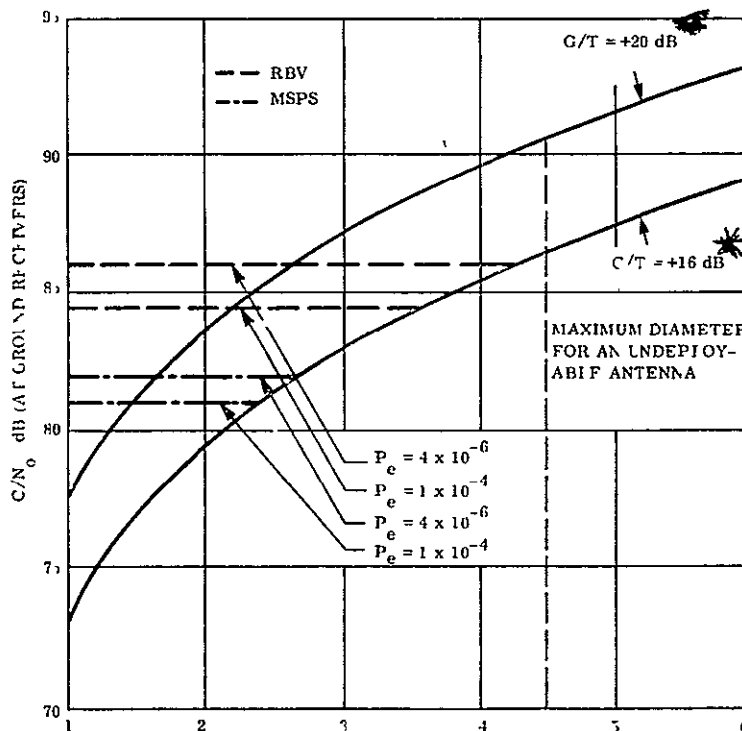


Figure 3 5-8 Carrier-to-Noise Spectral Density Versus Antenna Diameter

### 3.5.4 GROWTH POWER SYSTEMS

The feasibility of using Radioisotope Thermoelectric Generators (RTG's) as power sources on orbiting spacecraft was demonstrated on Nimbus III. The two RTG's used were SNAP-19's which are capable of supplying 25 watts each. However, in order to power the entire spacecraft subsystems as well as the sensor payloads the development of larger units will be required. This development is currently underway and will result in the design of an RTG with modular growth capacity. This unit is known as the Multi-Hundred Watt RTG (MHW-RTG).

\*ATS F/G characteristics assumed.

Table 3 5-4. ERTS to DRS Link Calculations

Item	2.0-Foot Parabola	3.0-Foot Parabola	4.5-Foot Parabola
$P_T$ , ERTS transmitter power	+13 dBw	+13 dBw	+13 dBw
$G_T$ , ERTS antenna gain	+31.5 dB	+35 dB	+38.5 dB
$L_T$ , ERTS transmission losses	<u>-1.0 dB</u>	<u>-1.0 dB</u>	<u>-1.0 dB</u>
EIRP, effective isotropic radiated power	+43.5 dBw	+47.0 dBw	+50.5 dBw
Path Loss = $-37.8 - 20 \log D$ $-20 \log F$ , $D = 24,600 \text{ nm}$ $F = 8.0 \text{ GHz}$	-203.6 dB	-203.6 dB	-203.6 dB
Polarization loss*	-3.0 dB	-3.0 dB	-3.0 dB
Pointing loss	-1.0 dB	-1.0 dB	-1.0 dB
Atmospheric loss	<u>-1.0 dB</u>	<u>-1.0 dB</u>	<u>-1.0 dB</u>
Link loss	-208.6 dB	-208.6 dB	-208.6 dB
$G/T$ , overall gain to equiva- lent temperature ratio at 8.0 GHz	+16 dB	+16 dB	+16 dB
K, Boltzman's Constant	-228.6 dB	-228.6 dB	-228.6 dB
$C/N_o$	+79.5 dB	+83.0 dB	+86.5 dB

Table 3.5-4. ERTS to DRS Link Calculations (Cont'd)

	2.0-Foot Parabola	3.0-Foot Parabola	4.5-Foot Parabola
$P_T$ , ERTS transmitter power	+13 dBw	+13 dBw	+13 dBw
$G_T$ , ERTS antenna gain	+31.5 dB	+35 dB	+38.5 dB
$L_T$ , ERTS transmission losses	<u>-1.0 dB</u>	<u>-1.0 dB</u>	<u>-1.0 dB</u>
EIRP, effective isotropic radiated power	+43.5 dBw	+47.0 dBw	+50.5 dBw
Path Loss = $-37.8 - 20 \log D$ $-20 \log F$ , $D = 24,600 \text{ nm}$ $F = 8.0 \text{ GHz}$	-203.6 dB	-203.6 dB	-203.6 dB
Polarization loss*	-3.0 dB	-3.0 dB	-3.0 dB
Pointing loss	-1.0 dB	-1.0 dB	-1.0 dB
Atmospheric loss	<u>-1.0 dB</u>	<u>-1.0 dB</u>	<u>-1.0 dB</u>
Link loss	-208.6 dB	-208.6 dB	-208.6 dB
$G/T$ , overall gain to equivalent temperature ratio at 8.0 GHz using the 30-foot parabola	+16 dB	+16 dB	+16 dB
$K$ , Boltzman's Constant	-228.6 dB	-228.6 dB	-228.6 dB
$C/N_o$	+79.5 dB	+83.0 dB	+86.5 dB

\*3.0-dB polarization loss due to the linear feed of ATS F&G 30-foot paraboloid. An improvement in link performance of up to 3.0-dB can be obtained by providing a circularly polarized X-band feed to the ATS-G feed system.

11 February 1970

The Multi-Hundred Watt Radioisotope Thermoelectric Generator (MHW-RTG) is being developed by the General Electric Company for the Atomic Energy Commission. The MHW-RTG design is currently in Phase I and the performance characteristics are therefore not final but may be considered to be representative of the generator which is anticipated for flight in the post 1973 time period.

An artist's conception of the MHW is shown in Figure 3 5-9 identifying the component parts. The MHW is basically two 1,000 watt cylindrical heat sources supported on a common centerline and surrounded by 12 thermoelectric panels arrayed to form a hexagonal prism.

The 144 watt, 30 volts reference design generator can be increased in power to approximately 216 watts with the addition of another 1,000 watt heat source and a proportionate increase in thermoelectric panels.

Minor variations in output power can be made by adjusting the number of thermoelectric panels and/or heat source fuel loading. The design characteristics are given in Table 3 5-5.

Table 3 5-5 Summary of MHW-RTG Reference Design Characteristics

<u>PERFORMANCE</u>		<u>CONVERTER</u> (Continued)	
Power	114 watts BOM 178 watts after 1 year 111 watts EOM (12 years)	Thermoelectric Couples	
Voltage	30 Vdc	Number	288 (Series-Parallel)
Fuel Loading	2000 watts (2-1000 watt heat sources)	Material	SiC (#07 Silicon)
Weight	9.7 lb	Leg Dimensions	N-leg 0.8 in long, by 0.0188 in <sup>2</sup> P-leg 0.8 in long, by 0.0208 in <sup>2</sup>
T <sub>hot</sub> junction	1100°C (2012°F) BOM	Hot Spots	SiMo
T <sub>cold</sub> junction	61.9°F BOM	Number of Panels	12 - 24 Couples/Panel
Conversion Efficiency	7.2% BOM	Insulation	Inde-Tyax Foli
Specific Power	2.11 watts/lb	Heat Source Cavity	Slid for 6.06 in dia Heat Source
<u>GEOMETRY</u>		<u>HEAT SOURCE</u>	
Diameter	11.85 in across diagonals (max)	Quantity	Two
Length	20.0 in	Fuel	Pu-238 Solid Solution Ceramic
Configuration	6-sided structure no fins	Geometry	4.0 in dia X 8.26 in long
<u>CONVERTER</u>		Installation in Converter	In-line Heat Source Axial Preload
End Closures	Spoked Titanium	Materials	TZM Liner WC 3015 or TZM Impact Shell Pyrolytic Graphite Insulation WC 3015 Outer Shell
Load Structures	6 Titanium Longerons	On Pad Cooling	Water 10 ft/sec 1/4 in Tubes Welded to Cladding Separate Loop for Each Heat Source
Radiators	Beryllium - Iron Titanate Coating c > 0.85	Vented	Yes

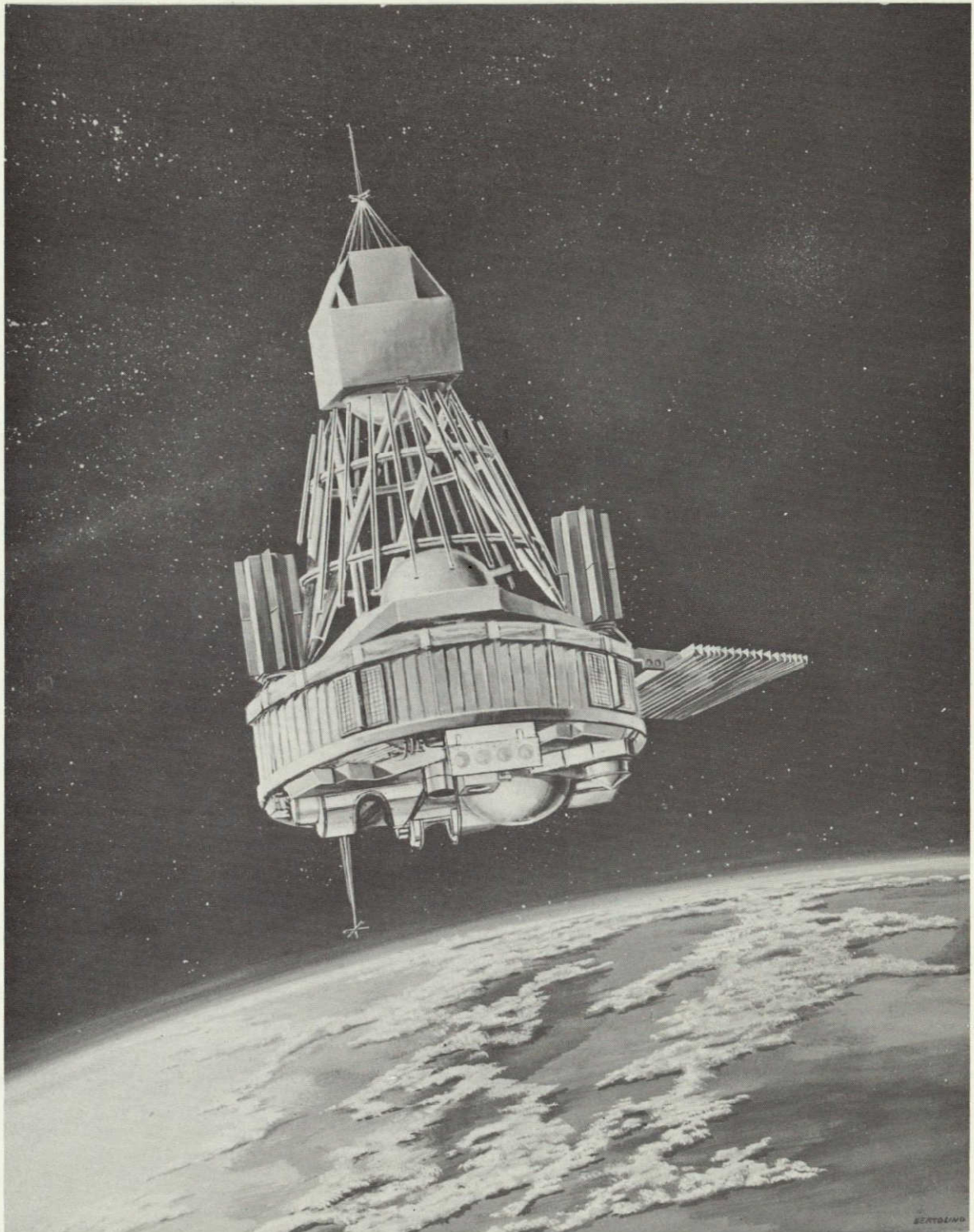


Figure 3.5-9. Multi-Hundred Watt Radioisotope Thermoelectric Generator

A major advantage of the MHW-RTG for the ERTS mission is the modular flexibility of the MHW-RTG to supply power to the vehicle in increments of 144 watts, thereby allowing a considerable degree of flexibility in the design of the experiments. An artist's concept of the MHW-RTG in a finned geometry configuration is shown in Figure 3.5-10. Two generators would be providing 288 watts total electrical power at the beginning of the mission in this configuration.

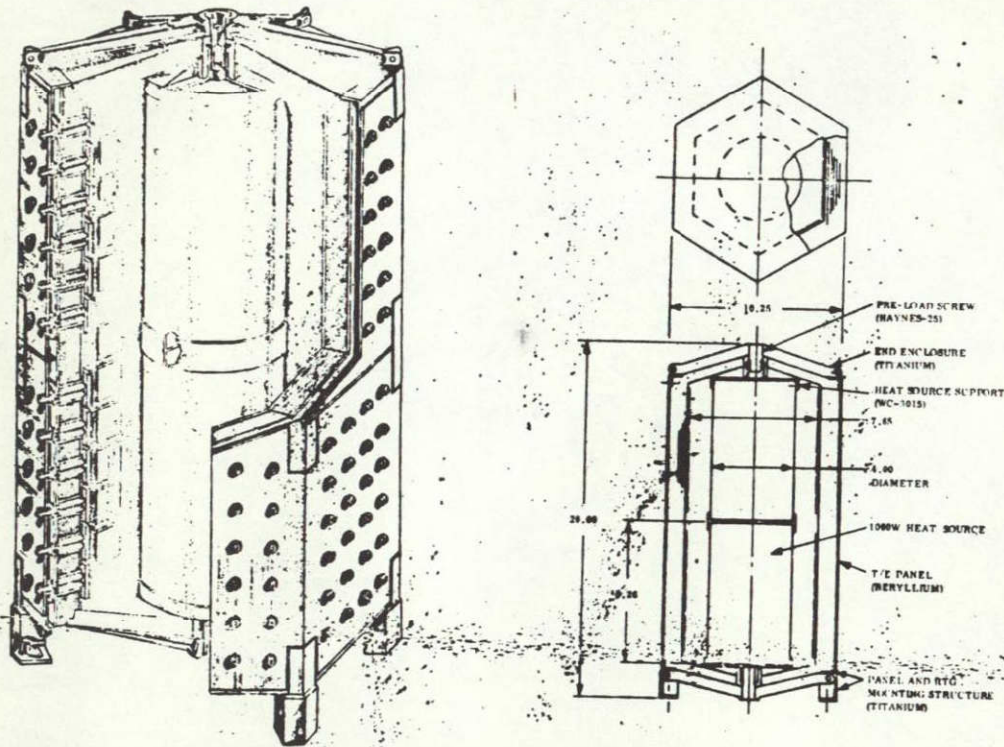


Figure 3.5-10. Multi-Hundred Watt Radioisotope Thermoelectric Generator in Finned Geometry Configuration

By examining the ERTS launch configuration, it is clear that the largest volume available for a parabolic dish antenna is located above the attitude control system. A layout was prepared (Figure 3.5-11) which indicates that a 54-inch diameter dish could be accommodated. It would be pointed by means of a two-axis gimbal, which, for conservatism, was assumed to be as large as the unit used in the Apollo command module. In order that the antenna beam clear the solar array at all times, it would be necessary to extend the entire assembly some 7.5 feet. In order to survive the launch environment, the gimbal and antenna will be latched to the spacecraft to minimize vibrational effects until orbit is achieved and then deployed.

### 3.5.5 ALTERNATE ORBITS

The ERTS Attitude Control System can operate effectively at orbit altitude between 300 and 2000 nm and at eccentricities between 0 and 0.15. This has been shown in many studies of this subsystem. It has also been evaluated as a function of ascending node time, ranging



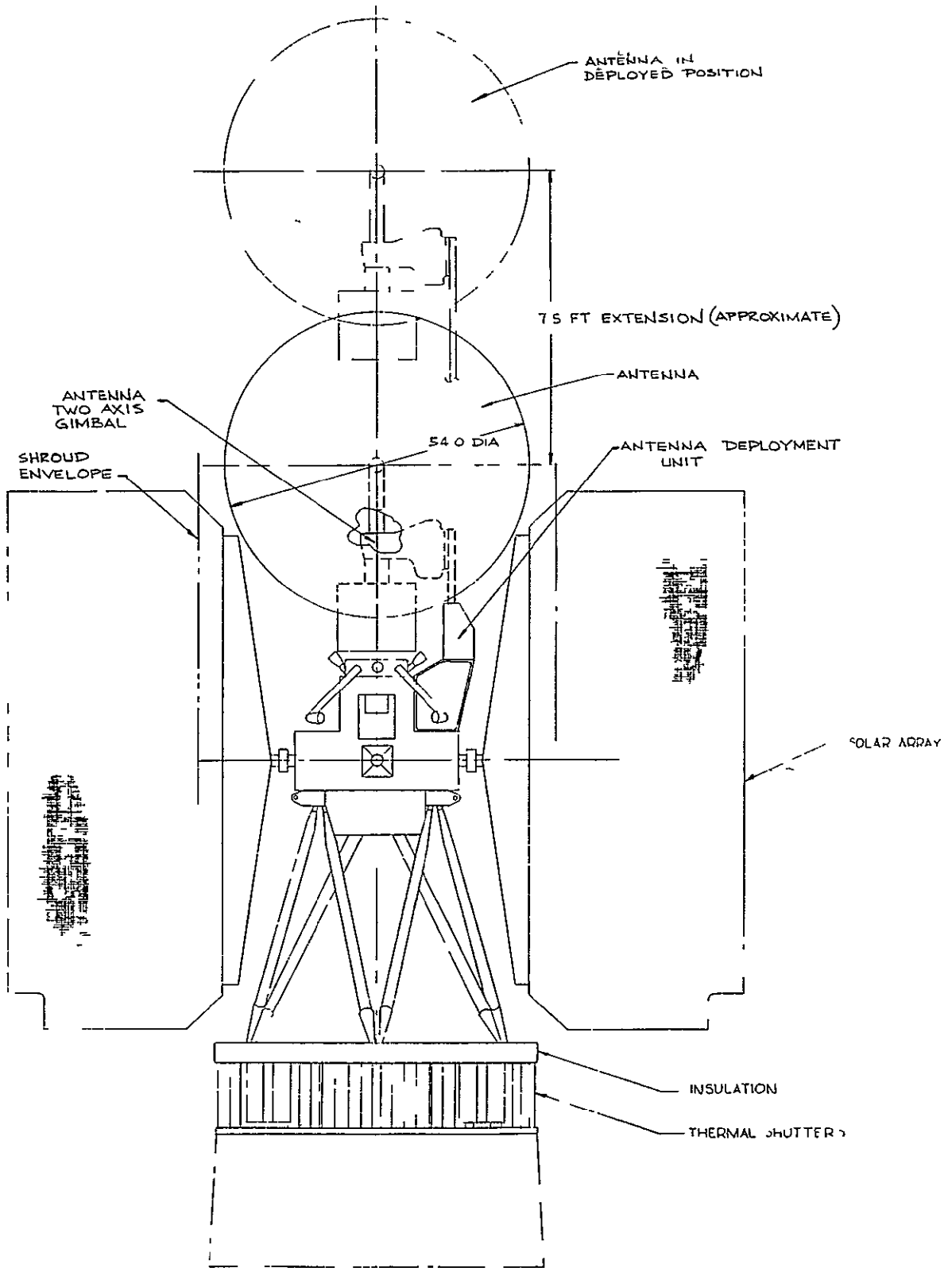


Figure 3 5-11 ERTS Relay Antenna Concept

11 February 1970

from mid-morning to high noon (Nimbus orbit) through mid-evening (ERTS A/B). To complete the cycle, a study was performed on the feasibility of operating this subsystem in a twilight orbit (6 AM - 6 PM). This orbit has the same altitude, inclination and launch direction as a high-noon orbit. The twilight orbit provides the opportunity to operate with a fixed solar array. The angle between the sunline and the surface of the solar array (commonly called the beta angle) then becomes a function of the orbit inclination and the time of year. This is illustrated in Figure 3.5-12. The array is located so that its sensitive surface is in the orbit plane.

This orbit offers the additional advantages of

1. Reducing the number of battery modules required.
2. Reducing the number of thermal shutters needed.
3. Eliminating the need for the solar array drive.
4. Maximizing the solar array power output.
5. Improving system reliability.
6. Reducing spacecraft weight.

The disadvantages are that there is no pitch momentum bias mode (which is a back-up mode not essential), and there may be some impact on experiment design.

The study results indicated that the ERTS spacecraft can easily fly in a twilight orbit, thus proving the extreme versatility of the vehicle.

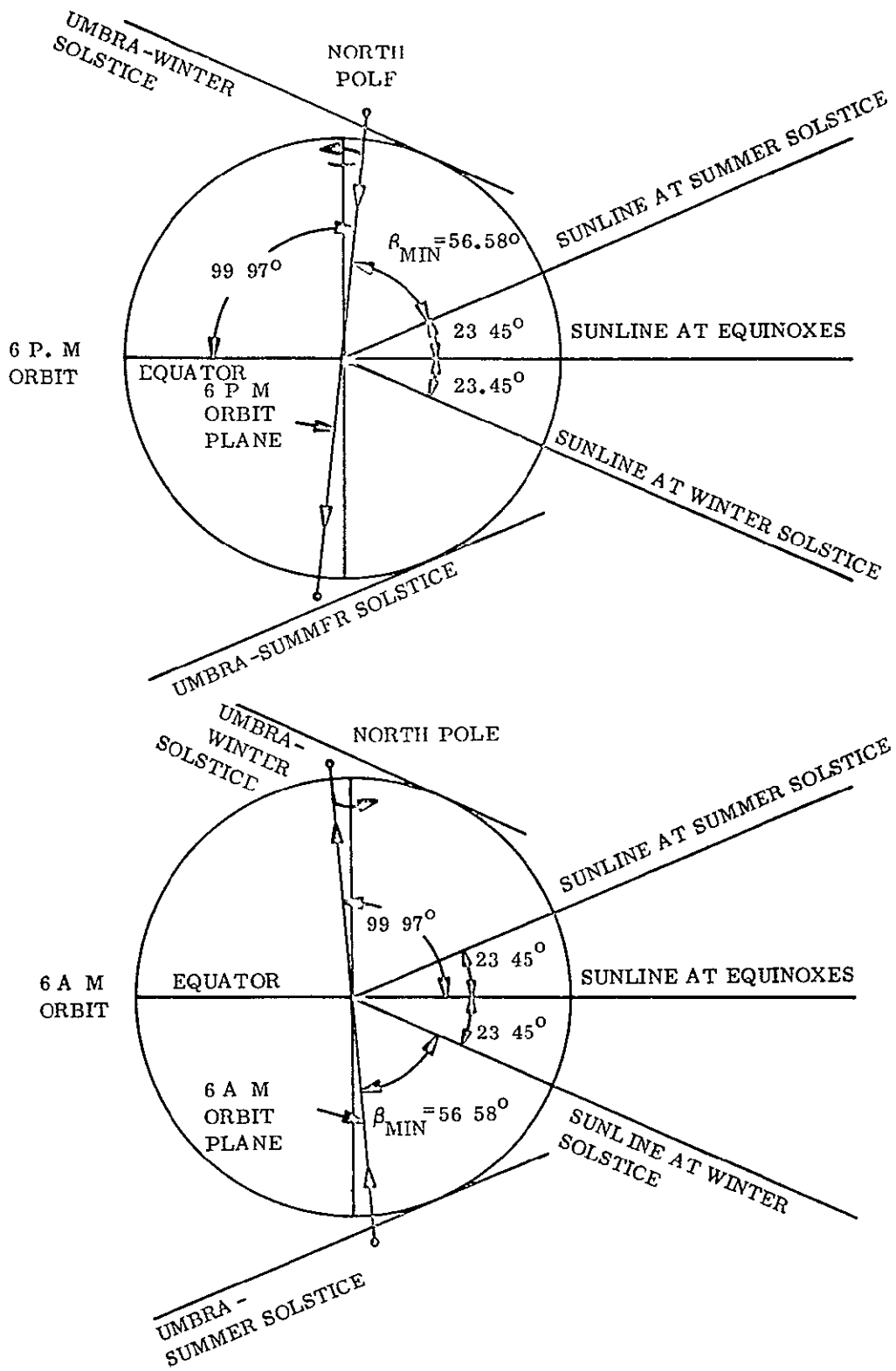


Figure 3 5-12 Twilight Orbits

# SECTION 4

## SYSTEM STUDIES

4.1	ERTS System Reliability . . . . .	4-2
	4.1.1 Summary . . . . .	4-2
	4.1.2 Principles of Reliability Assessment . . . . .	4-5
	4.1.3 Source of Failure Rate Data . . . . .	4-5
	4.1.4 Subsystem Reliability Assessments . . . . .	4-6
4.2	Orbit Analysis . . . . .	4-21
	4.2.1 Introduction . . . . .	4-21
	4.2.2 Nominal Orbit Selection . . . . .	4-22
	4.2.3 Drag Decay . . . . .	4-28
	4.2.4 Nominal Ground Track Control . . . . .	4-32
	4.2.5 Orbit Error Analysis . . . . .	4-35
	4.2.6 Operational Ground Track Control . . . . .	4-43
	4.2.7 Launch Window Analysis . . . . .	4-48
4.3	Image Location and Coverage . . . . .	4-75
	4.3.1 General . . . . .	4-75
	4.3.2 Units . . . . .	4-76
	4.3.3 Gains . . . . .	4-76
	4.3.4 Implementation and Relative Error Effects . . . . .	4-78
	4.3.5 First-Order Error Equation, Its Solution, and Attitude Determination Sensor Requirements . . . . .	4-79
	4.3.6 Basic Coverage . . . . .	4-82
	4.3.7 Rate Requirements . . . . .	4-86
	4.3.8 Requirements Summary . . . . .	4-91
4.4	Time Annotation . . . . .	4-92
	4.4.1 General . . . . .	4-92
	4.4.2 Approaches to Time Annotation . . . . .	4-94
	4.4.3 Discussion of Approaches . . . . .	4-95
	4.4.4 Baseline Approach . . . . .	4-98
4.5	Mission Simulation . . . . .	4-100
	4.5.1 Simulation Problem (Introduction) . . . . .	4-100
	4.5.2 Simulation Model . . . . .	4-100
	4.5.3 Simulation Cases . . . . .	4-104
	4.5.4 Specific Study Results . . . . .	4-109
4.6	Wideband Video Tape Recorders Management . . . . .	4-137
	4.6.1 Recorder Management . . . . .	4-137
	4.6.2 Tape Handling Requirements . . . . .	4-140
	4.6.3 Design Approach . . . . .	4-142

SECTION 4  
SYSTEM STUDIES

As part of the three-month ERTS Phase B/C SSD study numerous overall system and mission analyses and trade studies have been performed. These studies impact the evolution of the selected spacecraft design and operational concepts as well as other ERTS system elements. Several of these study areas are being continued and extended in support of the ongoing ground data handling system design. This section reports the results of those studies affecting the spacecraft system design. They are presented in the following groupings

1. Spacecraft Reliability Assessment
2. Orbit Analysis
3. Image Location and Coverage
4. Time Annotation
5. Mission Simulation
6. WBVTR Management

The reliability assessment examined the individual spacecraft subsystem designs proposed for ERTS A/B and arrived at the overall spacecraft reliability for a one year mission. This assessment was, of course, enhanced through the extensive use of redundancy in the proposed system design.

The orbit analyses performed have established the requirements for the spacecraft orbit adjust subsystem in terms of its functional capability, sizing and operational features. Also, the operational requirements and procedures have been developed for the establishment and maintenance of ground track control.

Image location requirements have been analyzed in order to arrive at the system error allocations and, in turn, these allocations reflected as requirements on the spacecraft and ground systems for attitude sensing and time correlation. Attitude control requirements, although specified by the government, have also been reviewed to assure consistency with the mission coverage requirements.

Several approaches to the time annotation of data collected by individual sensors and subsystems have been traded-off in order to select a system approach which will achieve the time correlation required for overall system operation.

Extensive mission simulations have been performed in order to fully understand the overall system operation, to establish design requirements, and to evaluate the capability of the proposed designs. These simulations have, for example, been used to produce worst-case power profiles for sizing the power system and for worst-case operational sequences to establish stored requirements.

The problems in operational management of the spacecraft Wideband Video Tape Recorders (WBVTR's) have been investigated and the requirements for recorder status and control established. These requirements dictate the spacecraft functional capability for effective orbital operations.

#### 4.1 ERTS SYSTEM RELIABILITY

##### 4.1.1 SUMMARY

All subsystems except for the payload were analyzed to assess the reliability of the ERTS spacecraft. For each subsystem reliability is defined as the probability that the subsystem will operate for one year without degradation affecting the ERTS mission. These subsystems and their reliabilities R are

Attitude Control	- R = .815
Electrical Integration	- R = .962
Orbit Adjust	- R = .992
Power	- R = .959
Structures	- R = .999+
C. &D. H	- R = .945

The overall system reliability is the product of these subsystem reliabilities It is

$$R_{\text{ERTS}} = .71$$

##### 4.1.1.1 ERTS System Reliability

A simplified reliability block diagram for the ERTS system is given in Figure 4 1-1. It shows the major blocks within each subsystem. Many of these blocks contain internal redundancy. Reliabilities shown are for a one year mission.

##### 4.1.1.2 Redundancy

Redundancy is widely used in the ERTS system to minimize the probability of catastrophic failure. The reliability block diagrams for the various subsystems show redundancy between components. Internal redundancy is discussed in the text. The present discussion is a summary of redundancy. It must be emphasized that degraded modes of operation are not included in this reliability assessment (with the exception of the wide band transmitter as discussed in the C&DH subsystem analysis). Redundancy is considered in this discussion only if the redundant mode of operation allows full capability for performing the ERTS mission. Redundancy incorporated into the design of the spacecraft subsystems is briefly described in the following sections

C&DH Subsystem. Functional redundancy is widely used in this subsystem. Both the MSFN and STADAN systems may be used to transmit commands to the command

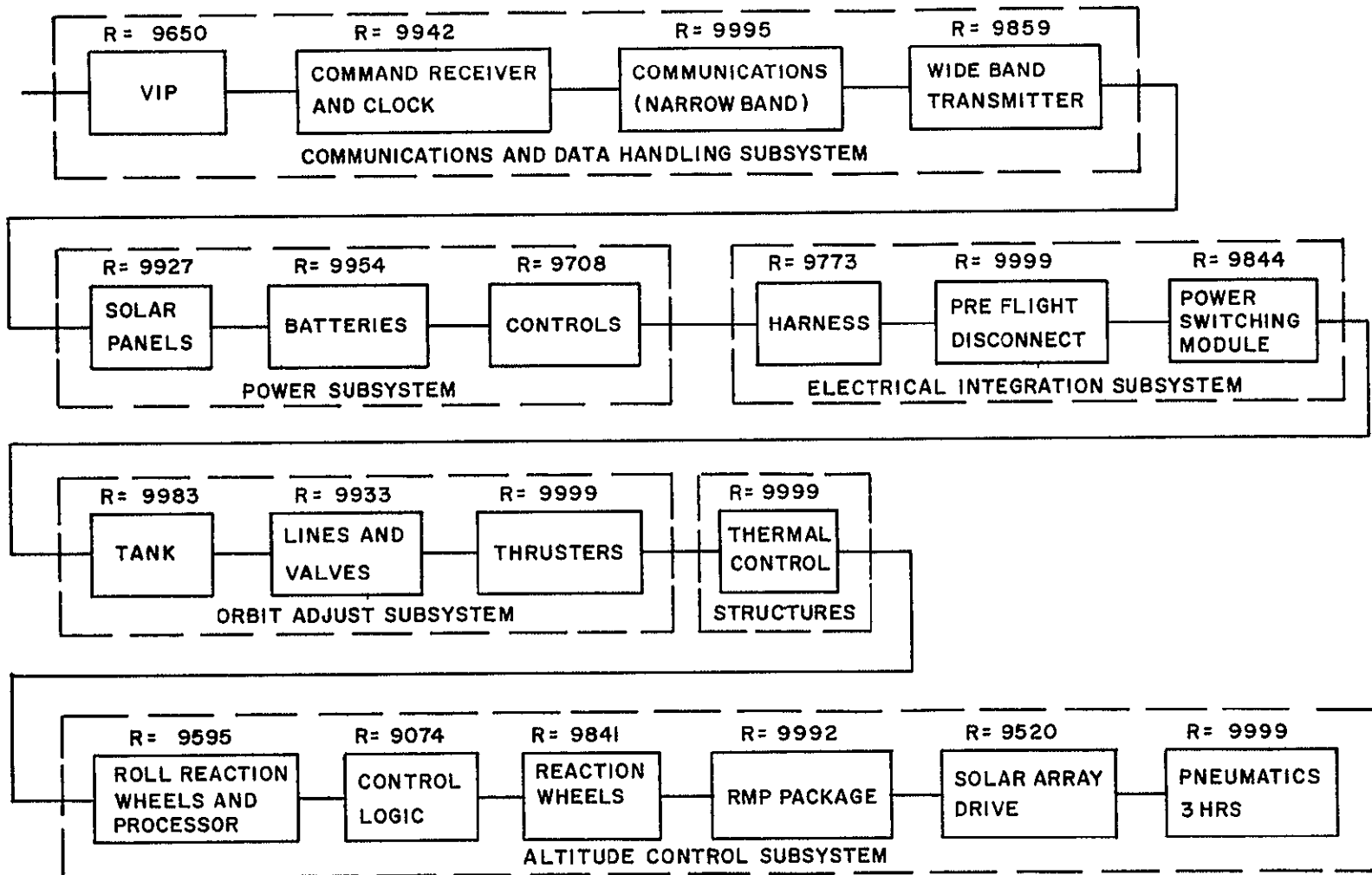


Figure 4.1-1. Simplified ERTS System Reliability Block Diagram

11 February 1970

Within each of the S-Band and VHF systems there is redundancy of receivers and demodulators. Broadcasting of "housekeeping" data can be accomplished through either the S-Band or VHF systems. The wide-band system transmits payload data on either PCM or video channels simultaneously and the redundant configuration permits a degraded mode of operation in which either channel may be used, but not both simultaneously. The VIP is designed to permit functional redundancy between the memory and the eleven stage counter

In addition to the functional redundancy which has been described in the C&DH subsystem, substantial block redundancy (two identical components) has been incorporated into the system design. Many block redundant components are "standby", that is, they are unpowered until needed, which reduces the probability that the redundant component will fail. The components employed in a standby redundant configuration are the S-Band and VHF command receivers and demodulators; the command matrix drivers and decoders, all clock components, the VHF transmitters, the USB transponders, and the premodulation processors. Components in a parallel redundant configuration (both powered) are S-band and VHF command receiver systems (each containing internal standby redundancy), the command integrators, the power supplies and command decoders, and (in the VIP) multiplexers, coders, formatter logic units, and reprogrammers.

Power Supply Subsystem. The solar array contains complex internal redundancy. The failure of single cells or single strings do not cause loss of the mission. Up to 9 string failures are permitted without loss of the solar array. The redundant configuration of the batteries permits the loss of 3 of 8 batteries without loss of the mission. Within the power control module, the auxiliary regulators and pulse width modulators are in parallel redundancy.

Attitude Control Subsystem. The reaction wheel scanners with signal processors are in parallel redundancy. The Rate Measuring Packages are in standby redundancy. The pneumatics are required for acquisition and are required for reacquisition, but the pneumatics are backed up by the Magnetic Moment Assembly in the wheel unloading mode. In addition several limited, but nevertheless mission useful, functionally redundant modes exist.

Structures Subsystem. In this subsystem, the thermal control components are the only ones considered as potentially contributing to unreliability. In the active thermal control system, there are springs backing up the bellows in each assembly to hold the shutters in a predetermined "fail-safe" position if the bellows fail. Each shutter assembly thus has high reliability, and the complete failure of a single assembly would probably not degrade the operation of the spacecraft. Thus the shutter assemblies may be considered redundant to each other. The passive thermal control system is not considered to have any significant failure mode.

Orbit Adjust Subsystem. This highly reliable system contains parallel redundant explosive valves, normally closed. The solenoid valves on the engines are two-seat, two-coil valves providing internal redundancy against leakage.



#### 4.1.2 PRINCIPLES OF RELIABILITY ASSESSMENT

In the components list for each subsystem, either a failure rate or a one year reliability is given for each component. The appearance of a failure rate implies that component is assumed to have an exponential distribution of time-to-failure, so that the R for time t is

$$R = e^{-\lambda t}$$

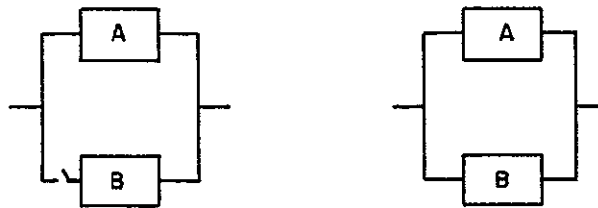
Components which do not have an exponential distribution of time-to-failure have a one year reliability given in the component lists.

Reliability for the case of standby redundancy is computed assuming that the standby component has a failure rate during its dormant or unpowered life equal to 10% of its normal "active" failure rate. If component A with failure rate  $\lambda_A$  is the active component and component B with failure rate  $\lambda_B$  is in standby, the reliability R of this redundant pair for time period T is

$$R = e^{-\lambda_A T} + \frac{\lambda_A}{\lambda_A + .1\lambda_B} R_S (e^{-\lambda_B T} - e^{-(\lambda_A + .1\lambda_B) T}),$$

where  $R_S$  is the reliability of the switch.

Standby redundancy is shown in the reliability block diagrams with a broken line indicating switching. Standby and parallel redundancy are diagrammed as follows



For all subsystems, reliability is computed assuming a required mission time of one year.

#### 4.1.3 SOURCE OF FAILURE RATE DATA

Reliability assessments for ERTS are in large part based on assessments of the Nimbus B spacecraft and the Nimbus D attitude Control Subsystem performed by Operations Research Inc. (ORI) which reported these assessments in Technical Reports 469 and 541. The notations ORI 469 and ORI 541 used in the present document refer to these reports.

The basic ground rule followed by ORI in their reliability assessment was the use of MIL-HDBK-217A failure rates at ground environment improved by one order of magnitude to

account for parts screening and the use of preferred parts. The rationale for the use of these failure rates is given in ORI 541, pp 30 and 31. For consistency, this ground rule was followed in the present report where piece-part analysis was performed or where vendors performed assessments using unimproved MIL-HDBK-217A rates. Exceptions to the use of ORI or MIL-HDBK-217A rates. Exceptions to the use of ORI or MIL-HDBK-217A rates are noted in components lists and discussed in the text for the subsystems where they appear.

#### 4.1.4 SUBSYSTEM RELIABILITY ASSESSMENTS

The subsystem reliability assessments performed on the phase B/C Spacecraft System Studies are summarized in the following sections.

##### 4.1.4.1 Structures Subsystem

Aside from the thermal control components, the probability of failure of this subsystem is assumed to be negligible. The reliability assessment of the thermal controls follows the assessment performed by Operations Research Inc. on the Nimbus B thermal controls and discussed in ORI Technical Report 469, pp. 57-60.

On the spacecraft, 16 bays have shutter assemblies. For each assembly, the failure rate is based on the following parts count

<u>Part</u>	<u>Failure Rate <math>\lambda \times 10^{-6}</math></u>
Bellows	1.2
Rack and four pinion gears	.6
Eight bearings	1.6
Spring	<u>.01</u>
	$\lambda = 3.41 \times 10^{-6}$

The reliability of a single bellows assembly for one year is .97057.

The bellows system in the shutter assembly is backed up by a spring to provide fail-safe operation. The failure rate of this spring is  $.01 \times 10^{-6}$ /hour, and its reliability is .999912. Thus the reliability of a shutter assembly including the spring backup is

$$R_{\text{assembly}} = 1 - (1 - .97057)(1 - .999912) = .999997$$

The probability that all 16 assemblies work throughout one year is

$$R = R_{\text{assembly}}^{16} = .99998.$$

There are 15 compensation loads. Each load contains three heaters in parallel redundancy. Each heater operates for 2000 hours. The failure rate of a heater is  $22.0 \times 10^{-6}$  failures/hour (PRC data at 50 percent confidence).

11 February 1970

In each load, one heater of three is required. If R denotes the reliability of a single heater, the probability  $P_{1/3}$  that at least one of three operates is

$$P_{1/3} = R^3 + 3 R^2 (1-R) + 3R (1 - R)^2$$

The reliability of a single heater is

$$R = e^{-22.0 \times 10^{-6} \times 2000} = .95695,$$

and, owing to the two-fold redundancy,

$$P_{1/3} = .99992.$$

This is the reliability of a compensation load.

It is conservatively assumed that at least 2 loads could fail without causing spacecraft failure. The probability that at least 13 loads succeed is

$$P_{13/15} = P_{1/3}^{15} + 15 P_{1/3}^{14} (1 - P_{1/3}) + 105 P_{1/3}^{13} (1 - P_{1/3})^2$$

$$P_{13/15} > .9999$$

The thermal control for the Attitude Control Subsystem has a negligible probability of failure (ORI 469, Table 30). Thus the reliability of the overall thermal control system exceeds 9999

#### 4.1 4.2 C&DH Subsystem

The C&DH subsystem is quite large and complex. As the subsequent discussion will show, a great deal of redundancy is utilized to minimize the probability of degraded performance or failure. The success of redundancy in the design is shown by the achievement of the very high subsystem reliability of 9453 for successful performance for a one year mission

It should be emphasized that this reliability is the probability of achieving all mission requirements. In addition, one degraded mode has been considered, it is discussed following the discussion of subsystem reliability.

The components of the C&DH subsystem are shown in Table 4.1.4-1. In this table the VIP appears as a single component, it is broken down in Table 4.1.4-2

The Versatile Information Processor is built by Radiation Inc. Its components are shown in Table 4.1 4-2

TABLE 4.1.4-1. COMPONENTS OF C&amp;DH SUBSYSTEM

Symbol	Component	Failure Rate or One-Yr Reliability	Source, Comments
A	VIP	R=0.965006	Radiation Inc.
B	VHF Transmitter	1.1064	ORI 469, p. 202, reduced by one order of magnitude
C	PM Transponder	3.25	Collins Radio
D	Summing Networks	0.0823 each	ORI 469, p. 201, reduced by one order of magnitude Compare ORI 541, p. 87
E	VCO (5)	0.1784 each	ORI 469, p. 186, reduced by one order of magnitude
F	Buffer	0.0823	Assumed equivalent to 1 summing network
G	S-Band Receiver	1.6048	ORI 469, p. 113, assumed equivalent to VHF Rcvr
H	Demodulator	3.8295	ORI 469, p. 113
I	VHF Receiver	1.6048	ORI 469, p. 113
J	Integrator	1.5	Estimated
K	Power Supply Unit	5.834	Rates supplied by vendor.
L	Comdec	3.6475	Conservatively based on MIL-HDBK-217A Reduced
M	Matrix Driver and Decoder	3.341	by one order of magnitude for ERTS
N	Comstor Logic	1.457	↓
O	Comstor Memory	3.177	
P	OSC	1.069	
Q	Frequency Generator	2.795	
R	TC Generator	2.49	
S	Filter	0.005	ITT
T	Modulator	0.8452	Piece part analysis

TABLE 4.1.4-1. COMPONENTS OF C&amp;DH SUBSYSTEM (Continued)

Symbol	Component	Failure Rate or One-Yr Reliability	Source, Comments
U	Power Amplifier	0.5291	HAC
V	Antenna	0.03	Estimate
W	Switch	0.02	MIL-HDBK-217A

TABLE 4.1.4-2. COMPONENTS OF THE VIP

Symbol	Component	One-Year Reliability for Single Component
A	Memory	0.5978
B	Memory Sequencer	0.9660
C	11 Stage Counter	0.9969
D	Multiplexer	0.9887
E	Redundant Multiplexer Circuits	0.9508
F	Coder	0.9737
G	Formatter Logic	0.9342
H	Reprogrammer	0.9180
I	Transmitter	0.9825
J	Isolator	0.9903
K	Switching Circuit	0.9999

The reliability block diagram of the VIP is shown in Figure 4.1.4-1.

The mathematical model for the reliability of the VIP is based on the assumption that all components are powered throughout the mission. The formula for the reliability of the VIP (letting  $R_X$  denote the one year reliability of component X, where the symbol is given in Table 4.1.4-2) is

$$R_{VIP} = \left[ 1 - (2R_A - R_A^2) (2R_B - R_B^2) \right] \left[ 1 - (2R_C - R_C^2) \right] \\ \times R_D (2R_E - R_E^2) (2R_F - R_F^2) (2R_G - R_G^2) \\ \times (2R_H - R_H^2) (2R_I - R_I^2) R_J R_K$$

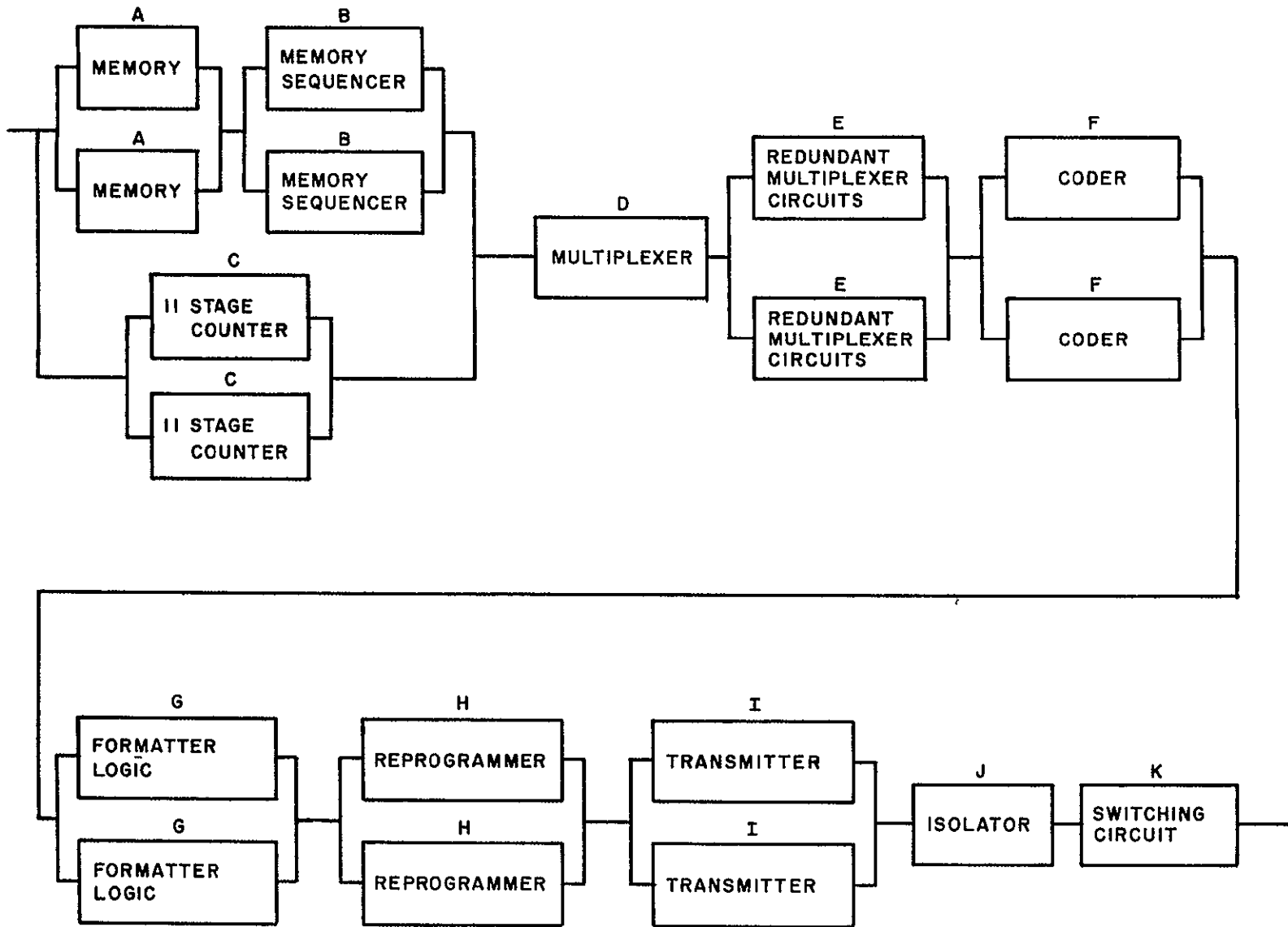


Figure 4.1.4-1. Reliability Block Diagram for VIP

The reliability of the VIP for 1 year is .965006.

The reliability block diagram for the entire C&DH subsystem is given in Figure 4.1.4-2.

The mathematical formula for the overall reliability of the C&DH subsystem uses the symbols for components given in Table 4.1.4-1 and Figure 4.1.4-2. For convenience of notation, let

$$R_X = e^{-\lambda_X T} = \text{reliability of component X with failure rate } \lambda_X \text{ for time}$$

$$\Phi(\lambda) = 2e^{-\lambda T} - e^{-2\lambda T} = \text{reliability of parallel redundant components with failure rate } \lambda$$

$$\Theta(\lambda) = e^{-\lambda T} + 10e^{-.02 \times 10^{-6} \times T} \left( e^{-\lambda T} - e^{-1.1\lambda T} \right) = \text{reliability of primary plus standby paths with failure rate } \lambda, \text{ where paths are identical}$$

The reliabilities of components S, T, U, and W are computed assuming a "powered" time of 1/2 year.

The subsystem reliability R is given by the following formula

$$R = \left[ 1 - (1 - \Theta(\lambda_G + \lambda_H)) (1 - \Theta(\lambda_I + \lambda_H)) \right] \Phi(\lambda_J) \\ \times \Theta(\lambda_K + \lambda_L) \Theta(\lambda_M) \Theta(\lambda_P) \Theta(\lambda_Q) \Theta(\lambda_R) \Phi(\lambda_N) \\ \times \Phi(\lambda_O) \Theta(\lambda_B) \Theta(\lambda_C) \Theta(2\lambda_D + 5\lambda_E) \Theta(\lambda_F) \\ \times R_A R_T^2 R_U^2 R_V R_W (2R_S^2 R_W^2 - R_S^4 R_W^4)$$

$$R = .94534$$

A degraded mode of operation was identified for the wideband transmitter. In normal operation, both MSS PCM data and RBV video data may be transmitted simultaneously. In the degraded mode, either may be transmitted upon command, but not both. The probability of operating at least in this degraded mode is .95840. This probability includes the probability of complete success (.9453) plus the probability of degraded operation only (0.0131). This degraded mode of operation replaces the configuration (in Figure 4.1.4-2).

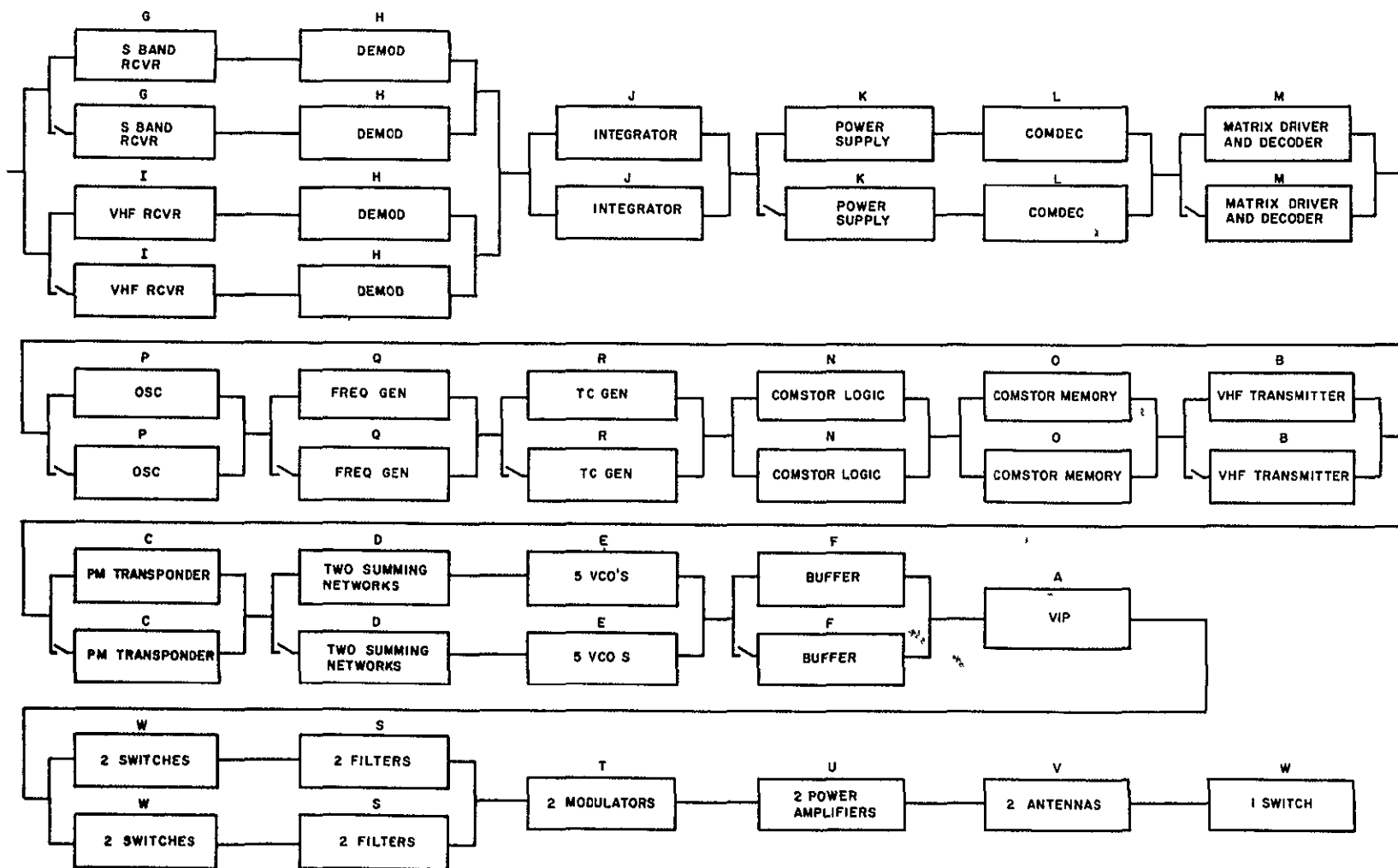
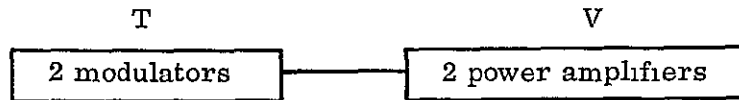
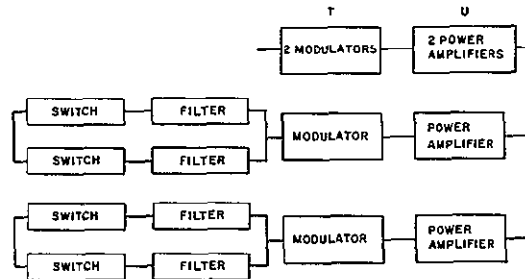


Figure 4.1.4-2. C&DH Subsystem Reliability Block Diagram.





with the configuration



with operating times adjusted to meet the requirements of degraded operation

#### 4 1.4 3 Attitude Control Subsystem

The Attitude Control Subsystem is designed to achieve its function with maximum reliability. All components are space qualified and have a demonstrated long life. Built-in redundancy minimizes the risks associated with single-point failures in the RMP, the reaction wheel scanner, the signal processor, and the yaw reaction wheel.

The yaw rate gyro is used for acquisition only. Its probability of success during this mode exceeds 0.99995.

The pneumatics are required for acquisition, orbit adjust, and wheel unloading. Their operating time for these tasks is estimated as 3 hours. The pneumatics are available as backup for the yaw reaction wheel. The use of the pneumatics in wheel unloading is backed up by the magnetic moment assembly.

To compute the reliability of the pneumatics, it is assumed that they are required for a total of 3 hours plus the expected time  $t_B$  used to backup the yaw reaction wheel if the reaction wheel fails. The expected time of failure, given that failure occurs in time  $T$  is between  $0.4T$  and  $0.5T$ . Assuming a 10 percent duty cycle during wheel unloading, the operating time of the pneumatics is 3 hours if the yaw reaction wheel succeeds and  $3 + (0.1 \text{ by } 0.6 \text{ by } 8760)$  if the yaw reaction wheel fails.

Failure rates for the components of the Attitude Control Subsystem are shown in Table 4.1 4-3. The failure rate of the wheels (pitch, roll, and yaw) is based on the following accumulated flight data (per wheel)

OAO and Nimbus 113400 hours in flight with no failure

OGO 63492 hours in flight with no failure

OGO 203057 hours on test with no failure

TABLE 4.1.4-3. ACS FAILURE RATES

Symbol	Component Name	Failure Rate $\lambda \times 10^{-6}$ or One-Year Reliability	Source and Comments
A	Reaction Wheel	3.9749	ORI 541, Table 9A
B	Signal Processor	7.6428	ORI 541, Table 9A
C	Control Logic	11.094	ORI 541, Table 9A, (eliminating A1 and A6/A7)
D	Rate Measuring Package (RMP)	4.5031	ORI 541, Table 9
E	Yaw Rate Gyro	37.7486	ORI 541, Table 9
F	Magnetic Moment Assembly	0.1065	Piece Part Analysis
G	Yaw Reaction Wheel	1.823	See Text
H	Pitch Reaction Wheel	1.823	See Text
I	Solar Array Drive	$\lambda = 5.384 \times 10^{-6}$ electronics $R \approx 0.998$ (mech)	ORI 541, Table 9  ORI 469, p. 69, modified with $\mu = 36$ months
J	Initiation Timer	3.4934	ORI 541, Table 9
K	Pneumatics	6.87	ORI 469, Table 30
L	Roll Reaction Wheels (2)	1.823 each	See Text

The calculated failure rate is  $1.823 \times 10^{-6}$  failures/hour/wheel.

The failure rate of the Magnetic Moment Assembly is based on the following parts count

Part	N	$\lambda \times 10^7$	$N \lambda \times 10^7$
Permanent Magnets	3	0.0102	0.03
Coils	3	0.3 (est)	0.9
Capacitors	2	0.02	0.04
Relays	8	0.01	0.08
Resistors	3	0.005	0.15

$$\lambda = 0.1065 \times 10^{-6}$$

This parts count utilizes MIL-HDBK-217A rates reduced by one order of magnitude.

The failure rate of the mechanical aspect of the solar array drive may be derived using the same approach as ORI (Technical Report 469, p. 69). Nimbus flight experience indicates that the mean life for this component is not less than 30 months. Assuming that the time to failure is normally distributed with standard deviation equal to 20 percent of the mean, we find that one year is three standard deviations below the mean life, so that the probability of failing in one year is less than .002.

A reliability block diagram of the Attitude Control Subsystem is shown in Figure 4.1.4-3.

The mathematical model for the reliability of the attitude control subsystem follow (T = 8760)

$$R = R_C R_I R_H R_L^2 \left[ 1 - (1 - R_A R_B)^2 \right] \left[ R_G e^{-3\lambda K} + (1 - R_G) e^{-528.6 \lambda K} \right] \left[ e^{-\lambda DT} + 10 (e^{-\lambda DT} - e^{-1.1\lambda D^T}) \right]$$

The one-year reliability of the subsystem, following the order of the given formula, is

$$R = (0.9074) (0.9520) (0.9842) (0.9686) \times (0.9906) (0.99992) (0.9992)$$

$$R = 0.81499 \text{ (one year)}$$

#### 4.1.4.4 Orbit Adjust Subsystem

Table 4.1.4-4 shows the components appearing in the Orbit Adjust Subsystem. The table shows failure rates in terms of failures per hour or failures per cycle except in the case of ordnance valves, for which the probability Q of failure is given. In addition, the number of cycles of operation required during a one year mission are shown.

The solenoid valves are two-coil, two-seat valves affording maximum protection against leakage mode of failure. The normally closed explosive valves are in parallel redundancy.

For components with failure rates given in terms of failures per cycle, the exponential approximation is used

$$R = e^{-\lambda N}$$

where N denotes the number of cycles. For one shot devices,  $R = 1 - Q$ .

The mathematical formula for the reliability R of this subsystem is

$$R = R_A^3 R_B R_C R_D^{35} R_E R_F^2 R_H (2R_G - R_G^2)$$

The reliability is 0.9917 for one year.

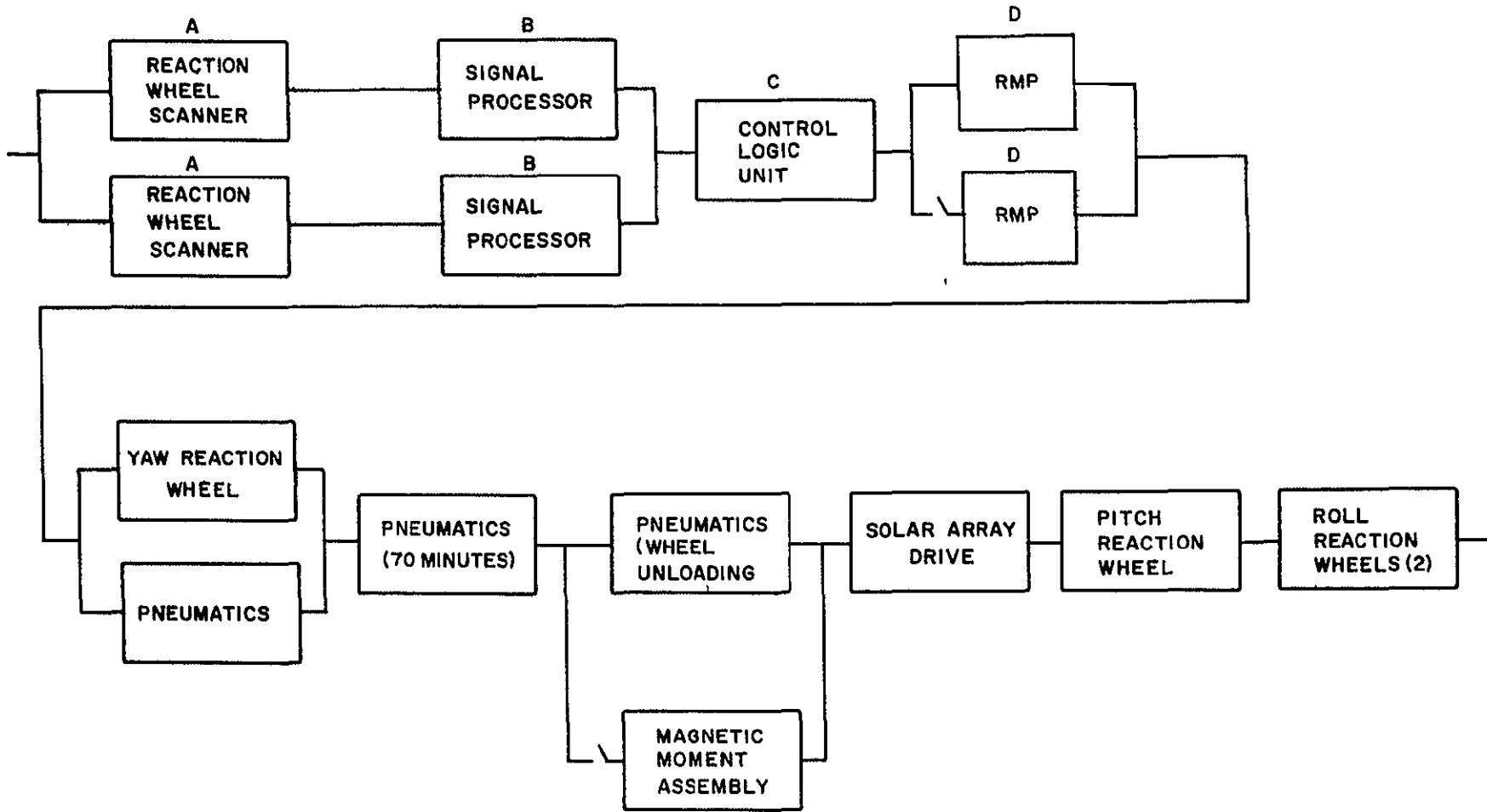


Figure 4.1.4-3. Attitude Control Subsystem Reliability Block Diagram

TABLE 4.1 4-4. COMPONENTS OF ORBIT ADJUST SUBSYSTEM

Symbol	Component	Quantity	Failure Rate X 10 or Q (each)	Duty Cycle	Sources
A	Fill or drain valve	3	$0.113 \times 10^{-6}$ per hour	8760 hrs	TRW (ATS-F/G) 6/67
B	Pressure Tank	1	$0.15 \times 10^{-6}$ per hour	8760 hrs	Ham. St., United A/C (ERTS-OAS), 12/63
C	Pressure Tank Bladder	1	$17.5 \times 10^{-6}$ per cycle	22 cycles	Same
D	Lines and Fittings	35	$0.003 \times 10^{-6}$ per hour	8760 hrs	GE (OAO) 5/68
E	Filter	1	$0.3 \times 10^{-6}$ per hour	8760 hrs	Marquardt Corp. (ATS-F/G) 7/67
F	Thruster	2	$0.38 \times 10^{-6}$ per cycle	22 cycles	Ham. Std., United A/C (ERTS-OAS), 12/63 (without solenoid)
G	N/C Ordnance Valve	2	Q = .0001	One-shot	Marquardt Corp. (ATS-F/G), 7/67
H	Solenoid Valve	2	$0.12 \times 10^{-6}$ per cycle	22 cycles	GE(OAO) 5/68

These results, using the above failure rates, are found to be quite consistent with the independent reliability analysis performed by Rocket Research Corporation and contained in Volume 2, Section 6, Appendix.

#### 4.1.4.5 Power Subsystem

The reliability analysis presented follows that performed by Operations Research Inc (Tech. Rept. 469), which in turn is based on assessments performed by RCA upon the solar panels and battery modules. The numerical results presented here are based on a re-evaluation of the reliability of solar panels and batteries.

One of the most significant contributors to unreliability in the assessment performed by RCA and used by ARI is the solar array. The derivation of the low number is based on a cell failure rate of  $250 \times 10^{-9}$  failures per temperature cycle. Recent data (RCA Internal Correspondence dated Nov. 18, 1968) indicates a failure rate of  $30 \times 10^{-9}$  failures per hour. Based on this data, the solar array has a one year reliability greater than .998 with up to 9 string losses permitted.

On the basis of Nimbus experience, batteries are considered to experience failures which are predominantly "chance" rather than "wear-out" in nature during a one year mission. The PRC reliability report based on actual flight data shows that "battery packs" have experienced four failures in  $7.94 \times 10^5$  hours of flight. From this data, the failure rate of a battery is estimated very conservatively as  $5.8816 \times 10^{-6}$ /hour at 50 percent confidence.

Adding to this the failure rate for battery electronics used by ORI ( $7.5 \times 10^{-6}$ /hour) and the failure rate of one diode, we have a failure rate of  $13.3866 \times 10^{-6}$ /hour for each battery. This approach assumes that the failure mode of a battery throughout one year is primarily exponential with negligible effect of wear-out. The reliability calculated for each battery is 0.90255. But only 5 of 8 are required. The probability that 5 of 8 batteries will survive for one year is 0.99543.

There are two power-control modules one is required throughout the one year mission, the other is required about 10 percent of this time. The failure rates used in computing reliability are based on ORI Tech. Rept. 469, Table 23. The failure rates used for the auxiliary regulator, the shunt dissipator, bus comparison, and PWM are the same as those used by ORI. The filter and storage block contains 5 capacitors and two choke inductors with a total failure rate of  $0.0598 \times 10^{-6}$ /hour. The remaining circuitry has a failure rate conservatively estimated as  $0.7973 \times 10^{-6}$ /hour. To find the total reliability for one year of operation of both power control modules, the reliability of a single module is computed for one year and also computed for .1 year, these two results are multiplied to obtain an overall reliability for the two modules of .97081.

The components of the Power Subsystem are shown in Table 4.1.4-5.

TABLE 4.1.4-5. POWER SUBSYSTEM

Symbol	Component	Failure Rate $\lambda \times 10^{-6}$ or Reliability R	Source
A	Solar Panels	R = 0.9927	ORI 469, Table 24, Modified by RCA Int Corresp. See text.
B	Battery Modules	R = 0.9954 (5 of 8 succeed)	See text.
C	Power Control Modules	R = 0.97081 Total	ORI 469, Table 23, See text for application.
D	Aux. Load Control and Aux. Load Panels	R > 0.99995	GE PIR 4341-24 (Nimbus B Program)
E	Unfold Timer	R = 0.9996 per timer	GE PIR's 4341-26 and 4341-43 (Nimbus B Program)

The reliability block diagram of the Power Subsystem is given in Figure 4.1 4-4.

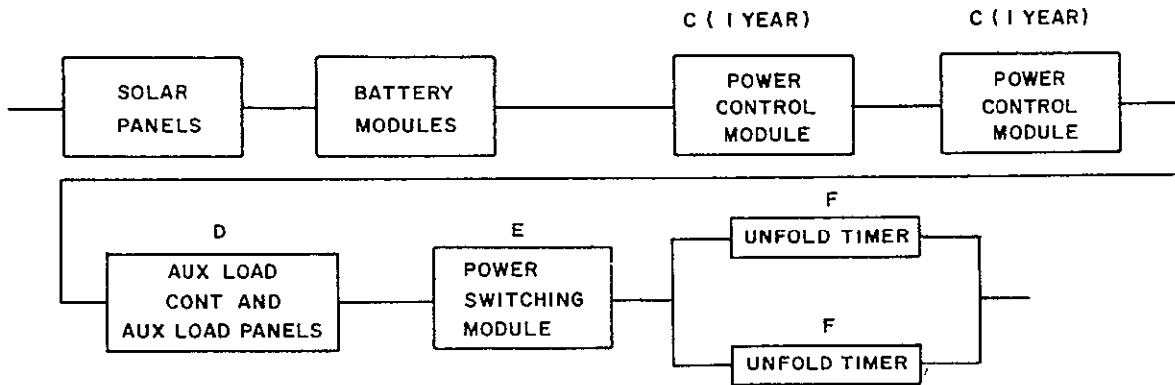


Figure 4.1.4-4. Power Subsystem Block Diagram

The formula for subsystem reliability R is

$$R = R_A R_B R_C R_D R_E (2R_F - R_F^2)$$

$$R = 0.95926$$

#### 4.1.4.6 Electrical Integration Subsystem

The Electrical Integration Subsystem contains the Power Switching Module, the electrical harness, and the pre-flight disconnect. Its reliability for a one year mission is 0.9621

The pre-flight disconnect is used only once before launch. Because of the very short operating time, its probability of failure is considered to be negligible

The Power Switching Module contains the parts shown in Table 4.1.4-6. The diodes appear in 160 redundant pairs, with total reliability 0.99999. The failure rate of the remainder of the Power Switching Module is  $1.7919 \times 10^{-6}$ /hour. The overall reliability of this module is 0.9844.

TABLE 4 1.4-6. POWER SWITCHING MODULE

Part Type	N	$\lambda \times 10^6$	$N \lambda \times 10^6$
Diodes	320	0.0333	160 redundant pairs, R 0.99999
Resistors	4	0.00048	0.00192
Power resistors	12	0.12	1.44
Holding relays	12	0.0005	0.006
Latching relays	34	0.001	0.034
Connectors (50 pins)	10	0.031	<u>0.31</u>
			$\lambda = 1.7919 \times 10^{-6}$
			R = 0.984425

The electrical harness comprises 436 connectors with an average of 20 pins each. The failure rate for such a connector is  $.006 \times 10^{-6}$ /hour, from MIL-HDBK-217A, reduced one order of magnitude. Thus the overall failure rate of the harness is  $2.616 \times 10^{-6}$ /hour and its reliability is 0.97734.

The overall reliability of the Electrical Integration Subsystem is

$$R = (0.9844)(0.97734) = 0.9621.$$

These failure rates are based on MIL-HDBK-217-A rates, reduced by one order of magnitude to account for screening.



## 4.2 ORBIT ANALYSIS

### 4.2.1 INTRODUCTION

During the course of the Phase B/C ERTS studies, extensive orbital analyses have been performed which have led to the definition of an orbit and an orbit control procedure that will permit attainment and maintenance of all ERTS orbital and ground trace swath control requirements for a minimum of one year. The altitude of the orbit is 492.35 nautical miles and the orbit is inclined by 99.088 degrees to the earth's equator (retrograde). The nominal eccentricity of this sun synchronous orbit is zero, its orbit period is 6196.015 seconds and the time at the descending node is, nominally 9 30 A.M. The entire earth (except small portion centered about each pole) could be surveyed every 18 days (251 revolutions) with the orbit. The orbit's ground track (and the subsatellite's swath) is controlled via a hydrazine fueled orbit adjust system that can either add or remove orbit velocity through the controlled firing of "one-pound" thrusters. This control is necessary for removing launch vehicle injection errors and for compensating energy losses due to atmospheric drag decay.

There are five basic requirements that must be met thru proper selection and control of the ERTS orbital parameters. They are as follows:

1. **Adjacent Ground Trace Control.** It is required that the subsatellite swath (100 nautical miles) of adjacent ground traces as generated on successive days overlap by  $\approx 10$  percent ( $\approx 10$  nautical miles). The swath should progress in a westward direction. This requires that the orbit selected should generate its ground tracks such that the ground trace of the first orbital revolution should be no more than 1.5 degrees (90 nautical miles at the equator) west of the first ground tracks from the previous day.
2. **Ground Track Control on Successive Coverage Cycles.** Each coverage cycle consists of 251 orbit ground tracks equally spaced, nominally, around the equator. Even after launch vehicle injection errors are removed, perturbations to the orbit and therefore to the ground track spacing are produced via atmospheric drag force, orbit determination and orbit adjust system impulse uncertainties. In the presence of these perturbations it is necessary to maintain sufficiently accurate control of the ground tracks (via orbit parameter control) such that a given subsatellite swath (e.g. rev. 10) during one coverage cycle coincides by  $\pm 10$  nautical miles with the same subsatellite swath (rev. 10) during any of the other 20 coverage cycles. Thus the corresponding (same rev. number) ground tracks must lie no more than 10 nautical miles away from each other during the entire year.
3. **Lighting Conditions at Satellite Nadir.** To maintain earth surface illumination conditions at satellite nadir within limits suitable for payload operation (sufficient solar illumination) and data interpretation (nearly constant illumination with sufficient shadowing) a sun synchronous orbit with a nominal descending node time of 9 30 A.M. is required.
4. **Eccentricity.** It is desired to maintain the scale variations in sensor imagery to less than 10 percent between maximum and minimum altitude (10 percent of 492 nautical miles), or  $\pm 25$  nautical miles. An eccentricity of .006 corresponds to an apogee-perigee difference

of  $\pm 23.7$  nautical miles and satisfies this requirement, neglecting the oblateness of the earth. Since the oblateness introduces a 9 nautical mile ( $\pm 4.5$  nautical miles) difference in altitude between equator and maximum latitude ( $\approx 81$  degrees), only an additional  $\pm 20$  nautical miles can be allotted to eccentricity-induced apogee-perigee differences

5. It is required that the above four requirements be maintained for a minimum of one full year.

Each of the five requirements discussed in the immediately preceding paragraphs imposes its own special requirements and restrictions on the orbit and on the techniques for control of the orbit. From requirements 1 and 3 comes the nominal orbit, from requirement 2 the need for orbit control, for the orbit adjust subsystem and for the development of operational procedures and techniques for control, from requirement 4, a bound or limitation (potentially) on the techniques used in removing injection errors and making up drag decay losses, and from requirement 5 comes the total velocity impulse to be provided by the orbit adjust subsystem.

#### 4.2.2 NOMINAL ORBIT SELECTION

Overall mission requirements considering the payload sensors resolution capability, imagery scale, space to ground communications, etc. have lead to the selection of an orbital altitude to be in the range of 500 nautical miles \* It is found that at an altitude of  $\approx 481.6$  nautical miles, an exactly repeating ground trace, every day, can be obtained. Fourteen separate ground tracks are generated, and then repeated, each day. By moving to a slightly higher or lower altitude, the ground tracks no longer exactly repeat, but will shift gradually each day until complete earth coverage is eventually obtained. With the altitude greater than 481.6 nautical miles, day to day ground track progression is to the west. This occurs because the orbit period is increased, it takes longer to make a revolution about the earth and the earth rotates to the east thru a slightly larger angle between equatorial crossings of the satellite.

Thus, the nominal orbit altitude will be slightly higher than 481 nautical miles. Using Equations 4.2.2-1 through 4.2.2-19 to be presented below, a set of nominal orbit parameters were computed and are given in Table 4.2-1. As shown, a 492.35 nautical miles altitude, 99.088 degree inclined orbit is selected.

To compute the nominal orbit, it is first necessary to determine the longitude shift,  $\Delta\phi_d$ , from one ascending node to the next as the satellite traverses the earth once. Once this is determined, the orbit period, the time for the satellite to make one revolution about the earth, that produces the desired  $\Delta\phi_d$  can then also be determined. Calculation of orbit altitude and inclination readily follows.

---

\*The selection of this altitude regime is not covered in this analysis. However, previous studies at GE are in agreement with NASA's selection of  $\sim 500$  nautical miles as the optimum ERTS A/B altitudes.

In selecting  $\Delta\phi_d$ , requirement 1, adjacency of day to day ground traces is the controlling factor. Figure 4.2-1 shows a set of ground traces falling on one segment of the equator. Identical patterns will be found for any other equatorial segment of length  $\Delta\phi_d$ . In the figure a "REV 1" ground trace is seen to commence at 0 degrees longitude which is simply a reference point longitude. The satellite begins "REV 2"  $\Delta\phi_d$  degrees to the west, the earth has rotated  $\Delta\phi_d$  degrees to the east during the time it takes for the ERTS to make one revolution about the earth. After 14 revs. ("END OF REV 14") the satellite's ascending node has "travelled" slightly more than 360.

That is

$$14 \Delta\phi_d = 360 + \Delta\ell$$

where  $\Delta\ell$  is the distance between adjacent ground traces on successive days.

After 28 Revs, the ascending nodes have "travelled" thru  $720 + 2 \Delta\ell$  degrees. From equation (1), an expression for  $\Delta\phi_d$  is derived

$$\begin{aligned} \Delta\phi_d &= (360 + \Delta\ell) / M \\ \Delta\phi_d &= 25.7142857 + \frac{\Delta\ell}{M} \end{aligned} \quad (4.2.2-2)$$

where

M

is the number of revs in one day (M = 14 for ERTS) and 25.7142857 is simply the quotient of 360/14. It is seen that the nodal longitude shift,  $\Delta\phi_d$ , should be slightly larger than 25.7142857 degrees. In order that a repeating situation be generated, it is necessary the broken-lined nodal traces in Figure 4.2-1, as they move to the west, eventually fall on the solid-lined trace "REV 2". When this happens, repeatability begins and a new coverage cycle is initiated. This is most easily accomplished by making  $\Delta\ell$  of such magnitude that when divided into  $\Delta\phi_d$ , the quotient is an integer. Mathematically, this is expressed by

$$\Delta\ell = \frac{\Delta\phi_d}{N} \quad (4.2.2-3)$$

where

N is the number of segments into which  $\Delta\phi_d$  is divided. Substituting (4.2.2-2) into (4.2.2-3) yields a general expression for  $\Delta\ell$

$$\Delta\ell = (360 + \Delta\ell) / MN \quad (4.2.2-4)$$

or

$$\Delta\ell = 360 / (MN - 1) \quad (4.2.2-5)$$

With  $M = 14$ ,  $N = 18$ , as in the case of ERTS,  $\Delta\ell = 1.434262$  degrees and the total number of revs in one coverage cycle is  $MN - 1$ . To determine  $\Delta\phi_d$ , the following rearrangement of equation (3) is used

$$\Delta\phi_d = N \cdot \Delta\ell \quad (4.2.2-6)$$

and  $\Delta\phi_d = 25.816733$  degrees. As an interesting check, the product of  $M \cdot \Delta\phi_d$  is 361.434262 degrees, thus verifying that  $\Delta\ell$  can also be expressed by the term  $(M \cdot \Delta\phi_d - 360)$ .

With  $\Delta\ell = 1.434262$  degrees, the distance at the equator is 86.06 nautical miles, giving  $\approx 14$  percent overlap of subsatellite swaths. If N is set equal to 17, instead of 18,  $\Delta\ell$  is found to be 1.5189873 degrees and the distance between adjacent tracks at the equator is 91.14 nautical miles, less than 9 percent overlap occurs. Figure 4.2-2 shows pictorially the definition of overlap.

It should be noted that there are actually only 13 17/18 orbital revs per one day with the  $N = 18$ ,  $M = 14$  ERTS orbit. Figure 4 2-1 shows "REV 252" ending at 25.816733 degrees West. This is the first complete rev of the second coverage cycle. "REV 251" is the last rev of the preceding coverage cycle, it completes that coverage cycle.

With  $\Delta\phi_d$  determined, the altitude and inclination can now be calculated. An expression relating  $\Delta\phi_d$  with orbit period,  $\tau$ , is given by the following expression for nodal longitude shift

$$\Delta\phi_d = -\tau (w_e - \dot{\Omega}_o) \quad (4.2.2-7)$$

Solving for  $\tau$  yields ( $\tau_d$  indicates the desired value of  $\tau$ )

$$\tau_d = \frac{-\Delta\phi_d}{w_e - \dot{\Omega}_o} \quad (4.2.2-8)$$

where  $w_e$  is the earth's angular rate about its spin axis,  $\tau$  is the nodal period and  $\dot{\Omega}_O$  is the precession rate of the orbit plane due to earth oblateness.  $\Delta \dot{\Omega}_O$  is the total precession angle per orbit. The minus sign indicates a drift to the west.

The general expression for  $\tau$  is

$$\tau = \tau_{\text{KEP}} \left[ 1 - \frac{J}{4} \left( \frac{R}{a} \right)^2 (7 \cos^2 i - 1) \right] \quad (4.2.2-9)$$

where  $J$  is the second order zonal harmonic of the earth model,  $R$  is earth's equatorial radius, and  $a$  is orbit's semi-major axis.  $\tau_{\text{KEP}}$ , the Keplerian orbit period, is given by

$$\tau_{\text{KEP}} = 2\pi \sqrt{\frac{R}{g}} \left( \frac{a}{R} \right)^{3/2} \quad (4.2.2-10)$$

where  $g$  is the gravitational acceleration on the earth's surface at the equator.

Nodal precession rate,  $\dot{\Omega}_O$ , is given by

$$\dot{\Omega}_O = -J \sqrt{\frac{g}{R}} \left( \frac{R}{a} \right)^{7/2} \cos i \quad (\text{rad/sec}) \quad (4.2.2-11)$$

The minus sign indicates precession to the west

$\dot{\Omega}_O$ , for sun-synchronous conditions ( $\dot{\Omega}_{\text{SS}}$ ) must be 0.98560912 degree per day to the east, therefore,  $\cos i < 0$ ,  $i > 90^\circ$ .

Solving for  $\cos i$  yields

$$\cos i = \frac{-\dot{\Omega}_{\text{SS}}}{J} \sqrt{\frac{R}{g}} \left( \frac{a}{R} \right)^{7/2} \frac{1}{57.2957795} \quad (4.2.2-12)$$

In this equation,  $\dot{\Omega}_{\text{SS}} = 1.1407513 \times 10^{-5}$  deg/sec. The right hand side of equation 4.2.2-8 is completely determined when  $\dot{\Omega}_{\text{SS}}$  is substituted for  $\dot{\Omega}_O$ . Square equation (4.2.2-12) and substitute it into equation (4.2.2-9), along with equation (4.2.2-10) and set it equal to  $\tau_d$  (Equation 4.2.2-9). This yields a complete expression for  $\tau$  as a function of semi-major axis,  $a$

$$\tau_d = -2\pi \sqrt{\frac{R}{g}} \left( \frac{a}{R} \right)^{3/2} \left[ 1 - \frac{J}{4} \left( \frac{R}{a} \right)^2 \left\{ 7 \frac{\dot{\Omega}_{\text{SS}}^2}{J^2} \frac{R}{g} \left( \frac{a}{R} \right)^7 \left( \frac{1}{57.2957795} \right)^2 - 1 \right\} \right] \quad (4.2.2-13)$$

$$= -2\pi \sqrt{A} X^{3/2} \left[ 1 - \frac{7A}{4J} \frac{\dot{\Omega}_{\text{SS}}^2}{\gamma} X^5 + \frac{J}{4} \left( \frac{1}{X} \right)^2 \right] \quad (4.2.2-14)$$

where  $A = \frac{R}{g}$ ,  $X = \frac{a}{R}$  and  $\gamma = 57.2957795$ .

The required value of period,  $\tau_d$  is 6196.015 sec.

Slight variations to the semi-major axis,  $a$ , produce the following changes in  $\tau_d$

$$\Delta\tau_d = -3\pi\sqrt{A} X^{\frac{1}{2}} \left[ 1 - \frac{J}{4} \left(\frac{1}{X}\right)^2 \left\{ 7 \frac{\Omega_{SS}^2}{J^2} A X^{\frac{7}{2}} \frac{1}{\gamma} - 1 \right\} \right] \Delta X \quad (4.2.2-15)$$

$$- 2\pi\sqrt{A} X^{3/2} \left[ -\frac{35}{4} X^4 \frac{\Omega_{SS}^2}{\gamma J^2} A - \frac{J}{2} \frac{1}{(X)^3} \right] \Delta X$$

Using equations (4.2.2-14) and (4.2.2-15) iteratively, the value of semi-major axis,  $a$ , that produced  $\tau_d = 6196.015$  and  $\phi_d = 25.816733$  was determined to be 23917335. feet (3936.287 nautical miles).  $a$  is then substituted into equation (4.2.2-12) to compute the nominal inclination,  $i_{SS}$ , (that value of  $i$  that yields the sun-synchronous precession rate for the nominal semi-major axis) which is found to be 99.088 degrees.

The orbit altitude,  $h$ , is defined as

$$h = a - R \quad (4.2.2-16)$$

which is 2991597. feet or 492.35 nautical miles, where  $R$ , the equatorial radius, equals 20925738 feet. This altitude is neither equatorial altitude nor the altitude at any other specific point. It is simply a convenient designation since both  $R$  and  $a$  are constant.

Due to the flattening of the earth, the actual altitude will vary by up to 10 nautical miles. Also, the radial distance (distance satellite is from the center of the earth) will vary, slightly, according to the following expression

$$\Delta r = Ja \left[ \left(\frac{R_e}{a}\right)^2 (\sin^2 i \cos 2w) \frac{1}{6} \right] \quad (4.2.2-17)$$

where  $w$  is the angular distance travelled from the equator. The extremes in  $\Delta r$  occur when  $w = 0$  and  $w = 90$  degrees. It is computed as  $\pm .795$  nautical miles.

The actual earth radius,  $R_e$ , is defined as a function of geocentric latitude,  $\theta$ , by

$$R_p = \frac{R \sqrt{1 - \epsilon^2}}{1 - \epsilon^2 \cos^2 \theta} \quad (4.2.2-18)$$

where

$$\epsilon^2 = 1 - (1 - f)^2, \quad f = 1/298.3 \quad (4.2.2-19)$$

The maximum latitude,  $\theta_{MAX}$ , is  $(180 - i_{SS})$  degrees. Since  $i_{SS} = 99.088$ ,  $\theta_{MAX} = 80.912$ , and  $R_e$  is 3432.665 nautical miles. With  $r$  (at  $w = 90^\circ$ ) =  $a - \Delta r = 3537.492$ , the actual altitude,  $h_{90}$ , at  $w = 90^\circ$  is 502.83 nautical miles. At the equator,  $h_E$  is  $h + \Delta r = 493.145$  nautical miles. (Note here that  $r$  is geocentric radius.)

Figure 4.2-3 shows the actual altitude and radial distance variations with angular travel. Also shown is the semi-major axis and orbit altitude.

Additional perturbations to the orbit were examined. They included solar-lunar gravitation perturbations and solar radiation pressure. The purpose of examining these perturbation sources was to determine if there is a secular perturbation to an orbit parameter (e.g. nodal precession rate) that could be compensated for via a slight change to one or more of the nominal orbits' parameters (e.g. inclination).

Solar and lunar gravitation attractions principally affect the eccentricity and the orientation of the orbit plane. Very small cyclic variations to the orbit period sometimes results. This perturbation was analyzed with the use of a general perturbation computer program, the perturbations are assumed constant over one orbit and the integrated effect used to update the orbit parameters for the next orbital rev.

As a result of this analysis, a secular perturbation to the orbit inclination was observed. It decreased at an approximately linear rate to 99.045 degrees,  $\Delta i = -.043$  degrees/year. This altered the orbit plane's nodal precession rate which also decreased linearly. An ascending node error then builds up as a function of time squared. At the end of a year this error is 0.8 degrees. This represents 3.2 minutes of error in local time at ascending node as well as an error of 48 nautical miles in ground track longitude. The ground track error can be compensated for by decreasing the nominal orbital altitude by approximately .015 nautical miles, the nodal timing error being accepted. Another approach is to alter the initial inclination by increasing it .021 degrees, to 99.109 degrees. Now, after a half year the nodal error would be 0.2 degrees, at which time the inclination would be down to  $\approx 99.088$  degrees. The nodal error will then drift back to zero degrees at the end of a year. Either approach is acceptable but further analysis is required to select the best method for compensation.

The influence of solar radiation pressure on the orbit was examined via a computer program that uses a finite perturbation technique. The program was modified to allow representation of the solar radiation as a constant inertial acceleration on the ERTS during its sunlit portions of the orbit. The total radiation pressure force,  $F_R$  is represented by

$$F_R = C_S P_R A_E \quad (4.2.2-20)$$

where  $P_R$  is the solar pressure at the earth ( $9.85 \times 10^{-7}$  pounds per square foot),  $A_E$  is the projected area of the ERTS satellite and  $C_S$  a coefficient representing the effectiveness of the impinging radiation on the surface of the satellite.  $C_S$  is chosen as 2 (specular reflection), to represent the worst case conditions.

No change to any of the orbit parameters was observed as a result of this analysis.

Some data from the Nimbus B2 satellite was examined to determine what perturbations to the Nimbus orbit has occurred. The Nimbus orbit is approximately 100 nautical miles higher than ERTS where atmospheric drag perturbations are negligible, thus, the effects of other perturbations will not be obscured by drag decay. From reference 3, the apogee and perigee altitudes on May 15, 1969 were given as 1135 KM/1075 KM. On July 30, the apogee/perigee difference was increased by 10 KM, they were 1140/1070 KM. Three months later, the apogee/perigee had returned to their original values.

The apogee/perigee differences observed are most likely attributable to solar radiation pressure although further examination of the data is required to substantiate this conclusion. The most important conclusion drawn from this data is in that perturbations to the in-plane orbit parameters (eccentricity and semi-major axis) are extremely small. When compared to the expected drag forces to be experienced by the ERTS satellite, these other perturbations (excepting solar-lunar gravity) are considered negligible.

#### 4.2.3 DRAG DECAY

There are two major areas of study involved in drag decay analyses selection of an atmospheric model for the time period of interest (1972-1973), and the calculation of ballistic coefficient,  $W/C_D A$ .

##### 4.2.3.1 Density

The atmosphere model agreed upon with GSFC is the U.S. Standard Atmosphere Supplements, 1966. The independent variable is exospheric temperature. Tables are provided which relate altitude and exospheric temperature to atmospheric density. The equations used and the appropriate constants are given in reference 1. The effects taken into account are the 11 year solar cycle variation (characterized by the 10.7 cm solar flux in units of  $10^{-22}$  watts/m<sup>2</sup>/cycle/sec), the semi-annual variation to the 11 year cycle, the diurnal variation which includes the "diurnal bulge" (atmosphere bulges out slightly at maximum temperature points), the local hour angle to the sun and the satellites latitude, and the geomagnetic activity. The exospheric temperature calculation,  $T_{\infty}$  is used to enter the tables given in the Atmosphere Supplement. The satellites' altitude, which varies with latitude (see Figure 4.2-3) is also used in the tables. Reference 2, a NASA document, has additional equations in which it is possible to compute the density directly instead of through the tables.

Temperature and the density calculations were made for single orbits at 8 different times of the year, thru 1972 and 1973. The "mean density"  $\bar{\rho}$  is obtained by integrating the density profile over a complete orbit. That is

$$\bar{\rho} = \left( \sum_{i=1}^n \rho_i' \Delta t_i \right) / \tau \quad (4.2.3-21)$$



where  $\rho_1 \Delta t_1$  is the effective density over a small (1<sup>th</sup>) segment of the orbit. The orbit is divided into n segments.  $\tau$  is the total orbit period. The mean density as obtained in this manner is plotted in Figure 4.2-4. Subsequently, these densities, together with  $C_{DA}$ , will be used to generate the drag force, orbit altitude decay rate, and orbit velocity loss.

#### 4.2.3.2 Ballistic Coefficient

Calculation of ballistic coefficient,  $W/C_{DA}$  depends on satellite weight, W, and the summation of all the  $C_{DA}$ 's. Each package on the ERTS has a cross sectional area normal to the velocity and a corresponding drag coefficient depending on the shape of the particular package. The following drag coefficients have been used

<u>Shape</u>	<u><math>C_D</math></u>
Planes	2.8
Cylinders	2.2
Spheres	2.0
Shear	0.075

These coefficients assume the velocity (wind) vector is normal to the plane or the cylindrical axis of rotation. Since the solar paddles rotate with respect to the velocity vector, the solar paddles'  $C_D$  is integrated over one revolution. In this case, the drag is then found to be attenuated by a factor of  $2/\pi$

The shear force, or skin friction, is that drag force occurring on surfaces that are parallel to the velocity direction, and it is necessary to estimate the surface areas involved. The total contribution of this effect to the total drag force is slightly less than 2.0 percent

Table 4.2-2 shows the  $C_{DA}$  calculations for each of the major ERTS components and structure. The total effective  $C_{DA}$  is seen to be 173.2 square feet.

#### 4.2.3.3 Altitude Decay Rate

The gradual loss in altitude due to atmospheric drag can be computed, quite accurately, as derived in the following equations. (The accuracy, of course, is limited by  $W/C_{DA}$  and density uncertainties.) The drag force,  $F_D$ , is

$$F_D = \frac{1}{2} \bar{\rho} V^2 C_{DA} \quad (4.2.3-22)$$

where V is orbital velocity = 24253 fps or 7392 m/s. In the calculations performed during ERTS study,  $C_{DA}$  and V were assumed constant. The velocity actually varies by 20 fps between the equator and the pole. This variation ( $\pm 10$  fps) is negligible when computing drag force since it represents only  $\pm .04$  percent of the mean orbital velocity.

$C_D A$  also varies because the solar paddles are essentially inertially oriented over a given rev., and can more accurately be expressed as

$$C_D A = 82.3 + |142.8 \sin w| \quad (4.2.3-23)$$

Thus, for example, when at the equator, at the equinox, the paddle faces are 90 degrees from the velocity vector, i.e. edge into the wind, and they generate the minimum drag force. At maximum latitude ( $w = 90$  degrees) the full paddle surfaces are normal to the velocity vector. However, the temperature variation over an orbit is a function of the hour angle to the sun. Higher temperatures are observed on the daylight side of the earth, rather than on the darkside, and produce a far greater density variation than does the altitude change (913 KM to 932 KM) between equator and pole. Thus the solar paddles go thru their entire excursion during both the maximum density and minimum density regions. Thus the effect of varying  $C_D A$  will essentially cancel over each orbit.

The expression for altitude loss per orbit is obtained by equating the rate of energy loss due to drag force with rate of orbital energy loss due to changes in semi-major axis.

The drag force energy loss  $dE/dt$ , for a circular orbit is

$$\begin{aligned} \frac{dE}{dt} &= \vec{F} \cdot \vec{V} \\ dE/dt &= -F_D V \\ &= -1/2 V^3 C_D A \end{aligned} \quad (4.2.3-24)$$

where the angle between  $F_D$  and  $V$  is the flight path angle and is assumed to be essentially zero.

In terms of orbital energy,  $E_o$ ,

$$E_o = -\frac{m\mu}{2a}, \quad (4.2.3-25)$$

and the time rate of change of energy with change in semi major axis,  $da/dt$ , is

$$\frac{dE_o}{dt} = \frac{m\mu}{2a^2} \frac{da}{dt} \quad (4.2.3-26)$$

where  $\mu$  is the gravitational constant ( $R^2 g$ )

Equating the right hand sides of equations (24) and (26) yields the following integral equation for da

$$\int_{a_0}^{a_1} \frac{da}{a^{\frac{1}{2}}} = - \int_0^{\tau} \mu^{\frac{1}{2}} \bar{\rho} \frac{C_D A}{m} dt \quad (4.2.3-27)$$

where the substitution  $V^2 = \mu/a$  has been made and  $a_1 - a_0$  is the change in semi major axis,  $\Delta a$  over one orbit rev. Integrating yields

$$2(a_1^{\frac{1}{2}} - a_0^{\frac{1}{2}}) = \mu^{\frac{1}{2}} \bar{\rho} \frac{C_D A}{m} \tau \quad (4.2.3-28)$$

Letting  $a_1 = a_0 + \Delta a$  to obtain  $2 \left[ (a_0 + \Delta a)^{\frac{1}{2}} - a_0^{\frac{1}{2}} \right]$  on the l.h.s of (4.2.3-28), expanding the first term and retaining only the first order term in  $\Delta a$  since  $\Delta a \ll a_0$ , yields  $\Delta a/a_0^{\frac{1}{2}}$  for the left hand side of (28).  $\Delta a$  then becomes

$$\Delta a = \mu^{\frac{1}{2}} a_0^{\frac{1}{2}} \bar{\rho} \frac{C_D A}{m} \tau \quad (4.2.3-29)$$

which can be rearranged, using the  $V^2$  expression above, to give

$$\Delta a = V_0 a_0 \bar{\rho} \frac{C_D A}{m} \tau \quad (4.2.3-30)$$

where the subscript zero indicates values at the beginning of the orbit. This analysis assumes circular or nearly circular orbits which decay very gradually with no change in eccentricity or velocity path angle. These are valid assumptions for the ERTS orbit.

The altitude decay rate per day is obtained by multiplying  $\Delta a$  of Equation 4.2.3-30 by 13-17/18, the number of revs per day.

From Figure 4.2-4,  $\bar{\rho}$  is obtained, and a curve of altitude decay rate,  $\dot{h}$  vs time of year can be drawn. This is shown in Figure 4.2-5. For a spring 1972 launch, the average decay rate over the year is approximately .0066 nautical miles per day which amounts to 2.42 nautical miles per year. A spring 1973 launch would have an average daily decay rate of about .0056 nautical miles per day or 2.05 nautical miles per year.

#### 4.2.4 NOMINAL GROUND TRACK CONTROL

The orbit/ground track control problem can now be examined in detail and a mechanism for describing the deviations of day to day ascending node locations from their nominal no-drag locations can be formulated. The nominal control technique is to insert the ERTS into an orbit whose semi-major axis,  $a$ , is slightly higher, by  $\Delta h$ , than the semi-major axis corresponding to the nominal altitude. The satellite decays down to the nominal altitude,  $h_n$ , and continues to an altitude  $h_n - \Delta h$ . At this point an orbit adjust velocity impulse is applied and the satellite raised back up to an altitude  $h_n + \Delta h$ . The decay time,  $t_d$ , is expressed as  $\Delta h/\dot{h}$  where  $\dot{h}$  is the mean altitude decay rate which is assumed to be constant over the small altitude range  $\Delta h$  ( $< 1.0$  nautical miles). It is desired to space the orbit adjust maneuvers at least 18 days (one coverage cycle) apart. Figure 4.2-5 shows that it will probably be necessary to select a mean decay rate prior to each orbit adjust in order to plan the control of the next decay cycles ground track variations.

##### 4.2.4.1 Graphical Description

A convenient method for pictorially describing the ground track variation with altitude decay is shown in Figure 4.2-6, a and b. The top half of the figure shows ascending node deviations from those nodes that would be obtained for  $h_n$  and as shown in Figure 4.2-1. The bottom of the figure shows how the deviations would appear on a display as given in Figure 4.2-1. The solid lines show the evenly spaced nominal ascending node points, the broken lines show the actual node points.

The parabolic curve at the top of Figure 4.2-6 shows how the first rev. of each day deviated from the nominal ascending node point. Using the numbers shown, rev. 1 on day two (BEGIN REV 15) crosses the equator  $\approx .42$  nautical miles west of the nominal point. This is shown also on the bottom of the figure, although not to scale. The deviations between broken and solid lines have been exaggerated to enhance clarity. In this case the distance between adjacent ground traces is 86.48 nautical miles ( $86.06 + .42$ ). Day 3's rev begins 791 nautical miles west of the nominal day 3 first rev. However, the distance between adjacent ground traces is only 86.43 nautical miles. The mean altitude on day 2 is lower than day 1's, therefore, the adjacent traces are not as far apart even though the total deviation from the no-drag nominal increases. At the end of last rev on day 9 (begin Rev 1, day 10) the satellite is at the nominal altitude but the node point is 2.002 nautical miles from the no decay nominal. At this point the distance between adjacent ground tracks is minimum, 86.085 nautical miles. During the second half of the decay cycle, the first half phenomena is reversed. The distance between adjacent tracks becomes smaller and is always less than 86.06 nautical miles. On day 18, it is 85.64 nautical miles ( $86.06 - .42$ ).

If the orbit adjust maneuver raised the altitude back up to exactly  $h_n + \Delta h$  at the start of the second coverage cycle, ALL the ground tracks and subsatellite swaths will be identical during the second coverage cycle to those of the first coverage cycle. There would be no variation between corresponding revs of successive coverage cycles! (This assumes of course the same decay rate during both decay cycles).

The above example used an altitude decay rate,  $\dot{h}$ , of 0.006 nm. Figure 4.2-7 shows the altitude decay curve when  $\dot{h} = .004$  and  $.008$  nm. Note that the  $\Delta h$ 's have been adjusted to obtain exactly 18 day decay cycles. In dashed lines is shown 2 additional situations, where  $\Delta h$  is maintained constant (.054 nm as in the .006 nm/day  $\dot{h}$ ) but  $\dot{h} = .004$ , and  $.008$  nm/day. The middle one is simply a repeat of Figure 4.2-6. This shows the effect of  $\dot{h}$  errors.

As a final consideration, a two coverage cycle, 36 day decay cycle, is examined, and shown on Figure 4.2-7 for  $\dot{h} = .006$  nm. Now there will be deviations between corresponding rev numbers on successive coverage cycles. For this case the maximum deviation occurs for REV 1 of day 1 and REV 1 of day 19. The distance is 8.008 nm. The maximum distance between adjacent ground tracks is .82 nm, twice that of the 18 day,  $\dot{h} = .006$  nm, decay cycle. It will be shown in the following section that adjacent distances (day to day) are a function of  $\Delta h$ , while the distances  $\Delta s$  (cycle to cycle) are a function of  $\Delta h^2$ .

The traces shown in figures 4.2-6 and 4.2-7 are very useful for examining the effects of errors in  $\Delta h$  due to orbit determination errors and orbit adjust residuals. These considerations will be examined in detail in section 4.2.5 covering error analyses.

#### 4.2.4.2 Mathematical Description of Altitude Effects on Ground Track Deviations

The equations from which altitude-ground track deviations curves of the preceding section were generated will now be derived.

The basic approach in this analysis is to take the longitude change per orbit,  $\Delta \phi_d$  as given in equation (4.2.2-7) and determine the variation  $\Delta(\Delta \phi_d)$  due to orbit period variations. Then the errors in orbit period  $\Delta \tau$  due to altitude variations  $\Delta h$  as in equation (4.2.2-15) will be determined. Thus, the variation in ground track with altitude  $\Delta(\Delta \phi_d)/\Delta(\Delta h)$  will be determined.

Differentiating equation (4.2.2-7) yields

$$\frac{d(\Delta \phi_d)}{d\tau} = - (w_e - \dot{\Omega}_o) \quad (4.2.4-31)$$

or

$$\Delta(\Delta \phi_d) = \Delta \phi_d \delta \tau / \tau \quad (4.2.4-32)$$

Equation (4.2.2-15),  $\Delta \tau$  as used in this analysis requires only the differential of the Keplerian term  $2\pi \sqrt{a^3/\mu}$ , the first term in equation (4.2.2-15). The second term is only .06 percent of the first. Therefore, represent  $\delta \tau$  as

$$\frac{\Delta \tau}{\tau} = \frac{3}{2} \frac{\Delta a}{a} \quad (4.2.4-33)$$

and  $\Delta(\Delta\phi_d)$  in degrees is

$$\Delta(\Delta\phi_d) = \frac{3}{2} \frac{\Delta a}{a} \Delta\phi_d \quad (4.2.4-34)$$

At the equator, 1 degree  $\approx$  60 nm, also, there are 13-17/18 revs per day. Thus  $\delta(\Delta\phi_d)$  per day in nm is computed to be

$$\Delta(\Delta\phi_d) = 8.23 \Delta a \quad (4.2.4-35)$$

where  $\Delta a$  is in nm.

This equation applies to a constant  $\Delta a$ , or  $\Delta h$ . The designation  $\Delta h$  will be used for convenience. For nominal operation, the desired  $\Delta h$ , when the total decay time is  $t_d$ , is

$$\Delta h = \frac{1}{2} t_d \dot{h} \quad (4.2.4-36)$$

The average altitude deviation during decay from  $h_n + \Delta h$  to  $h_n$  is  $\Delta h/2$ . Equation (35) applies for one day, for  $t$  days,  $\Delta(\Delta\phi_d)$  is

$$\Delta(\Delta\phi_d) = 8.23 \Delta h t \quad (4.2.4-37)$$

Let  $\Delta(\Delta\phi_d)$  be designated as  $\Delta S$ . The maximum value of  $\Delta S$  occurs when  $t = t_d/2$  (the time to decay thru  $\Delta h$ ).

$$\Delta S_{MAX} = 8.23 \frac{\Delta h}{2} \frac{t_d}{2} \quad (4.2.4-38)$$

where  $\Delta h$  is divided by two since the average  $\Delta h$  during decay from  $h_n + \Delta h$  to  $h_n$  is  $\Delta h/2$ . Thus an expression for  $\Delta S_{MAX}$  is

$$\Delta S_{MAX} = 2.06 \Delta h t_d \quad (4.2.4-39)$$

A more useful expression results if  $t_d$  is eliminated and  $\Delta S_{MAX}$  is made a function of  $\Delta h$  and  $\dot{h}$  only. Such an expression will be much more useful for error analysis studies to be considered in section 4.2.6. Using equation (4.2.4-36) to eliminate  $t_d$  in equation 4.2.4-39 yields

$$\Delta S_{MAX} = \frac{4.12 \Delta h^2}{\dot{h}} \quad (4.2.4-40)$$

This expression was used to generate the curves given in Figures 4.2-6 and 4.2-7.

## 4 2 5 ORBIT ERROR ANALYSIS

The nominal orbit decay rate and ground track variations have been defined. Control of the orbit and its ground trace would be a simple matter were it not for the imperfections in the performance of other system elements. The launch vehicle will inject the ERTS into an orbit with some probability of error, the orbit adjust system will leave small residual velocity errors in the orbit, the tracking network will determine the orbit quite accurately but with some residual uncertainty, and the altitude decay rate will vary from its predicted value. In addition, the attitude control systems' pitch nozzle may perturb the orbit when performing attitude control maneuvers. Before an analysis of the altitude decay/ground track variation phenomena can be analyzed, it is necessary to delineate the contributions of all these error sources to the subsequent orbital motion and ground track variation.

It will be necessary, therefore, to specify all the orbit adjust system velocity requirements before the frequency and magnitude of  $\Delta V$  maneuvers are defined. The orbit adjust residual errors can then be defined.

4 2 5 1 O/A Subsystem  $\Delta V$  Requirements

The ERTS orbit adjust system employs a monopropellant hydrazine fueled propulsion system operating in a blowdown pressurant mode feeding two "one-pound" thrusters which are aligned in opposite directions along the vehicle X axes. Thus velocity corrections can be made in either direction along the velocity vector, to either increase or decrease orbital energy. The thruster whose propellant is expelled along the minus X axis is canted upward from the -X axis by about 21.5 degrees (angle depends on final c.m. location) to allow the thrusters' plume to clear paddle latch mechanism and struts. A complete description of this subsystem and the geometry of its thrusters with respect to the spacecraft axes is contained in Volume II Section 6.

## 4.2.5.1.1 Launch Vehicle Injection Errors

The 99 percent probability injection errors from the DELTA launch vehicle have been specified as follows:

<u>Parameter</u>	<u>99 Percent Probable Minimum</u>	<u>99 Percent Probable Minimum</u>
Apogee altitude (nm)	- 3 0	+11 0
Perigee altitude (nm)	-11 0	+ 3 0
Orbit Eccentricity		0 0011
Orbit Inclination (degrees)	- 0 03	+ 0 03
Orbit Period (minutes)	- 0 3	+ 0 3

The altitude errors and resulting period errors propagate to almost 60 nm of ground track error after one day if not removed. This is prohibitive considering the tight tolerances on the ground track control requirements. The maximum altitude error to be removed is 14 nm. Combinations of two extremes of errors (e.g. -11, +3 or 11, -3, or 11, -11)

cannot occur since the maximum apogee/perigee difference can only be 8 nm as indicated by the maximum eccentricity of 0.0011. Depending on where in the orbit the altitude errors are removed, the maximum apogee/perigee difference cannot exceed 22 nm (8 nm from maximum insertion eccentricity and 14 nm from maximum altitude correction). This is well within the 47 nm allowance required ( $e \leq 0.006$ ).

The inclination errors propagate to only 5 minutes of error in the time at the ascending node after one full year. This is considered quite tolerable in the light of the 30 minute launch window tolerance. It is necessary therefore only to remove the altitude induced launch vehicle errors. The following analysis shows that this will require 21.7 feet/sec of velocity impulse. From the vis viva integral, the impulsive velocity required to remove altitude errors when thrusting at an apse is derived. The vis viva integral is

$$V^2 = \frac{2\mu}{r} - \frac{\mu}{a}$$

which assumes the satellite is at apogee,  $r_a$  is perigee distance. Differentiation yields

$$2 \frac{\Delta V}{V} = - \frac{2\mu}{V^2 r_a} \frac{\Delta r_a}{r_a} + \frac{\mu}{V^2 a} \frac{\Delta a}{a}$$

However,  $r_a$  will not change when the impulse is applied at  $r_a$ . Also, for a near circular orbit  $V^2 = \mu/a$ . The actual velocity varies by only  $\pm 50$  fps from the mean velocity of 24250 fps when the orbit eccentricity is about 0.002. Thus approximating  $V$  by  $\sqrt{\mu/a}$  is valid. Then, for  $\Delta V$

$$\Delta V = \frac{1}{2} V \frac{\Delta a}{a} \quad (4.2.5-42)$$

The coefficient is then 3.1 fps of  $\Delta V$  for each nm of semi-major axis change or 1.55 fps for each nm of altitude change. Since, in this example, the apogee distance does not change, the perigee must change by 2 nm to get 1 nm of semi-major axis change. It can be shown that identical results are obtained if the impulse is applied at perigee and the same assumptions of near circularity are made. Thrusting over an extended orbital arc or applying impulses at points between apogee and perigee produces only second order deviations in the value of the coefficient.

#### 4.2.5.1.2 Drag Induced Altitude Decay

Figure 4.2-5 shows the mean altitude decay rate to be 0.066 nm per day or 2.42 nm/year. The required velocity impulse to make up for this energy loss is 7.5 fps per year. Again the coefficient of 3.1 fps of  $\Delta V$  per nm of semi-major change is used. Here the altitude of the entire orbit decreases, not just at one point, thus altitude decay and semi-major axis decrease are the same and 3.1 fps/nm is required to restore the energy lost.



#### 4.2.5.1.3 Attitude Control Effects

When the attitude control system engines are fired and a pure couple is not generated, then a change to the orbit velocity vector is produced. If the resultant  $\Delta V$  change is normal to the orbit plane, as is the case for the roll control jets, a change in inclination, or line of nodes, or both takes place. Over 4 fps of  $\Delta V$  is necessary in order to change either by 0.01 degrees. Considering that the total impulse from the roll control jets over one year will be less than 3 fps, and there is some distribution of roll jet firings throughout the orbit much less than 0.01 degrees change would be expected. Thus roll jet induced changes to the velocity vector are negligible.

Pitch attitude control correction impulses from the pitch control nozzles (aligned along the  $\pm X$  axis) coincide nominally with the velocity vector and will increase or decrease this velocity slightly with each gating (firing). If the number of positive and negative firings are not equal, their effect must be compensated. Analyses have shown that an uncompensated "gating" or firing, would be expected approximately once every three orbits. Depending on spacecraft mass distribution, the cross products of inertia could in the worst case produce as much as one uncompensated gate per orbit. Each firing or gating produces a thrust level of 0.195 pounds for fifty milliseconds, resulting in an impulse of 0.00975 pounds-sec. With an ERTS mass of 49 slugs, the  $\Delta V$  per gate is  $\approx 2.0 \times 10^{-4}$  fps. In one year (5090 orbits) this amounts to 1.0 fps at one gate every orbit and 0.34 fps at one gate every three orbits. (Flight data shows Nimbus B2 gates on the average of once every third or fourth orbit with the same jet used for all the gatings.) Therefore, a worst case allotment of one fps per year of  $\Delta V$  will be provided by the Orbit Adjust System.

#### 4.2.5.1.4 Additional Losses

There are a number of other sources of relatively small  $\Delta V$  requirements. There are predictable efficiency losses due to the canted engine (7-8 percent). Also, a 4-5 percent loss results from the thrusting over a 30 to 50 degree arc that is necessary for removing the injection errors with the "one-pound" thrusters. With an average thrust level from the orbit adjust system of 0.75 pounds during injection error removal, 27 minutes of total thrusting time is required to impart 25 fps of orbit velocity change. Two equal duration burns would each cover 47 degrees of orbital arc. A low thrust, finite differencing computer program simulation was used to evaluate the efficiency loss due to continuous thrust operation. As a reference point for comparison, the program was also used to compute the orbit change when the total  $\Delta V$  impulse was applied at perigee. This was done by increasing the thrust level by a factor of  $10^3$  and reducing thrust duration by an equal amount. Comparison between the two cases showed the 4 to 5 percent difference. Also the 3.1 fps/nm coefficient was verified.

System error sources of a random or statistical nature produce additional requirements. The sources of these errors are

- 1) Thrust vector uncertainty of 0.25 degrees
- 2) Final alignment to c.m. could alter cant angle by a maximum 1.78 degrees. These two error sources produce a velocity make-up requirement of about 1.0 percent.

- 3) Attitude control system errors - The yaw angle could build up to 10 degrees during long duration burns used for injection error removal. The average loss in efficiency (a cosine effect) is less than 1.0 percent. Pitch and roll errors of up to 5 degrees might occur and will produce a 2.5 percent loss if the pitch error adds directly to increase the effective cant angle by 5 degrees. The attitude errors, root sum squared are 2.7 percent.

The root sum square of the errors produced during the long duration burn for removing injection error, is 2.9 percent.

During drag make-up, thrusting is over a very short arc ( $\sim 3$  deg) and no inefficiency is attributed to the continuous thrust effect. However, the canted nozzle is required for all drag make-up  $\Delta V$  maneuvers since it adds  $\Delta V$  to the orbital velocity vector, again a 7 percent loss in efficiency is experienced.

An additional  $\Delta V$  margin ( $\approx 30$  percent) to allow for other contingencies is provided. This amounts to just over 10 fps. Table 4-2-4 summarizes all the Orbit Adjust System  $\Delta V$  requirements. The total  $\Delta V$  capability to be provided by the system is 45 fps.

It should be pointed out that uncertainties in metering and commanding the required  $\Delta V$  impulse from the O/A subsystem will contribute to  $\Delta V$  residuals but not necessarily to additional  $\Delta V$  requirements. On a short duration burn, a 6 percent uncertainty in the  $\Delta V$  impulse is possible (3 $\sigma$ ). RSS'ed with the 1 percent errors in thrust vector control, a 6.1 percent total uncertainty might be experienced when performing drag make-up maneuvers.

Total impulse uncertainties due to such things as propellant temperature variations and unavailable propellant caused by inefficient propellant expulsion have been taken into account by the orbit adjust subsystem allotment of hydrazine propellant and are not included here.

#### 4-2-5-2 Launch Vehicle Injection Error Removal Techniques

Before orbit correction residuals can be determined, it is necessary to formulate a technique for removing the injection errors. Then the errors that result, when this technique is employed, can be determined. There is no attempt made to optimize the technique for the purpose of minimizing correction residuals. Rather, the philosophy is to keep the number of O/A burns to a minimum, to allow for performing these burns in view of a ground station, and to limit the duration of each burn to prevent excessive attitude control error buildup during the burn.

An approach which meets this philosophy requires, in the worst case, two major burns of 12 to 14 minutes duration each, and a third trim maneuver burn of less than a minute duration. These first two burns will remove almost all of the injection errors. The third burn, if necessary, would minimize the orbit error remaining subsequent to the final O/A correction  $\Delta V$  maneuver.

The O/A thrust level for the first burn is expected to average about 0.8 pounds. With the ERTS mass at about 49 slugs, 13 fps of  $\Delta V$  ( $\approx 1/2$  the maximum injection error  $\Delta V$ ) can be imparted in  $\approx 800$  seconds. During this time the yaw attitude error can build up to 10

degrees, pitch and roll to 5 degrees. At the completion of the burn, the orbit will again be determined via the ground tracking and data system and the effectiveness of the burn determined. Performance of the attitude control system will be assessed and most of the attitude control system errors determined. The orbit determination data would aid in determining thrust vector errors. Actual propellant impulse,  $I_{sp}$ , would also be deduced.

The performance of the second burn can now be predicted to a high degree of accuracy. None of these errors, individually, should exceed 1 percent and the accuracy of the second burn should be predictable to within 1.5 percent. In order to prevent over-correction, the second burn's  $\Delta V$  will be intentionally biased short of the total  $\Delta V$  error by an amount proportional to the expected uncertainty in the burn. The uncertainty in the burn should be no more than 1.5 percent of the total velocity impulse imparted by the burn.

The third burn will remove the bias together with any residuals from the second burn. The resulting altitude errors, expected to be very small, will be superimposed on the altitude decay loss and will eventually be removed by the first drag make-up orbit adjust.

It is proposed that the same engine be used for removing all of the altitude injection error, no attempt will be made to circularize the orbit via burns with both thrusters. Thus, the planned bias should further prevent the need for thrusting in both directions.

#### 4 2 5 3 Orbit Correction Residuals

To gain a complete understanding of the expected extremes on the ground track generation process, it is necessary to include all the possible sources of error that contribute to  $\Delta h$  errors. The errors in  $\Delta h$  are made up of the residuals following an orbit adjust correction. The principle sources of error result from orbit adjust corrections and from orbit determination uncertainties. Orbit adjust errors are in the form of  $\Delta V$  residuals that result in  $\Delta h$  being either too large or too small. Orbit determination uncertainties result in an inaccurate computation of the required change in semi-major axis and consequently a  $\Delta V$  command that is in error. Uncompensated pitch attitude control impulses will be taken into account as part of the uncertainty in altitude decay rate.

#### 4 2 5 3 1 Orbit Adjust Subsystem Correction Residuals

Two separate sets of residuals will be generated, one following corrections to remove launch vehicle injection errors, the other following a drag make-up O/A maneuver.

In Section 4 2 5 2, the technique for removing launch vehicle injection errors was described. Assuming that worst case errors occur, (25 fps  $\Delta V$  correction necessary) the first burn, of 800 seconds duration will have removed 13 fps of velocity error. The performance will then be examined via telemetry observation and from ground tracking orbit determinations. The second burn will require removal of most of the remaining 12 fps. The accuracy of the second burn will now be predictable to within 1.5 percent. The bias will be 1.5 percent of 12 fps or 0.18 fps. The maximum residual is 36 fps, which is twice the bias. This assumes errors in the burn are in the same direction as the bias. The maximum error on the short duration burns are 6.1 percent (Section 4 2 5 1 4). Thus a maximum ( $3\sigma$ ) residual of

$\approx 0.022$  fps can be expected due to the O/A subsystem upon removal of launch vehicle injection errors. From equation (4.2.5-42), the equivalent residual semi-major axis error produced by this velocity residual is  $.0071$  nm.

The drag make-up correction residuals will again be 6.1 percent of the  $\Delta V$  impulse. This impulse magnitude is dependent upon the  $\Delta h$  to be provided which, in turn, is dependent on time lapse between drag make-up corrections. Using 7.5 fps per year as the basic  $\Delta V$  requirement, a correction every 18-day (one coverage cycle) would require 0.375 fps, while 36-day decay time would require, on the average, 0.75 fps. The residual velocity errors are then 0.023 fps and 0.046 fps. The equivalent semi-major axis errors are 0.0074 nm and 0.0148 nm.

#### 4.2.5.3.2 Orbit Determination Uncertainties

Orbit determination uncertainties lead to orbit correction residuals that appear as altitude errors. Again, two sets of numbers will be generated, one for launch vehicle injection error removal, the other for drag make-up corrections. It is assumed that many of the MSFN - 30 foot dish tracking stations will be available for orbit determination purposes following launch vehicle injection and up until the time ERTS is placed into its nominal orbit. This will provide extensive coverage of all operations and should provide a very accurate determination of the orbit.

Subsequent to launch vehicle injection error removal, it has been assumed that only the MSFN tracking station at Corpus Christi, Texas will be dedicated full time to the ERTS mission.

Early in the study, information was provided by GSFC's Tracking and Data Systems Branch that indicated the total ERTS orbit position uncertainty would be on the order of 100m ( $1\sigma$ ) based on one day of tracking with the 30' MSFN stations and about 260m ( $1\sigma$ ) based on one day of tracking data from the Texas station. For preliminary analysis, 30 semi-major axis uncertainties were derived and were used for ground track control analysis presented in Section 4.2.6. Subsequent to this analysis, a complete 6 x 6 covariance matrix of orbit parameter uncertainties were received from GSFC, one for each of the two tracking situations. The semi-major axis errors were computed from the two covariance matrices using standard statistical techniques (as described in Section 4.2.5.3.4). Assuming the matrices as shown in Tables 4.2-4 and 4.2-5 are correct, the  $\delta a$ 's resulting from them appear to be prohibitively large, three times as large as the preliminary  $\delta a$ 's from 260m error from Texas, and six times as large as the preliminary  $\delta a$  error from the 30' MSFN stations. The preliminary  $\delta a$ 's therefore were used for the orbit control studies presented in Section 4.2.6. These studies were begun prior to reception of the covariance matrix. Since the preliminary  $\delta a$ 's were found to provide marginal but adequate performance, it was felt that repeating the studies with the larger  $\delta a$ 's would only confirm the conclusion that orbit determination uncertainties represent the largest single contribution to the problem of maintaining ground track control. It is therefore recommended that the ERTS orbit determination procedure (number of stations, data processing, filter, etc.) for the operational phase of the ERTS mission be reviewed for any reasonable improvements in the estimation of semi-major axis. In Section 4.2.6.2, consideration is given to techniques for prediction of ground track

nodal crossings and decay rates, and for planning orbit adjust maneuvers, which should allow satisfactory performance with the orbit determination capability as presently estimated via the covariance matrices provided by GSFC

The semi-major axis error was obtained from the 100m and 260m position uncertainty designated as  $\delta P$ , in the following manner. It was assumed that only 60 percent of the error was along the in-track direction. The time to traverse this distance is  $0.6\delta P/V$  where the time computation is essentially independent of errors in velocity,  $V$ . The semi-major axis error,  $\delta a$ , is then computed from equation (4.2 4-33) which rearranged yields:

$$\delta a = \frac{2}{3} \frac{a \delta \tau}{\tau}$$

During launch vehicle injection error removal, where  $\delta P = 100$  m,  $\delta \tau$  is computed to be .024 sec ( $3\sigma$ ) and  $\delta a$  to be 0.0102 nm ( $3\sigma$ ).

During the rest of the ERTS mission,  $\delta P = 260$ m  $\delta \tau$  is computed to be 0.624 seconds ( $3\sigma$ ) and  $\delta a$  to be 0.27 nm ( $3\sigma$ )

#### 4 2 5 3 3 Total Correction Residuals

The total errors in semi-major axis at the conclusion of an orbit adjust velocity impulse maneuver is the root sum square of the two individual sources

$$\delta a_R = \sqrt{(\delta a)_{O/A}^2 + (\delta a)_{O/D}^2} \quad (4 2 5-43)$$

When removing launch vehicle injection errors, the values for  $(\delta a)_{O/A}$  and  $(\delta a)_{O/D}$  ( $\delta a$  from orbit adjust and from orbit determination residuals respectively) were shown to be

$$(\delta a)_{O/A} = 0.0071 \quad (\delta a)_{O/D} = 0.0102 \text{ nm}$$

The total error,  $(\delta a)_R$  is 0.0124 nm

When making up drag losses the values for  $(\delta a)_{O/A}$  and  $(\delta a)_{O/D}$  were shown to be

$$(\delta a)_{O/A} = 0.0074 \text{ (18-day)} \quad (\delta a)_{O/D} = 0.0267$$

$$(\delta a)_{O/A} = 0.0148 \text{ (36-day)}$$

The total RSS errors are 0.0277 nm and 0.0305 nm for the 18 day and 36 day durations between burns, respectively

These  $(\delta a)_R$  errors will be used in Section 4 2 6 to examine the effect of corrections residuals on the subsequent ground track (subsattellite swath) generation

First, though, a discussion of the method used in deriving  $(\delta a)_{O/D}$  from the GSFC provided covariance matrix will be given.

#### 4.2.5.3.4 Covariance Matrix Orbit Determination Uncertainties

The covariance matrices provided by GSFC, Tracking and Data Systems, are as shown in Tables 4.2-4 and 4.2-5. The nominal orbit elements associated with matrices are shown in Table 4.2-6. Also shown are other useful orbit parameters computed from the elements.

The purpose of this section is to show how the standard deviation of the semi-major axis  $\delta a$  was computed from the covariance matrix,  $\sigma_{cov}^2$ . The matrix  $\sigma_{cov}^2$  was computed in an Earth-centered equatorial inertial coordinate system,  $(X, Y, Z)$ .

$$\sigma_{cov}^2 = f(X, Y, Z, \dot{X}, \dot{Y}, \dot{Z}) \quad (4.2.5-44)$$

The sensitivity coefficients relating errors in semi-major axis to errors in  $X, Y, \dots, Z$  is required. Designate the resulting matrix as  $[\Delta a]$ . Then  $\sigma_{\delta a}^2$ , the variance, is computed from

$$\sigma_{\delta a}^2 = [\Delta a]^{1 \times 6} [\sigma_{cov}^2]^{6 \times 6} [\Delta a]^T{}^{6 \times 1} \quad (4.2.5-45)$$

The matrix  $[\Delta a]$  is a  $1 \times 6$  while  $[\sigma_{cov}^2]$  is a  $6 \times 6$ .

$[\Delta a]$  is computed as follows, from the vis-viva integral

$$\frac{\mu}{a} = \frac{2\mu}{r} - V^2 \quad (4.2.5-46)$$

Taking partial derivatives we obtain

$$\frac{-\mu}{a^2} \delta a = \frac{-2\mu}{r^2} \delta r - \frac{2V}{V^2} \delta V \quad (4.2.5-47)$$

or

$$\delta a = 2 \delta r + 2 \frac{r}{V} \delta V \quad (4.2.5-48)$$

where  $r = a$ ,  $\mu/a = V^2$  for orbits of very small eccentricity Using

$$r^2 = X^2 + Y^2 + Z^2 \quad (4.2.5-49)$$

and

$$V^2 = X^2 + Y^2 + Z^2 \quad (4.2.5-50)$$

we can obtain the appropriate partials for equation (48) They are

$$\partial r = \frac{X}{r} X + \frac{Y}{r} Y + \frac{Z}{r} \partial Z \quad (4.2.5-51)$$

and

$$\partial V = \frac{X}{V} \partial X + \frac{Y}{V} \partial Y + \frac{Z}{V} \partial Z \quad (4.2.5-52)$$

Substituting these into equation (48) yields for  $[\Delta a]$

$$\Delta a = \left[ 2 \frac{X}{r} \quad 2 \frac{Y}{r} \quad 2 \frac{Z}{r} \quad 2 \frac{\gamma}{V} \frac{X}{V} \quad 2 \frac{\gamma}{V} \frac{Y}{V} \quad 2 \frac{\gamma}{V} \frac{Z}{V} \right] \quad (4.2.5-53)$$

If six orbit parameters were being determined, then  $[\Delta a]$  would be a 6x6 matrix and  $\sigma^2 \delta a$  would also be a 6x6 covariance matrix. As is used here, however,  $[\Delta a]$  is a 1x6. After  $[\Delta a]$  multiplied by  $[\sigma^2 \text{cov}]$ , a 1x6 row matrix results. When this matrix is multiplied by  $[\Delta a]^T$  a single number results, namely the variance of  $\delta a$ ,  $\sigma^2 \delta a$ . The square root of a  $\sigma^2 \delta a$  is the "1 $\sigma$ " value of  $\delta a$ .

From the MSFN stations' covariance matrix,  $\delta a$  is computed to be 133 feet, or 0.022 nm. The "3 $\sigma$ " value for  $\delta a$  is then 0.066 nm. In section 4.2.5.3.2  $\delta a$ ,  $3\sigma$ , was computed as 0.0102 nm.

Using the Texas station generated covariance matrix,  $\delta a$  was computed to be 148 feet,  $\delta a = 0.0244$  nm,  $1\sigma$  or 0.073 nm,  $3\sigma$ .

#### 4.2.6 OPERATIONAL GROUND TRACK CONTROL

In Section 4.2.4, the influence of altitude decay on the ground tracks was shown. The parameter  $\Delta s$  (Equations 4.2.4-37 through 4.2.4-40) was shown to be a measure of a ground tracks deviation for an unperturbed no-drag nominal track. Now the effects of errors in  $\Delta h$ , to be designated as  $\delta a_R$ , on ground track control will be shown. Also shown will be the effects of errors in predicting  $\bar{h}$ . Decay cycles of 18, 27 and 36 days, nominal, will be examined. Nominal decay rates,  $\dot{h}$ , will be .005 nm/day and .0075 nm/day. Only the  $\delta a_R$  residuals after a drag make-up are considered since  $\delta a_R$  is smaller following launch vehicle injection error removal and applies for only one decay cycle. Altitude decay rate uncertainties are

estimated to be 15 percent. This estimation is based on data obtained from the U.S. Standard Atmosphere Supplements, and on the consideration that continued operation of ERTS at nearly constant altitude will produce determinations of  $h$  with sufficient accuracy to allow accurate prediction of  $h$  over the next decay cycle.

The first part of this study concerns the ground track deviations over one decay cycle only. Bounds are then placed on maximum decay time and/or maximum  $\delta a_R$ . The second part discusses control philosophy based on successive decay cycle control.

#### 4.2.6.1 Ground Track Variation Through a Single Decay Cycle

Figures 4.2-8 through 4.2-13 completely summarize the total extremes in ground track variation for the assumed three sigma errors,  $\delta a_R$  and  $\delta \dot{h}$ . Each figure shows the nominal decay cycle curve and two curves for the  $\pm 15$  percent  $\delta \dot{h}$  error. Also shown is the decay curve for  $\delta a_T = \Delta h \pm \delta a_R$  for  $\delta \dot{h} = 0$ , and for  $\delta \dot{h} = \pm 15$  percent ( $\delta a_T$  is the total semi-major axis deviation from the nominal semi-major axis.) When  $\delta a_R$  is positive, the worst case  $\Delta S$  occurs for  $\delta \dot{h}$  negative, and vice versa.

Figures 4.2-8 and 4.2-9 show the 18-day decay cycle for  $\dot{h} = 0.005$  nm/day and  $0.0075$  nm/day respectively.  $\delta a_R = \pm 0.0277$  nm. Figures 4.2-10 and 4.2-11 show the 27 day decay cycle for  $\dot{h} = 0.005$  nm/day and  $0.0075$  nm/day respectively for  $\delta a_R = \pm 0.0291$  nm. Figures 4.2-12 and 4.2-13 show the 36 day decay cycle for  $\dot{h} = 0.005$  nm/day and  $\dot{h} = 0.0075$  nm/day respectively for  $\delta a_R = \pm 0.0305$  nm/day.

Note here that decay cycle is defined as the time to decay from  $\Delta h + \delta a_R$  to  $-(\Delta h + \delta a_R)$ . The time at the start of decay is denoted as "REV No 1 on day 1". The time ticks shown on the curves are for REV No 1 on the day shown. The maximum ground track errors will then occur between the day 1 and day 19 ground track ticks since it is the 18 day coverage cycle duration that governs ground track requirements.

The following observations are made regarding the ground track errors. Figures 4.2-8, and 4.2-9 show the  $\Delta S$  between days 1 and 19 are the same,  $\pm 4.15$  nm regardless of the  $\dot{h}$  and  $\delta a_R$ 's polarity. With the  $\delta \dot{h}$  errors superimposed on the  $\delta a_R$ 's this statement is no longer quite true, with maximum  $\Delta S$  now being about  $\pm 5$  nm. These two figures indicate that a nominal 18 day decay cycle appears feasible with the orbit determination errors assumed (preliminary numbers, not covariance matrix). In Section 4.2.6.2, the philosophy for determining when in the decay cycle the O/A  $\Delta V$  maneuvers should be performed, is discussed. Figures 4.2-8 and 4.2-9 show two extremes for decay time if the O/A adjusts are to be made when  $\Delta S$  returns to zero; 34 days for  $\delta a_R = +0.0277$ ,  $\delta \dot{h} = -15$  percent,  $\dot{h} = 0.005$  and 6 days if  $\delta a_R = -0.0277$ ,  $\delta \dot{h} = +15$  percent,  $\dot{h} = 0.005$  nm/day.

Figure 4.2-10 ( $\dot{h} = 0.005$  nm/day, 27 day decay cycle), shows the  $\Delta S$  between days 1 and 19 to nominally be  $3.35$  nm. The same distance also occurs between days 10 and 28, (actually, end of day 10 and end of day 27). When  $\delta a_R$  and  $\delta \dot{h}$  errors are superimposed,  $\Delta S$  between day 1 and 19 become  $+7.6$  nm for the positive  $\delta a_R$  and  $-7.8$  nm for minus  $\delta a_R$ .



Figure 4.2-11 ( $\dot{h} = 0.0075$  nm/day, 27 day decay cycle) shows nominal  $\Delta S$  to be +5.2 nm and the extremes to be 9.3 nm ( $+\delta a_R$ ) and -9.38 nm ( $-\delta a_R$ ). Note that if careful control of the orbit is not maintained, the total  $\Delta(\Delta S)$  error is greater than 10 nm. That is the net difference in  $\Delta S$  between the 19 day points for the two extremes is  $\approx 15.0$  nm,  $\dot{h} = .005$  nm/day, and  $\approx 18.5$  nm,  $\dot{h} = .0075$  nm/day. From Figures 4.2-10 and 4.2-11, the extremes on decay time are 45 days and 13 days

Figure 4.2-12 ( $\dot{h} = .005$  nm/day, 36 day decay cycle) shows the nominal  $\Delta S$  between days 1 and 19 to be 6.67 nm and increasing to 7.8 nm when  $\delta h = -15$  percent. With  $\delta a_R$  of 0.303 nm added to  $\Delta h$ ,  $\Delta S$  becomes 11.0 nm. Superimposing  $\delta h$  of -15 percent on  $\delta a_R$  results in  $\Delta S$  of 12.2 nm. It is shown therefore, that the ground track requirements of 10 nm maximum distance between the same "REV number ground track" on any coverage cycle cannot be met under the assumed errors  $\delta a_R$  and  $\delta \dot{h}$ . Figure 4.2-13 shows the same conclusions with  $\dot{h} = .0075$ , except that the  $\Delta S$  distances are even larger.

With the -15 percent for  $\delta \dot{h}$ , the maximum  $\delta a$  that gives 10 nm of  $\Delta S$  is 0.105 nm for nominal  $\dot{h}$  of .005 nm/day. Therefore with  $\Delta h$  nominally at .09 nm the maximum  $\delta a_R$  is 0.015 nm/day. The orbit adjust system error for a 36 day decay cycle was shown to be 0.0148 nm. This leaves virtually nothing for orbit determination errors. Therefore, in order to use a 36 day decay cycle at  $\dot{h} = .005$ , system errors must be significantly reduced. At  $\dot{h} = .0075$  nm/day, no errors at all are permitted for a 36 day decay cycle.

Figure 4.2-13 ( $\dot{h} = .0075$ , 36 day decay cycle) is shown for completeness of data presentation. With no errors at all, the total  $\Delta S$  allotment of 10 nm is used just for nominal decay cycle control. Any errors at all result in  $\Delta S$  of greater than 10 nm. Thus, it is concluded from Figures 4.2-12 and 4.2-13 that the 36 day decay cycle is not feasible for ground track control.

From Figures 4.2-10 and 4.2-11, a nominal 27 day decay cycle appears feasible with proper control. Depending on  $\dot{h}$ , some duration greater than 27 days may be possible at given times of the year.

This entire section thus far has considered only the 10 nm ground track requirement on successive coverage cycles. The requirement for  $\approx 10$  percent overlap of adjacent swaths on successive days designated  $\Delta \ell$  will now be considered. This effect is essentially independent of  $\dot{h}$ , the maximum distance occurs on the first day of a decay cycle since  $\delta a_T$  is largest at this point. From equation (4.2.4-35) the distance  $\Delta S$  is given as

$$\Delta S_{\Delta \ell} = 8.23 \delta a$$

The nominal  $\Delta \ell$ , at nominal altitude (semi-major axis) is 86.06 nm. This leaves 3.94 nm for  $\Delta S_{\Delta \ell}$  if 90 nm maximum is permitted between adjacent ground tracks. From equation 4.2.4-35 computed to 0.478 nm. This is far in excess of any  $\delta a_T$  thus far encountered. Therefore, the requirement for 10 percent overlap on a day to day basis will always be achieved for the assumptions made in this analysis.

#### 4.2.6.2 Ground Track Control

Having determined how the various decay cycle durations, decay rates and systems errors influence ground track position over one decay cycle, it is now necessary to devise a method for establishing and controlling the decay cycles from one cycle to the next.

The ideal situation is one where the nominal cycle, for the  $\dot{h}$  associated with the particular time of the year, would be obtained through the operation of an error free system. Even though this is not realizable, the nominal decay curve can still be used as a reference. All deviations produced in the ground tracks due to system errors could be measured from this reference. Therefore, as an initial ground rule, the orbit adjust maneuvers should be planned to return the ERTS satellite to an altitude that would place it on the nominal decay cycle curve. It is assumed that at no time would correction residuals be so large as to allow the subsequent  $\Delta S$  to exceed 10 nm. This could happen only when the altitude is too high. If this did occur an orbit adjust would be necessary to lower the altitude, a decidedly inefficient maneuver.

Figure 4.2-14 shows functionally the data from Figure 4.2-8, the 18 day decay cycle with  $\dot{h} = .005$  nm and  $\Delta h$  nominally 0.045 nm at the start of decay. This figure will be used for discussing control philosophy. Assume  $\delta a_R = .0277$  nm so that the  $\Delta h + \delta a_R$  solid line curve is being traversed. After 18 days (start of day 19), the actual  $\Delta h$  is only -0.02 nm and the ground track for REV 1 of the "second" coverage cycle is shifted +4.1 nm from the "first" coverage cycle's. (Note that first and second will be used for discussion purposes, this does not imply the first or second coverage cycle after injection into orbit.) An orbit adjust would not be useful at the end of this first coverage cycle since an orbit adjust does not instantly affect  $\Delta S$ , but only the  $\Delta h$  (vertically on the graph). Decay until at least day 27 would be recommended since only then is it possible to return to the nominal curve. If a perfect O/A maneuver were performed on day 27 such that the satellite is now following exactly the nominal decay curve, the satellite altitude would now be nominal, at  $h_H$ . But this is at the middle of decay cycle and another orbit adjust would be required 9 days later. Therefore, it seems prudent to delay the orbit adjust maneuver for three additional days, at which point  $\Delta S$  is zero. Now a perfect return to the nominal curve would allow 18 days of decay prior to the next orbit adjust.

Now, consider the control philosophy if  $\delta a_R$  had been -.0277 nm. The decay cycle curve returns to  $\Delta S = 0$  in only eight days. An orbit adjust at this point might be difficult to make with any degree of accuracy since orbit determination/ground track prediction errors may not be reduced to a sufficiently small uncertainty. Therefore, it is probably better to wait for some longer time, perhaps till start of day 19, then attempt to return to the nominal cycle (dotted line on the  $-\Delta S$  side of plot.) However, another O/A maneuver with  $\delta a_R$  being negative might result in the entire second cycle being spent in the  $-\Delta S$  region. This is not desirable since another O/A may be required a few days later to prevent  $\Delta S$  from becoming too negative and the 10 nm requirement being exceeded.

Two possible solutions to the problem have been considered. One most applicable to the  $-\delta a_R$  case would attempt to optimize the time between day 8 and day 19 for making the maneuver, such that sufficient orbit determination accuracy is obtained while minimizing the possibility of remaining in the  $-\Delta S$  region.

The other solution which pertains to both positive and negative  $\delta a_R$  is to simply box in a 10 nm  $\Delta S$  area (as shown on the figure) and require that at no time will any part of the decay cycle be permitted to exceed these bounds. Note that the  $\Delta S$  limits are not  $\pm 10$  nm from the reference ( $\Delta S = 0$ ) point. If they were, then it is possible that a given rev. number during one coverage cycle, if at +10 nm, might during some other coverage cycle be at -10 nm. In this case there would be a 20 nm separation between the corresponding revs.

The last facet of orbit control to be considered is the determination of the actual decay curve and computation of the next orbit adjust maneuver.

A suggested technique for determining the decay cycle curve in the presence of orbit determination errors is to examine the nodal crossing points back in time to the beginning of the decay cycle. This information, being "after the fact", should be very accurate, then the total decay cycle curve can be drawn. As an example, consider Figure 4.2-15, which is effectively a rotation of the decay cycle curves. Note that  $\Delta h$  and time are synonymous when  $\dot{h}$  is constant. All the decay cycle curves of Figures 4.2-7 through 4.2-13 could have had their ordinates labeled as time or the ratio of time to altitude rate,  $\dot{h}$ , instead of altitude. On Figure 4.2-15, the solid line is the predicted  $\Delta S$  versus time based on data from which the orbit adjust maneuver was computed. The circled points represent the actual nodal positions,  $\Delta S$ . Eventually the curve will be accurately constructed and prediction into the future is obtained by extending the actual curve. On Figure 4.2-15 some  $\Delta S$  violation zones are shown. The cross-hatched regions at the top and bottom represent areas outside of the 10 nm  $\Delta S$  variation permissible. The dashed line regions contain lines of constant  $\dot{h}$  which indicate that if the curve enters this region, the cross-hatched areas will be traversed before  $\Delta h$  gets to zero. Final location of the center of this zone along  $\pm \Delta S$  must be determined from analysis, but there would probably be more of the acceptable region to the  $+\Delta S$  side since the nominal decay cycle extends into this region even when there are no  $\delta a_R$  errors.

The operational system would not use the graphical display, per se, for orbit control. The data on the curve would be mechanized in the operational software. Graphical displays could be included as part of the software's output as a convenient aid for the ground controllers. The actual curve could also be combined with the nodal crossing points predicted by propagating orbit determination data ahead in time, in order to aid in reducing those errors. With data of this form available, it now becomes possible to predict orbit adjust maneuvers well in advance. As a check on the predicted O/A maneuver, all 251 rev number  $\Delta S$ 's from all the previous coverage cycles would be stored. When the orbit adjust maneuver is planned, the new 251 coverage cycle's in nodal positions would be computed assuming worst case errors. Then comparisons are made with all the previous cycles to see that no rev number's ground track will be more than 10 nm from its corresponding rev number on any other coverage cycle.

Analyses of this suggested approach to the orbit control problem should be performed in order to fully evaluate its capabilities. Simulations should be performed which include errors in orbit determination and orbit adjust maneuvers, to determine how the ground track errors accrue over the 20 coverage cycles in a year. Ultimately the total control concept would be evolved.

From this analysis of operational ground track control studies, it is concluded that 18 to 27 day decay cycles are feasible and that all orbit and subsatellite swath requirements can be met. Orbit determination capability should be reviewed for further possible improvement. Although details of the control philosophy remain to be defined, an approach that appears promising has been formulated.

#### 4.2.7 LAUNCH WINDOW ANALYSIS

The ERTS launch window is defined to place the time at the descending node to be between 9 30 and 10 00 hours. The effect of the one-half hour window produces variations to the beta angle, the shadow duration and solar elevation angle at ERTS nadir.

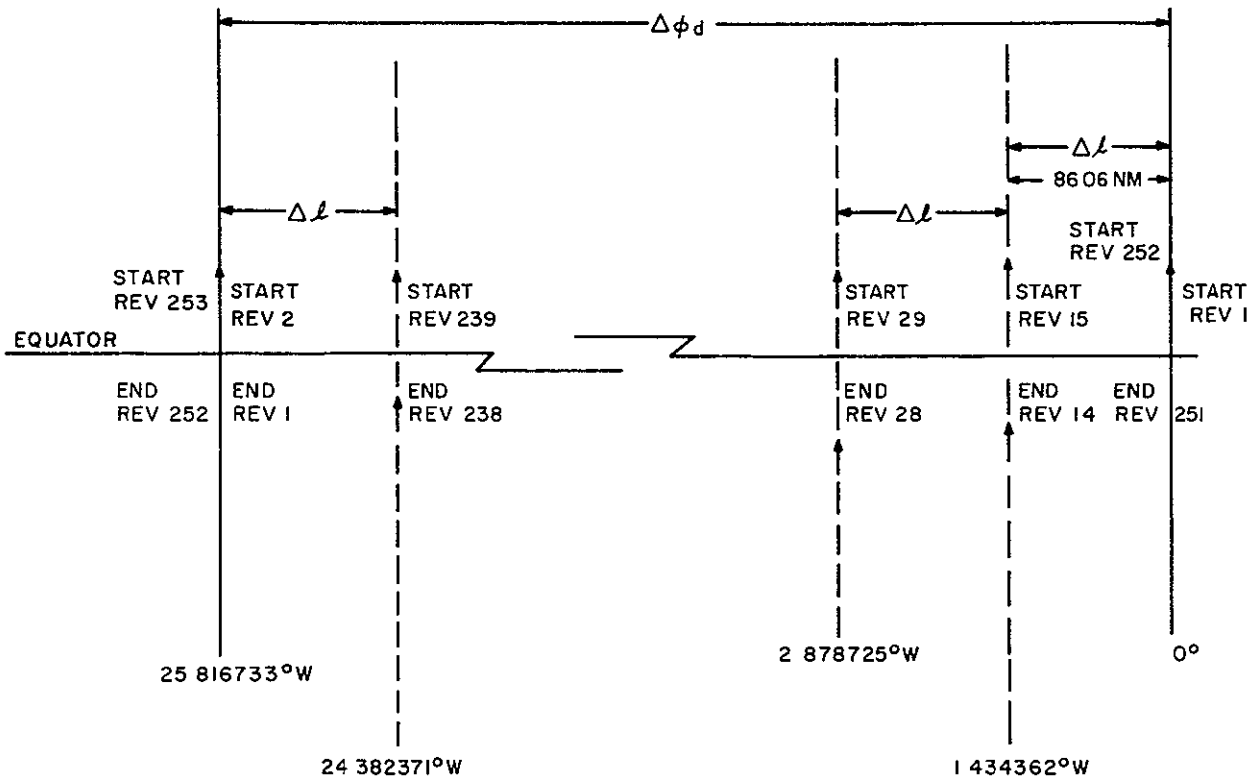
The beta angle is defined as the acute angle between the ERTS orbit plane and the sun-line. It can also be defined as the complement of the angle between the ERTS orbit plane's normal and the sun-line. Figure 4.2-16 shows the beta angle history for both bounds on the launch window. Variations of between 6 to 7.5 degrees is seen.

ERTS will pass through the earth's shadow on every orbit. The time spent in the shadow, nominally (9 30 descending node) varies between 29 and 32.6 minutes. Figure 4.2-17 shows an increase of 1 to 2 minutes if launch is at the end of the launch window (10 00 descending node time).

The beta angle and shadow duration variations affect principally the thermal and power subsystems

The solar elevation angle is the angle between the sun-line and the local horizon at Satellite Nadir. In Figures 4 2-18 and 4 2-19, the complete yearly history of solar elevation angle variation with latitude is shown for the two ends of the launch window. Of interest is the latitudes  $30^{\circ}$ N and  $50^{\circ}$ N since these encompass most of continental United States. The effect of the launch window on solar elevation angle at these two latitudes is shown in Figure 4.2-20. Variations of at least two degrees but not more than 6 degrees is seen. The effect of the increased angle at the end of the launch window on payload operation is expected to be minor.

$\Delta\phi_d$  LONGITUDE SHIFT FROM ONE ASCENDING NODE TO NEXT  
 $\Delta l$  LONGITUDE SHIFT FROM ONE DAY TO NEXT (ADJACENT TRACKS)  
 NOMINAL  $\Delta\phi_d = 25.816733$  DEGREES  
 $\Delta l = 1.434362$  DEGREES



ORBIT PROVIDES  
 14% SIDELAP  
 REPEATING GROUND TRACE-18 DAYS

Figure 4.2-1. Definition of Ground Track Longitude Separation

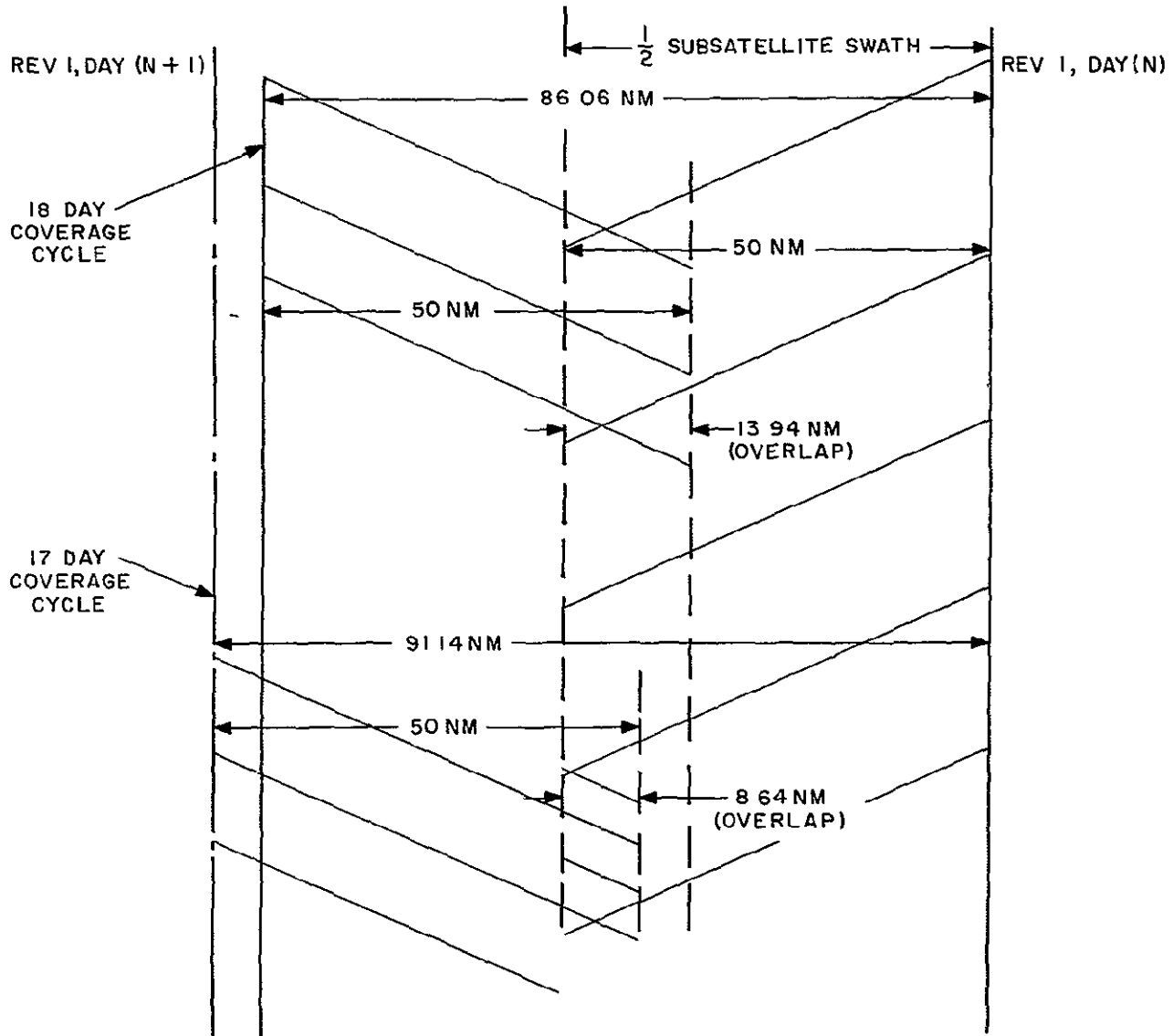


Figure 4.2-2. Definition of Subsatellite Swath Overlap

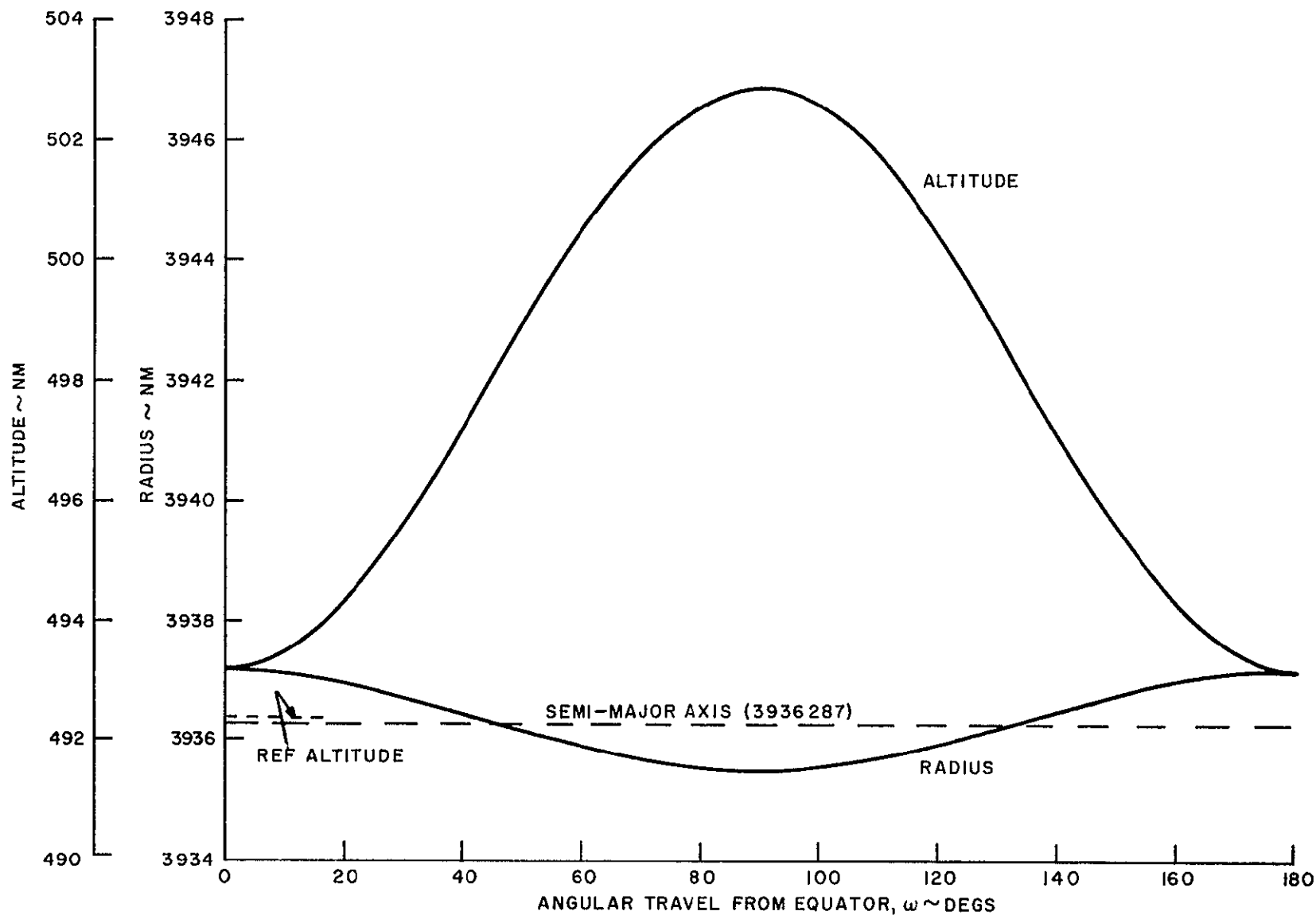


Figure 4 2-3 ERTS Nommal Orbit Altitude and Radius Versus Angular Travel

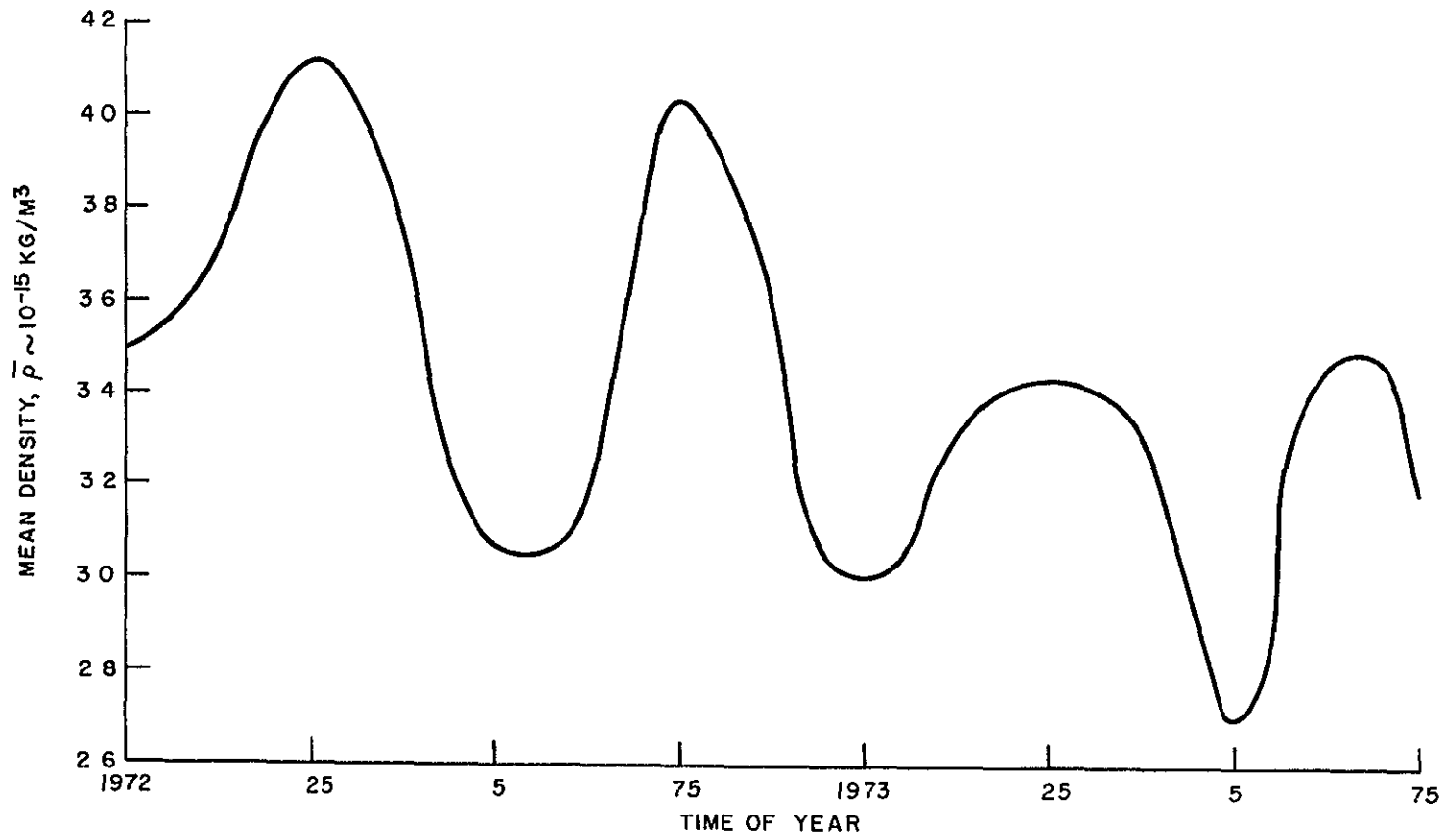


Figure 4 2-4 Variation of ERTS Mean Density During 1972-1973



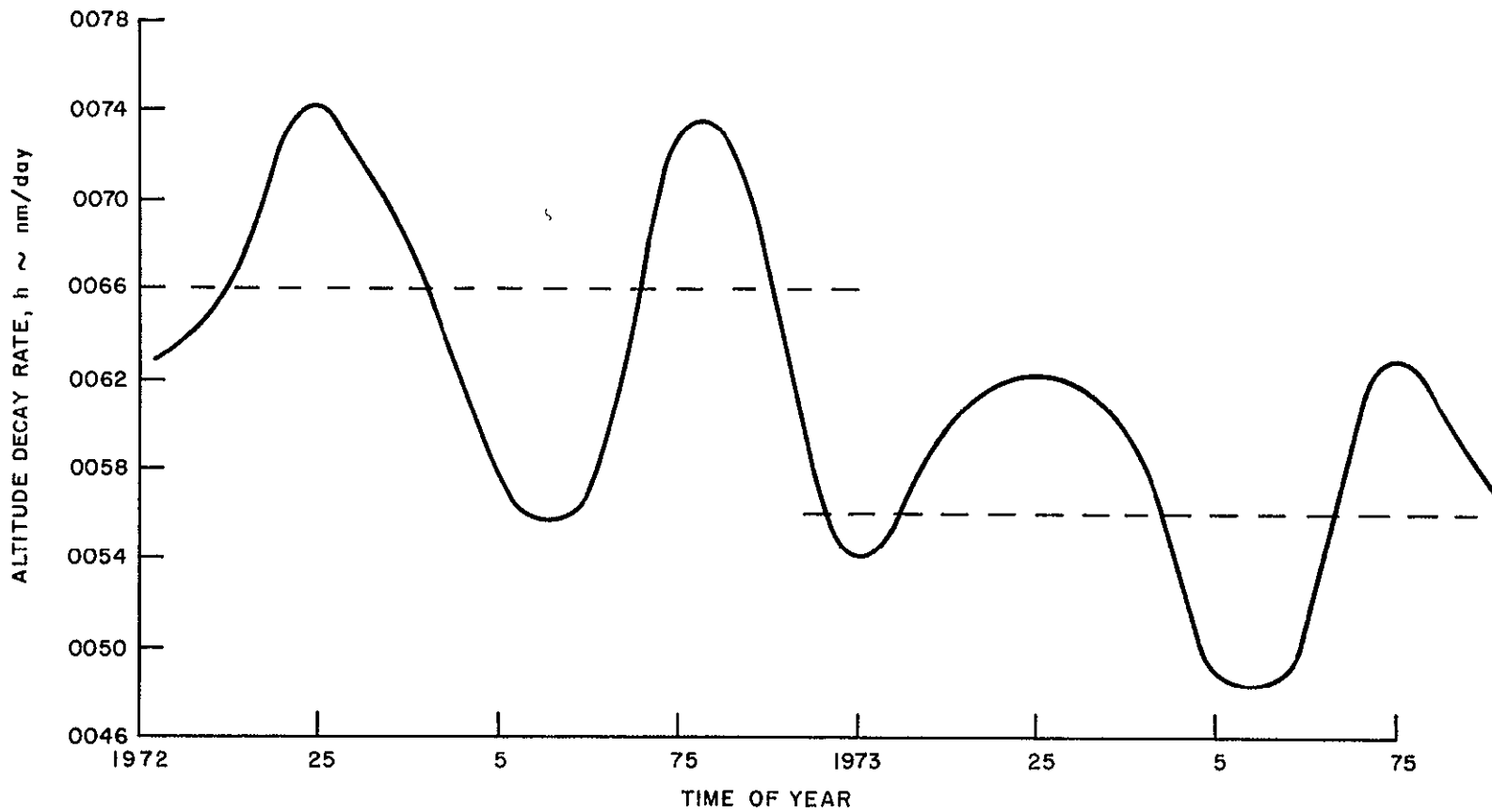


Figure 4.2-5. Variation of Mean Altitude Delay Rate With Time of Year

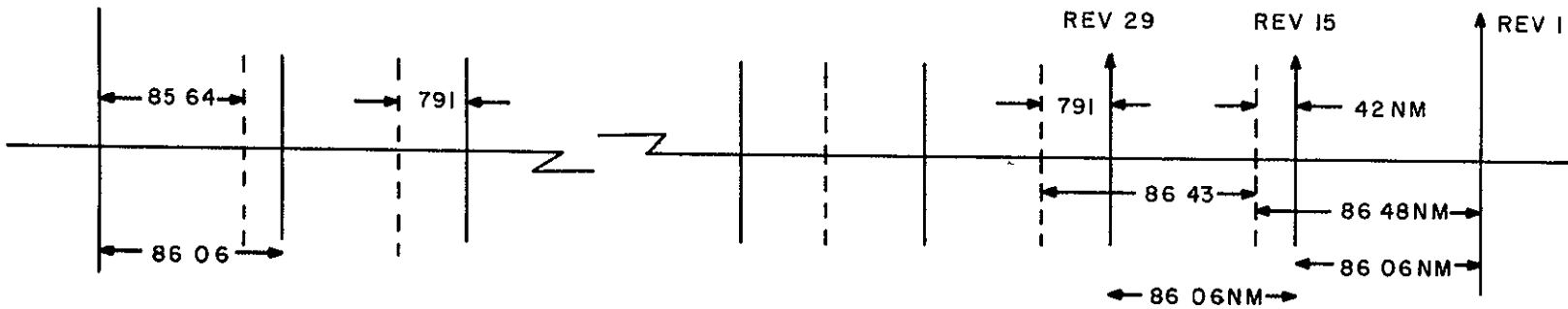
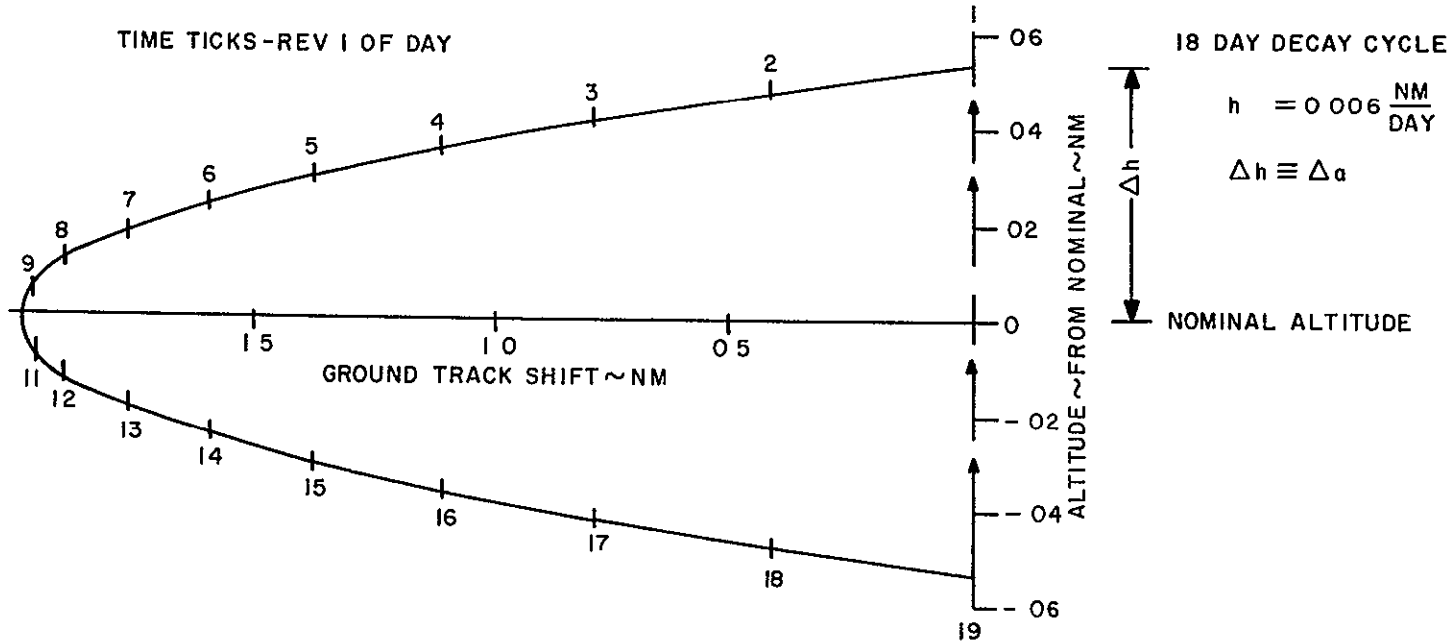


Figure 4.2-6. Description of Ground Track Variation With Altitude Decay

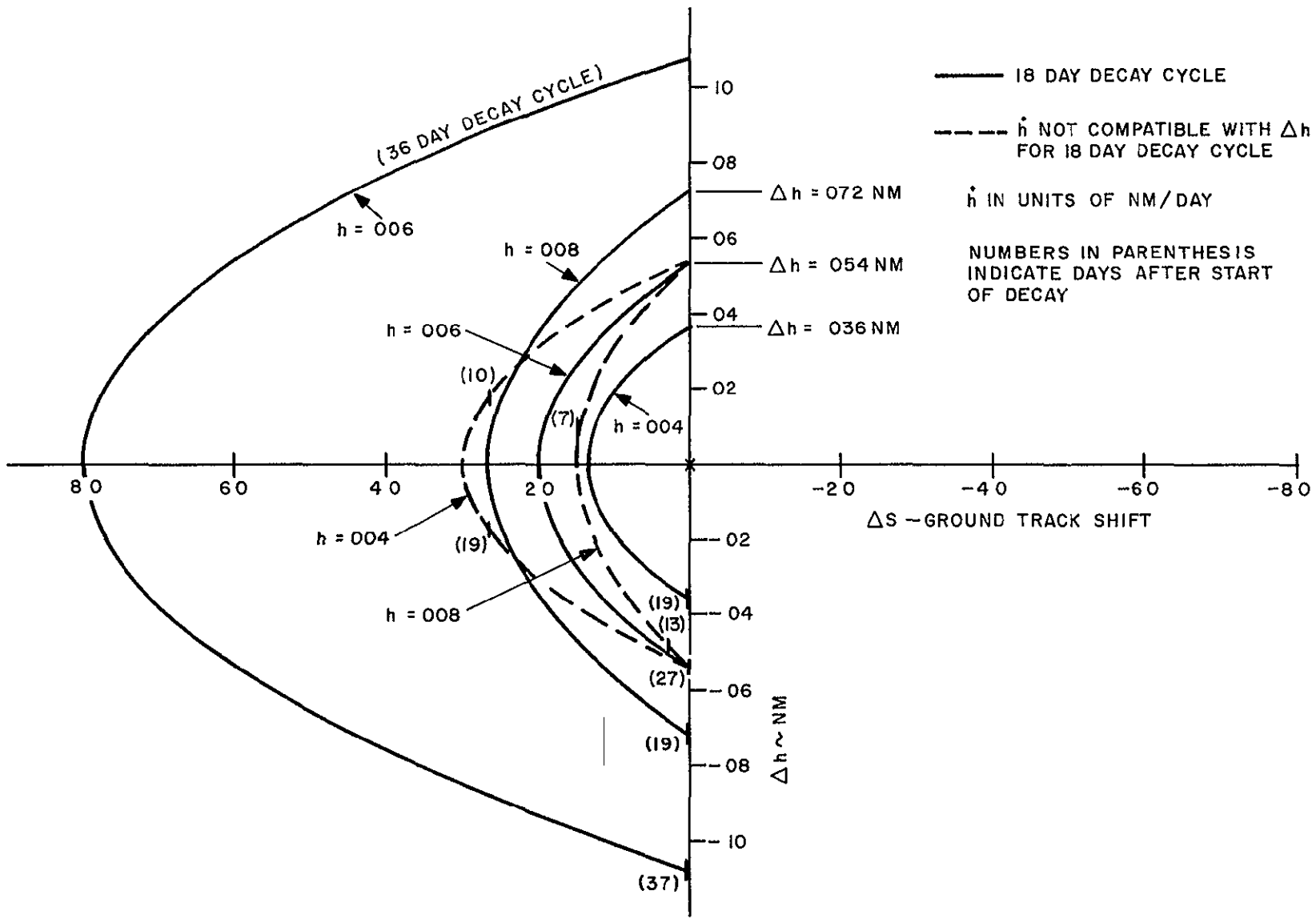


Figure 4 2-7 Variation of Ground Track Node Position With Altitude Decay

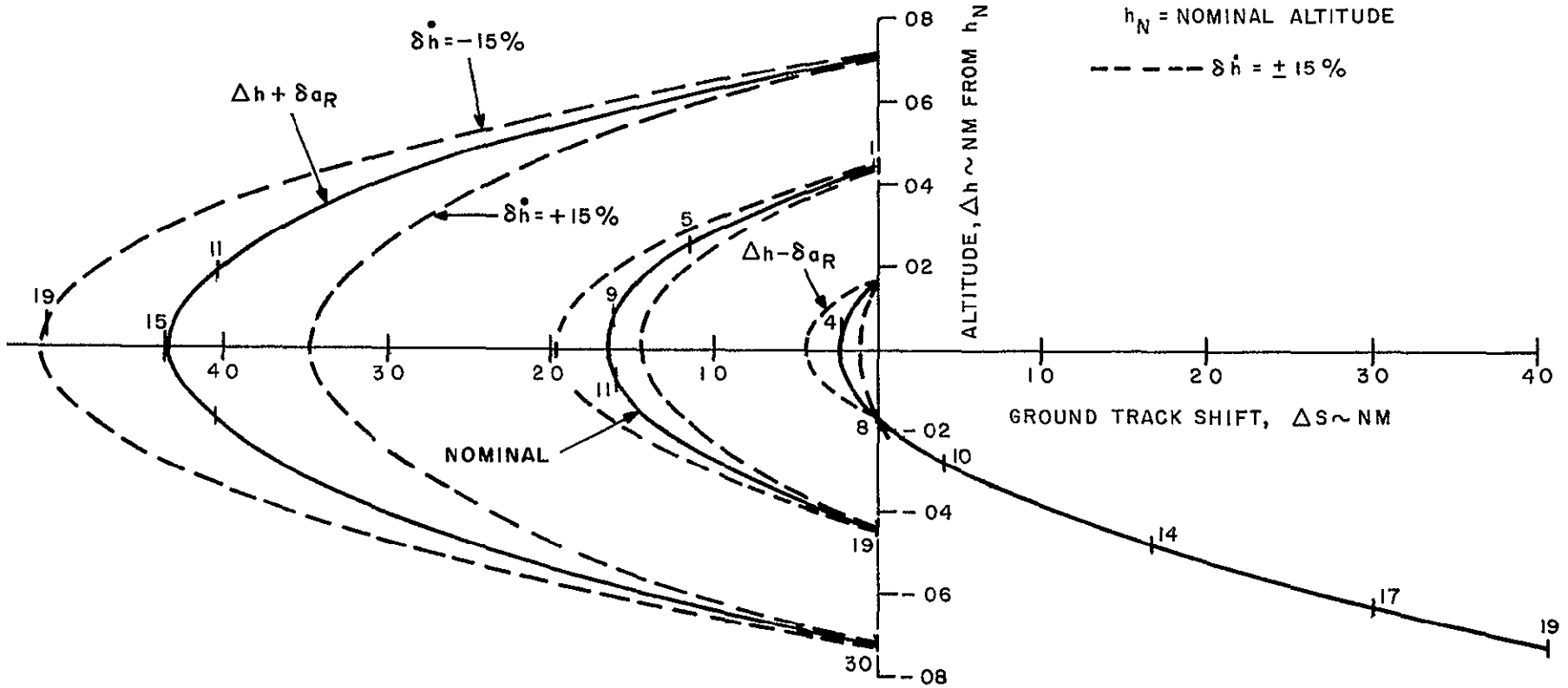


Figure 4.2-8 18 Day Decay Cycle Curve,  $h = .005 \text{ nm/day}$

11 February 1970

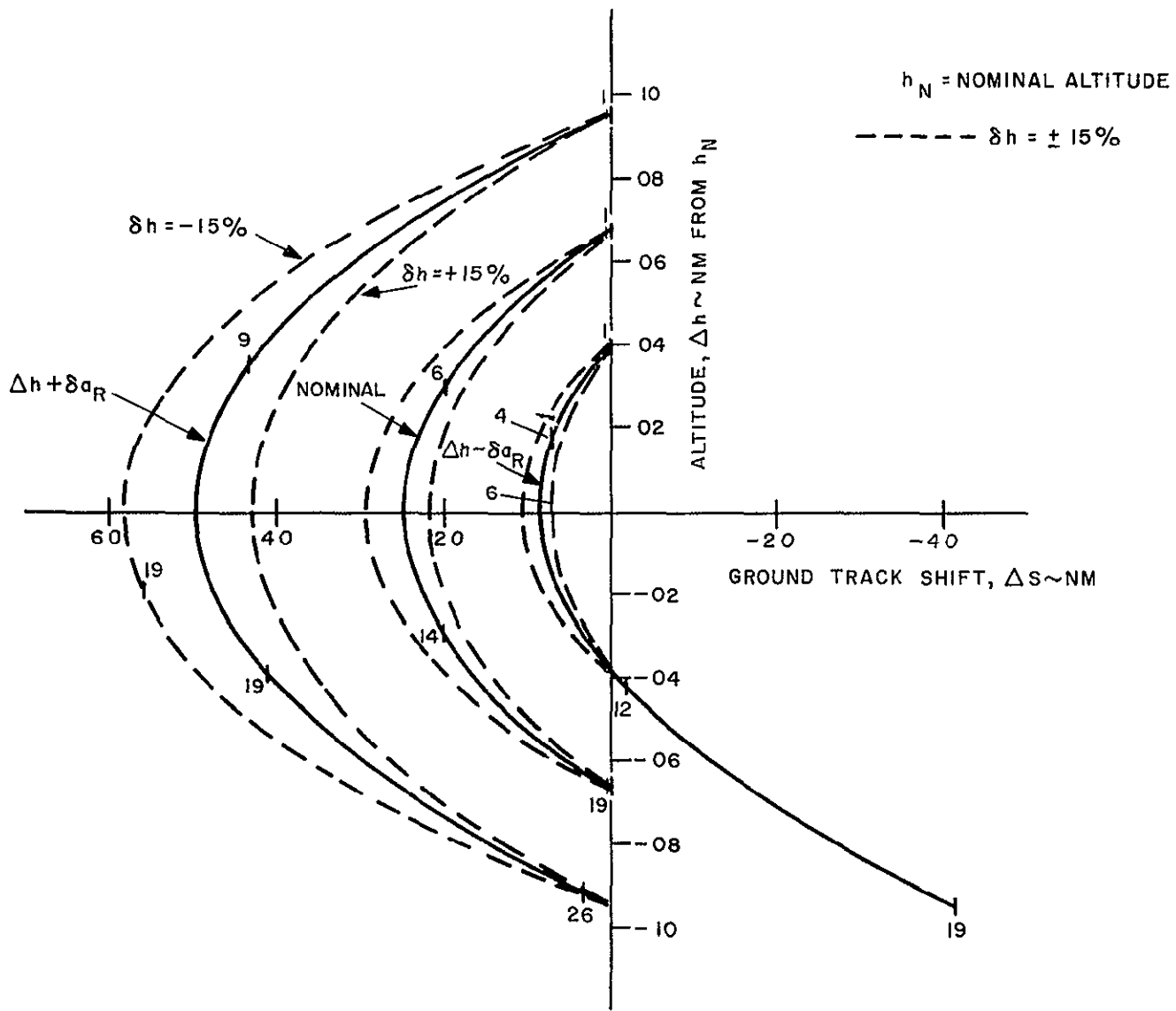


Figure 4.2-9. 18 Day Decay Cycle Curve,  $h = .0075 \text{ nm/day}$

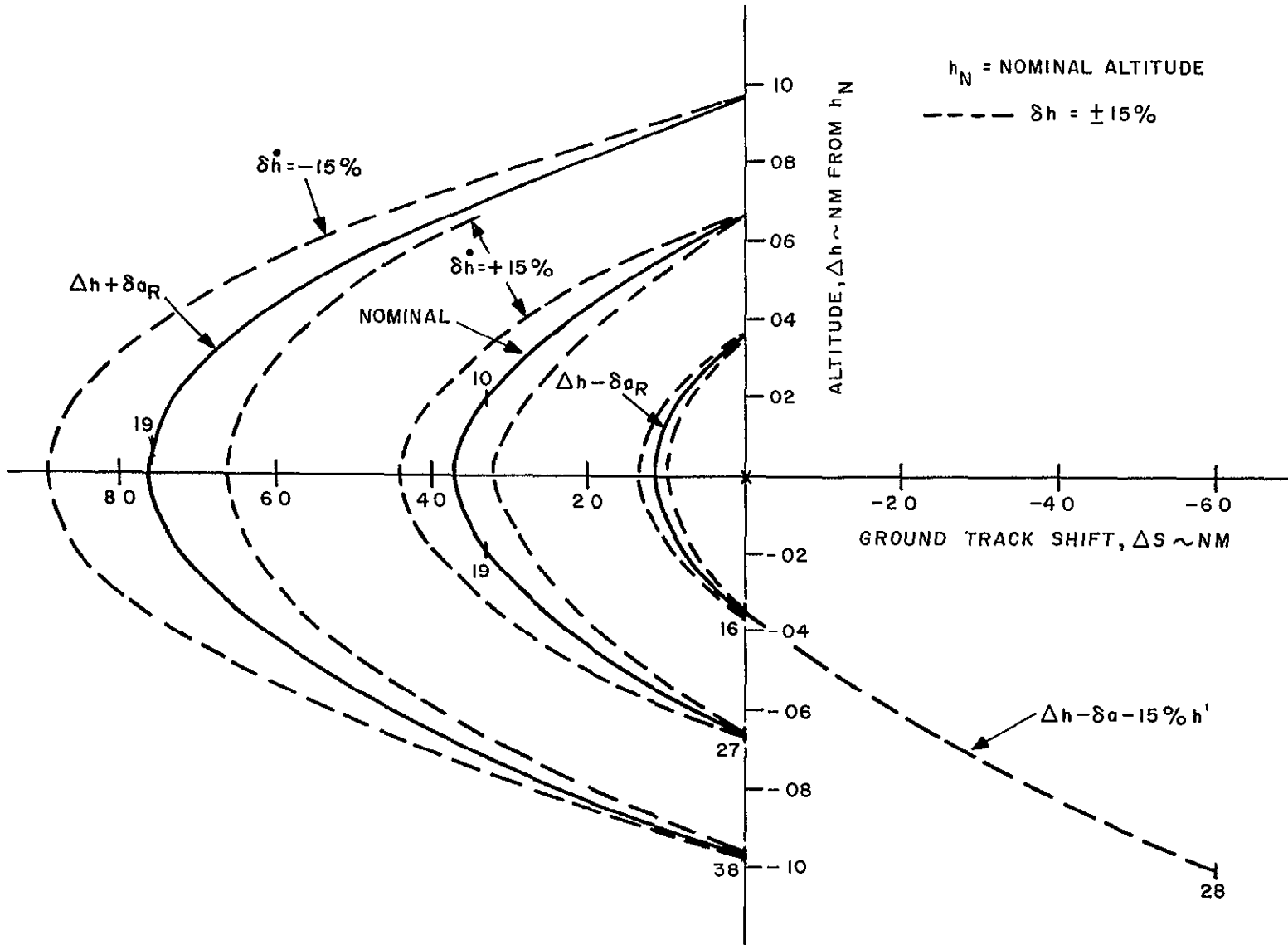
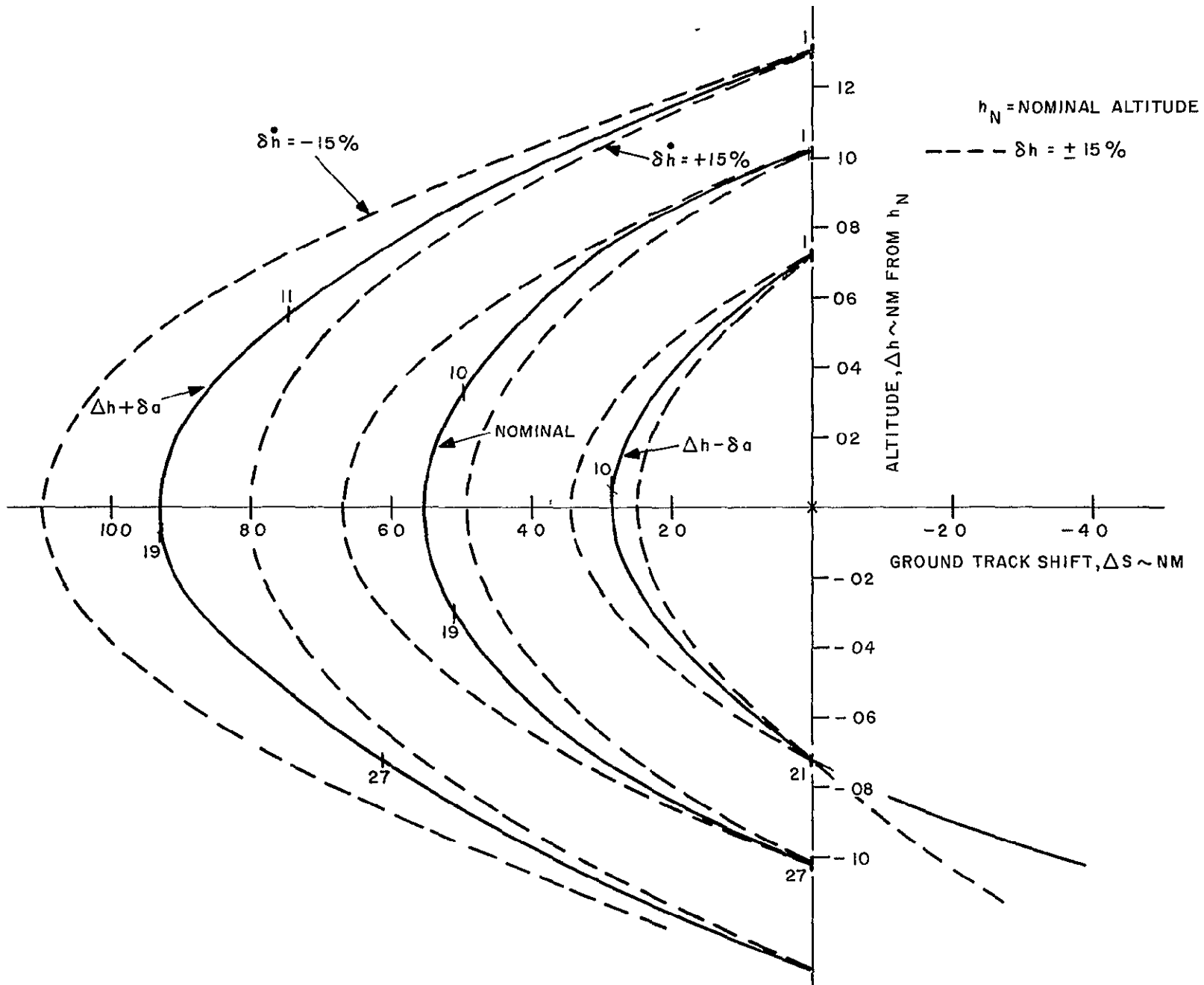


Figure 4.2-10. 27 Day Decay Cycle Curve,  $h = .005 \text{ nm/day}$

Figure 4.2-11. 27 Day Decay Cycle Curve,  $h = .0075 \text{ nm/day}$

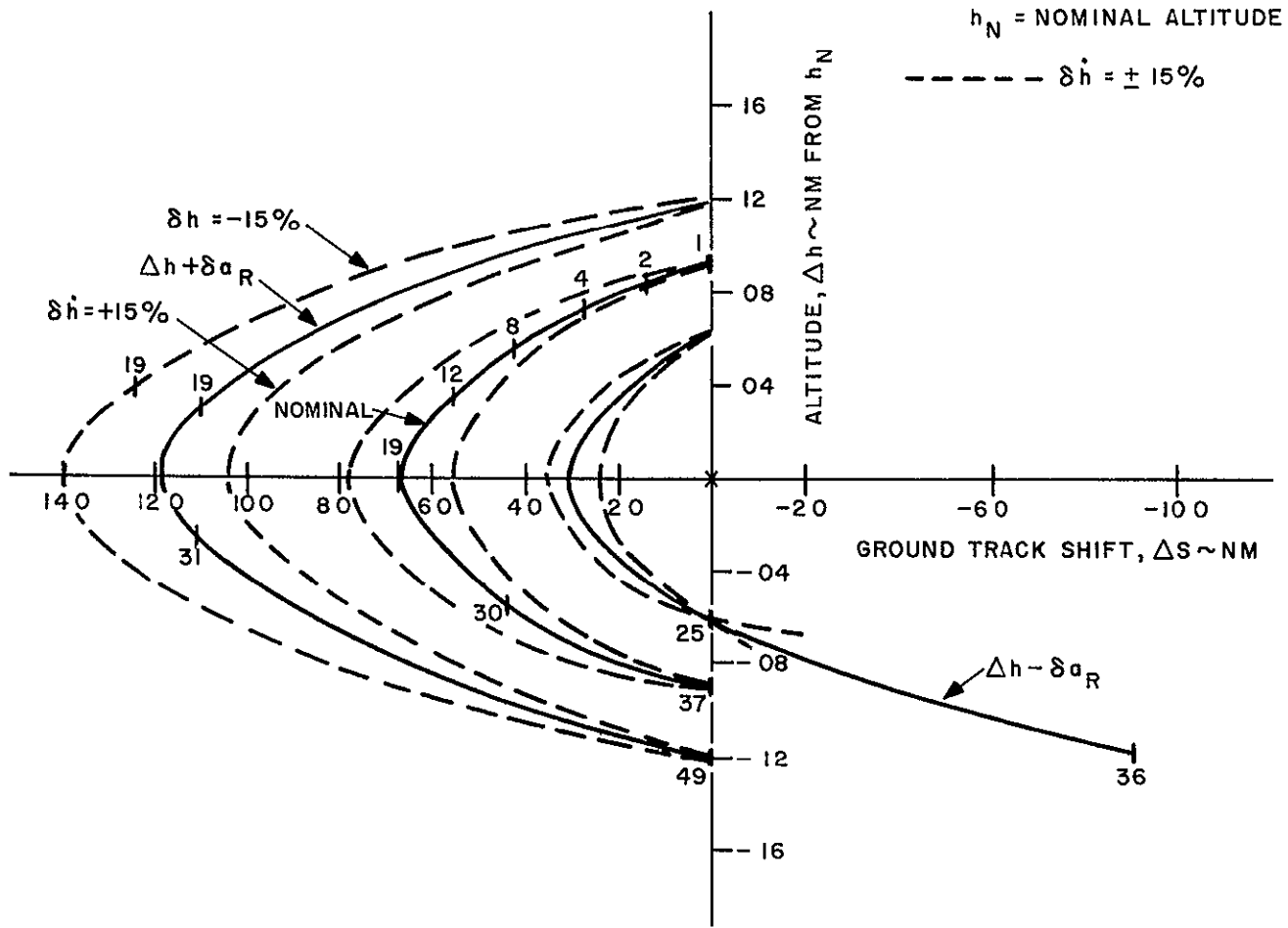
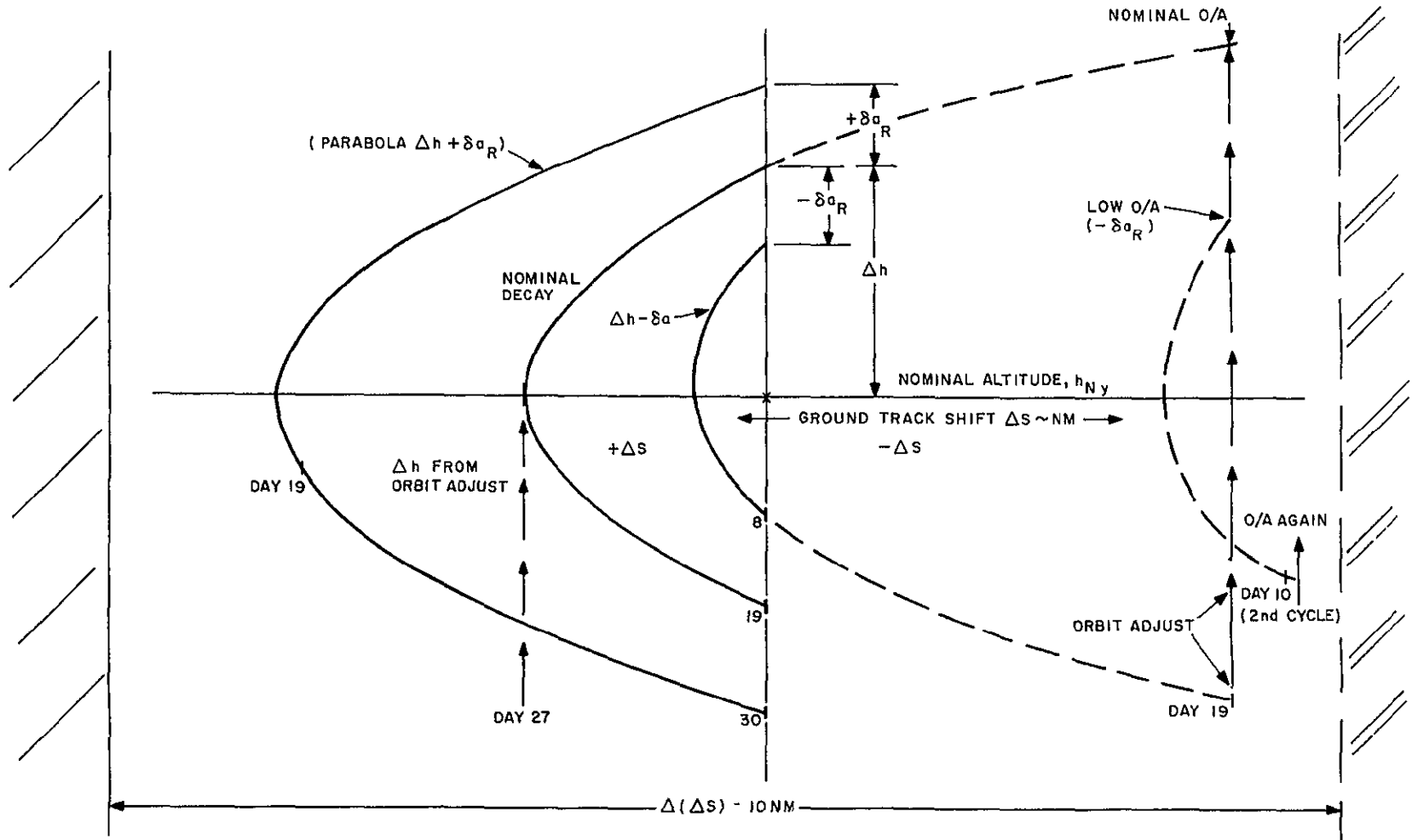


Figure 4.2-12. 36 Day Decay Cycle Curve,  $h = .005 \text{ nm/day}$







11 February 1970

Figure 4.2-14. Orbit Adjust Control of Orbit Decay Cycle

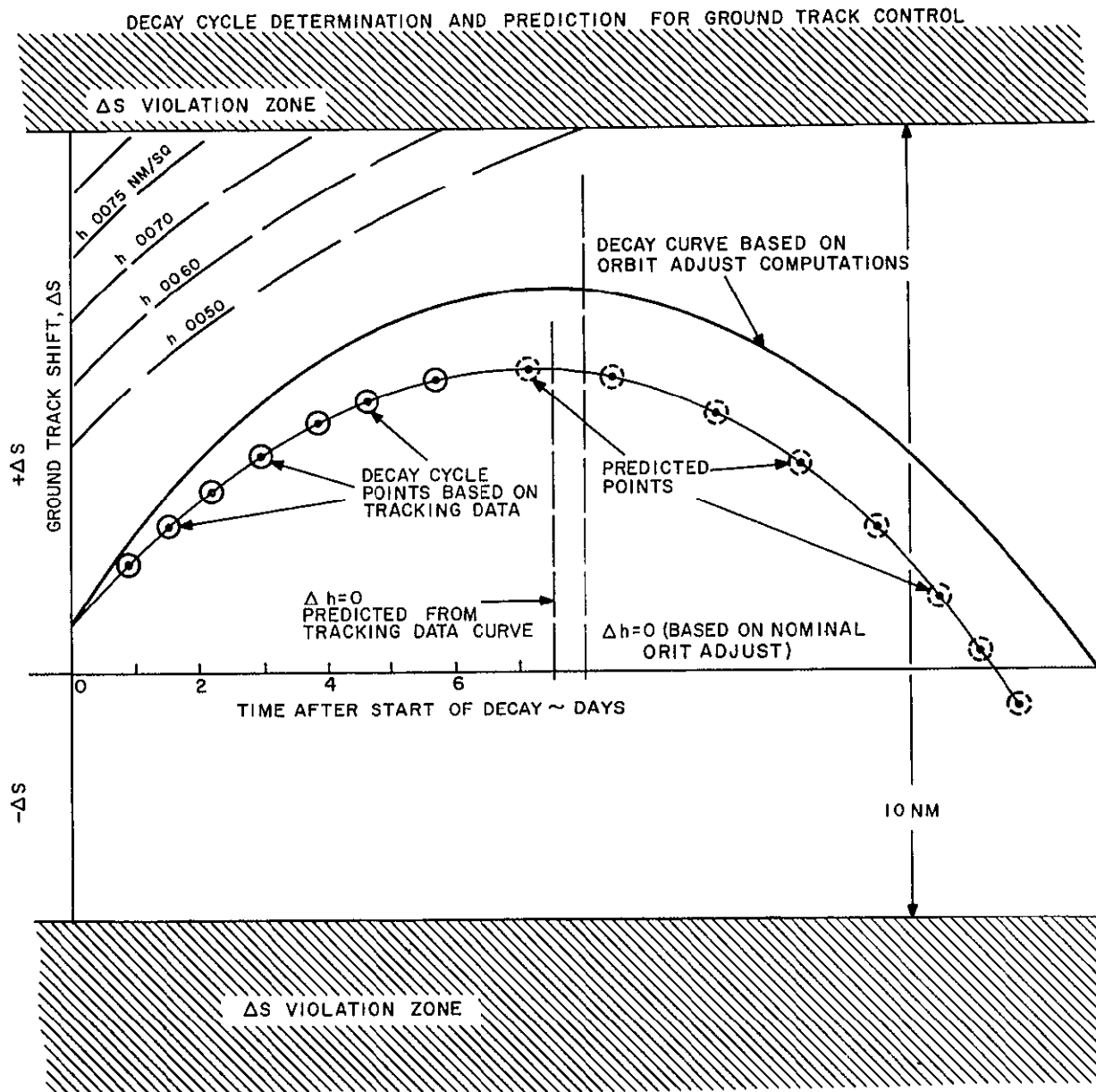


Figure 4.2-15. Decay Cycle Determination and Prediction for Ground Track Control

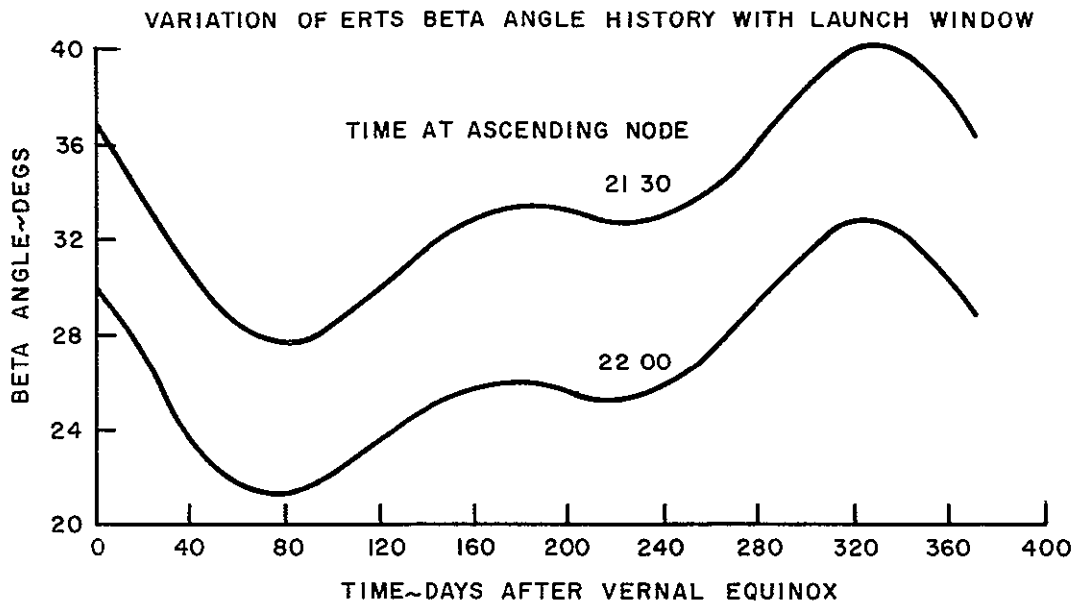


Figure 4.2-16. Variation of ERTS Beta Angle History With Launch Window

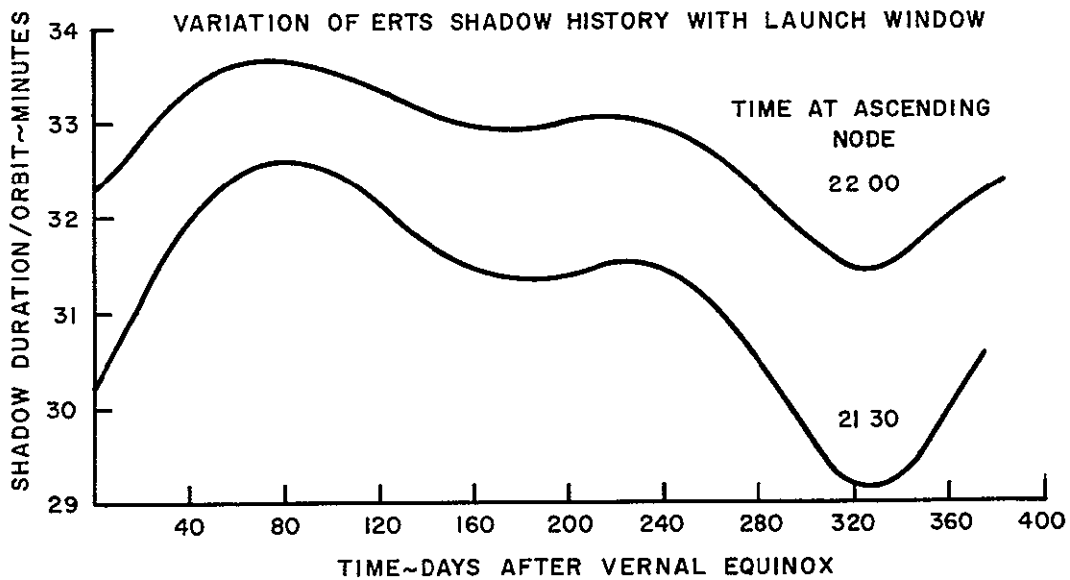


Figure 4.2-17. Variation of ERTS Shadow History With Launch Window

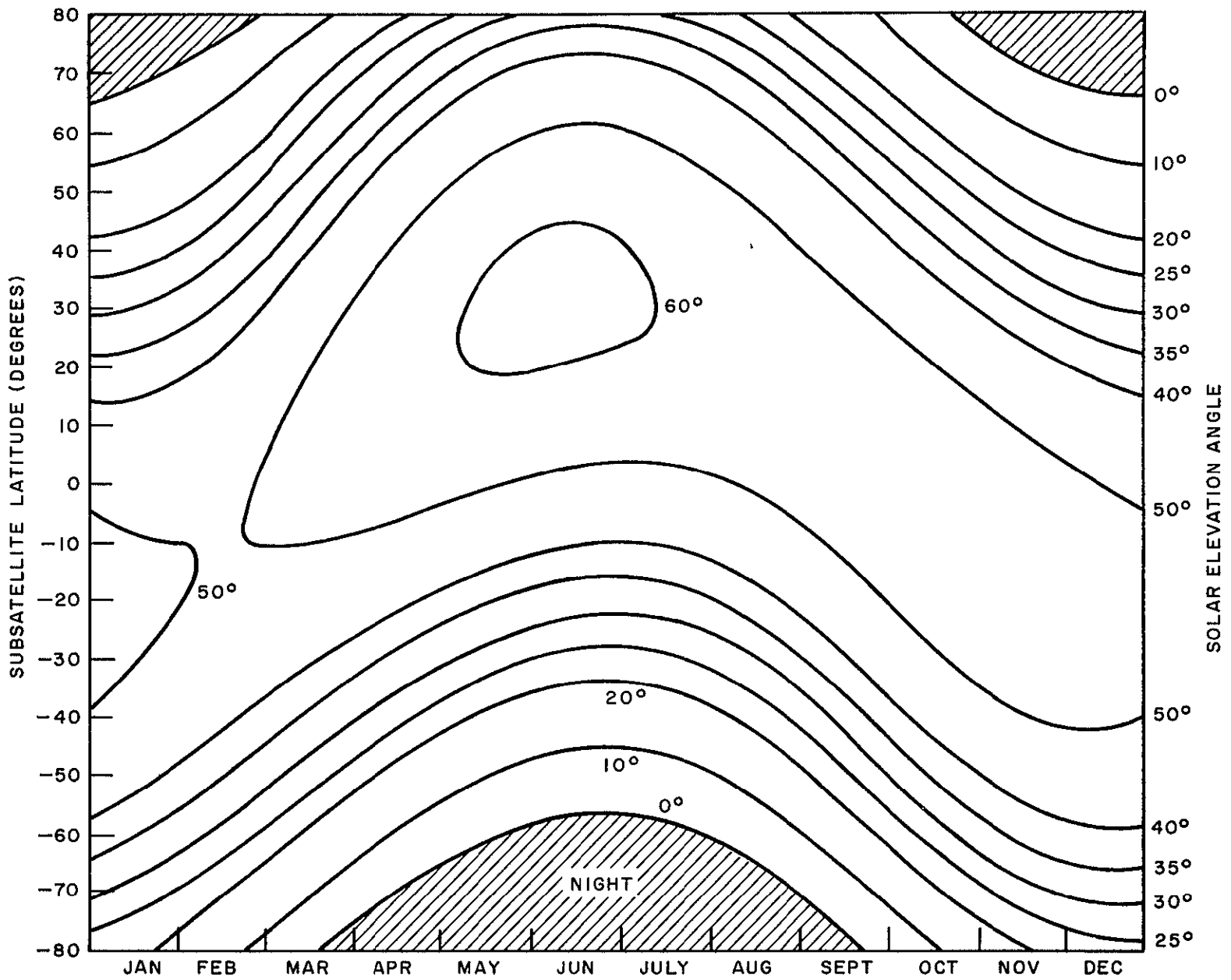


Figure 4.2-18. Solar Elevation Angle History as a Function of Subsatellite Latitude - Ascending Node at 2130 Hours

11 February 1970

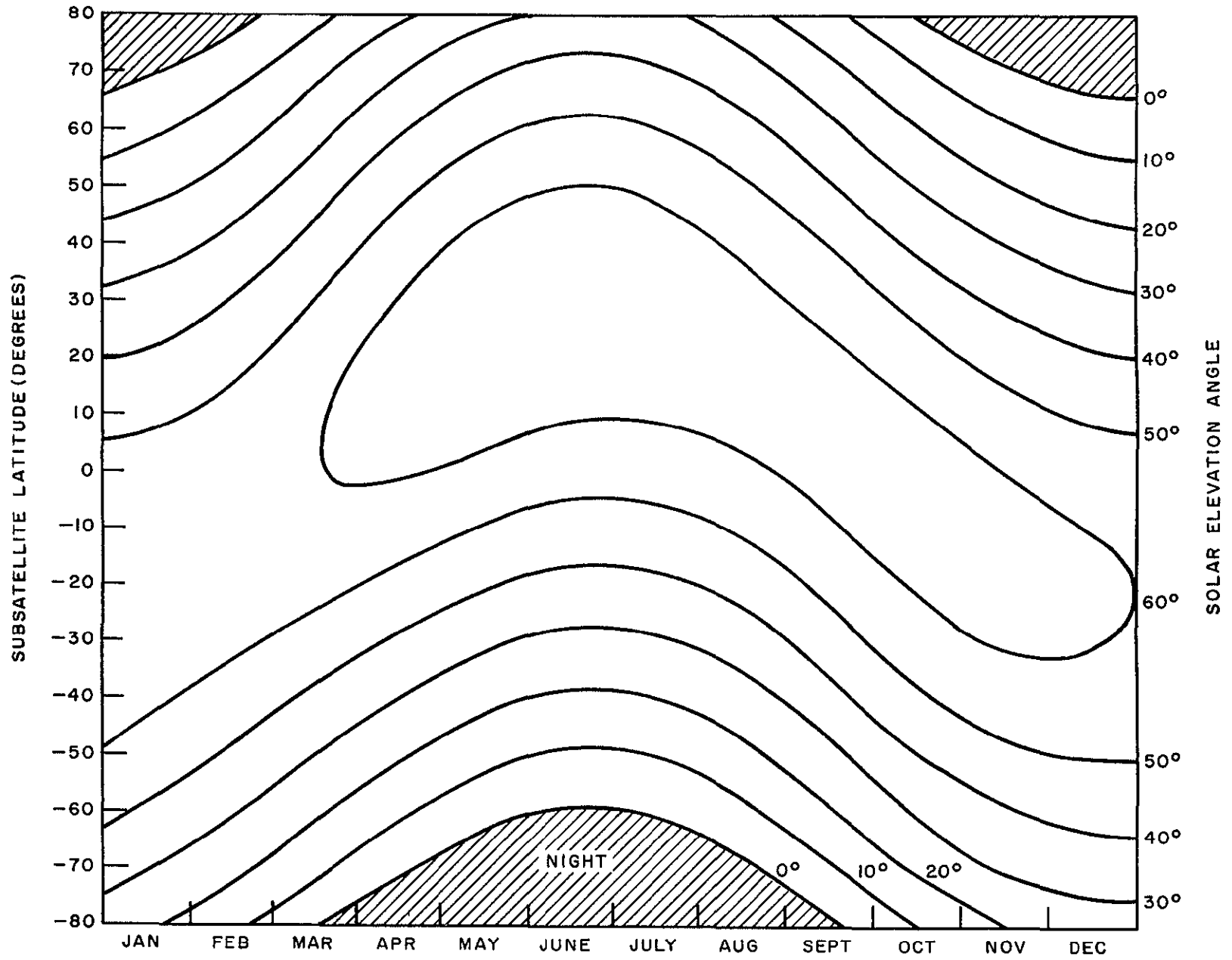


Figure 4.2-19. Solar Elevation Angle History as a Function of Subsatellite Latitude - Ascending Node at 2200 Hours

11 February 1970

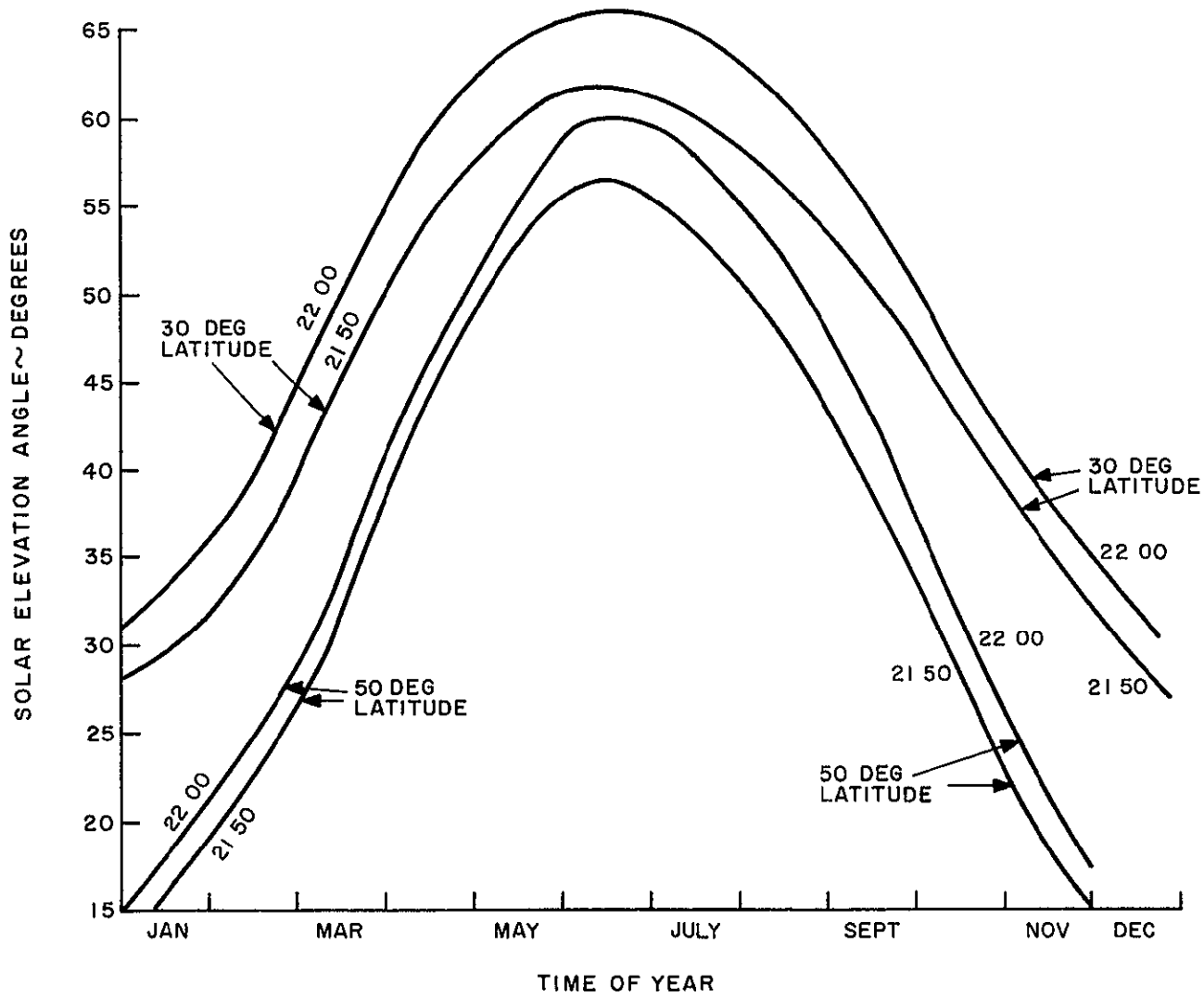


Figure 4.2-20. Effect of 30 Minute Launch Window on Solar Elevation Angle at 30 Degrees and 50 Degrees North Latitude

TABLE 4.2-1. NOMINAL ORBIT

<u>Orbit Parameters</u>	
Altitude*	492.35 nm
Inclination	99.088 degrees
Period	6196.015 seconds
Eccentricity	0
Time at Ascending Node	21 30
Coverage Cycle Duration	18 days (251 revs)
Distance Between Adjacent Ground Tracks	= 86.06 nm

\*Altitude Defined As

Semi-Major Axis Minus Equatorial Radius



TABLE 4.2-2.  $C_D A$  CALCULATIONS

Item	Normal Force			Sheer Force		
	Area (sq ft)	$C_D$	$C_D A$ (sq ft)	Area (sq ft)	$C_D$	$C_D A$ (sq ft)
Ground Plane	0.1	2.2	0.2	0		
Paddles	51.0	$2.8(\frac{2}{\pi})$	90.9	0		
Trans Section	6.2	2.8	17.4	0		
+ Drives	0.43	2.2	0.9			
ACS	4.5	2.8	12.6	8.64 (Sides) 4.1 (top)	0.075	0.6 0.3
Truss Tubes	3.0	2.2	6.6	0		
Aux. Load Panels	0.7	2.8	2.0	0		
ACS I/F Panels	1.2	2.8	3.4			
O/A						
Module	0.19	2.8	0.5	0		
Tank (partially blocked)	0.167	2.0	0.3	0		
Torus Ring	6.1	2.2	13.4			
WBRE'S	2.0	2.8	5.6	35.	0.075	2.6
Sensors, etc.	5.7	2.8	15.9			
			<u>169.7</u>			<u>3.5</u>
Total $C_D A$	173.2 sq ft					

TABLE 4.2-3. ORBIT ADJUST SUBSYSTEM  $\Delta V$  REQUIREMENTS

		$\Delta V$ FPS
A. INJECTION ERROR REMOVAL		
1.	Nominal - (Remove 14. nm Altitude Error)	21.7
2.	Predictable Losses in Efficiency	
A.	Thruster Cant Angle of $21.5^\circ$ (7% Loss)	1.5
B.	Continuous Thrusting Arc (5% Loss)	1.1
	Subtotal	24.3
3.	Error Sources	
A.	Thrust Alignment	
1.	Thrust Vector $.25^\circ$ } 2. $1.78^\circ$ C.G. Pointing } 1%	
B.	Attitude Control	
	Pitch, Roll $5^\circ$ (added Cant Angle)	2.5%
	Yaw 0 to $10^\circ$ , Avg. of $\approx 5^\circ$	1.0%
	RSS of Error Sources	2.9%
	Total $\Delta V$ Injection Error Removal	<u>25.0</u>
B. DRAG MAKE-UP		
1.	Decay Rate (2.42 nm/Yr.)	7.5
2.	Losses	
A.	Cant Angle - 7%	<u>0.5</u>
	Subtotal	8.0
3.	Error Sources	
A.	Thrust Alignment	1% 0.1
B.	Attitude Control	Negligible
	Total $\Delta V$ for Drag Make-Up	<u>8.1</u>
C. ATTITUDE CONTROL EFFECTS		
1.	Pitch Error Corrections	1.0
D. ADDITIONAL MARGIN ( $\approx 30\%$ )		<u>10.9</u>
TOTAL $\Delta V$		45.00 FPS

TABLE 4.2-4. COVARIANCE MATRIX - MSFN (METERS AND CENTIMETERS)

$0.461297 \times 10^3$	$0.102584 \times 10^3$	$-0.372790 \times 10^3$	$0.318797 \times 10^2$	$-0.255107 \times 10^2$	$-0.316175 \times 10^2$
	$0.238453 \times 10^3$	$-0.343637 \times 10^3$	$0.123967 \times 10^2$	$-0.310654 \times 10^2$	$0.269304 \times 10^2$
		$0.355040 \times 10^4$	$-0.178066 \times 10^3$	$0.260083 \times 10^3$	$-0.470579 \times 10^2$
	SYMMETRIC		$0.106002 \times 10^2$	$-0.123284 \times 10^2$	$0.208299 \times 10^0$
				$0.199287 \times 10^2$	$-0.487497 \times 10^1$
					$0.101861 \times 10^2$

TABLE 4.2-5. COVARIANCE MATRIX - CORPUS CHRISTI (METERS AND CENTIMETERS)

$0.239313 \times 10^4$	$0.164108 \times 10^4$	$-0.786428 \times 10^4$	$0.402627 \times 10^3$	$-0.594417 \times 10^3$	$0.482858 \times 10^2$
	$0.140231 \times 10^4$	$-0.614073 \times 10^4$	$0.278678 \times 10^3$	$-0.459570 \times 10^3$	$0.888044 \times 10^2$
	SYMMETRIC	$0.633764 \times 10^5$	$-0.336738 \times 10^4$	$0.448782 \times 10^4$	$-0.323752 \times 10^3$
			$0.189397 \times 10^3$	$-0.234938 \times 10^3$	$0.104348 \times 10^2$
				$0.323595 \times 10^3$	$-0.227993 \times 10^2$
					$0.122504 \times 10^2$

TABLE 4.2-6. ORBIT PARAMETERS FOR COVARIANCE MATRICES

Elements		
Semi-Major Axis	=	7296.757 km
Eccentricity	=	0.0001
Inclination	=	99.0 degrees
Right Ascension of Ascending Node	=	300.25 degrees
Argument of Perigee	=	0.0 degrees
Mean Anomaly	=	180. degrees
Calculated Parameters		
Radial Distance $\hat{=}$ Semi-Major Axis	=	23939491. ft
Velocity	=	24249 ft/sec
X	=	12059997. ft
Y	=	20679890. ft
Z	=	0.
$\dot{X}$	=	3275.38 ft/sec
$\dot{Y}$	=	1910.92 ft/sec
$\dot{Z}$	=	-23950.4 ft/sec

11 February 1970

#### 4.3 REFERENCES

1. Memorandum for Record - "Proposed Constants and Equations for ERTS-A and ERTS-B Atmospheric Density Model" - Memorandum from Walter D. Bradley to Thomas M. Ragland - dated November 24, 1969.
2. "Models of Earth's Atmospheres, 120 KM to 1000 KM", NASA SP-8021 - May 1969.
3. GSFC Operations Control Center - "Satellite Situation Reports" - May 31, 1969 through December 15, 1969.

### 4.3 IMAGE LOCATION AND COVERAGE

The studies in this section relate largely to attitude control and attitude determination requirements. Sections 4.3.1 through 4.3.5 analyze the problem of spatially locating information contained in ERTS imagery to an accuracy of 2 nautical miles. This analysis results in the specification of attitude determination requirements for the spacecraft. Section 4.3.6 investigates the effect of the basic coverage requirements on the control system pointing requirements. Section 4.3.7 summarizes the effects of spacecraft attitude rates on ERTS imagery. Finally, Section 4.3.8 summarizes the attitude control and attitude determination requirements.

#### 4.3.1 GENERAL

Attitude sensors and telemetry provisions to determine attitude to an accuracy sufficient to locate any point on a 100- by 100-nautical mile picture with an accuracy of less than 2 nautical miles is required for ERTS-A and B.

To proceed to a timely solution allowing specification of the accuracy requirement to be met by the attitude determination sensor, an assumption was made in interpreting this requirement. The assumption is that this requirement must be met with a geometrically accurate payload sensor. This requirement then becomes a system/attitude sensor requirement which is not dependent upon the characteristics of any particular payload sensor.

Errors in spatially correlating the imagery obtained to the Earth's surface arise from effects external to the sensor, such as Earth curvature, atmospheric refraction, and terrain relief. Errors in the imagery also arise from effects internal to the sensor, such as lens and scan anomalies. For the purposes of this study, it is assumed that both of these effects will be controlled through an effective sensor implementation and data processing system such that the indeterminate components of these errors will result in picture distortions which are of the order of the ground resolution of the sensor at maximum contrast.

Both the RBV's and the MSS have ground resolutions of 230 to 240 feet from the ERTS altitude. With the assumption that sensor associated random distortions are limited to a ground resolution element (230 feet), it will be shown that position location to an accuracy of 2 nautical miles is essentially independent of the payload sensor.

The total mapping accuracy study to be completed in April 1970 will result in a value for indeterminate sensor distortions based on the analyses performed in that study. When such distortion estimates are available the error analysis will be updated, and the attitude sensor specification and its expected performance will be investigated for margin.

The image location requirement for a 100- by 100-nautical mile picture clearly relates to the RBV's. In consideration of the MSS, where no picture is formed in a conventional sense, the assumption is made that meeting the requirement for an RBV picture results in meeting it for an MSS strip. This is true simply because the MSS is very slightly less sensitive to yaw errors.

### 4.3.2 UNITS

In determining the accuracy requirement for an attitude determination sensor, statistical quantities are involved. Precisely, the accuracy requirement will be in terms of the three-sigma (99.7 percent) value required in three axes (roll, pitch and yaw), where roll and pitch determine the local vertical and yaw determines the heading angle. The 2-nautical mile accuracy is assumed to be a three-sigma value.

As specified in the Design Study Specification, the operational ephemeris location of ERTS will not be known closer than  $\pm 0.16$  statute mile. The precise interpretation is that the in-track position error is 0.16 statute mile, one-sigma, and the cross-track and altitude errors are 50 meters, one-sigma. The three-sigma ephemeris errors are

In-track	Cross-track	Altitude
2534 feet	482 feet	482 feet

The three-sigma accuracy and one-sigma ephemeris assumption is the most pessimistic interpretation.

Timing errors produce location errors due to two types of velocities present in the system. The orbital velocity transferred to the sub-vehicle point produces location errors similar to the effects of ephemeris errors when timing errors exist in the knowledge of shutter time. Angular velocities of the spacecraft frame produce location errors similar to attitude sensor errors when camera shutter operation is not perfectly correlated with the attitude sensor data.

The units employed in this analysis are feet (for ephemeris), minutes of arc (for attitude), and milliseconds (for time errors), and they are three-sigma statistical quantities.

### 4.3.3 GAINS

To set up the error equation, it is necessary to relate ephemeris to surface position, attitude angles to surface position, and time to surface position. These gains then have the units foot per foot, foot per arc-minute, and foot per second, and they allow expression of all error sources in terms of feet on the Earth's surface.

Ephemeris when applied to ERTS would be a table of coordinates with equal time intervals as the argument. To obtain such a table, the ERTS vehicle must be tracked and "fixes" must be obtained. Since the ERTS cannot be tracked continuously, the motion between fixes and tracking times must be modeled. Such modeling requires estimates of the harmonics of the Earth's gravitational field. Once modeled, the series represents the gravitational potential of the Earth so that the Earth's oblateness and its pear shape are represented. (The GSFC Earth model employs 14 to 15 terms.) The effects of drag must also be modeled.

Two types of errors due to ephemeris exist. First, the actual table data can be in error, i.e., at a precise time, the vehicle position as listed in the table has only a finite degree of certainty. Tracking errors usually result in three definable position uncertainties along



11 February 1970

the track, cross-track, and altitude, along the track uncertainties are the largest. Second, the knowledge of time is uncertain, i.e., the table of ephemeris is entered with some basic uncertainty in the argument.

For ephemeris errors when a local vertical sensor is employed, the projection of position from the orbit to the surface is reduced by the ratio of the Earth radius to the orbit radius. For the case of ERTS, this reduction is 7/8. When celestial references are used to determine attitude, the local vertical must be determined from the ERTS position in orbit, and the local vertical thus determined has an error dependent upon the ephemeris error. When this effect is considered, the ephemeris error when projected to the surface has a gain of nearly 1.1.

Attitude when applied to ERTS would be the orientation of the payload sensor with respect to the local vertical and the orbital velocity direction. Attitude errors are small angle perturbations about the references. The gains relate the linear displacement in feet at the Earth's surface to orientation errors about the references.

At ERTS nominal altitude, the length of the arc of 1 minute of central angle is 877 feet. Thus, the first order effect of 1 arc minute of roll or pitch error is 877 feet of surface position error of the sub-vehicle point. At the corner of a picture, a yaw error works through a radius of 70.7 nautical miles. An arc minute of yaw error produces a corner displacement of 125 feet.

Orientation errors are of two types orientation sensor errors and boresight errors. To appreciate these two types of error sources, it is necessary to define the vehicle axes. Let the vehicle control axes be defined as the axes of the orientation sensors. (These axes are not necessarily orthogonal except to first-order effects.) Now let the payload axes be defined as the axes of the sensor/sensors. (These axes are orthogonal since internal sensor anomalies are considered separately.)

Orientation sensor errors are the uncertainties within the sensor (including its data processing) and include non-orthogonalities when more than one sensing head is used.

Boresight errors are the uncertainties which are present between the control axes defined by the orientation sensors and the payload axes defined by the operational sensor or sensors.

Statistically, boresight errors are equal to the mean value of the random process associated with orientation determination and can be estimated statistically. The mean value,  $\bar{X}$ , is  $\int_{-\infty}^{\infty} x f(x) dx$ . Statistically, sensor errors are equal to the square root of the variance where the variance is the mean-squared value of the random process about the mean. The variance,  $\sigma^2$ , is given as  $\int_{-\infty}^{\infty} (x - \bar{X})^2 f(x) dx$ . The mean squared value of the random process,  $X^2$ , is given by  $\int_{-\infty}^{\infty} x^2 f(x) dx$  and is equal to the variance plus the square of the mean value.

MEAN SQUARED VALUE = VARIANCE + MEAN VALUE SQUARED

$$\overline{x^2} = \sigma^2 + \overline{x}^2$$

The high gain associated with orientation errors and the a priori knowledge of the cost to improve the attitude determination system suggests that to use the mean squared value of the sensor rather than the variance as the limiting sensor accuracy may be an expensive accuracy criterion, particularly since the mean value (boresight error) will be readily determined from an averaging of a limited number of ground truth operations. This is comparable to sighting in a gun with a few, measurable trial shots.

The sub-vehicle point velocity in the orbit plane is 21,195 feet per second. The surface velocity (a function of latitude, earth rate, and earth radius) is zero at the poles and 1,520 feet per second at the equator. The error in surface position due to timing error in milliseconds is

In-track                      21.1 ft/msec

East-West (at equator)    1.5 ft/msec

The vehicle attitude rates will never exceed 0.04 degree per second. This is equivalent to 2.4 arc minutes per second or 2100 feet per second in roll and pitch and 300 feet per second at a picture corner in yaw:

Roll/pitch                    2.1 ft/msec

Yaw                            .3 ft/msec

#### 4.3.4 IMPLEMENTATION AND RELATIVE ERROR EFFECTS

The ephemeris errors are considered to be basic system constraints to which a portion of the 2-nautical mile location error must be allocated. The altitude error, to the first order, is assumed to have zero again.

The timing error of interest is the error in determining the shutter operation. Exposure times are 8, 12, and 16 milliseconds. It is reasonable to assume that the system can determine the time of shutter operation to an accuracy commensurate with the exposure time, i.e., the location of the frame center should be as precise as the time of exposure of one part of the picture to any other. The uncertainty in the knowledge of the time of shutter operation is on the order of 10 milliseconds. (Section 4.4 of this volume discusses the approach to achieving this timing information.)

Based upon a 10-millisecond timing error and a picture taken at or near the equator, the position errors of the picture center due to ephemeris and time errors for a local vertical sensor implementation are as follows

In-track	Ephemeris	2216 feet
	Time (velocity)	212 feet
	Time (pitch attitude rate)	21 feet
Cross-track	Ephemeris	422 feet
	Time (velocity)	15 feet
	Time (roll attitude rate)	21 feet

Combining the errors statistically, (both in-track and cross-track) and then geometrically as orthogonal components of an error magnitude results in

$$(\text{Error})^4 = (2216^2 + 212^2 + 21^2)^2 + (422^2 + 15^2 + 21^2)^2$$

$$\text{Error} = 2220 \text{ feet}$$

To make a point, in statistic combination of variances, an order-of-magnitude difference in the standard deviation of two error sources results in the neglecting of that error source with the smaller standard deviation.

With an in-track ephemeris error of 2216 feet, which is non-reducible from an operational system standpoint, a limited number of error sources with an order-of-magnitude lower standard deviation may be ignored.

The assumption in Section 4.3.1 was that if sensor external errors and sensor internal errors are limited to one resolution element (230 feet) on the ground, then these two error sources may be ignored when considering ephemeris and attitude errors. From the above, this assumption is justified.

#### 4.3.5 FIRST-ORDER ERROR EQUATION, ITS SOLUTION, AND ATTITUDE DETERMINATION SENSOR REQUIREMENTS

As indicated in the previous section, there is only one significant error source that must be included in the First-Order Error Equation for attitude errors. This is the in-track ephemeris error, which produces a surface projected error of 2216 feet along the track.

11 February 1970

The three attitude errors are the errors in roll, pitch and yaw. Let these errors be  $E_R$ ,  $E_P$  and  $E_Y$ , respectively. In terms of the Allowable Error ( $E_A$ ) these quantities are related by

$$E_A^4 = \left\{ (2216)^2 + (877E_P)^2 + (88E_Y)^2 \right\}^2 \\ + \left\{ (877E_R)^2 + (88E_Y)^2 \right\}$$

The allowable error is at a corner, and the contribution of yaw error has been geometrically projected to in-track and cross-track components. The allowable error is a scalar quantity.

Two approaches to a solution are possible. First, the allowable error can be reduced from 2 nautical miles by the mean value of attitude error, the expected boresight errors between the payload sensor axes, and the attitude determination sensor axes. The solution would be in terms of the standard deviation of the random variables  $E_R$ ,  $E_P$  and  $E_Y$ . Second, the allowable error can remain at 2 nautical miles where it is assumed that the mean values of  $E_R$ ,  $E_P$  and  $E_Y$  are compensated out by a ground command bias. Such an assumption implies that ground truth data is used to determine the boresight error. During early portions of the mission, the attitude data available with the picture data will not be sufficiently accurate to locate any point with an accuracy of 2 nautical miles because the boresight compensation bias will not have been incorporated. Once truth data is produced to allow mean value (boresight) compensation, the attitude data available with picture data will allow location to 2 nautical miles, and all early data can then be post-adjusted to meet the location accuracy specified.

The error allocation for the post-launch boresight error between the payload and the attitude determination sensor will be 3 arc minutes or 0.05 degree in all three axes. This is not the alignment tolerance between the payload and the attitude determination sensor during spacecraft assembly it is the sum of assembly alignment inaccuracy and any launch induced misalignment. It is felt that such post-launch precision can be achieved by mounting both the orientation and payload sensors to a common support structure, but with difficulty for both payloads (RBV's and MSS). To compensate for the optimism of the 3-arc minutes, a pessimistic rationale will be employed in the allocation of error to boresight sources.

The boresight error is assumed to be 3 arc minutes (optimistic), but the worst case will be used where the 3 arc minutes of boresight error is assumed to exist simultaneously in each axis (pessimistic). The boresight error,  $E_B$ , is

$$E_B = \left[ (3(877))^2 + (3(877))^2 + (3(125))^2 \right]^{\frac{1}{2}} \\ = 3913 \text{ feet}$$

Without in-flight boresight removal, the allowable error is 2 nautical miles less 3913 feet or 8247 feet. With in-flight boresight removal the allowable error is 2 nautical miles or 12160 feet.

The object is to solve the error equation

$$E_A^4 = \left\{ (2216)^2 + (877E_P)^2 + (88E_Y)^2 \right\}^2 + \left\{ (877E_R)^2 + (88E_Y)^2 \right\}^2$$

for two values of  $E_A$  to determine how much roll, pitch and yaw error can be tolerated, with and without in-flight ground truth operations. To solve the equation, we must have two additional equations which relate the roll, pitch and yaw errors to each other

The ratio of the errors are dependent upon the implementation employed.

For a celestial sensor,  $E_R$ ,  $E_P$ , and  $E_Y$  should all be equal. The error equation can then be solved for the per axis error in attitude. The in-track error due to ephemeris error must be increased, as previously noted. The value then is 2534 feet.

$$E_A^4 = \left\{ (2534)^2 + (877E)^2 + (88E)^2 \right\}^2 + \left\{ (877E)^2 + (88E)^2 \right\}^2$$

The solution with calibration is 0.2 degree, and without calibration it is 0.126 degree.

For a local vertical sensor,  $E_R$  and  $E_P$  should be equal. Furthermore, a state-of-the-art limit is 0.10 degree in each axis. The solution of the error equation with these conditions results in the yaw attitude precision requirement.

	<u>Earth Sensor Implement</u>		
	<u>Allowable Error</u> $E_A$	<u>Axis</u>	<u>Assumption</u> $E_R = E_P = 0.1^\circ$
With Calibration	12,160 feet	Roll/Pitch Yaw	0.10° 1.67°
Without Calibration	8,247 feet	Roll/Pitch Yaw	0.10° 0.80°

11 February 1970

The Yaw axis requirement indicates that with some in-flight ground truth data to determine boresight errors between the attitude determination sensor and the payload sensor, the normal yaw-axis control will provide yaw precision that is more than adequate in conjunction with a local vertical sensor of 0.1 degree accuracy. In summary, the attitude determination sensing system accuracy requirements are

1. For a celestial reference system, the three-sigma accuracy must be 0.2 degree with in-flight calibration and 0.126 degree without. This accuracy must be achievable irrespective of available star density variations due to orbit motion, earth occultation, and solar or lunar interference.
2. For a local vertical system, the three-sigma accuracy must be better than 0.1 degree. This accuracy must be achievable over an off-null range of one degree and independent of solar interference effects.

The selection of a sensor satisfying these requirements is discussed in Section 3.3.5 of Volume II of this design study report.

#### 4.3.6 BASIC COVERAGE

A basic requirement for ERTS is to direct the two primary sensor system FOV's to the local vertical and the velocity vector.

In the case of the RBV camera system, it is required that montage photographs be produced with minimum misalignment between contiguous pictures. To produce such a montage, both image overlaps and sidelaps must be provided. An orbit adjust system is provided to initiate and adjust, if necessary, the satellite track to provide image sidelaps from adjacent orbits.

In the case of the multi-spectral point scanner, it is required that the vehicle orbital pitch rate be regular and provide, in conjunction with a single-degree-of-freedom driven mirror, continuous coverage of the subsatellite swath.

Because coverage connotes pointing and not knowledge of pointing, it is necessary to consider the actual achieved orientation accuracy.

Also, there exists a tradeoff between satellite orientation control and orbit parameter adjustment. To the first order, pitch orientation control and along-track ephemeris are related through RBV overlaps, while roll orientation control and cross-track ephemeris are related through RBV sidelaps. Similar interrelationships exist for the MSS coverage of the subsatellite swath.

The ERTS orbit parameters are adjusted to provide a nominal 10 percent sidelap between contiguous subsatellite swaths in the absence of any attitude error, while the actual subsatellite swaths coincide by  $\pm 10$  miles in any one full coverage period.

The ERTS orbit has a semi-major axis of 3936 nautical miles with an orbit period, ascending node to ascending node, of 6196 seconds. The geographic longitude of ERTS ascending node shifts 25.8167 degrees to the west between each subsequent ascending node.

Contiguous subsatellite swaths occur every 14 revolutions and are separated in longitude by 1.4338 degrees. Since a nautical mile is one minute of longitude, the contiguous subsatellite swaths are separated by 86.028 nautical miles at the equator. Table 4.3-1 shows the ascending node longitude history for an initial ascending node in the prime (Greenwich) meridian plane. At the end of 18 days, or the completion of 251 orbits, the coverage period is completed, and the ascending node is again in the prime meridian plane.

The problem of sidelaps is a question of precision of the ascending node geographic longitude shift in 14 orbits and roll/yaw pointing accuracy to achieve the desired coverage

The problem of subsatellite track coincidence is a question of precision of the ascending node geographic longitude shift in 251 orbits. Track coincidence and the orbit adjust system are discussed in Section 4.2. However, the  $\pm 10$  miles allowable in 18 days results in an allowable deviation of the center of contiguous subsatellite swaths (tracks separated by 14 revolutions or about one day) of 0.55 mile.

It will be assumed that the orbit adjust system will not be required to operate more often than once in 18 days and that the error in ascending node shift results in the center of contiguous subsatellite swaths being separated by 86.028 nautical miles to within 0.55 nautical mile.

TABLE 4.3-1. ERTS LONGITUDE OF ASCENDING NODE

Orbit	Degrees West Longitude
0	0.0000
1	25.8167
2	51.6334
-	- - -
13	335.6171
14	1.4338
15	27.2505
--	- - -
250	334.1833
251	0.0000

The coverage problem will be investigated for both sensor systems.

For the RBV, the contiguous geometry at the equator is shown in Figure 4.3-1. The interpretation of the sidelaps requirement is that the 10 percent sidelaps must exist to provide for orientation errors and guarantee that for maximum error at least adjacent pictures are butting.

Under "All Nominal" conditions the sidelap at the equator is

$$\begin{aligned} \text{Sidelap} &= \frac{(100\text{nm}) \cos 99^\circ - 86.028 \text{ nm}}{86.028 \text{ nm}} 100\% \\ &= 14.810\% \end{aligned}$$

To investigate off-nominal conditions, it is assumed that orbit errors produce a 10-mile error in 18 days. It is then possible that the 86.028 nautical miles between swath center lines can for example increase to 86.584 nautical miles. The remaining allowable error under these conditions at the equator is

$$\begin{aligned} E_A &= (98.769 - 86.584) \text{ nm} \\ &= 12.185 \text{ nm} \\ &= 74,100 \text{ feet} \end{aligned}$$

To the first order, one arc minute error in roll produces a loss of 877 feet in sidelap, and one minute of error in yaw produces a loss of 88 feet in sidelap. This is shown in Figure 4.3-2.

Considering of course that only part of the total allowable error can be allocated to either of the adjacent orbit passes, and allowing twice the roll error for yaw, the result is

$$877 (E_R) + 88 (E_Y) < \frac{74,100}{\sqrt{2}}$$

$$E_Y = 2E_R$$

$$E_R < 49.6 \text{ arc minutes}$$

$$E_R < 0.83 \text{ degree}$$

$$E_Y < 1.66 \text{ degree}$$



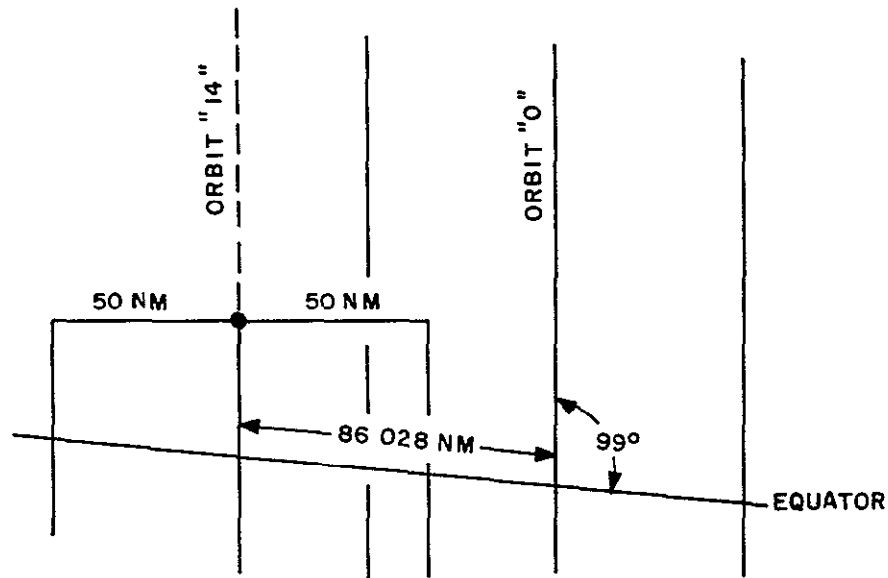


Figure 4.3-1. ERTS Contiguous Geometry

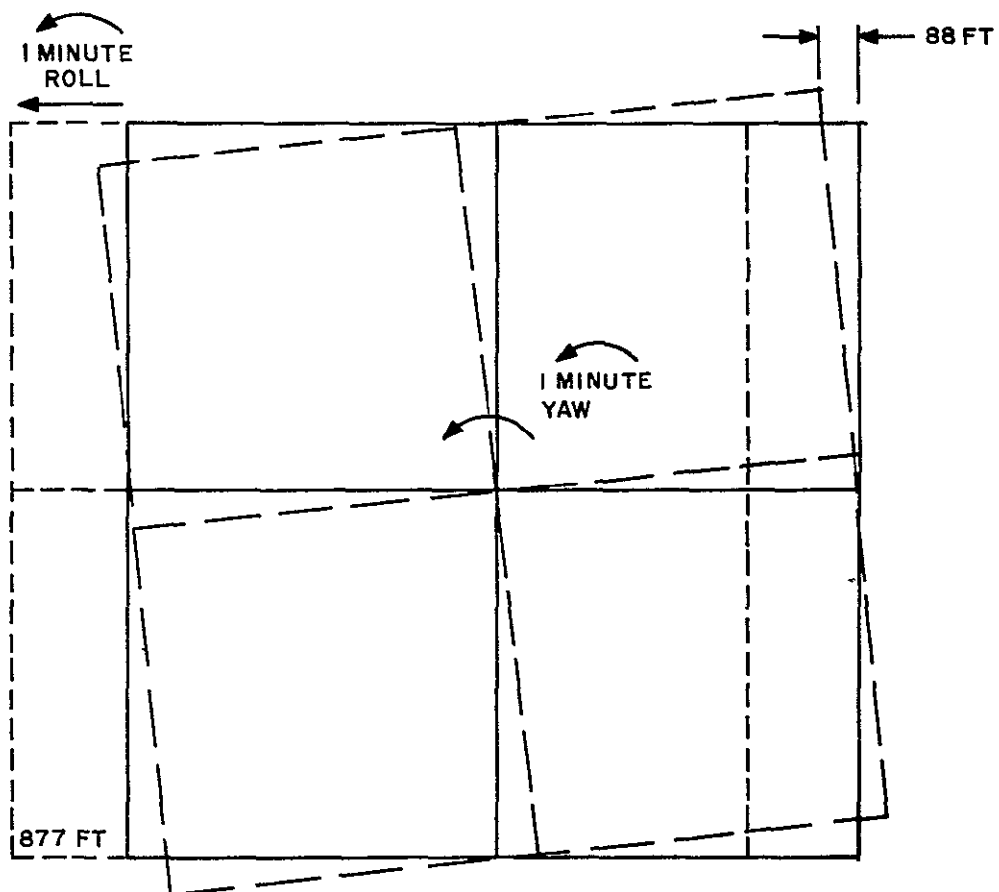


Figure 4.3-2. First-Order Effects of Roll and Yaw Error on Sidelap

11 February 1970

There is no stated overlap requirement. However, if the basic or automatic shutter mode takes a "picture" every 25 seconds, there is a nominal overlap of

$$\begin{aligned}\text{Overlap} &= 100 \text{ nm} - (0.0581^\circ/\text{sec}) (25 \text{ sec}) (60 \text{ nm}/(^\circ)) \\ &= (100 - 87.2) \text{ nm} = 12.8 \text{ nm}\end{aligned}$$

The allowable error is

$$E_A = (12.8 \text{ nm})$$

Picture timing errors between subsequent shutter operations will produce a loss of overlap of 0.3486 nautical mile for every one-tenth second of error. Timing accurate to one part in 250 seems reasonable and will be assumed. (Knowledge of shutter operation time is accurate to 10 milliseconds.)

Yaw error affects overlap as it does sidelap. A pitch orientation error produces 0.144 nautical miles of overlap loss per minute of arc or 8.65 nautical miles per degree.

The allowable overlap loss is  $12.8/\sqrt{2}$  nautical miles. If 0.35 nautical mile is dedicated to shutter timing errors, 8.72 nautical miles is available to pitch attitude error.

$$E_P = \frac{8.72}{8.65} (^\circ) = 1.01 (^\circ)$$

In summary, the most severe pointing requirement to achieve coverage is in roll and yaw, it is 0.83 degree in roll and 1.66 degrees in yaw to achieve butting of adjacent pictures. To ensure  $1-\frac{1}{2}$  nautical mile actual picture sidelap, a roll accuracy of 0.70 degree and a yaw accuracy of 1.40 degrees are required. Pitch accuracy could be relaxed, but with similar implementations, pitch precision of 0.70 degree is implied.

The pointing requirement is 0.70 degree in roll and pitch and 1.40 degrees in yaw and is a requirement on the Attitude Control System. This requirement is in addition to the attitude knowledge discussed in Section 4.3.4.

#### 4.3.7 RATE REQUIREMENTS

A basic requirement for ERTS is to provide rate error of less than 0.04 degree per second, exclusive of orbital rate.

In addition, as a design goal, a rate error of less than 0.015 degree per second is desired for the MSPS.

The rate requirements are due to the finite shutter time of the RBV cameras and the scan implementation of the MSS where the sub-vehicle point velocity is used to provide a "continuous" strip film.

11 February 1970

The RBV's have moving slit focal plane shutters that move parallel to the track. The exposure time is 8, 12, or 16 milliseconds. For continuous coverage, a picture is taken every 25 seconds. Picture size is 11.5 degrees by 11.5 degrees.

A total RBV distortion of 1 percent is expected. This corresponds to 1 nautical mile or 6080 feet. If the spacecraft induced distortions are held to 1 percent of the total distortion or less, these distortions will be negligible.

The MSS has a swipe width of 1380 feet. The swipe is accomplished by a cross-track (roll) sweep of 11.5 degrees in 43 milliseconds, with a return sweep in 24 milliseconds. There are 2640 ground elements per sweep. The detector optical resolution is 230 feet in diameter.

The nominal orbital pitch rate is 0.0581 degree per second, with a nominal in-track surface velocity of 21,195 feet per second

#### 4.3.7.1 Rate Effects on the RBV's

For a roll or pitch rate error of  $\theta_E$  degrees per second, the displacement error while the shutter is open is

$$\theta_E = \dot{\theta}_E T_S$$

For the case where  $T_S$  is 20 milliseconds

$$\theta_E = 20 \times 10^{-3} \dot{\theta}_E$$

On the assumption that such error displacement due to rate is to be 10 percent of the total distortion figure

$$\theta_E = \frac{(0.01) (6080 \text{ ft.})}{\sqrt{2} (877 \text{ ft./min})}$$

Then

$$\dot{\theta}_E = \frac{60.8}{(\sqrt{2}) (877) (0.02)} \text{ min/sec} = 2.5 \text{ min/sec}$$

$$\dot{\theta}_E < 0.04^\circ/\text{sec.}$$

Or, from the viewpoint of smear, a rate of 0.04 degree per second existing in either roll or pitch will produce a smear of 33.6 feet, which seems quite commensurate with the beam focus resolution of 230 feet.

## 4.3.7.2 Rate Effects on the MSS

The MSS has four bands for ERTS A. Each band uses six detectors which are scanned simultaneously. Each detector has an instantaneous FOV of 240 feet. (ERTS B has a fifth band with two detectors and instantaneous FOV of 720 feet, which is not as critical.)

The nominal scan is shown in the Figure 4.3-3.

The swipe width is 21,195 feet per second by 0.065 second, or 1380 feet, which is provided by the MSS design of six detectors in a line array. If the maximum constant rate is 0.04 degree per second, the image location error from the start of one swipe to the next is

$$\begin{aligned} \text{Error} &= (.065 \text{ second}) (0.04 \text{ degree/second}) (60 \text{ min/degree}) (877 \text{ ft/min}) \\ &= 141 \text{ feet} \end{aligned}$$

The width distortion is

$$\text{Distortion} = 43/67 \times 141 \text{ feet} = 90 \text{ feet}$$

It is felt that the 141-foot gap or overlap between swipes is excessive for a basic sensor detector FOV of 240 feet. Overlap should be held to no more than 20 percent, and preferably to about 10 percent. For a 20 percent gap or overlap, the maximum allowable rate is

$$\begin{aligned} \theta_E &= \frac{48}{141} (0.04 \text{ degree/second}) \\ &= 0.0136 \text{ degree/second} \end{aligned}$$

Previous considerations have been of the effects of a constant rate existing in the vehicle frame during an RBV exposure time or during an MSS mirror deflection. Low frequency vehicle frame oscillations about null will have grossly the same worst case effects as a constant rate when the exposure or sweep period is small compared to the period of the oscillation.

In the case of the RBV, shutter a jitter frequency of 786 radians per second would produce a half sine wave position motion during the time of exposure. The jitter rate allowable at this frequency without exceeding the position error of  $2.74 \times 10^{-4}$  degree is 0.338 degree per second.

In the case of the MSS sweep, a jitter frequency of 146 radians per second would produce a half sine wave position motion during the sweep. To keep the position error below 10 percent of a detector instantaneous FOV, the jitter rate allowable at this frequency is 0.105 degree per second.

The allowable jitter rate magnitude as a function of frequency is shown in Figure 4.3-4.

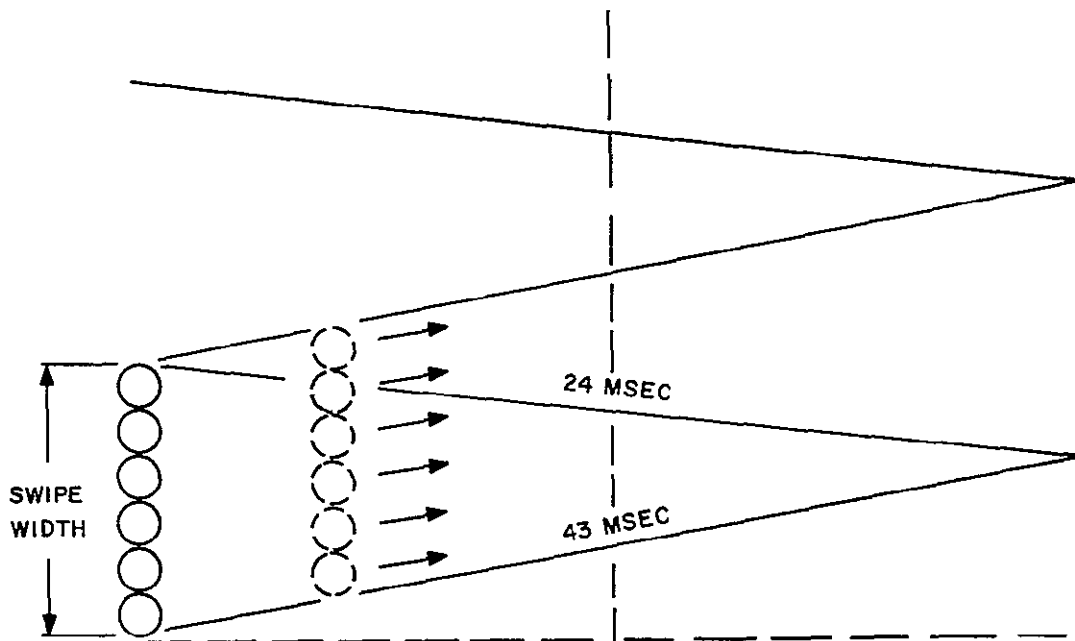


Figure 4.3-3. Nominal Scan

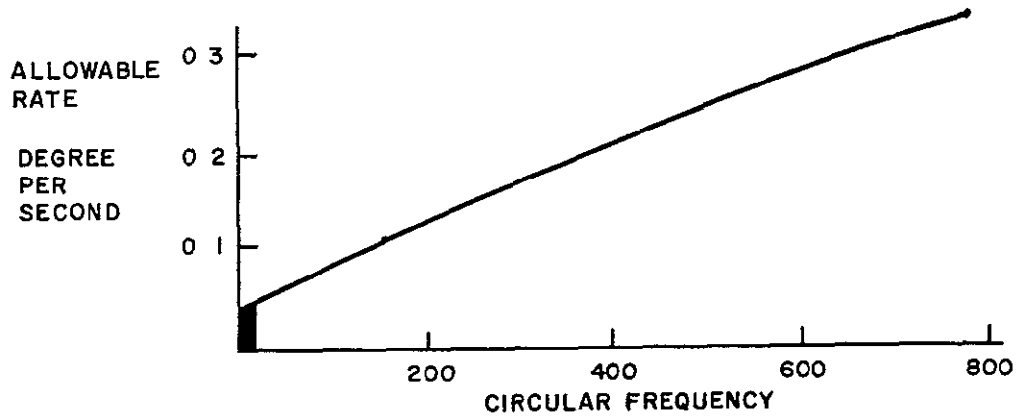


Figure 4.3-4. Allowable Jitter Rate Magnitude as a Function of Frequency

11 February 1970

The approximate controller bandwidth is the dark area. A measurement of the vehicle rates performed by a finite bandwidth instrument or by an infinite bandwidth instrument limited by TM sample rate can ensure that the peak rate is not exceeded for any frequency within its sensitivity.

In the case of high frequency oscillations (those frequencies above the controller bandwidth) instrumentation to measure the instantaneous rate through all these frequencies is very expensive. It is therefore desirable to ascertain the need, i.e., what is the probability that higher frequency oscillations above the controller bandwidth can exist at a sufficient amplitude to produce deleterious effects on the payload sensors.

The source of such oscillations is the structural compliance of the spacecraft, and the higher the frequency the more local the effect. In the present ERTS configuration, high frequency oscillations at the payload would be due to the local structure of the sensor ring. Lower frequency effects would be due to oscillations in the sensor ring/control ring structure or due to bending modes in the articulated solar array.

The cause of such oscillations is not the momentum wheel control actuators because the actuator effects are within the controller bandwidth. Environmental disturbances, also by definition, are within the controller bandwidth. Rather, the oscillations are primarily produced by the RCS. Discrete jet actuation occurring either as a result of orbit control thrusting or momentum wheel unloading are the causes.

At high frequency, the angular acceleration required to maintain a rate amplitude increases linearly with the frequency. This can be seen from the expressions

$$\theta = \frac{A}{\omega} \sin \omega t$$

$$\dot{\theta} = A \cos \omega t$$

$$\ddot{\theta} = A \omega \sin \omega t$$

In order that the displacement be large enough to affect the payload with increasing frequency, the rate amplitude must increase. As a consequence, the acceleration must increase as the square of frequency. For vibrations to shake the massive payload, the large accelerations of high frequency requires large forces, these do not exist in the RCS.

Lower frequency oscillations can produce significant displacement amplitudes with lower accelerations (forces). Primarily, the solar array bending modes when excited by discrete operation of the RCS can be of concern. For ERTS, these frequencies are between one and two cycles per second, and any measure of attitude control subsystem rate performance measurements should include these frequencies.

The instantaneous rate limit should be 0.04 degree per second over a frequency range of zero to 10 cps, with a goal of 0.014 degree per second.

#### 4.3.8 REQUIREMENTS SUMMARY

The ephemeris error for in-track must be less than 0.16 statute mile, one sigma, for cross-track and altitude it must be 50 meters, one sigma. The time of the RBV shutter operations must be known to an accuracy of 10 milliseconds, three-sigma.

The attitude determination sensor should have an accuracy of 0.126 degree, three sigma in all three axes for a celestial type of implementation, for a local vertical type of implementation it should have an accuracy of 0.100 degree in roll and pitch and 0.800 degree in yaw.

Both types of attitude determination systems must retain relative alignment with the payload sensors of 3 arc minutes ( $0.05^\circ$ ). This alignment is the alignment accuracy achieved after the spacecraft has experienced the launch force and vibration environment.

In-flight calibration to remove the mean value of the attitude determination system error (the boresight error) can be performed with ground truth. Such an operation can be looked upon as either improving the image location accuracy to a value less than 2 nautical miles or allowing larger margins for the attitude determination sensor. With in-flight boresighting, a celestial type system is required to have an accuracy of 0.200 degree. A local vertical sensor would retain an accuracy requirement of 0.100 degree, but yaw accuracy could be as imprecise as 1.670 degrees.

The Attitude Control System will point the vehicle to the local vertical and in the direction of flight. Such pointing allows the coverage of the Earth's surface by the RBV pictures and the MSS scan. To guarantee that the pictures and the scan do cover the total Earth's surface without gaps, roll pointing must be performed to an accuracy of 0.83 degree, and pitch to 1.01 degrees. To ensure at least  $1-\frac{1}{2}$  nautical mile overlap to facilitate montage construction, the roll/pitch pointing accuracy should be 0.70 degree, and the yaw pointing accuracy should be better than 1.4 degrees.

The allowable rates present on the spacecraft are determined from the RBV exposure time and the MSS active scan time. For a 20-millisecond exposure time and a maximum displacement of 431 feet for the RBV the vehicle rate should be less than 0.0400 degree per second. For a 43-millisecond active scan time and a maximum error in scan start position of one-fifth of one detector instantaneous field of view, the vehicle rate should be less than 0.0136 degree per second.

The attitude determination sensor requirements, along with the precision in the knowledge of time of RBV shutter operations, will meet the image location requirement. The Attitude Control System requirements for pointing precision and allowable instantaneous rates are in substantial agreement with the ERTS specification.

## 4 4 TIME ANNOTATION

### 4.4.1 GENERAL

A basic requirement for the ERTS mission is to provide "attitude sensors and telemetry provisions to determine attitude to an accuracy sufficient to locate any point on a 100 x 100 nautical mile picture with an accuracy of less than two (2) nautical miles. The above concept for determining the location of any point in the imagery is based on a computation of locations, using spacecraft attitude, ephemeris position and universal time as input parameters " Therefore, as part of the overall image location/time/position correlation, the time at which the sensors were operated must be known to some finite accuracy. In the image location error study (Section 4.3 of this volume), it was shown that for timing errors on the order of 10 milliseconds, the time error contribution to image position location is negligibly small. This section addresses the problems in achieving this accuracy

In order to process imagery within the GDHS, it is necessary to construct an Image Annotation Tape (IAT) containing information such as spacecraft latitude and longitude corresponding to the center of each frame of imagery In order to develop this tape and have it available for processing when the video tapes are received at the NDPF, the spacecraft NB telemetry must contain the times at which the RBV shutter operated. (It will be assumed that the strip MSS imagery will be framed to correspond to the RBV images and thus the annotation data for it will be required for the same times as the RBV shutter operation.)

Based on currently available information on the RBV camera system, no entirely suitable telemetry signal has been defined that precisely defines shutter operating time (An ideal signal would be a bi-level, digital B type signal whose transition occurs at the center of shutter travel ) Therefore, the assumption is made that a suitable signal, compatible with the ERTS telemetry system, ultimately will be available. Even with the availability of such a signal, several problems exist in determining its time of occurrence.

The RBV shutter timing is derived from the spacecraft 1 Hz timing signal from the ERTS Command Clock subsystem. However, it may be delayed by some measureable amount from the leading edge of this square due to internal delays in the RBV system Variations in actual shutter operation (motion) will occur because of mechanical delays which change with time or age. This variation in shutter operation has been estimated to be 1 millisecond at the start of life and extending to 10 milliseconds at the end of one year. Depending on how shutter telemetry signal is derived, this variation may not be sensed. If it is not sensed, the possibility exists that it could be calibrated out of the system during normal operation. Another source of shutter timing variation exists due to rephasing of the camera system with the WBVTR. A possible 800  $\mu$  second delay per picture cycle can be incurred The total timing variation due to this could be as much as 38.4 milliseconds for a 20 minute maximum continuous operating cycle This variation will only occur



when the system is operated in the record mode. Thus, the worst case shutter time variation variation from these two causes could be 48.4 milliseconds. This is shown in Figure 4.4-1.

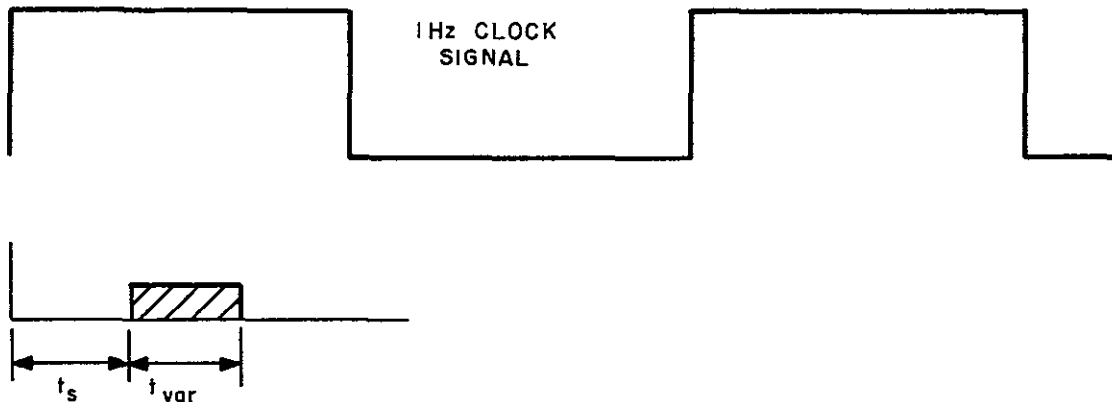


Figure 4.4-1. RBVC Shutter Operating Time Variation

The ERTS telemetry subsystem is also synchronized to the 1 Hz timing signal and if proper attention is taken in assigning the time slot(s) for sampling this RBV shutter signal, reasonable knowledge of its time occurrence can be deduced.

The VIP Telemetry System reads one digital word (10 bits, which could be 10 different bi-level events) into the ITS formatter at a 1 kilobit per second rate. Therefore, it takes 10 milliseconds to read one digital word into the formatter. The 10 bits are clocked in during the last half of the last bit time at the end of a 10 millisecond period. Therefore, the time of occurrence of event is only determinable to this 10 millisecond period. To measure time occurrence of events more accurately than this would require the use of additional equipment which is not now necessary for proper system performance. To be certain the RBVC shutter pulse will be observed and to determine to better than 48 milliseconds when it occurred, even in the 20 minute continuous record mode, will require either multiple sampling of this telemetry output or the selective placement of the three shutter pulses - one from each camera. (It is assumed that the mechanical delays of each are approximately the same, and the build-up of time of shutter operation are identical since the one count down chain controls the entire camera system.) One sampling approach is shown in Figure 4.4-2. The shutter telemetry output would be sampled during one bit of several successive 10 bit digital words. (Five are shown in the example.) The sampling rate for the words shown would be once per second and their time sequence of occurrence would be such that they would be sampled during the interval when the camera shutter could occur. From the resulting telemetry we could determine within one word time (10 milliseconds for a 1 kbps bit rate) when the shutter occurred. Thus, except for errors within the camera between actual shutter travel and the telemetry signal which acknowledges this level, we are able to determine the shutter operating time to  $\pm 5$  milliseconds.

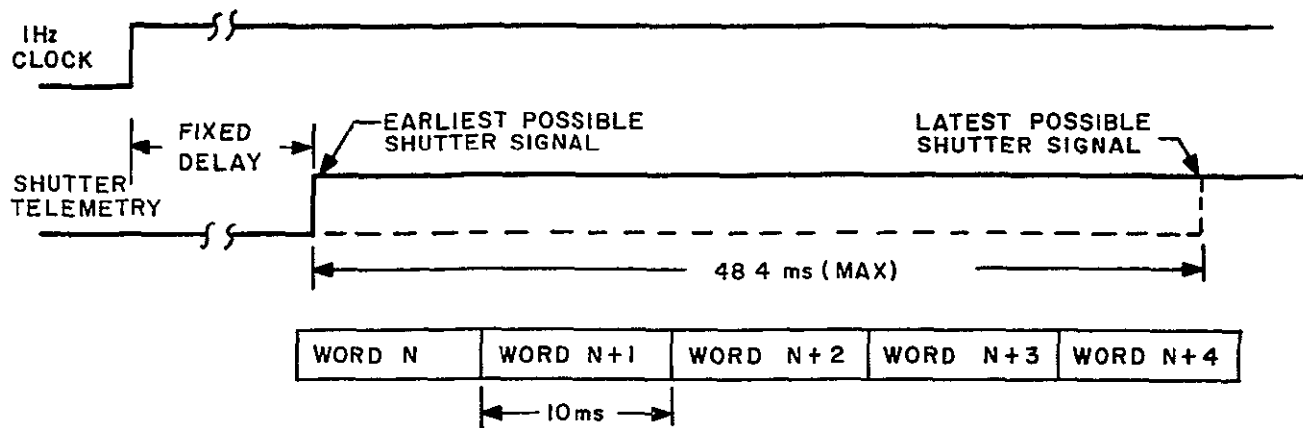


Figure 4.4-2. Shutter Pulse Sampling

Monitoring operation of the MSS involves other considerations. The MSS is not synchronized to the ERTS Command Clock and the sensor can start operation at any time for the real time mode. Therefore, a telemetry output sampled once per second will not have any significant use in determining when the sensor operated any better than within one second. To accurately determine sensor start time requires the knowledge of when the command was received and acted upon. The presence of sensor video output can be an aid here. For stored command operation, the execution time of the command can accurately be determined by knowing where in COMSTOR the command is located. However, this requires a good bit of "bookkeeping" to be done on the ground to keep track of not only when the start commands were sent, but of all the system delays and error sources.

To insure that the sensor video data can be correlated with sensor operate signals (RBVC) or to determine operation time for MSS, time information relating to sensor operation must be stored in some form with the sensor video data. If this is not done, the possibility exists that data will be received without knowing its timing (and therefore, position). To prevent this, several approaches to overall time annotation were evaluated. Common to all approaches is the requirement or assumption that RBV shutter telemetry output is available which relates the initial operation of the sensor to spacecraft time. This is the primary source of information on sensor operation and is used to make up image annotation tapes in advance of receipt of video tapes, as well as time correlating sensor data with NB telemetry support data.

#### 4.4.2 APPROACHES TO TIME ANNOTATION

Four basic approaches were considered for obtaining time information as a function of sensor operation. These approaches are:

1. Record all narrowband (NB) telemetry data on the auxiliary track of the wideband video tape recorder (WBVTR) when recording sensor data.

- a. Real Time - on the ground
  - b. Stored Mode - on the spacecraft (stripped off, sent down via USB, and remerged on the ground with the sensor data)
2. Record the pulse width modulated time code from the ERTS command clock on the auxiliary track of the WBVTR when recording sensor data.
    - a. Real Time - on the ground
    - b. Stored Mode - on the spacecraft (stripped off, sent down via USB, and remerged on the ground with the sensor data).
  3. Record WWV on the auxiliary track of the ground tape recorder in either the real time or stored mode of operation.
  4. Add time code to the sensors.

The fourth approach is the only one requiring an additional modification to the sensors.

#### 4.4.3 DISCUSSION OF APPROACHES

The four approaches considered will be discussed relative to the impact each causes to various sections of the total ERTS System. Each approach offers a feasible concept for the time correlation process. They differ in the amounts of data to be processed or handled and the spacecraft and/or ground equipment required.

1. Record all NB telemetry on the auxiliary track of the WBVTR when recording sensor data.

This approach requires the addition of a buffer amplifier to the spacecraft, so that the single telemetry output channel may be split 3 ways. One to its present path, i.e., the NB link, and the second and third outputs to the auxiliary tracks of the two WBVTR's during the time sensor data is being recorded. During playback the NB telemetry will be stripped off, transmitted to the ground via the USB link and recorded on the same VTR as the sensor data. In the real time mode, the NB telemetry will be recorded on the ground VTR. Two subcarrier oscillators are required in the premodulation processor (PMP) for adding these signals to the USB system. Figure 4.4-3 is a block diagram of this approach.

To recover the sensor operation time, the NB telemetry data recorded with the sensor data must be decommutated and processed. This means that the same telemetry data will be processed twice - the first time is the normal processing as the data is received via the NB system, and the second time when the same telemetry data is stripped from the auxiliary track of the ground VTR.

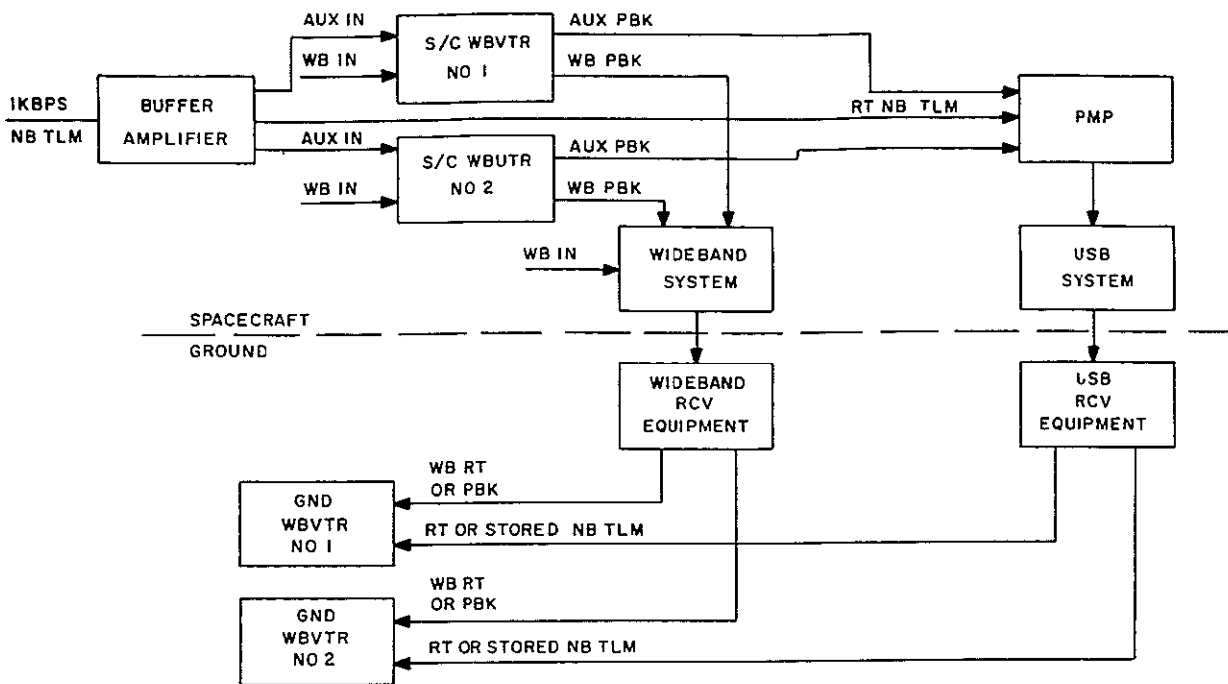


Figure 4.4-3. Time Annotation Approach No.1

2. Record the pulse width modulated time code from the ERTS command clock on the auxiliary track of the WBVTR when recording sensor data.

The comments and discussion for the first approach are pertinent here. The only difference is that the time code from the command clock would be buffered and divided three ways. The time code would be sent down to the ground via the USB link in real-time as well as during playback of stored data. This is shown in Figure 4.4-4.

This approach simplifies time location since only the time code has to be decoded. This is a much simpler operation than processing the entire telemetry matrix. Note that as an alternate for real-time data, time code could be put on at the ground station. It would then be necessary to correlate spacecraft and ground time codes

- 3 Record WWV on the auxiliary track of the ground VTR - real time/stored.

This approach eliminates the need for the storing of any type of data on the WBVTR auxiliary tracks. The WWV time of data reception is placed on the auxiliary track of the ground VTR for either real-time or stored data. However, the ground "bookkeeping" becomes quite complex. For recorded data, a complete log of start and stop times of the

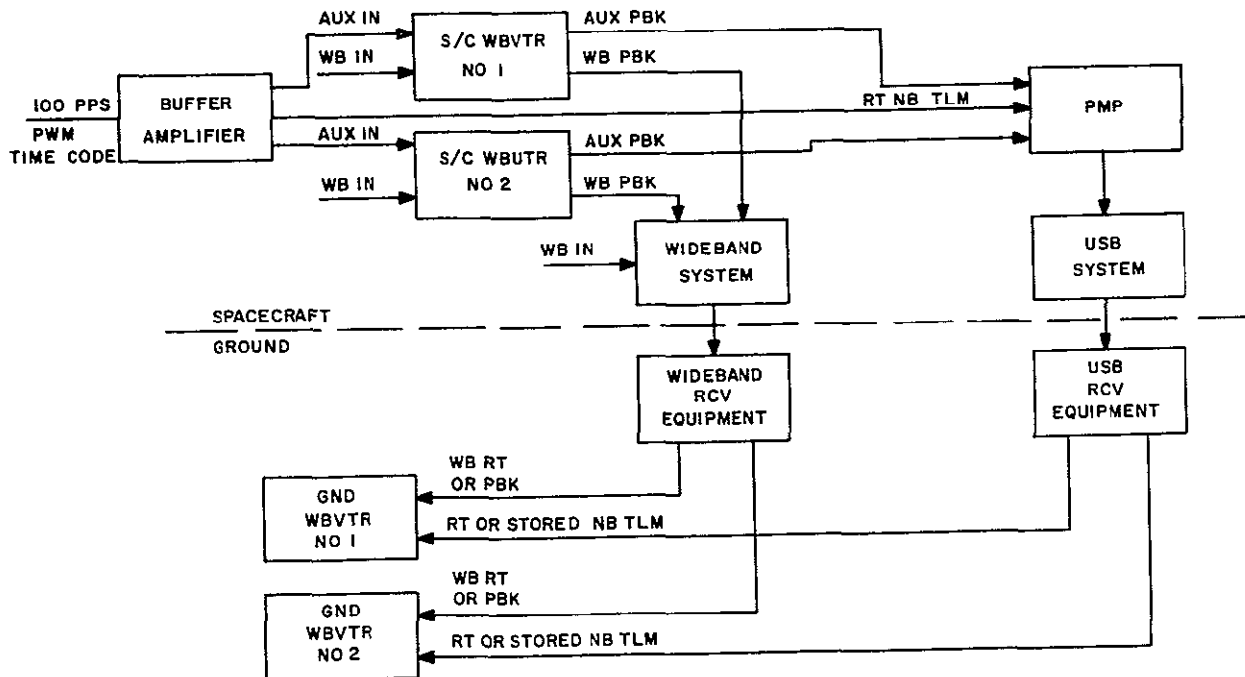


Figure 4.4-4. Time Annotation Approach No. 2

sensors must be maintained for the entire length of the tape. The amount of data played back and at what times must be logged so as to be able to identify where and when the data was taken. Figure 4 4-5 shows the signal flow for this approach

#### 4. Add time code to the sensors.

This approach has the advantage of keeping the video data and the time of its occurrence together. No other auxiliary tracks or data to be stripped and merged are required. It requires the buffering of several ERTS command clock signals so as to make them available to the sensors. Typical signals to be used are time code, 500 Hz and the 1.0 Hz signals. A modification to both the RBV and MSS would be required.

In the case of the RBV, the preferred approach would be to insert the spacecraft time code (modified to give better than one second resolution) just prior to or following the video for each picture. Ideally, the method of implementation should (1) allow for ease in detection and stripping of this time code during video to film conversion, and (2) provide for visual identification in the resulting image. Thus, any and every image would contain an inseparable identifier. The code could also be sampled by the spacecraft telemetry to identify shutter operating time.

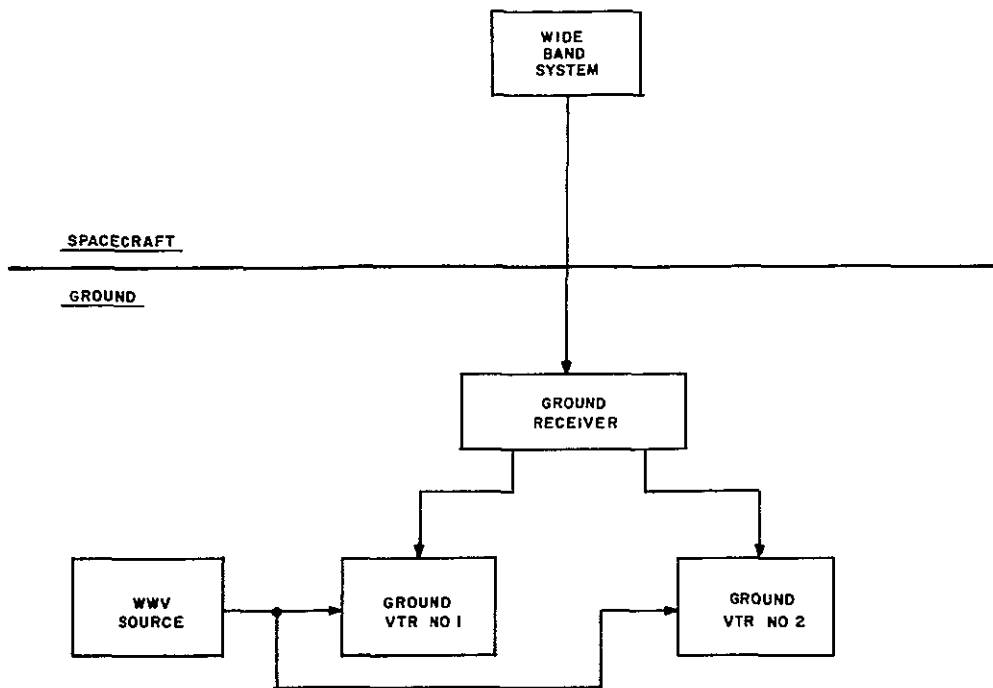


Figure 4.4-5. Time Annotation Approach No.3

For the MSS, time code could be inserted during the retrace time between active scan lines. This could be done during each retrace or periodically every few scan lines. Again, the ideal implementation should be easily detectable electronically or visually

#### 4.4.4 BASELINE APPROACH

Table 4.4-1 summarizes the advantages and disadvantages for each approach. Approach 4, adding time code to the sensors, is the recommended approach. It simplifies the spacecraft, the ground processing and overall produces a more reliable annotation system. It does, however, depend on sensor modification.

In the case of the RBV camera, an implementation scheme is currently under study by RCA. However, no decision has yet been reached to incorporate this scheme. In accordance with the design study specifications, an alternate approach has been selected as a baseline that is compatible with current sensor definition. On the basis of minimum system complexity, the approach of adding time code to the auxiliary tracks of the WBVTR's is the baseline approach. This approach permits accurate time correlation of sensor video and information contained in the NB telemetry data. The additional spacecraft equipment required is a buffer amplifier and IRIG SCO's for the USB premodulation processor. On the ground, the subcarriers will be stripped from the USB signal and added to another track on the ground VTR which is recording wideband sensor data.

TABLE 4.4-1. TIME ANNOTATION APPROACH EVALUATION

Approach	Advantages	Disadvantages
1. Record all TLM data on auxiliary track of WBVTR	<ol style="list-style-type: none"> <li>1. All support data with video on a one-to-one correspondence</li> <li>2. Enables correlation between time and sensor start</li> </ol>	<ol style="list-style-type: none"> <li>1. Requires duplicate processing of TLM data</li> <li>2. Requires either time on OCC ground station or additional TLM station at NDPF</li> <li>3. Requires 2 NB channels for transmission to ground</li> <li>4. Data must be stripped and transmitted via NB link</li> <li>5. Data must be merged on GNDVTR</li> </ol>
2. Record time code on auxiliary track of WBVTR	<ol style="list-style-type: none"> <li>1. Enables correlation between time and sensor start</li> <li>2. Records only necessary data</li> </ol>	<ol style="list-style-type: none"> <li>1. Requires stripping and merging process as approach 1.</li> <li>2. Requires 2 NB channels</li> <li>3. Time code must be merged on GNDVTR</li> </ol>
3. Record WWV on ground VTR auxiliary track	<ol style="list-style-type: none"> <li>1. Eliminates need for spacecraft auxiliary tracks or additional NB channels</li> <li>2. No merging or stripping required</li> </ol>	<ol style="list-style-type: none"> <li>1. All video and TLM data must be normalized to WWV time prior to any pre- or final processing</li> <li>2. OCC "bookkeeping" required for every inch of WB tape</li> <li>3. All system errors must be precisely known</li> </ol>
4. Add time code to sensors	<ol style="list-style-type: none"> <li>1. No bookkeeping</li> <li>2. No other data to be processed</li> <li>3. No additional NB channels needed</li> <li>4. Time and data inseparable</li> </ol>	<ol style="list-style-type: none"> <li>1. Modify sensors.</li> </ol>

## 4 5 MISSION SIMULATION

### 4 5 1 SIMULATION PROBLEM

The primary ERTS mission is to gather multispectral data via earth imaging sensors in a manner that will effectively satisfy an overall coverage requirement. Since the system will be capable of acquiring useable data only under certain conditions (i.e., proper scene illumination, availability of desired terrain, etc.), the operation of the sensors will be scheduled accordingly. The schedule against which the system must operate while in orbit then will levy certain requirements on the spacecraft subsystem design, ground support capability, and operational support procedures.

The capability to simulate the on-orbit profile of the ERTS system operations for what is considered to be a typical and realistic set of conditions was developed. The results of these simulations have provided a data base from which design requirements were derived. The adoption of this approach has insured that all subsystem designs are compatible with the overall ERTS mission.

The basic problem simulated was the on-orbit operation of the sensor payloads, the management of the onboard recorder resource, and the management of the acquisition of data by the ground sites. Of primary importance in the design of the simulation capability was to incorporate the ability to consider both the operational capabilities of the system and the constraints and limitations of both the system and the mission. Since much of the overall operational philosophy was not solidified at the time of this design, a need for flexibility in specifying the parameters and conditions of the simulation cases was mandatory. The resulting simulation capability provided a versatile tool that enabled not only a baseline profile to be generated but also provided the capability to investigate the significance of variation in the basic parameters and conditions of the mission/system.

### 4 5 2 SIMULATION MODEL

The simulation capability is a computer aided process. The basic model is designed around four basic types of mission/system descriptors:

1. Prioritized world coverage map
2. Orbital ground trace
3. Data acquisition site coverage
4. Spacecraft and sensor capabilities and constraints

#### 4 5 2 1 Prioritized Coverage Map

To simulate the anticipated preferences for specific geographical coverage by ERTS, the capability was provided to partition the world map into homogeneous regions. The boundary of each region is a variable and each region is assigned to one of eight different categories. Since it is expected that the desire to image certain areas will be greater than for



others, the categories were assigned a relative priority structure. Figure 4.5-1 presents the prioritized map used for this simulation. The finest granularity of region segmenting was at a region level. Although it is expected that finer coverage region definition will be employed operationally, it is felt that the map used here does present a realistic coverage requirement distribution on which to develop design profiles.

#### 4.5.2.2 Orbital Ground Trace

Although the simulation model can handle any specified orbit, the unique features of the ERTS orbit (i.e., 18 day repeat cycle, sun synchronous) allows for some simplifications to be made in the simulation. With this orbit it is necessary to only examine the operations for a single 18 day cycle. The sun synchronous condition simplifies the accounting for variations resulting from effects of time of year. Effectively, different times of year result in a translation of the region of acceptable sun angle within an orbit and can be assumed to be essentially a fixed translation for all orbits within an 18 day cycle. On figure 4.5-1 the descending ground traces for a typical day in an 18 day cycle are shown. The particular case shown is for "day 9" of the cycle. For each successive day, in a cycle the ground trace overlay would shift approximately 1.5 degrees west at the equator and on the 19th day the ground trace pattern will essentially be the same as day 1.

#### 4.5.2.3 Data Acquisition Site Coverage

Three data acquisition sites capable of receiving the wideband sensor video data were used (Alaska, Corpus Christi, and NTTF). It was assumed that data could be transmitted to the ground sites during any pass over the site (day or night). Although the simulation model can handle any station cone angle, it was assumed for these cases that wideband data could be received any time the spacecraft was at an elevation of more than 5 degrees from the site. Figure 4.5-1 shows the ground station cones for 5 degrees elevation angles. In addition to the three wideband acquisition sites, Rosman is also shown.

Where two or more sites can see the spacecraft at the same time, it was assumed that both sites could receive the video data simultaneously.

#### 4.5.2.4 Spacecraft/Sensor Considerations

The operations of the sensors must be scheduled in a manner that will return imagery over the land areas of interest. The ERTS system has been designed to provide the capability to image the ground during the appropriate daylight portion of the orbit and to store this data for future transmission to earth during those times when not in contact with a ground station. During a contact with a data acquisition station, either data from real time operations of the sensors or the dumping of previously recorded data can be scheduled.

The simulation problem is to generate the schedules for the operations of sensors, on board recorders, data transmission cycles, and spacecraft subsystem support requirements in a manner that best satisfies the coverage requirement. The resultant schedules from the simulation must be feasible for the ERTS System to perform. This requires that the simulation process consider the capabilities of the spacecraft/sensor system and any

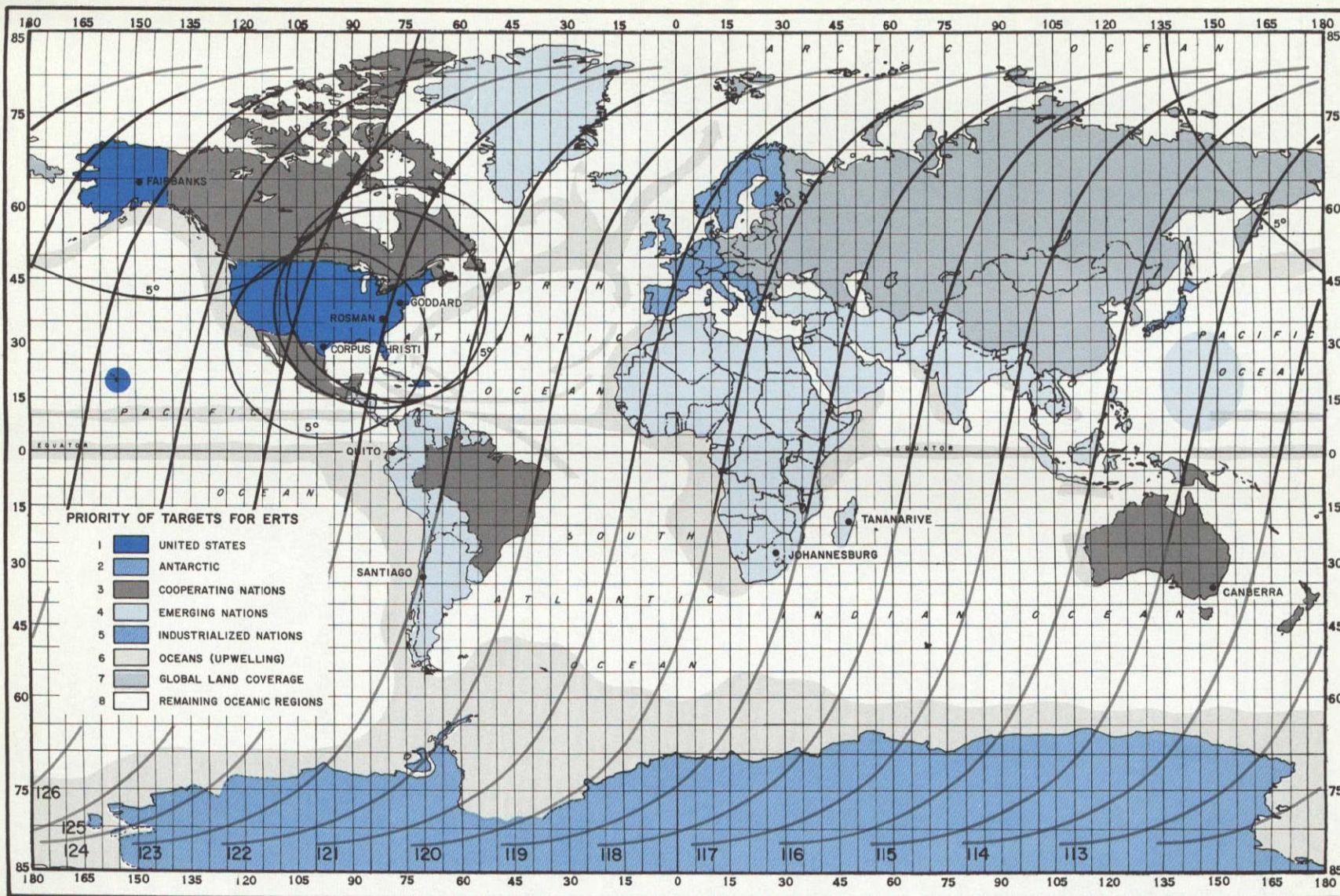


Figure 4.5-1. World Coverage Map

11 February 1970

limitations or constraints imposed on its operations either by the spaceborne system itself, the ground support constraints, or because of operational ground rules. The simulation is capable of handling spacecraft and sensor parameters such as

- 1 On board wideband tape recorder capacity
- 2 Maximum allowable operation time per orbit
- 3 Sensor operating sequences
- 4 Sun angle limits for sensor operations
- 5 Real time or recorded operations
- 6 Selective inhibiting of specific operations or groups of operations

Figure 4.5-2 depicts the simulation tool from a logic flow point of view

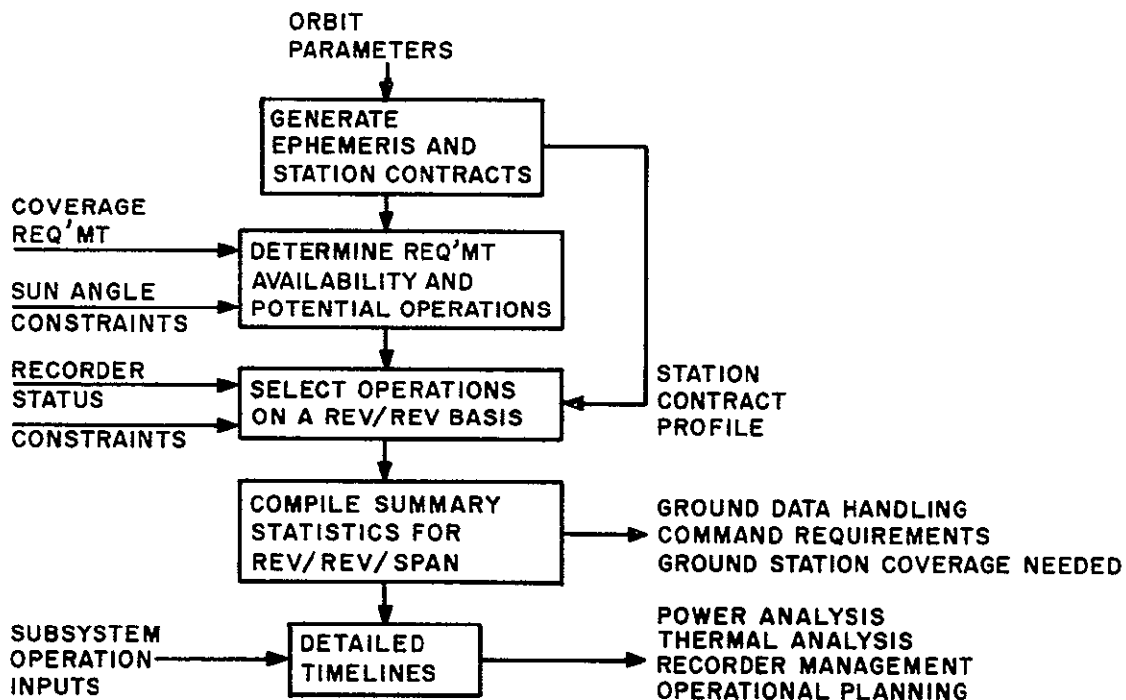


Figure 4 5-2. Simulation Logic Flow

#### 4 5 3 SIMULATION CASES

##### 4 5 3 1 Purpose

Simulated mission operations were used to support the spacecraft design and are continuing to establish the ground support requirements. The specific results obtained for use in the spacecraft design include

- 1 Maximum daily payload operations
- 2 Maximum number of stored commands for payload operations between ground station acquisitions
- 3 Recorder usage

Specific results being obtained for ground data handling system design include

- 1 Maximum daily payload operations
- 2 Command requirements
- 3 Ground station coverage planned

##### 4 5 3 2 Inputs

The simulated mission operations, that were conducted to establish worst case requirements for the spacecraft design, used the following parameters and operational ground rules

- 1 Orbital parameters (ground traces shown in Figure 4 5-1)

inclination	99 088 °
altitude	492 35 nm
period	6196 0 sec
descending node time	0930

- 2 Land mass coverage

complete global coverage over an 18 day cycle

consider no cloud restrictions

land priority structure used if required (priority structure is shown in Figure 4 5-1)

schedule coverage above 60°N latitude on alternate revs only\*

sensors continue to operate between land masses whenever their off period would be less than 2 minutes

2 Payload Operation

Simultaneous MSS and RBV operation are scheduled whenever the following three conditions are met

- (a) sensor operation allowable for sun angle  $\geq 35^\circ$  (Summer solstice case shown in Figure 4.5-1, by darker portion of orbit traces)
- (b) a real time link or WBVTR available
- (c) the subsatellite point is overland, coastal waters or major island groups

3 Data Acquisition Stations

Alaska, Corpus and NTTTF/Rosman

unrestricted wideband link operation within 5° elevation cone

Minimum station contact of two minutes required in order to schedule WBVTR playback

unrestricted use of in-cone time (i.e., ground station support whenever required)

4 Spacecraft recording capability

2 WBVTRS

30 minute capacity each

no operating life restrictions

4.5 3.3 Mission Profiles

Simulated mission operations using the above ground rules have been performed for 18 day periods at summer solstice, vernal equinox and winter solstice. The autumnal equinox is nearly identical to the vernal equinox, therefore, changes in payload operation can be projected for a full year of operation.

Mission operations data has been summarized in three tables. Table 4 5-1 contains the information for summer solstice, Table 4 5-2 for fall and spring, and Table 4 5-3 for winter operations.

\*Above 60°N latitude, alternate contiguous subsatellite swaths provide the required coverage including overlap. Therefore, complete coverage can be obtained in 18 days by scheduling alternate rev operation. Elimination of this duplicate coverage permits more effective use of the Alaska ground station and in recovering data from other areas of the world.

Table 4 5-1 Operations Summary 18-Day, Summer Solstice

Day	I Available Land Mass Sun Angle 35°			II Available Land Mass Sun Angle 35° Duplicate Coverage Removed - > 60°			III Actual Scheduled Mission Operations			IV Available Land Mass Missed
	Total	Total Real Time	Total Remote	Total	Total Real Time	Total Remote	Total	Total Real Time	Total Recorded	Total
1	182 4	42 9	139 5	156 9	30 5	126 4	139 3	30 5	108 8	18 6
2	183 3	45 5	139 8	159 4	37 5	121 9	143 4	37 5	105 9	16 0
3	177 6	41 8	135 8	151 7	30 4	121 3	136 9	30 4	106 5	14 7
4	180 4	42 2	138 2	152 1	34 4	117 7	137 1	34 4	102 7	15 0
5	183 0	44 5	138 5	156 2	33 1	123 1	137 1	33 1	104 0	19 1
6	186 5	43 0	143 5	156 3	33 4	123 3	135 2	33 4	101 8	21 5
7	192 0	43 4	148 6	164 9	34 2	130 7	139 3	34 2	105 1	25 6
8	187 9	39 3	148 6	159 1	30 1	129 1	137 0	30 1	106 9	22 2
9	183 6	46 3	147 3	170 7	37 9	132 8	147 1	40 7	106 4	24 5
10	187 9	40 2	147 7	160 8	33 1	127 7	141 2	33 1	108 1	19 6
11	184 7	40 1	144 6	161 4	33 3	128 1	136 2	33 3	101 9	26 2
12	181 3	40 0	141 3	153 6	29 4	124 2	133 3	29 4	103 9	20 3
13	174 8	40 8	134 0	150 2	33 8	116 4	126 9	33 8	93 1	23 3
14	171 9	41 0	130 9	145 6	30 4	115 2	128 0	30 4	97 6	17 6
15	171 7	41 6	130 1	147 2	34 3	113 9	128 8	34 3	94 5	19 4
16	164 9	38 5	126 4	141 3	29 3	112 0	127 0	29 3	97 7	14 3
17	170 0	40 7	129 3	145 1	33 2	111 9	131 8	33 2	98 6	13 3
18	166 9	40 2	126 7	144 1	31 6	112 5	134 4	31 6	102 8	9 7

(TIMES IN MINUTES)

Table 4.5-2 Operations Summary 18-Day, Vernal/Autumnal Equinox

Day	I Available Land Mass Sun Angle 35°			II Available Land Mass Sun Angle 35° & Duplicate Coverage Removed - > 60°			III Actual Scheduled Mission Operations			IV Available Land Mass Missed
	Total	Total Real Time	Total Remote	Total	Total Real Time	Total Remote	Total	Total Real Time	Total Recorded	Total
1	123 6	11 9	111 7	Same as Column I			115 8	11 9	103 9	7 8
2	131 3	17 2	114 1				122 9	17 2	105 7	8 4
3	125 6	15 7	110 0				117 3	15 7	101 6	8 3
4	123 9	15 6	108 3				114 9	15 6	99 3	9 0
5	121 8	16 5	105 3				112 3	16 5	95 8	9 5
6	122 7	15 8	107 0				112 8	15 8	97 0	10 0
7	121 0	14 3	106 7				111 7	14 3	97 4	9 3
8	120 5	13 6	106 9				110 2	13 6	96 6	10 3
9	127 6	20 6	107 0				112 9	20 6	92 3	14 7
10	121 1	16 0	105 1				106 1	16 0	90 1	15 0
11	119 5	14 8	104 7				105 6	14 8	90 8	13 9
12	116 8	14 5	102 3				102 5	14 5	88 0	14 3
13	114 0	16 0	98 0				100 3	16 0	84 3	13 7
14	110 0	14 7	95 3				96 9	14 7	82 2	13 1
15	113 9	15 7	98 2				100 0	15 7	84 3	13 9
16	110 0	13 6	96 4				98 8	13 6	85 2	11 2
17	113 9	14 0	99 9				103 6	14 0	89 6	10 3
18	113 4	14 0	99 4				98 7	14 0	84 7	14 7

(TIMES IN MINUTES)

Table 4 5-3 Operations Summary 18-Day Winter Solstice

Day	I Available Land Mass Sun Angle 35°			II Available Land Mass Sun Angle 35° Duplicate Coverage Removed - >60°			III Actual Scheduled Mission Operations			IV Available Land Mass Missed
	Total	Total Real Time	Total Remote	Total	Total Real Time	Total Remote	Total	Total Real Time	Total Recorded	Total
1	67 9	1 2	66 7	Same as Column I			67 9	1 2	66 7	0
2	77 4	2 6	74 8	NOTE			77 4	2 6	74 8	0
3	75 1	1 7	73 4	Lower latitude limit for a sun elevation angle $\geq 35^\circ$ is -65 7° All of Antarctica is below this latitude Sensor operations should be possible for lower sun angles over this region because of the increased reflectivity of the area These operations are not shown on this table because of the ground rule of sun angle $\geq 35^\circ$ Alternate rev operation would be scheduled for mission operations over Antarctica			75 1	1 7	73 4	0
4	72 3	2 5	69 8				72 3	2 5	69 8	0
5	70 3	3 1	67 2				70 3	3 1	67 2	0
6	71 2	2 2	69 0				71 2	2 2	69 0	0
7	68 9	1 9	67 0				68 9	1 9	67 0	0
8	66 3	0 5	65 8				66 3	0 5	65 8	0
9	71 1	3 9	67 2				71 1	3 9	67 2	0
10	64 5	0 5	64 0				64 5	0 5	64 0	0
11	57 9	0 9	57 0				57 9	0 9	57 0	0
12	55.4	0.9	54 5				55 4	0 9	54 5	0
13	54 7	2.4	52 3	54 7	2 4	52 3	0			
14	51 1	0.9	50 2	51 1	0 9	50 2	0			
15	55 6	2.1	53 5	55 6	2 1	53 5	0			
16	56 7	0.5	56 1	56 6	0 5	56 1	0			
17	61 8	0 9	60 9	61 8	0 9	60 9	0			
18	60 5	1 5	59 0	60 5	1 5	59 0	0			

(TIMES IN MINUTES)



These tables show (I), the total land mass covered for a sun angle  $\geq 35^\circ$ , (II), the total land mass covered for a sun angle  $> 35^\circ$  less the duplicate coverage that exists in 18 days at latitudes greater than  $60^\circ$ , and (III), scheduled mission operations. Each of these three major columns further shows the breakdown of this coverage by real time, remote coverage and their totals. A fourth major column, (IV), shows the total land mass missed because of combined recorder/ground station limitations.

Examination of the maximum case of payload operations is required as a worst case input to power analysis, thermal analysis, and ground operations. As expected, the maximum payload operations occur during summer solstice. Average daily operations during this season are approximately 135 minutes. Average daily operations for Spring/Fall and Winter seasons are 108 and 64 minutes respectively. Note that summer operations are double those for winter and 25 percent higher than the equinox case. Within summer solstice, day 9 operations (147 minutes), represents the absolute worst case.

Day 9 is examined in detail in the timelines shown in Figure 4 5-3. These timelines show by rev, the latitude and time at which primary ground station coverage is available and the mission operations planned. Subsystem payload operation required to perform the mission operations is shown, including warmup/starting times and recorder operations of rewind, record and playback. Rev summaries of total operating times, frames of data taken, and recorder management are shown.

#### 4 5 3 4 Summary

Maximum payload operations occur during summer solstice due to the fact that most of the world's land mass is in the Northern Hemisphere. Maximum payload operations occur during day 9 of this period, and this day has been examined in detail through the use of a timeline. It should be noted that these represent worst case conditions. Under more realistic conditions cloud coverage restrictions would have been used. Operationally, areas of cloud cover would be inhibited to eliminate useless tape recorder operation. Also, the total world land mass has been attempted during all seasons. It is assumed that preference would likely be given to the Northern Hemisphere during the summer growing season at the expense of Southern Hemispheric coverage. However, the worst case results from the mission simulation studies are the inputs used in the specific studies that follow.

### 4 5.4 SPECIFIC STUDY RESULTS

#### 4 5 4 1 Power Analysis Input

The power subsystem was evaluated using the maximum daily payload operation. The detailed timeline for this day (Day 9) was used as an input to the power analysis computer program. The mode of operation of all individual payload equipments and the time of day or night these operations occur were inputted to this computer program to develop the detailed load profile.

Power status results, for this simulated worst case day, are discussed in Volume II Section 8.3.



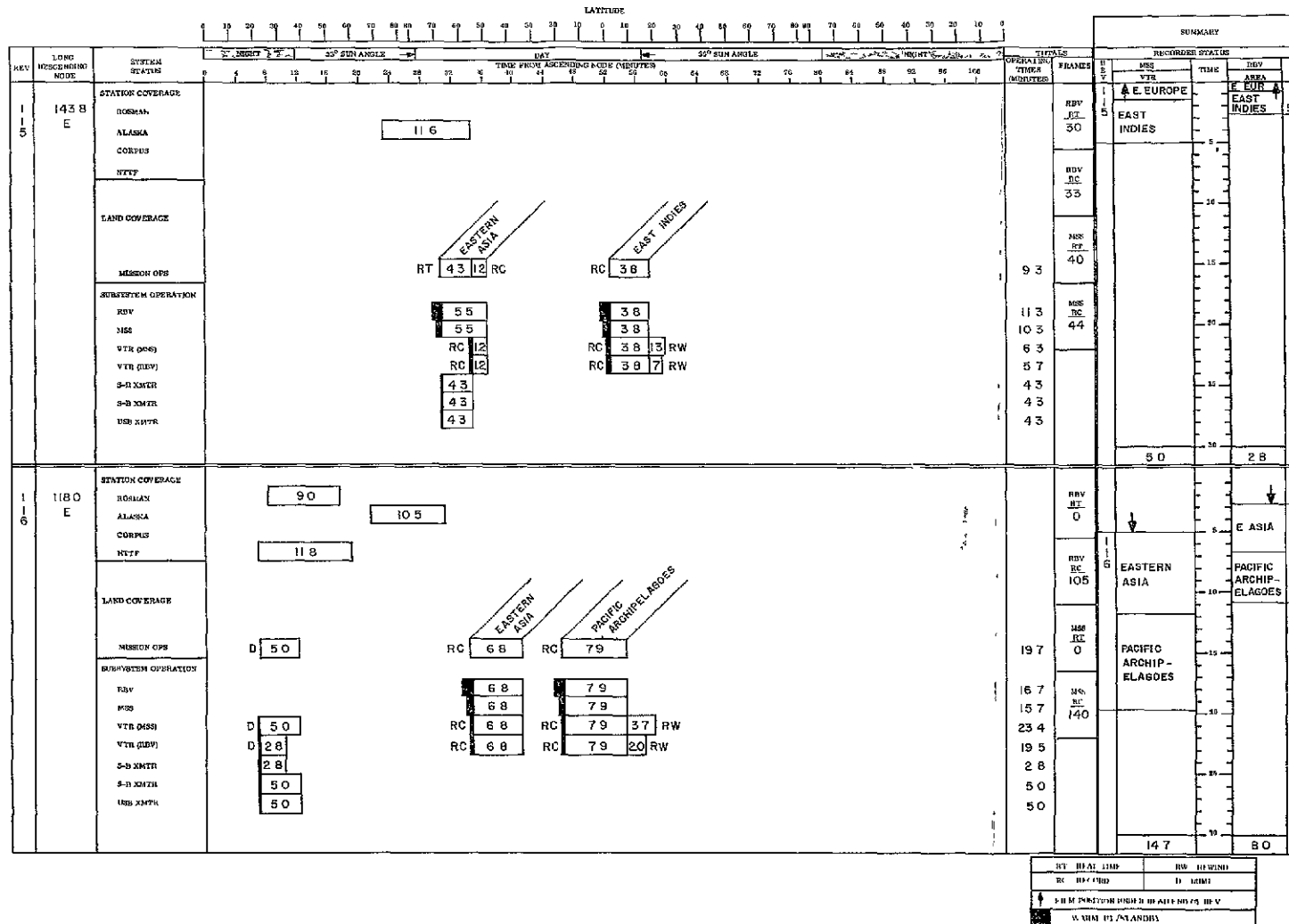
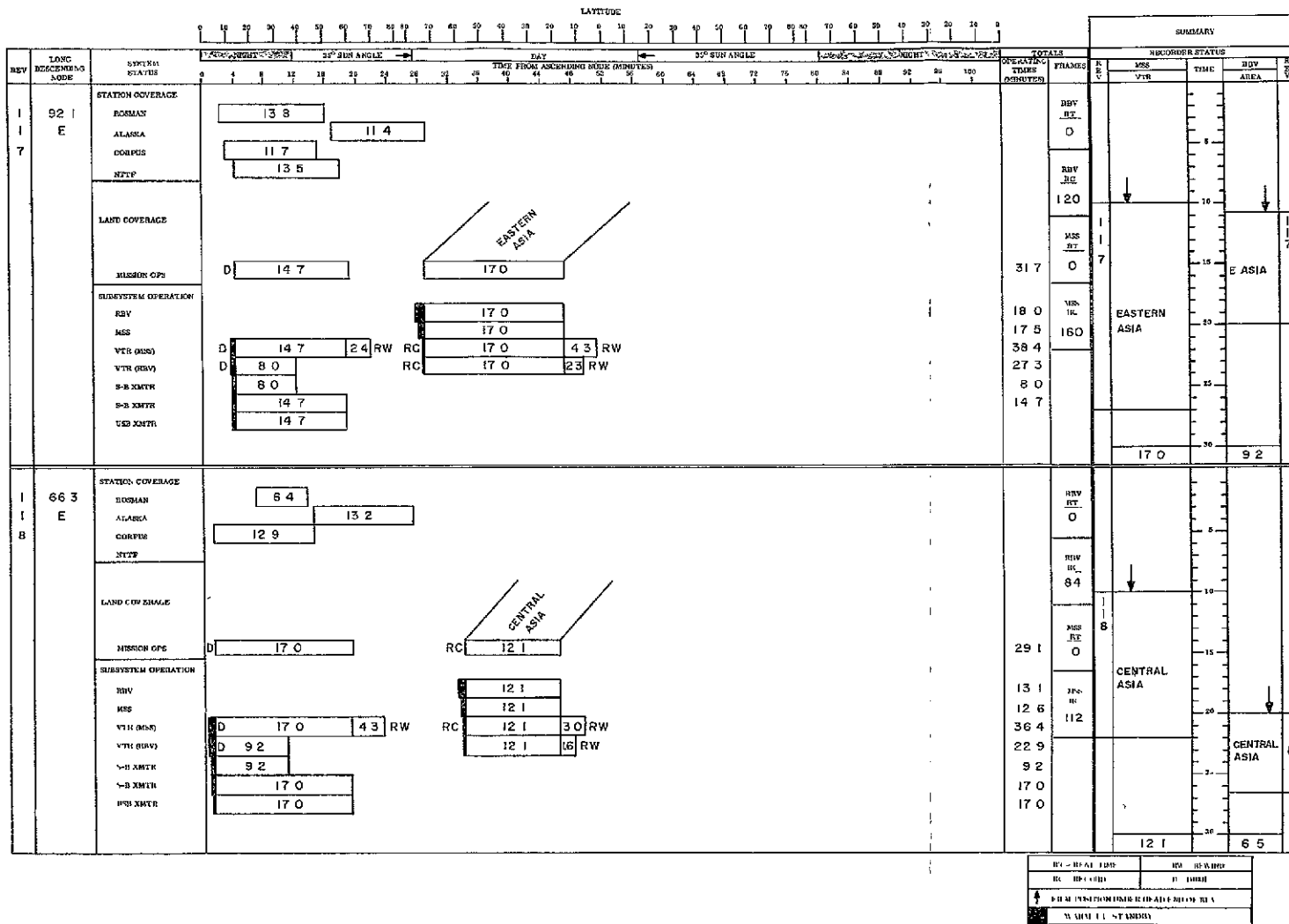


Figure 4.5-3 Mission Timeline-Day 9 (Sheet 2 of 7)

FOLDOUT FRAME

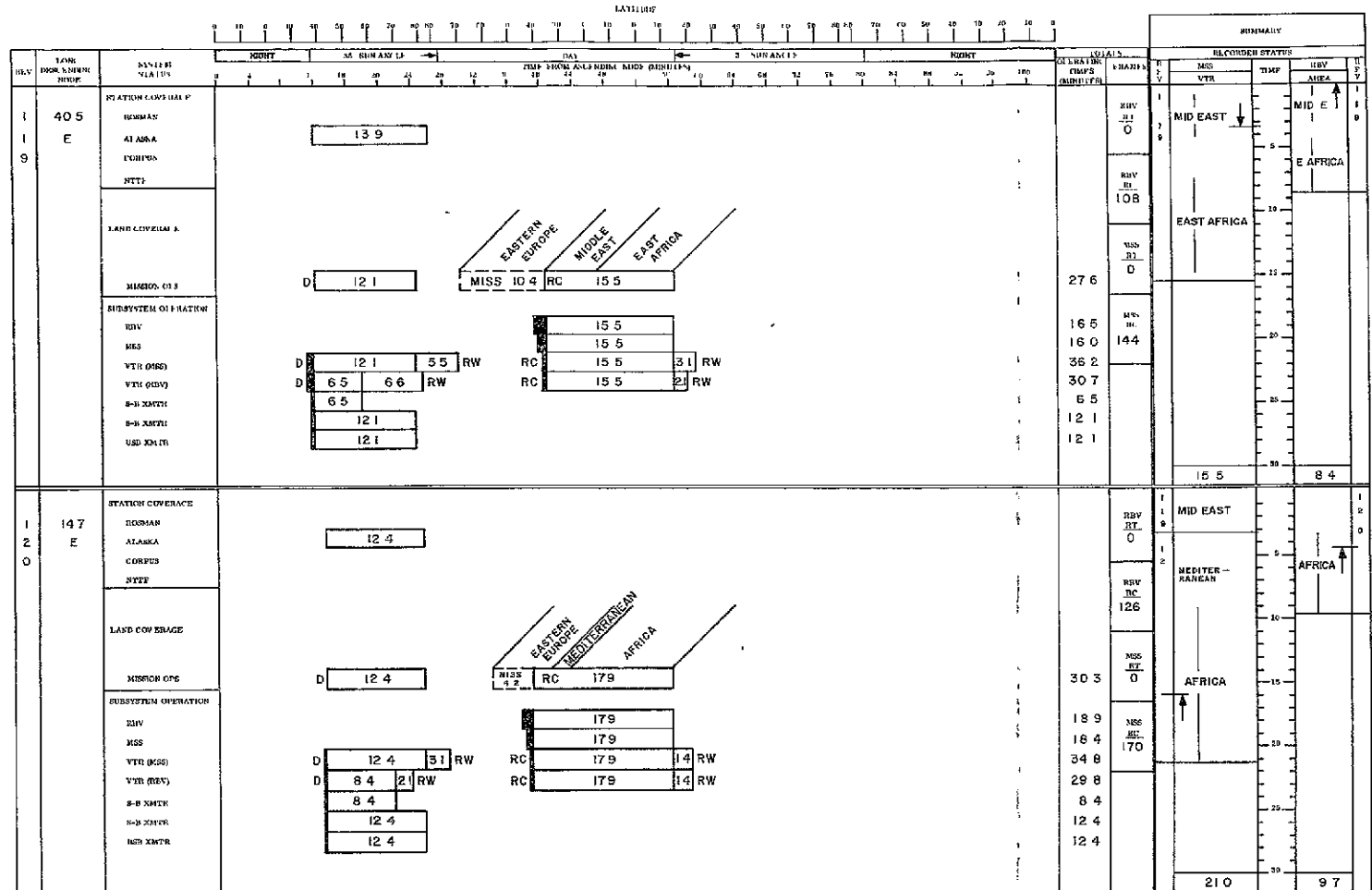
FOLDOUT FRAME



FOI DOUT FRAME

Figure 4.5-3. Mission Timeline-Day 9 (Sheet 3 of 7)

FOLDOUT FRAME



RT - REAL TIME      RW - REVISED  
 RC - RECORD      D - DUMP  
 ↑ FILM POSITION UNDER HEAD END OF REV  
 WARM-UP/STANDBY

FOLDOUT FRAME

Figure 4 5-3 Mission Timeline-Day 9  
 (Sheet 4 of 7)

4-117/118  
 FOLDOUT FRAME



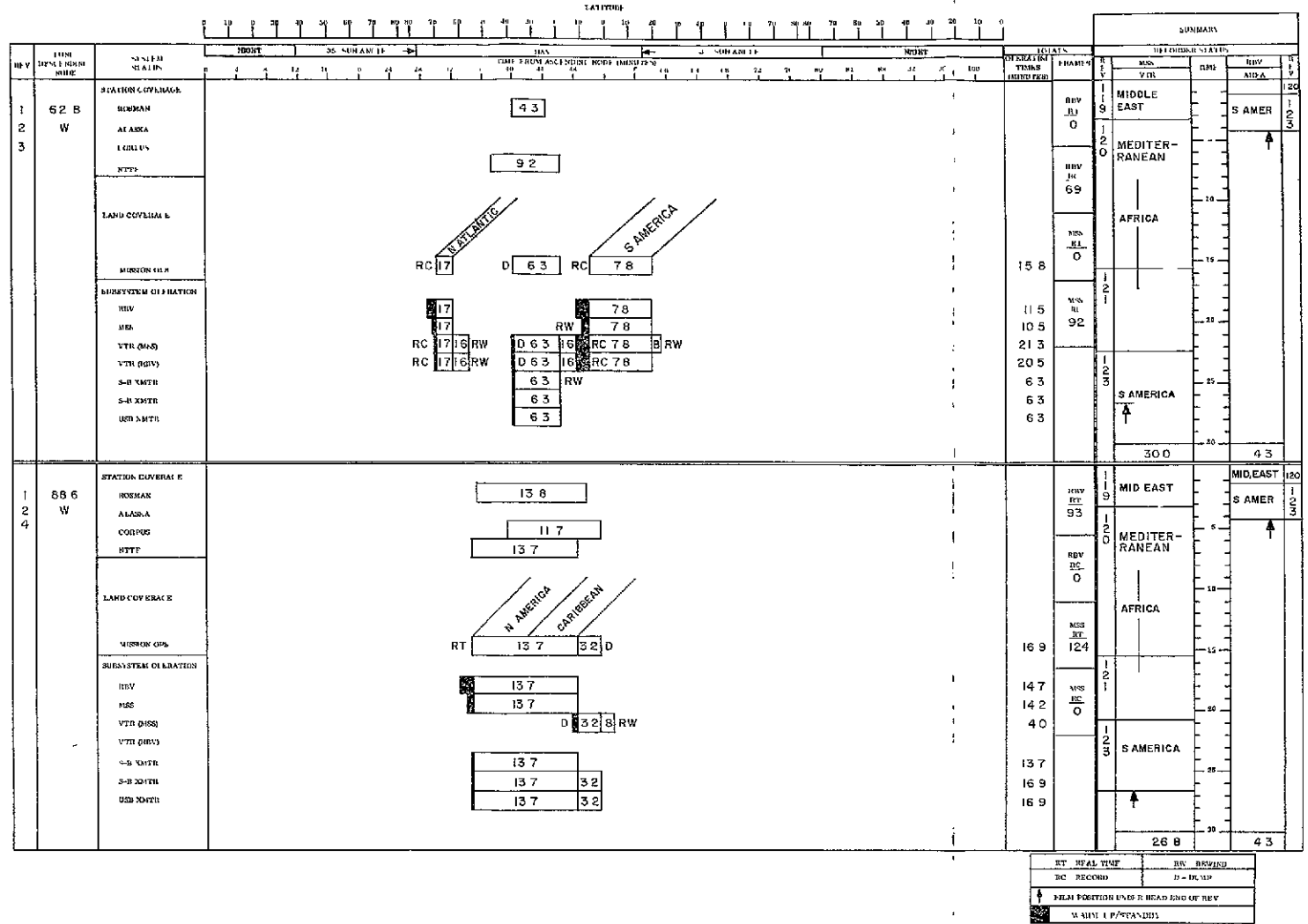
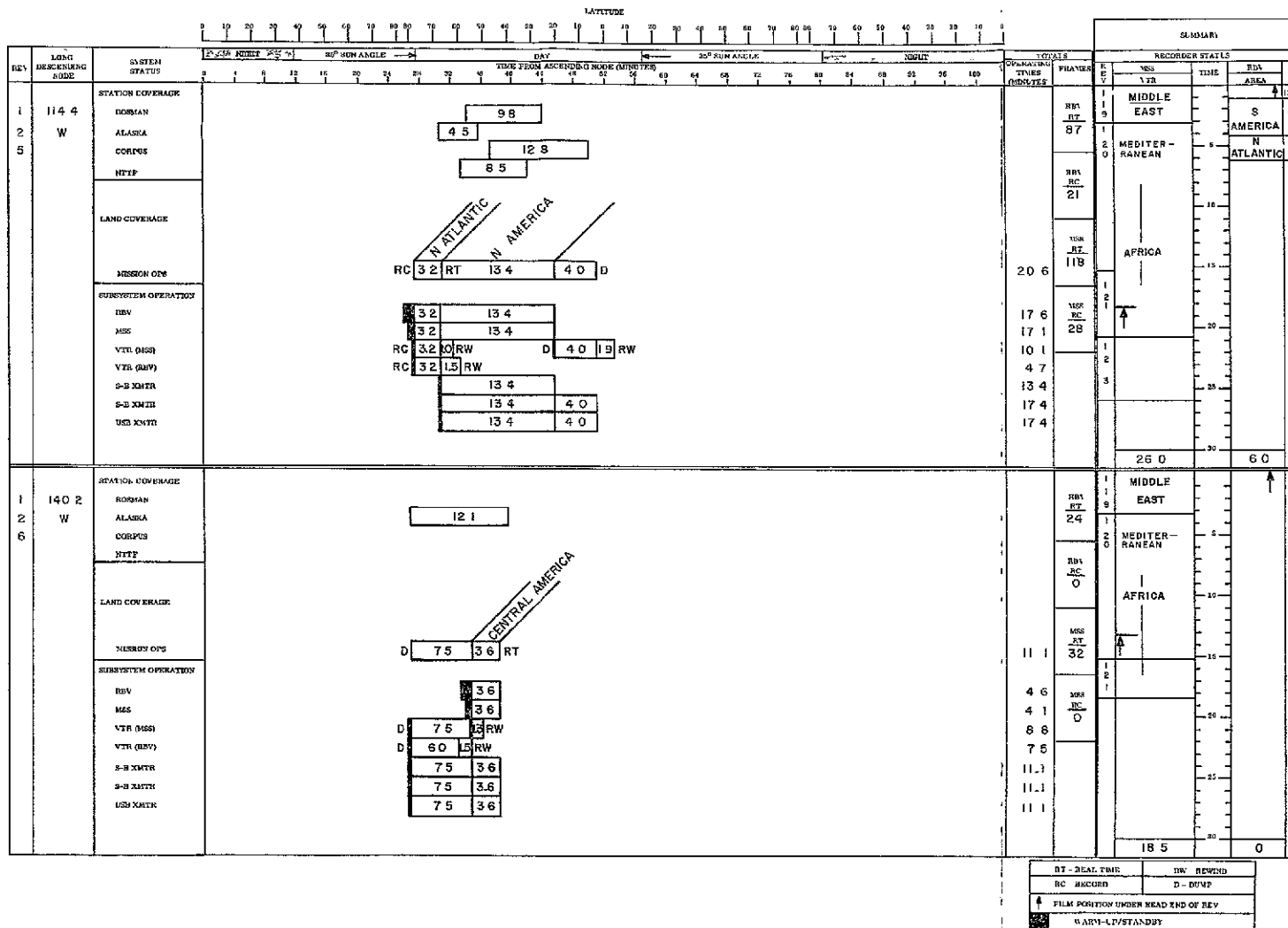


Figure 4 5-3 Mission Timeline-Day 9 (Sheet 6 of 7)

FOLDOUT FRAME

FOLDOUT FRAME



FOLDOUT FRAME

Figure 4.5-3 Mission Timeline-Day 9 (Sheet 7 of 7)

FOLDOUT FRAME



#### 4 5.4.2 Thermal Analysis Input

The worst case system operations for heating occurs not on the longest payload operating rev (27+min) but on a series of successive long operating revs. This is due to the thermal lag in the system in that it cannot return to its starting point in a single rev. Therefore, the input to thermal analysis from the mission simulation studies is to find the greatest accumulation of payload operating time in consecutive revs. This also occurs in Day 9

Thermal analysis for this mission simulation is contained in Volume II, 7.

#### 4.5 4 3 Command Storage Requirements

##### 4 5 4 3 1 Period Requiring Greatest Number of Stored Commands

The maximum loading on command storage occurs when the greatest number of remote payload sequences are required between station contacts. Mission simulation studies considering station contacts and payload sequences required have shown that this could occur on Days 8, 13, 14, 15, 16 and 17 (of each 18-day series) during spring, summer and fall periods. Table 4.5-4 summarizes the command sequences required, for the "dead" rev station contact period, for summer solstice.

##### 4.5.4.3.2 Sequences required for Maximum Case

Day 13, requiring 5 stored command sequences, is typical of the maximum cases and is illustrated in Figure 4.5-4. The following brief sequence of events occurs for this period

Mission Operation	Rev	Duration	Event	Place
Station Contact	8	11 5	Comd. Loading	Alaska
1st Payload Operational Seq	8	8 6	RBV/MSS Recorded Ops	Eastern Europe
2nd Payload Operational seq	8	9 7	RBV/MSS Recorded Ops	Africa
3rd Payload Operational Seq.	9	12.8	RBV/MSS Recorded Ops	W. Europe
4th Payload Operational Seq.	10	0 9	RBV/MSS Recorded Ops	N. Atlantic

TABLE 4 5-4 NUMBER OF PAYLOAD SEQUENCES REQUIRED - "DEAD" REV STATION CONTACT PERIOD

Day	Station Contact Rev	Payload Sequences by Rev					Mission Ops Area	Total Sequences Required
		8	9	10	11	12		
1	9	1					Europe/Africa N Atlantic S America N Atlantic	4
	12		1		1	1		
2	9	1					Europe/Africa N Atlantic S America --	3
	12		1		1	1		
3	9	1					Europe/Africa -- S America N Atlantic	3
	12		0		1	1		
4	9	1					Europe/Africa -- S America --	2
	12		0		1	0		
5	9	1					Europe Africa -- S America N Atlantic	4
	12	1		0		1		
6	9	1					Europe Africa -- N Atlantic S America --	4
	12	1		0		1		
7	9	1					Europe Africa -- S America N Atlantic	4
	12	1		0		1		
8	9	1					Europe Africa S America N Atlantic S America --	5
	12	1		1		1		
9	9	1					Europe/Africa S America --	2
	11		1			0		

Day	Station Contact Rev	Payload Sequences by Rev					Mission Ops Area	Total Sequences Required
		8	9	10	11	12		
10	9	1					Europe/Africa S America N Atlantic	3
	11			1		1		
11	9	1					Europe/Africa S America --	2
	11			1		0		
12	9	1					Scandinavia Europe/Africa S America N Atlantic	4
	11			1		1		
13	8	1					Europe Africa Europe/Africa N Atlantic S America --	5
	11	1		1		1		
14	8	1					Europe Africa Europe/Africa S America N Atlantic	5
	11	1		1		1		
15	8	1					Europe Africa Europe/Africa N Atlantic S America --	5
	11	1		1		0		
16	8	1					Europe/Africa W Europe W Africa S America N Atlantic	5
	11	1		1		1		
17	8	1					Europe/Africa W Europe Africa N Atlantic S America --	5
	11	1		1		0		
18	8	1					Europe/Africa W Europe S America N Atlantic	4
	11	1		1		1		

11 February 1970

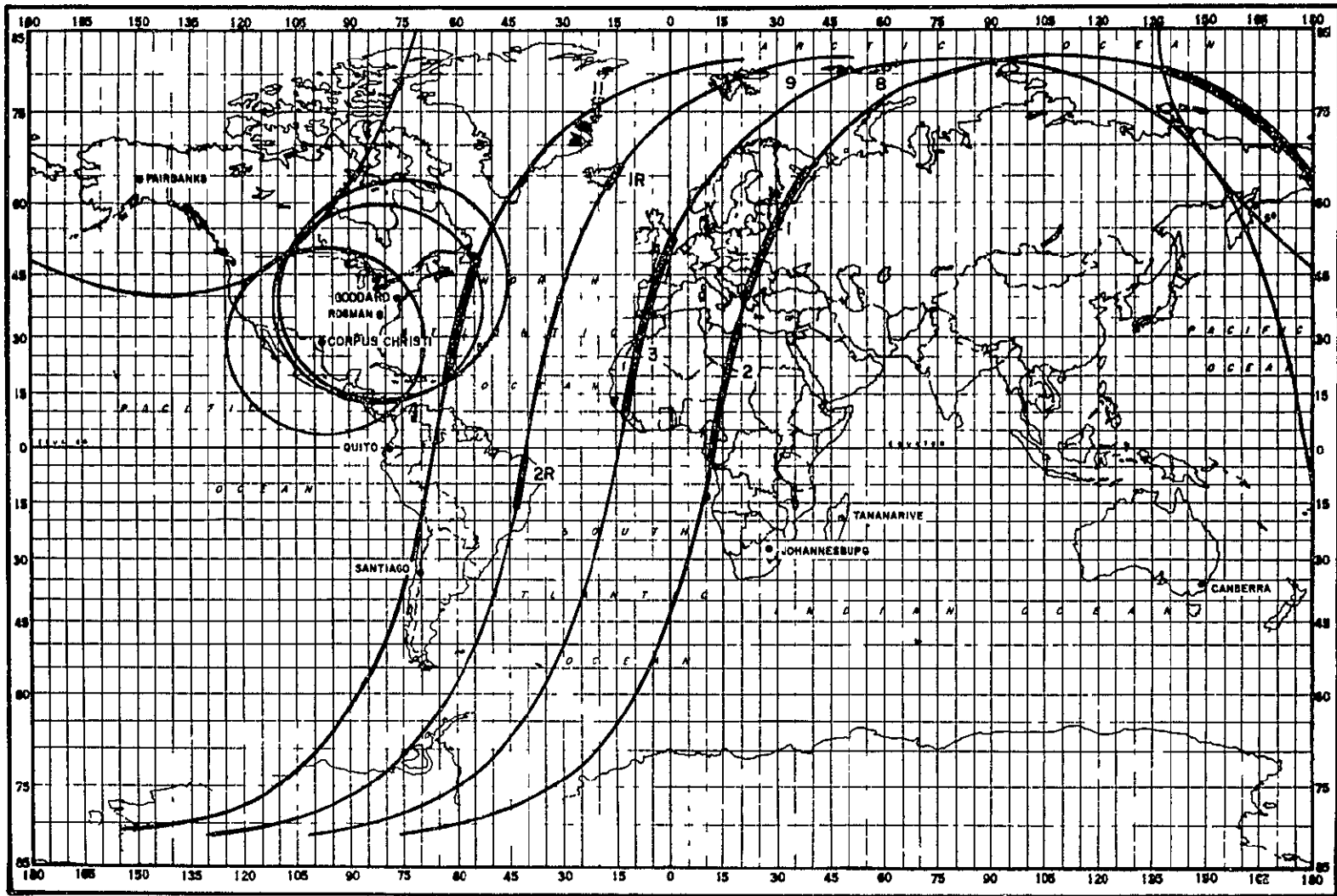


Figure 4 5-4 Operating Profile Requiring Maximum Stored Commands (No Clouds)

Mission Operation	Rev	Duration	Event	Place
5th Payload Operational Seq	10	3 8	RBV/MSS Recorded Ops	S. America
Station Contact	11	9 3	Comd Loading	Rosman

Note The small tip of Scandanavia on rev 9, and N Atlantic on rev 11 are not scheduled on Day 13 as they are above 60°N. They were scheduled on Day 12 and N. Atlantic is scheduled on Day 14 Scandanavia is out of view on Day 14

Note that the total operations scheduled in Figure 4.5-4 cannot be performed as they exceed the tape recorder capacity by 5 8 minutes even assuming a completely empty recorder at the beginning of the sequence Therefore, some coverage would not be scheduled For worst case sizing of the stored command requirements, it is assumed that this reduction in coverage would not decrease the number of payload sequences scheduled

#### 4 5 4 3 3 Cloud Coverage Consideration

Operational planning will inhibit sensor operations over large cloud masses where it is unlikely that any significant amount of useful data would be collected Such a situation is hypothesized in Figure 4 5-5 Large areas of clouds are considered to be present over the Mediteranean Sea, Southern Europe and Northwestern Asia This cloud pattern segments the operations planned during rev 8 and 9 Thus, the following payload sequences would be required

- Rev 8 one sequence for Central Europe  
one sequence for Central Western Africa
- Rev 9 one sequence for W Europe  
one sequence for West Africa
- Rev 10 one sequence for N. Atlantic  
one sequence for S America

For this condition, which represents a worst case in terms of the number of operating sequences during dead revs and considers major cloud scheduling, six payload sequences are required

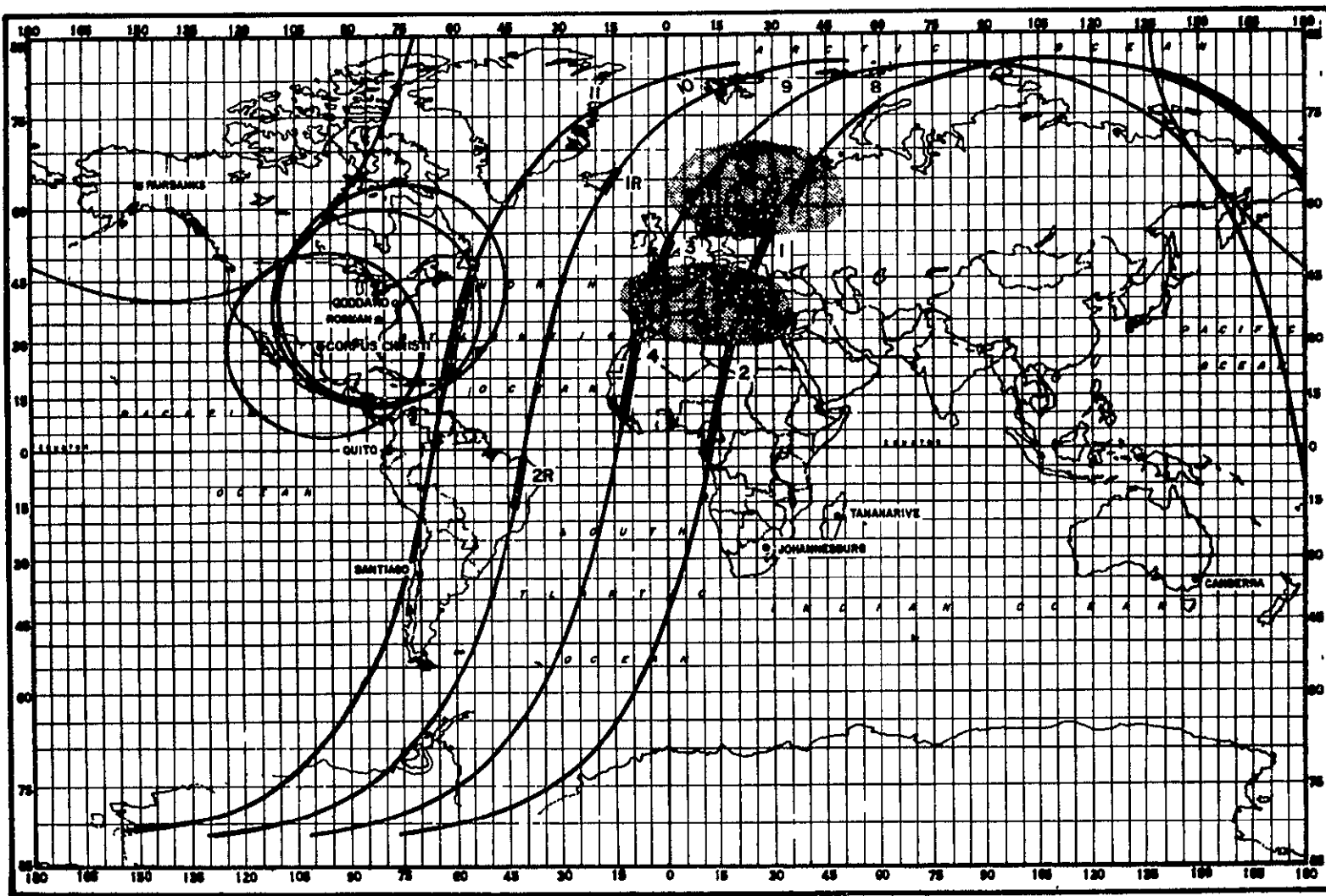


Figure 4. 5-5 Operating Profile Requiring Maximum Stored Commands (With Clouds)

## 4 5 4 3 4 Payload Command Sequence Content

For remote payload operation a command sequence consists of turning both sensors and WBVTR's on and off. A prerequisite is that the RBV, MSS and WBVTR's have been previously set to the desired operating mode (i.e., record mode, continuous operation, etc.). Once this has been accomplished each operates automatically throughout the coverage area and does not require additional commands. A payload command sequence requires the following commands:

<u>Time</u>	<u>Command</u>	<u>Response</u>	<u>Stored Commands</u>
T-50	MSS ON RBV STDBY	MSS turns on RBV in standby	1
T-5	VTR (MSS) RECD	WBVTR (MSS) startup	1
T-0	(AUTO)	RBV begins operating sequence, MSS recording data	0
T+2	VTR (RBV) STDBY	WBVTR (RBV) in standby	1
T+9 5	(AUTO)	WBVTR (RBV) in record	0
T+14 5	(AUTO)	RBV SHUTTER	0
T+25 0	(AUTO)	WBVTR (RBV) in standby	0
≈	(RBV CYCLE REPEATS, MSS RECORDING CONTINUES, UNTIL END OF PASS IS REACHED )		0
T+( <sup>END OF</sup> PASS)	VTR (MSS) OFF	WBVTR (MSS) turns OFF	1
T+( <sup>END OF</sup> PASS)+1	VTR (RBV) OFF	WBVTR (RBV) turns OFF	1
T+( <sup>END OF</sup> PASS)+2	MSS and RBV OFF	MSS and RBV turn OFF	1
		TOTAL	6

## 4 5 4 3 5 Command Recycle

Command recycle capability exists for each stored command \* When the recycle bit is set in the command word, command execution will occur again after the specified recycle time span has elapsed Continued reexecution will occur at this  $\Delta$  recycle time This command feature is used to re-execute sensor and VTR commands This is shown in Figure 4 5-5 where the recycle command indicated by an "R" is used to re-execute the payload sequences 1 and 2 given over Europe and Africa to occur again over the North Atlantic and South America respectively Note that recycle commands are scheduled so that the second recycle execution will occur after a station commanding pass For example in Figure 4 5-5, the first recycle is used for the payload sequence for the North Atlantic This payload sequence would be re-executed during rev 12 but it is removed during station passes occurring on either revs 11 or 12

## 4 5 4 3 6 Stored Commands Required - Maximum Case

Combining the number of commands required for a payload sequence, the number of payload sequences required, the command recycle capability and restrictions, plus the stored commands required for vehicle operation, provide the worst case number of command storage spaces filled Since the first command recycle executions should not occur earlier than 2 revs from the initial execution (for this case), then revs 8 and 9 of Day 13 require 2 stored sequences each and rev 10 with two sequences required will be recycle commands from rev 8

Therefore, 4 sequences containing 6 commands are required for payload operation for a total of 24 stored commands One command is required to turn on both S-Band transmitter heater power and one to rewind the MSS recorder, prior to station contact Vehicle operation requires 4 stored commands for scanner turn on/off at sunrise/sunset

Thus adequate command storage exists for the worst case mission operations

## 4 5 4 3 7 Growth

Should the stored command requirements increase beyond the present capacity of 30 stored commands, greater efficiency in the use of commands could be achieved by using a sequencer to program a combined RBV/MSS/WBVTR turn-on operation The sequencer operation would be initiated by a single stored command Turn off would be handled similarly. Thus, a payload sequence after presetting the sensors to the desired operating modes would consist of only two commands Also the segment switches on the solar array drive are being investigated for the ACS scanner on/off commands in place of stored commands This further reduces the stored command requirement.

---

\*The recycle function is described in detail in Volume II Section 4 4 2 2

4 5 4 4 Ground Data System Sizing

Much of the activity required of the ERTS ground support system is very dependent on the way the spacecraft/sensor system will be operated in orbit. The mission simulation capability has been used to develop two sizing studies to date:

- 1 NASA Data Processing Facility Loading Requirements
- 2 Estimation of the number of wide band video tapes to be received from Acquisition sites

At the current time, operational procedure definition and ground system timelines are being studied employing the simulated profiles as a primary input. The following two sections present a brief summary of the results of the two sizing studies. Final results will be included in the final study report in April.

## 4 5 4 4 1 NDPF Loading Requirements

This study examined various loading requirements for the NDPF. The cases selected were based on our orbit studies, the design study specification (S-701-P-3), and conversations with NASA personnel. The results are summarized below:

Operations Mode	Minutes Per Day	Images Per Day	Images Per Week
1 Real-Time, US (incl Alaska)	18	315	2,205
2 Real-Time, All Land with coverage cones	44	740	5,180
3 Real-Time, US plus one hour	78	1,316	9,212
4 30 minute recorder limited, attempt global land coverage	135	2,268	15,876
5 Three ground station contact limit, no recorder limit, attempt global land coverage	208	3,495	24,465
6 Average 20 min/rev operation	280	4,704	32,928

To convert minutes of operation (M) to number of images (I) produced, the following is used:

$$\begin{aligned}
 I &= M \left( \frac{\text{min}}{\text{day}} \right) \times 60 \left( \frac{\text{sec}}{\text{min}} \right) \times \left( \frac{1}{25} \right) \left( \frac{\text{operation}}{\text{sec}} \right) (X)^7 \left( \frac{\text{images}}{\text{operation}} \right) \\
 &= 16.8 M \left( \frac{\text{images}}{\text{days}} \right)
 \end{aligned}$$



Line 1 is Case A described in section 7.14 of the design study specification and must be throughputed in a 40-hour week at minimum cost. Line 3 is Case B and we must tradeoff throughput rate vs hardware and manpower. No specific time is specified for processing Case B other than the obvious 168 hour/week physical limit.

In performing the trades for Case B design, the following considerations are being included:

1. Equipment cost and amortization
2. Shift bonus costs
3. Growth (say to line 2 plus one hour or line 4)
4. Maintenance of complex equipment

Table 4.5-5 is the conversion of operating times to various product rates.

#### 4.5.4.4.2 Estimation of Number of Wideband Tapes to be Received from Acquisition Sites

Information was generated to estimate the number of wideband data tapes produced daily as a preliminary basis for sizing GDHS design. The estimates are worst case and are based on the day 9 summer solstice operating profile. The following assumptions were made in computing the estimates:

1. A 30-minute record capacity exists on the ground WBVTR's at the acquisition sites.
2. Data received on different passes will be recorded on a single tape if space exists.
3. Data will be received at Alaska, Corpus Christi, and the NTTF.
4. All acquisition passes (both day and night) were considered available for data receipt.
5. The basic profile considered sensor operations compatible with the compatibility of the S/C system, therefore, the total amount of data gathered exceeds the Case B coverage requirement as stated in the specification.

Table 4.5-6 shows the breakdown of data receiving passes at each of the three acquisition sites as a function of rev. All numbers relating to the amount of data is shown in minutes. For each pass, whether data is real time or dumped recorder is indicated. The status of the WBVTR's at the sites after each pass is also shown.

Table 4.5-7 summarizes the wideband tapes recorded per day as a function of site, tape ID#, amount of data on tape, and the passes (rev) from which data was recorded.

TABLE 4 5-5 PRODUCTION RATES

		Case A	Case B	Recorder Limit
1	Images/day	315	1,316	2,268
2	Images/week	2,205	9,212	15,876
3	Color neg, RBV/week (20% of line 2/3 x 3/7)	63	263	453
4	Color neg, MSS/week (line 3 x 2)	126	526	906
5	Total, line 3 + line 4	189	789	1,359
6	Precision B&W neg/week (5% of line 2)	110 3	460 6	793 8
7	Precision Color net/week (3/7 of line 6)	47 3	197 4	340 2
8	Photogrammetrically Proc Sets/week 5% of line 2)	110 3	460 6	793 8
	B&W Images/hr - 40 hr week	55 1	230 3	396 9
	- 80 hr week	27 6	115 2	198 5
	- 168 hr week	13 4	56 1	96 8
<u>Production Processing</u>				
9	B&W Bulk/week	22,030	92,120	158,760
10	Color Bulk/week	1,890	7,890	13,590
11	Precision B&W/week	1,103	4,604	7,938
12.	Precision Color/week	473	1,974	3,402
<u>Annual Storage</u>				
13	B&W Masters	114,600	479,000	825,500
14	Color Masters	9,800	41,000	70,700
15	B&W Precision	5,700	24,200	41,300
16	Color Precision	2,460	10,300	17,700
17	Photogrammetrically Proc Sets	5,700	24,200	41,300

TABLE 4 5-6 SENSOR DATA RECORDED BY GROUND STATIONS

Rev	Alaska Pass			Corpus Pass			NTTF Pass		
	Rt	Dump	WBVTR Status	Rt	Dump	WBVTR Status	Rt	Dump	WBVTR Status
1	5.7	5 0	10 7	-	-	-	-	-	-
2	-	12 4	23 1	-	-	-	-	-	-
3	3.3	-	26 4	-	-	-	-	-	-
4	-	-	-	-	-	-	-	6 9	6 9
5	-	2.0	28 4*	-	10 7	10 7	-	13 5	20 4
6	-	5 1	5.1	-	12 9	23 6*	-	-	-
7	-	12 1	17 2	-	-	-	-	-	-
8	-	12 3	29 5*	-	-	-	-	-	-
9	-	5 6	5 6	-	-	-	-	-	-
10	-	-	-	-	-	-	-	-	-
11	-	-	-	-	-	-	-	9 2	29.6*
12	-	-	-	10 0	-	10 0	13 8	-	13 8
13	4 5	-	10 1	8 8	4 0	22 8*	8 5	-	22 3*
14	3.3	8 0	21 4*	-	-	-	-	-	-

\*Indicates that tape cannot accommodate all data from next pass and thus is demounted and ready for shipment to NDPF

TABLE 4 5-7 SUMMARY OF GROUND RECORDED TAPES

Site (Tape ID#)	Amount of Data Min	Passes Recorded (Rev)
Alaska (1)	28 4	1, 2, 3, 5
Alaska (2)	29.5	6, 7, 8
Alaska (3)	21.4	9, 13, 14
Corpus (1)	23.6	5, 6
Corpus (2)	22 8	12, 13
NTTF (1)	29 6	4, 5, 11
NTTF (2)	23 3	12, 13

Based on the above data, a maximum of 14 wideband tapes (7 RBV, 7 MSS) would be required per day. For Case B coverage (a total of approximately 78 min/day as opposed to the approximate 147 min/day as shown), a maximum of 12 tapes would be required per day. This would reduce to a total of 8 tapes per day (4 from Alaska, 2 from Corpus, and 2 from NTTF), if a carry-over of more than a day is permitted for the Corpus and NTTF stations.

The absolute minimum number of tapes based on data volumes and tape capacity would be 6 per day. This assumes a total of 78 minutes of operations per day and would allow approximately 12 minutes for redundant recording by two sites simultaneously. This is not considered practical because of the tape packing density and does not allow adequate room for data segmenting information, headers, etc.

Table 4 5-8 summarizes the various cases vs the tape requirements.

TABLE 4 5-8 MISSION OPERATING CASES VS TAPE REQUIREMENTS

Case	Alaska	Corpus	NTTF	Total
1 Data dumped every pass (20 passes/day) New tape each pass*	22	8	10	40
2 Worst case mission profile (New tape each pass)	20	8	10	38
3 Worst case mission profile (Tape packing)	6	4	4	14
4. Case B profile (Tape packing, contiguous pass)	4	4	4	12
5 Case B profile (Tape packing, day and night passes NTTTF and Corpus packed)	4	2	2	8
6 Absolute minimum number tapes (data volume)	2	2	2	6

\*A total of 20 passes over the acquisition sites occurred on the day considered. Case 1 assumed that data would be received at each of these passes and a new tape would be used each time.

As can be seen from Table 4 5-8, the number of tapes required per day vary significantly depending on assumptions. It appears that (if tape packing is employed) Cases 3, 4, and 5 would most likely occur with Case 3 and 4 being the most probable. Therefore, for design purposes, the Ground Data Handling System should expect approximately 10-12 wideband video tapes per day from acquisition sites.

## 4 6 WIDEBAND VIDEO TAPE RECORDERS MANAGEMENT

### 4 6 1 RECORDER MANAGEMENT

Management of the use of the onboard wideband video tape recorders is necessary for three basic reasons

1. The sensors can produce more data than the recorder is capable of storing.
2. The full contents of the recorder cannot be dumped during the limited time of a station contact.
3. The lifetime of the recorder is limited.

In order to effectively manage the use of the recorder, the Mission Scheduling function in the Operations Control Center (OCC) must maintain an accurate status of the recorder at all times. The primary status information is

- 1 How much, and what data is currently on the tape,
- 2 What is the physical position of the tape at all times,
3. What is the current status of the recorder capability (i. e. , does a degraded mode exist, what are the actual tape speeds, etc.)
- 4 What operational mode is the recorder currently in

The results of the mission simulations presented in Section 4 5 indicate that typical ERTS operations would include the following types of recorder usage

1. Record data remotely during an orbit and completely dump this data at the next available station pass.
2. Record data remotely during an orbit, or a series of orbits, but be unable to dump all the recorded data during the available station passes on these orbits.

The first of these two cases is obviously the simplest from a recorder management standpoint. The operational sequence would entail the recording of data for some period of time, a rewind of the recorder after recording has ceased by an amount corresponding to the recorded operation, and a dump operation during the pass during which all the previously recorded data is returned to the ground. The tape can either be rewound to the beginning of tape at this time and readied for the next recording operation, or not rewound but readied at its current position for the next recording operation, if sufficient tape still remains on the reel from this point to accept the next anticipated recorded operation. The latter of these two situations could be employed if one wants to wait to verify that the dumped data was received properly since the next record cycle would not erase this data and a retransmission at a later time would still be feasible. The approach might also be employed to limit concentrated usage of a specific section of the tape (the front end) thus possibly reducing potential tape failures attributed to effects resulting from multiple recordings on the tape.

The second operational sequence where all previously recorded data can not be transmitted to the ground during the station pass presents a more complex recorder management problem. It is anticipated that the majority of the remote operations will be between 2 and 10 minutes each. It is possible, however, to have more than one of these operational sequences occur during a single orbit. A typical station pass might be on the order of 10 minutes. Therefore, hopefully, all the data from at least a single operational sequence could be returned during a single station pass. However, it is likely that additional data will be recorded before all the data recorded on the previous orbit is played back. In this type of situation it becomes extremely important to ensure that the new data to be recorded does not in any way interfere with previously recorded data that still needs to be transmitted to the ground. To properly manage the recorder usage under these conditions requires that the OCC maintain an accurate image of the recorder tape situation at all times.

Figure 4 6 1-1 graphically depicts a typical operational sequence for two orbits. It was assumed that the tape was clean at the beginning of the pass in rev N. Two remote operational sequences (A&B) were scheduled on rev N. The available dump time during the station pass on rev N however was only sufficient to transmit the recorded data from operation A. Therefore at the beginning of the remote operations planned for rev N+1 (operational sequences C&D), the recorder tape still contains untransmitted data from operation B. The recording of data from operations C and D must then be recorded on the tape exclusive of where operation B is contained. As is shown it was elected to record operation C behind operation B and to record operation D over the area where the already transmitted operation A was contained.

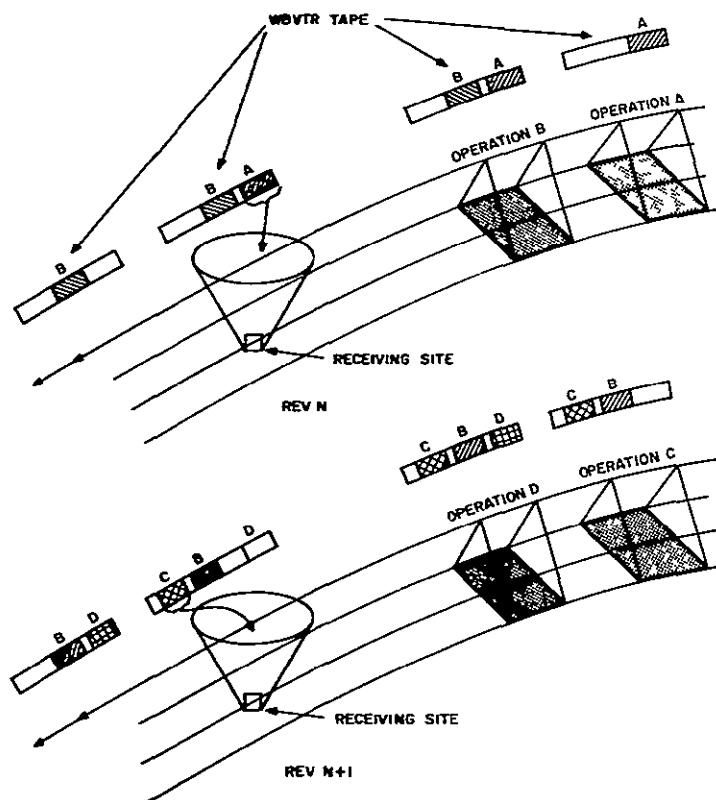


Figure 4 6 1-1 Typical Operational Sequence for Two Orbits

11 February 1970

The station pass on rev N+1 is such that only operation C can be transmitted to the ground. This, therefore, was scheduled and at the beginning of rev N+2, the tape contains recorded, but still untransmitted data from operations B and D.

This type of sequence will generally continue to occur for a period of a few orbits (see Section 4.5) until sufficient dump time becomes available to allow all the recorded data to be transmitted to the ground. At this point the situation as described in case 1 will prevail again for a series of orbits until a case 2 condition arises again. Typically one finds a single case 1 series of orbits and a single case 2 series of orbits in any given day. The case 2 condition arises generally around those orbits that contain no or very short station passes.

In the previous discussion the recorder management problem was examined from the standpoint of mission operations and recorder usage requirements. At this point some key considerations can be noted.

1. Since the recorder has a limited storage capacity, certain potential remote sensor operations over available coverage requirement must be inhibited (see Section 4.5). This implies that at times the full capacity of the recorder will be used and all the data on the resulting fully loaded tape will not as yet have been transmitted to the ground.
2. Generally, the data on the tape will be in segments related to specific operational sequences and these segments will generally be on the order of 2 to 10 minutes of data each.
3. The order of the individual segments on the tape may not necessarily be time-sequenced since, to maximize the efficiency of the use of the tape, data will be recorded on a space available basis (i. e., if a 3-minute recorded operation is planned, the current tape content status will be examined to determine the best area on the tape to record the operation).
4. Since ground site contact time and the availability of station passes relative to desired recording cycles constrains what can be recorded, the efficient use of the available ground contact time is mandatory. The current content of the tape must be examined to determine which specific recorded data segment(s) are best scheduled for transmission during the anticipated pass. The transmission of partial segments is not desirable and therefore should not be scheduled if possible.

The key to effective tape recorder management is the capability to have accurate knowledge of and control over the tape content. The system must have

1. The ability to move the tape to a predetermined position prior to an operational record sequence, and,
2. The ability to move the tape to a predetermined position prior to a recorder dump sequence over a data acquisition site.

In order to position the tape to satisfy the above two conditions, the OCC will require knowledge of a tape position vs sensor operation history. This profile will allow for correlation of the video with tape position. The OCC must also maintain an accurate history of tape position vs video data dumped. Finally, the OCC must have accurate knowledge of the actual position of the tape at any point in time.

#### 4.6.2 TAPE HANDLING REQUIREMENTS

Accurate knowledge of the status of the onboard wideband tape recorder is necessary. The questions which need to be examined are:

1. How accurately must the knowledge of tape position be for both monitoring and controlling, and
2. How can this information be obtained on the ground.

##### 4.6.2.1 Accuracy of Tape Position

Tape-positioning accuracy requirements are directly related to how the video data is recorded on the tape. The tape must be positioned properly (1) to allow recording of additional data without destroying previous records, and (2) to allow for readout of a total previously recorded operational sequence. Improper tape positioning in either the record or dump mode can result in the loss of data.

The configuration of data on the tape will be different depending on whether the data is from the RBV or the MSS. During RBV operations in the recorded mode, the camera controls the motion of the tape. The cameras are readout during part of the camera operating sequence. During the readout phase the tape is set into motion and the data recorded. At the completion of the readout, the tape is stopped and not moved again until the next camera readout cycle. Figure 4.6.2-1 graphically depicts the configuration of the tape resulting from an RBV operating sequence.

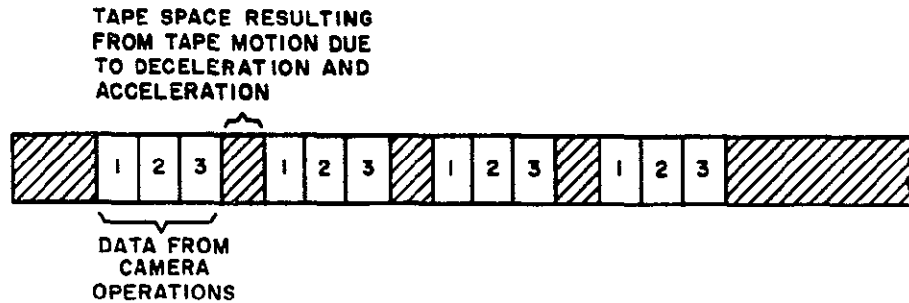
The operation of the MSS in the recording mode is such that data is continuously being outputted from the sensor. This data is continuously recorded for the duration of the operating cycle. The configuration of the resulting MSS tape is also shown in Figure 4.6.2-1.

The tape is moving at 12 ips during all recording operations. The amount of tape required to record the readouts of the 3 RBV cameras is 126 inches. The space between camera readout data due to tape movement during deceleration and start up is 36 inches. For the MSS data, the data recorded from two operating sequences will contain a buffer area between them on tape. This can be assumed to be at least 36 inches also due to normal tape movement due to deceleration and acceleration of the tape.

The recorder management function will require that the tape be capable of being positioned to a point within a buffer area between recorded data such that the first data following the buffer area can be readout when the tape is up to speed. The characteristics of the recorder are such that it takes 0.4 seconds from receipt of "record" command until the tape is up to speed and an additional 2.8 seconds to synchronize the recorder so data can be recorded. A total of 33.6 inches of tape is moved during this time period.



RBV



MSS

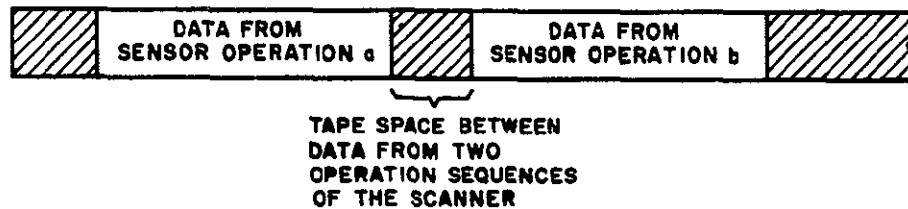


Figure 4 6 2-1 Wideband Tape Content Configurations

The amount of tape moved from the time the command to stop is received until the tape has stopped depends whether the tape was moving at the low or high rate. If it was moving at the 12 ips rate, then 2.4 inches of tape is moved, if at the 48 ips, then 9.6 inches is moved.

The total amount of tape moved during a record to standby to record cycle is 36 inches. It can therefore be expected that a buffer area of at least 36 inches will occur between any recorded two segments of recorded data.

The positioning of the tape in anticipation of a data dump cycle requires that the tape be up to speed at the point data is encountered. To allow for normal start up movement, the tape position must be positioned to at least 2.4 inches ahead of the data (Figure 4. 6. 2-2). This results in a tape positioning procedure capable of positioning the tape within a pre-determined 36 inch segment. Given that the midpoint of this segment will be nominally sought, the accuracy must be such that the tape can be position to within  $\pm 16.8$  inches of the nominal.

#### 4 6 2 2 Monitoring Tape Position

Two means are currently available for monitoring tape position. Position data is available as a normal telemetry point in form of the tape footage indicator. This data point however will not be sufficient to position within the required  $\pm 16.8$  inches because it is accurate to approximately 5% of the total tape length (1440 inches of tape).

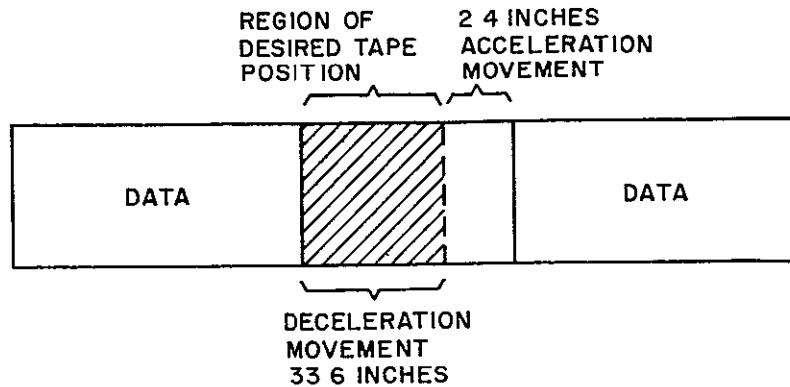


Figure 4.6.2-2. Tape Position Regions

The tape also contains a search track with a prerecorded code of tape position data. This track contains prerecorded unique 12 bit words every 6 inches along the tape. The monitoring of this information will allow for a measurement of tape position to within an accuracy of 6 inches. This accuracy falls well within the required  $\pm 16.8$  inches and thus is an acceptable monitor for tape position location.

#### 4.6.3 DESIGN APPROACHES

##### 4.6.3.1 Tape Position Monitoring

Two primary approaches were evaluated to transfer this data from the spacecraft to the OCC where it is ultimately needed:

1. Dump the search track on a separate subcarrier during the normal tape dump operation, and
2. Monitor the search track and merge the position data into the normal PCM telemetry data.

The first of these approaches although the simplest to implement from the spacecraft point of view was eliminated for the following reasons:

1. The only-time tape-position data would be available is during a dump operation.
2. The complexity of the problem of handling the signal at the remote site and transmitting it back to the OCC in real time during the dump operation.
3. The inability to effectively apply corrective measures (fine-tune tape repositioning) if it was found that the tape was not positioned properly prior to start of the dump operation.
4. Inability to accurately determine the location of recorded but yet untransmitted data since accurate tape position data is only available for data that has been dumped.

The approach of merging into the PCM telemetry provides several desirable features although it does require the addition of some specific circuitry to the spacecraft. The features that prompted the selection of this approach are as follows:

1. Tape position data available for all tape recorder modes.
2. Inclusion of this data in the normal PCM telemetry requires no special ground data handling procedures.
3. Actual tape position can be viewed from real time telemetry prior to a planned tape dump and fine repositioning can be effected if required prior to dumping.
4. Since tape position data is monitored during remote recorded sensor operations, an evaluation of the playback PCM telemetry will provide an accurate knowledge of recorder content status.

#### 4.6.3.2 Search Track Telemetry Processor

The implementation of this design approach is described in Volume IIE, Section 5.11 of the Phase D Technical proposal. A summary bilevel output signal from each Wideband Video Tape Recorder auxiliary track is inputted to a processor which performs the necessary storage and synchronization to permit the telemetry system (VIP) to read the twelve-search track data bits serially. The VIP will read the processor 10 bits at a time using two channels separated in time by ten milliseconds. The processor inhibits any new data transfers into the output for 30 ms  $\pm$  5 ms after the VIP starts to read the data. After the VIP reads the data it is retained in the processor unless updated with new search track data.

A Forward/Reverse signal is provided so that the processor correctly formats the data when the tape is operating in either direction. The format is such that the search track data is always read out to the VIP as if the tape were in forward motion.

A stop/start signal will be provided so that the processor will be able to store the last search-track data output and inhibit subsequent data during the tape deceleration. The first search-track data output after a tape start, however, will not necessarily be valid.

Search-track data will be presented to the processor at two speeds which correspond to tape speeds of 12 IPS and 48 IPS. The 12-bit data repetition time is shown in Figure 4.6.3-1.

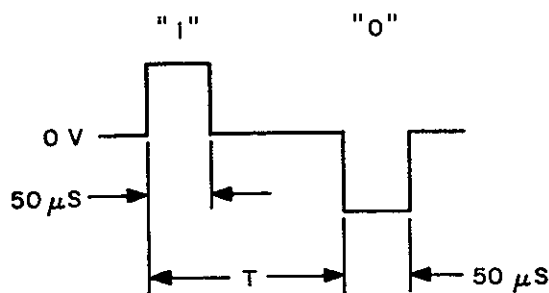
#### 4.6.3.3 Positioning of the Tape

In addition to obtaining an accurate knowledge of the tape position at any time, effective recorder management requires the capability to accurately reposition the tape to a predetermined position. The tape must be positioned in two situations:

1. To move the tape to appropriate position in order to dump the desired video data to the data acquisition site, and,
2. To move the tape to the appropriate position that allows data to be recorded on the allocated space.

The first situation requires that the tape be positioned far enough in advance of the data scheduled to be dumped such that, with the normal tape start up movement, the tape will be moving at the dump speed when the first data is encountered. It is desirable to position the tape relatively close to this limit position to eliminate the unnecessary waste of station contact time. In addition, the positioning of the tape too far in advance of the limit position could result in video data from the previous segment on the tape being dumped to the site. Although this is not expected to be catastrophic, it is not a desirable condition.

The second tape movement situation requires that the tape be positioned such that when the record operation is initiated, it occurs in an area of the tape that doesn't contain data that still must be transmitted. This means that the planned recorded operation must be evaluated and the required tape space allocated within the space available.



TAPE SPEED	
12 IPS	48 IPS
$T = 400 \mu S$	$T = 100 \mu S$

Figure 4 6 3-1 12-Bit Data Repetition Time

In both of the tape movement situations, the desired position, which can be expressed in terms of a search track word, will be known in advance in the OCC. The OCC will also have an accurate knowledge of the current tape position or the estimated tape position prior to the expected tape repositioning. As pointed out earlier, there will exist a minimum of 36 inches of buffer area between any two segments of video. Actual tape movement during start up motion is approximately 2.4 inches. Thus, positioning the tape in either of the two tape positioning situations to a point within the 36-inch buffer, not closer than 3 inches of the video on either side, should satisfy all conditions. It is anticipated, however, that an additional amount of tape will be moved to provide a larger buffer region between separate operational sequence segments.

Since dump operations will generally be scheduled to accommodate data from a complete operational sequence, it can be expected that the region within which the tape must be positioned will be larger than the minimum 30 inches as previously defined.

Two basic approaches to commanding position were considered.

1. Using an on command to start tape motion (either fast or normal, forward or rewind) followed by an off command scheduled to occur a specific time later.

2. Providing the capability to command the recorder to move the tape directly to the predetermined position and automatically return to the standby condition.

The first of these approaches requires the use of two discrete commands. If the movement was implemented by use of stored program commands, the desired position can be achieved to within a  $\pm 24$  inches. This results from the fact that the granularity with which two commands can be specified is one second. Movement initiated by real time commands can achieve a granularity of  $\sim 0.4$  seconds from a STADAN site and  $\sim 0.25$  seconds from a MSFN site. The positioning accuracy in these cases are  $\pm 9.6$  and  $\pm 6$  inches respectively.

The utilization of this approach for large tape movements via stored command and allowing for fine repositioning with real time commands if required as a result of the real time TLM evaluation will then provide tape position capability within the desired accuracy. This approach can be implemented without modification or additional hardware for either the WBVTR or spacecraft.

The second approach provides the capability for positioning of the tape to approximately the accuracy of the word displacement on the search track. This approach, however, requires that additional capability be added to the spacecraft. Conceptually, a quantitative command would be sent which defines the desired tape position (search track word). A comparison would be made between this word and the search-track word as monitored during tape movement. The recorder would be stopped when coincidence occurs. Since the capability to monitor the search track for position data is required, some of the circuitry required to implement this approach can be considered to exist. Nevertheless, the former approach provides the desired positioning capability with no additional equipment and therefore is selected.

**GENERAL  ELECTRIC**  
**SPACE DIVISION**  
**SPACE SYSTEMS ORGANIZATION**



NATIONAL AERONAUTICS AND SPACE ADMINISTRATION  
WASHINGTON D C 20546

REPLY TO  
ATTN OF SRB/TAG

AUG 14 1970


TO: US/Director, Scientific & Technical  
Information Division

FROM: SRB/Program Manager  
Earth Resources Flight Programs

SUBJECT: Transmittal of ERTS Phase B/C Final Reports

Attached herewith is one complete set of ERTS definition/preliminary design final reports by TRW and General Electric. It is desired that these reports be forwarded to the Clearinghouse for Scientific and Technical Information.

It is recommended that Clearinghouse number(s) be assigned to these reports as soon as possible since we expect considerable demand for the studies from ERTS experimenters responding to Memo Change No. 28, and other Government agencies.

  
T. A. George

Attachment

*This is the DRF*

*STAR -  
NICK-00*

*CR # 109907*

ROUTING SLIP

MAIL CODE	NAME	Action
		Approval
USI	Mr. Watson	Call Me
		Concurrence
		File
		Information
		Investigate and Advise
		Note and Forward
		Note and Return
		Per Request
		Per Telephone Conversation
		Recommendation
		See Me
		Signature
		Circulate and Destroy

Jim -

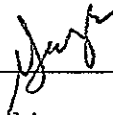
Here is a mess -- a clean mess as far as processing goes

Please get them in STAR ASAP and then to the CFSTI Sauter et al will have a stroke when they have to reproduce them but that's their problem

Ted's rather obscure release to the CFSTI is interpreted by me as OK for STAR announcement I have talked with him and that's what he intends

Please call if this mess is a dirty one

Thx.



NAME F G Drobka	TEL NO (or code) & EXT 26150
CODE (or other designation) USI	DATE Aug 14



**NASA  
FORMAL  
REPORT**

N 70-34454

12M

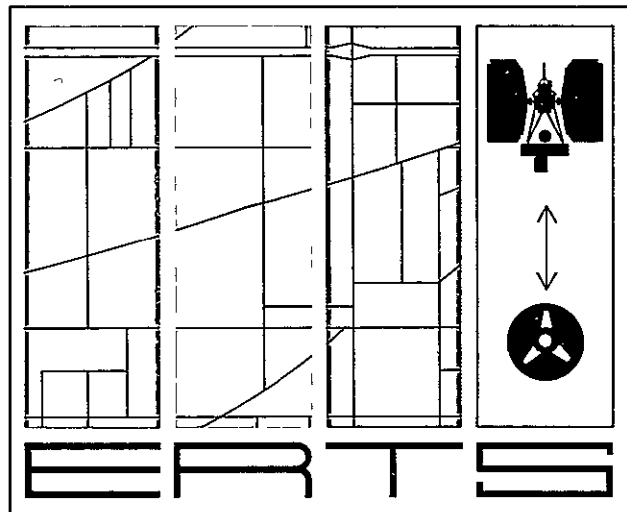
Document No 70SD4207

11 February 1970



# EARTH RESOURCES TECHNOLOGY SATELLITE SPACECRAFT SYSTEM DESIGN STUDIES FINAL REPORT

VOLUME I  
SYSTEMS STUDIES



Reproduced by  
**NATIONAL TECHNICAL  
INFORMATION SERVICE**  
Springfield, Va. 22151

Prepared For  
**GODDARD SPACE FLIGHT CENTER**  
GREENBELT, MARYLAND 20771



DOCUMENT NO. 70SD4207  
11 FEBRUARY 1970

**EARTH RESOURCES TECHNOLOGY SATELLITE  
SPACECRAFT SYSTEM DESIGN STUDIES  
FINAL REPORT**

**VOLUME I  
SYSTEMS STUDIES**

**PREPARED FOR.  
GODDARD SPACE FLIGHT CENTER  
GREENBELT, MARYLAND 20771**

**UNDER  
CONTRACT No NAS 5-11529**

**GENERAL  ELECTRIC**

**SPACE SYSTEMS ORGANIZATION  
Valley Forge Space Center  
P O Box 8555 • Philadelphia, Penna 19101**

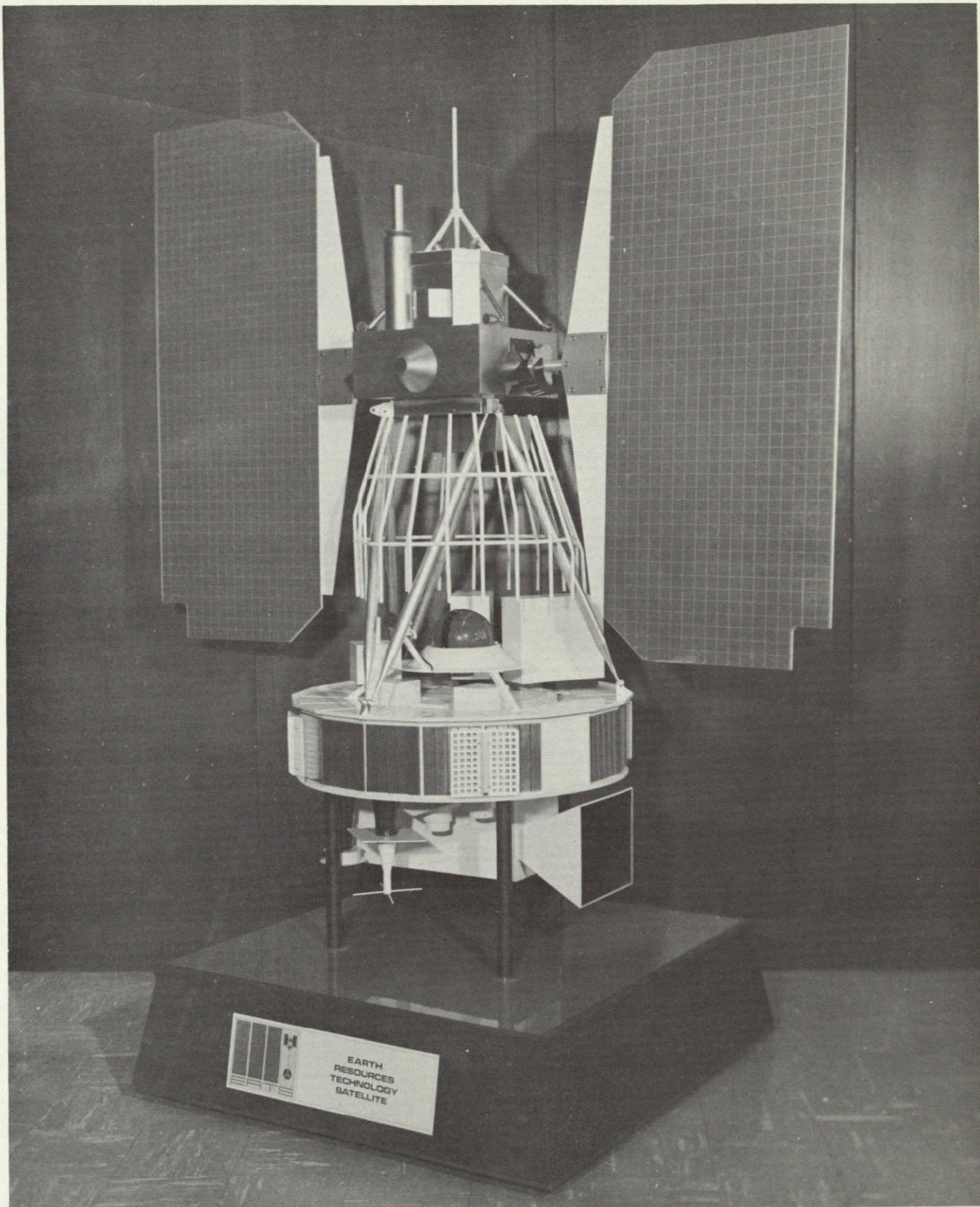


# TABLE OF CONTENTS

Section		Page
1	INTRODUCTION	
	1.1 Study Objective . . . . .	1-1
	1.2 Summary . . . . .	1-1
2	STUDY REQUIREMENTS	
	2.1 Study Tasks . . . . .	2-1
	2.2 Supplementary Study Documents . . . . .	2-1
3	BASELINE SPACECRAFT SYSTEM DESIGN	
	3.1 Introduction . . . . .	3-1
	3.2 Spacecraft System Design . . . . .	3-1
	3.2.1 System Functional Relationships . . . . .	3-1
	3.2.2 Payload Characteristics Summary . . . . .	3-6
	3.2.3 ERTS Spacecraft Configuration . . . . .	3-13
	3.2.4 Electrical and Functional Description . . . . .	3-16
	3.2.5 Subsystem Overview . . . . .	3-24
	3.3 Hardware Matrix . . . . .	3-68
	3.4 Launch Vehicle Study Result . . . . .	3-77
	3.4.1 General . . . . .	3-77
	3.4.2 ERTS/Delta Electrical Integration . . . . .	3-79
	3.5 Growth . . . . .	3-86
	3.5.1 General . . . . .	3-86
	3.5.2 Growth Missions . . . . .	3-86
	3.5.3 Spacecraft Growth . . . . .	3-92
	3.5.4 Growth Power Systems . . . . .	3-100
	3.5.5 Alternate Orbits . . . . .	3-105
4	SYSTEM STUDIES	
	4.1 ERTS System Reliability . . . . .	4-2
	4.1.1 Summary . . . . .	4-2
	4.1.2 Principles of Reliability Assessment . . . . .	4-5
	4.1.3 Source of Failure Rate Data . . . . .	4-5
	4.1.4 Subsystem Reliability Assessments . . . . .	4-6
	4.2 Orbit Analysis . . . . .	4-21
	4.2.1 Introduction . . . . .	4-21
	4.2.2 Nominal Orbit Selection . . . . .	4-22
	4.2.3 Drag Decay . . . . .	4-28
	4.2.4 Nominal Ground Track Control . . . . .	4-32
	4.2.5 Orbit Error Analysis . . . . .	4-35
	4.2.6 Operational Ground Track Control . . . . .	4-43
	4.2.7 Launch Window Analysis . . . . .	4-48

## TABLE OF CONTENTS (Continued)

Section	Page
4.3 Image Location and Coverage . . . . .	4-75
4.3.1 General . . . . .	4-75
4.3.2 Units . . . . .	4-76
4.3.3 Gains . . . . .	4-76
4.3.4 Implementation and Relative Error Effects . . . . .	4-78
4.3.5 First -Order Error Equation, Its Solution, and Attitude Determination Sensor Requirements . . . . .	4-79
4.3.6 Basic Coverage . . . . .	4-82
4.3.7 Rate Requirements . . . . .	4-86
4.3.8 Requirements Summary . . . . .	4-91
4.4 Time Annotation . . . . .	4-92
4.4.1 General . . . . .	4-92
4.4.2 Approaches to Time Annotation . . . . .	4-94
4.4.3 Discussion of Approaches . . . . .	4-95
4.4.4 Baseline Approach . . . . .	4-98
4.5 Mission Simulation . . . . .	4-100
4.5.1 Simulation Problem (Introduction) . . . . .	4-100
4.5.2 Simulation Model . . . . .	4-100
4.5.3 Simulation Cases . . . . .	4-104
4.5.4 Specific Study Results . . . . .	4-109
4.6 Wideband Video Tape Recorders Management . . . . .	4-137
4.6.1 Recorder Management . . . . .	4-137
4.6.2 Tape Handling Requirements . . . . .	4-140
4.6.3 Design Approach . . . . .	4-142

## LIST OF ACRONYMS

NDPF	NASA Data Processing Facility
NTTF	NASA Tracking and Training Facility
WBVTR	Wide Band Video Tape Recorder
MSS	Multi-Spectral Scanner
RBV	Return Beam Vidicon
WB	Wide Band
RBVC	Return Beam Vidicon Camera
DCS	Data Collection System
OCC	Operations Control Center
TLM	Telemetry
NB	Narrow Band
MSFN	Manned Space Flight Network
nm	Nautical Mile
M	Meters
PCM	Pulse Code Modulated
I/O	Input/Output
STADAN	Satellite Tracking and Data Acquisition Network
AGE	Aerospace Ground Equipment (also equivalent to GSE or STE)
PMP	Premodulation Processor
CIU	Command Integration Unit
COMDEC	Command Decoder
PCM/FSK	Pulse Code Modulated/Frequency Shift Keyed
Nort	Nortronics
FHC	Fairchild-Hiller Corp
Cal Comp	California Computer Co
PCM/PSK	Pulse Code Modulated/Phase Shift Keyed
IRLS	Interrogation, Recording and Location Subsystem
ITP	Integrated Test Plan
BIT	Bench Integrated Test
T/V	Thermal Vacuum
WTR	Western Test Range
GFE	Government Furnished Equipment
C&DH	Command and Data Handling Subsystem
VIP	Versatile Information Processor
SASS	Solar Array Sun Sensor
RWS	Reaction Wheel Scanner
SAD	Solar Array Drive
ADP	Automatic Data Processing
SWR	Standing Wave Ratio
RDT	Raw Data Tape
RMP	Rate Measuring Package
YIRU	Yaw Inertial Reference Unit
LN	Lead Network
RSAD	Right Solar Array Drive
HAC	Horizon Attitude Computer
ACS	Attitude Control Subsystem
PSA	Pneumatic Subassembly





## SECTION 1 INTRODUCTION

The Phase B/C study for the Earth Resources Technology Satellite, ERTS-A and -B has been successfully completed with the establishment of a spacecraft baseline design meeting the overall ERTS mission requirements.

The evolution of the design from the initial goals, requirements, analysis, conceptual design and definition of hardware to meet the criteria has culminated in a Phase D proposal being submitted with this final Phase B/C Spacecraft System Design Report.

### 1.1 STUDY OBJECTIVE

The primary objective of this study is to develop an observatory spacecraft capable of meeting the performance requirements of the ERTS mission. In attaining this objective, it was necessary to perform the analyses delineated in the NASA Study Specification S-701-P-3 and other analyses and design tasks as the study progressed.

### 1.2 SUMMARY

This final study report delineates the activities that have taken place since contract inception. A complete report of the analyses, studies, design tradeoffs and the final spacecraft baseline design is included.

This report consists of three volumes. Volume I discusses the study requirements for Phase B/C along with the specific study tasks that were performed during the spacecraft phase of the study.

The Baseline Spacecraft Design is presented in summary fashion, including the overall performance, payload characteristics, configuration of the spacecraft and an overview of each subsystem making up the spacecraft and its associated Aerospace Ground Equipment (AGE).

This baseline design includes a high percentage of space-qualified hardware including the basic structure design, attitude control subsystem, power subsystem, thermal subsystem, and electrical integration subsystem. These subsystems are basically the Nimbus design, or modifications thereof, for the ERTS application. In addition, the Orbit Adjust Subsystem was selected from those flown on other space programs and the Communications and Data Handling Subsystem components were defined to utilize, where possible, flight proven designs or modifications to space-qualified hardware. The remainder of Volume I is devoted to the following spacecraft system level study reports

1. System Reliability - The System Reliability Study includes the analysis and subsystem reliability block diagrams for each spacecraft subsystem with the subsystem and system reliability numbers for a one-year operation.

11 February 1970

2. Orbit Analysis - The Orbit Analysis Study is an analytical treatise on the selection of the orbital parameters for the ERTS mission. The analysis resulted in establishing the requirements for controls to achieve and maintain the orbit.
3. Image Location - The analysis in this area is due to the necessity of locating a given image within 2nm in a 100 x 100 nm frame. The results of this analysis established the attitude control and attitude determination requirements for the spacecraft.
4. Time Annotation - The Time Annotation requirement is associated with the previous analysis on image location. This study included analysis on different methods of processing time information with image information aid in the location of a given image.
5. Mission Simulation - The Mission Simulation task developed the operational concepts for the ERTS mission. Mission time lines established the duty cycle for the payload and associated equipment, this in turn, established the power requirements and consequently the power subsystem performance. The same information was required to establish the thermal control performance requirements. Hence, an analysis of the coverage, ground trace, data acquisition, data transmission and payload capabilities and constraints contribute greatly to the baseline spacecraft design.

Volume II of this study report covers detailed study and analysis tasks which led to each subsystem baseline design. The introduction to Volume II includes a brief summary description of the Spacecraft System, which is presented in much more detail in Section 3 of this Volume.

Volume III is dedicated solely to the Study Performance Assurance Tasks. It includes Quality Program Plans, Parts, Materials and Processer Plans, Configuration Management Plan, Process Control, Failure Analysis and Reporting, Compliance of Existing Hardware to ERTS Requirements, and, the ERTS Reliability Program Plan. Two copies of GE SSO Quality Assurance Procedures are included with two copies of applicable specifications as other supporting documentation.

Appendices are included at the end of the section to which they apply.

The Baseline System Design Description appears in this study report and in the Phase D proposal. This was done intentionally to clearly establish and have available for the reader, the baseline designs resulting from the study on which the Phase D proposal is based. Detailed component descriptions appear only in the respective proposal volumes, thus avoiding unnecessary duplication of written material. Summaries of the subsystem

11 February 1970

analyses and studies, reported in detail in the study report, have been included in the Proposal for convenience of the reader. Subsystem descriptions are similarly detailed in the study report and either summarized or repeated in the proposal as is required for clarity.

# SECTION 2

## STUDY REQUIREMENTS

2.1	Study Tasks . . . . .	2-1
2.2	Supplementary Study Documents . . . . .	2-1

## SECTION 2

## STUDY REQUIREMENTS

The Phase B&C study requirements are specified in NASA/GSFC's Design Study Specifications for the Earth Resources Technology Satellite, ERTS A and B, dated April 1, 1969, re-issued October 1969 (S-701-D-3). These requirements were analyzed in detail and specific study tasks identified as part of GE's proposal to the government for the ERTS Phase B/C Study. \* Having been awarded this study, the General Electric Company has diligently pursued these tasks, as well as many others which it considered pertinent and in the government's best interest in performing a comprehensive and complete design study.

2.1 STUDY TASKS

For convenience in locating the specific section(s) of the SSD final report in which each study task is addressed, Table 2-1 has been prepared. The task numbers (assigned by GE) use the first four digits to reference the appropriate paragraphs of the Design Study Specification and the final two digits as sequence numbers. The tasks derive from those contained in GE's proposal in two respects

1. The 14XXXX and subsequent tasks are not included since they are part of the GDHS final report to be submitted in April.
2. Additional tasks have been added that are of interest to the government, but not specifically included in the reference proposal.

2.2 SUPPLEMENTARY STUDY DOCUMENTS

During the course of the study, the government has made many advisory documents, reports, articles and memos available to the General Electric Company to supplement the information contained in the design study specification and to generally aid in performance of the study. A list of the documents received is contained in Table 2-2. In addition to the title, author and data received, a document number used for internal control is included.

---

\* MSD Proposal No. N-21611, Volume V - Revision B, 14 November 1969

TABLE 2-1. SUMMARY TASK DESCRIPTION REFERENCE

Task No.	Task Description	Location in SSD Final Report
710001	<p>Show capability of the proposed spacecraft to satisfy payload requirements.</p> <ul style="list-style-type: none"> <li>● Configuration layouts</li> <li>● Thermal analysis</li> <li>● Mechanical and structural analysis</li> <li>● Integration into a final spacecraft design which supports the payload requirements.</li> </ul>	Volume I Section 3.2.3
710002	<p>Identify specification items not compatible with existing designs. Determine where spacecraft design changes are required to achieve compatibility. Where appropriate, recommend payload changes to GSFC.</p> <ul style="list-style-type: none"> <li>● Establish whether MSPS can use an existing Nimbus D Clock signal</li> <li>● Determine modifications required to the Power Subsystem to accommodate the WBVTR's and RBV camera transients</li> <li>● Review all other payload characteristics for spacecraft compatibility. Resolve incompatibilities if they exist.</li> </ul>	Volume I Section 3.2.2
713001	<p>Review basic DCS conceptual approach, define and justify departures if required. Outline functional and operational system concept, conceptual designs and prepare preliminary specifications and optimize costs.</p> <ul style="list-style-type: none"> <li>● Review the basic conceptual approach for definition and evaluation of successful reception, platform distribution, overall system accuracy, clock accuracy, ERP, spacecraft and platform antennas, reliability and cost.</li> <li>● Recommend any departures from the concept if required.</li> <li>● Outline functional and operational systems concepts.</li> <li>● Prepare a conceptual design of the DCS</li> <li>● Prepare preliminary specifications for the DCP and the spacecraft equipment.</li> </ul>	Separate Report

TABLE 2-1. SUMMARY TASK DESCRIPTION REFERENCE (Contd.)

Task No	Task Description	Location in SSD Final Report
714001	<p>Study an additional spacecraft configuration which excludes the WBVTR's.</p> <ul style="list-style-type: none"> <li>● Provide overall spacecraft configuration layout</li> <li>● Evaluate thermal and mechanical provisions of configuration</li> <li>● Provide mass properties</li> <li>● Revise command/telemetry functions and determine impact on these subsystems</li> <li>● Evaluate effect on overall wideband telemetry system</li> <li>● Develop alternate power profiles and evaluate effect</li> <li>● Evaluate implications to the GDHS</li> </ul>	Deleted from Study requirements
720001	<p>Investigate equipment capability for 1 year life. Identify elements that might prevent achievement of 1 year life. Investigate sizing expendables, redundancy, recommend design solutions.</p> <ul style="list-style-type: none"> <li>● Identify equipment whose reliability fails to meet reliability allocation</li> <li>● Recommend design study of equipment for Phase D</li> <li>● Evaluate ability of Orbit Adjust system to meet 1 year life requirement</li> <li>● Review existing Nimbus analysis of pneumatics storage vs 1 year life requirement</li> </ul>	Volume I Section 4.1
730001	<p>Study mechanical, thermal and structural provisions for payload.</p> <ul style="list-style-type: none"> <li>● Modify component and payload arrangement layouts</li> <li>● Perform dynamic and stress analysis of primary crossbeam structural members</li> </ul>	Volume II Section 2.4.5  Section 2.4.7

TABLE 2-1. SUMMARY TASK DESCRIPTION REFERENCE (Contd.)

Task No.	Task Description	Location in SSD Final Report
730002	<p>Study sensor alignment provisions and perform alignment error analysis for individual sensors.</p> <ul style="list-style-type: none"> <li>● Perform analyses and provide the mechanical design to assure required sensor alignments</li> </ul> <p>(Note Overall system performance, including effects of misalignment is included in Task 151001)</p>	Volume II Section 2.3.4
None	Demonstrate Flexibility of Spacecraft Design.	Volume II Section 2
740001	Review the results of the Nimbus study "Thorad/Delta Launch Vehicle Study for Nimbus E Spacecraft" for applicability to ERTS.	Volume I Section 3.2 7
741001	<p>Study and indicate moments and products of inertia.</p> <ul style="list-style-type: none"> <li>● Provide periodic Mass Properties Reports which list weight, moments and products of inertia of the spacecraft and payload</li> <li>● Determine spacecraft control system tolerance to uncompensated momentum and magnetic moment</li> </ul>	Volume II Section 2  Volume II Section 5.4.5
751001	<p>Study compatibility with Orbit Adjust system.</p> <ul style="list-style-type: none"> <li>● Compute rate and attitude errors during the orbit adjust maneuver</li> <li>● Determine what control system design changes, if any, are required to achieve a pointing accuracy compatible with the orbit adjust maneuver.</li> </ul>	Volume II Section 5.4.3



TABLE 2-1. SUMMARY TASK DESCRIPTION REFERENCE (Contd )

Task No.	Task Description	Location in SSD Final Report
751002	<p>Study attitude determination for image location Identify problems and hardware associated with meeting goals.</p> <ul style="list-style-type: none"> <li>• Define techniques for accurately determining the attitude of the spacecraft in order to determine the location of an image in photographs taken from orbital altitude to within less than 2 nautical miles in a 100 x 100 nautical mile picture.</li> <li>• Define requirements for and select attitude sensor for this purpose.</li> </ul>	<p>Volume I Section 4.3</p> <p>Volume II Section 5.4.9</p>
751003	<p>Determine location of imagery using ground features, predicted satellite performance and imagery information.</p> <ul style="list-style-type: none"> <li>• Investigate visibility and identifiability of control-point images on RBV and MSPS imagery</li> <li>• Evaluate time and pointing errors for manual image identification and location</li> <li>• Evaluate time and pointing errors for automatic image matching of RBV/MSPS imagery</li> <li>• Determine extent and type of positioning to be performed</li> </ul>	<p>Later (April)</p>
751004	<p>Update control system block diagram Analyze results of computer simulations performed on Nimbus program. Select analyses applicable to ERTS to demonstrate control system performance to ERTS requirements</p>	<p>Volume II Section 5.4.2 and 5.3</p>
751005	<p>Define yaw sun sensor control back-up mode.</p> <ul style="list-style-type: none"> <li>• Identify the components and techniques to be used to control the yaw axis in the event of failure of the rate measuring package (gyrocompass)</li> </ul>	<p>Volume II Section 5.4.4</p>

12

TABLE 2-1. SUMMARY TASK DESCRIPTION REFERENCE (Contd.)

Task No.	Task Description	Location in SSD Final Report
None	System Design Changes to Achieve Desired Attitude Rate.	5.4.2.3.2
None	Provide Block Diagram of Control System and Demonstrate Performance.	5.3
None	Recommend Control System Provisions during Orbit Adjust.	5.4.3.3
761001	<p>Determine and recommend number and type of command functions for payload and spacecraft operation, and indicate availability of command status telemetry monitoring.</p> <ul style="list-style-type: none"> <li>● Update list of command functions required for proper operation of the spacecraft and payload sensors</li> <li>● Determine requirement for telemetry</li> </ul>	<p>Volume II Section 4</p> <p>Volume II Section 4 Appendix</p>
761101	<p>Consider command storage requirements and provisions for multiple executions of stored commands and define interface requirements</p> <ul style="list-style-type: none"> <li>● Rewrite specification reflecting any changes</li> <li>● Update definition of the command storage interface</li> <li>● Document the provisions for overriding of stored commands</li> <li>● Update the command addressing technique</li> <li>● Document the inherent reliability, flexibility, and adaptability</li> </ul>	Volume II Section 4
761201	<p>Investigate techniques for providing "Fail Safe" design to prevent non-reversible command action.</p> <ul style="list-style-type: none"> <li>● Select the optimum technique to insure that no single occurrence of an erroneous command can initiate a non-reversible command</li> </ul>	Volume II Section 4

TABLE 2-1. SUMMARY TASK DESCRIPTION REFERENCE (Contd.)

Task No.	Task Description	Location in SSD Final Report
762001	<p>Define NB telemetry system and determine capacity, sampling rate, flexibility and growth capability Consider existing VHF or UHF transmission system.</p> <ul style="list-style-type: none"> <li>• Obtain specifications of existing spacecraft PCM systems</li> <li>• Determine their ability to handle all housekeeping data and data from the Attitude Determination System</li> <li>• Study the formatting, flexibility and growth capability of the selected PCM unit</li> <li>• Define the system capability, sampling rate available, provisions for digital words, single bit indicators, sampling flexibility, growth provisions and the total bit rate for each available format</li> <li>• Choose an existing PCM/PM transmitter which meets the requirement of a received bit error rate of 1 in <math>10^6</math> or less for real time telemetry</li> </ul>	Volume II Section 4
763101	<p>Perform W/B Telemetry RF downlink power calculations for two stated conditions.</p> <ul style="list-style-type: none"> <li>• Determine the optimum parameters of the system components</li> </ul>	Volume II Section 4
763102	<p>Prepare system design and block diagram, estimate size, weight and power input requirements and specify the transmitter to be used.</p> <ul style="list-style-type: none"> <li>• Study and verify the GSFC baseline system configuration in order to achieve the desired operational features at minimum cost, within the allowable time</li> <li>• Prepare specifications for system components</li> <li>• Refine the estimated physical characteristics of the system components</li> </ul>	Volume II Section 4

TABLE 2-1. SUMMARY TASK DESCRIPTION REFERENCE (Contd.)

Task No.	Task Description	Location in SSD Final Report
763103	<p>Study the expected degradation of the wideband sensor data.</p> <ul style="list-style-type: none"> <li>● Identify sources of degradation to the sensor output data</li> <li>● Select the optimum system configuration</li> </ul>	Volume II Section 4
763104	<p>Evaluate both PCM and FM S-band transmitter designs.</p> <ul style="list-style-type: none"> <li>● Survey vendors for transmitters meeting ERTS specified requirements</li> <li>● Select design for the ERTS program</li> </ul>	Volume II Section 4
763105	<p>Evaluate Breadboard PCM and FM modulators.</p> <ul style="list-style-type: none"> <li>● Provide modulator breadboards</li> <li>● Test to verify electrical specifications of wideband telemetry link</li> </ul>	Volume II Section 4
763106	<p>Study, define, and evaluate diplexer and shaped antenna system for W/B telemetry.</p> <ul style="list-style-type: none"> <li>● Analysis of candidate designs</li> <li>● Definition of antenna system configuration</li> </ul>	Volume II Section 4
763201	<p>Study scanner and TV data links Recommend cross strapping to achieve maximum redundancy</p> <ul style="list-style-type: none"> <li>● Study switching and command functions, for interconnecting the RBV sensor, MSPS sensor, tape recorders, and wideband transmitters and antennas</li> <li>● Recommend detailed interconnection switching subsystem</li> </ul>	Volume II Section 4

TABLE 2-1. SUMMARY TASK DESCRIPTION REFERENCE (Contd.)

Task No	Task Description	Location in SSD Final Report
763202	<p>Perform overall study of wideband communication system design including verification of selected multiplexing techniques.</p> <ul style="list-style-type: none"> <li>• Determine data characteristics of object plane MSPS and RBV sensor signals</li> <li>• Perform communication system studies of Object Plane MSPS and of RBV to verify the selected multiplex techniques and parameters, recording techniques and carrier modulation techniques</li> <li>• Consider implementation factors (size, weight, power, development time and effort), and growth capacity</li> </ul>	Volume II Section 4
764001	<p>Verify minitrack link calculations</p> <ul style="list-style-type: none"> <li>• Perform RF downlink power calculations</li> </ul>	Volume II Section 4
765101	<p>Determine that the system design is compatible with the wideband tape recorder characteristics.</p> <ul style="list-style-type: none"> <li>• Study specification of GFE WBVTR</li> <li>• Establish requirements imposed on ERTS by WBVTR</li> <li>• Prepare report</li> </ul>	Volume II Section 4
765201	<p>Study application of existing flight proven recorders to ERTS.</p> <ul style="list-style-type: none"> <li>• Study use of redundant recorders</li> <li>• Analyze suitability of Nimbus Recorders to ERTS mission</li> <li>• Conduct survey of available off the shelf recorders</li> <li>• Prepare specification</li> <li>• Prepare report</li> </ul>	Volume II Section 4

TABLE 2-1. SUMMARY TASK DESCRIPTION REFERENCE (Contd.)

Task No.	Task Description	Location in SSD Final Report
766001	<p>Define the clock subsystem and determine its accuracy, stability, reliability and suitability for ERTS mission.</p> <ul style="list-style-type: none"> <li>● Identify all timing requirements of ERTS</li> <li>● Document the accuracy and tolerances with which universal time may be annotated with picture data</li> <li>● Study the provisions for resetting the clock and accelerating it through one year of time</li> <li>● Investigate methods for uniquely identifying the camera exposure time with the spacecraft clock</li> </ul>	<p>Volume II Section 4</p> <p>Volume I Section 4. 4</p>
767001	<p>Study the baseline GSFC combined TT&amp;C system in order to implement the design.</p> <ul style="list-style-type: none"> <li>● Investigate techniques to integrate STADAN/VHF and MSFN/USB dual command capability</li> <li>● Determine modifications required to existing command hardware</li> <li>● Determine specifications for new command hardware required for integrated dual command capability.</li> <li>● Determine specifications for 1.024 MHz subcarrier oscillator and bi-phase modulator</li> <li>● Determine optimum modulation indices for 1.024 MHz subcarrier data and range-and-range rate signal using USB transmitter</li> <li>● Determine degradation caused by transmitting NB telemetry recorder playback on 136 MHz beacon</li> <li>● Prepare detailed specification for the subsystem components.</li> <li>● Perform link calculations to determine output power requirements for USB transmitters</li> </ul>	<p>Volume II Section 4</p>

TABLE 2-1 SUMMARY TASK DESCRIPTION REFERENCE (Contd.)

Task No.	Task Description	Location in SSD Final Report
770001	<ul style="list-style-type: none"> <li>● Evaluate characteristics of USB antenna</li> <li>● Prepare detailed specifications on components in the optimized system</li> <li>● Recommend alternate system and component configurations as required</li> <li>● Evaluate thermal, mechanical and electrical integration of USB equipment into spacecraft</li> <li>● Evaluate requirements and designs for AGE and ground station equipment associated with USB equipment</li> </ul> <p>Command RF Power.</p> <p>Develop power profiles and typical sequences, and analyze system performance against these</p> <ul style="list-style-type: none"> <li>● Update existing power profiles</li> <li>● Assess the margin of the Nimbus/ERTS power subsystem</li> <li>● Determine power subsystem load capability in relationship to the demands</li> </ul>	<p>Volume II Section 4</p> <p>Volume I Section 4</p> <p>Volume I, Sect. 4 5 Volume II, Section 8.4.1</p>
770002	<p>Study effects of season and other causes of sun angle variation on power system performance.</p> <ul style="list-style-type: none"> <li>● Investigate and document seasonal variations and changing shadow patterns</li> <li>● Update solar array I-V curves</li> </ul>	<p>Volume 2 Section 8.4.2</p>
770003	<p>Determine payload regulation and conversion requirements and provide subsystem design compatible with these requirements</p> <ul style="list-style-type: none"> <li>● Relate to the Nimbus D/ERTS power subsystem capabilities</li> </ul>	<p>Volume II Section 8.4.4</p>

TABLE 2-1. SUMMARY TASK DESCRIPTION REFERENCE (Contd )

Task No.	Task Description	Location in SSD Final Report
780001	<p>Consider satellite configuration on overall basis for thermal requirements.</p> <ul style="list-style-type: none"> <li>● Update existing ERTS studies</li> <li>● Identify any required design or hardware changes</li> <li>● Update heat rejection capability of Attitude Control System</li> <li>● Verify overall thermal design of the ACS</li> <li>● Determine maximum and minimum orbital temperature excursions for equipment in sensory ring and center section</li> <li>● Define the payload/spacecraft thermal interface</li> </ul>	Volume II Section 7
780002	<p>Investigate specific problems associated with payload or with proposed spacecraft configuration.</p> <ul style="list-style-type: none"> <li>● Investigate localized payload problems</li> <li>● Determine the thermal interaction between the orbit adjust engine and the spacecraft</li> <li>● Determine the effects of orbital adjust engine plume impingement on spacecraft structure, equipment and thermal coatings</li> </ul>	Volume II Section 7
791001	<p>Specify the orbit adjust system to permit attainment of the stated specification requirements.</p> <ul style="list-style-type: none"> <li>● Update the existing preliminary specifications</li> <li>● Revise the specification of total <math>\Delta V</math></li> <li>● Investigate the effects of thrust duration, pointing accuracy, impulse uncertainty and cross coupling of <math>\Delta V</math>'s</li> </ul>	Volume I Section 4. 2



TABLE 2-1. SUMMARY TASK DESCRIPTION REFERENCE (Contd.)

Task No.	Task Description	Location in SSD Final Report
791002	<p>Estimate the injection residuals after a nominal orbit adjust.</p> <ul style="list-style-type: none"> <li>● Update estimates of injection residuals</li> <li>● Determine range of expected orbit adjust system residuals</li> <li>● Apportion of errors between the orbit adjust system and orbit determination capability</li> </ul>	Volume 1 Section 4.2
791003	<p>Specify the orbit adjust operational/procedural sequence necessary for removal of the injection errors.</p> <ul style="list-style-type: none"> <li>● Refine operational/procedural sequence</li> </ul>	Volume 1 Section 4.2
791004	<p>Design orbit adjust propulsion subsystem and generate subsystem and component specifications.</p> <ul style="list-style-type: none"> <li>● Consider alternate propulsion configurations</li> <li>● Relate effective thermal control to the spacecraft</li> <li>● Perform a comprehensive analysis of propulsion performance</li> <li>● Update the selection of all propulsion components</li> <li>● Prepare the subsystem specification</li> <li>● Identify long lead items</li> <li>● Write component specifications and vendor work statements</li> </ul>	Volume II Section 6
791005	<p>Verify the 496 nm, 99.04° retrograde circular orbit as optimum for ERTS coverage requirements.</p>	Volume I Section 4.2
791006	<p>Predict the variations in orbital parameters expected for a one year operation subsequent to removal of initial injection errors, and predict the need for subsequent orbit adjust maneuvers.</p> <ul style="list-style-type: none"> <li>● Update predictions based on residual errors subsequent to orbit adjust maneuvers</li> </ul>	Volume 1 Section 4.2

TABLE 2-1. SUMMARY TASK DESCRIPTION REFERENCE (Contd.)

Task No.	Task Description	Location in SSD Final Report
791007	<p>Verify the present GSFC assumption that orbit maintenance for drag decay over a 1-year lifetime is required.</p> <ul style="list-style-type: none"> <li>● Re-run digital computer programs to re-confirm conclusions as ballistic coefficients, density and residual orbit errors become more firm</li> </ul>	Volume I Section 4.2
791008	<p>Examine the effects of launch window duration and inclination errors on variations in "Beta" angle, subsatellite solar elevation angle and shadow history.</p> <ul style="list-style-type: none"> <li>● Evaluate the effect of a launch at the end of the launch window on the subsatellite's sun elevation angle, the beta angle and the shadow history</li> <li>● Evaluate the effects of inclination errors on the same three conditions (solar elevation, beta angles, and shadow history)</li> <li>● Evaluate injection inclination errors versus reduced orbit adjust system propellant requirements</li> </ul>	Volume I Section 4.2
791009	<p>Determine the optimum method for computing the required orbit adjust <math>\Delta V</math>, based on orbit determination data, and gradual accumulation of ground track errors.</p> <ul style="list-style-type: none"> <li>● Investigate alternate techniques for devising the best way of determining the actual ERTS orbit period, or ascending node longitude shift</li> <li>● Develop logic from which velocity impulse commands are ordered and monitored</li> <li>● Minimize effects of orbit determination errors</li> </ul>	Volume I Section 4.2

TABLE 2-1. SUMMARY TASK DESCRIPTION REFERENCE (Contd.)

Task No.	Task Description	Location in SSD Final Report
100001	<p>Prepare hardware availability matrix for major spacecraft assemblies</p> <ul style="list-style-type: none"> <li>● Update the matrix of ERTS major hardware</li> <li>● Determine extent of re-design to accommodate ERTS requirements</li> <li>● Overview of hardware availability</li> </ul>	Volume I Section 3.3
110001	<p>Review hardware for compliance with reliability, quality and testing requirements</p> <ul style="list-style-type: none"> <li>● Review all related hardware documents</li> <li>● Report on reliability, quality and test review ERTS hardware.</li> </ul>	Volume III Section 8
110002	<p>Develop reliability model and make numerical assessment for proposed hardware.</p> <ul style="list-style-type: none"> <li>● Report the nature of the model developed for the ERTS design</li> <li>● Discuss "weak" system links</li> </ul>	Volume I Section 7
110003	<p>Study configuration management and failure reporting procedures, and determine compliance with Goddard management instructions.</p> <ul style="list-style-type: none"> <li>● Review the existing Nimbus Configuration Management and Failure Reporting systems</li> <li>● Measure these against the requirements of existing policies specified for the Phase D proposal</li> </ul>	Volume III Section 7
110004	<p>Prepare parts and material lists, procurement specifications, and sources of supply</p> <ul style="list-style-type: none"> <li>● Update approved parts, materials and processes lists</li> </ul>	Volume III Sections 3 and 4

TABLE 2-1. SUMMARY TASK DESCRIPTION REFERENCE (Contd.)

Task No.	Task Description	Location in SSD Final Report
110005	<p>Develop the following performance assurance documentation for the ERTS-A and B Phase D Proposal.</p> <ul style="list-style-type: none"> <li>● Reliability Program Plan</li> <li>● Quality Program Plan</li> <li>● Test Monitor and Control Program Plan</li> <li>● Configuration Management Plan</li> <li>● Soldering Program Plan</li> <li>● Failure Reporting Plan</li> </ul>	<p>Volume III</p> <p>Vol. III, Sect. 9 Vol. III, Sect. 2 Vol. III, Ap. 2C Vol. III, Sect. 5 Vol. III, Sect. 6 Vol. III, Sect. 7</p>
120001	<p>Provide outline of integration, test, and launch support plan, including facility requirements. Define and justify any deviations from environmental test specifications, functions not testable during all-up test, proposed sequence, basic test philosophy.</p> <ul style="list-style-type: none"> <li>● Revise and update outlines of Phase D plans contained in Volume IV</li> <li>● Use Nimbus Test and Launch Support experience as well as existing Nimbus plans, test reports and procedures</li> </ul>	<p>Volume II Section 10</p>
130001	<p>Describe GSE, its application, and define new requirements and develop hardware matrix</p> <ul style="list-style-type: none"> <li>● Identify all GSE end items</li> <li>● Determine applicability of existing GSE hardware</li> <li>● Define design modifications</li> <li>● Establish new design items</li> <li>● Establish source and usage of all GSE end items</li> <li>● Summarize the study (Ref 767001)</li> </ul>	<p>Volume II Section 11</p>

TABLE 2-2. SUPPLEMENTARY STUDY DOCUMENT

Document/ Drawing No	Title	Author	Date Received
RM-001	General Environmental Test Specification for Spacecraft and Components	GSFC	17 November 1969
RM-002	GSFC Specification Contractor-Prepared Monthly, Periodic, Periodic, and Final Reports	GSFC	
RM-003	MSS Multiplexer/Modem Demultiplexer Final Study Report	SBRC	10 November 1969
RM-004	MSS Ground Recording And Processing Study Report	SBRC	10 November 1969
RM-005	MSS Processing Techniques Study Constraints	SBRC	5 November 1969
RM-006	Optimization of a Multispectral Scanner For ERTS	Hughes	4 November 1969
RM-007	Attachment II (Section 1.4.5) Design Study Spec S-701-P-3	GSFC	10 November 1969
RM-008	Attachment III (Section 1.4.8) Design Study Spec S-701-P-3	GSFC	10 November 1969
RM-009	GSFC Specification Multispectral Scanner Sys.	GSFC	4 November 1969
RM-010	Appendix A Revision GSFC MSS Spec	GSFC	5 November 1969
RM-011	Ground Display Equipment Interface Requirements B1-Weekly Report No. 7	GSFC	10 November 1969
RM-012	Ground Display Equipment Interface Requirements B1-Weekly Report No. 8	GSFC	10 November 1969
RM-013	MSS Design Study	SBRC	10 November 1969
RM-014	First Quarterly Report on Wideband Video Recorder	RCA	10 November 1969
RM-015	Multi-Spectral Picture Registration Study	RCA	10 November 1969

TABLE 2-2. SUPPLEMENTARY STUDY DOCUMENTS (Cont'd.)

Document/ Drawing No.	Title	Author	Date Received
RM-016	U. S. Government Memorandum Meeting on Nov. 10, 1969 concerning ERTS Unified S-Band Link	Tracking and Data Systems Manager for ERTS	28 November 1969
RM-017	MSS Monthly Progress Report No. 1	Hughes	28 November 1969
RM-018	Memorandum for Record Proposed Constants and Equations For ERTS A and ERTS B Atmospheric Density Model	A Fuchs R. Strafella	1 December 1969
RM-019	Memorandum From Tracking and Data Systems Mgr.	Bradley	3 December 1969
RM-020	RBV Shutter Drive Schematic	RCA	2 December 1969
RM-021	RBV Progress Report October 1969	RCA	5 December 1969
RM-022	RBV Design Study Report AED-R-3413 Dated January 1969	RCA	25 November 1969
RM-023	USB Acquisition Techniques	GSFC	5 December 1969
RM-024	S-Band Xmtr - Design Study Report and First Quarterly Report - 16 June 1969 to 16 Sept. '69	ITT	12 December 1969
RM-025	RBVC Drawings 1976466 Camera Electronics Assy 1976467 Camera Controller Assy 1976696 Sensor Outline 2" RBV	RCA	25 November 1969
RM-026	MSS Radiometer Drawing - 24391	HAC	
RM-027	Design Study Specifications For ERTS April 1969 Revised October 1969	NASA	

11 February 1970

TABLE 2-2. SUPPLEMENTARY STUDY DOCUMENTS (Cont'd.)

Document/ Drawing No	Title	Author	Date Received
RM-028	Second Quarterly Report For Design, Fabrication Development and Test of 4 MHz Video Recorder/ Reproducer	RCA	4 November 1969
RM-030	Thor Delta Performance Preliminary Mission Analysis	GSFC	17 December 1969
RM-031	Preliminary Specs for Triple Line Transmitter and Receivers (1969)	RAD	18 December 1969
RM-032	Dual Line Receiver and Driver Bulletin	TI	18 December 1969
RM-033	MSS Radiometer Interface Control Drawing	SBRC	18 December 1969
RM-034	Ground Display Equipment Interface Requirements B1-Weekly Report No. 9	GSFC/ Westinghouse	17 December 1969
RM-035	Ground Display Equipment Interface Requirements B1-Weekly Report No 10	GSFC/ Westinghouse	17 December 1969
RM-036	Ground Display Equipment Interface Requirements B1-Weekly Report No. 11	GSFC	17 December 1969
RM-037	MSS December Interface Meeting (Vu-Graph)	HAC	18 December 1969
RM-038	MSS Interface Specification	HAC	18 December 1969
RM-039	RBV's Monthly Progress Report No. 1	RCA	18 December 1969
RM-040	Two inch Return Beam Vidicon Camera System	RCA	18 December 1969
RM-041	Minutes of MSS Interface Meeting Held at HAC 12/18/69	HAC	22 December 1969
RM-042	Preliminary Statement of RBV Camera Mounting and Alignment Constraints	RCA	23 December 1969

TABLE 2-2. SUPPLEMENTARY STUDY DOCUMENTS (Cont'd )

Document/ Drawing No.	Title	Author	Date Received
RM-043	NASA Memorandum 29DEC69 Subject Manpower Phasing Plan for ERTS/6DHS M and O Type Personnel, GSFC Furnished	NASA	
RM-044	VIDEO Tape Recorder Power Profiles	GSFC	9 January 1970
RM-045	MSS Thermal Analysis	GSFC	9 January 1970
RM-046	MSS Monthly Progress Report No. 2	Hughes	9 January 1970
RM-047	RBV Interface Action Items	RCA	9 January 1970
RM-048	Data System Development Plan NASCOM Network Revision 4, Section I Revision 5, Section I Revision 5, Section II	GSFC	12 January 1970
RM-049	2" RBV Envelope Drawing - Three Sensors	RCA	9 January 1970
RM-050	MSS Spacecraft Wiring	Hughes	14 January 1970
RM-051	USB Ranging Spectra	GSFC	15 January 1970
RM-052	Management, Processing, and Discrimination of Sensory Data for ERTS	ARA	20 January 1970
RM-053	Changes to Specification S-701-P-3 Section 2.14	GSFC	16 January 1970
RM-054	MSS/ERTS Interface	GSFC/Hughes	26 January 1970
RM-055	MSS Monthly Progress Report No 3	SBRC	26 January 1970
RM-056	RBV Monthly Progress Report No. 2	RCA	23 January 1970
RM-057	RBV Power Profiles Faceplate Temperature Control Function	RCA	30 January 1970



## SECTION 3

### BASELINE SPACECRAFT SYSTEM DESIGN

3.1	Introduction . . . . .	3-1
3.2	Spacecraft System Design . . . . .	3-1
3.2.1	System Functional Relationships . . . . .	3-1
3.2.2	Payload Characteristics Summary . . . . .	3-6
3.2.3	ERTS Spacecraft Configuration . . . . .	3-13
3.2.4	Electrical and Functional Description . . . . .	3-16
3.2.5	Subsystem Overview . . . . .	3-24
3.3	Hardware Matrix . . . . .	3-68
3.4	Launch Vehicle Study Result . . . . .	3-77
3.4.1	General . . . . .	3-77
3.4.2	ERTS/Delta Electrical Integration . . . . .	3-79
3.5	Growth . . . . .	3-86
3.5.1	General . . . . .	3-86
3.5.2	Growth Missions . . . . .	3-86
3.5.3	Spacecraft Growth . . . . .	3-92
3.5.4	Growth Power Systems . . . . .	3-100
3.5.5	Alternate Orbits . . . . .	3-105

## SECTION 3

### BASELINE SPACECRAFT SYSTEM DESIGN

#### 3.1 INTRODUCTION

The basic requirements specified by NASA for the ERTS A&B Spacecraft System Design (SSD) have been studied in detail. The results of these studies are reported in this and subsequent volumes. The culmination of these studies is a proposed spacecraft design which optimally satisfies the ERTS A&B requirements. This section provides a top level summary description of the proposed ERTS A&B spacecraft design which has evolved. Detail discussion, analysis and trade studies which have led to this selection and more detailed subsystem and component descriptions are contained in subsequent sections.

A matrix of all major spacecraft components and Aerospace Ground Equipment (AGE) end items follows. This identifies all hardware, quantities, source, design status, and flight experience.

Next, the selected launch vehicle and shroud is presented.

The final section considers growth beyond ERTS A&B. Growth missions, and in particular, the oceanographic mission, are discussed briefly. Then spacecraft growth, based on logical extensions of the proposed baseline design, is considered which meet the projected needs of an ongoing Earth Resources program.

#### 3.2 SPACECRAFT SYSTEM DESIGN

This section provides a summary description of the spacecraft system design which was selected as a result of the Phase B/C study effort. Compared to the baseline design presented in General Electric's proposal of June 1969, the most significant changes have occurred in the telemetry, tracking and command equipment. These changes result from the requirement to operate compatibly with both STADAN and MSFN ground stations. Even with these changes, the basic requirements specified by NASA are met largely by existing designs or straightforward modifications of existing designs.

##### 3.2.1 SYSTEM FUNCTIONAL RELATIONSHIPS

The functional relationship between the ERTS Spacecraft subsystems is designed to provide maximum mission performance. The overall Spacecraft system is comprised of nine subsystems.

1. Structures
2. Communications and Data Handling
3. Attitude Control
4. Orbit Adjust

5. Thermal
6. Power
7. Electrical Integration
8. Aerospace Ground Equipment (AGE)
9. Payload (GFE)

The overall system is illustrated in a simplified block diagram, Figure 3.2.1-1. This figure delineates, in accessible form, the main functional elements within each subsystem. Table 3.2.1-1 summarizes the functional relationships among the subsystems

The overall configuration of the spacecraft is shown in Figure 3.2.1-2. The cross-section layouts show the ERTS B Multispectral scanner with the radiative cooler. The ERTS A configuration is identical except for the deletion of this cooler. The selection and arrangement has evolved through careful study using established guidelines which will assure successful integration of a payload consisting of several earth viewing sensors

The high resolution payload sensors for ERTS A&B require an extremely stable, low rate, and highly accurate platform to realize their maximum capability. The attitude control system requirements compatible with these sensor requirements has been specified as less than 0.7 degrees pointing control with error rates of less and 0.04 degree per second and as a goal 0.015 degrees per second

The Nimbus D derived ERTS attitude control subsystem has the capability to meet these requirements. This control subsystem is based on a flight proven design which has demonstrated its capability to operate for several years in orbit. Modifications to meet ERTS requirements include simple switching changes to the logic, adjustment of loop gains and the provision of a redundant yaw gyro.

In addition to the pointing requirements, a requirement exists for locating any point on a 100 by 100 nm image with an accuracy of less than 2 nm. This position location accuracy requires precise attitude knowledge which is provided by an attitude sensor. The sensor selected is a passive radiometric balance type of earth sensor which is developed and fully qualified. This sensor provides pitch and roll attitude to better than 0.1 degree. The only significant modification is the lens design which is changed to accommodate the ERTS altitude. Yaw attitude data is determined from processing of existing spacecraft telemetry

The mission coverage requirements for precisely controlled and repeating observation by the relatively narrow field of view sensors necessitate the inclusion of an orbit adjust subsystem in the spacecraft. This system must remove initial launch vehicle injection errors to establish the precise ERTS orbital parameters and must make adjustments throughout the one year life of the mission in order to maintain the orbital parameters under disturbing influences such as aerodynamic drag. A simple monopropellant blowdown

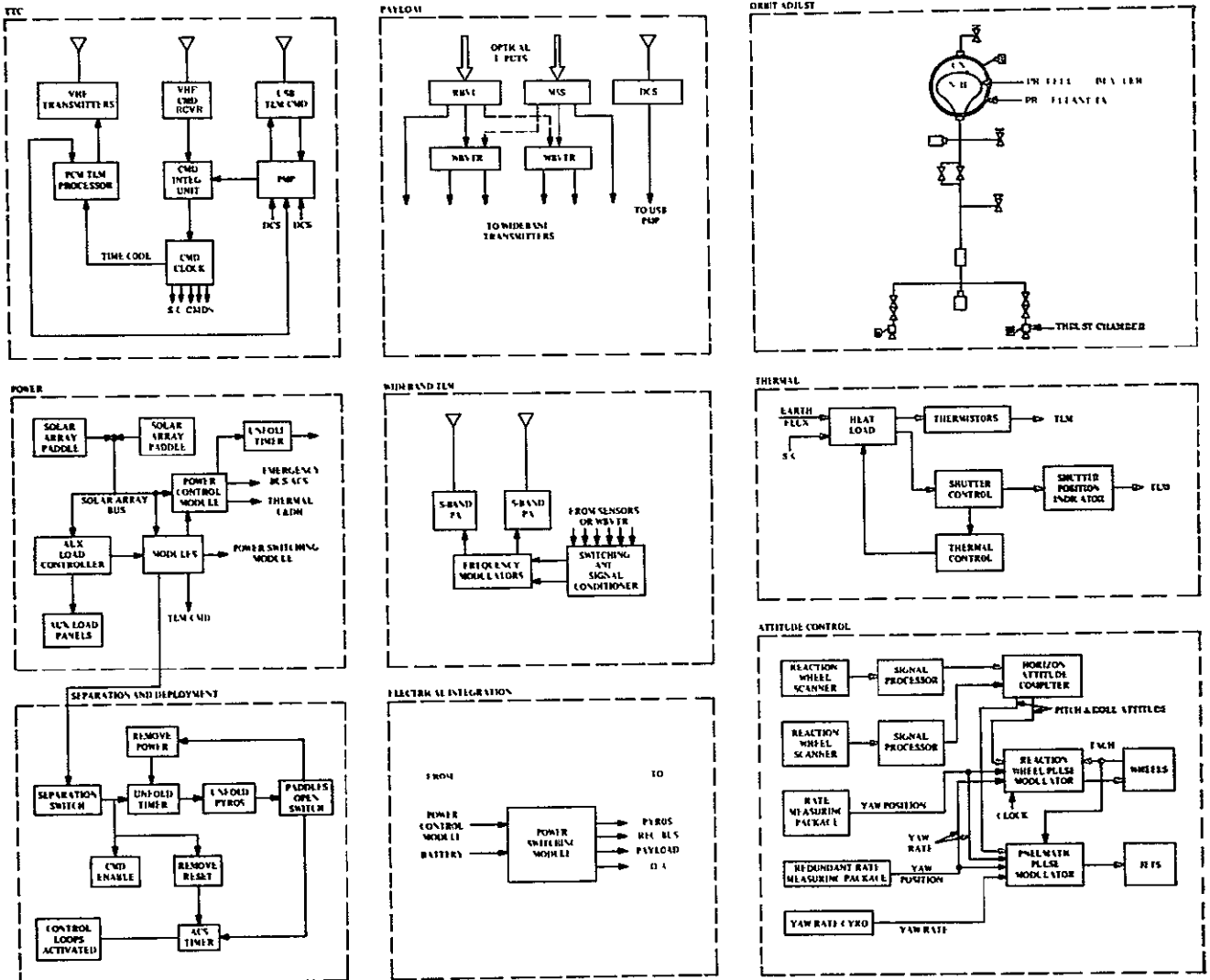


Figure 3.2.1-1. ERTS Simplified Block Diagram

Table 3 2 1-1 Functional Relationships

Requires	Subsystem	Provides
<ul style="list-style-type: none"> <li>• Power</li> <li>• Commands                             <ul style="list-style-type: none"> <li>- On-Off</li> <li>- Operations Modes</li> </ul> </li> <li>• Data from Payload</li>   <li>• Status from all Subsystems</li> <li>• Power</li>   <li>• Commands</li> <li>• Power</li>   <li>• Commands</li> <li>• Power</li>   <li>• Commands for auxiliary loads</li> <li>• Commands for On-Off Control</li>   <li>• Power</li> <li>• Ground Data from (DCP)</li> <li>• Spacecraft Stability Control</li> <li>• Operational Control</li>   <li>• Structural Support</li> <li>• Commands</li>   <li>• Power</li> <li>• Temperature Status</li> </ul>	<p><u>COMMUNICATIONS AND DATA HANDLING</u></p> <p><u>Wide-Band Telemetry</u></p> <p>The wideband telemetry provides the transmission channel for the MSS and RBV data and accepts the stored data from the WBVTR. Transmission of the PCM (MSS) data or the Video (RBV) data can be on either channel of the redundant system.</p> <p><u>Narrow Band Telemetry, Tracking and Command</u></p> <p>The Narrow Band Telemetry Tracking and Command equipment provide the means for tracking the vehicle, commanding the vehicle and its equipment, and telemetering housekeeping data. Uplink and downlink is available both through MSFN and STADAN stations.</p> <p><u>ORBIT ADJUST</u></p> <p>The orbit adjust subsystem provides the means to correct for initial injection errors and to provide orbit maintenance due to drag.</p> <p><u>ATTITUDE CONTROL</u></p> <p>The attitude control subsystem acquires and maintains three axis stabilization of the spacecraft and provides a stable platform for sensor operation. Also through utilization of the Attitude sensor, image location within <math>\pm 2</math> nm is achieved.</p> <p><u>POWER</u></p> <p>Primary power is generated by the solar array panels with excess power dissipated in the auxiliary loads. Battery charging is controlled by circuitry in each storage module and regulated voltages are provided by redundant pulse width modulators in the Power Control Modules. Automatic switchover is available in each Power Control Module.</p> <p><u>PAYLOAD</u></p> <p>The spacecraft payload consists of three RBV's, two WBVTR's, the DCS receiver and antenna and the MSS. These provide the data for multi-spectral analysis of the selected coverage areas.</p> <p><u>ELECTRICAL INTEGRATION</u></p> <p>The electrical integration subsystem distributes the power and signals throughout the spacecraft.</p> <p><u>THERMAL</u></p> <p>The thermal subsystem provides thermal control for the sensory ring, the ACS, the equipment mounted within, below, and above the sensory ring.</p>	<ul style="list-style-type: none"> <li>• Data link to Corpus Christi NTTF and Alaska</li>   <li>• Implements Command functions for all subsystems</li> <li>• Communications</li> <li>• Tracking Beacon</li> <li>• MSFN/STADAN Command Compatibility</li>   <li>• <math>\Delta V</math> for orbit correction</li>   <li>• Control stability for sensors</li> <li>• Status to Telemetry</li> <li>• Data for image location</li>   <li>• Regulated and Unregulated power for all Subsystems</li>   <li>• Image data via wideband telemetry</li> <li>• DCS data via USB telemetry</li> <li>• Stored data from the WBVTR's</li>   <li>• Power switching</li> <li>• Signal switching</li> <li>• All electrical I/F's</li>   <li>• Passive control</li> <li>• Active control</li> <li>• Thermal sensing for various subsystems</li> </ul>

hydrazine system was selected which provides a thrust level of about one pound. This level allows launch vehicle injection corrections to be made in a reasonably short time, still permits the metering of relative small corrections for drag make-up, and is compatible with the ACS control torques. A modular packaging concept has been employed, allowing the complete orbit adjust subsystem to be assembled and tested as an integral unit prior to assembly to the spacecraft. Interfaces are especially simple. The selected system uses components which are all flight qualified. The total  $\Delta V$  requirement for one year has been derived and is 45 fps.

The Communications and Data Handling (C&DH) system is unique in that it must be compatible with two different NASA ground networks, STADAN and MSFN/USB, and also must routinely transmit data at the highest rate and bandwidth ever required for any previous NASA program. For the Telemetry, Tracking and Command (TT&C) portion of this subsystem, dual equipments are required. To operate with the MSFN/USB requires the use of the Apollo USB type equipment which operates at 2106.4 MHz (command uplink) and at 2287.5 MHz down for TLM. The STADAN TT&C operates at 154.2 MHz for command and at 137.86 MHz for telemetry.

The proposed TT&C system uses existing designs for the command/clock and telemetry processor (VIP). A simple harness change allows the output data rate of the VIP to be reduced from 4 (as used on Nimbus D) to 1 kbps for ERTS. The VHF transmitters are based on existing designs, however the modulation is changed from AM to PM, and two power levels are provided. In order to make the USB command compatible with the existing command clock a command integrator unit (CIU) is used. Although a new design, it incorporates the state of the art circuitry and serves to demodulate and sub-bit decode the USB uplink command signal providing a compatible output at 200 kbps to the command clock. The VHF receivers have been modified to make them fully compatible with STADAN requirements. The USB transponders and the premodulation processor are based on Apollo designs but will require repackaging. The narrow band tape recorder designs are based on a currently qualified recorder. All antennas are existing designs currently used on NIMBUS D.

The wideband telemetry system accepts either RBV video at 3.5 MHz or MSS PCM at 15 Mbps. Switching and signal conditioning of the six possible data inputs (RBV or MSS, Realtime or Playback, WBVTR No. 1 or WBVTR No. 2) results in the selection of any two. These are processed through identical parallel modulator/power amplifier/antenna systems. Commandable 20/10 watt levels are provided in the TWT power amplifiers. Two shaped beam antennas provide a near constant earth illumination with > 4 dB gain over a +60 degree cone angle.

The relatively large power demands and varying duty cycles of the payload equipment plus the housekeeping loads of the spacecraft specify the energy and conversion requirements that the power system must satisfy. These are satisfied with the existing and flight proven Nimbus power system design, consisting of independently driven solar arrays, eight individual battery modules with a total capacity of 36 ampere-hours, an auxiliary load controller and two power control modules. The use of a second Power Control Module

(PCM) is the only change from the flight proven Nimbus system. This increases the peak capacity of the system to about 1000 watts (500 from each PCM) and allows the RBV and WBVTR's to operate from an isolated regulator system.

The thermal requirements for ERTS payload equipment ( $20^{\circ} \pm 10^{\circ} \text{C}$ ) are quite similar to existing Nimbus requirements ( $25^{\circ} \pm 10^{\circ} \text{C}$ ). They can be met with existing thermal control hardware (adjusted to operate at a lower nominal temperature) and previously used thermal control techniques. Flight experience with the proposed combination of passive, semiactive and active thermal control approaches has been highly successful.

In Table 3.2.1-2, the expected performance of the proposed spacecraft design is compared with the major ERTS A&B design requirements.

### 3.2.2 PAYLOAD CHARACTERISTICS SUMMARY

The ERTS payload consists of the Return Beam Vidicon Subsystem (RBV), the Multispectral Scanner Subsystem (MSS), the Wide Band Video Tape Recorder Subsystems (2) (WBVTR) and the Data Collection Subsystem (DCS). These provide the data for multispectral analysis of the selected coverage areas.

A summary of the pertinent characteristics of these components is shown in Table 3.2.2-1. The interfaces between these components is depicted, in a "top-level" basis, in Figure 3.2.2-1. All items shown except for the DCS and switching module are Government Furnished Equipment (GFE). The payload/spacecraft interface is at the input to the switching and signal conditioning module, and, for the DCS, at the output of the limiter.

The individual subsystems with the exception of DCS terminate their outputs in the Wide Band (S-Band) Transmitters. DCS data is received via the DCS antenna and receiver operating at 402.1 MHz and transmitted through the unified S-Band equipment. RBV and MSS outputs can be either transmitted direct (real time) or recorded for delayed playback. This is accomplished by using two identical WBVTR's on either line.

As a result of this interconnection scheme for the imaging sensors (RBV and MSS) the Wide Band Telemeter input is supplied with six types of outputs, namely

- RBV Video
  - Real Time Signal
  - WBVTR No. 1 - Playback Signal
  - WBVTR No. 2 - Playback Signal
- MSS Signal
  - Real Time Signal
  - WBVTR No. 1 - Playback Signal
  - WBVTR No. 2 - Playback Signal

Table 3.2 1-2 ERTS Spacecraft Requirements and Performance

	Design Requirement	ERTS Performance
<b>ORBIT</b>		
Sun Synchronous		Meets
Altitude	492 35 ± nm	Capable to correct worst case injection and maintenance for 1 year 30% margin built in. 100% margin with no redesign.
Inclination	98.086°	
Ascending Node Time	2130	
Eccentricity	0	
<b>PAYLOAD</b>		
Weight	450 pounds	530 pounds
Volume	12 ft <sup>3</sup>	37 ft <sup>3</sup>
Earth viewing	payload sufficient plus 25%	available
<b>ATTITUDE CONTROL</b>		
Attitude Accuracy	± 0.7° all axes	- 0.7° pitch & roll - 1.0° yaw
Attitude rate		
Requirement	0.04°/sec	Meets
Goal	0.015°/sec	0.02°/sec
Image Location	±2 NM	Meets using simple passive attitude sensor
<b>THERMAL</b>		
	20°C - 10°C	20°C - 10°C
<b>COMMUNICATIONS &amp; DATA HANDLING</b>		
<b>Command</b>		
Uplink Frequency		
STADAN	148-154 MHz	1.54 MHz
MSFN	2106.4 MHz	2106.4 MHz
Real Time Digital Commands	2-6	1 - total 480 external
Stored Digital Commands	10	10 plus recycle
Fall Safe Design	Required	Meets
<b>Narrow Band Telemetry</b>		
Downlink Frequency		
STADAN	136 - 138 MHz	137.86 MHz
MSFN	2287.5 MHz	2287.5 MHz
Data Accuracy	8 bits	10 bits
Real Time Data Rate	≤ 1 Kbs	1 Kbs
Playback Data Rate	2-0 Kbs	1 Kbs
Transmitter Power (Commandable)		300 MW
		1 Watt (Emergency)
<b>Wideband Telemetry</b>		
Downlink Frequency		
	26.5 MHz	26.5 MHz
	2229.5 MHz	2229.5 MHz
Bandwidth (RBV)	0 MHz	0 MHz
Transmitter Power (Commandable)	20 Watt	10 Watt & 10 Watt
Operating Elevation	0°	0°
Receiving Antenna		
	30 foot dish	either with
	85 foot dish	1 dB degradation
Bandwidth (MSS)	20 MHz	20 MHz
<b>Tracking</b>		
Minitrack System		
Transmitter Power		300 MW
<b>Timing</b>		
Common Spacecraft Clock	Provide all necessary timing signals	Meets
<b>Power</b>		
Payload Operation	20 Min/Orbit	15 Min/Orbit
<b>Lifetime</b>		
	One year in orbit	Meets

\* Can meet 20 min. per orbit by canting solar array - analysis verifies that 15 min/orbit is adequate  
 • Analysis shows mission requirements be met with ±1.0 yaw control. Can improve to 0.7 with subsystem modification



Table 3.2 2-1 ERTS Sensor Payload Summary

Multispectral Scanner		Return Beam Vidicon Camera Subsystem	Video Tape Recorder
	<u>Radiometer Head (1 required)</u>	<u>Camera Head (each) (3 required)</u>	<u>Tape Transport (2 required)</u>
Size (in.)	14H x 15W x 36L (ERTS-A) 14H x 15W x 48L (ERTS-B)	22L x 8 75H x 7 75W	21 5L x 14.8W x 6 5H
Weight (lb)	105 (ERTS-A) 120 (ERTS-B)	31 2	45
Power (Watts avg )	50 (ERTS-A) 55 (ERTS-B)	30	Record 85 Standby- 40 Rewind 40
	<u>MSS Signal Processor (1 required)</u>	<u>Electronics (each) (3 required)</u>	<u>Recorder Electronics (2 required)</u>
Size (in.)	Module 2/2	Module 3/3 (6x6x13 in.)	16 6L x 16W x 7 0H
Weight (lb)	10	12 0	25
Power (Watts)	15 (est)	15 (est)	30 (est)
		<u>Controller (1 required)</u>	
Size		Module 3/0 (6x6x6 5 in )	
Weight (lb)		7	
Power (Watts)		10 (est)	
		<u>Video Combiner (1 required)</u>	
Size		Module 3/0 (6x6x6 5 in )	
Weight (lb)		9	
Power (Watts avg )		5 (est)	
Commands Total	47	74	8 (tent )
Telemetry Points Total	50	54	24 (tent )

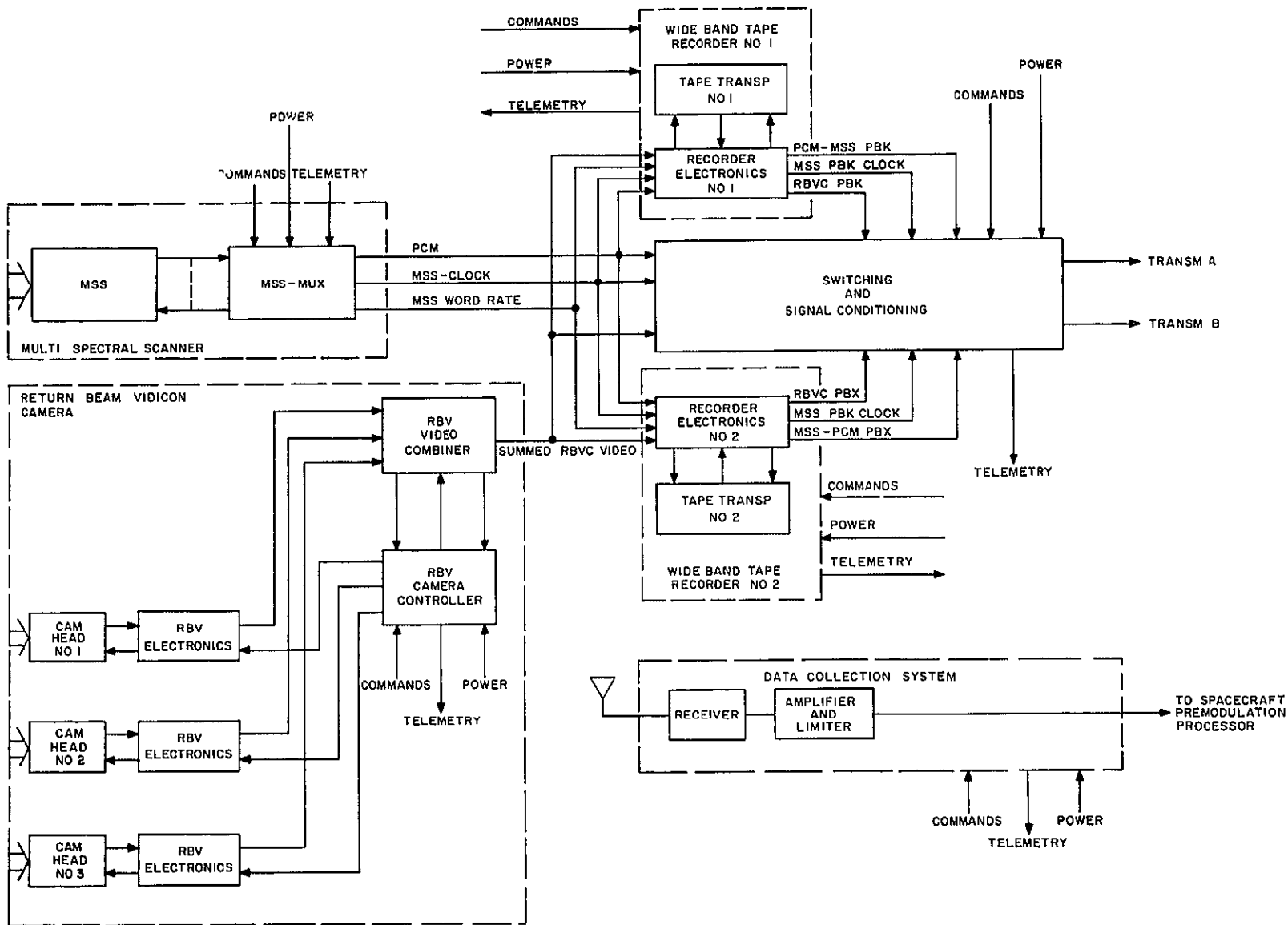


Figure 3.2.2-1 ERTS Payload Subsystems

Switching of these inputs is performed by the Wide Band Communication Subsystem and permits any two of the six inputs to be transmitted simultaneously.

### 3.2.2.1 Return Beam Vidicon Camera Subsystem

The RBV camera subsystem consists of

1. Camera Head (3 required)
2. Camera Electronics (3 required)
3. Camera Controller (1 required)
4. RBVC Video Combiner (1 required)

Except for the RBV Camera Heads all other units are in a form of standard Nimbus modules. Camera Heads are irregular in shape. The details on other RBVC modules is summarized in Table 3.2.2-1. In all other aspects, the modules conform to Nimbus D Experimenter's Handbook.

Return Beam Vidicon Camera Subsystem signal output is analog and is the result of time multiplexing the three individual camera outputs plus synchronizing signals. The baseband of this signal is from DC to about 3.5 MHz. The WBVTR subsystem accepts the RBVC signal, video, and records it in FM mode. Playback mode of RBVC video reconverts the FM tape readout back to an analog signal with less than 1 dB signal to noise degradation.

### 3.2.2.2 Multispectral Scanner Subsystem

The Multispectral Scanner Subsystem consists of only two units

1. Scanner Head (Radiometer)
2. MSS Multiplexer

The scanner head is irregular in shape and will have two possible configurations. The ERTS B configuration includes a passive radioactive cooler, required for the fifth spectral band. The ERTS A configuration excludes the fifth spectral band and associated cooler.

The MSS multiplexer is in a form of Nimbus 2/2 standard module, and its design conforms to Nimbus D Experimenter's Handbook.

Power consumption of MSS is 50 watts for ERTS A application and 55 watts for ERTS B, and includes 15 watts allotted to the MUX.

A summary of pertinent characteristics is shown in Table 3.2.2-1.

The data output after multiplexing emerge as a 15 Mbs PCM signal. In addition, two auxiliary signals are produced in the multiplexer, the 7.5 MHz MSS clock and MSS word

rate. These two are needed by the WBVTR in the encoder, where PCM to 8 level FM conversion is accomplished and thus permits the use of the same recorder for both MSS and RBV data

The playback signal from WBVTR in the MSS mode is 8 level FM and, therefore, it is reconverted back to PCM. This makes the direct and playback MSS PCM signals fully identical and therefore compatible with the wideband communication subsystem. The 7.5 MHz clock signal is also reconstructed so it can be used by the wideband communication subsystem if reclocking of PCM signal is desired.

### 3.2.2.3 Wideband Video Tape Recorder Subsystem

The Wide Band Video Tape Recorder Subsystem is provided for the enhancement of RBVC and MSS operational flexibility.

WBVTR's can be operated in either RBVC or MSS Record or Playback modes. The switching is provided internally in each WBVTR by means of commands applied from the spacecraft command subsystem.

Each WBVTR has two recording tracks. First track is compatible with either RBVC or MSS wideband signals. The second track is intended for auxiliary purposes, such as, telemetry, time code or other support purposes. It can be erased if desired, and also can be played back a number of times without erasing. Its frequency response is DC to 5 kHz and will accept  $\pm 0.75V$  amplitudes across 600 ohms input.

In playback the WBVTR also provides a search track signal output. This signal is recovered from a prerecorded track with data prerecorded at 6 inch intervals. Its intended use is for locating data. It may be readout during forward or rewind, fast or normal operation.

Physically, the WBVTR is subdivided into two functional units, the Tape Unit and Electronics. Power dissipation of the tape unit is complex, and has quite severe transient power demands, depending on the mode of operation. The electronics unit dissipates uniformly about 30 watts. The summary of WBVTR parameters is provided in Table 3.2.2-1.

### 3.2.2.4 Data Collection Subsystem (DCS)

The DCS for ERTS A&B consists of three segments. They are the Data Collection Platforms (DCP's), the Spacecraft Receiving Subsystem and the DCS Ground Preprocessing Equipment. The DCP's are collocated with sensors throughout the continental United States and its coastal waters. Each DCP accepts inputs from eight sensors. The analog inputs are multiplexed using time division multiplexing. Each input is then coded using Pulse Code Modulation (PCM). A convolutional encoder then encodes the pulse train before it is passed on to the FSK modulator and transmitter. The signal is transmitted to the spacecraft on a carrier at a frequency of 401.9 MHz.

The signal is received at the spacecraft through a crossed dipole antenna and passes to the DCS spacecraft receiver subsystem. The receiver is a double heterodyne receiver with a 3 dB overall noise figure, an IF bandwidth of 100 kHz and an output center frequency of

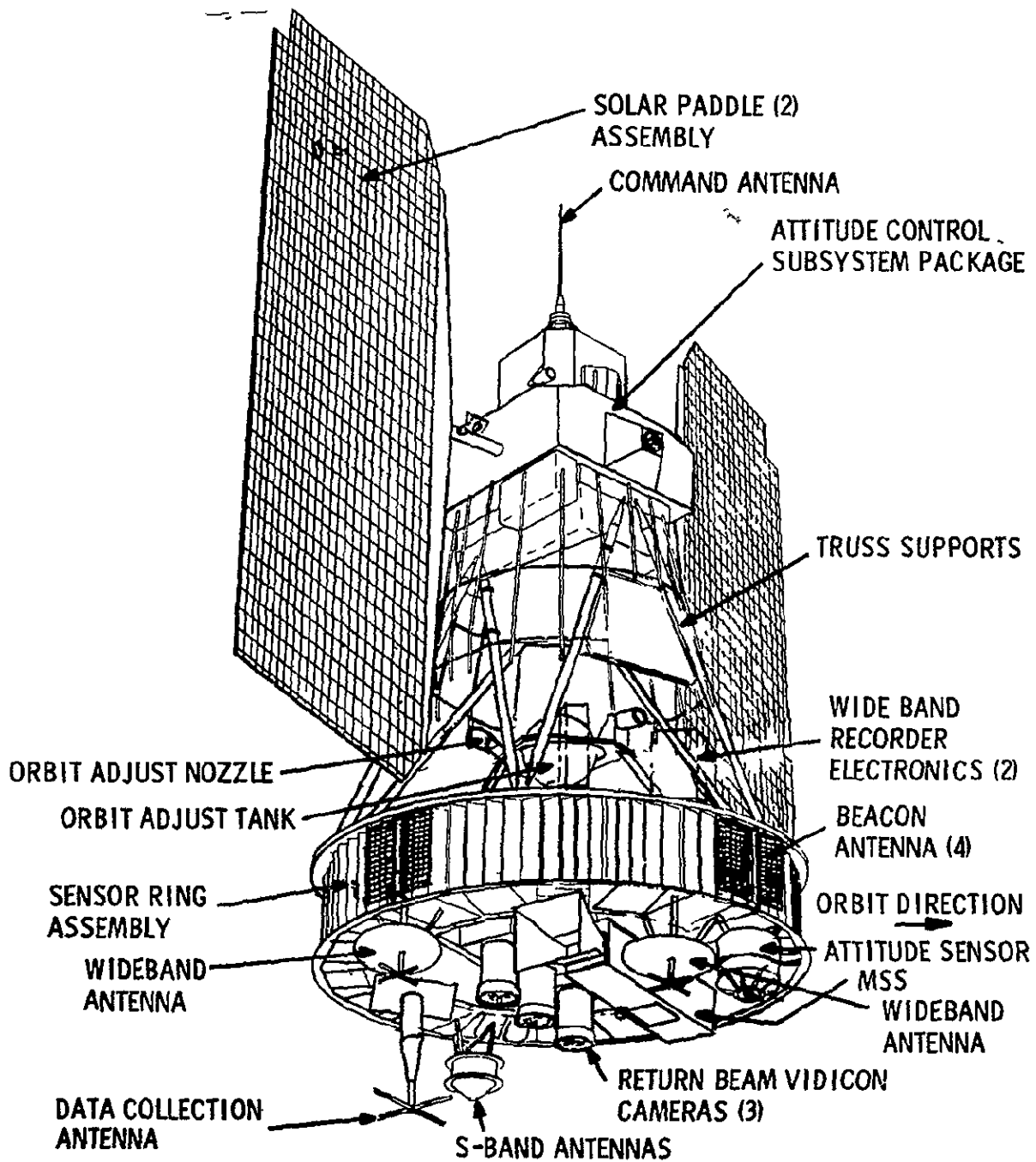


Figure 3.2.3-1. ERTS Configuration

1 024 MHz The 1 024 MHz signal is passed to the Unified S-Band (USB) premodulation processor where it is combined with other signals for relay to the ground over the USB downlink

At the three receiving sites (Alaska, Corpus Christi, and NTTF), the USB downlink signal is received and demodulated. The DCS signal is stripped out of the composite baseband and routed to the DCS ground preprocessing equipment. In the preprocessing equipment the PCM/FSK signal is detected and demodulated and then decoded and formatted for transmission over telephone lines to the Operation Control Center (OCC) and the NASA Data Processing Facility (NDPF). At the NDPF the data is formatted and prepared for dissemination to the users.

The system provides for a 1000 DCPs with 0.95 probability of receiving interference free data from each platform every 12 hours. The coding provided will assure that the probability of errors in a message being undetected is less than 0.05.

### 3.2.3 ERTS SPACECRAFT CONFIGURATION

The ERTS spacecraft provides payload accommodations and meets payload requirements for the ERTS A&B missions. The ERTS configuration is shown in Figure 3.2.3-1 in the orbit configuration. With the exception of the equipment arrangement in the sensory ring assembly, including the accommodation of the Orbit Adjust S/S Assembly and the payload equipment, this configuration is identical with the flight proven Nimbus spacecraft. The ERTS configuration is a two body spacecraft connected by a truss (set of 6 struts). The lower body is the sensory ring assembly which houses the payload and housekeeping subsystems, and the upper body is the attitude control package and solar array to provide orientation for the spacecraft and provide power for the spacecraft.

The ERTS configuration and packaging arrangement is defined in Figure 3.2.3-2, (drawing 47J220030). This drawing identifies the major elements of the baseline configuration.

The Attitude Control Subsystem package, identified in axis Y-Y profile of Figure 3.2.3-2, provides an unobstructed exposed mounting for the solar paddle sun sensors, horizon scanners and gas nozzles. The subsystem electronics, mechanical assemblies and pneumatics are internally packaged, as are the solar array drives. The command antenna and the upper part of the ground plane are mounted on the top surface of the ACS.

The solar arrays attach to the shaft projecting from the ACS package, Figure 3.2.3-2 axis Y-Y profile. In the launch configuration, the solar arrays are folded along the longitudinal axis to fit within the Sensory Ring envelope and is secured by a latching mechanism, Figure 3.2.3-2, axis X-X profile.

The truss structure provides a tripod connection between the ACS and the Sensory Ring Assembly, allowing alignment adjustment between the ACS and the Sensory Ring. See Figure 3.2.3-2, axis X-X profile. The truss also supports the command antenna lower ground plane, the auxiliary load panel and the ERTS/ACS connector IF panel.

The Sensory Ring Assembly is a torus structure with 18 modular bays for packaging equipment. The lower surface of the sensory ring provides mounting for payload equipment and antennas. The upper surface of the sensory ring provides mounting for spacecraft equipment. The center of the sensory ring has crossbeam assemblies to mount additional payload equipment and other non-modular spacecraft equipment.

Figure 3.2.3-2 presents the baseline packaging of the equipment in the Sensory Ring Assembly. Section A-A of the figure identifies the equipment packaged in each of the 18 peripheral bays and also defines the equipment packaged on the crossbeams, including

- 1 RBV Assembly (3 RBV's plus mounting plate)
2. WBVTR (2)
- 3 NBTR (2)
- 4 Power Switching Module (1)
- 5 Unfold Timer (1)
6. TLM Conversion Module (3)

On the top of the Sensory Ring, Section B-B of Figure 3.2.3-2, the following equipment is mounted

- 1 OA Subsystem Assembly
2. WBVTRE (2)
- 3 Magnetic Moment Assembly

Below the Sensory Ring, Section C-C of Figure 3.2.3-2, the following equipment is mounted

- 1 MSS
2. Wide Band WBV/PCM Antenna (2)
3. USB Antenna
- 4 DCS Antenna
5. Attitude Sensor

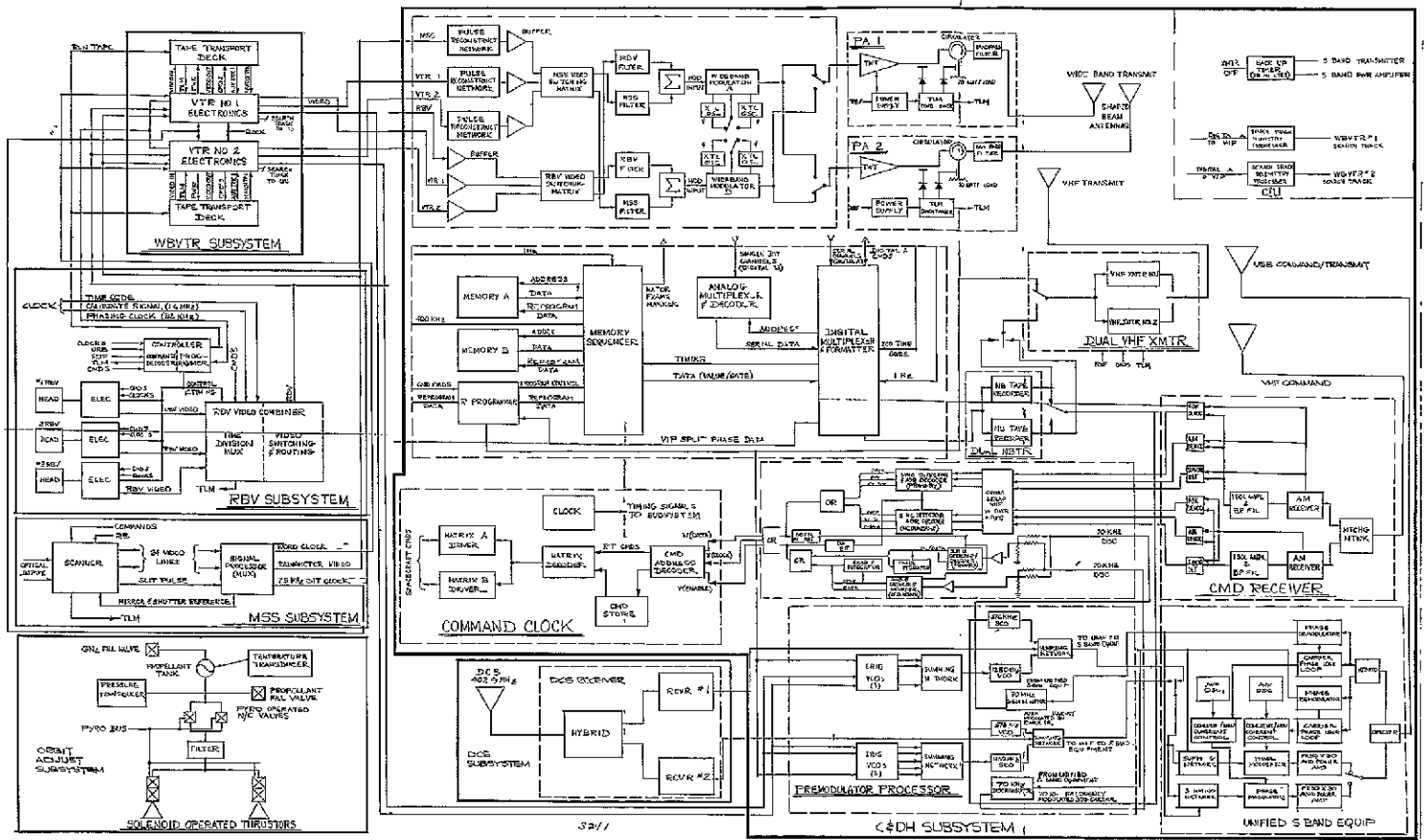


Figure 3.2.4-1 Electrical Block Diagram (Sheet 2 of 2)



Table 3 2.4-1 Spacecraft Regulated Power Demand  
for Various Operating Modes

<u>All Systems On</u>		
<u>Subsystem</u>	<u>Continuous</u>	<u>Peak</u>
Power	1.3	1.3
Attitude Control	35.5	99.5
Thermal Control	10.2	10.2
Command and Data Handling	55.9	102.0
Orbit Adjust Telemetry (turned on as required)	<u>negligible</u>	<u>1.8</u>
	102.9	217.8
<p>Note For end-of-life, thermal control requirements will be reduced to 1 watt System total becomes 93.7 watts for that condition</p>		
<u>Payload-Real Time</u>		<u>Peak</u>
DCS Receiver		1.0
Attitude Sensor		1.6
RBV		155.0
MSS (ERTS B)		70.0
WB PA & MOD (2)		<u>125.0</u>
		351.6
<u>Payload-Record</u>	<u>Peak 13.5 seconds</u>	<u>Peak 11.5 seconds</u>
DCS Receiver	1.0	1.0
Attitude Sensor	1.6	1.6
RBV	163.0 (Prepare)	145.0 (Readout)
MSS	70.0	70.0
WBVTR (2)	<u>118.0 (one on standby)</u>	<u>166.0 (both recording)</u>
	353.6	383.6
<u>Payload-Playback</u>	<u>RBV/MSS</u>	<u>MSS</u>
DCS Receiver	1.0	1.0
WBVTR	152.0	76.0
WB Power Amplifier & Modulator (2)	<u>125.0</u>	<u>45.0</u>
	278.0	122.0

Table 3.2.4-1 Spacecraft Regulated Power Demand  
for Various Operating Modes (Cont'd)

Note If RBV and MSS record simultaneously, one recorder will only playback 46% of total operate time because the RBV picture readout time is only 11.5 seconds out of the 25 second cycle. Therefore, the RBV recorder will be on standby power for 54% of that time

<u>Payload-Rewind</u>	<u>Watts</u>
DCS Receiver	1.0
WBVTR (2)	60.0 (1.15 minutes)
WBVTR (1)	<u>30.0 (2.5 minutes)</u>
	61 (1.15 minutes)/31 (2.5 minutes)

Minimum Satellite

<u>Service Subsystem</u>	<u>Watts</u>
Power	1.3
Attitude Control	35.5
Thermal Control	10.2
Communication and Data Handling	55.9
Compensation Heaters	36.9
Orbit Adjust Telemetry	1.8

Payload Subsystems

Attitude Sensor	0
RBV	0
MSS	0
WBVTR	0
WTMR	0
DCS Receiver	<u>0</u>
	141.6

Launch

<u>Subsystem</u>	<u>Watts</u>
Power	1.3
Attitude Control	64.8
Orbit Adjust Telemetry	1.8
Thermal Control	10.2
Compensation Heaters	0

Table 3 2.4-1 Spacecraft Regulated Power Demand  
for Various Operating Modes (Cont'd)Subsystem (Cont'd)

Communications and Data Handling	55.9
Attitude Sensor	0
RBV	0
MSS	0
WBVTR	0
WBTMR	0
DCS Receiver	<u>0</u>
	131.0 watts

Attitude Control Launch and Initial Stabilization

	<u>Launch</u>	<u>Initial Stabilization</u>
Control Logic and Signal Processors	8.8	8.8
Roll Flywheels and Scanners	1.5	30.0
Pitch Flywheel	-	15.0
Roll Flywheel	-	15.0
RMP	32.3	10.0
Initiation Timer	0.8	0.8
Solar Array Drives	13.0	24.0
Continuous Telemetry	1.7	1.7
Pneumatics	-	44.6
Yaw Axis Rate Gyro	<u>6.7</u>	<u>9.0</u>
	64.8	158.9

Regulated Power Requirements

<u>Power Subsystem</u>	<u>Orbital Average or Continuous</u>	<u>Peak</u>
Auxiliary Load Controller	0.65	0.65
Power Switching Module	0.65	0.65
Unfold Timer	<u>-</u>	<u>-</u>
	1.3 watts	1.3 watts

Table 3 2.4-1 Spacecraft Regulated Power Demand  
for Various Operating Modes (Cont'd)

Note Solar array, power control module, payload regulator module, and battery module regulated power requirements are included as internal subsystem losses. The power requirements shown above are mainly for telemetry circuits. Unfold timer pyrotechnic devices actuated off the unregulated pyro bus and the timing circuits off the regulated bus are automatically switched off when deployment is completed.

<u>Attitude Control Subsystem</u>	Orbital Average or <u>Continuous</u>	<u>Peak</u>
Control Logic and Signal Processors	7.3	8.8
Roll Flywheels and Scanners	2.2	10.8
Pitch Flywheel	1.1	10.0
Yaw Flywheel	0.3	10.4
RMP	9.4	10.0
Initiation Timer	0.8	0.8
Solar Array Drives	13.8	17.6
Telemetry Conversion Module	1.7	1.7
Pneumatics	<u>0.6</u>	<u>29.4</u> (2 axes)
	37.2 watts	99.5 watts

Note All other ACS equipment not utilized in normal orbital mode of operation.

<u>Thermal Control Subsystem</u>	Orbital Average or <u>Continuous</u>	<u>Peak</u>
Telemetry Conversion Modules (3)	2.25	2.25
Auxiliary Load Panels (2)	0.20	0.2
Attitude Control Subsystem	2.23	2.23
Orbit Adjust Heaters	3.00	3.0
Payload and Other	2.52	2.52
Compensation Heaters	<u>          </u>	<u>36.9</u>
	10.20 watts	50.1 watts

Note Continuous load of 10.2 watts is for temperature telemetry circuits. All but 1 watt will be switched off.

Table 3 2 4-1 Spacecraft Regulated Power Demand  
for Various Operating Modes (Cont'd)

Compensation heaters are cycled to maintain temperature as required. Will not normally be needed during normal full on operation. Generally only used after more than one orbit at low load conditions

<u>Communications &amp; Data Handling</u>	Orbital Average or <u>Continuous</u>	<u>Peak</u>
VHF Transmitter	0 5	12 0 (Emergency)
*VHF Command Receiver	2 0	2 0
USB Equipment		22.2
Premodulation Processor	1 6	4.0
PCM Telemetry Processor	6 8	6 8
*Command Clock	27 0	27 0
*Command Integration Unit	3.0	3.0
Narrow Band Tape Recorder (2)	<u>10.6</u>	<u>25.0</u>
Subsystem	55 9 watts	102 0 watts

\* Also connected to Emergency Bus. Narrowband tape recorders load based on one on standby and one recording for continuous demand and one recording and one in playback for peak demand.

<u>Attitude Sensor</u>	1 6 watt
<u>Data Collection System Receiver</u>	1 0 watt
<u>Return Beam Vidicon</u>	<u>Watts</u>
Camera Head (3 @ 30 w)	90 0
Camera Electronics (3 @ 15 w)	45 0
Camera Controller	10 0
Video Combiner	<u>10 0</u>
	155 0 watts

Note Shutter solenoid power is 30 amperes/100 ms at 26 volts. Can be connected to 26 to 39 volt bus

Table 3 2 4-1. Spacecraft Regulated Power Demand  
for Various Operating Modes (Cont'd)

Multispectral Scanner

Signal Processor	15.0	15.0
Scanner	<u>50.0</u> (ERTS A)	<u>55.0</u> (ERTS B)
	65.0 watts	70.0 watts

Wide Band Storage

Recorder Electronics (2) Each is	20.0
Video Tape Recorder (2) Each is	15.0 (Standby)
	63.0 (Record)
	56.0 (Playback)
	10.0 (Rewind)

Note Each recorder has a 250 watt transient decaying in 4 seconds to steady state standby level. Commands to turn on should have a 4 second interval between recorders.

Wide Band Telemetry

FM Modulator	5.0
S-Band Power Amplifier (2)	80.0 (RBV)
	<u>40.0</u> (MSS)
	125.0 watts

Orbit Adjust Subsystem

Telemetry Transducers (3)	1.5
Pressure Transducer	<u>0.3</u>
	1.8 watts

Note Solenoid valves, energized off unregulated pyro bus, require less than 10 watts. Pyrotechnic valves are actuated off the unregulated pyro bus. Transducers will be energized prior to launch and through removal of injection errors, then switched off until next operation.

### 3.2.5 SUBSYSTEM OVERVIEW

#### 3.2.5.1 Structures Subsystem Summary

##### 3.2.5.1.1 Structure and Spacecraft Arrangement

The ERTS spacecraft and structures subsystem meets the payload accommodation and requirements for the ERTS A and B missions. The ERTS spacecraft is shown in Figure 3 2.5-1 (isometric) and is similar to the Nimbus spacecraft. The spacecraft has four major configurational elements

1. The Attitude Control Subsystem (ACS), the upper structure that provides unobstructed exposed mounting for the solar paddle sun sensors, horizon scanners, and gas nozzles. The necessary electronics, mechanical drives and pneumatics are assembled internally, as is the drive for the solar array paddles. The command antenna and the upper part of its ground plane are mounted on the top surface.
2. The solar array paddles attach to the shaft projecting from the ACS housing. In the launch configuration, the solar array is folded along its longitudinal axis to fit within the Sensory Ring envelope and is secured to the truss structure by a latch mechanism. The spacecraft is mounted on an adapter structure, which, in turn, is bolted to the launch vehicle adapter ring.
3. A truss structure provides a tripod connection between the ACS and Sensory Ring assemblies, allowing the alignment required between the ACS and the sensors. The truss also supports the command antenna lower ground plane and the auxiliary load panel.
4. The Sensory Ring is a torus structure composed of 18 rectangular module bays, 13 inches in depth. The bays house the electronic equipment and battery modules. The lower surface of the torus provides mounting space for payload and antennas. A crossbeam structure, mounted within the center of the torus, provides support for additional payload equipment and tape recorders.
5. The Adapter (not shown) is the transition section between the spacecraft and the launch vehicle. The adapter is 24 inches high and interfaces with the spacecraft with a Marmon Band Separation device and with the launch vehicle with eight-1/2 inch diameter bolts on a 58 inch diameter bolt circle. The adapter also provides a support beam to accommodate payload sensor stimulators and antennas pickups and reradiators.

##### 3.2.5.1.2 Requirements

The structural subsystem primary functional requirements are to provide volume, strength and stiffness to

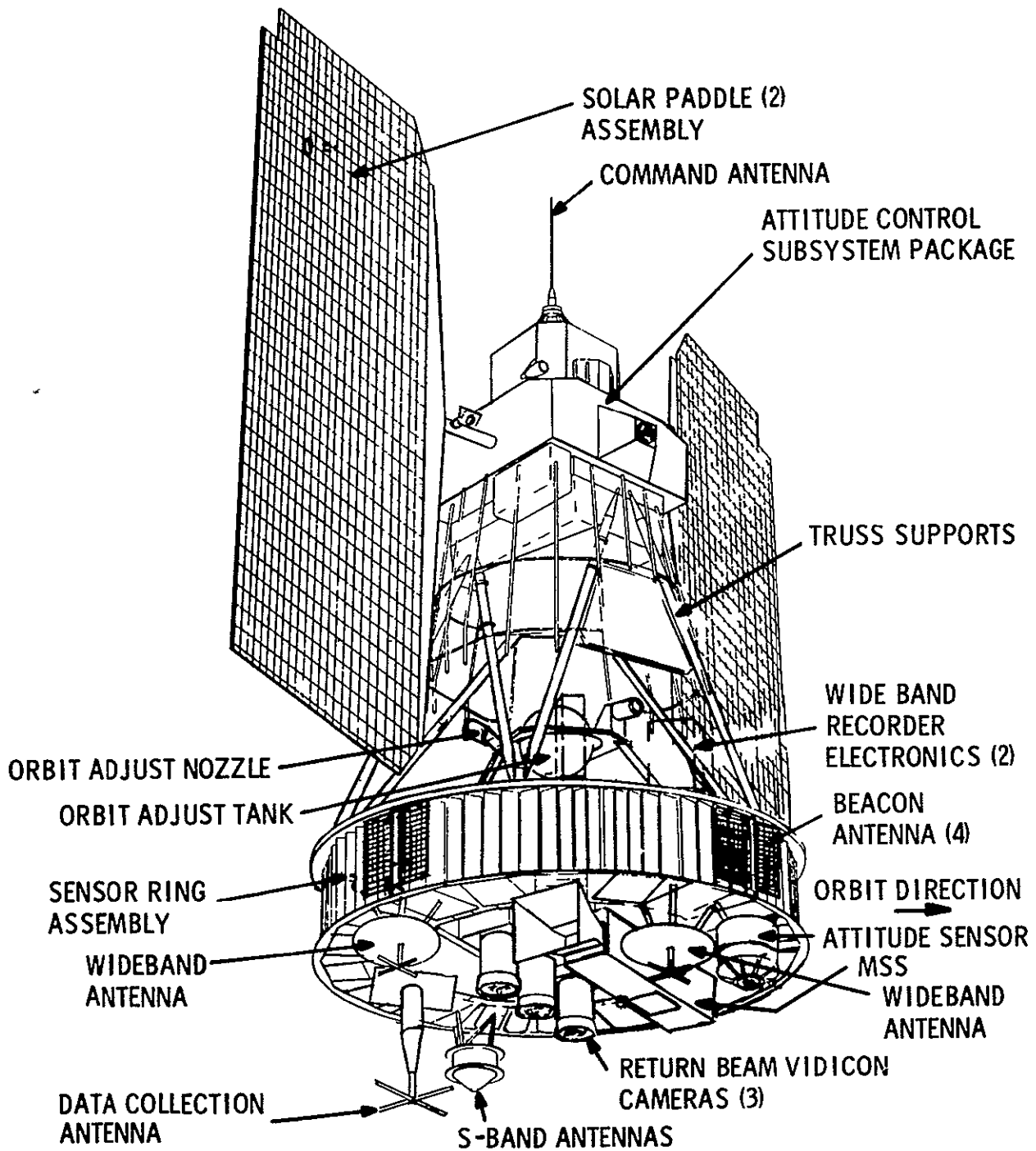


Figure 3. 2. 5-1. ERTS Spacecraft



1. Support the payload and all other subsystems throughout all phases of the mission. As well as the basic housekeeping subsystem accommodation, payload requirements are to accommodate 450 lbs and 12 cu ft of payload equipment
2. Maintain the location and alignment of components within the specified tolerances. The payload sensor and Attitude Control Subsystem Components require 0.1 degree alignment of the components with respect to the vehicle axes.
3. Be compatible with the Delta launch vehicle and SACS shroud. Spacecraft space envelope, static and dynamics, must have clearance of 0.25 inch with surrounding shroud structure during ground handling and launch through shroud separation. Spacecraft adapter must be primary load interface at 58 inch diameter bolt circle of eight bolts.
4. Withstand the environments through all mission phases. The principal requirements are to withstand launch environment of quasi-static and dynamic load requirements. All prelaunch phases will be attenuated with AGE as required.

#### 3.2.5.1.3 Structure Assemblies

The arrangement and major features of the structural assemblies and their function are provided in Figure 3 2 5-2 (Structural Isometric)

##### 3.2.5.1.3.1 Solar Paddle Assemblies

The structural subsystem interfaces with the Solar Paddle Assemblies and supports these assemblies during launch and in orbit. The in-orbit support is provided by the solar paddle to solar array drive interface which is a socket built into the paddle transition section engaged to the Solar Array Drive Shaft.

In a launch position, the solar paddle assemblies are secured by three points in a stowed position. The points are at the ends of the arrays shafts as described above and at the paddle unfold latch system which is attached to the sensory ring. In the launch configuration, the paddles are folded back along the hinge line and the paddles are connected to each other by hinge-like jaws (7) spaced along the paddle edge. The jaws are latched with pins that are connected to each other by a cable. The cable, at the lower end, has a rod anchored in the lower latch assembly and tensioned by a spring at the top. Unlatching occurs when a pyrotechnic cutter severs the anchor rod, permitting the cable to be pulled upward by the upper tension spring. This motion withdraws the pins from the jaws and each array unfolds by means of the paddle drive motor. The paddles are then latched in the full open position. Teflon lined guides are strategically located to prevent hangup of the array during deployment.

##### 3.2.5.1.3.2 Attitude Control Subsystem (ACS) Package

The structural subsystem interfaces with the ACS in order to control the interfaces of this package with the solar paddle assemblies. The truss tube support and special fittings on the ACS serve as lift lugs for the entire spacecraft.

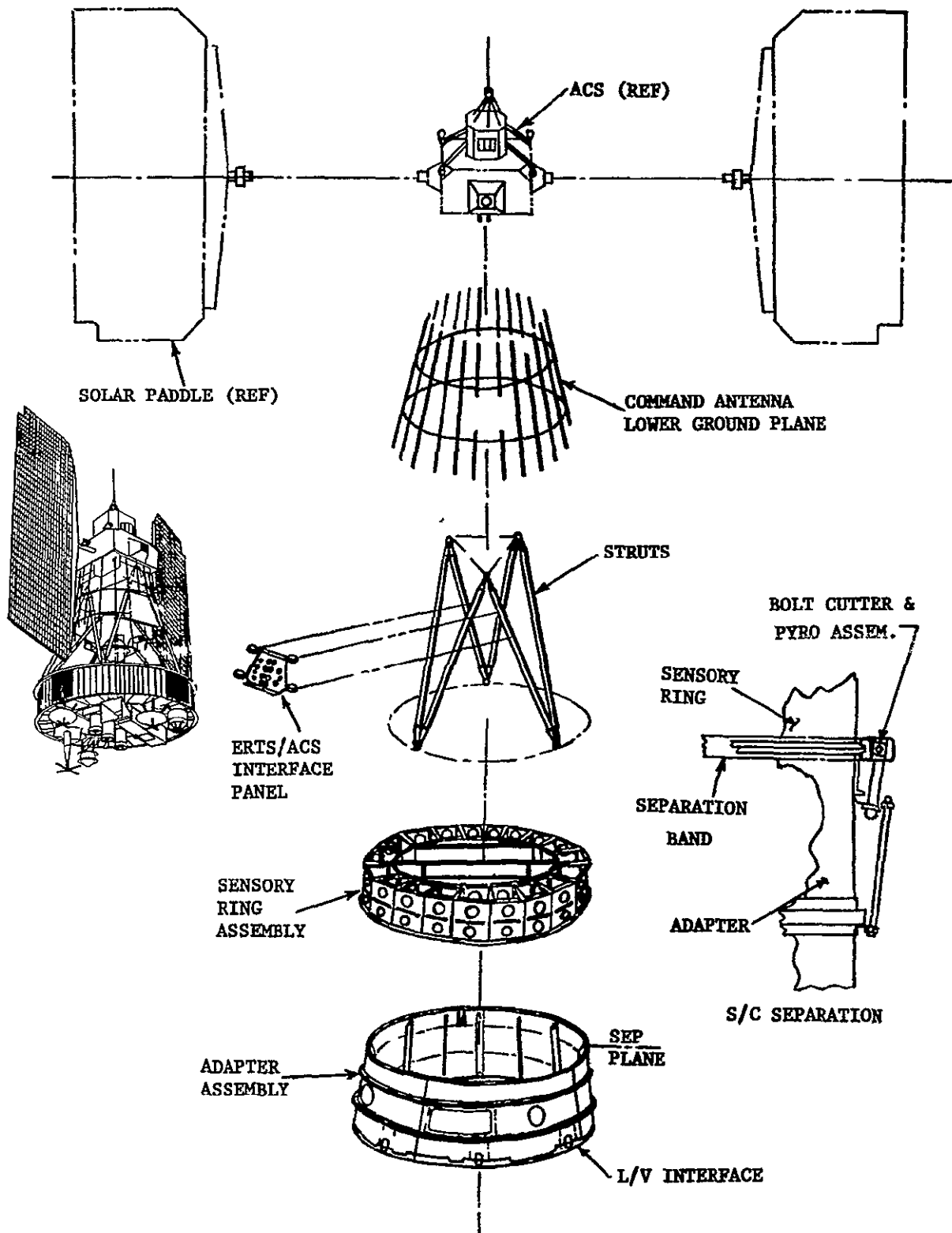


Figure 3.2.5-2. Arrangement and Major Features of the Structural Assemblies and their Function

### 3.2.5.1.3.3 Strut Support

The strut support consists of six tabular assemblies forming a stable framework to support and connect ACS package to the sensory ring assembly. The strut supports provide primary spacecraft structural continuity and provision to permit alignment adjustments of the ACS package to the vehicle axes. In the top spacecraft assembly, the following equipment is attached to the strut supports

1. Lower ground plane for VHF Receiver Antenna
2. ERTS/ACS connector interface panel
3. Electrical Power Subsystem Auxiliary Load Panels
4. ERTS/ACS Connecting Harness and Support

### 3.2.5.1.3.4 Sensory Ring Assembly

The Sensory Ring Assembly is the major element of the ERTS structural subsystem. This assembly supports and accommodates the required payload equipment and most of the supporting spacecraft subsystems.

The Sensory Ring structure will be the basic Nimbus Torus Ring. The Torus Ring structure is the basic structure which forms the 18 sided ring of the spacecraft. The Torus ring structure consists of 18 magnesium alloy separator castings, an upper ring, a lower ring, inner ring channels, and external and internal shear webs. The outboard lower ring is the separation interface with the spacecraft adapter and incorporates a Marmon Band Cross Section. Each equipment bay accepts electronic packages up to 13 inches high x 8 inches deep x 6 inches wide. Placement is achieved by means of evaluating component module size, thermal dissipation requirements and proximity of components that have inter-connecting functions.

The ERTS center cross beam structure will be the same for ERTS A and B vehicles and is unique for ERTS. The cross beam structure accommodates and supports some of the payload and spacecraft support components. One section of the cross beam structure supports the Return Beam Vidicon Cameras (3) on a common mounting. This common mounting plate is provided to achieve alignment between the RBV's of 30 secs before installation into the spacecraft. This structural plate is separate from the other cross beam structures in order to minimize induced spacecraft loads and deflections for maintaining alignment. The major section of the cross beam structure supports the following equipment

1. Wideband Video Tape Recorder (WBVTR) (2)
2. Narrow Band Tape Recorder (NBTR) (2)
3. Solar Paddle Unfold Timer (1)

4. Power Switching Module (1)
5. T/M Conversion Module (1)

The upper plane of the Sensory Ring is utilized to support and accommodate the Orbit Adjust (OA) Subsystem, the Wide Band Video Tape Recorder Electronics (WBVTRE) and the Magnetic Moment Assembly. The OA interface is a simple three point attachment of the mounting feet to pads on the upper plane of the Sensory Ring. The Structures Subsystem provides the support structure for the WBVTRE and the Magnetic Moment Assembly.

The lower plane of the Sensory Ring is utilized to support and accommodate the Multi-Spectral Scanner (MSS), Attitude Measurement Sensor (AMS), UHF-DCS Antenna, Wide Band Antenna (2), and the Unified S-Band Antenna. The support structure has stand-off configurations to provide the proper fields of view for the components. In addition, there is accommodation and interfaces for the thermal insulation for the lower surface of the Sensory Ring, the MSS and the AMS

#### 3.2.5.1.3.5 Adapter

The Adapter Structure provides structural continuity between the spacecraft and the launch vehicle during the launch phase of the mission. It also provides the separation function for the spacecraft. Additionally, the adapter supports and accommodates payload sensor stimulators (RVB and MSS), and antenna pickups and reradiators.

The Adapter is a shell structure with longitudinal stiffeners, and upper and lower closure rings that are machined from forgings to mate with the spacecraft sensory ring and the launch vehicle ring, respectively. Secondary structure is the adapter cross beams necessary to support the payload stimulators.

The separation function is provided by the following hardware

1. Two separation band halves
2. Two pyrotechnic bolt cutters and bolts
3. Marmon Band retaining cables
4. Four separation spring assemblies with guides and brackets
5. Four separation switches and brackets

The spacecraft and adapter are clamped together with the Marmon Band, which is pre-loaded by a force to prevent gapping at the separation plane. Separation springs are provided to produce a nominal zero tumble rate and specified separation velocity. Separation begins with the ignition of the pyrotechnic bolt cutters, which disconnects the Marmon

Band halves. The bands displace from the separation rings, but are retained with the adapter by the retaining cables. Four separation springs provide velocity to separate the spacecraft and the adapter. Four switches monitor the event.

### 3.2.5.2 Communications and Data Handling Subsystem

The Communications and Data Handling Subsystem is composed of the Wide Band Data Link, the Narrow Band Telemetry, Tracking and Command Link and the transmission link for the Data Collection System. With the exceptions of the Wide Band Equipment all equipment in this subsystem is either identical to flight proven equipment or a modification there-of.

#### 3.2.5.2.1 Wide Band Telemetry

The Wide Band Telemetry equipment is designed to transmit the data from the Multi-Spectral Scanner, Return Beam Vidicon Camera and the Wide Band Video Tape Recorders. The characteristics and requirements for the Wide Band Telemetry equipment have been derived from the mission image resolution requirements, the sensor signal characteristics, the available ground equipment as defined in the Design Study Specification S-701-P-3 and the analysis performed during the Phase B/C study. Figure 3.2.5-3 illustrates the Wide Band Telemetry hardware. This equipment interfaces with the ERTS spacecraft payload and the ground stations. The Power, Command and Telemetry interfaces are not shown. The WBVTR Search and Auxiliary Tracks contain low rate PCM data and are routed to the Narrow Band Communications. The subsystem consists of four (4) component types a redundant Signal Conditioner, a redundant Frequency Modulator, two (2) Power Amplifiers and two (2) Shaped Beam Antennas.

##### 3.2.5.2.1.1 Signal Conditioner

The Signal Conditioner interfaces with the payload. It accepts stored and real time signals from the MSS, the RBV, and the two (2) associated wide band video tape recorders. The unit is commanded by the spacecraft command/clock and selects pairs of input lines. The unit conditions the inputs as follows

	<u>15 MBS</u> <u>MSS (PCM)</u>	<u>(3.5 MHZ)</u> <u>RBV (Video)</u>
Impedance Matching	X	X
Digital Reconstruction	X	
Premodulation Filtering	X	X

The selected and conditioned MSS/RBV signals are routed to the Frequency Modulators.

##### 3.2.5.2.1.2 Frequency Modulator

The Frequency Modulator consists of two identical, commandable units. Each unit is capable of operation at either center frequency (2229.5 MHz or 2265.5 MHz) and will accept either MSS or RBV signals. The modulator routes a frequency modulated signal to the two Power Amplifiers. Cross strapping switches are employed at the output lines of both units for redundancy.

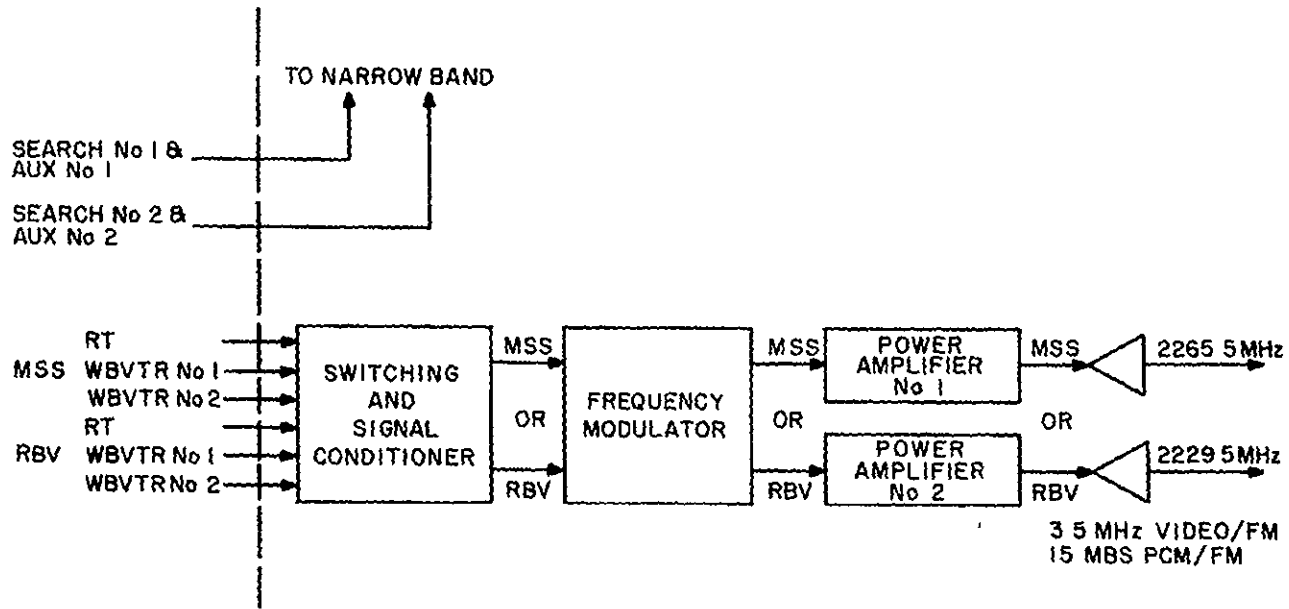


Figure 3.2.5-3. Wide Band Subsystem

### 3.2.5.2.1.3 Power Amplifier

Either of the two separate Power Amplifiers accepts the frequency modulated MSS or RBV inputs on command. The units contain TWT's with commandable (10 and 20 watt) power levels, R. F. band pass filters, a circulator for isolation and individual power supplies.

### 3.2.5.2.1.4 Shaped Beam Antennas

Two identical shaped beam antennas are located on the underside of the spacecraft. A simple, compact turnstile design is used. One antenna is dedicated to P. A No. 1 and the other is dedicated to P. A No. 2. Near constant earth illumination is achieved with a gain  $\geq$  4dB over a cone angle of  $\pm 60.6$  degrees.

### 3.2.5.2.2 Narrow Band Telemetry, Tracking and Command

The Narrow Band Telemetry, Tracking and Command equipment provides the means for collecting and transmitting housekeeping data from the spacecraft to the Ground Net, providing a tracking beacon for the spacecraft, receiving commands from either the MSFN or STADAN Net and implementing those commands aboard the spacecraft. In addition, it provides the link for transmitting data from the Data Collection System to the Ground Net.

Figure 3 2 5-4 illustrates the Narrowband Communications hardware. This equipment interfaces with other spacecraft subsystems and the ground stations. It consists of the items shown exclusive of the DCS receiver and antenna.

#### 3.2.5.2.2.1 PCM Telemetry Processor

The PCM Telemetry Processor samples the output of all the telemetry (housekeeping) sensors on board the spacecraft, it processes the data, and inserts it into a 1 KBPS output stream to be stored on the Narrow Band Digital Tape Recorder or transmitted real time. This unit is identical to the Nimbus D PCM Telemetry Processor.

The processor handles the following inputs

1. Analog and Digital spacecraft telemetry channels.
2. A command/clock generated Clocking Signal and a PWM serial time code.

#### 3.2.5.2.2.2 VHF Transmitter

This unit contains two (2) commandable transmitters each capable of two (2) power levels (300 mw for Real Time data and 1 watt for Play Back Data). The transmitter receives real time 2-phase TLM data from the PCM TLM Processor at a 1 KBS rate or it receives stored 2-Phase TLM data from either of two commandable Narrow Band Tape Recorders. This data phase modulates a 137.86 MHZ carrier in either one of the two transmitters. The transmitters interface with the VHF quadraloop antennas and supply carrier power for Minitrack.

#### 3.2.5.2.2.3 Command Clock

The Command Clock provides an accurate time base for spacecraft operations, generates time codes for transmission or storage, receives, processes and stores command infor-

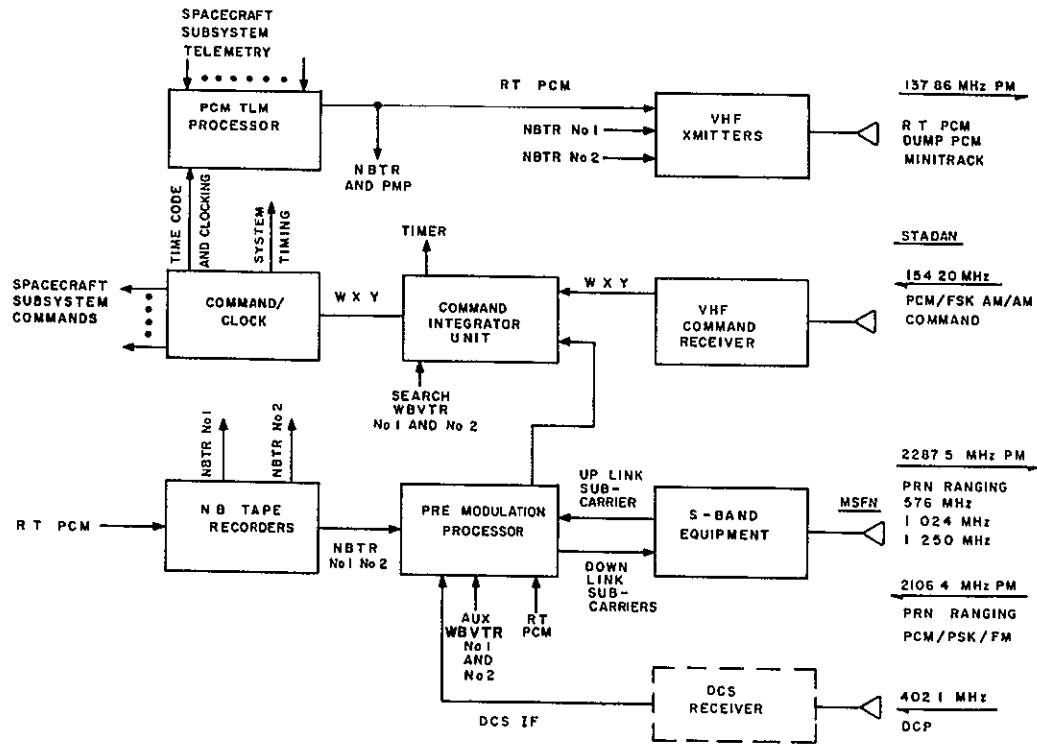


Figure 3.2.5-4. Narrow Band Communications



mation from the Command Integrator and executes these commands at predetermined times. The capability for 30 stored Commands and more than 256 real time digital commands exist within the component. The Command/Clock receives serial PCM data in a compatible format on three lines from the Command Integration unit: NRZ-L Data (w), NRZ-L Sync (x), and NRZ-L Enable (y). It also implements previously stored commands. It contains a command decoder and relay matrix drivers for command implementation. In addition, a self-contained clock generates system timing signals and a Time Code.

#### 3.2.5.2.2.4 Command Integrator Unit

The Command Integrator Unit accepts signals from the VHF Command Link at 128 bps or the USB Command Link at 1 kbps, operates on the signals and provides an acceptable input for the Command Clock. The resulting signal from the USB is sub-bit decoded to yield a 200 bps NRZ-L Data (w) plus Clock (x). An Enable (y) signal is also generated from the presence of the clock signal. This resulting signal is compatible with the clock input.

Provision is made to inhibit commands that are being transmitted from one site while commands are going in via another site. The design is also such that commands from the same site for another spacecraft will not be accepted.

In addition, the command integrator unit contains a back-up timer. This timer is initiated when the system is commanded on for payload operation and will turn off all equipment having the same duty cycle as the payload after 28 minutes. This will back-up the condition when a real time command fails to turn off the equipment after a station pass. In addition it contains a shift register for assembling the serial PCM data from the WBVTR search track.

#### 3.2.5.2.2.5 VHF Command Receiver

The receiver interfaces with the command stub antenna at a 154.20 MHz carrier frequency. The function of the receiver is to convert Commands, received at 128 bps, from the STADAN ground station into intelligence suitable for storage and/or execution. One channel remains on continuously. The receiver consists of two commandable units consisting of a Front end, AGC, and a Demodulator. The Demodulator generates, 1) an Enable (y) based on "presence of subcarrier", 2) a Clock (x) via detection of AM on the carrier, and 3) NRZ-L Data (w) via demodulation of the PCM/FM. The resultant signal (3 separate lines) is outputted to the C.I.U.

#### 3.2.5.2.2.6 Unified S-Band Equipment

The Unified S-Band Equipment consists of a diplexer, hybrid, transponder and mixing amplifiers. Commands are received from the MSFN site through the Unified S-Band Antenna at a 1 KBS rate to the diplexer, hybrid, receiver portion of the transponder. The receiver output goes into a 70 KHZ Discriminator packaged in the Premodulation Processor. Downlink information enters the equipment through a mixing amplifier, an S-Band transmitter, to a diplexer and out through the Antenna. The power output of the transmitter is 2 watts. This equipment is similar to equipment flight proven on Apollo.

### 3.2.5.2.2.7 Premodulation Processor

The PMP comprises a redundant subcarrier modulation and demodulation unit. It contains a 70 KHz FM discriminator for command demodulation and FM subcarrier modulators and pre-modulation filters to handle the following down-link TLM signals

1. Either of two (2) N B. Tape Recorders at 24 KBS
2. One (1) D C S I F at 100 KHz B W
3. One (1) R. T. TLM Channel at 1 KBS
4. Two (2) W. B. V T R Aux TLM Channels at 100 bps

### 3.2.5.2.2.8 Narrow Band Tape Recorders

The Narrow Band Digital Tape Recorder accepts NRZ-L data from the PCM Telemetry Processor at a 1 KBS rate. The data is recorded directly on the tape and played back at a 32 KBS rate. The data can be played back either over the VHF transmitter link or through the USB equipment to the ground net. The unit is similar to those flown on other space programs.

### 3.2.5.2.2.9 Antennas

The Narrow Band antennas have the following characteristics

#### VHF Beacon and Telemetry

Frequency - 137.86 MHz  
Pattern Coverage - Spherical  
Minimum Gain - -10 dB with 3 dB nulls

#### VHF Command

Frequency - 154.2 MHz  
Pattern Coverage - Spherical  
Minimum Gain - 0 dB with 20 dB nulls

#### Unified S-Band

Frequency - 2100 - 2300 MHz  
Pattern Coverage - Hemispherical  
Gain - 0 dB for  $\pm 60$  degree Cone

### 3.2.5.3 ERTS Attitude Control Subsystem (ACS)

The ERTS-ACS is a 3-axis, active control subsystem which maintains the spacecraft alignment with the local earth vertical and orbit velocity vectors. The ACS employs horizon scanners for local vertical roll and pitch attitude sensing, and rate gyros for sensing yaw rate and for use in a gyrocompassing mode to sense yaw attitude. The

11 February 1970

torquing is provided by a combination of reaction jets to provide net momentum control and large control torques when required and flywheels for fine control and residual momentum storage.

The ERTS-ACS is a flexible, long life, highly reliable system having several operational and backup modes. These modes are summarized in Figure 3.2.5-5. The summary discussion of these operational modes is presented in Section 3.2.5.3.3.

The ERTS-ACS consists of the following major elements

- Roll Reaction Wheel Scanner -2 per ACS, provides front and rear IR scanners whose output is proportional to pitch and roll errors. Scan function provided by reaction wheels which also provide momentum exchange.
- Control Logic Box - contains control electronics for the ACS functions as well as mode selection and switching.
- Yaw Gyrocompass -2 per ACS (redundant) serves as the primary yaw sensor providing an output proportional to yaw error and rate.
- Pitch and Yaw Reaction Wheels - provide momentum exchange about the pitch and yaw axes respectively.
- Pneumatics - provides high-torque reaction and wheel unloading
- Yaw Rate Gyro - used only during acquisition, senses yaw rate for improved yaw damping
- Solar Array Drive - provides controlled motion of the solar array to maintain solar array illumination
- Magnetic Moment Assembly - commandable magnetic dipole about pitch, roll and yaw to cancel spacecraft magnetic dipole
- Attitude Sensor - precise attitude measurement (0.1 degree) for use in image location

Back-up Modes  
Element Condition Shown Representative of Normal Mode

Control Loop	Control Loop Elements	Launch Mode	Acquisition Mode	Normal Mode	Orbit Adjust Mode	Gyrocompass Backup	Pitch Momentum Bias	IR Scanner Failure	MMA Unload	
Pitch	IR Scanners	Off	X	X	X	X	X	Switch in Pseudo Earth Pulse in Place of Failed Scanner	X	
	Control Electronics	Off	X	X	X	X	X	X	X	
	Reaction Wheel Pneumatics	Off	X	X	X	X	X+1100 RPM X(Unload)	X	X	
Roll	IR Scanners	Off	X	X	X	X	X	Switch Off Failed Scanner	X	
	Control Electronics	Off	X	X	X	X	X		X	X
	Reaction Wheel Pneumatics	Wheel Running	X	X	X	X	X		X	X
		Off	X	X(Unload)	X	X(Unload)	X(Unload)		X(Unload)	Off
Yaw	Yaw Gyrocompass No. 1	On	X	X	X	Off	Off	X	X	
	Yaw Gyrocompass No. 2	On	Off	Off	Off	X	Off	Off	Off	
	Yaw Rate Gyro	On	X	Off	On-Output Disabled	Off	Off	Off	Off	
	Control Electronics	Off	X	X	X	X	Off	X	X	
	Reaction Wheel Pneumatics	Off	X	X	Off	X	Off	X	X	
		Off	X	X	Off	X	Off	Off	Off	
Solar Array Drive (2)	Sun Sensor	↑ Off ↓	X	X	X	Each Paddle Driven Independently				
	Control Electronics		X	X	X					
	Servo Motor		X	X	X					
	Potentiometer (Position Readout Only)		X	X	X					
	Tachometer		X	X	X					

Figure 3.2, 5-5. ERTS - ACS Control Modes

The design of the ACS relies on the Nimbus designs. The components are similar to Nimbus except for the Magnetic Moment Assembly and the Attitude Sensor.

The proposed ACS is a self-contained, major spacecraft subassembly, which is assembled and thoroughly tested as a subsystem prior to mating with the spacecraft. Figure 3.2.5-6 is a photograph of the Nimbus Attitude Control Module having completed test and ready for integration into the spacecraft. The controls subsystem module has the shape of a square parallelepiped. Solar paddles for power generation are attached to shafts which emanate from opposing faces of this parallel piped, the shaft being driven by the solar array drive motors.

#### 3.2.5.3.1 Requirements - Summary

The ERTS mission requires that instrumentation aboard the spacecraft be able to measure spacecraft accuracy compatible with locating any point in a 100 x 100 nautical mile photograph to within 2 nautical miles.

- The ACS is required to maintain the alignment of the ERTS Spacecraft body axes to the local earth-vertical orbit-velocity orientation of the orbital reference axes to within 0.7 degree for each of the three body axes, with the instantaneous angular rates about the satellites body axes to be less than 0.04 degree per second, with a goal of less than 0.015 deg/sec. An analysis of these NASA requirements, in conjunction with the attitude control capabilities, led to the following attitude control performance requirements.
- Provide an Attitude Sensor with  $\pm 0.1$  degree pitch and roll measurement accuracy.
- Acquisition of the reference orientation from an initial orientation, and with angular rates of up to 2 deg/sec about each axis.
- Independent, single-axis rotation of the solar array paddles for sun-tracking to within  $\pm 10$  degrees of the pitch axis-sun line plane.
- Provide three axes stabilization during orbit adjust maneuver with accuracies of less than  $\pm 6$  degrees for pitch and roll and  $\pm 10$  degrees in yaw considering a 600 sec OA engine on-time. For longer OA engine on times, the pitch and roll accuracies remain the same, and the yaw error increases at a rate of 0.01 deg/sec.
- Reacquisition of the reference orientation from the same angular rates specified for acquisition and from any attitude should some disturbance temporarily interrupt the attitude stabilization. The ERTS-ACS shall provide this capability a minimum of four times.

#### 3.2.5.3.2 ERTS-ACS Description

The ERTS-ACS employs two infrared horizon scanners to provide pitch and roll attitude error sensing. The conical scan axes for the two scanner units are aligned parallel to the

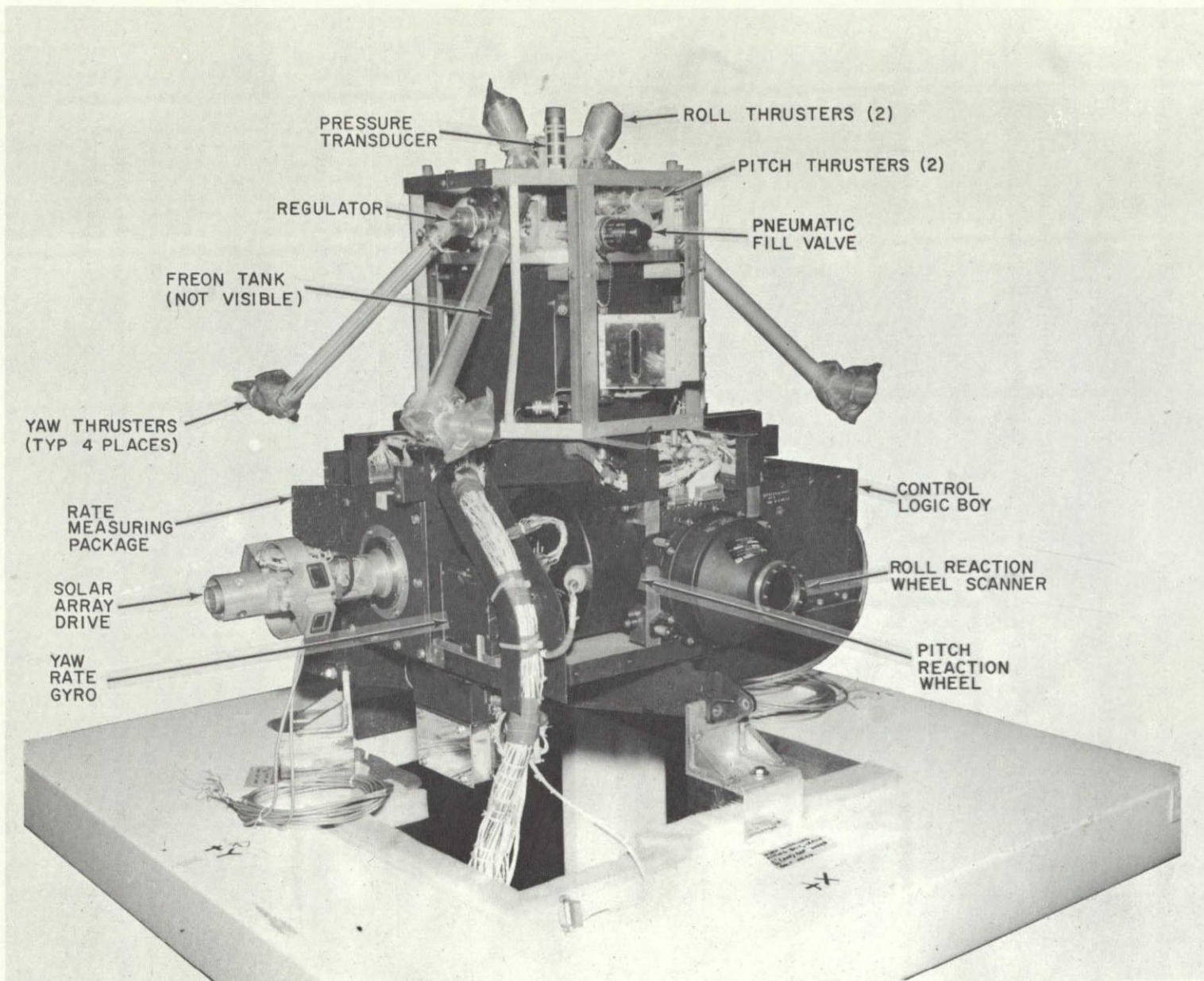


Figure 3.2.5-6. Nimbus Attitude Control Module

roll axis, one directed forward and one aft. The scanning motion is provided by the roll reaction wheels to which prisms are attached. A minimum scan speed (600 rpm) is maintained for each of the two wheels, which are rotated in opposite directions so that the net angular momentum along the roll axis is nominally zero. Roll momentum control is provided by speed variation of the wheels relative to each other. Figure 3.2.5-7 is the ACS block diagram.

The yaw channel error signals are derived from two sources, a yaw axis rate gyro or yaw gyrocompasses, determined by the commanded control mode. The various yaw control loop mechanizations provide for yaw rate damping as well as yaw attitude control.

Initial alignment of the pitch, roll and yaw spacecraft body axes to the reference orbital frame is effected by the use of the 3-axis, pneumatics-reaction wheel torquing subsystem. Acquisition about each of the three body axes occurs when the reaction wheels "capture" spacecraft control from the pneumatic jet torquers, reducing gas expenditure thereafter to periodic unloading of any momentum build-up in the reaction wheels.

The pitch and roll attitude control loop functions are identical for both the acquisition, orbit adjust, and normal orbit control modes. The yaw control loop, however, can be commanded to operate somewhat differently in the various modes, in order to achieve the required control. During the initial acquisition maneuvers, rate errors signals from the yaw axis rate gyro are fed directly to the pneumatics for corrective control action, while the yaw gyrocompass error signals are channeled to the yaw reaction wheel. The gyrocompass consists of a rate-integrating gyro, and gyro control electronics and is operated in a rate mode. It is mounted with its input axis in the roll-yaw plane tilted up 45 degrees from the positive roll axis towards the negative yaw axis. Its output signal contains components proportional to yaw attitude and rate as well as roll attitude and rate. Once the yaw reaction wheel is controlled by the gyrocompass attitude rate switching line, the yaw axis rate gyro and yaw pneumatics is disabled by command. Further yaw reaction wheel unloading is accomplished through the use of roll axis momentum unloading. During orbit adjust, the gyrocompass output is channeled directly to the yaw pneumatics in order to provide sufficient torque and rate limiting during this mode, and the yaw axis rate gyro is disabled.

The circuits used to control the pneumatic thrusters and reaction wheel drivers, provide as output, a constant amplitude pulse train whose duty cycle is proportional to the input error signal. Each circuit has a threshold, below which no output occurs, and a full on level, above which the device is saturated. No output corresponds to a zero duty cycle while saturation corresponds to a 100% duty cycle. This arrangement provides most of the benefits of proportional control while using simple on-off control elements.

### 3.2.5.3.3 ACS Control Modes - Summary

#### 3.2.5.3.3.1 Launch

During the launch and orbit injection phase, all pneumatic pulse modulators, pitch and yaw wheel pulse modulators, the fine roll error signal (that error signal being fed to the roll wheels), and the solar array drive control loop are inhibited.

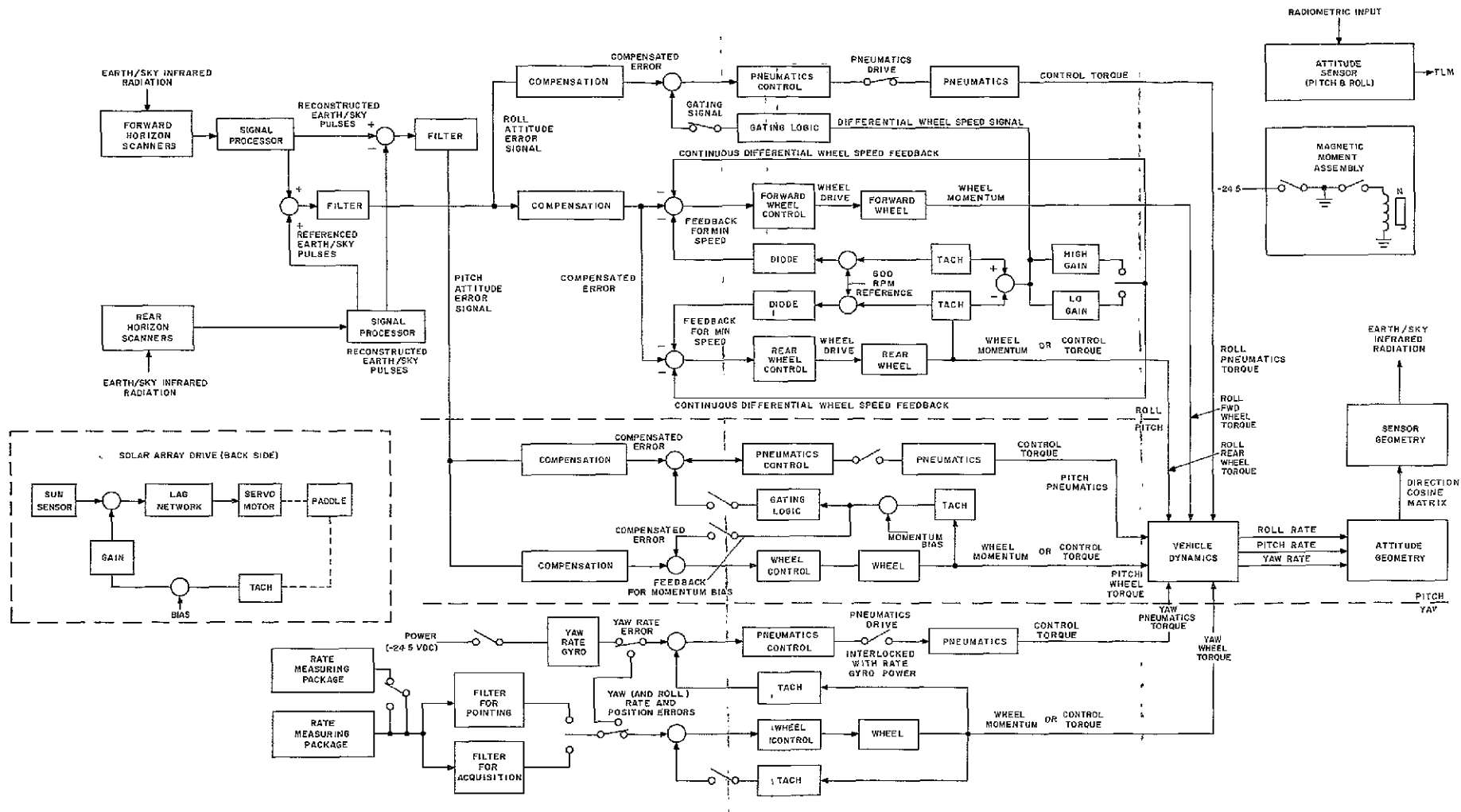


Figure 3 2 5-7 ERTS-ACS Block Diagram



The gyros are powered and the scanners are running at 600 rpm, during this phase of operation.

#### 3.2.5.3.3.2 Acquisition

Following orbit injection, the ACS is required to acquire the reference earth-vertical orbit-velocity orientation from any initial spacecraft orientation.

Following separation and time out of the 15 second timer, the inhibited elements of the ACS are enabled. Pitch and roll attitude error signals are provided by the IR horizon scanners, while yaw axis rate gyro and yaw gyrocompass provide yaw axis rate and attitude error signals.

The ACS, in this configuration, can acquire from any attitude with initial angular rates about any or all body axes up to 2 degree/sec. The presence of the yaw axis rate gyro in the yaw control loop assures that any initial yaw angular rates will be quickly reduced, since the yaw pneumatics will be activated for yaw rates greater than 0.1 degree per second.

The control laws are designed such that once the pitch, roll and yaw errors have been reduced to below the pneumatic modulator threshold levels, torquing control will gradually and smoothly be transferred to the reaction wheel system. This transfer occurs automatically and is referred to as wheel capture.

#### 3.2.5.3.3.6 Back Up Modes - Summary

The ERTS-ACS possesses several, inherent, back up modes, which enhance its high reliability and long life capability.

- The yaw gyrocompass is block redundant.
- Capability is provided to switch out either of the IR Horizon Scanners and simultaneously supply a "pseudo earth pulse" to the pitch Horizon Attitude Computer. In this mode, the ACS will continue to function within requirements.
- The Magnetic Moment Assembly can unload wheel momentum in the event of pneumatic loss.
- The system can be switched to the orbit adjust mode to compensate for a yaw wheel failure.
- The Pitch Momentum Bias mode provides for a back up of the total yaw control loop.

#### 3.2.5.3.3.3 Normal

The ACS provides automatic transition from the acquisition mode to the normal orbit operation in pitch and roll without the requirement of orbit adjust commands. The mechanization of the yaw control loop includes both an acquisition orbit adjust and a normal mode.

The normal mode control in yaw provides tighter yaw control than is possible while the ACS is subjected to acquisition constraints. Yaw momentum build up is removed by the roll pneumatics and yaw attitude and rate sensing is provided by the yaw gyrocompass, the yaw axis rate gyro and yaw pneumatics are turned off (by a single command) after wheel capture has occurred

#### 3.2.5.3.3.4 Orbit Adjust

During this mode, disturbances to the ACS are caused as a result of mis-alignment of the orbit adjust engine thrust vector relative to the spacecraft center of mass. The pitch and roll control axes will function in their normal mode, and will go automatically to pneumatic control. The yaw axis will be commanded to the orbit adjust mode, in which the output of the yaw gyrocompass is switched (acquisition) to the yaw pneumatics, and the yaw axis rate gyro output is disabled. Upon completion of the orbit adjust, the yaw axis is commanded to the acquisition mode and then to the normal mode.

- In a low voltage condition, the pneumatic solenoid supply voltage is automatically turned off, placing the ACS in a "wheels only" operating state. This insures that spurious pneumatic operation will not occur during a low voltage condition

#### 3.2.5.3.3.5 Solar Array Control Loop

The solar array control loops independently drive the two solar paddles which provides accurate paddle illumination and inherent redundancy. Sun sensors provide closed-loop tracking of the sun during sunlit portions of the orbit.

A geared ac servomotor is the primary drive mechanism for each solar paddle. A constant nominal rate command ( $\omega_P$ ) of 3.33 deg/min is provided at all times, subject to override by the sun sensor error signal when the sun is in view. The measured paddle rate is compared with the commanded rate, and the rate error signal is amplified by a relative angle-rate gain. The resulting equivalent angle error signal is summed with the output of the sun sensor.

#### 3.2.5.4 Orbit Adjust Subsystem Design Summary

The Orbit Adjust Subsystem is shown schematically on Figure 3.2.5-8 and in assembled form on Figure 3.2.5-9 and 3.2.5-10. It is a single module for ease of integration into the ERTS spacecraft.

The propellant and nitrogen gas pressurant are stored in a single tank, separated by a positive expulsion bladder. Two manually operated fill valves are provided for pressurant and propellant loading and unloading. Immediately downstream of the propellant fill valve are two paralleled normally closed explosively actuated valves. Operation of either of these valves arms the subsystem after launch. Just beyond this point in the propellant line is a third manually operated valve. This valve is used as a test port for functional checks of the downstream portion of the subsystem without operating the normally closed explosive valves. All three manually operated fill and test valves are capped after closing to minimize the possibility of leaks. The propellant is filtered through a 25 micron absolute filter in the manifold. In addition, there are pressurant valve inlet filters of the same 25 micron size.

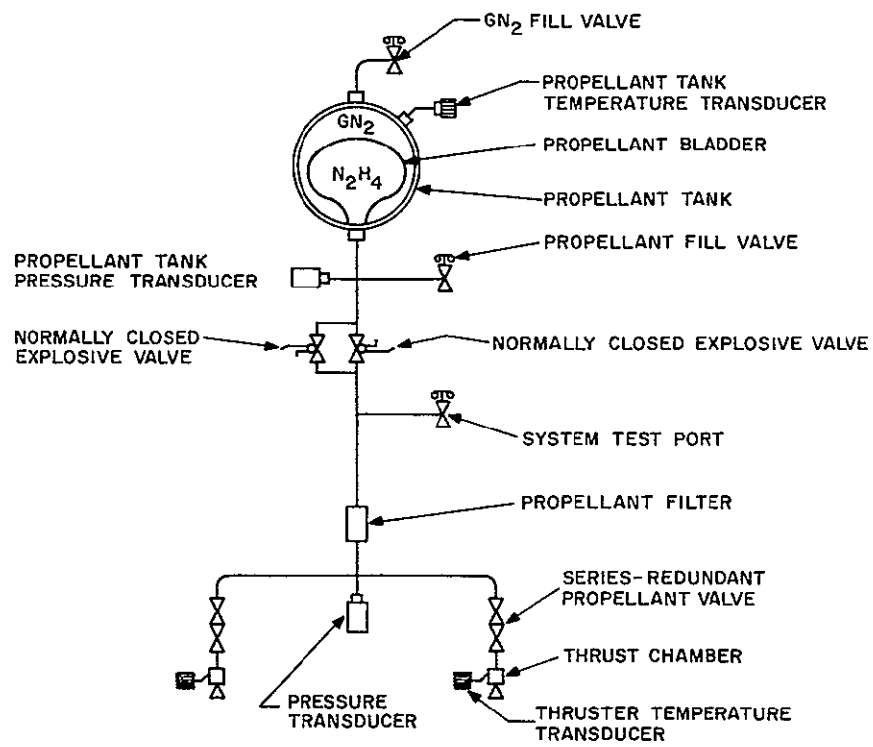


Figure 3.2.5-8. Orbit Adjust Subsystem - Schematic

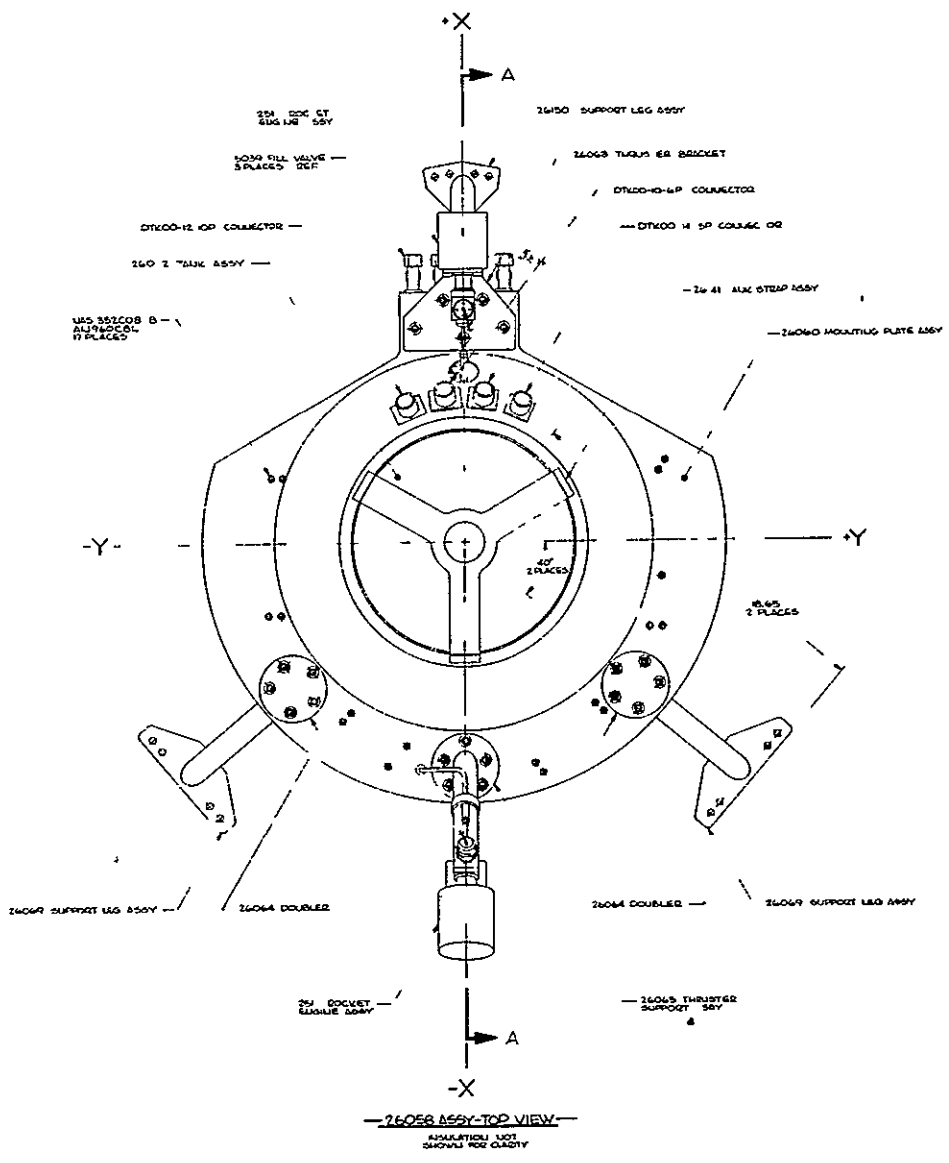


Figure 3.2.5-9. Orbit Adjust Subsystem - Assembled Top View



These valves are solenoid operated and series redundant. They consist of two complete valves assembled in a common housing. Operation of the solenoid valves by an electrical command fires the thruster assemblies. With the temperature of the subsystem at a nominal 70°F, the initial thrust is nominally 0.870 pounds force, decaying to 0.568 pounds force as the propellant is consumed from the storage tank. Subsystem instrumentation includes two pressure transducers to monitor propellant tank pressure and propellant manifold pressure and temperature transducers mounted on the external surface of the tank and on each of the thruster catalyst chambers. A "cocoon" of insulation is used around the subsystem module to maintain acceptable temperature limits (4°C to 49°C) in the worst case orbit plus firing duty cycle conditions. This insulation covers all but the mounting feet, thrusters, and bottom of the module.

Thruster identification and spacecraft axes definition are shown on Figure 3.2.5-11. The subsystem is mounted in the spacecraft so that the thrusters are located on the -x and x roll axis. The modular design of the subsystem readily enables alignment of the thruster axis to within a 0.100 inch radius sphere about the measured CM of the spacecraft. One thruster is canted upwards at an angle of approximately 20° so that its exhaust plume will not impinge upon the spacecraft struts and the paddle latch mechanism. Because of subsystem is designed as a module, it can be readily subjected to testing prior to installation on the spacecraft. This all-brazed propellant feed system minimizes leaks and heavy connecting fittings. The total subsystem weight is 31.7 pounds fully fueled with 10.1 pounds of hydrazine. The hydrazine thrusters of the subsystem are designed for and have been tested for operational firing modes ranging from 1.0 to 0.1 pounds force thrust for pulses varying from 1 second to 8 hours. Thrusters of this design have accumulated as much as 114 hours of burn time under vacuum conditions. The operational requirements for the Orbit Adjust Subsystem at an average thrust level of 0.75 pounds force include firings for durations as long as 18 minutes. Firings for drag makeup, however, will be as short as 12 seconds.

All components of the Orbit Adjust Subsystem were selected to take advantage of previously documented experience with components which satisfy the subsystem requirements. Extensive qualification testing is not required. A component matrix is shown on Table 3.2.5-1. The propellant tank, supplied by Pressure Systems, Inc. has undergone extensive qualifications for Mariner Mars '69 flight. Some redesign of the propellant tank is required to accommodate the higher operating pressures required for the ERTS Orbit Adjust Subsystem. This redesign will be verified by additional qualification testing. In addition, the bladder material will be replaced with ethylene-propylene, although the same design, and fabrication techniques will be used. The propellant solenoid valve, manufactured by the Panther-Hannefin Corp. are of a soft seat, Belleville actuation solenoid design. The explosively actuated valves are a normally closed design wherein the squib exhaust gases push a piston which shears a tube, pushing the sheared section clear of the flow path. The propellant filter is manufactured by Vacco Valve Company. The filter is a stocked, etched disc type. The pressure transducers, manufactured by the Instrument Systems Division of the Whittaker Corporation, are a bonded strain gage type. The temperature transducer selected to monitor the subsystem temperature is also manufactured by the Whittaker Corporation and uses a platinum resistance thermometer and a central signal conditioning unit.

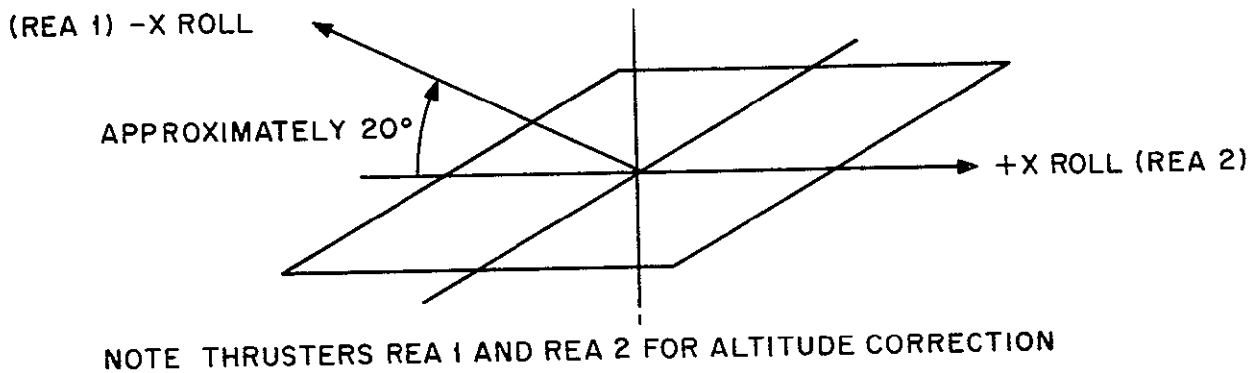
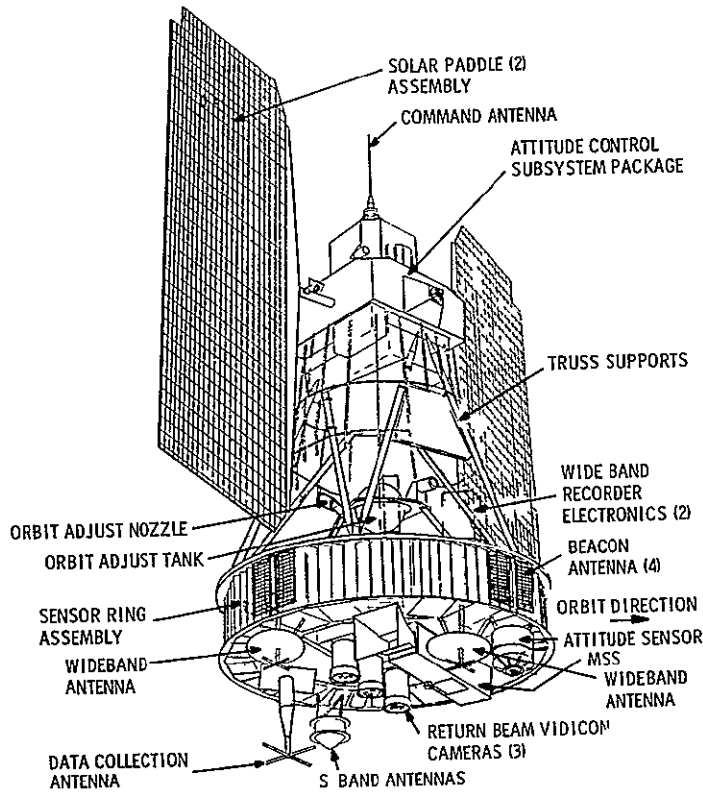


Figure 3.2.5-11. Thruster Identification and Spacecraft Axes

Table 3 2 5-1 Components Matrix

Component	Qty	Vendor	Previous Use (Qualification)
Propellant tank	1	Pressure Systems, Inc.	Mariner '64, '69
Thruster	2	Rocket Research Corp.	
NC explosive valve	2	Pyronetics, Inc.	
Fill and test valve	3	Rocket Research Corp.	
Filter	1	Vacco Valve Co.	Classified Program
Pressure transducer	1	Whittaker Corp., Instrument Systems Division	
Temperature transducer	3	Whittaker Corp., Instrument Systems Division	
Propellant valve	2	Parker - Hannecm Corp.	

In summarizing its performance capabilities, the Orbit Adjust Subsystem is designed to operate in a blowdown mode, resulting in a decreasing level of thrust during the one year spacecraft life. As orbit adjustments are performed, propellant is consumed, and the pressure drops, resulting in decreased thrust. The mission requires 2169 pound-seconds total impulse. Figure 3.2.5-12 shows that with the subsystem at 70°F, the thrust will decrease from 0.870 pounds force to 0.568 pounds force

#### 3.2.5.5 Thermal Subsystem Description Summary

The ERTS thermal control subsystem is required to maintain the temperature of the payload environment to  $20^{\circ} \pm 10^{\circ}\text{C}$ , and the temperature of the attitude control subsystem component mounting structure to  $25^{\circ} \pm 10^{\circ}\text{C}$ . Temperature control is accomplished by different means in each of the four major regions of the spacecraft, utilizing a combination of thermally actuated shutters, low duty cycle compensation electric heaters, radiator plates, thermal radiation and rigid conductor coupling, multilayer insulation, thermal coatings, and mass thermal capacity.

##### 3.2.5.5.1 Sensory Ring

Figure 3.2.5-13 shows the plan form of the sensory ring and lists the components included in its 18 equipment bays. Heat from this equipment is conducted to the periphery of the ring, where it is radiated from the spacecraft through shutters that are opened or closed according to the temperature of the bay. Multilayer insulation covers the top and bottom of the ring to isolate it from the external environment and channel the component heat to the shutter regulated radiating surfaces. These radiating surfaces are coated with white paint



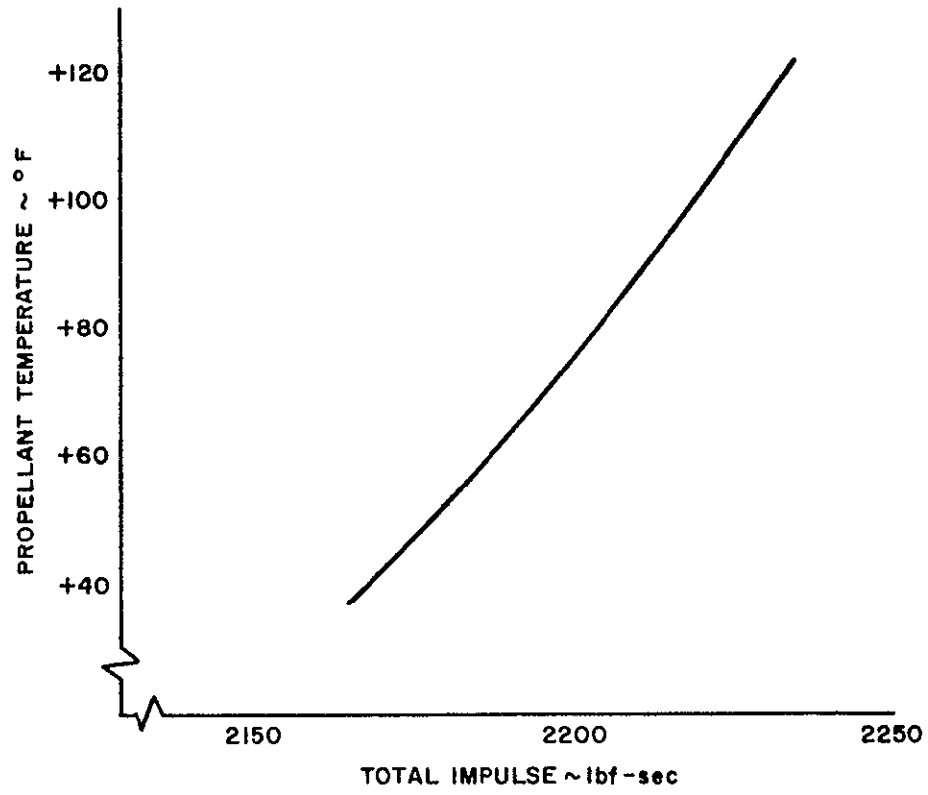


Figure 3. 2. 5-12. . System Operating Characteristics

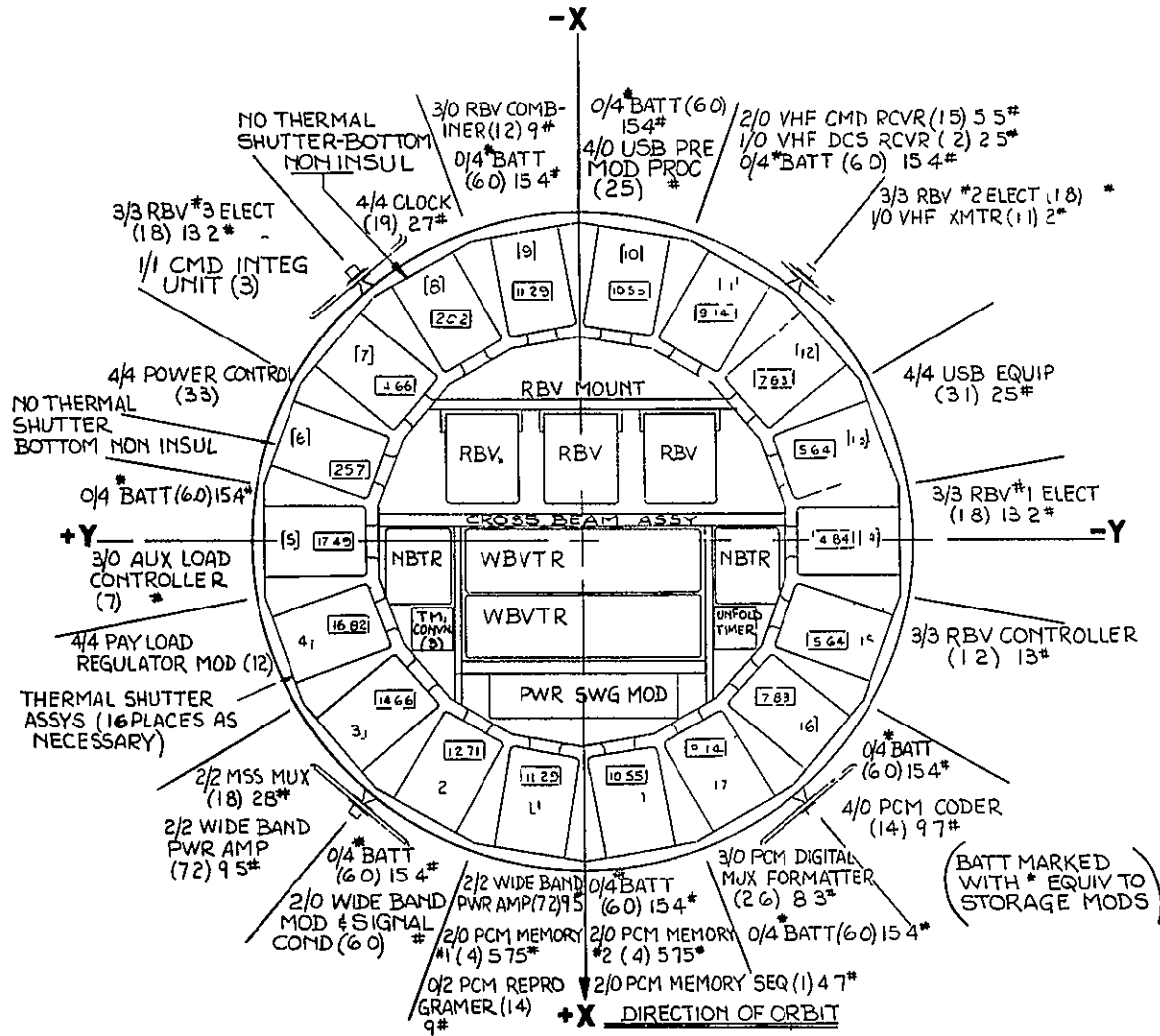


Figure 3.2.5-13. Sensory Ring

( $\alpha_s \leq 0.2$ ,  $\epsilon \geq 0.85$ ) to maximize IR heat rejection and minimize solar and albedo heat absorption. During low duty cycle periods when component heat may not be sufficient to maintain minimum temperature with closed shutters, electric heaters are activated by command to supplement the heat balance.

#### 3.2.5.5.2 Sensory Ring Center Section

Figure 3.2.5-14 shows that the Multi-Spectral Scanner and Return Beam Vidicon Cameras are mounted on the structural beams of the sensory ring center section. These beams also support the Wideband Video Tape Recorders, the Narrow Band Tape Recorders, and several other components. The heat dissipated by this equipment is radiated away, from the MSS directly, from the cavity surrounding the RBVs, from the radiator plate attached to the structure at the +X side of the MSS instrument mount, and through the insulation that covers the top of the center section. The heat dissipated by this equipment varies from an orbit average of 87.8 watts during an orbit with 25.8 minutes of payload operation, to an average of 11.2 watts during an orbit with no payload operation.

Temperature control of these center section components is accomplished by sizing the radiating areas to reject a carefully selected orbit average heat load, using insulation over the components to restrict other heat flow paths. Compensation heaters supply auxiliary heat and thereby prevent component subcooling below 10°C during those low duty cycle orbits when the component heat dissipation is below the radiation heat rejection capability. The radiating areas are chosen so that the component mounting interface temperature will not exceed 30°C for the worst case series of high duty cycle orbits, considering both radiation heat rejection and component mass heat capacity. Components mounted in the center section will be coated with black paint ( $\epsilon = 0.9$ ) to maximize radiation exchange, and the external radiator plate will be coated with white paint ( $\alpha_s = 0.2$ ,  $\epsilon = 0.85$ ) to provide high radiating capacity and minimize solar absorption. Silver filled silicone grease will be used to prevent high thermal path resistance in the vacuum environment at all attachment connections.

The orbit adjust subsystem is mounted over the center section. It is covered by the center section top insulation blanket and maintained above its minimum allowable temperature of 4.5° by radiation and conduction from the center section equipment and the sensory ring structure. The thrusters are exposed, but are raised to satisfactory pre-operation temperature by built in 1.5 watt heaters.

#### 3.2.5.5.3 Above Sensory Ring

Figure 3.2.5-15 shows the location of the wideband video tape recorder electronics boxes. These packages are insulated and radiate their heat through windows cut in the insulation blankets. The insulation on the sides of the boxes is faired into the top insulation of the sensory ring so that radiation can freely exchange between the bottom of the boxes and the ring. Black paint is used on these internal radiating surfaces, and white paint is used on the exposed box windows. The orbit average heat load can vary from 11 watts to 0. The window area is sized (40 square inches per box) so that the net heat rejection, after accounting for solar, albedo, and earth fluxes, is sufficient to prevent the box from exceeding 30°C during the worst case series of orbits, when accounting for both duty cycle timing and component mass heat capacity. 3.5 watts compensation heat per box is required to prevent these components from cooling below 10°C during orbits when the recorders are not operated.

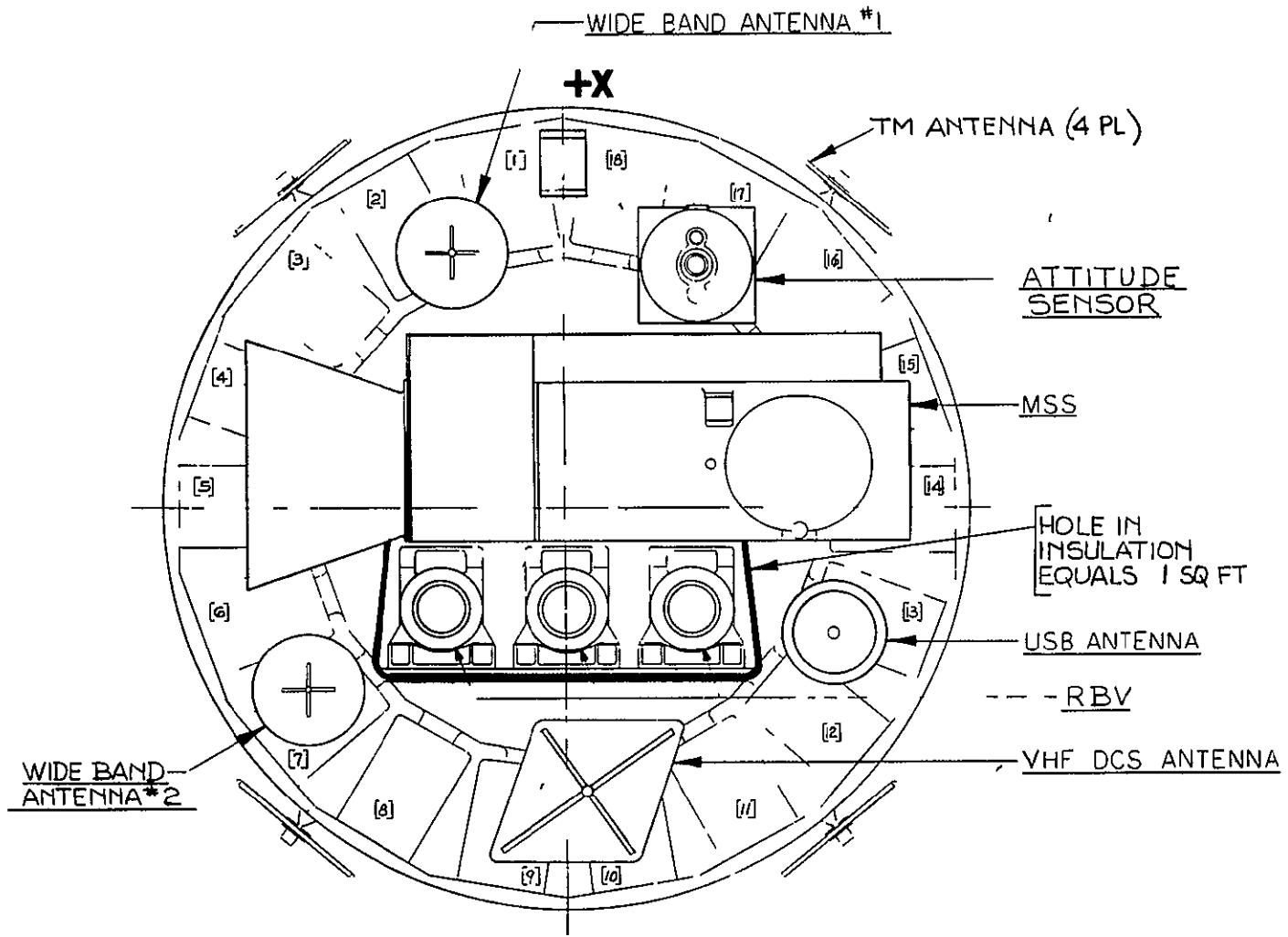


Figure 3.2.5-14. Sensory Ring Center Section

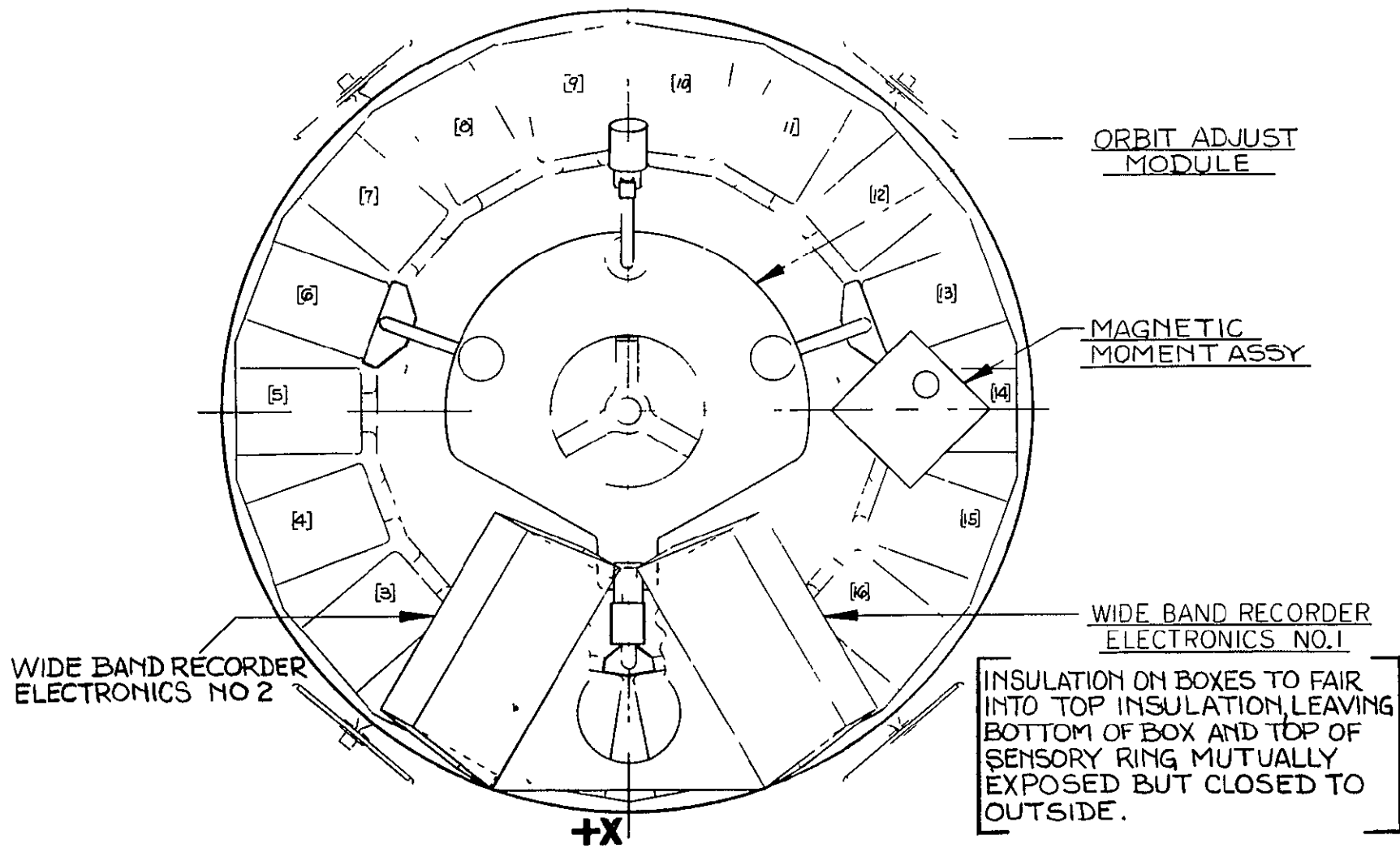


Figure 3.2.5-15. Top View, Sensory Subsystem

#### 3.2.5.5.4 Attitude Control System

The attitude control system is a separate and distinct structural assembly located above the Sensory Subsystem and attached to it by six (6) structural tubes. The ACS also provides support to and actuation of the solar arrays. ACS thermal control for ERTS is the same as for Nimbus D. This system is designed to accommodate a wide range of orbit Beta ( $\beta$ ) angles. Temperature of the ACS is provided by passive and semi-passive techniques, similar to the sensory ring. A unique aspect of the ACS thermal design is the enclosed shutter assembly. The shutter assembly is located between the equipment mounting deck and a dust cover/heat sink as shown previously in Figure 3.2.5-14. This dust cover, suspended from the lower surface of the ACS, is painted black on the inside and white on the outside.

The white paint on the outside causes the dust cover to operate at low temperatures. The low temperature and black paint on the inside provide an adequate heat sink for the components mounted above, which radiate to the cover through the shutter blades.

Parametric analyses performed by the subsystem contractor and extended by GE for ERTS show that temperature control to  $25 \pm 10^\circ\text{C}$  can be maintained in the 37 degree Beta angle orbit. Average temperatures will be about  $5^\circ\text{C}$  higher (to  $26^\circ\text{C}$ ) than for the  $0^\circ\beta$  angle operation with Nimbus. This extension includes the small radiation blockage effect of the WBRE boxes mounted on top of the sensory ring.

#### 3.2.5.6 Power Subsystem

The power subsystem provides the electrical power required to operate the spacecraft and its subsystems from transfer to internal power prior to launch through the one year design point. The subsystem is comprised of the following components listed in Table 3.2.5-2.

The solar array/battery system provides power through a regulated bus to sustain orbital operations. The battery complement provides sufficient energy to support the spacecraft during launch, ascent and acquisition phases prior to deployment of the solar array. A block diagram of the subsystem is shown in Figure 3.2.5-16 and the component characteristics are summarized in Table 3.2.5-2. The deployment mechanism is included as part of the structure subsystem and the solar array drive is considered as part of the Attitude Control Subsystem. The total weight of the power subsystem, as defined above, is 254 pounds.

##### 3.2.5.6.1 Functional Description

During the launch sequence, the solar arrays are in the stowed position and the batteries deliver power to the unregulated bus through the Power Control module. Upon separation of the adapter from the spacecraft, relays are energized in the Unfold Timer which causes the paddle unfold pyros to fire at predetermined intervals. When the cables are cut the unfold motor is started, deploying the solar arrays. They then begin tracking the sun, with its acquisition, the solar array assumes the power generating function for the spacecraft.

During sunlight periods the solar array delivers power to the unregulated bus in the Power Control Module at a voltage of from about -30 to -39 volts. The lower limit is set by the battery discharge voltage as -30 volts is approached load sharing occurs and the batteries begin to discharge. A

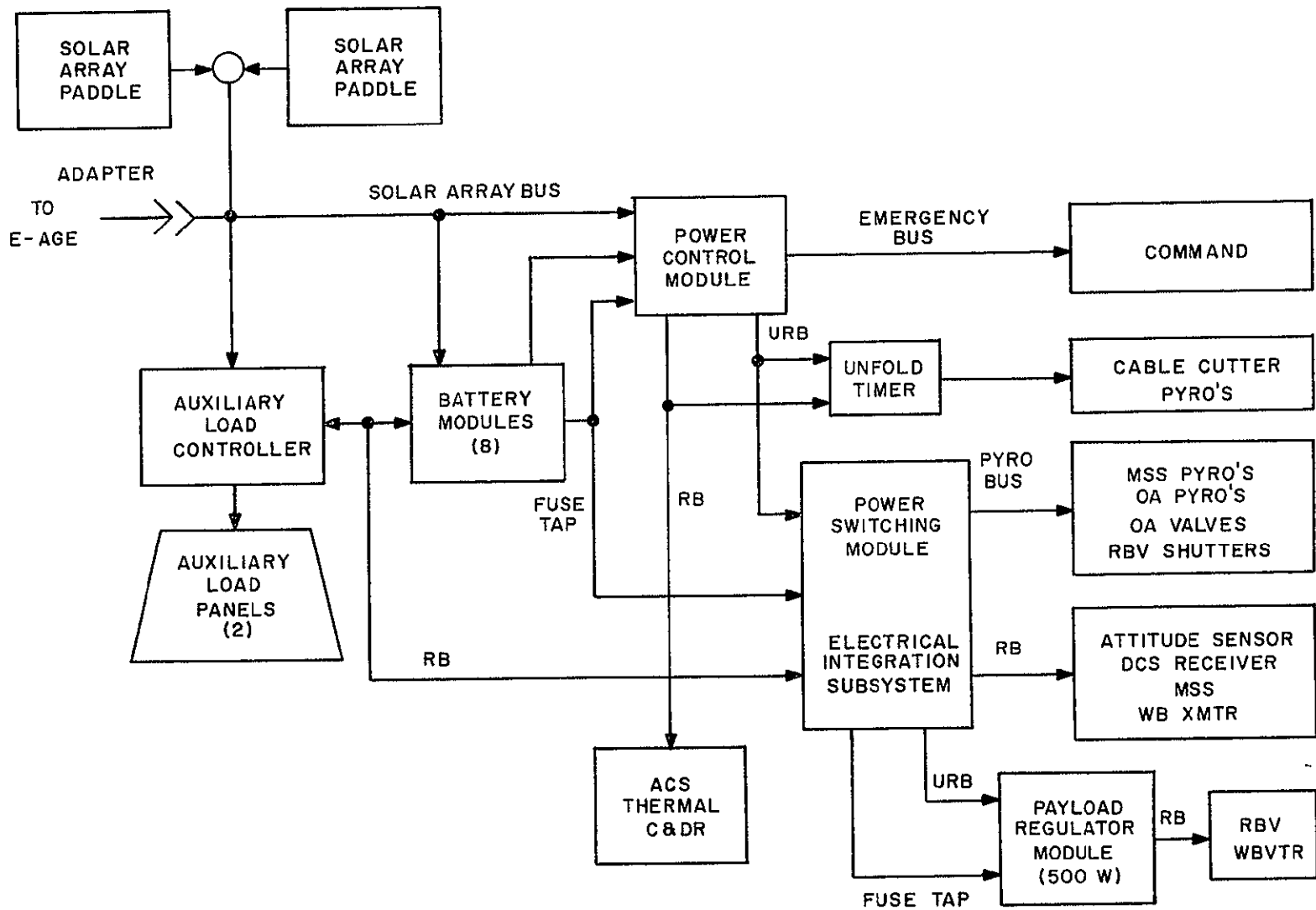


Figure 3.2.5-16. Block Diagram, ERTS Power Subsystem

Table 3 2 5-2 Power Subsystem Components

Item	Need Modification	Weight Pounds Each	Dimensions Each	Max Power Dissipated Watts	Make/buy	Comments
Solar Paddle (2)	No	36.4	38 4" X 96" (25 ft <sup>2</sup> )	-	RCA	Same as Nimbus D/E
Battery Modules (8)	No	15.5	0/4	7.6	RCA	Same as Nimbus D/E
Power Control Module (1)	No	21.3	4/4	41	RCA	Same as Nimbus D/E
Aux Load Controller (1)	No	6.0	3 0	0.6	Make	Same as Nimbus D/E
Aux Load Panel (2)	No	5.0	10" (top) X 15 X 1 3/4 16" (bottom)	200	Make	Same as Nimbus D/E
Unfold Timer (1)	No	3.5	6 3/4" X 5 1/2" X 3 1/4"	-	Make	Same as Nimbus D/E
Payload Regulator Module (1)	No	21.3	4/4	41	RCA	Same as Power Control Module
<b>Total</b>		<b>253.9</b>				



approached load sharing occurs and the batteries begin to discharge. Above -39 volts voltage limiters, located in each of the battery modules, automatically shunt excessive current from the solar array bus up to a maximum of 12 amperes. Additional power management functions are carried out by the commandable auxiliary load controller which causes power to be drained from the solar array bus to one of the auxiliary load panels. These auxiliary loads are generally required only when normal spacecraft loads are very light, solar array output is high, and it is desired to reduce the power dissipated in the battery modules through the shunt resistors.

In addition to battery cells and shunt elements the battery modules contain the charge control electronics, a battery on/off relay and a 15 cell tap for providing large surges of current directly to the regulated bus in case of emergencies.

The power control module contains two redundant pulse width modulated regulators which supply the -24.5 volt regulated bus, two redundant auxiliary regulators supplying a -23.5 volt bus, a trickle charge override switch to override the trickle charge on the battery modules, 8 battery isolation diodes, a regulated bus comparator, the shunt dissipation driver, and fuse blow inputs for the 15 cell battery tap.

The power control module feeds regulated -24.5 volt power to the ACS, thermal control, command and data handling subsystem and the power switching module. It also feeds unregulated power to the Unfold Timer and the Power Switching Module. The emergency bus, from the auxiliary regulators, is used by the command subsystem for receiver and clock operation.

The power switching module contains pyro firing circuitry and relays for control of input power to the commandable subsystems as well as the Payload Regulator Module.

The Payload Regulator Module is identical to the Power Control Module and contains redundant PWM regulators for providing -24.5 volts to the RBV cameras and wideband video tape recorders.

When the power required by the spacecraft subsystems is in excess of that which the solar array can provide, as evidenced by the array voltage dropping to the battery discharge voltage (less the drop across the isolation diodes) the batteries will discharge and load sharing will occur between batteries and solar array. Should the drain be excessive, such as might occur during a short, and the regulated bus voltage drop to less than 18 volts, the 15 cell battery fuse tap is activated and 15 cells discharge directly onto the regulated bus. This will blow the fuse or clear the short by burning it out.

During eclipse periods the batteries discharge onto the unregulated bus through the isolation diodes located in the Power Control Module to supply spacecraft loads. Batteries are recharged by voltage limited temperatures compensated charge controllers located in the individual modules. Each module also contains circuitry to reduce the charge to a trickle rate should battery temperature increase to 45°C. The trickle charge can be overridden by the trickle charge override function located in the power control module. Battery charging

occurs when the solar arrays receive solar energy. Should the charge controller not prove effective in controlling overcharge, the auxiliary load panels are activated to drain off excess power.

### 3.2.5.7 Electrical Integration

The electrical integration subsystem includes the distribution harness and the following components Preflight Disconnect, Power Switching Module. Electromagnetic interface considerations are also discussed as part of this subsystem.

The Harness provides the electrical interfaces between the payload sensors and all spacecraft components. It is a critical element in the performance of the communications subsystems and also in the minimization of interference between components. The functions of the Harness Subsystem include the following

1. Provides signal interconnections between spacecraft service subsystems and sensors
2. Distribution of regulated and unregulated power
3. Collection of telemetry data
4. Distribution of commands
5. Provides ground reference for all components

The primary design objectives established for the harness are

- 1 To provide accessibility to all components during test while the vehicle is in an operating mode
2. To minimize the noise radiated from and the noise picked up by the harness
3. To limit the voltage drop in the power harness to 1% of the supply voltage
4. To provide an adequate transfer function for all signals
5. To provide selective redundancy for critical vehicle functions
6. To minimize subsystem weight
7. To minimize the magnetic moment of the harness

Design features of the Harness which will attain these objectives are as follows

1. The component accessibility achieved through judicious harness routing in the component area.

2. Requirements for shielding, shield termination, and routing of harness have been specified. Critical signals are run as twisted lines or coaxial cables.
3. Wire gauge for each power line and return will be sized to limit the IR drop to less than 1%.
4. Minimization of harness weight will be a key factor in the design of the Telemetry and Command Subsystem Harnesses and in the design of the Power Subsystem Harness.
5. The selection of nonmagnetic connectors and the twisting of the Power Distribution wires will minimize the contribution of the harness to the magnetic moment of the spacecraft.

Physically, the Harness divides into 1) Sensory Ring Harness, top and bottom, to include both the spacecraft and sensor subsystem segments, 2) the Attitude Controls Interface Harness, routed up the struts, and 3) the Adapter Harness.

The major portion of the Harness is located at the top of the sensory ring with interconnections to the bottom loaded sensor equipment being routed down through the cross beam area just inboard of the modules. Connector breakouts to the sensory ring modules are routed along the castings between the modules to facilitate installation and removal of modules. The Solar Array and Attitude Control Subsystem interface segments are routed and clamped external to the truss tubes.

Functionally, the harness can be engineered as follows

- Power
- Separation
- Command
- Telemetry
- Thermal
- Communication
- Sensor

Each of the functional harnesses is analyzed for signal level and frequency content to determine shielding and routing requirements to minimize electromagnetic interference. When Harness separation for EMI purposes is impractical due to physical space limitation, the harness segments will be individually shielded for maximum isolation. The functional harness segments will be segmented to facilitate fabrication, test, and installation.

Table 3 2 5-3 shows a summary of the major harness segments, including an approximation of the number of connectors. The estimated weight of the harness subsystem is 135 pounds. Major portion of the weight data is derived from actual Nimbus data thus offering more accuracy to the estimate.

Table 3 2 5-3 Harness Summary

Subsystem Power & Separation	Number of Harness* Segments	Number of Connectors**
Power	18	114
Command	8	57
PCM Telemetry	19	118
Thermal	6	6
Power Switching Mod (Switched Power and Signals)	1	20
DCS	2	4
Wideband Telemetry	12	33
Narrowband Recorder	12	33
RBV	9	27
MSS	2	6
Adapter	7	18
Total	96	436
*Includes 31 coaxial segments		
**Includes intrasubsystem interface connectors		

### 3 2 5 7 1 Power Switching Module

The power switching module is the interface between power, spacecraft loads, and command subsystems. The major functions are to provide power and signal switching, load fault protection, and to provide voltage for limiting the unregulated voltage applied to the orbit adjust solenoid valves. Telemetry circuits are necessary to indicate switch position, pyro firing events, and system bus voltages.

11 February 1970

The pyro firing relays and small signal relays are housed in separate rf compartments. Fuses and telemetry circuits are mounted on circuit boards. Power command and telemetry circuits are electrically input.

The power switching module is 13 by 13 by 3-3/4 inches, and is designed for mounting on the ERTS sensory ring cross-beam, where its central location will optimize the interconnecting harness, which interfaces with all major subsystems.

### 3 2 5 7 2 Preflight Disconnect Component

The preflight disconnect component provides for remote disconnect of power and monitor circuits (required during the pre-launch phase only) between the adapter and spacecraft prior to launch. Demating prior to launch eliminates the requirement for an umbilical quick-pull type disconnect which would be demated and operation of the shroud or adapter, in flight, thus enhancing the overall reliability of the separation sequence.

The preflight disconnect is a motor-driven plug which remains in the adapter, and the associated receptacle is spring-mounted on its base to provide movement in the event of slight misalignment during mating. The plug can be remotely mated or demated to make or break connections to externally located ground equipment.

### 3.2.5.8 AGE

Equipment under the general category of Aerospace Ground Equipment (AGE) includes all mechanical and electrical spacecraft oriented equipment required to support sub-system and system level testing, handling, transportation, checkout, servicing, stimulation and simulation, packaging and maintenance of the satellite during its complete ground mission profile including factory, remote test facility, and field operations.

The AGE required to support the ERTS Program is logically divided into two categories Mechanical AGE and Electrical AGE. There are numerous individual equipment items in each of these categories. For summary purposes, these items have been consolidated into functional groups. Table 3 2 5-4 is a tabulation of these functional equipment groups and a summary of equipment items as functions included in each group.

The AGE design approach capitalizes upon the successful AGE designs previously used for Nimbus A, C, B, and B2 and currently in use or planned for use on the Nimbus series D, E and F programs. The degree of Nimbus design and hardware utilization is shown by end item categories for Electrical and Mechanical AGE in Table 3 2 5-5, AGE Status Summary

Table 3 2.5-4 ERTS AGE Summary

Equipment Group No	Nomenclature	Function/Equipment Items
<b><u>Mechanical AGE</u></b>		
M1	Attitude Control Subsystem BTE	A group of mechanical AGE required to support test of the ACS. Equipment includes RWS simulators, ACS support fixture SPSS simulators, alignment fixture, RAD alignment targets, ACS handling sling, RCS T/V test equipment, and vibration fixture, RAD shaft dual indicator, RAD shaft drive fixture, RWS shipping containers, solar paddle transition simulator.
M2	Orbit Adjust Subsystem BTE	The following items of mechanical AGE are required: OA shipping container, OA alignment targets, OA handling fixture.
M3	Payload Subsystem BTE	A group of mechanical AGE including RBV handling fixture, RBV S/A alignment fixture, RBT removal, check of calibration fixture.
M4	Spacecraft Handling and Transportation Equipment	A group of mechanical AGE including a Test and Calibration Dolly, Spacecraft Dolly and Sensory S/S Fixture, Utility Dolly, Cover Sling, Hydraset, S/C Cover Mounting Ring, Sensor Ring 1 in Sling, Transport Trailer, Spacecraft Spacer, S/C Humidity Covers, Spacecraft Sling, Spacecraft Cover, Flight adapter handling fixture, and AGE packaging.
M5	Spacecraft Checkout Equipment	Spacecraft checkout equipment includes the following: Matchmate Tool, Leak Test Equipment, Alignment Equipment, Mass Property Meas Equip, Wt and c g Separation Rate Fixture, Paddle Hub Clamp, RFI Sling, Vibration Fixtures, ambient check of calibration adapter.
M6	Spacecraft Servicing Equipment	A group of mechanical AGE including Nitrogen gas, charging equipment, S/C access ladders and platforms, S/C cleaning kit, S/C mechanics tool kit, S/C accountability kit, orbit adjust fuel servicing equipment.
M7	Spacecraft Thermal-Vacuum Equipment	A group of special support and check of calibration equipment required for spacecraft T/V testing.
<b><u>Electrical AGE</u></b>		
E1	Electrical Systems Test Set	Controls and Monitors spacecraft operation during integration and systems test. Supplies ground power, performs battery charging, verifies attitude control S/S, Power S/S, and unfold, MSS and OA EED Circuitry. Controls Sun, Earth, and Attitude Sensor Simulators. Provides hardwire command signals. Provides special test signals and verifies responses. Controls RBV and MSS-Go/NoGo targets. Provides troubleshooting capability. Contains Protective circuitry to assure spacecraft electrical test safety.
E2	Test Ground Station	Generates and verifies RF Commands (VHF and USB) to spacecraft. Receives, records, processes, and displays real time and stored telemetry. Verifies PRN and DCS performance. Receives and records RBV and MSS data. Processes RBV and MSS Data with GFE Test equipment. Provides troubleshooting, debugging evaluation and statistical analysis.
E3	Auxiliary Test Equipment	A group of equipment providing: RBV Collimator and MSS Target Controls, Solar Array Simulation, Solar Array Testing, RF Test Equipment, Test Antennas, RF Dummy Loads and Protection, Ambient Test Cables, Test Tees and Breakout Boxes, and Passive Simulation of spacecraft and adapter loads.
E4	Environmental Electrical Support Equipment	A group of equipments providing: Thermal Vacuum Test support including Power and Control of Heater arrays, Thermal vacuum Test Cables, Temperature monitoring thermocouples, and special test modules.
E5	Field Operations Equipment	A group of equipment including: Blockhouse Console to power and monitor spacecraft during prelaunch and launch operation, Attitude Controls Stimulator Control Console, Simulators to electrically check Launch Vehicle interfaces, and special test modules.
E6	Subsystem Bench Test Equipment	Subsystem Bench Test Equipment to functionally test the following subsystems: ACS, Power S/S, Command S/S, TLM S/S, RBV S/S (GFE); MSS S/S (GFE); DCS and Wide Band Comm. S/S.

11 February 1970

Equipment Category	Design Sources		
	Nimbus	Mod Nimbus	New
<b>Mechanical</b>			
1. ACS Bench Test Equipment	11	1	1
2. Orbit Adjust BTE	1	1	2
3. Payload Subsystem BTE	7	-	3
4. Spacecraft Handling and Transportation Equipment	13	-	-
5. Checkout Equipment	6	2	-
6. Servicing Equipment	1	4	-
7. Spacecraft Thermal Vacuum Equipment	1	1	2
<b>Electrical</b>			
1. Electrical Systems Test Set	5	5	1
2. Test Ground Station	-	-	1
3. Auxiliary Equipment	3	6	1
4. Environmental Test Support Equipment	1	2	-
5. Field Operations Equipment	1	5	-
6. Subsystem Bench	3	1	4

Table 3 2 5-5 AGE Status Summary

Utilization of the basic Nimbus D spacecraft as a bus with integrated ERTS payloads and the orbit adjust subsystem incorporated minimizes the number of new AGE designs in both the electrical and mechanical areas.

The individual payload subsystems and their associated equipment, the Communications and Data Handling subsystem and to a lesser degree, the orbit-adjust subsystem, comprise the major differences between Nimbus and the proposed ERTS spacecraft which affect AGE.

Highlights of the approach to AGE for ERTS are as follows

1. Maximum utilization of the spacecraft telemetry system is made for performance monitoring and fault diagnosis. This minimizes the number of hardware test points required.
2. Fault isolation to the black box level is attained through the use of supplementary test tees and breakout boxes.
3. In the interest of cost effectiveness and the versatility achieved by direct operator control, test equipment is manual. Interlock circuitry is provided to preclude spacecraft damage through incorrect sequences of operation. The exception is that telemetry and command data is processed by computer in the Test Ground Station.
4. Wherever feasible, identical equipment supports factory, field, and prelaunch operations to produce correlatable data.
5. Sensor, payload, and critical control components are aligned at the control package and sensory ring subassembly level and these subassemblies are aligned to each other at spacecraft assembly. Following environmental tests, alignments is rechecked in the optical facility to insure that components have remained within requirements.
6. As a result of measured results closely confirming calculated results early in the Nimbus program, moments of inertia are calculated only.
7. The spacecraft is transported with the yaw axis horizontal in a transporter having passive environmental control except for humidity which is controlled by continuous purge.
8. Spacecraft payloads are stimulated and calibrated as an "all-up" system in ambient and vacuum-thermal environments during system test.
9. Hard points for handling the assembled spacecraft are provided on sensory ring.
10. Handling equipment is designed to a minimum static limit loading of 3g at yield or 4.5g at ultimate, whichever is less and is proof loaded to a static load of 2g.



11 February 1970

### 3.3 HARDWARE MATRIX

Table 3.3-1 is a compilation of the major spacecraft components that will be used for the Earth Resources Technology Satellite (ERTS). Since the Observatory design has been predicated upon an existing spacecraft which already meets many of the ERTS mission requirements, most of the ERTS hardware is identical or requires very little design modification. The table is presented in the format designated in Attachment VI (Section 1.4.16) of S-701-P-3, Design Study Specifications for the Earth Resources Technology Satellite ERTS "A" and "B".

It can be seen from the Spacecraft Hardware Table that approximately 56 percent of the line items listed will require no change from the existing design in order to be used for ERTS, and another 21 percent will require only minor design modifications. The remaining line items (23 percent) require new designs and will be procured from well established, technically competent subcontractors or produced in-house. This approach allows for maximum control of the relatively few newly designed components for the ERTS program.

Implementation of the actual hardware procurement program will follow well established and proven procedures, utilizing for the most part, the same material sources and subcontractors found to be most suitable on the Nimbus program. In-house fabrication and test functions will be performed with the same (or newly built but equivalent) equipment and facilities and by the personnel previously trained and experienced on Nimbus.

Table 3 3-1 Preliminary Availability Status Information on Potential ERTS Hardware

MAJOR SPACECRAFT ASSEMBLY NOMENCLATURE	ANTICIPATED SOURCE	NEW DESIGN REQUIRED?	USE EXISTING DESIGN WITH		QUANTITY FOR ERTS A, -B, & SPARES			UNITS AVAILABLE FOR ERTS		ERTS ESTIMATED COST	FLIGHT HISTORY	
			NO CHANGE	MINOR CHANGE	REQUIRED	AVAILABLE	TO BE FABRICATED	SERIAL NUMBERS	PROGRAM ACCOUNTABILITY			
<u>Structure Subsystem</u>												
• Structure	GE	No	X		2	0	2			See Phase D Proposal Volume III	Nimbus II III	
• Sensory S/S Primary Structure		Yes		X	2	0	2	-				
• Sensory S/S Secondary Structure	GE	Yes		X	2	0	2		-			
• Paddle Unfold Switch	Micro Switch	No	X		3	0	3	-			Nimbus II III	
• Cable Cutter & Squibs Assembly	Atlas Chemical Company	No	X		18	0	18 (14 spares)	-			Nimbus II III	
• Load Cells	GE	No	X		2	0	2				Nimbus II, III	
• Paddle Latch Hardware	GE	No	X		2	0	2				Nimbus II III	
• Bolt Cutter Assembly & Squibs	Atlas Chemical Company	No	X		4	0	4				Nimbus II, III	
• Adapter Primary Structure	GE	No		X	2	0	2	--			Nimbus II III	
• Adapter Secondary Structure	GE	No		X	2	0	2				Nimbus II, III	
• Separation Band	GE	No	X		2	0	2	-	--		Nimbus II, III	
• Separation Springs	GE	No		X	12	0	12	-	--		Nimbus II, III	
• Paddle Dampers	GE	No	X		4	0	4		--		Nimbus II, III	
• Separation Switches	Micro Switch	No	X		14	0	14	-	-		Nimbus II, III	
• ACS Shroud Stimulators	GE	No	X		12	0	12	--	--		Nimbus II, III	
• Adapter Co/No-Go Targets	GE	Yes			2 sets	0	2 sets	-	--		Nimbus II, III	
• WB Antenna Pickup & Re-radiator	GE	Yes			2	0	2	-	--		Nimbus II, III	
• USB Antenna Pickup & Re-radiator	GE	No		X	2	0	2	--	--		Nimbus II III	

Table 3.3-1 Preliminary Availability Status Information on Potential ERTS Hardware (Cont)

MAJOR SPACECRAFT ASSEMBLY NOMENCLATURE	ANTICIPATED SOURCE	NEW DESIGN REQUIRED?	USE EXISTING DESIGN WITH		QUANTITY FOR ERTS-A, -B, & SPARES			UNITS AVAILABLE FOR ERTS		ERTS ESTIMATED COST	FLIGHT HISTORY
			NO CHANGE	MINOR CHANGE	REQUIRED	AVAILABLE	TO BE FABRICATED	SERIAL NUMBERS	PROGRAM ACCOUNTABILITY		
<u>C&amp;DH Subsystem</u>											
• Command Clock	Gal Comp	No	X		2	0	2(a)	(a)	Nimbus E/F	See Phase D Proposal Volume III	Nimbus D
• VHF Command Receiver	RCA	Yes			2	0	2(b)	--	--		
• PCM Telemetry Processor	Radiation	No	X		2	0	2(a)	(e)	Nimbus E/F		Nimbus D
• N/B Tape Recorders	Leach	No		X	4	0	4(b)	-	-		
• VHF Transmitter	Radiation	No		X	2	0	2(b)	-	-		
• W/B FM Modulator	GE	Yes			2	0	2(b)				
• W/B Power Amp	Watkins Johnson	Yes			4	0	4(b)		-		
• Pramod Processor	Motorola	Yes			2	0	2(b)	-	-		
• Unified S-Band Equip	Motorola	Yes			2	0	2(b)		-		
• Conditioner Box	GE	Yes			2	0	2(b)	-	-		
• Command Integrator	GE	Yes			2	0	2(b)	-	-		
• W/B Antenna	GE	Yes			4	0	4	-	-		
• Command Antenna	GE	No		X	2	0	2	--	-		
• Quadraloop Antenna	GE	No		X	8	0	8	-	-		
• USB Antenna	GE	No			2	0	2		--		
<u>ACS Subsystem</u>											
• ACS Structure	Fairchild	No			2	0	2	--	--		
• Thermal Control Assembly	Fairchild	No	X		2	0	2(a)	(a)	Nimbus E/F		Nimbus D
• Pitch Flywheel	Bendix	No	X		2	0	2(a)	(a)	Nimbus E/F		Nimbus II III D
• Yaw Flywheel	Bendix	No	X		2	0	2(a)	(a)	Nimbus E/F		Nimbus II, III D

11 February 1970

Table 3 3-1 Preliminary Availability Status Information on Potential ERTS Hardware (Cont)

MAJOR SPACECRAFT ASSEMBLY NOMENCLATURE	ANTICIPATED SOURCE	NEW DESIGN REQUIRED?	USE EXISTING DESIGN WITH		QUANTITY FOR ERTS A, -B, & SPARES			UNITS AVAILABLE FOR ERTS		ERTS ESTIMATED COST	FLIGHT HISTORY
			NO CHANGE	MINOR CHANGE	REQUIRED	AVAILABLE	TO BE FABRICATED	SERIAL NUMBERS	PROGRAM ACCOUNTABILITY		
<u>ACS Subsystem (Cont.)</u>											
• Pneumatics Assembly	TRW	No	X		2	0	2(a)	(f)	Nimbus E/F	See Phase D Proposal Volume III	Nimbus D
• Solar Array Drive (SAD)	TRW	No	X		5	0	5(a)	(g)	Nimbus E/F		Nimbus D
• Rate Measuring Package (RMP)	Sperry	No	X		4	0	4(a)	(a)	Nimbus E/F		Nimbus III, D
• Yaw Rate Gyro	Northrup	No	X		2	0	2(a)	(a)	Nimbus E/F		Nimbus-Nimbus D
• Harness	GE	No		X	2 sets	0	2 sets	--	-		Nimbus II, III, D
• Attitude Sensor	Quantic	No		X	2	0	2(b)	-	--		
• Initiation Timer	GE	No	X		2	0	2	--	--		Nimbus D
• Magnetic Moment Assy	Ithaco	No	X		2	0	2(a)	-	-		Nimbus D
• Roll Reaction Wheel Scanner	Bendix	No	X		4	0	4(a)	(a)	Nimbus E/F		Nimbus D
• Control Logic Box	Ithaco	No		X	2	0	2(b)	--	-		Nimbus D
• Signal Processor	Ithaco	No	X		4	0	4(a)	(h)	-		Nimbus D
<u>Orbit Adjust Subsystem</u>											
• Propellant Tank	Rocket Research	No		X	2	0	2(b)	--			Classified Prog
• Thruster Assembly	Rocket Research	No	X		2	0	2(b)	-			Classified Prog
• Structure	Rocket Research	No	X		2	0	2(b)	--	--		Classified Prog
• Other Components	Rocket Research	No	X		2	0	2(b)	--	--		Classified Prog
<u>Thermal Subsystem</u>											
• Thermal Radiation Plates	GE	Yes			4	0	4	--			
• Temperature Controller Assembly	GE	No	X		36	0	36 (4 spares)	--	-		Nimbus II III, D
• Shutter Position Indicator Assembly	GE	No	X		32	0	32	-	-		Nimbus II III, D

TABLE 3.3-1. PRELIMINARY AVAILABILITY STATUS INFORMATION ON POTENTIAL ERTS HARDWARE

MAJOR SPACECRAFT ASSEMBLY NOMENCLATURE	ANTICIPATED SOURCE	NEW DESIGN REQUIRED?	USE EXISTING DESIGN WITH		QUANTITY FOR ERTS-A, -B, & SPARES			UNITS AVAILABLE FOR ERTS		ERTS ESTIMATED COST	FLIGHT HISTORY
			NO CHANGE	MINOR CHANGE	REQUIRED	AVAILABLE	TO BE FABRICATED	SERIAL NUMBERS	PROGRAM ACCOUNTABILITY		
<u>Thermal Subsystem (Cont )</u>											
• Insulation	GE	Yes			3 sets	0	3 sets(c)	-	--	See Phase D Proposal Volume III	Nimbus II, III, D
• Shutter Assemblies	GE	No	X		36	0	36(4 spares)	--	--		Nimbus II, III, D
• Compensating Loads	GE	No	X		65	0	65(5 spares)	--	--		Nimbus II, III, D
• Thermal Coatings & Tapes	GE	No			As Required			-	-		Nimbus II, III, D
<u>Power Subsystem</u>											
• Solar Paddles	RCA-AED	No	X		4	0	4	-	-		Nimbus II, III, D
• Storage Modules	RCA-AED	No	X		17	0	17(a)	(d)	Nimbus E/F		Nimbus II, III, D
• Power Control Module	RCA-AED	No	X		2	0	2(a)	(a)	Nimbus E/F		Nimbus II, III, D
• P/L Regulator Module	RCA-AED	No	X	Identical To Power Control Module	2	0	2(a)	(a)	Nimbus E/F		Nimbus II, III, D
• Auxiliary Load Panel	GE	No	X		4	0	4(a)	(a)	Nimbus E/F		Nimbus II, III, D
• Auxiliary Load Controller	GE	No	X		2	0	2(a)	(a)	Nimbus E/F		Nimbus II, III, D
• Separation Unfold/Timer	GE	No	X		2	0	2(a)	(a)	Nimbus E/F		Nimbus II, III, D
<u>Electrical Integration Subsystem</u>											
• Spacecraft Harnesses	GE	Yes			2 sets	0	2 sets	--	--		Nimbus II, III, D
• Flight Adapter Harnesses	GE	Yes		X	2 sets	0	2 sets	--	--		Nimbus II, III, D
• Power Switching Module	GE	Yes			2	0	2	--	--		
• T/M Conversion Modules	GE	No	X		6	0	6	--	--		Nimbus II, III, D
• Thermistors	GE	No	X		180	0	180	--	--		Nimbus II, III, D
• Preflight Disconnect	GE	No	X		2	0	2	--	--		Nimbus II, III, D

(a) - Nimbus F and ERTS B share common backup

(b) - Qual Model Refurbished for Spares

(c) - Shells only required for Spares

(d) - ERTS Provides 1 Spare

(e) - PCM Telemetry Processor Memory

(F) - ERTS Provides Spare Regulator

(g) - ERTS Provides 1 Spare

(h) - ERTS Provides Circuit Cards For Signal Processor

### 3.4 LAUNCH VEHICLE STUDY RESULTS

#### 3.4.1 GENERAL

A study was performed under Program Directive Number 55 (Nimbus E/F) dated June 6, 1969 (NASA Contract #11570) to "Determine the impact on the Nimbus E/F spacecraft design using a Thorad/Delta launch vehicle for launching of the spacecraft with a payload as defined in GSFC Nimbus "E" configuration modified to include addition of the T&DR system and deletion of the SDR system " The study considered the mechanical and electrical interfaces, and the support equipment (AGE). In the course of the study, various "Delta" problems arose for which "Nimbus" solutions were obvious. These problems were identified and proposed solutions were recommended.

This study was reviewed to determine the applicability of the results with respect to the ERTS spacecraft and its electrical and mechanical interface requirements.

##### 3.4.1.1 Review Summary

The study was reviewed against the ERTS requirements. The conclusion reached was that while most of the potential mechanical and electrical problems identified for the Nimbus E/Delta L/V interface are extremely minor and readily solvable there is one area which was not completely resolved. This area is the inadequate clearance between the upper-paddle latch of the spacecraft and the Delta shroud.

This clearance problem is created by the method of shroud attachment to the launch vehicle. The Delta configuration has the shroud mounted directly to the forward end of the launch vehicle. The spacecraft adapter is mounted to a two-inch adapter ring (or spacer) which in turn mounts to the forward end of the Delta. Because of this ring and the manner and position of mounting the shroud, the upper end of the paddle assembly protrudes into the conical portion of the shroud, thus creating an interference problem. Figure 3.4-1 illustrates this problem. Both Nimbus "B" and Nimbus "D" were mounted to two-inch spacer rings which were mounted on top of the Agena, however, the shroud used was attached to the top of this spacer resulting in an adequate clearance for the upper paddle latch.

Several methods by which this problem can be resolved are listed as follows:

- 1 Use a SACS type shroud with an SACS adapter ring (spacer) which raises the shroud 2 inches and attaches to the Delta booster, which requires modifying the front end of the Delta.
- 2 Use the present Delta shroud configuration except mounted to a new adapter ring.
- 3 Increase the length of the shroud by two inches.
- 4 Dimple the Delta shroud around the clearance problem area.

11 February 1970

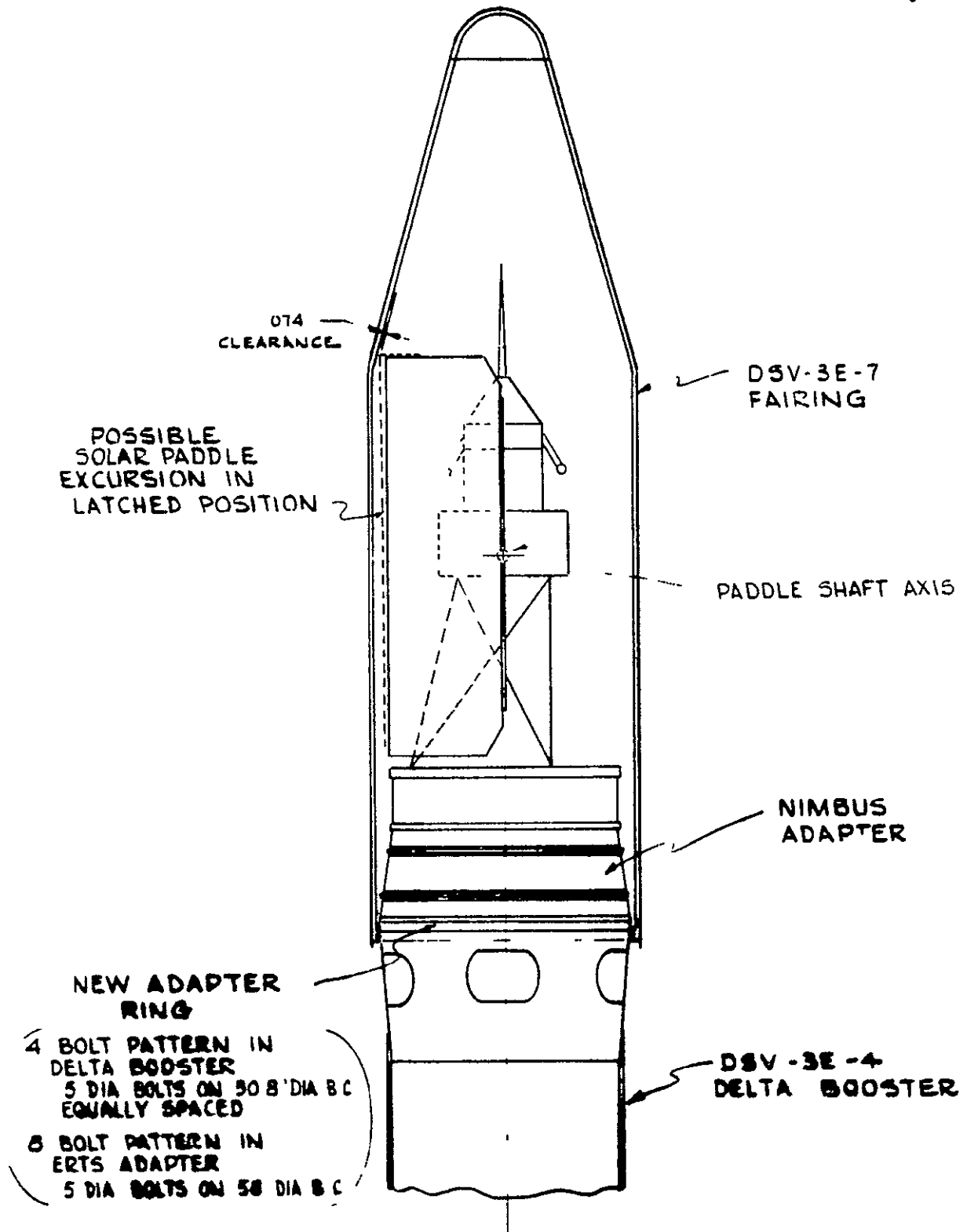


Figure 3.4-1. Paddle Assembly Protrudes into Conical Portion of Shroud

- 5 Design a new adapter to fit on top of the Delta booster, eliminating the need for an intermediate adapter ring (spacer)
- 6 Design a shorter adapter

### 3.4.1.2 Baseline Configuration

Figure 3.4-2 shows the recommended approach which is to modify the upper end of the Delta to accept the SACS ring, thus permitting the use of the SACS shroud. This change has been requested by the NASA/GSFC Nimbus E/F Project Office.

## 3.4.2 ERTS/DELTA ELECTRICAL INTEGRATION STUDY

### 3.4.2.1 Introduction

The Electrical Interface design of the ERTS Spacecraft and the Delta launch vehicle is presented in this section. As a result of this study, it has been determined that the ERTS Spacecraft can be made electrically compatible with the Delta Launch Vehicle if the following requirements are met by the Delta electrical system as follows:

1. Supply 24 amperes to the spacecraft separation pyros (bolt cutters) at the initiation of the separation event.
2. Accept and transmit five telemetry signals from the spacecraft flight adapter.
3. Provide the above telemetry monitors with regulated power.
4. The fairing should be RF transparent between 130 MHz through 2300 MHz in specific areas.
5. Relay contacts for the separation pyro circuitry should be "break-before-make".
6. The umbilical should be able to accommodate 47 pins + 20 percent spares for spacecraft functions.
7. RF compatibility.

### 3.4.2.2 Interface Description

An interconnection diagram of the proposed ERTS Delta Electrical Interface is shown in Figure 3.4-3. The Delta bulkhead connector functions are listed generically in Table 3.4-1.

### 3.4.2.3 Umbilical Pin Requirements

A review of the spacecraft blockhouse electrical interface requirements indicates that 47 pins plus 20 percent spares are required through the Delta umbilical.

Table 3.4-2 categorizes the functional requirements assigned to the umbilical pins.



11 February 1970

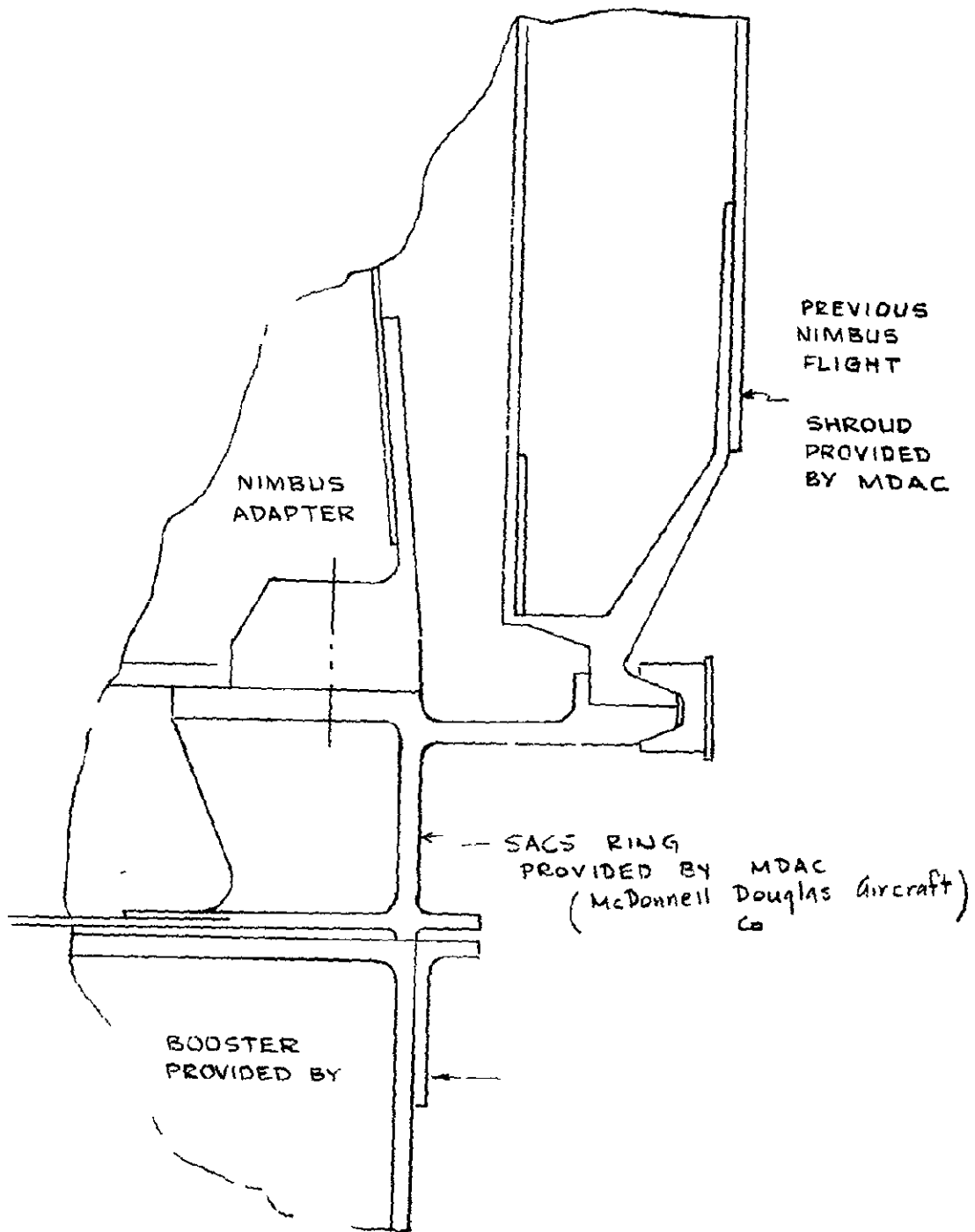


Figure 3.4-2 Delta Modified to Accept SACS Ring

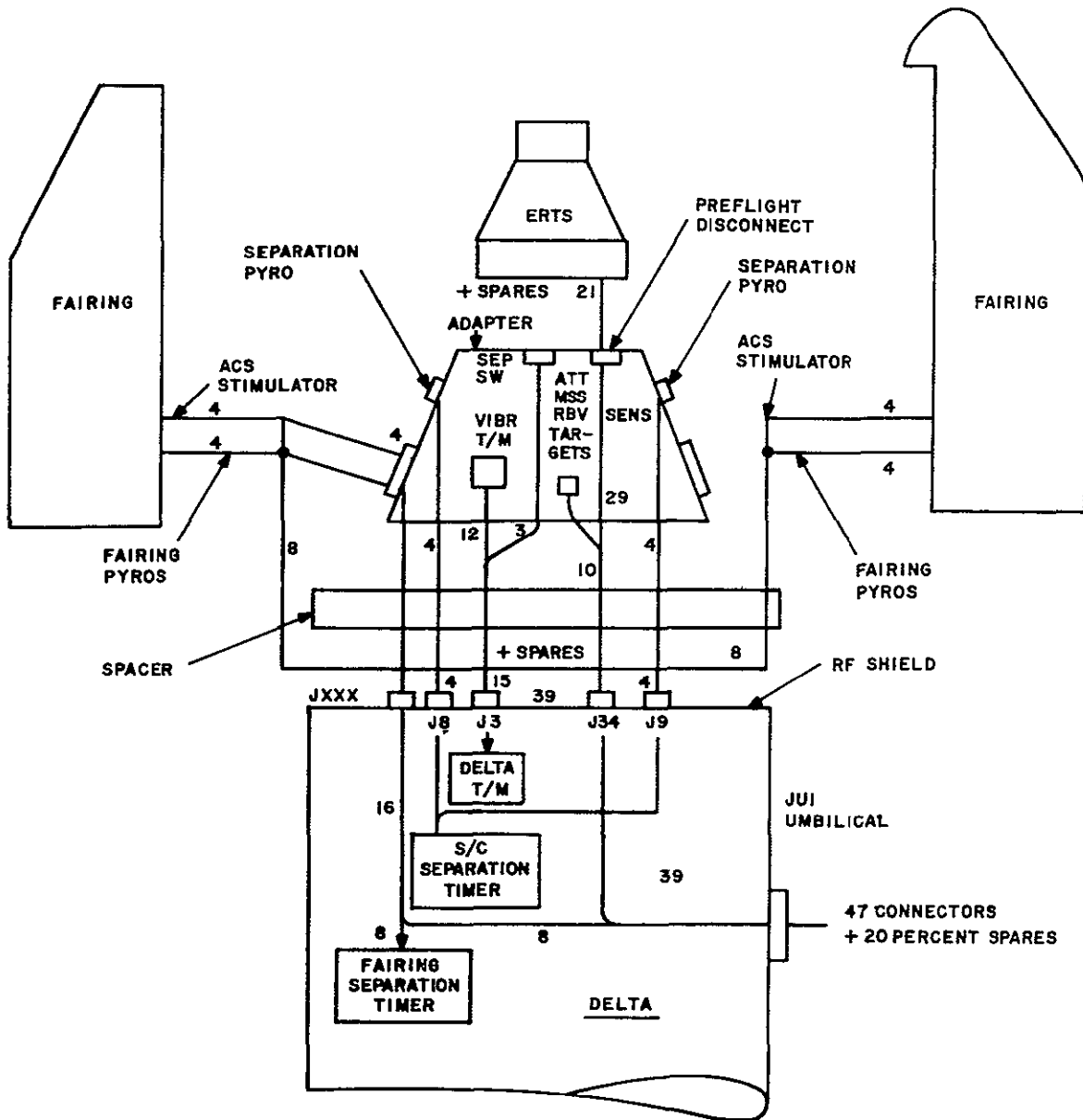


Figure 3.4-3. Interconnection Diagram Delta/ERTS Electrical Interface

Table 3 4-1 Spacecraft Adapter/Delta Connector Functions

Delta Connector Number	Minimum Number of Pins Required	Conductor Functions
J8	4	Power from Delta events timer to spacecraft separation pyros (1/2)
J9	4	Power from Delta events timer to spacecraft separation pyros (1/2)
J3	15 to 23 depending upon shield termination design	5 spacecraft telemetry monitors to Delta telemetry 3 Accelerometers 1 Vibration Sensor 1 Separation-Event Switch
J34	39 + spares	Spacecraft power, T/M & Control functions from Blockhouse & Experiment Target Power
JXXX	8 for ACS Simulators and 8 for Fairing pyros	Blockhouse Power to ACS Stimulators & Delta Events Timer to Fairing separation pyros

Table 3.4-2 Umbilical Pin Assignment Summary

Pins	Assignment
8	<u>Power</u>
	4      Spacecraft Power
	1      Gyro Heater
	2      T/M Power
	1      Unipoint Ground
10	<u>Control</u>
	3      Preflight Disconnect Control
	2      Dump ACS Pneumatics
	1      RMP Emergency OFF
	1      Umbilical Isolate Control
	1      Command Enable Control
	1      Separation Switch OFF Control
	1      All Batteries ON
18	<u>Targets</u>
	8      ACS Horizon Scanners
	2      RBV Cam 1
	2      RBV Cam 2
	2      RBV Cam 3
	2      MSS
	2      Attitude Sensor
11	<u>Telemetry</u>
	5      Preflight Disconnect Position & Voltage Monitor
	2      Spacecraft Voltage Monitor
	1      Gyro Temperature
	1      ACS Manifold Pressure
	2      ACS Tank Pressure & Temperature
47 Total + 20% spares	

11 February 1970

3.4.2.4 Electrical AGE

The electrical AGE required to support Spacecraft Delta electrical compatibility testing are listed in Table 3.4-3. This equipment is similar in all respects to that designed for Nimbus "D." No "new scope" pieces of AGE have been identified.

(Standard modifications to AGE resulting from different connector interfaces will be required.)

3.4.2.5 AGE Location at Launch Complex

Nimbus electrical AGE has historically been located in the Blockhouse and Launch PAD building in order to support launches from SLC-2E. Other than changes in cable length Blockhouse to SLC-2W vs SLC-2E and possible relocation of the Blockhouse Console within the Blockhouse, no other changes are foreseen. Since the distance from Blockhouse to SLC-2W is approximately 800 feet shorter than SLC-2E, no problem with AGE line driving capability should exist.

Table 3 4-3 Electrical AGE Required to Support L/V Compatibility Testing

Item	Function	Location
Blockhouse Console	Supply Spacecraft power & target control	In Blockhouse
Line Resistance Simulator	Simulate Blockhouse to Booster Electrical Line Resistance during equipment checkout	At PAD and Booster Facility
Boltcutter Bridgewire (GFE)	Simulate Spacecraft Separation Pyro Electrical Resistance	At PAD during vertical all systems test At Booster facility during compatibility checkout
AGE Simulator	Simulate Blockhouse Console and ACS Stimulator Control Console	At Booster Facility during compatibility checkout
ACS Stimulator Control Console	Control ACS Stimulators mounted in Faring	In Launch PAD Building
Spacecraft & Adapter Load Simulator	Simulate Spacecraft Electrical Loads and Interface	At Booster Facility during comps checkout At PAD during Horizontal all systems test
Interconnect Harnesses	Interconnect Spacecraft & Booster Flight hardware and AGE during non-flight configuration testing	At Booster Facility At PAD

### 3 5 GROWTH

#### 3 5 1 GENERAL

Because of the exploratory nature of the ERTS program, payload growth predictions for the future ERTS mission are extremely difficult. Additional knowledge is constantly being obtained from earth resource instrumented aircraft which will provide the answers to such specific questions as what spectral bands are most useful for agricultural mapping, to provide species identification and to provide yield estimates. A scanner with 24 bands will be operated from such aircraft to provide data to aid in making this selection. Questions concerning the utility of multi-frequency, dual polarization, microwave observations for the purpose of assessing sea state hopefully will be answered by ocean overflights. Thermal IR readings versus time-of-day, for various types of soil and varying amounts of moisture are being taken by the Universities of California and Michigan to assess the methods of IR observations for hydrology applications.

Apart from the aircraft earth resources program, considerable knowledge and experience will be obtained from related application spacecraft missions such as Apollo, Nimbus, ITOS, ATS, and of course, ERTS A/B. Missions planned include radiometric sensors for IR mapping and microwave radiometry for passive mapping, as well as a variety of spectrographic and imaging sensors. Many of these sensors and payloads, though not specifically optimized for the ERTS application missions, will enable a more accurate identification of required spatial and spectral resolution, problems of communication and data handling, optimum orbital characteristics, vehicle motion and attitude rates, etc., all of which directly affect designs of future growth payloads. Factors such as these are constantly being studied by NASA, GE, user agencies, and industry. From the assessments of these combined studies the optimum growth payloads will evolve.

#### 3 5 2 GROWTH MISSIONS

The growth area discussed in this section is based on advances in technology projected for the post-ERTS A/B period and is primarily concerned with oceanography. Emphasis has been given to the oceanographic area since it is an important area that is not specifically addressed by the ERTS A/B mission. Because of the importance of oceanographic processes on the natural resources of contiguous land masses, as well as due to their importance in their own right, the ERTS/Oceanographic payload ensemble will be discussed in some detail.

##### 3 5 2 1 ERTS - Oceanographic

The understanding of large-scale oceanographic processes is expected to have a tremendous economic and scientific impact in such diverse areas as weather prediction, shipping, and fishing industries. The study performed by GE for the Marine Council supported this contention. Thus, it is anticipated that a specific ERTS satellite beyond ERTS A/B in the early nineteen-seventies, may be devoted to an oceanographic mission. An appropriate payload for such a mission could consist of an Electrically Scanning Microwave Radiometer similar to the one to be flown on Nimbus E, WISP, a scanner operating in the Thermal IR region, and a data collection system to collect data from specially equipped ships. Each of these payload subsystems, its function, and its operation is described below. A typical Oceanographic ERTS configuration is shown in Figure 3 5-1.

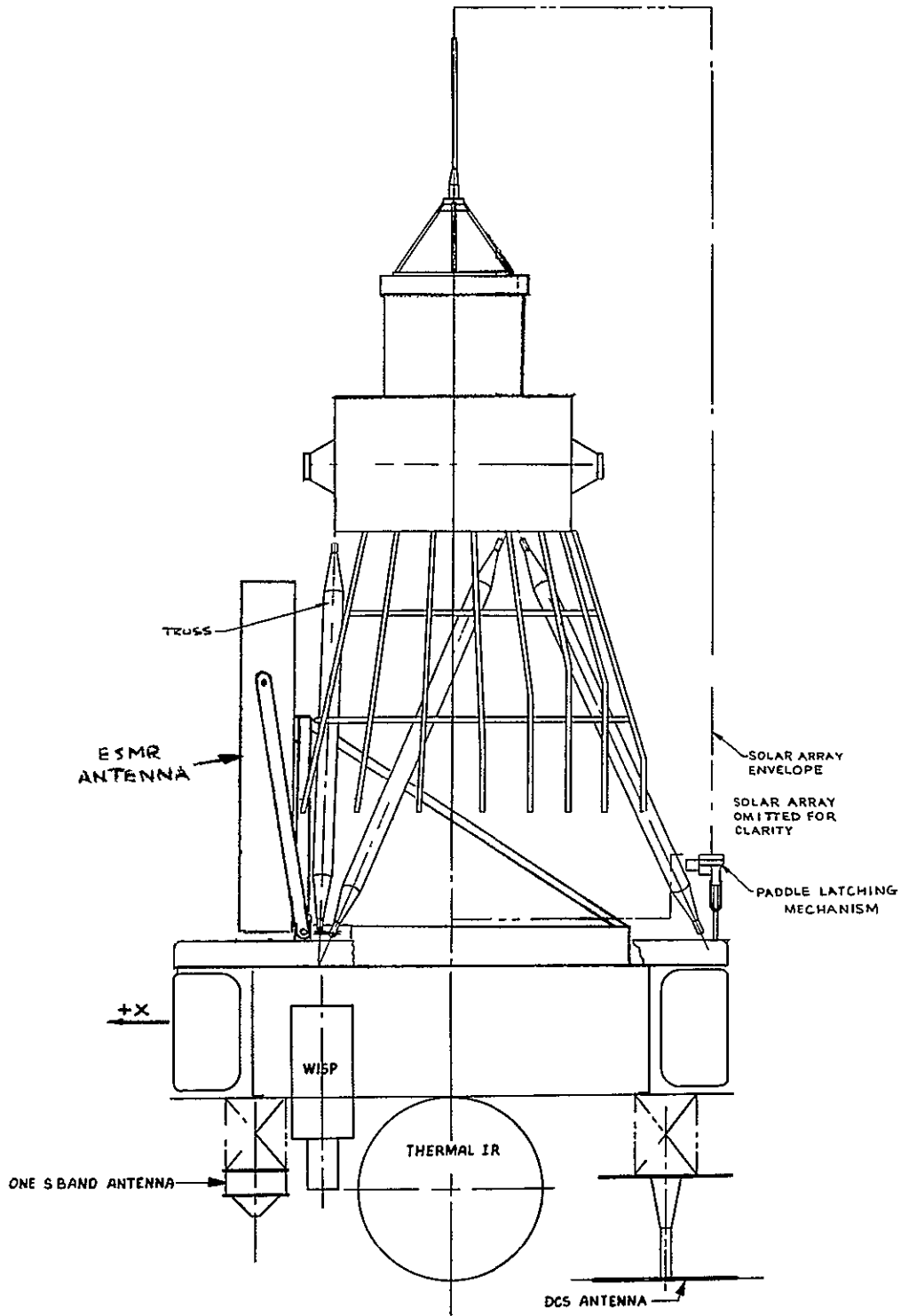


Figure 3.5-1 Oceanographic ERTS Configuration



### Wide-range Image Spectrophotometer (WISP)

The measurement of ocean color has potential applications for the fishing industries. The efficiency of fishing operations would increase considerably, if the search time for productive fishing grounds could be reduced. The forecasting of potentially productive areas hinges on deriving meaningful correlation between environmental conditions and the abundance of fish species. Such environmental conditions are sea temperatures, (as discussed below) and biological activity, which is reflected through the ocean color. Thus, synoptic observation of ocean color, with short response time data analysis, can be applied to identification of good fishing grounds. Monitoring of pollution and assimilation of waste discharged into the ocean are other possible applications.

The sensor selected for this application is WISP. WISP can operate with relatively poor angular resolution. It is this mode of operation where WISP can be a valuable ocean color sensor.

The Wide-range Image Spectrophotometer is a slit camera that has the capability of splitting the image into several regions and selectively scanning these regions.

An objective lens focuses the incident radiation on a narrow slit, which determines the field of view. The narrow dimension of the slit is oriented along the velocity vector and determines the resolution along the ground track. The long dimension is perpendicular to the direction of motion and determines the ground swath width. Radiation passing through the slit is converted into a beam of parallel rays by a collimating lens. A diffraction grating breaks up the beam according to wavelength, with different wavelength components leaving at different angles. Another lens assembly focuses these spectral components on the photosensitive surface of an imaging tube. Each component is focused in a unique location on the tube surface.

Selected regions can be electronically scanned to provide an image of the scene for each spectral band selected. The total number of bands that may be selected is fixed, that is, it is preselected by the sensor design. Selection of individual bands for data transmission may be accomplished by ground command. Thus, for spacecraft application where bandwidths are limited, only those spectral bands of current interest are used.

The overall performance of the WISP is governed largely by the characteristics of the tube selected as the detector. Both the image disector and FPS vidicon have been used to provide a relatively lightweight, low-power-consuming sensor. The sensitivity of the image disector and the spectral response of the FPS vidicon are the salient tube characteristics which limit the WISP performance. Other detectors, such as the image orthicon, could also be used, but with considerably increased weight and power requirements.

### Thermal IR - Sea Surface Temperature and Currents

Oceanographers have a strong interest in measuring the temperatures of the oceans, since the thermal structure is related to all marine processes, including the migration of marine life. Synoptic and repetitive measurement of the oceans temperatures is required and the word repetitive is to be stressed, since the large scale thermal features of the oceans change frequently.

11 February 1970

More specifically, cold upwelling regions are quite often biologically fertile areas and are good fishing grounds. Most of the time the sea currents boundaries are characterized by temperature differences. Thus, mapping of ocean currents, which is important to the shipping industry, can be carried out by temperature mapping.

In the thermal IR region, the emissivity of water is very close to unity. Thus, measuring radiation temperatures using an IR scanner is tantamount to measuring actual water temperatures. However, the atmospheric moisture content affects these measurements. Thus, it is proposed to use a two-channel scanner, one with ground resolution of the order of 0.5 mm, in the window band of 10.5 to 12.5 microns, and one with much poorer resolution, measuring in the 7-micron band, the absorption band of water vapor. The concept proposed is similar to that of THIR.

The Temperature Humidity Infrared Radiometer (THIR) is a relatively low resolution scanning radiometer which measures radiation in two IR bands: the "water vapor" band of 6.5 to 7.0 microns and the "window" of 10.5 to 12.5 microns.

The water-vapor channel has a field of view of 21 milliradians, and the atmospheric window channel has a field of view of 7 milliradians. The dynamic range of these channels is 0 to 270°K and 0 to 330°K respectively.

The sensor consists of two units, the scanner and the electronics module. The scanner provides the optical scan motion to produce cross-track scanning with reference to the satellite ground path of the radiometer instantaneous field of view. The scanner consists of the scan drive power supply, motor and mirror, the optical telescope, detectors pre-amplifiers, detector power supply, scan line synchronization pulse generators and amplifiers and housekeeping thermistors.

The electronic module contains the command power switching circuits, a dc-to-dc converter to power the electronics, the logic circuits to provide the signal format, the signal amplifiers, and the thermistor biasing circuits.

#### Electrically Scanning Microwave Radiometer

Data on sea state in all kinds of weather on an ocean-wide basis is of crucial importance to the shipping industry, and also in weather forecasting, since the energy exchange processes between the sea and the atmosphere have a strong influence on the weather.

The optical techniques, such as glitter analysis, are severely limited by the vast cloud cover which is quite prevalent over the marine areas of the earth. Thus, the application of microwave techniques, with its all weather capability, has great attraction.

A variety of observations and analytical studies have demonstrated the practicality of employing microwave sensors to monitor sea state, and also to monitor ice distribution. The oceans in the near polar regions are seasonally or perennially covered with sea ice. Adequate knowledge of the properties, distribution variability and behavior of the sea ice in these areas

11 February 1970

is presently lacking. The all-weather information on ice and icebergs, has applications for meteorological services, ice patrols and the shipping industries. Satellite data obtained with the existing meteorological satellites (TIROS, ESSA, Nimbus) are currently used, when available. Microwave radiometry has a great potential here, since the difference in brightness temperature (radiation temperature) between ice and water is very large ( $\sim 100^{\circ}\text{K}$ ). The microwave radiometer measures the radiation temperature of the surface. The electronically scanned antenna sweeps periodically in the direction transverse to the satellite forward velocity. The continuous forward overlay of such successive scans is obtained by the satellite motion.

Except for wavelength, the microwave radiometer will be a copy of that to be flown on Nimbus E. This applies especially to size, weight, configuration, structure and thermal design of the instrument. It consists of a receiver and an electrically scanning phased array antenna operating at a wavelength between 3-5cm. The following components will be contained in the flight instrument in addition to the basic antenna and receiver:

1. Beam steering network
2. Hot and cold calibration temperature sources
3. Data readout
4. Timing and control
5. Power supplies
6. Command

The antenna is perhaps the most critical component of the radiometer. Microwave radiometry of the earth from a satellite can be viewed as a radio-astronomy with one unique distinction. The earth has a roughly uniform temperature and fills nearly an entire hemisphere so that temperature differences of the order of a few degrees must be mapped with relatively high spatial resolution. This is very precise by the current standards of radioastronomy.

The antenna is capable of scanning through an angle of  $\pm 50^{\circ}$  with respect to the nadir and perpendicular to the direction of motion of the satellite. This will permit coverage of a large portion of the earth.

The most important characteristics of the proposed instrument are listed in Table 3-5-1. The 90 by 90 cm antenna requires that a system of deployment be used after satellite orbit is achieved. This system would be identical to the one used for Nimbus E.

#### Oceanographic Data Collection System

For oceanography applications, depth profile data from buoys and surface ships cannot only complement the broad coverage of surface data obtainable by remote sensing from satellites, but can also serve as ground (ocean) truth calibration marks when using satellite data.

Table 3 5-1 Specifications for ERTS Microwave Radiometer

RECEIVER	Central Frequency	10 GHz
	Bandwidth	100 MHz
	Noise Temperature	800 <sup>o</sup> K
	Integration Time	75 millsec
	$\Delta T_{rms}$	0.6 <sup>o</sup> K
	Absolute Accuracy	2 <sup>o</sup> K
	Dynamic Range	50-330 <sup>o</sup> K
	Dimensions less Antenna	15 by 20 by 32.5 cm Nimbus Module
	Calibration	Sky horn and internal hot blackbody (reference load)
ANTENNA	Type	Two dimensional phased array containing about 55 linear arrays
	Dimensions	90 by 90 by 10 cm
	Resolution	2.7 <sup>o</sup> at 3 dB points broadside 3.5 <sup>o</sup> at 3 dB points at scan angle of $\pm 50^o$
	Loss	1.5 dB
	Polarization	Receives component with electric field parallel to earth's surface at all scan angles
	Sidelobe Contribution	5 percent or less of total received power
	Scan Angle	$\pm 50^o$
	Scan Period	3.2 sec
	Total Experiment Weight	25 kg
	Total Experiment Power Requirement	25 watts
Telemetry	10 bit word read each 80 milliseconds Serial readout	

Note (Calculated for 600 km circular orbit, 90 x 90 cm antenna and a 3 cm wavelength)

1. Hydrological Measurements Remote stations will be useful in transmitting data with respect to existing water supply, the quality of ground and surface water, and the advent of flood conditions. Measurements in this category include water stage or stream level, discharge rate, water temperature, evaporation, water content of snow, and precipitation. In addition, the soil conditions of moisture, temperature, and evapotranspiration will be important.
2. Oceanography Water temperature profile, salinity, surface turbulence, etc., are considered standard candidates for the buoy. More specialized measurements include acoustical sound level at selected frequency intervals, biological content of the surface water, and depth soundings. A potentially valuable application that has gained recent interest is the monitoring of ice conditions in sea passages in the Arctic Circle, such as the Amundsen Gulf, in North Canada. Extensive oil deposits in the Arctic region depend on a real-time knowledge of the navigability of those passages for their successful exploitation and thus could benefit from a large network of remote stations.

### 3.5.3 SPACECRAFT GROWTH

#### 3.5.3.1 General

Increasing demands on the spacecraft's supporting subsystems by the various sensor configurations have led to studies in areas such as power, attitude control, structure (for more viewing area), and communications. The results of these studies will be discussed in the following paragraphs.

#### 3.5.3.2 Power

The introduction of additional sensors and the use of high power consuming data systems requires an increase in the available electrical power. Increased power may also be required because of more sustained payload operation.

The Bi-fold Advanced Solar Array considered for Nimbus by NASA/GSFC presents an approach that is directly applicable to growth ERTS spacecraft. Figure 3.5-2 shows a photograph of the engineering model of these solar-array paddles attached to a Nimbus spacecraft model.

A bi-fold solar array version of ERTS is a logical extension of the basic Nimbus configuration. The obvious modification is the array, each half of which contains an additional panel that is stowed by folding it against the main panel. Due to the extra weight of the additional panel, local structural "beef-ups" will be necessary. These include increasing the truss tube size and strengthening the latch mechanism.

An engineering model of bi-fold panels was designed, fabricated and tested by Fairchild-Hiller Corporation, with no failure. Another similar design was prepared by GE. Either version appears suitable for an ERTS growth application. The electrical power considerations were studied by RCA Corporation\* and GE.

---

\*Study of Power Supply Configurations for Advanced Nimbus Missions, RCA-AED  
Report No. R-3431, (Contract No. NAS5-11549)

11 February 1970

(This page left blank intentionally )

Figure 3 5 2

Figure 3.5-3 is a plan view of the bi-fold paddle showing a possible 94-series cell string layout on the auxiliary platform. The corresponding nominal case, beginning-of-life, bi-fold current voltage curves at three temperatures are shown in Figure 3.5-4. The bi-fold array increases the array power capacity by 84 percent

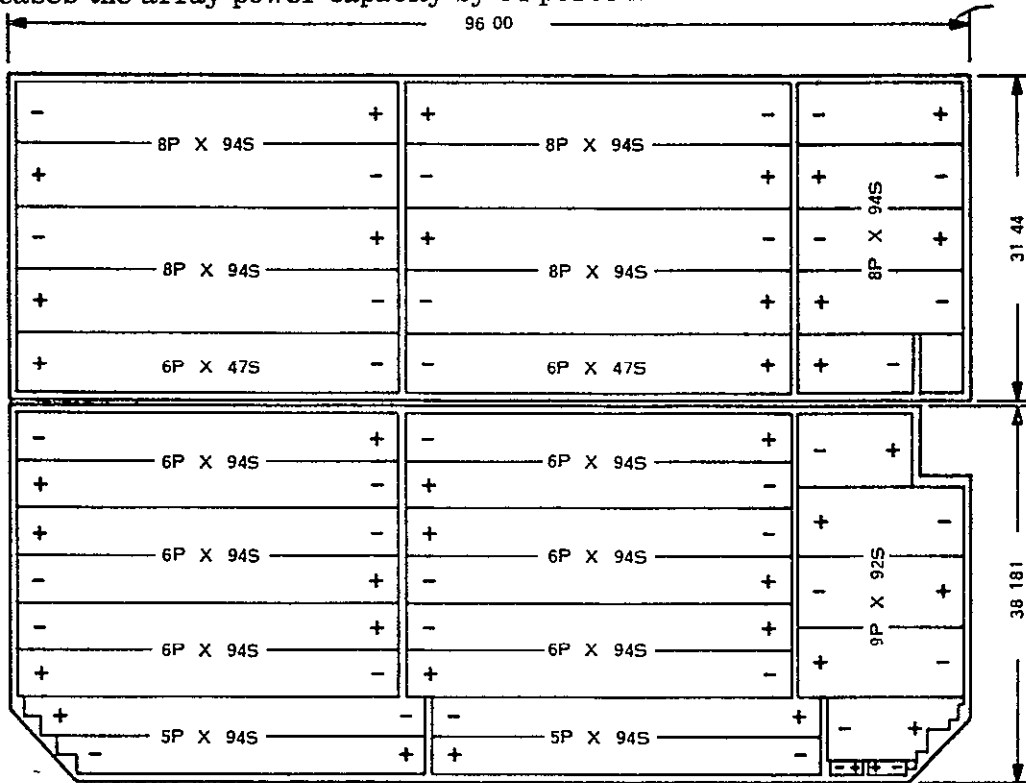


Figure 3.5-3 Typical Solar Cell Layout on Bi-Fold Paddles

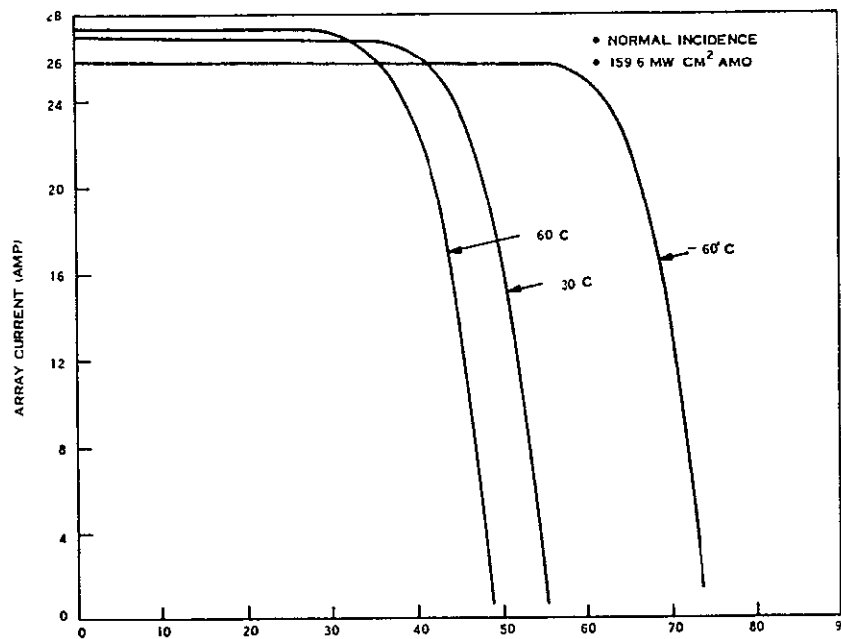


Figure 3.5-4 Solar Array I-V Curves, Nonimal Case, Beginning of Life

### 3 5 3 3 Attitude Control

The ERTS attitude control system was evaluated for its ability to control a 3000 pound, 9-foot diameter advance earth resources satellite. The size and weight of this version were based on the maximum size and weight capability, of the Atlas/Centaur launch vehicle. This spacecraft was considered to have the basic ERTS orbital parameters and configuration while incorporating advanced bi-fold-solar paddles and a nine-foot diameter sensory ring.

The study results indicated that, with the exception of control of the yaw axis, the ERTS attitude control system can control a vehicle of this size to less than  $\pm 1^\circ$  in pitch and roll. Because of the increased yaw inertia of this configuration, the yaw flywheel inertia must be increased by a factor of three to avoid cyclic disturbances by the pneumatic gating threshold at a frequency which could quickly deplete the available gas supply. With this modification, the pointing error in this axis should remain below  $1^\circ$ . Another modification which is required involves the canting of the roll nozzles to avoid plume impingement on solar panels.

### 3 5 3 4 Structure/Configuration

A spacecraft configuration study was made to investigate and evaluate concepts of ring design and the ring/adapter/fairing interfaces for a nine-foot diameter ERTS spacecraft.

Figure 3 5-5 shows four different ring configurations studied. Table 3 5-2 lists the capacity of each of these configurations in terms of bays and total number of 1/0 type modules (i.e., 6 x 2 x 6.5 inches) the particular configuration can hold. The last column refers to the number of 1/0 modules which can be accommodated between the inner radius and the outer radius of the sensory ring, which is known as the inboard depth.

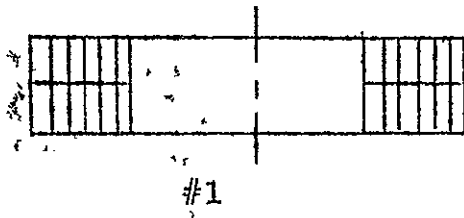
Table 3 5-2 Module Capacity

Configuration Number	Total Modules	Bays	No of Modules, Inboard Depth
Existing	144	18	4
1	324	27	6
2	360	18	4
		27	4
3	330	33	5
4	336	42	4

All of these configurations are a simple ring except Number 2 which is a "wedding cake" design using the existing ring as the top layer.

Structurally Configuration 1 is regarded as superior since the crossbeam span is less than for Configurations 3 and 4 and the truss attachment points are only a few inches inboard of





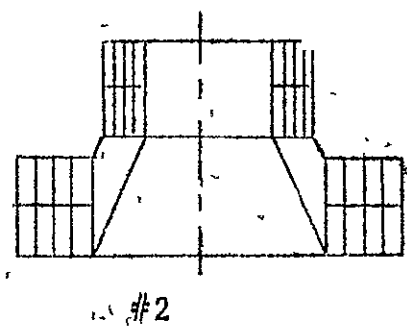
27 bays 6/6

324 total 1/0 spaces

I.R. = 30"

O.R. = 42"

} neglecting  
structure



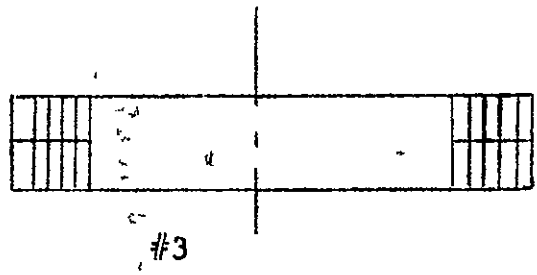
18 bays 4/4

& 27 bays 4/4

360 total 1/0 spaces

I.R. = 19.9"

O.R. = 38.0"

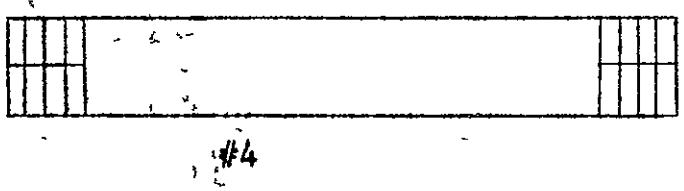


33 bays 5/5

330 total 1/0 spaces

I.R. = 36.7"

O.R. = 46.7"



42 bays 4/4

336 total 1/0 spaces

I.R. = 46.80"

O.R. = 54.80"

NOTE: I.R. = Inner Radius  
O.R. = Outer Radius

Figure 3.5-5. Conceptual Sensory Ring Configurations

the sensory ring. It is structurally desirable to have as small a distance as possible from these truss attachment points to the separation flange at the lower outside edge of the sensory ring, since this is a primary load path for several major loading conditions. Thermally, Configuration No. 3 is the best, but No. 1 can be modified to provide the needed additional thermal dissipation.

Overall, Configuration No. 1 was judged the best choice as a growth configuration, with No. 3 rated as second choice. The factors leading to this judgment are summarized in Table 3.5-3.

Table 3.5-3

Configuration Number	Pro	Con
1	Simple ring adequate space for sensors-truss points close to ring lowest weight	Outboard web extensions and radiator required
2	Lowest inertias - more than adequate thermal dissipation	More complex, heavier ring crossbeam area quite crowded, sensor mounting difficult, somewhat short of sensor mounting area More structural elements than computer can handle
3	Simple ring best thermal match-ample space for sensors	Ring too far from truss, crossbeam more flexible.
4	Simple ring - excess space for sensors	Ring furthest from truss points. Crossbeam, not ring, is primary structure Tight shroud clearance

### 3.5.3.5 Communications/Data Relay

The data requirements of earth observation satellites have continuously grown and, with the advent of the Earth Resources Program, will soon exceed the data capacity of existing and contemplated storage devices. The gathering of such large amounts of data results in the need for either more dedicated ground stations or continuous real-time data relay to the ground via a synchronous data relay satellite system. The latter approach eases or eliminates the storage requirement. In addition, the ability to have real-time command and control of the experiments and spacecraft subsystems can significantly improve the performance of the spacecraft in meeting the mission requirements.

The main advantages of the use of a synchronous satellite relay link for transmission of ERTS wideband sensor signals (RBV and/or MSS) include the following

1. A continuous link is provided so that on-board recording of wideband sensor signals is not required. (The WBVTR is considered the weakest link in the present wideband sensor subsystem of ERTS.)
2. Because of the continuous link, more data could be returned during a given mission life
3. The elimination of the WBVTR should result in improved quality of the received wideband signals.

For proper viewing of the relay satellite the ERTS relay link antenna must be capable of coverage over all portions of a sphere except that portion bonded by the earth's horizon. This coverage may be stated as an elevation angle of  $120^{\circ}$  and azimuth of  $360^{\circ}$ . Elevation is measured from the yaw axis, azimuth in a plane perpendicular to this axis. The variation of these two angles during a two-day period is shown in Figure 3 5-6. Comparable angles for a pitch-roll gimbal can be calculated.

Figure 3 5-7 is a block diagram showing the elements of the ERTS to DRS link. The relay unique equipment is shown in dotted lines. The output of the wideband sensor will be sampled and encoded by the Data Encoder. The encoder output is used to drive the modulator, which, in turn, modulates the X-band TWT RF amplifier. The modulation format tentatively selected is PCM-PM for the sensors. The ERTS antenna is coarsely pointed by pre-programmed commands, and, through the use of a monopulse acquisition and tracking system, will acquire and track the DRS via the beacon signal transmitted from the DRS.

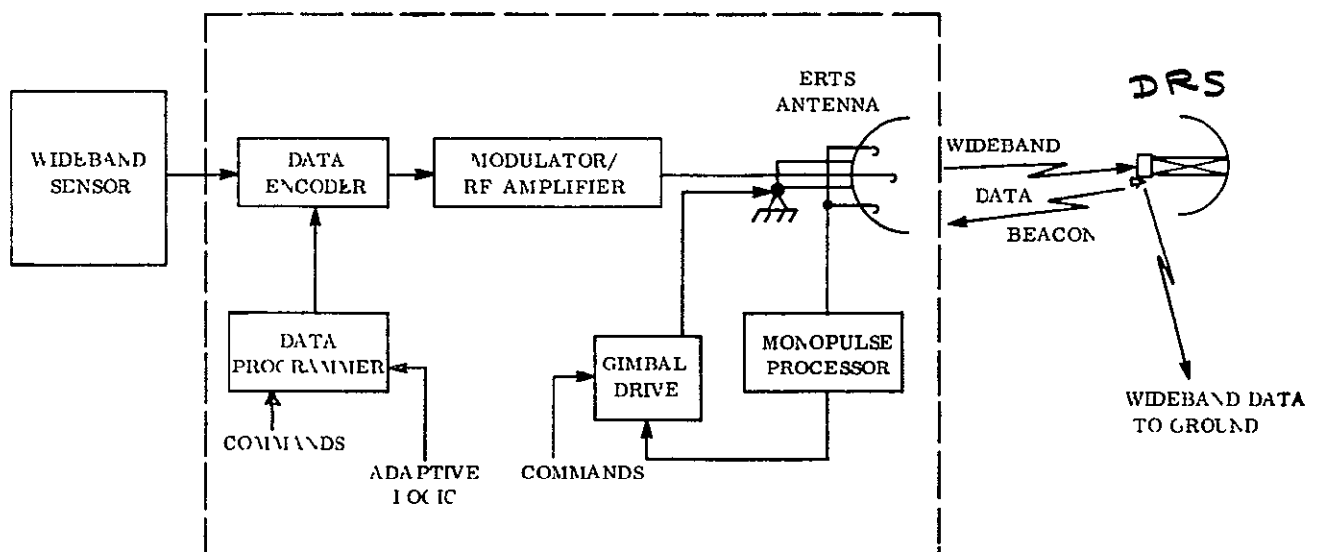


Figure 3 5-7 System Block Diagram

Table 3.5-4 shows the link calculations for three ERTS high-gain antenna sizes 2-, 3-, and 4.5-foot in diameter. The results are plotted in Figure 3.5-8 to show the variation of  $S/N_0$ , at the ground receiver, with the ERTS antenna diameter as the variable, this was done for two values of DRS G/T. The lower curve is for a G/T of +16 dB, while the other curve is for a G/T of +20 dB, this is to show the effect the G/T of the DRS system has on the antenna size required for ERTS.

The  $C/N_0$  required for each of the two ERTS sensors considered is shown for two different error rates (1)  $P_e = 4 \times 10^{-6}$  and (2)  $P_e = 10^{-4}$ . Figure 3.5-8 shows that to transmit the MSS data during the times of mutual visibility between ERTS and DRS, an antenna with a diameter of about 2.5 to 3.0 feet (with a 20-watt transmitter) is required. To relay the RBVC data, however, requires the use of an antenna between 3.5 and 4.5 feet. This is with a G/T of +16 dB.\* Considering a G/T of +20 dB reduces the antenna sizes to 1.5 to 2.0 feet for MSS data and about 2.2 to 2.6 feet for RBVC data.

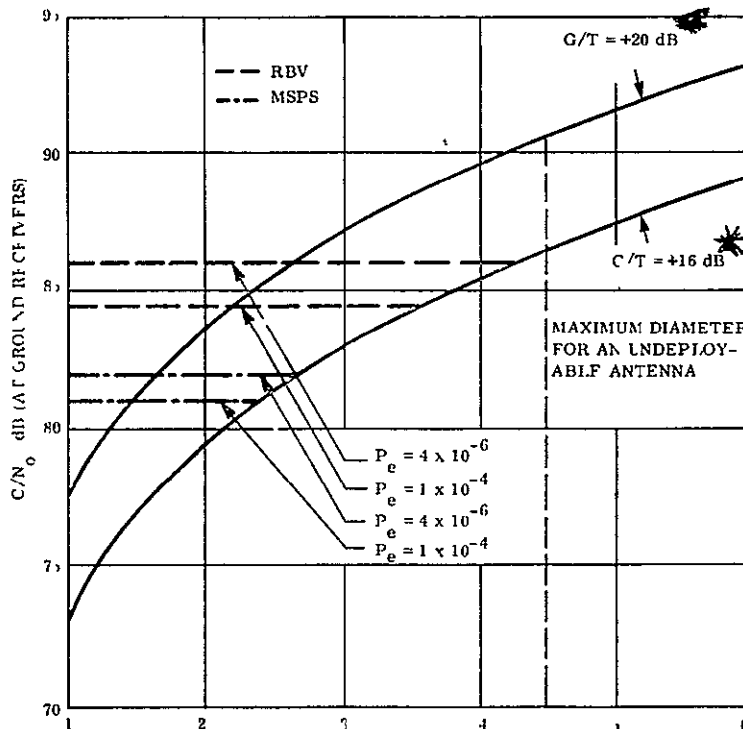


Figure 3.5-8 Carrier-to-Noise Spectral Density Versus Antenna Diameter

### 3.5.4 GROWTH POWER SYSTEMS

The feasibility of using Radioisotope Thermoelectric Generators (RTG's) as power sources on orbiting spacecraft was demonstrated on Nimbus III. The two RTG's used were SNAP-19's which are capable of supplying 25 watts each. However, in order to power the entire spacecraft subsystems as well as the sensor payloads the development of larger units will be required. This development is currently underway and will result in the design of an RTG with modular growth capacity. This unit is known as the Multi-Hundred Watt RTG (MHW-RTG)

\*ATS F/G characteristics assumed.

Table 3.5-4. ERTS to DRS Link Calculations

Item	2.0-Foot Parabola	3.0-Foot Parabola	4.5-Foot Parabola
$P_T$ , ERTS transmitter power	+13 dBw	+13 dBw	+13 dBw
$G_T$ , ERTS antenna gain	+31.5 dB	+35 dB	+38.5 dB
$L_T$ , ERTS transmission losses	<u>-1.0 dB</u>	<u>-1.0 dB</u>	<u>-1.0 dB</u>
EIRP, effective isotropic radiated power	+43.5 dBw	+47.0 dBw	+50.5 dBw
Path Loss = $-37.8 - 20 \log D$ $-20 \log F$ , $D = 24,600 \text{ nm}$ $F = 8.0 \text{ GHz}$	-203.6 dB	-203.6 dB	-203.6 dB
Polarization loss*	-3.0 dB	-3.0 dB	-3.0 dB
Pointing loss	-1.0 dB	-1.0 dB	-1.0 dB
Atmospheric loss	<u>-1.0 dB</u>	<u>-1.0 dB</u>	<u>-1.0 dB</u>
Link loss	-208.6 dB	-208.6 dB	-208.6 dB
G/T, overall gain to equiva- lent temperature ratio at 8.0 GHz	+16 dB	+16 dB	+16 dB
K, Boltzman's Constant	-228.6 dB	-228.6 dB	-228.6 dB
$C/N_o$	+79.5 dB	+83.0 dB	+86.5 dB

Table 3.5-4. ERTS to DRS Link Calculations (Cont'd)

	2.0-Foot Parabola	3.0-Foot Parabola	4.5-Foot Parabola
$P_T$ , ERTS transmitter power	+13 dBw	+13 dBw	+13 dBw
$G_T$ , ERTS antenna gain	+31.5 dB	+35 dB	+38.5 dB
$L_T$ , ERTS transmission losses	<u>-1.0 dB</u>	<u>-1.0 dB</u>	<u>-1.0 dB</u>
EIRP, effective isotropic radiated power	+43.5 dBw	+47.0 dBw	+50.5 dBw
Path Loss = $-37.8 - 20 \log D$ $-20 \log F$ , $D = 24,600 \text{ nm}$ $F = 8.0 \text{ GHz}$	-203.6 dB	-203.6 dB	-203.6 dB
Polarization loss*	-3.0 dB	-3.0 dB	-3.0 dB
Pointing loss	-1.0 dB	-1.0 dB	-1.0 dB
Atmospheric loss	<u>-1.0 dB</u>	<u>-1.0 dB</u>	<u>-1.0 dB</u>
Link loss	-208.6 dB	-208.6 dB	-208.6 dB
G/T, overall gain to equiva- lent temperature ratio at 8.0 GHz using the 30-foot parabola	+16 dB	+16 dB	+16 dB
K, Boltzman's Constant	-228.6 dB	-228.6 dB	-228.6 dB
$C/N_o$	+79.5 dB	+83.0 dB	+86.5 dB
*3.0-dB polarization loss due to the linear feed of ATS F&G 30-foot paraboloid. An improvement in link performance of up to 3.0-dB can be obtained by providing a circularly polarized X-band feed to the ATS-G feed system.			

The Multi-Hundred Watt Radioisotope Thermoelectric Generator (MHW-RTG) is being developed by the General Electric Company for the Atomic Energy Commission. The MHW-RTG design is currently in Phase I and the performance characteristics are therefore not final but may be considered to be representative of the generator which is anticipated for flight in the post 1973 time period.

An artist's conception of the MHW is shown in Figure 3 5-9 identifying the component parts. The MHW is basically two 1,000 watt cylindrical heat sources supported on a common centerline and surrounded by 12 thermoelectric panels arrayed to form a hexagonal prism.

The 144 watt, 30 volts reference design generator can be increased in power to approximately 216 watts with the addition of another 1,000 watt heat source and a proportionate increase in thermoelectric panels.

Minor variations in output power can be made by adjusting the number of thermoelectric panels and/or heat source fuel loading. The design characteristics are given in Table 3 5-5.

Table 3 5-5 Summary of MHW-RTG Reference Design Characteristics

<u>PERFORMANCE</u>		<u>CONVERTER (Continued)</u>	
Power	114 watts BOM 138 watts after 1 year 111 watts FOM (12 years)	Thermoelectric Couples	
Voltage	30 Vdc	Number	288 (Series-Parallel)
Fuel Loading	2000 watts (2 1000 watt heat sources)	Material	Silicene (80% Silicon)
Weight	59.7 lb	Leg Dimensions	N-leg 0.8 in long, by 0.0188 in <sup>2</sup> P-leg 0.8 in long, by 0.0208 in <sup>2</sup>
Hot Junction	1100°C (2012°F) BOM	Heat Sources	12 - 24 Couples/Panel
Cold Junction	61.0°F BOM	Insulation	Inde-lype Foil
Conversion Efficiency	7.2% BOM	Heat Source Convty	Sized for 60°C in dia Heat Source
Specific Power	2.11 watts/lb		
<u>GEOMETRY</u>		<u>HEAT SOURCE</u>	
Diameter	11.85 in across diagonals (max)	Quantity	Two
Length	20.0 in	Fuel	Pu-238 Solid Solution Ceramic
Configuration	6 sided structure no fins	Geometry	4.0 in dia X 8.28 in long
		Installation in Converter	In-line Heat Source Axial Preload
		Materials	TZM Liner WC 3015 or TZM Impact Shell Pyrolytic Graphite Insulation WC 3015 Outer Shell
<u>CONVERTER</u>		On Pad Cooling	Water 10 ft/sec 1/4 in Tubes Welded to Cladding Separate Loop for Each Heat Source
End Closures	Spoked Titanium	Ventid	Yes
Load Structures	6 Titanium Longerons		
Radiators	Beryllium - Iron Titanate Coating ε > 0.85		

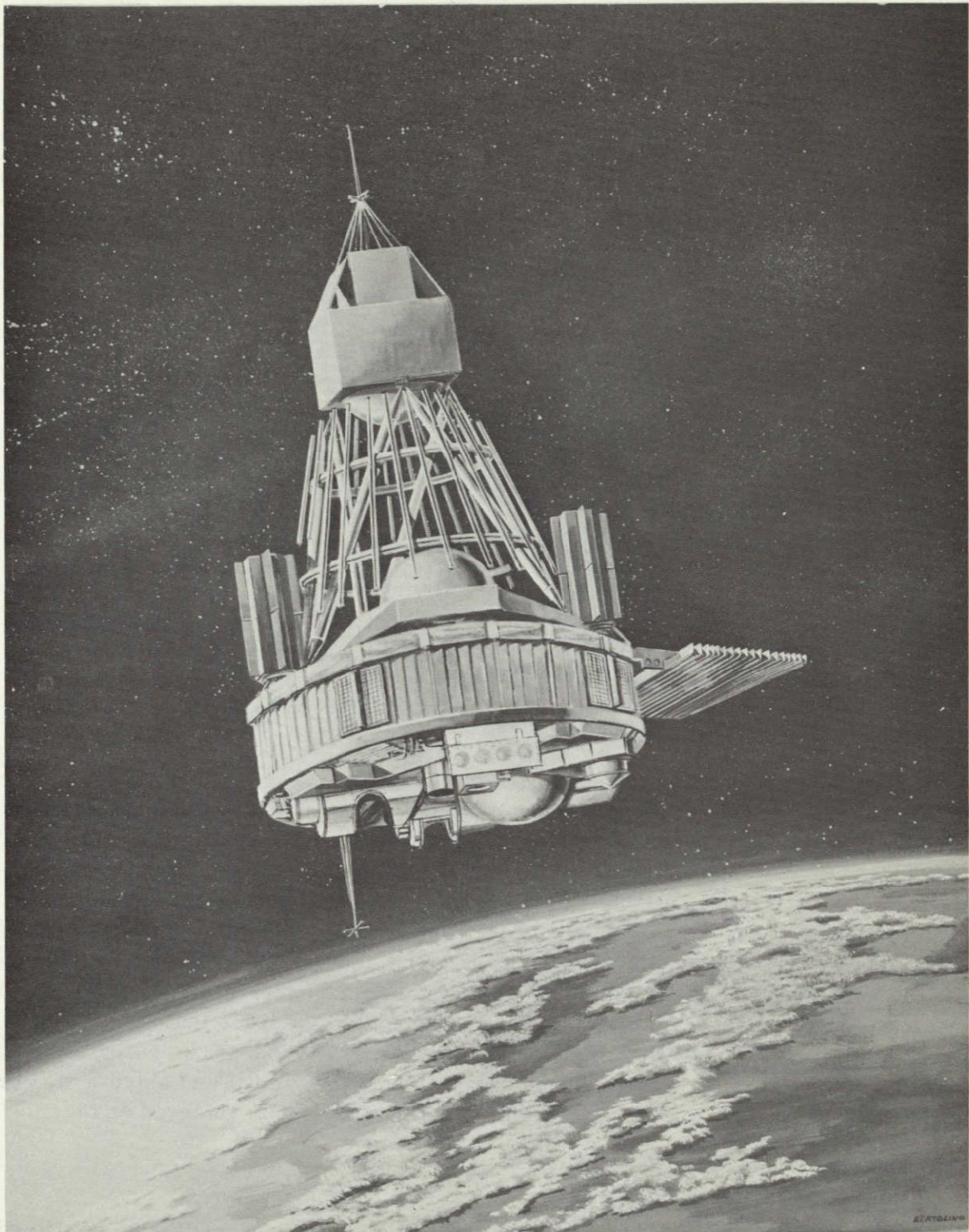


Figure 3.5-9. Multi-Hundred Watt Radioisotope Thermoelectric Generator



A major advantage of the MHW-RTG for the ERTS mission is the modular flexibility of the MHW-RTG to supply power to the vehicle in increments of 144 watts, thereby allowing a considerable degree of flexibility in the design of the experiments. An artist's concept of the MHW-RTG in a finned geometry configuration is shown in Figure 3.5-10. Two generators would be providing 288 watts total electrical power at the beginning of the mission in this configuration.

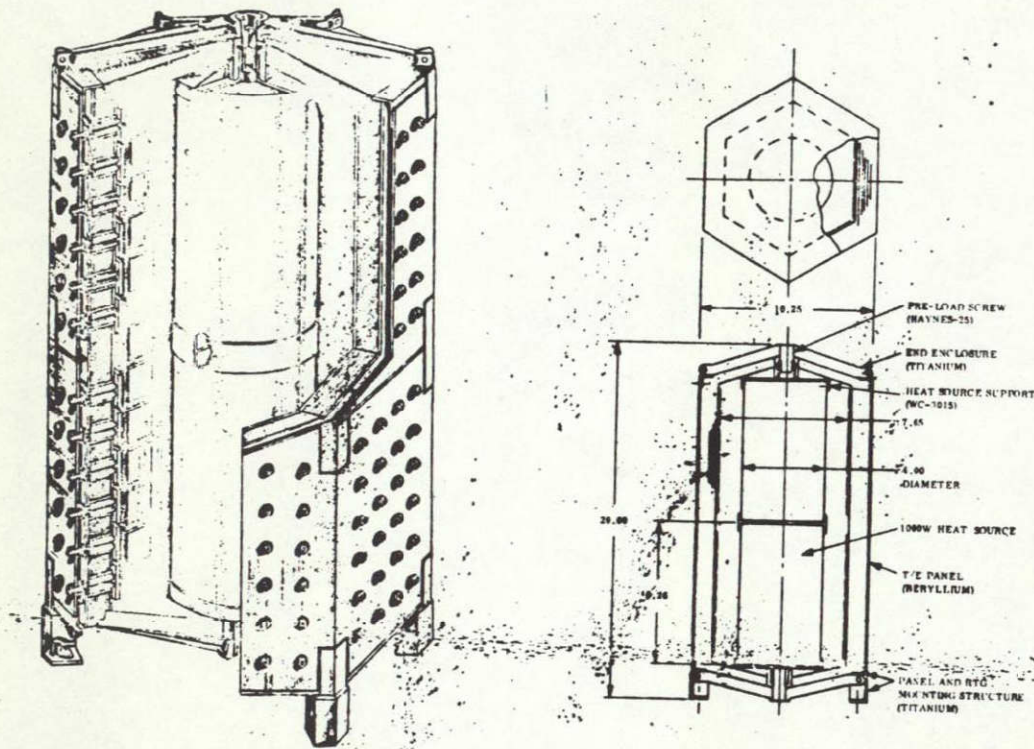


Figure 3.5-10. Multi-Hundred Watt Radioisotope Thermoelectric Generator in Finned Geometry Configuration

By examining the ERTS launch configuration, it is clear that the largest volume available for a parabolic dish antenna is located above the attitude control system. A layout was prepared (Figure 3.5-11) which indicates that a 54-inch diameter dish could be accommodated. It would be pointed by means of a two-axis gimbal, which, for conservatism, was assumed to be as large as the unit used in the Apollo command module. In order that the antenna beam clear the solar array at all times, it would be necessary to extend the entire assembly some 7.5 feet. In order to survive the launch environment, the gimbal and antenna will be latched to the spacecraft to minimize vibrational effects until orbit is achieved and then deployed.

### 3.5.5 ALTERNATE ORBITS

The ERTS Attitude Control System can operate effectively at orbit altitude between 300 and 2000 nm and at eccentricities between 0 and 0.15. This has been shown in many studies of this subsystem. It has also been evaluated as a function of ascending node time, ranging

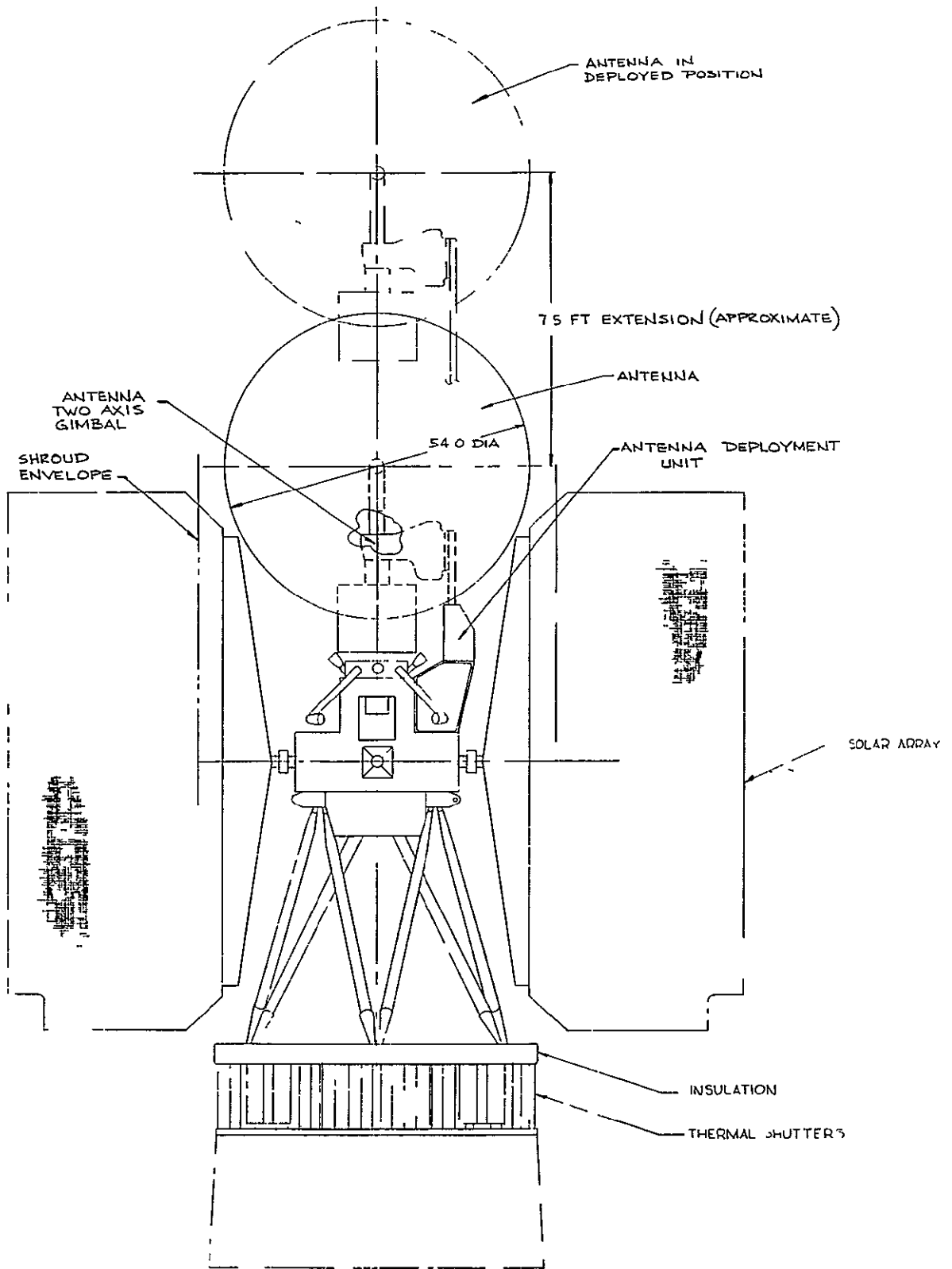


Figure 3 5-11 ERTS Relay Antenna Concept

11 February 1970

from mid-morning to high noon (Nimbus orbit) through mid-evening (ERTS A/B). To complete the cycle, a study was performed on the feasibility of operating this subsystem in a twilight orbit (6 AM - 6 PM). This orbit has the same altitude, inclination and launch direction as a high-noon orbit. The twilight orbit provides the opportunity to operate with a fixed solar array. The angle between the sunline and the surface of the solar array (commonly called the beta angle) then becomes a function of the orbit inclination and the time of year. This is illustrated in Figure 3.5-12. The array is located so that its sensitive surface is in the orbit plane.

This orbit offers the additional advantages of

1. Reducing the number of battery modules required.
2. Reducing the number of thermal shutters needed.
3. Eliminating the need for the solar array drive.
4. Maximizing the solar array power output.
5. Improving system reliability.
6. Reducing spacecraft weight.

The disadvantages are that there is no pitch momentum bias mode (which is a back-up mode not essential), and there may be some impact on experiment design.

The study results indicated that the ERTS spacecraft can easily fly in a twilight orbit, thus proving the extreme versatility of the vehicle.

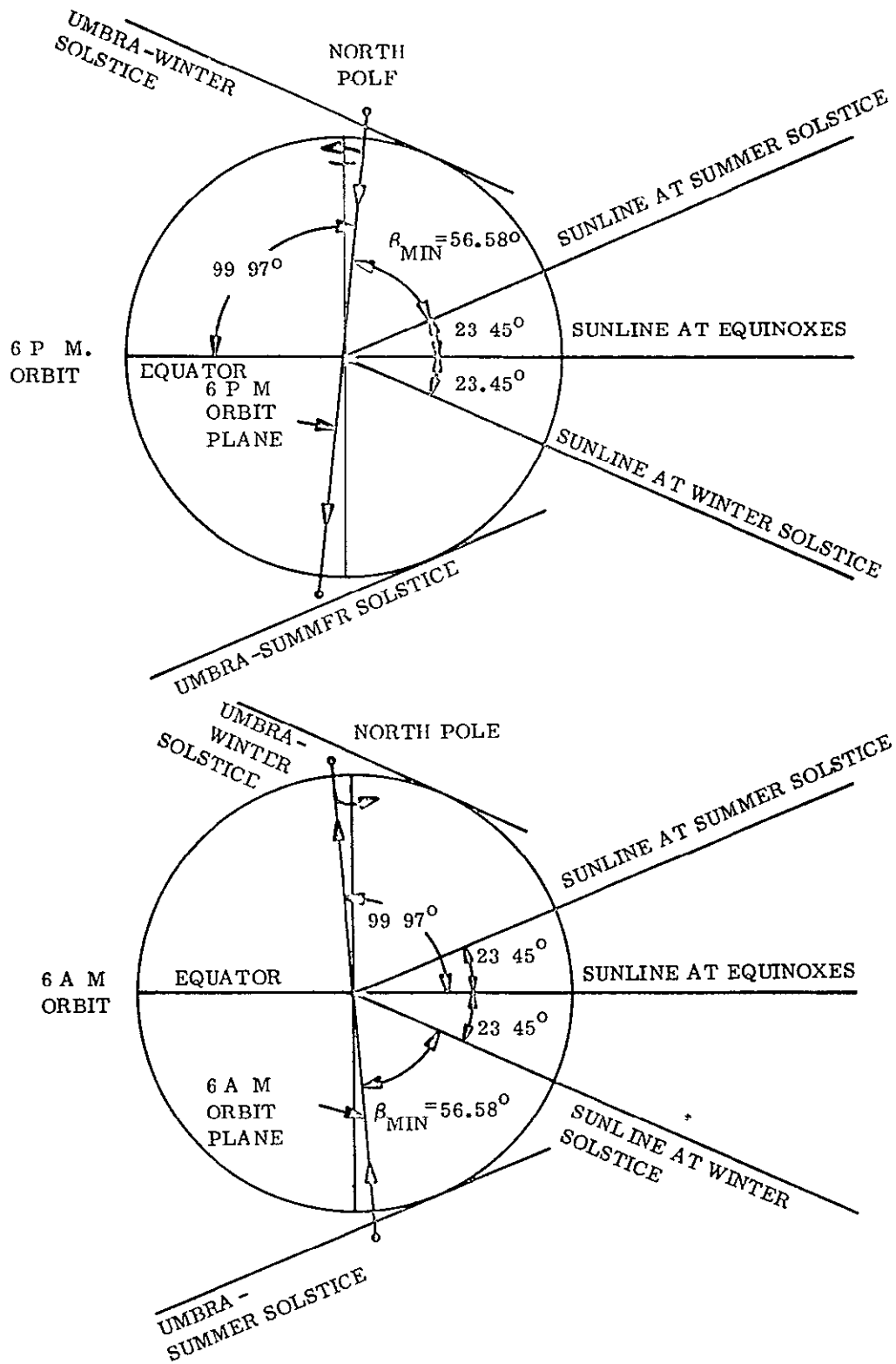


Figure 3.5-12 Twilight Orbits

# SECTION 4

## SYSTEM STUDIES

4.1	ERTS System Reliability . . . . .	4-2
	4.1.1 Summary . . . . .	4-2
	4.1.2 Principles of Reliability Assessment . . . . .	4-5
	4.1.3 Source of Failure Rate Data . . . . .	4-5
	4.1.4 Subsystem Reliability Assessments . . . . .	4-6
4.2	Orbit Analysis . . . . .	4-21
	4.2.1 Introduction . . . . .	4-21
	4.2.2 Nominal Orbit Selection . . . . .	4-22
	4.2.3 Drag Decay . . . . .	4-28
	4.2.4 Nominal Ground Track Control . . . . .	4-32
	4.2.5 Orbit Error Analysis . . . . .	4-35
	4.2.6 Operational Ground Track Control . . . . .	4-43
	4.2.7 Launch Window Analysis . . . . .	4-48
4.3	Image Location and Coverage . . . . .	4-75
	4.3.1 General . . . . .	4-75
	4.3.2 Units . . . . .	4-76
	4.3.3 Gains . . . . .	4-76
	4.3.4 Implementation and Relative Error Effects . . . . .	4-78
	4.3.5 First-Order Error Equation, Its Solution, and Attitude Determination Sensor Requirements . . . . .	4-79
	4.3.6 Basic Coverage . . . . .	4-82
	4.3.7 Rate Requirements . . . . .	4-86
	4.3.8 Requirements Summary . . . . .	4-91
4.4	Time Annotation . . . . .	4-92
	4.4.1 General . . . . .	4-92
	4.4.2 Approaches to Time Annotation . . . . .	4-94
	4.4.3 Discussion of Approaches . . . . .	4-95
	4.4.4 Baseline Approach . . . . .	4-98
4.5	Mission Simulation . . . . .	4-100
	4.5.1 Simulation Problem (Introduction) . . . . .	4-100
	4.5.2 Simulation Model . . . . .	4-100
	4.5.3 Simulation Cases . . . . .	4-104
	4.5.4 Specific Study Results . . . . .	4-109
4.6	Wideband Video Tape Recorders Management . . . . .	4-137
	4.6.1 Recorder Management . . . . .	4-137
	4.6.2 Tape Handling Requirements . . . . .	4-140
	4.6.3 Design Approach . . . . .	4-142

## SECTION 4

## SYSTEM STUDIES

As part of the three-month ERTS Phase B/C SSD study numerous overall system and mission analyses and trade studies have been performed. These studies impact the evolution of the selected spacecraft design and operational concepts as well as other ERTS system elements. Several of these study areas are being continued and extended in support of the ongoing ground data handling system design. This section reports the results of those studies affecting the spacecraft system design. They are presented in the following groupings

1. Spacecraft Reliability Assessment
2. Orbit Analysis
3. Image Location and Coverage
4. Time Annotation
5. Mission Simulation
6. WBVTR Management

The reliability assessment examined the individual spacecraft subsystem designs proposed for ERTS A/B and arrived at the overall spacecraft reliability for a one year mission. This assessment was, of course, enhanced through the extensive use of redundancy in the proposed system design.

The orbit analyses performed have established the requirements for the spacecraft orbit adjust subsystem in terms of its functional capability, sizing and operational features. Also, the operational requirements and procedures have been developed for the establishment and maintenance of ground track control.

Image location requirements have been analyzed in order to arrive at the system error allocations and, in turn, these allocations reflected as requirements on the spacecraft and ground systems for attitude sensing and time correlation. Attitude control requirements, although specified by the government, have also been reviewed to assure consistency with the mission coverage requirements.

Several approaches to the time annotation of data collected by individual sensors and subsystems have been traded-off in order to select a system approach which will achieve the time correlation required for overall system operation.

Extensive mission simulations have been performed in order to fully understand the overall system operation, to establish design requirements, and to evaluate the capability of the proposed designs. These simulations have, for example, been used to produce worst-case power profiles for sizing the power system and for worst-case operational sequences to establish stored requirements.

The problems in operational management of the spacecraft Wideband Video Tape Recorders (WBVTR's) have been investigated and the requirements for recorder status and control established. These requirements dictate the spacecraft functional capability for effective orbital operations.

#### 4.1 ERTS SYSTEM RELIABILITY

##### 4.1.1 SUMMARY

All subsystems except for the payload were analyzed to assess the reliability of the ERTS spacecraft. For each subsystem reliability is defined as the probability that the subsystem will operate for one year without degradation affecting the ERTS mission. These subsystems and their reliabilities R are

Attitude Control	- R = .815
Electrical Integration	- R = .962
Orbit Adjust	- R = .992
Power	- R = .959
Structures	- R = .999+
C. &D. H	- R = .945

The overall system reliability is the product of these subsystem reliabilities It is

$$R_{\text{ERTS}} = .71$$

##### 4.1.1.1 ERTS System Reliability

A simplified reliability block diagram for the ERTS system is given in Figure 4 1-1. It shows the major blocks within each subsystem. Many of these blocks contain internal redundancy. Reliabilities shown are for a one year mission.

##### 4.1.1.2 Redundancy

Redundancy is widely used in the ERTS system to minimize the probability of catastrophic failure. The reliability block diagrams for the various subsystems show redundancy between components. Internal redundancy is discussed in the text. The present discussion is a summary of redundancy. It must be emphasized that degraded modes of operation are not included in this reliability assessment (with the exception of the wide band transmitter as discussed in the C&DH subsystem analysis). Redundancy is considered in this discussion only if the redundant mode of operation allows full capability for performing the ERTS mission. Redundancy incorporated into the design of the spacecraft subsystems is briefly described in the following sections

C&DH Subsystem. Functional redundancy is widely used in this subsystem. Both the MSFN and STADAN systems may be used to transmit commands to the command

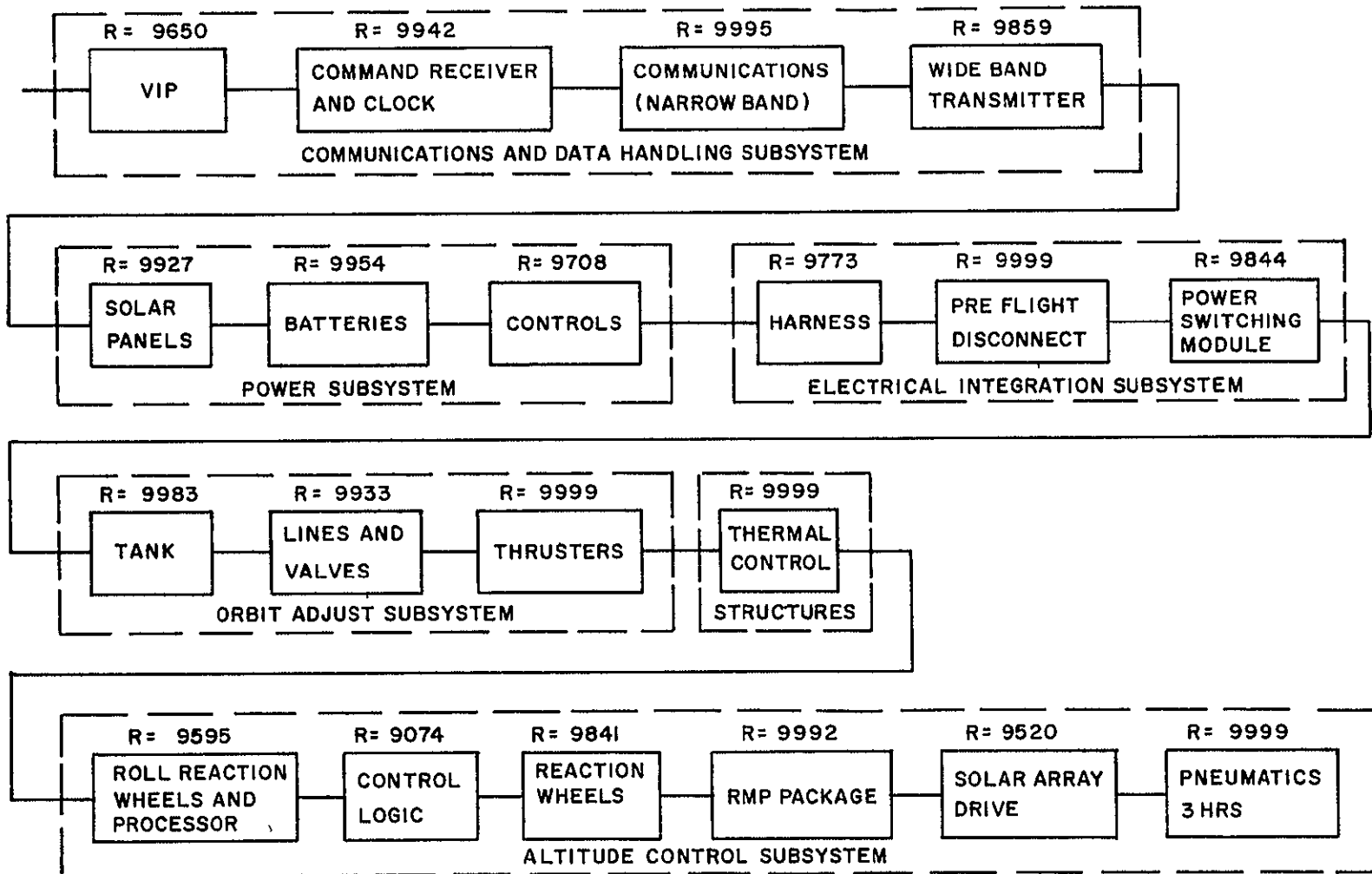


Figure 4.1-1. Simplified ERTS System Reliability Block Diagram



Within each of the S-Band and VHF systems there is redundancy of receivers and demodulators. Broadcasting of "housekeeping" data can be accomplished through either the S-Band or VHF systems. The wide-band system transmits payload data on either PCM or video channels simultaneously and the redundant configuration permits a degraded mode of operation in which either channel may be used, but not both simultaneously. The VIP is designed to permit functional redundancy between the memory and the eleven stage counter.

In addition to the functional redundancy which has been described in the C&DH subsystem, substantial block redundancy (two identical components) has been incorporated into the system design. Many block redundant components are "standby", that is, they are unpowered until needed, which reduces the probability that the redundant component will fail. The components employed in a standby redundant configuration are the S-Band and VHF command receivers and demodulators, the command matrix drivers and decoders, all clock components, the VHF transmitters, the USB transponders, and the premodulation processors. Components in a parallel redundant configuration (both powered) are S-band and VHF command receiver systems (each containing internal standby redundancy), the command integrators, the power supplies and command decoders, and (in the VIP) multiplexers, coders, formatter logic units, and reprogrammers.

Power Supply Subsystem The solar array contains complex internal redundancy. The failure of single cells or single strings do not cause loss of the mission. Up to 9 string failures are permitted without loss of the solar array. The redundant configuration of the batteries permits the loss of 3 of 8 batteries without loss of the mission. Within the power control module, the auxiliary regulators and pulse width modulators are in parallel redundancy.

Attitude Control Subsystem. The reaction wheel scanners with signal processors are in parallel redundancy. The Rate Measuring Packages are in standby redundancy. The pneumatics are required for acquisition and are required for reacquisition, but the pneumatics are backed up by the Magnetic Moment Assembly in the wheel unloading mode. In addition several limited, but nevertheless mission useful, functionally redundant modes exist.

Structures Subsystem. In this subsystem, the thermal control components are the only ones considered as potentially contributing to unreliability. In the active thermal control system, there are springs backing up the bellows in each assembly to hold the shutters in a predetermined "fail-safe" position if the bellows fail. Each shutter assembly thus has high reliability, and the complete failure of a single assembly would probably not degrade the operation of the spacecraft. Thus the shutter assemblies may be considered redundant to each other. The passive thermal control system is not considered to have any significant failure mode.

Orbit Adjust Subsystem. This highly reliable system contains parallel redundant explosive valves, normally closed. The solenoid valves on the engines are two-seat, two-coil valves providing internal redundancy against leakage.

#### 4 1.2 PRINCIPLES OF RELIABILITY ASSESSMENT

In the components list for each subsystem, either a failure rate or a one year reliability is given for each component. The appearance of a failure rate implies that component is assumed to have an exponential distribution of time-to-failure, so that the R for time t is

$$R = e^{-\lambda t}$$

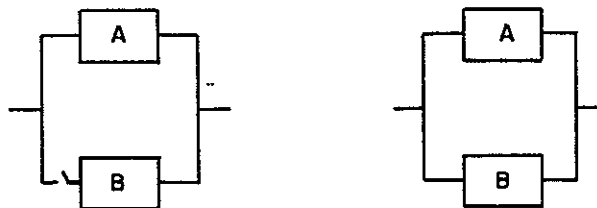
Components which do not have an exponential distribution of time-to-failure have a one year reliability given in the component lists.

Reliability for the case of standby redundancy is computed assuming that the standby component has a failure rate during its dormant or unpowered life equal to 10% of its normal "active" failure rate. If component A with failure rate  $\lambda_A$  is the active component and component B with failure rate  $\lambda_B$  is in standby, the reliability R of this redundant pair for time period T is

$$R = e^{-\lambda_A T} + \frac{\lambda_A}{\lambda_A - .9\lambda_B} R_S (e^{-\lambda_B T} - e^{-(\lambda_A + .1\lambda_B) T}),$$

where  $R_S$  is the reliability of the switch.

Standby redundancy is shown in the reliability block diagrams with a broken line indicating switching. Standby and parallel redundancy are diagrammed as follows



For all subsystems, reliability is computed assuming a required mission time of one year

#### 4 1.3 SOURCE OF FAILURE RATE DATA

Reliability assessments for ERTS are in large part based on assessments of the Nimbus B spacecraft and the Nimbus D attitude Control Subsystem performed by Operations Research Inc. (ORI) which reported these assessments in Technical Reports 469 and 541. The notations ORI 469 and ORI 541 used in the present document refer to these reports.

The basic ground rule followed by ORI in their reliability assessment was the use of MIL-HDBK-217A failure rates at ground environment improved by one order of magnitude to

account for parts screening and the use of preferred parts. The rationale for the use of these failure rates is given in ORI 541, pp 30 and 31. For consistency, this ground rule was followed in the present report where piece-part analysis was performed or where vendors performed assessments using unimproved MIL-HDBK-217A rates. Exceptions to the use of ORI or MIL-HDBK-217A rates. Exceptions to the use of ORI or MIL-HDBK-217A rates are noted in components lists and discussed in the text for the subsystems where they appear.

#### 4 1.4 SUBSYSTEM RELIABILITY ASSESSMENTS

The subsystem reliability assessments performed on the phase B/C Spacecraft System Studies are summarized in the following sections.

##### 4.1.4.1 Structures Subsystem

Aside from the thermal control components, the probability of failure of this subsystem is assumed to be negligible. The reliability assessment of the thermal controls follows the assessment performed by Operations Research Inc. on the Nimbus B thermal controls and discussed in ORI Technical Report 469, pp. 57-60.

On the spacecraft, 16 bays have shutter assemblies. For each assembly, the failure rate is based on the following parts count.

<u>Part</u>	<u>Failure Rate <math>\lambda \times 10^{-6}</math></u>
Bellows	1.2
Rack and four pinion gears	.6
Eight bearings	1.6
Spring	<u>.01</u>
	$\lambda = 3.41 \times 10^{-6}$

The reliability of a single bellows assembly for one year is .97057.

The bellows system in the shutter assembly is backed up by a spring to provide fail-safe operation. The failure rate of this spring is  $.01 \times 10^{-6}$ /hour, and its reliability is .999912. Thus the reliability of a shutter assembly including the spring backup is

$$R_{\text{assembly}} = 1 - (1 - .97057) (1 - .999912) = .999997$$

The probability that all 16 assemblies work throughout one year is

$$R = R_{\text{assembly}}^{16} = .99998.$$

There are 15 compensation loads. Each load contains three heaters in parallel redundancy. Each heater operates for 2000 hours. The failure rate of a heater is  $22.0 \times 10^{-6}$  failures/hour (PRC data at 50 percent confidence).

In each load, one heater of three is required. If R denotes the reliability of a single heater, the probability  $P_{1/3}$  that at least one of three operates is

$$P_{1/3} = R^3 + 3 R^2 (1-R) + 3R (1-R)^2$$

The reliability of a single heater is

$$R = e^{-22.0 \times 10^{-6} \times 2000} = .95695,$$

and, owing to the two-fold redundancy,

$$P_{1/3} = .99992.$$

This is the reliability of a compensation load.

It is conservatively assumed that at least 2 loads could fail without causing spacecraft failure. The probability that at least 13 loads succeed is

$$P_{13/15} = P_{1/3}^{15} + 15 P_{1/3}^{14} (1 - P_{1/3}) + 105 P_{1/3}^{13} (1 - P_{1/3})^2$$

$$P_{13/15} > .9999$$

The thermal control for the Attitude Control Subsystem has a negligible probability of failure (ORI 469, Table 30). Thus the reliability of the overall thermal control system exceeds 9999

#### 4.1.4.2 C&DH Subsystem

The C&DH subsystem is quite large and complex. As the subsequent discussion will show, a great deal of redundancy is utilized to minimize the probability of degraded performance or failure. The success of redundancy in the design is shown by the achievement of the very high subsystem reliability of 9453 for successful performance for a one year mission

It should be emphasized that this reliability is the probability of achieving all mission requirements. In addition, one degraded mode has been considered, it is discussed following the discussion of subsystem reliability.

The components of the C&DH subsystem are shown in Table 4.1.4-1. In this table the VIP appears as a single component, it is broken down in Table 4.1.4-2.

The Versatile Information Processor is built by Radiation Inc. Its components are shown in Table 4.1 4-2.

TABLE 4.1.4-1. COMPONENTS OF C&amp;DH SUBSYSTEM

Symbol	Component	Failure Rate or One-Yr Reliability	Source, Comments
A	VIP	R=0.965006	Radiation Inc.
B	VHF Transmitter	1.1064	ORI 469, p. 202, reduced by one order of magnitude
C	PM Transponder	3.25	Collins Radio
D	Summing Networks	0.0823 each	ORI 469, p. 201, reduced by one order of magnitude Compare ORI 541, p. 87
E	VCO (5)	0.1784 each	ORI 469, p. 186, reduced by one order of magnitude
F	Buffer	0.0823	Assumed equivalent to 1 summing network
G	S-Band Receiver	1.6048	ORI 469, p. 113, assumed equivalent to VHF Rcvr
H	Demodulator	3.8295	ORI 469, p. 113
I	VHF Receiver	1.6048	ORI 469, p. 113
J	Integrator	1.5	Estimated
K	Power Supply Unit	5.834	Rates supplied by vendor. Conservatively based on MIL-HDBK-217A. Reduced by one order of magnitude for ERTS.
L	Comdec	3.6475	
M	Matrix Driver and Decoder	3.341	
N	Comstor Logic	1.457	
O	Comstor Memory	3.177	
P	OSC	1.069	
Q	Frequency Generator	2.795	
R	TC Generator	2.49	
S	Filter	0.005	ITT
T	Modulator	0.8452	Piece part analysis

TABLE 4 1 4-1. COMPONENTS OF C&DH SUBSYSTEM (Continued)

Symbol	Component	Failure Rate or One-Yr Reliability	Source, Comments
U	Power Amplifier	0.5291	HAC
V	Antenna	0.03	Estimate
W	Switch	0.02	MIL-HDBK-217A

TABLE 4 1.4-2. COMPONENTS OF THE VIP

Symbol	Component	One-Year Reliability for Single Component
A	Memory	0.5978
B	Memory Sequencer	0.9660
C	11 Stage Counter	0.9969
D	Multiplexer	0.9887
E	Redundant Multiplexer Circuits	0.9508
F	Coder	0.9737
G	Formatter Logic	0.9342
H	Reprogrammer	0.9180
I	Transmitter	0.9825
J	Isolator	0.9903
K	Switching Circuit	0.9999

The reliability block diagram of the VIP is shown in Figure 4.1 4-1.

The mathematical model for the reliability of the VIP is based on the assumption that all components are powered throughout the mission. The formula for the reliability of the VIP (letting  $R_X$  denote the one year reliability of component X, where the symbol is given in Table 4.1.4-2) is

$$R_{VIP} = [1 - (2R_A - R_A^2)(2R_B - R_B^2)] [1 - (2R_C - R_C^2)] \\ \times R_D (2R_E - R_E^2)(2R_F - R_F^2)(2R_G - R_G^2) \\ \times (2R_H - R_H^2)(2R_I - R_I^2) R_J R_K$$

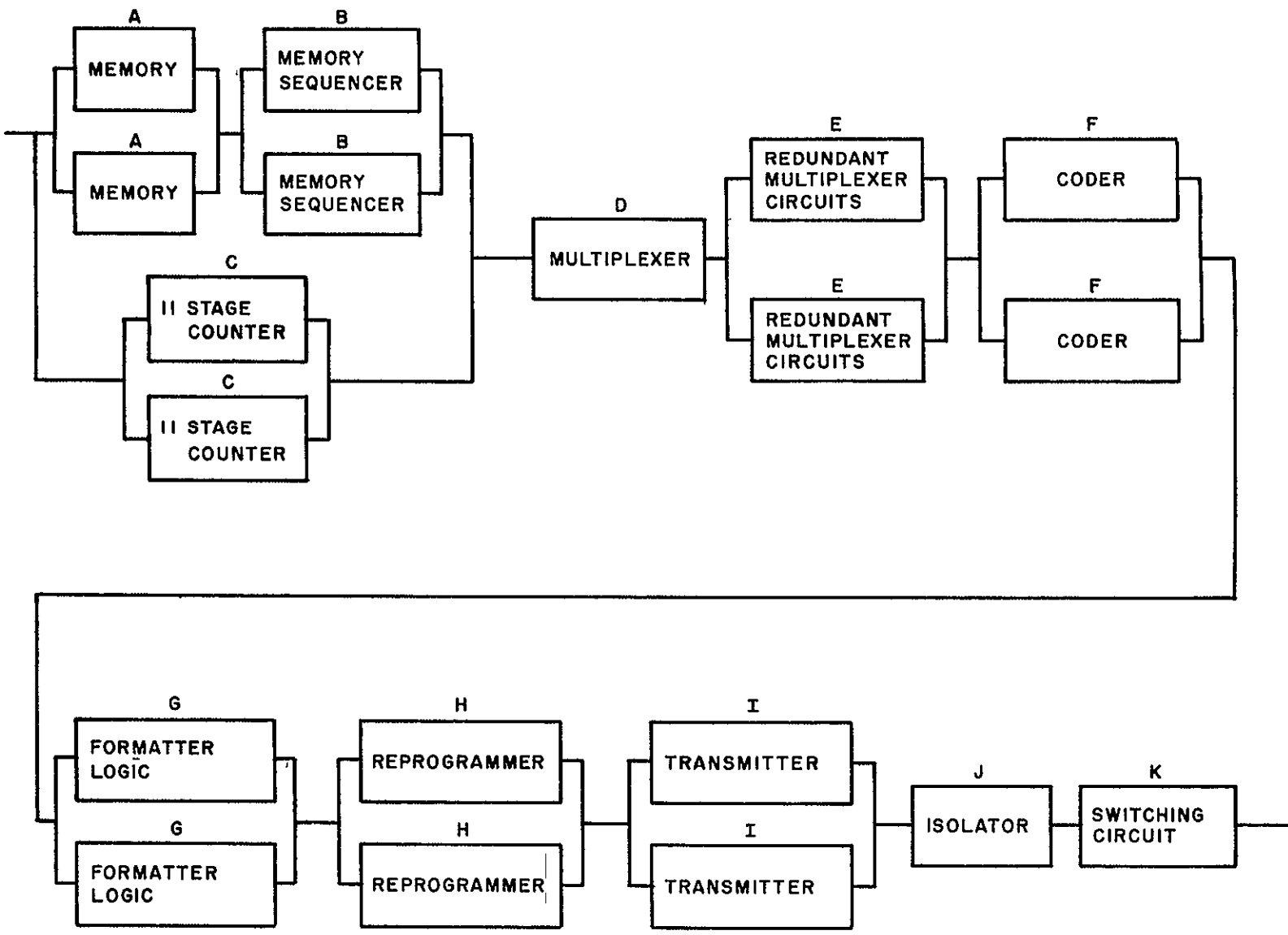


Figure 4.1.4-1. Reliability Block Diagram for VIP

The reliability of the VIP for 1 year is .965006

The reliability block diagram for the entire C&DH subsystem is given in Figure 4.1.4-2

The mathematical formula for the overall reliability of the C&DH subsystem uses the symbols for components given in Table 4.1.4-1 and Figure 4.1.4-2. For convenience of notation, let

$$R_x = e^{-\lambda_x T} = \text{reliability of component X with failure rate } \lambda_x \text{ for time}$$

$$\Phi(\lambda) = 2e^{-\lambda T} - e^{-2\lambda T} = \text{reliability of parallel redundant components with failure rate } \lambda$$

$$\Theta(\lambda) = e^{-\lambda T} + 10e^{-0.2 \times 10^{-6} \times T} \left( e^{-\lambda T} - e^{-1.1\lambda T} \right) = \text{reliability of primary plus standby paths with failure rate } \lambda, \text{ where paths are identical}$$

The reliabilities of components S, T, U, and W are computed assuming a "powered" time of 1/2 year.

The subsystem reliability R is given by the following formula

$$R = \left[ 1 - (1 - \Theta(\lambda_G + \lambda_H)) (1 - \Theta(\lambda_I + \lambda_H)) \right] \Phi(\lambda_J) \\ \times \Theta(\lambda_K + \lambda_L) \Theta(\lambda_M) \Theta(\lambda_P) \Theta(\lambda_Q) \Theta(\lambda_R) \Phi(\lambda_N) \\ \times \Phi(\lambda_O) \Theta(\lambda_B) \Theta(\lambda_C) \Theta(2\lambda_D + 5\lambda_E) \Theta(\lambda_F) \\ \times R_A R_T^2 R_U^2 R_V R_W (2R_S^2 R_W^2 - R_S^4 R_W^4)$$

$$R = .94534$$

A degraded mode of operation was identified for the wideband transmitter. In normal operation, both MSS PCM data and RBV video data may be transmitted simultaneously. In the degraded mode, either may be transmitted upon command, but not both. The probability of operating at least in this degraded mode is .95840. This probability includes the probability of complete success (.9453) plus the probability of degraded operation only (0.0131). This degraded mode of operation replaces the configuration (in Figure 4.1.4-2).



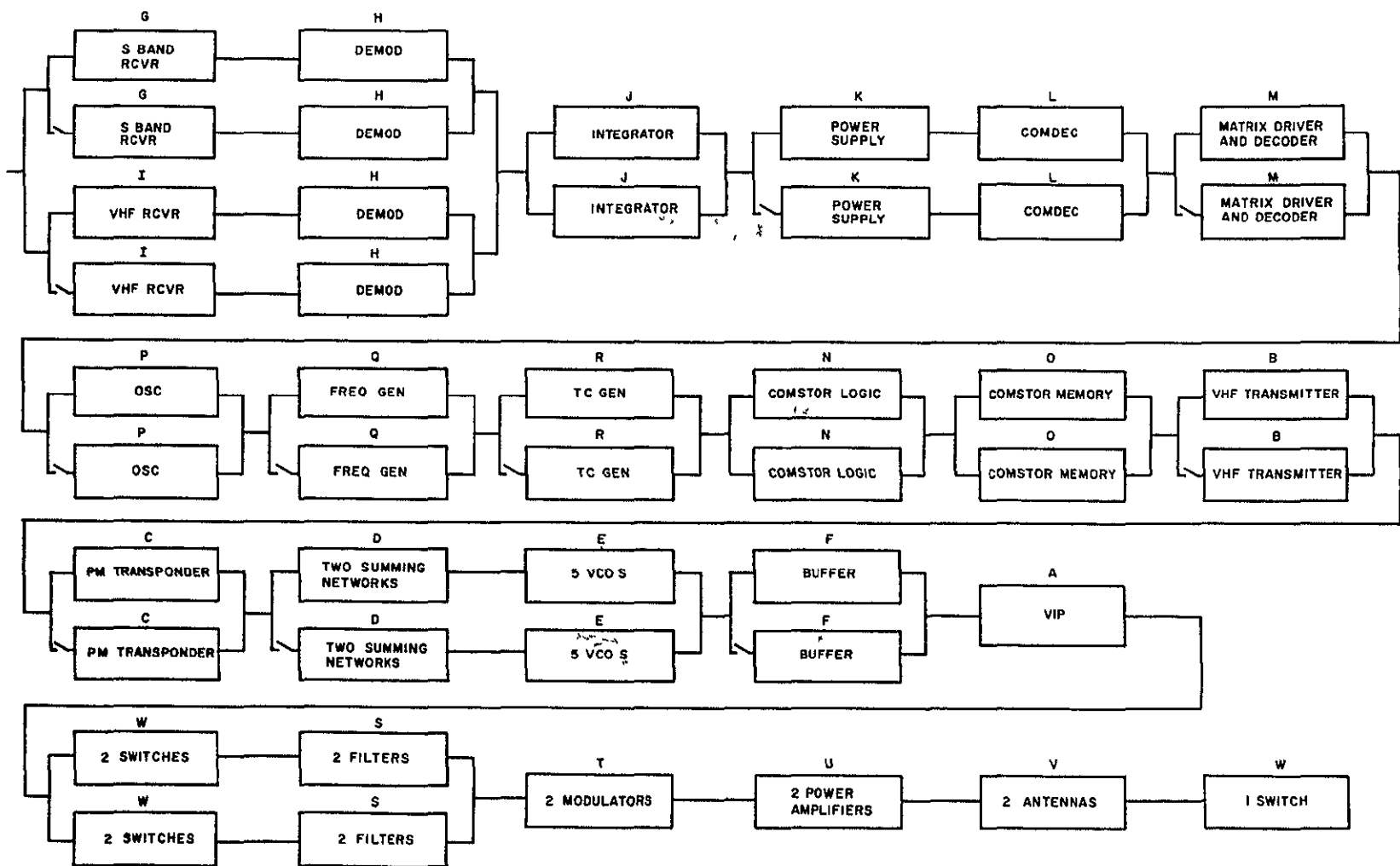
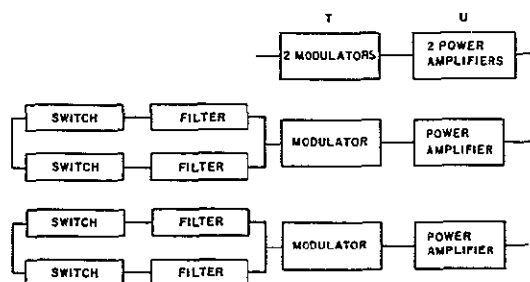


Figure 4.1.4-2. C&DH Subsystem Reliability Block Diagram.



with the configuration



with operating times adjusted to meet the requirements of degraded operation.

#### 4.1.4.3 Attitude Control Subsystem

The Attitude Control Subsystem is designed to achieve its function with maximum reliability. All components are space qualified and have a demonstrated long life. Built-in redundancy minimizes the risks associated with single-point failures in the RMP, the reaction wheel scanner, the signal processor, and the yaw reaction wheel.

The yaw rate gyro is used for acquisition only. Its probability of success during this mode exceeds 0.99995.

The pneumatics are required for acquisition, orbit adjust, and wheel unloading. Their operating time for these tasks is estimated as 3 hours. The pneumatics are available as backup for the yaw reaction wheel. The use of the pneumatics in wheel unloading is backed up by the magnetic moment assembly.

To compute the reliability of the pneumatics, it is assumed that they are required for a total of 3 hours plus the expected time  $t_B$  used to backup the yaw reaction wheel if the reaction wheel fails. The expected time of failure, given that failure occurs in time  $T$  is between  $0.4T$  and  $0.5T$ . Assuming a 10 percent duty cycle during wheel unloading, the operating time of the pneumatics is 3 hours if the yaw reaction wheel succeeds and  $3 + (0.1 \text{ by } 0.6 \text{ by } 8760)$  if the yaw reaction wheel fails.

Failure rates for the components of the Attitude Control Subsystem are shown in Table 4.1.4-3. The failure rate of the wheels (pitch, roll, and yaw) is based on the following accumulated flight data (per wheel)

OA0 and Nimbus 113400 hours in flight with no failure

OGO 63492 hours in flight with no failure

OGO 203057 hours on test with no failure

TABLE 4.1.4-3: ACS FAILURE RATES

Symbol	Component Name	Failure Rate $\lambda \times 10^{-6}$ or One-Year Reliability	Source and Comments
A	Reaction Wheel	3.9749	ORI 541, Table 9A
B	Signal Processor	7.6428	ORI 541, Table 9A
C	Control Logic	11.094	ORI 541, Table 9A, (eliminating A1 and A6/A7)
D	Rate Measuring Package (RMP)	4.5031	ORI 541, Table 9
E	Yaw Rate Gyro	37.7486	ORI 541, Table 9
F	Magnetic Moment Assembly	0.1065	Piece Part Analysis
G	Yaw Reaction Wheel	1.823	See Text
H	Pitch Reaction Wheel	1.823	See Text
I	Solar Array Drive	$\lambda = 5.384 \times 10^{-6}$ electronics $R \approx 0.998$ (mech)	ORI 541, Table 9 ORI 469, p. 69, modified with $\mu = 36$ months
J	Initiation Timer	3.4934	ORI 541, Table 9
K	Pneumatics	6.87	ORI 469, Table 30
L	Roll Reaction Wheels (2)	1.823 each	See Text

The calculated failure rate is  $1.823 \times 10^{-6}$  failures/hour/wheel.

The failure rate of the Magnetic Moment Assembly is based on the following parts count:

Part	N	$\lambda \times 10^7$	$N \lambda \times 10^7$
Permanent Magnets	3	0.0102	0.03
Coils	3	0.3 (est)	0.9
Capacitors	2	0.02	0.04
Relays	8	0.01	0.08
Resistors	3	0.005	0.15

$$\lambda = 0.1065 \times 10^{-6}$$

This parts count utilizes MIL-HDBK-217A rates reduced by one order of magnitude.

The failure rate of the mechanical aspect of the solar array drive may be derived using the same approach as ORI (Technical Report 469, p. 69) Nimbus flight experience indicates that the mean life for this component is not less than 30 months. Assuming that the time to failure is normally distributed with standard deviation equal to 20 percent of the mean, we find that one year is three standard deviations below the mean life, so that the probability of failing in one year is less than .002

A reliability block diagram of the Attitude Control Subsystem is shown in Figure 4.1.4-3.

The mathematical model for the reliability of the attitude control subsystem follows (T = 8760)

$$R = R_C R_I R_H R_L^2 \left[ 1 - (1 - R_A R_B)^2 \right] \left[ R_G e^{-3\lambda K} + (1 - R_G) e^{-528.6 \lambda K} \right] \left[ e^{-\lambda DT} + 10 (e^{-\lambda DT} - e^{-1.1 \lambda D^T}) \right]$$

The one-year reliability of the subsystem, following the order of the given formula, is

$$R = (0.9074) (0.9520) (0.9842) (0.9686) \times (0.9906) (0.99992) (0.9992)$$

$$R = 0.81499 \text{ (one year)}$$

#### 4.1.4.4 Orbit Adjust Subsystem

Table 4.1.4-4 shows the components appearing in the Orbit Adjust Subsystem. The table shows failure rates in terms of failures per hour or failures per cycle except in the case of ordnance valves, for which the probability Q of failure is given. In addition, the number of cycles of operation required during a one year mission are shown.

The solenoid valves are two-coil, two-seat valves affording maximum protection against leakage mode of failure. The normally closed explosive valves are in parallel redundancy.

For components with failure rates given in terms of failures per cycle, the exponential approximation is used

$$R = e^{-\lambda N}$$

where N denotes the number of cycles. For one shot devices,  $R = 1 - Q$ .

The mathematical formula for the reliability R of this subsystem is

$$R = R_A^3 R_B R_C R_D^{35} R_E R_F^2 R_H (2R_G - R_G^2)$$

The reliability is 0.9917 for one year.

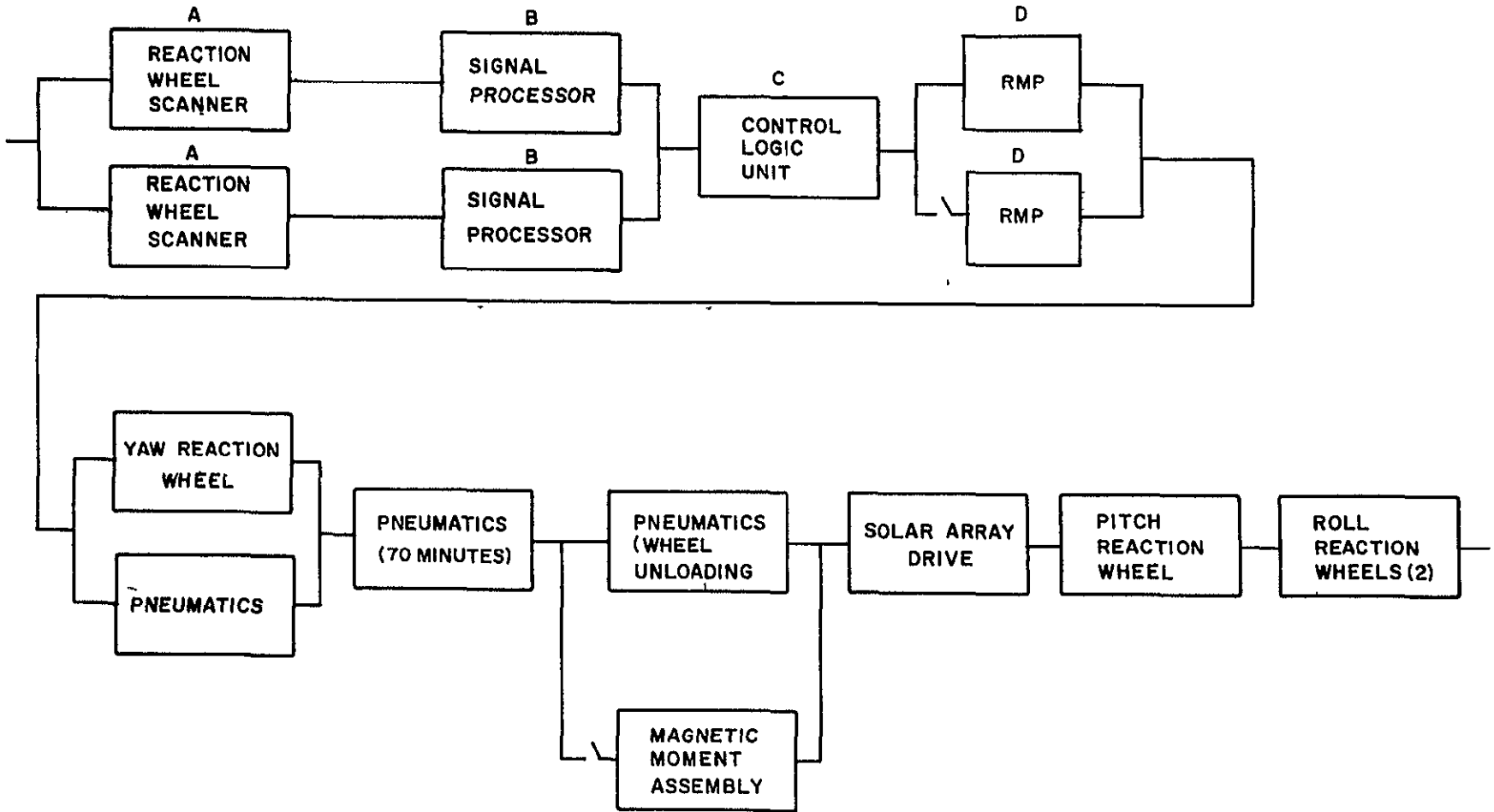


Figure 4.1.4-3. Attitude Control Subsystem Reliability Block Diagram

TABLE 4 1 4-4. COMPONENTS OF ORBIT ADJUST SUBSYSTEM

Symbol	Component	Quantity	Failure Rate X 10 or Q (each)	Duty Cycle	Sources
A	Fill or drain valve	3	$0.113 \times 10^{-6}$ per hour	8760 hrs	TRW (ATS-F/G) 6/67
B	Pressure Tank	1	$0.15 \times 10^{-6}$ per hour	8760 hrs	Ham. St., United A/C (ERTS-OAS), 12/63
C	Pressure Tank Bladder	1	$17.5 \times 10^{-6}$ per cycle	22 cycles	Same
D	Lines and Fittings	35	$0.003 \times 10^{-6}$ per hour	8760 hrs	GE (OAO) 5/68
E	Filter	1	$0.3 \times 10^{-6}$ per hour	8760 hrs	Marquardt Corp (ATS-F/G) 7/67
F	Thruster	2	$0.38 \times 10^{-6}$ per cycle	22 cycles	Ham. Std., United A/C (ERTS-OAS), 12/63 (without solenoid)
G	N/C Ordnance Valve	2	Q = .0001	One-shot	Marquardt Corp. (ATS-F/G), 7/67
H	Solenoid Valve	2	$0.12 \times 10^{-6}$ per cycle	22 cycles	GE(OAO) 5/68

These results, using the above failure rates, are found to be quite consistent with the independent reliability analysis performed by Rocket Research Corporation and contained in Volume 2, Section 6, Appendix.

#### 4.1.4.5 Power Subsystem

The reliability analysis presented follows that performed by Operations Research Inc. (Tech Rept. 469), which in turn is based on assessments performed by RCA upon the solar panels and battery modules. The numerical results presented here are based on a re-evaluation of the reliability of solar panels and batteries.

One of the most significant contributors to unreliability in the assessment performed by RCA and used by ARI is the solar array. The derivation of the low number is based on a cell failure rate of  $250 \times 10^{-9}$  failures per temperature cycle. Recent data (RCA Internal Correspondence dated Nov. 18, 1968) indicates a failure rate of  $30 \times 10^{-9}$  failures per hour. Based on this data, the solar array has a one year reliability greater than .998 with up to 9 string losses permitted.

On the basis of Nimbus experience, batteries are considered to experience failures which are predominantly "chance" rather than "wear-out" in nature during a one year mission. The PRC reliability report based on actual flight data shows that "battery packs" have experienced four failures in  $7.94 \times 10^5$  hours of flight. From this data, the failure rate of a battery is estimated very conservatively as  $5.8816 \times 10^{-6}$ /hour at 50 percent confidence.

Adding to this the failure rate for battery electronics used by ORI ( $7.5 \times 10^{-6}$ /hour) and the failure rate of one diode, we have a failure rate of  $13.3866 \times 10^{-6}$ /hour for each battery. This approach assumes that the failure mode of a battery throughout one year is primarily exponential with negligible effect of wear-out. The reliability calculated for each battery is 0.90255. But only 5 of 8 are required. The probability that 5 of 8 batteries will survive for one year is 0.99543.

There are two power-control modules one is required throughout the one year mission, the other is required about 10 percent of this time. The failure rates used in computing reliability are based on ORI Tech. Rept. 469, Table 23. The failure rates used for the auxiliary regulator, the shunt dissipator, bus comparison, and PWM are the same as those used by ORI. The filter and storage block contains 5 capacitors and two choke inductors with a total failure rate of  $0.0598 \times 10^{-6}$ /hour. The remaining circuitry has a failure rate conservatively estimated as  $0.7973 \times 10^{-6}$ /hour. To find the total reliability for one year of operation of both power control modules, the reliability of a single module is computed for one year and also computed for .1 year, these two results are multiplied to obtain an overall reliability for the two modules of .97081.

The components of the Power Subsystem are shown in Table 4.1 4-5.

TABLE 4.1.4-5. POWER SUBSYSTEM

Symbol	Component	Failure Rate $\lambda \times 10^{-6}$ or Reliability R	Source
A	Solar Panels	R = 0.9927	ORI 469, Table 24, Modified by RCA Int. Corresp. See text.
B	Battery Modules	R = 0.9954 (5 of 8 succeed)	See text.
C	Power Control Modules	R = 0.97081 Total	ORI 469, Table 23, See text for application.
D	Aux. Load Control and Aux. Load Panels	R > 0.99995	GE PIR 4341-24 (Nimbus B Program)
E	Unfold Timer	R = 0.9996 per timer	GE PIR's 4341-26 and 4341-43 (Nimbus B Program)

The reliability block diagram of the Power Subsystem is given in Figure 4.1 4-4.

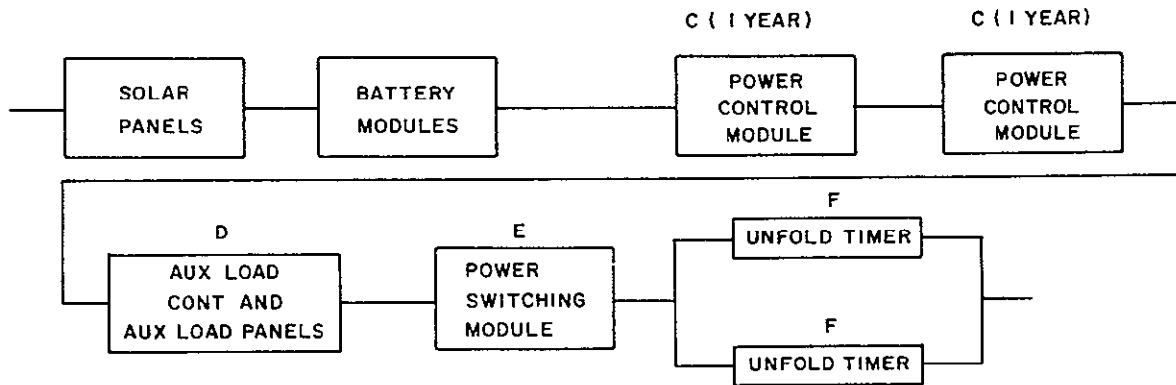


Figure 4 1 4-4. Power Subsystem Block Diagram

The formula for subsystem reliability  $R$  is:

$$R = R_A R_B R_C R_D R_E (2R_F - R_F^2)$$

$$R = 0.95926$$

#### 4.1.4.6 Electrical Integration Subsystem

The Electrical Integration Subsystem contains the Power Switching Module, the electrical harness, and the pre-flight disconnect. Its reliability for a one year mission is 0.9621

The pre-flight disconnect is used only once before launch. Because of the very short operating time, its probability of failure is considered to be negligible.

The Power Switching Module contains the parts shown in Table 4.1.4-6. The diodes appear in 160 redundant pairs, with total reliability 0.99999. The failure rate of the remainder of the Power Switching Module is  $1.7919 \times 10^{-6}$ /hour. The overall reliability of this module is 0.9844.



TABLE 4.1.4-6 POWER SWITCHING MODULE

Part Type	N	$\times 10^6$	$N \lambda \times 10^6$
Diodes	320	0.0333	160 redundant pairs, R 0.99999
Resistors	4	0.00048	0.00192
Power resistors	12	0.12	1.44
Holding relays	12	0.0005	0.006
Latching relays	34	0.001	0.034
Connectors (50 pins)	10	0.031	<u>0.31</u>
			$\lambda = 1.7919 \times 10^{-6}$
			R = 0.984425

The electrical harness comprises 436 connectors with an average of 20 pins each. The failure rate for such a connector is  $.006 \times 10^{-6}$ /hour, from MIL-HDBK-217A, reduced one order of magnitude. Thus the overall failure rate of the harness is  $2.616 \times 10^{-6}$ /hour and its reliability is 0.97734.

The overall reliability of the Electrical Integration Subsystem is

$$R = (0.9844)(0.97734) = 0.9621.$$

These failure rates are based on MIL-HDBK-217-A rates, reduced by one order of magnitude to account for screening.

## 4.2 ORBIT ANALYSIS

### 4.2.1 INTRODUCTION

During the course of the Phase B/C ERTS studies, extensive orbital analyses have been performed which have led to the definition of an orbit and an orbit control procedure that will permit attainment and maintenance of all ERTS orbital and ground trace swath control requirements for a minimum of one year. The altitude of the orbit is 492.35 nautical miles and the orbit is inclined by 99.088 degrees to the earth's equator (retrograde). The nominal eccentricity of this sun synchronous orbit is zero, its orbit period is 6196.015 seconds and the time at the descending node is, nominally 9 30 A.M. The entire earth (except small portion centered about each pole) could be surveyed every 18 days (251 revolutions) with the orbit. The orbit's ground track (and the subsatellite's swath) is controlled via a hydrazine fueled orbit adjust system that can either add or remove orbit velocity through the controlled firing of "one-pound" thrusters. This control is necessary for removing launch vehicle injection errors and for compensating energy losses due to atmospheric drag decay.

There are five basic requirements that must be met thru proper selection and control of the ERTS orbital parameters. They are as follows:

1. **Adjacent Ground Trace Control.** It is required that the subsatellite swath (100 nautical miles) of adjacent ground traces as generated on successive days overlap by  $\approx 10$  percent ( $\approx 10$  nautical miles). The swath should progress in a westward direction. This requires that the orbit selected should generate its ground tracks such that the ground trace of the first orbital revolution should be no more than 1.5 degrees (90 nautical miles at the equator) west of the first ground tracks from the previous day.
2. **Ground Track Control on Successive Coverage Cycles.** Each coverage cycle consists of 251 orbit ground tracks equally spaced, nominally, around the equator. Even after launch vehicle injection errors are removed, perturbations to the orbit and therefore to the ground track spacing are produced via atmospheric drag force, orbit determination and orbit adjust system impulse uncertainties. In the presence of these perturbations it is necessary to maintain sufficiently accurate control of the ground tracks (via orbit parameter control) such that a given subsatellite swath (e.g. rev. 10) during one coverage cycle coincides by  $\pm 10$  nautical miles with the same subsatellite swath (rev. 10) during any of the other 20 coverage cycles. Thus the corresponding (same rev. number) ground tracks must lie no more than 10 nautical miles away from each other during the entire year.
3. **Lighting Conditions at Satellite Nadir.** To maintain earth surface illumination conditions at satellite nadir within limits suitable for payload operation (sufficient solar illumination) and data interpretation (nearly constant illumination with sufficient shadowing) a sun synchronous orbit with a nominal descending node time of 9 30 A.M. is required.
4. **Eccentricity.** It is desired to maintain the scale variations in sensor imagery to less than 10 percent between maximum and minimum altitude (10 percent of 492 nautical miles), or  $\pm 25$  nautical miles. An eccentricity of .006 corresponds to an apogee-perigee difference

of  $\pm 23.7$  nautical miles and satisfies this requirement, neglecting the oblateness of the earth. Since the oblateness introduces a 9 nautical mile ( $\pm 4.5$  nautical miles) difference in altitude between equator and maximum latitude ( $\approx 81$  degrees), only an additional  $\pm 20$  nautical miles can be allotted to eccentricity-induced apogee-perigee differences.

5. It is required that the above four requirements be maintained for a minimum of one full year.

Each of the five requirements discussed in the immediately preceding paragraphs imposes its own special requirements and restrictions on the orbit and on the techniques for control of the orbit. From requirements 1 and 3 comes the nominal orbit, from requirement 2 the need for orbit control, for the orbit adjust subsystem and for the development of operational procedures and techniques for control, from requirement 4, a bound or limitation (potentially) on the techniques used in removing injection errors and making up drag decay losses, and from requirement 5 comes the total velocity impulse to be provided by the orbit adjust subsystem.

#### 4.2.2 NOMINAL ORBIT SELECTION

Overall mission requirements considering the payload sensors resolution capability, imagery scale, space to ground communications, etc. have lead to the selection of an orbital altitude to be in the range of 500 nautical miles \* It is found that at an altitude of  $\approx 481.6$  nautical miles, an exactly repeating ground trace, every day, can be obtained. Fourteen separate ground tracks are generated, and then repeated, each day. By moving to a slightly higher or lower altitude, the ground tracks no longer exactly repeat, but will shift gradually each day until complete earth coverage is eventually obtained. With the altitude greater than 481.6 nautical miles, day to day ground track progression is to the west. This occurs because the orbit period is increased, it takes longer to make a revolution about the earth and the earth rotates to the east thru a slightly larger angle between equatorial crossings of the satellite.

Thus, the nominal orbit altitude will be slightly higher than 481 nautical miles. Using Equations 4.2.2-1 through 4.2.2-19 to be presented below, a set of nominal orbit parameters were computed and are given in Table 4.2-1. As shown, a 492.35 nautical miles altitude, 99.088 degree inclined orbit is selected.

To compute the nominal orbit, it is first necessary to determine the longitude shift,  $\Delta\phi_d$ , from one ascending node to the next as the satellite traverses the earth once. Once this is determined, the orbit period, the time for the satellite to make one revolution about the earth, that produces the desired  $\Delta\phi_d$  can then also be determined. Calculation of orbit altitude and inclination readily follows.

---

\*The selection of this altitude regime is not covered in this analysis. However, previous studies at GE are in agreement with NASA's selection of  $\sim 500$  nautical miles as the optimum ERTS A/B altitudes.

In selecting  $\Delta\phi_d$ , requirement 1, adjacency of day to day ground traces is the controlling factor. Figure 4.2-1 shows a set of ground traces falling on one segment of the equator. Identical patterns will be found for any other equatorial segment of length  $\Delta\phi_d$ . In the figure a "REV 1" ground trace is seen to commence at 0 degrees longitude which is simply a reference point longitude. The satellite begins "REV 2"  $\Delta\phi_d$  degrees to the west, the earth has rotated  $\Delta\phi_d$  degrees to the east during the time it takes for the ERTS to make one revolution about the earth. After 14 revs. ("END OF REV 14") the satellite's ascending node has "travelled" slightly more than 360.

That is

$$14 \Delta\phi_d = 360 + \Delta\ell$$

where  $\Delta\ell$  is the distance between adjacent ground traces on successive days

After 28 Revs, the ascending nodes have "travelled" thru  $720 + 2 \Delta\ell$  degrees. From equation (1), an expression for  $\Delta\phi_d$  is derived

$$\begin{aligned} \Delta\phi_d &= (360 + \Delta\ell) / M \\ \Delta\phi_d &= 25.7142857 + \frac{\Delta\ell}{M} \end{aligned} \quad (4.2.2-2)$$

where

M

is the number of revs in one day (M = 14 for ERTS) and 25.7142857 is simply the quotient of 360/14. It is seen that the nodal longitude shift,  $\Delta\phi_d$ , should be slightly larger than 25.7142857 degrees. In order that a repeating situation be generated, it is necessary the broken-lined nodal traces in Figure 4.2-1, as they move to the west, eventually fall on the solid-lined trace "REV 2". When this happens, repeatability begins and a new coverage cycle is initiated. This is most easily accomplished by making  $\Delta\ell$  of such magnitude that when divided into  $\Delta\phi_d$ , the quotient is an integer. Mathematically, this is expressed by

$$\Delta\ell = \frac{\Delta\phi_d}{N} \quad (4.2.2-3)$$

where

N is the number of segments into which  $\Delta\phi_d$  is divided. Substituting (4.2.2-2) into (4.2.2-3) yields a general expression for  $\Delta\ell$

$$\Delta\ell = (360 + \Delta\ell) / MN \quad (4.2.2-4)$$

or

$$\Delta\ell = 360 / (MN - 1) \quad (4.2.2-5)$$

With  $M = 14$ ,  $N = 18$ , as in the case of ERTS,  $\Delta\ell = 1.434262$  degrees and the total number of revs in one coverage cycle is  $MN - 1$ . To determine  $\Delta\phi_d$ , the following rearrangement of equation (3) is used

$$\Delta\phi_d = N \cdot \Delta\ell \quad (4.2.2-6)$$

and  $\Delta\phi_d = 25.816733$  degrees. As an interesting check, the product of  $M \cdot \Delta\phi_d$  is 361.434262 degrees, thus verifying that  $\Delta\ell$  can also be expressed by the term  $(M \cdot \Delta\phi_d - 360)$ .

With  $\Delta\ell = 1.434262$  degrees, the distance at the equator is 86.06 nautical miles, giving  $\approx 14$  percent overlap of subsatellite swaths. If N is set equal to 17, instead of 18,  $\Delta\ell$  is found to be 1.5189873 degrees and the distance between adjacent tracks at the equator is 91.14 nautical miles, less than 9 percent overlap occurs. Figure 4.2-2 shows pictorially the definition of overlap.

It should be noted that there are actually only 13 17/18 orbital revs per one day with the  $N = 18$ ,  $M = 14$  ERTS orbit. Figure 4.2-1 shows "REV 252" ending at 25.816733 degrees West. This is the first complete rev of the second coverage cycle. "REV 251" is the last rev of the preceding coverage cycle, it completes that coverage cycle.

With  $\Delta\phi_d$  determined, the altitude and inclination can now be calculated. An expression relating  $\Delta\phi_d$  with orbit period,  $\tau$ , is given by the following expression for nodal longitude shift

$$\Delta\phi_d = -\tau (w_e - \dot{\Omega}_o) \quad (4.2.2-7)$$

Solving for  $\tau$  yields ( $\tau_d$  indicates the desired value of  $\tau$ )

$$\tau_d = \frac{-\Delta\phi_d}{w_e - \dot{\Omega}_o} \quad (4.2.2-8)$$

where  $w_e$  is the earth's angular rate about its spin axis,  $\tau$  is the nodal period and  $\dot{\Omega}_O$  is the precession rate of the orbit plane due to earth oblateness.  $\Delta \dot{\Omega}_O$  is the total precession angle per orbit. The minus sign indicates a drift to the west.

The general expression for  $\tau$  is

$$\tau = \tau_{KEP} \left[ 1 - \frac{J}{4} \left( \frac{R}{a} \right)^2 (7 \cos^2 i - 1) \right] \quad (4.2.2-9)$$

where  $J$  is the second order zonal harmonic of the earth model,  $R$  is earth's equatorial radius, and  $a$  is orbit's semi-major axis.  $\tau_{KEP}$ , the Keplerian orbit period, is given by

$$\tau_{KEP} = 2\pi \sqrt{\frac{R}{g}} \left( \frac{a}{R} \right)^{3/2} \quad (4.2.2-10)$$

where  $g$  is the gravitational acceleration on the earth's surface at the equator.

Nodal precession rate,  $\dot{\Omega}_O$ , is given by

$$\dot{\Omega}_O = -J \sqrt{\frac{g}{R}} \left( \frac{R}{a} \right)^{7/2} \cos i \text{ (rad/sec)} \quad (4.2.2-11)$$

The minus sign indicates precession to the west

$\dot{\Omega}_O$ , for sun-synchronous conditions ( $\dot{\Omega}_{SS}$ ) must be 0.98560912 degree per day to the east, therefore,  $\cos i < 0$ ,  $i > 90^\circ$ .

Solving for  $\cos i$  yields

$$\cos i = \frac{-\dot{\Omega}_{SS}}{J} \sqrt{\frac{R}{g}} \left( \frac{a}{R} \right)^{7/2} \frac{1}{57.2957795} \quad (4.2.2-12)$$

In this equation,  $\dot{\Omega}_{SS} = 1.407513 \times 10^{-5}$  deg/sec. The right hand side of equation 4.2.2-8 is completely determined when  $\dot{\Omega}_{SS}$  is substituted for  $\dot{\Omega}_O$ . Square equation (4.2.2-12) and substitute it into equation (4.2.2-9), along with equation (4.2.2-10) and set it equal to  $\tau_d$  (Equation 4.2.2-9). This yields a complete expression for  $\tau$  as a function of semi-major axis,  $a$

$$\tau_d = -2\pi \sqrt{\frac{R}{g}} \left( \frac{a}{R} \right)^{3/2} \left[ 1 - \frac{J}{4} \left( \frac{R}{a} \right)^2 \left\{ 7 \frac{\Omega_{SS}^2}{J^2} \frac{R}{g} \left( \frac{a}{R} \right)^7 \left( \frac{1}{57.2957795} \right)^2 - 1 \right\} \right] \quad (4.2.2-13)$$

$$= -2\pi \sqrt{A} X^{3/2} \left[ 1 - \frac{7A}{4J} \frac{\dot{\Omega}_{SS}^2}{\gamma^2} X^5 + \frac{J}{4} \left( \frac{1}{X} \right)^2 \right] \quad (4.2.2-14)$$

where  $A = \frac{R}{g}$ ,  $X = \frac{a}{R}$  and  $\gamma = 57.2957795$ .

The required value of period,  $\tau_d$  is 6196.015 sec.

Slight variations to the semi-major axis,  $a$ , produce the following changes in  $\tau_d$

$$\Delta\tau_d = -3\pi\sqrt{A} X^{\frac{1}{2}} \left[ 1 - \frac{J}{4} \left(\frac{1}{X}\right)^2 \left\{ 7 \frac{\dot{\Omega}_{SS}^2}{J^2} A X^7 \frac{1}{\gamma} - 1 \right\} \right] \Delta X \quad (4.2.2-15)$$

$$- 2\pi\sqrt{A} X^{3/2} \left[ -\frac{35}{4} X^4 \frac{\dot{\Omega}_{SS}^2}{\gamma J} A - \frac{J}{2} \frac{1}{X^3} \right] \Delta X$$

Using equations (4.2.2-14) and (4.2.2-15) iteratively, the value of semi-major axis,  $a$ , that produced  $\tau_d = 6196.015$  and  $\phi_d = 25.816733$  was determined to be 23917335. feet (3936.287 nautical miles).  $a$  is then substituted into equation (4.2.2-12) to compute the nominal inclination,  $i_{SS}$ , (that value of  $i$  that yields the sun-synchronous precession rate for the nominal semi-major axis) which is found to be 99.088 degrees.

The orbit altitude,  $h$ , is defined as

$$h = a - R \quad (4.2.2-16)$$

which is 2991597. feet or 492.35 nautical miles, where  $R$ , the equatorial radius, equals 20925738 feet. This altitude is neither equatorial altitude nor the altitude at any other specific point. It is simply a convenient designation since both  $R$  and  $a$  are constant

Due to the flattening of the earth, the actual altitude will vary by up to 10 nautical miles. Also, the radial distance (distance satellite is from the center of the earth) will vary, slightly, according to the following expression

$$\Delta r = Ja \left[ \left(\frac{R_e}{a}\right)^2 (\sin^2 i \cos 2w) \frac{1}{6} \right] \quad (4.2.2-17)$$

where  $w$  is the angular distance travelled from the equator. The extremes in  $\Delta r$  occur when  $w = 0$  and  $w = 90$  degrees. It is computed as  $\pm .795$  nautical miles.

The actual earth radius,  $R_e$ , is defined as a function of geocentric latitude,  $\theta$ , by

$$R_p = \frac{R \sqrt{1 - \epsilon^2}}{1 - \epsilon^2 \cos^2 \theta} \quad (4.2.2-18)$$

where

$$\epsilon^2 = 1 - (1 - f)^2, \quad f = 1/298.3 \quad (4.2.2-19)$$

The maximum latitude,  $\theta_{MAX}$ , is  $(180 - i_{SS})$  degrees. Since  $i_{SS} = 99.088$ ,  $\theta_{MAX} = 80.912$ , and  $R_e$  is 3432.665 nautical miles. With  $r$  (at  $w = 90^\circ$ ) =  $a - \Delta r = 3537.492$ , the actual altitude,  $h_{90}$ , at  $w = 90^\circ$  is 502.83 nautical miles. At the equator,  $h_E$  is  $h + \Delta r = 493.145$  nautical miles. (Note here that  $r$  is geocentric radius.)

Figure 4.2-3 shows the actual altitude and radial distance variations with angular travel. Also shown is the semi-major axis and orbit altitude.

Additional perturbations to the orbit were examined. They included solar-lunar gravitation perturbations and solar radiation pressure. The purpose of examining these perturbation sources was to determine if there is a secular perturbation to an orbit parameter (e.g. nodal precession rate) that could be compensated for via a slight change to one or more of the nominal orbits' parameters (e.g. inclination).

Solar and lunar gravitation attractions principally affect the eccentricity and the orientation of the orbit plane. Very small cyclic variations to the orbit period sometimes results. This perturbation was analyzed with the use of a general perturbation computer program, the perturbations are assumed constant over one orbit and the integrated effect used to update the orbit parameters for the next orbital rev.

As a result of this analysis, a secular perturbation to the orbit inclination was observed. It decreased at an approximately linear rate to 99.045 degrees,  $\Delta i = -.043$  degrees/year. This altered the orbit plane's nodal precession rate which also decreased linearly. An ascending node error then builds up as a function of time squared. At the end of a year this error is 0.8 degrees. This represents 3.2 minutes of error in local time at ascending node as well as an error of 48 nautical miles in ground track longitude. The ground track error can be compensated for by decreasing the nominal orbital altitude by approximately .015 nautical miles, the nodal timing error being accepted. Another approach is to alter the initial inclination by increasing it .021 degrees, to 99.109 degrees. Now, after a half year the nodal error would be 0.2 degrees, at which time the inclination would be down to  $\approx 99.088$  degrees. The nodal error will then drift back to zero degrees at the end of a year. Either approach is acceptable but further analysis is required to select the best method for compensation.

The influence of solar radiation pressure on the orbit was examined via a computer program that uses a finite perturbation technique. The program was modified to allow representation of the solar radiation as a constant inertial acceleration on the ERTS during its sunlit portions of the orbit. The total radiation pressure force,  $F_R$  is represented by

$$F_R = C_S P_R A_E \quad (4.2.2-20)$$

where  $P_R$  is the solar pressure at the earth ( $9.85 \times 10^{-7}$  pounds per square foot).  $A_E$  is the projected area of the ERTS satellite and  $C_S$  a coefficient representing the effectiveness of the impinging radiation on the surface of the satellite.  $C_S$  is chosen as 2 (specular reflection), to represent the worst case conditions.



No change to any of the orbit parameters was observed as a result of this analysis.

Some data from the Nimbus B2 satellite was examined to determine what perturbations to the Nimbus orbit has occurred. The Nimbus orbit is approximately 100 nautical miles higher than ERTS where atmospheric drag perturbations are negligible, thus, the effects of other perturbations will not be obscured by drag decay. From reference 3, the apogee and perigee altitudes on May 15, 1969 were given as 1135 KM/1075 KM. On July 30, the apogee/perigee difference was increased by 10 KM, they were 1140/1070 KM. Three months later, the apogee/perigee had returned to their original values.

The apogee/perigee differences observed are most likely attributable to solar radiation pressure although further examination of the data is required to substantiate this conclusion. The most important conclusion drawn from this data is in that perturbations to the in-plane orbit parameters (eccentricity and semi-major axis) are extremely small. When compared to the expected drag forces to be experienced by the ERTS satellite, these other perturbations (excepting solar-lunar gravity) are considered negligible.

#### 4.2.3 DRAG DECAY

There are two major areas of study involved in drag decay analyses selection of an atmospheric model for the time period of interest (1972-1973), and the calculation of ballistic coefficient,  $W/C_D A$ .

##### 4.2.3.1 Density

The atmosphere model agreed upon with GSFC is the U.S. Standard Atmosphere Supplements, 1966. The independent variable is exospheric temperature. Tables are provided which relate altitude and exospheric temperature to atmospheric density. The equations used and the appropriate constants are given in reference 1. The effects taken into account are the 11 year solar cycle variation (characterized by the 10.7 cm solar flux in units of  $10^{-22}$  watts/m<sup>2</sup>/cycle/sec), the semi-annual variation to the 11 year cycle, the diurnal variation which includes the "diurnal bulge" (atmosphere bulges out slightly at maximum temperature points), the local hour angle to the sun and the satellites latitude, and the geomagnetic activity. The exospheric temperature calculation,  $T_{\infty}$  is used to enter the tables given in the Atmosphere Supplement. The satellites' altitude, which varies with latitude (see Figure 4.2-3) is also used in the tables. Reference 2, a NASA document, has additional equations in which it is possible to compute the density directly instead of through the tables.

Temperature and the density calculations were made for single orbits at 8 different times of the year, thru 1972 and 1973. The "mean density"  $\bar{\rho}$  is obtained by integrating the density profile over a complete orbit. That is

$$\bar{\rho} = \left( \sum_{i=1}^n \rho_i \Delta t_i \right) / \tau \quad (4.2.3-21)$$

where  $\rho_1 \Delta t_1$  is the effective density over a small (1<sup>th</sup>) segment of the orbit. The orbit is divided into n segments.  $\tau$  is the total orbit period. The mean density as obtained in this manner is plotted in Figure 4.2-4. Subsequently, these densities, together with  $C_{DA}$ , will be used to generate the drag force, orbit altitude decay rate, and orbit velocity loss.

#### 4.2.3.2 Ballistic Coefficient

Calculation of ballistic coefficient,  $W/C_{DA}$  depends on satellite weight, W, and the summation of all the  $C_{DA}$ 's. Each package on the ERTS has a cross sectional area normal to the velocity and a corresponding drag coefficient depending on the shape of the particular package. The following drag coefficients have been used

<u>Shape</u>	<u><math>C_D</math></u>
Planes	2.8
Cylinders	2.2
Spheres	2.0
Shear	0.075

These coefficients assume the velocity (wind) vector is normal to the plane or the cylindrical axis of rotation. Since the solar paddles rotate with respect to the velocity vector, the solar paddles'  $C_D$  is integrated over one revolution. In this case, the drag is then found to be attenuated by a factor of  $2/\pi$ .

The shear force, or skin friction, is that drag force occurring on surfaces that are parallel to the velocity direction, and it is necessary to estimate the surface areas involved. The total contribution of this effect to the total drag force is slightly less than 2.0 percent.

Table 4.2-2 shows the  $C_{DA}$  calculations for each of the major ERTS components and structure. The total effective  $C_{DA}$  is seen to be 173.2 square feet.

#### 4.2.3.3 Altitude Decay Rate

The gradual loss in altitude due to atmospheric drag can be computed, quite accurately, as derived in the following equations. (The accuracy, of course, is limited by  $W/C_{DA}$  and density uncertainties.) The drag force,  $F_D$ , is

$$F_D = \frac{1}{2} \bar{\rho} V^2 C_{DA} \quad (4.2.3-22)$$

where V is orbital velocity = 24253 fps or 7392 m/s. In the calculations performed during ERTS study,  $C_{DA}$  and V were assumed constant. The velocity actually varies by 20 fps between the equator and the pole. This variation ( $\pm 10$  fps) is negligible when computing drag force since it represents only  $\pm .04$  percent of the mean orbital velocity

$C_D A$  also varies because the solar paddles are essentially inertially oriented over a given rev., and can more accurately be expressed as

$$C_D A = 82.3 + |142.8 \sin w| \quad (4.2.3-23)$$

Thus, for example, when at the equator, at the equinox, the paddle faces are 90 degrees from the velocity vector, i.e. edge into the wind, and they generate the minimum drag force. At maximum latitude ( $w = 90$  degrees) the full paddle surfaces are normal to the velocity vector. However, the temperature variation over an orbit is a function of the hour angle to the sun. Higher temperatures are observed on the daylight side of the earth, rather than on the darkside, and produce a far greater density variation than does the altitude change (913 KM to 932 KM) between equator and pole. Thus the solar paddles go thru their entire excursion during both the maximum density and minimum density regions. Thus the effect of varying  $C_D A$  will essentially cancel over each orbit.

The expression for altitude loss per orbit is obtained by equating the rate of energy loss due to drag force with rate of orbital energy loss due to changes in semi-major axis.

The drag force energy loss  $dE/dt$ , for a circular orbit is

$$\begin{aligned} \frac{dE}{dt} &= \vec{F} \cdot \vec{V} \\ dE/dt &= -F_D V \\ &= -1/2 V^3 C_D A \end{aligned} \quad (4.2.3-24)$$

where the angle between  $F_D$  and  $V$  is the flight path angle and is assumed to be essentially zero.

In terms of orbital energy,  $E_o$ ,

$$E_o = -\frac{m\mu}{2a}, \quad (4.2.3-25)$$

and the time rate of change of energy with change in semi major axis,  $da/dt$ , is

$$\frac{dE_o}{dt} = \frac{m\mu}{2a^2} \frac{da}{dt} \quad (4.2.3-26)$$

where  $\mu$  is the gravitational constant ( $R^2 g$ )

Equating the right hand sides of equations (24) and (26) yields the following integral equation for da

$$\int_{a_0}^{a_1} \frac{da}{a^{\frac{1}{2}}} = - \int_0^{\tau} \mu^{\frac{1}{2}} \bar{\rho} \frac{C_D A}{m} dt \quad (4.2.3-27)$$

where the substitution  $V^2 = \mu/a$  has been made and  $a_1 - a_0$  is the change in semi major axis,  $\Delta a$  over one orbit rev. Integrating yields

$$2(a_1^{\frac{1}{2}} - a_0^{\frac{1}{2}}) = \mu^{\frac{1}{2}} \bar{\rho} \frac{C_D A}{m} \tau \quad (4.2.3-28)$$

Letting  $a_1 = a_0 + \Delta a$  to obtain  $2 \left[ (a_0 + \Delta a)^{\frac{1}{2}} - a_0^{\frac{1}{2}} \right]$  on the l.h.s of (4.2.3-28), expanding the first term and retaining only the first order term in  $\Delta a$  since  $\Delta a \ll a_0$ , yields  $\Delta a/a_0^{\frac{1}{2}}$  for the left hand side of (28).  $\Delta a$  then becomes

$$\Delta a = \mu^{\frac{1}{2}} a_0^{\frac{1}{2}} \bar{\rho} \frac{C_D A}{m} \tau \quad (4.2.3-29)$$

which can be rearranged, using the  $V^2$  expression above, to give

$$\Delta a = V_0 a_0 \bar{\rho} \frac{C_D A}{m} \tau \quad (4.2.3-30)$$

where the subscript zero indicates values at the beginning of the orbit. This analysis assumes circular or nearly circular orbits which decay very gradually with no change in eccentricity or velocity path angle. These are valid assumptions for the ERTS orbit.

The altitude decay rate per day is obtained by multiplying  $\Delta a$  of Equation 4.2.3-30 by 13-17/18, the number of revs per day.

From Figure 4.2-4,  $\bar{\rho}$  is obtained, and a curve of altitude decay rate,  $\dot{h}$  vs time of year can be drawn. This is shown in Figure 4.2-5. For a spring 1972 launch, the average decay rate over the year is approximately .0066 nautical miles per day which amounts to 2.42 nautical miles per year. A spring 1973 launch would have an average daily decay rate of about .0056 nautical miles per day or 2.05 nautical miles per year.

#### 4.2.4 NOMINAL GROUND TRACK CONTROL

The orbit/ground track control problem can now be examined in detail and a mechanism for describing the deviations of day to day ascending node locations from their nominal no-drag locations can be formulated. The nominal control technique is to insert the ERTS into an orbit whose semi-major axis,  $a$ , is slightly higher, by  $\Delta h$ , than the semi-major axis corresponding to the nominal altitude. The satellite decays down to the nominal altitude,  $h_n$ , and continues to an altitude  $h_n - \Delta h$ . At this point an orbit adjust velocity impulse is applied and the satellite raised back up to an altitude  $h_n + \Delta h$ . The decay time,  $t_d$ , is expressed as  $\Delta h/\dot{h}$  where  $\dot{h}$  is the mean altitude decay rate which is assumed to be constant over the small altitude range  $\Delta h$  ( $< 1.0$  nautical miles). It is desired to space the orbit adjust maneuvers at least 18 days (one coverage cycle) apart. Figure 4.2-5 shows that it will probably be necessary to select a mean decay rate prior to each orbit adjust in order to plan the control of the next decay cycles ground track variations.

##### 4.2.4.1 Graphical Description

A convenient method for pictorially describing the ground track variation with altitude decay is shown in Figure 4.2-6, a and b. The top half of the figure shows ascending node deviations from those nodes that would be obtained for  $h_n$  and as shown in Figure 4.2-1. The bottom of the figure shows how the deviations would appear on a display as given in Figure 4.2-1. The solid lines show the evenly spaced nominal ascending node points, the broken lines show the actual node points.

The parabolic curve at the top of Figure 4.2-6 shows how the first rev. of each day deviated from the nominal ascending node point. Using the numbers shown, rev. 1 on day two (BEGIN REV 15) crosses the equator  $\approx .42$  nautical miles west of the nominal point. This is shown also on the bottom of the figure, although not to scale. The deviations between broken and solid lines have been exaggerated to enhance clarity. In this case the distance between adjacent ground traces is 86.48 nautical miles ( $86.06 + .42$ ). Day 3's rev begins .791 nautical miles west of the nominal day 3 first rev. However, the distance between adjacent ground traces is only 86.43 nautical miles. The mean altitude on day 2 is lower than day 1's, therefore, the adjacent traces are not as far apart even though the total deviation from the no-drag nominal increases. At the end of last rev on day 9 (begin Rev 1, day 10) the satellite is at the nominal altitude but the node point is 2.002 nautical miles from the no decay nominal. At this point the distance between adjacent ground tracks is minimum, 86.085 nautical miles. During the second half of the decay cycle, the first half phenomena is reversed. The distance between adjacent tracks becomes smaller and is always less than 86.06 nautical miles. On day 18, it is 85.64 nautical miles ( $86.06 - .42$ ).

If the orbit adjust maneuver raised the altitude back up to exactly  $h_n + \Delta h$  at the start of the second coverage cycle, ALL the ground tracks and subsatellite swaths will be identical during the second coverage cycle to those of the first coverage cycle. There would be no variation between corresponding revs of successive coverage cycles! (This assumes of course the same decay rate during both decay cycles).

The above example used an altitude decay rate,  $\dot{h}$ , of 0.006 nm. Figure 4.2-7 shows the altitude decay curve when  $\dot{h} = .004$  and  $.008$  nm. Note that the  $\Delta h$ 's have been adjusted to obtain exactly 18 day decay cycles. In dashed lines is shown 2 additional situations, where  $\Delta h$  is maintained constant (.054 nm as in the .006 nm/day  $\dot{h}$ ) but  $\dot{h} = .004$ , and  $.008$  nm/day. The middle one is simply a repeat of Figure 4.2-6. This shows the effect of  $\dot{h}$  errors.

As a final consideration, a two coverage cycle, 36 day decay cycle, is examined, and shown on Figure 4.2-7 for  $\dot{h} = .006$  nm. Now there will be deviations between corresponding rev numbers on successive coverage cycles. For this case the maximum deviation occurs for REV 1 of day 1 and REV 1 of day 19. The distance is 8.008 nm. The maximum distance between adjacent ground tracks is .82 nm, twice that of the 18 day,  $\dot{h} = .006$  nm, decay cycle. It will be shown in the following section that adjacent distances (day to day) are a function of  $\Delta h$ , while the distances  $\Delta s$  (cycle to cycle) are a function of  $\Delta h^2$ .

The traces shown in figures 4.2-6 and 4.2-7 are very useful for examining the effects of errors in  $\Delta h$  due to orbit determination errors and orbit adjust residuals. These considerations will be examined in detail in section 4.2.5 covering error analyses.

#### 4.2.4.2 Mathematical Description of Altitude Effects on Ground Track Deviations

The equations from which altitude-ground track deviations curves of the preceding section were generated will now be derived.

The basic approach in this analysis is to take the longitude change per orbit,  $\Delta \phi_d$  as given in equation (4.2.2-7) and determine the variation  $\Delta(\Delta \phi_d)$  due to orbit period variations. Then the errors in orbit period  $\Delta \tau$  due to altitude variations  $\Delta h$  as in equation (4.2.2-15) will be determined. Thus, the variation in ground track with altitude  $\Delta(\Delta \phi_d)/\Delta(\Delta h)$  will be determined.

Differentiating equation (4.2.2-7) yields

$$\frac{d(\Delta \phi_d)}{d\tau} = - (w_e - \dot{\Omega}_o) \quad (4.2.4-31)$$

or

$$\Delta(\Delta \phi_d) = \Delta \phi_d \delta \tau / \tau \quad (4.2.4-32)$$

Equation (4.2.2-15),  $\Delta \tau$  as used in this analysis requires only the differential of the Keplerian term  $2\pi \sqrt{a^3/\mu}$ , the first term in equation (4.2.2-15). The second term is only .06 percent of the first. Therefore, represent  $\delta \tau$  as

$$\frac{\Delta \tau}{\tau} = \frac{3}{2} \frac{\Delta a}{a} \quad (4.2.4-33)$$

and  $\Delta(\Delta\phi_d)$  in degrees is

$$\Delta(\Delta\phi_d) = \frac{3}{2} \frac{\Delta a}{a} \Delta\phi_d \quad (4.2.4-34)$$

At the equator, 1 degree  $\approx$  60 nm, also, there are 13-17/18 revs per day. Thus  $\delta(\Delta\phi_d)$  per day in nm is computed to be

$$\Delta(\Delta\phi_d) = 8.23 \Delta a \quad (4.2.4-35)$$

where  $\Delta a$  is in nm.

This equation applies to a constant  $\Delta a$ , or  $\Delta h$ . The designation  $\Delta h$  will be used for convenience. For nominal operation, the desired  $\Delta h$ , when the total decay time is  $t_d$ , is

$$\Delta h = \frac{1}{2} t_d \dot{h} \quad (4.2.4-36)$$

The average altitude deviation during decay from  $h_n + \Delta h$  to  $h_n$  is  $\Delta h/2$ . Equation (35) applies for one day, for  $t$  days,  $\Delta(\Delta\phi_d)$  is

$$\Delta(\Delta\phi_d) = 8.23 \Delta h t \quad (4.2.4-37)$$

Let  $\Delta(\Delta\phi_d)$  be designated as  $\Delta S$ . The maximum value of  $\Delta S$  occurs when  $t = t_d/2$  (the time to decay thru  $\Delta h$ ).

$$\Delta S_{MAX} = 8.23 \frac{\Delta h}{2} \frac{t_d}{2} \quad (4.2.4-38)$$

where  $\Delta h$  is divided by two since the average  $\Delta h$  during decay from  $h_n + \Delta h$  to  $h_n$  is  $\Delta h/2$ . Thus an expression for  $\Delta S_{MAX}$  is

$$\Delta S_{MAX} = 2.06 \Delta h t_d \quad (4.2.4-39)$$

A more useful expression results if  $t_d$  is eliminated and  $\Delta S_{MAX}$  is made a function of  $\Delta h$  and  $\dot{h}$  only. Such an expression will be much more useful for error analysis studies to be considered in section 4.2.6. Using equation (4.2.4-36) to eliminate  $t_d$  in equation 4.2.4-39 yields

$$\Delta S_{MAX} = \frac{4.12 \Delta h^2}{h} \quad (4.2.4-40)$$

This expression was used to generate the curves given in Figures 4.2-6 and 4.2-7.

#### 4 2 5 ORBIT ERROR ANALYSIS

The nominal orbit decay rate and ground track variations have been defined. Control of the orbit and its ground trace would be a simple matter were it not for the imperfections in the performance of other system elements. The launch vehicle will inject the ERTS into an orbit with some probability of error, the orbit adjust system will leave small residual velocity errors in the orbit, the tracking network will determine the orbit quite accurately but with some residual uncertainty, and the altitude decay rate will vary from its predicted value. In addition, the attitude control systems' pitch nozzle may perturb the orbit when performing attitude control maneuvers. Before an analysis of the altitude decay/ground track variation phenomena can be analyzed, it is necessary to delineate the contributions of all these error sources to the subsequent orbital motion and ground track variation.

It will be necessary, therefore, to specify all the orbit adjust system velocity requirements before the frequency and magnitude of  $\Delta V$  maneuvers are defined. The orbit adjust residual errors can then be defined.

##### 4 2 5 1 O/A Subsystem $\Delta V$ Requirements

The ERTS orbit adjust system employs a monopropellant hydrazine fueled propulsion system operating in a blowdown pressurant mode feeding two "one-pound" thrusters which are aligned in opposite directions along the vehicle X axes. Thus velocity corrections can be made in either direction along the velocity vector, to either increase or decrease orbital energy. The thruster whose propellant is expelled along the minus X axis is canted upward from the -X axis by about 21.5 degrees (angle depends on final c.m. location) to allow the thrusters' plume to clear paddle latch mechanism and struts. A complete description of this subsystem and the geometry of its thrusters with respect to the spacecraft axes is contained in Volume II Section 6.

##### 4.2.5.1.1 Launch Vehicle Injection Errors

The 99 percent probability injection errors from the DELTA launch vehicle have been specified as follows:

<u>Parameter</u>	<u>99 Percent Probable Minimum</u>	<u>99 Percent Probable Minimum</u>
Apogee altitude (nm)	- 3 0	+11 0
Perigee altitude (nm)	-11 0	+ 3 0
Orbit Eccentricity		0 0011
Orbit Inclination (degrees)	- 0 03	+ 0 03
Orbit Period (minutes)	- 0 3	+ 0 3

The altitude errors and resulting period errors propagate to almost 60 nm of ground track error after one day if not removed. This is prohibitive considering the tight tolerances on the ground track control requirements. The maximum altitude error to be removed is 14 nm. Combinations of two extremes of errors (e.g. -11, +3 or 11, -3, or 11, -11)



cannot occur since the maximum apogee/perigee difference can only be 8 nm as indicated by the maximum eccentricity of 0.0011. Depending on where in the orbit the altitude errors are removed, the maximum apogee/perigee difference cannot exceed 22 nm (8 nm from maximum insertion eccentricity and 14 nm from maximum altitude correction). This is well within the 47 nm allowance required ( $e \leq 0.006$ ).

The inclination errors propagate to only 5 minutes of error in the time at the ascending node after one full year. This is considered quite tolerable in the light of the 30 minute launch window tolerance. It is necessary therefore only to remove the altitude induced launch vehicle errors. The following analysis shows that this will require 21.7 feet/sec of velocity impulse. From the vis viva integral, the impulsive velocity required to remove altitude errors when thrusting at an apse is derived. The vis viva integral is

$$V^2 = \frac{2\mu}{r} - \frac{\mu}{a}$$

which assumes the satellite is at apogee,  $r = r_a$  is perigee distance. Differentiation yields

$$2 \frac{\Delta V}{V} = - \frac{2\mu}{V^2 r_a} \frac{\Delta r_a}{r_a} + \frac{\mu}{V^2 a} \frac{\Delta a}{a}$$

However,  $r_a$  will not change when the impulse is applied at  $r_a$ . Also, for a near circular orbit  $V^2 = \mu/a$ . The actual velocity varies by only  $\pm 50$  fps from the mean velocity of 24250 fps when the orbit eccentricity is about 0.002. Thus approximating  $V$  by  $\sqrt{\mu/a}$  is valid. Then, for  $\Delta V$

$$\Delta V = \frac{1}{2} V \frac{\Delta a}{a} \quad (4.2.5-42)$$

The coefficient is then 3.1 fps of  $\Delta V$  for each nm of semi-major axis change or 1.55 fps for each nm of altitude change. Since, in this example, the apogee distance does not change, the perigee must change by 2 nm to get 1 nm of semi-major axis change. It can be shown that identical results are obtained if the impulse is applied at perigee and the same assumptions of near circularity are made. Thrusting over an extended orbital arc or applying impulses at points between apogee and perigee produces only second order deviations in the value of the coefficient.

#### 4.2.5.1.2 Drag Induced Altitude Decay

Figure 4-2-5 shows the mean altitude decay rate to be 0.066 nm per day or 2.42 nm/year. The required velocity impulse to make up for this energy loss is 7.5 fps per year. Again the coefficient of 3.1 fps of  $\Delta V$  per nm of semi-major change is used. Here the altitude of the entire orbit decreases, not just at one point, thus altitude decay and semi-major axis decrease are the same and 3.1 fps/nm is required to restore the energy lost.

#### 4.2.5.1.3 Attitude Control Effects

When the attitude control system engines are fired and a pure couple is not generated, then a change to the orbit velocity vector is produced. If the resultant  $\Delta V$  change is normal to the orbit plane, as is the case for the roll control jets, a change in inclination, or line of nodes, or both takes place. Over 4 fps of  $\Delta V$  is necessary in order to change either by 0.01 degrees. Considering that the total impulse from the roll control jets over one year will be less than 3 fps, and there is some distribution of roll jet firings throughout the orbit much less than 0.01 degrees change would be expected. Thus roll jet induced changes to the velocity vector are negligible.

Pitch attitude control correction impulses from the pitch control nozzles (aligned along the  $\pm X$  axis) coincide nominally with the velocity vector and will increase or decrease this velocity slightly with each gating (firing). If the number of positive and negative firings are not equal, their effect must be compensated. Analyses have shown that an uncompensated "gating" or firing, would be expected approximately once every three orbits. Depending on spacecraft mass distribution, the cross products of inertia could in the worst case produce as much as one uncompensated gate per orbit. Each firing or gating produces a thrust level of 0.195 pounds for fifty milliseconds, resulting in an impulse of 0.00975 pounds-sec. With an ERTS mass of 49 slugs, the  $\Delta V$  per gate is  $\approx 2.0 \times 10^{-4}$  fps. In one year (5090 orbits) this amounts to 1.0 fps at one gate every orbit and 0.34 fps at one gate every three orbits. (Flight data shows Nimbus B2 gates on the average of once every third or fourth orbit with the same jet used for all the gatings.) Therefore, a worst case allotment of one fps per year of  $\Delta V$  will be provided by the Orbit Adjust System.

#### 4.2.5.1.4 Additional Losses

There are a number of other sources of relatively small  $\Delta V$  requirements. There are predictable efficiency losses due to the canted engine (7-8 percent). Also, a 4-5 percent loss results from the thrusting over a 30 to 50 degree arc that is necessary for removing the injection errors with the "one-pound" thrusters. With an average thrust level from the orbit adjust system of 0.75 pounds during injection error removal, 27 minutes of total thrusting time is required to impart 25 fps of orbit velocity change. Two equal duration burns would each cover 47 degrees of orbital arc. A low thrust, finite differencing computer program simulation was used to evaluate the efficiency loss due to continuous thrust operation. As a reference point for comparison, the program was also used to compute the orbit change when the total  $\Delta V$  impulse was applied at perigee. This was done by increasing the thrust level by a factor of  $10^3$  and reducing thrust duration by an equal amount. Comparison between the two cases showed the 4 to 5 percent difference. Also the 3.1 fps/nm coefficient was verified.

System error sources of a random or statistical nature produce additional requirements. The sources of these errors are

- 1) Thrust vector uncertainty of 0.25 degrees
- 2) Final alignment to c.m. could alter cant angle by a maximum 1.78 degrees. These two error sources produce a velocity make-up requirement of about 1.0 percent

- 3) Attitude control system errors - The yaw angle could build up to 10 degrees during long duration burns used for injection error removal. The average loss in efficiency (a cosine effect) is less than 1.0 percent. Pitch and roll errors of up to 5 degrees might occur and will produce a 2.5 percent loss if the pitch error adds directly to increase the effective cant angle by 5 degrees. The attitude errors, root sum squared are 2.7 percent.

The root sum square of the errors produced during the long duration burn for removing injection error, is 2.9 percent.

During drag make-up, thrusting is over a very short arc ( $\sim 3$  deg) and no inefficiency is attributed to the continuous thrust effect. However, the canted nozzle is required for all drag make-up  $\Delta V$  maneuvers since it adds  $\Delta V$  to the orbital velocity vector, again a 7 percent loss in efficiency is experienced.

An additional  $\Delta V$  margin ( $\approx 30$  percent) to allow for other contingencies is provided. This amounts to just over 10 fps. Table 4.2-4 summarizes all the Orbit Adjust System  $\Delta V$  requirements. The total  $\Delta V$  capability to be provided by the system is 45 fps.

It should be pointed out that uncertainties in metering and commanding the required  $\Delta V$  impulse from the O/A subsystem will contribute to  $\Delta V$  residuals but not necessarily to additional  $\Delta V$  requirements. On a short duration burn, a 6 percent uncertainty in the  $\Delta V$  impulse is possible (3 $\sigma$ ). RSS'ed with the 1 percent errors in thrust vector control, a 6.1 percent total uncertainty might be experienced when performing drag make-up maneuvers.

Total impulse uncertainties due to such things as propellant temperature variations and unavailable propellant caused by inefficient propellant expulsion have been taken into account by the orbit adjust subsystem allotment of hydrazine propellant and are not included here.

#### 4.2.5.2 Launch Vehicle Injection Error Removal Techniques

Before orbit correction residuals can be determined, it is necessary to formulate a technique for removing the injection errors. Then the errors that result, when this technique is employed, can be determined. There is no attempt made to optimize the technique for the purpose of minimizing correction residuals. Rather, the philosophy is to keep the number of O/A burns to a minimum, to allow for performing these burns in view of a ground station, and to limit the duration of each burn to prevent excessive attitude control error buildup during the burn.

An approach which meets this philosophy requires, in the worst case, two major burns of 12 to 14 minutes duration each, and a third trim maneuver burn of less than a minute duration. These first two burns will remove almost all of the injection errors. The third burn, if necessary, would minimize the orbit error remaining subsequent to the final O/A correction  $\Delta V$  maneuver.

The O/A thrust level for the first burn is expected to average about 0.8 pounds. With the ERTS mass at about 49 slugs, 13 fps of  $\Delta V$  ( $\approx 1/2$  the maximum injection error  $\Delta V$ ) can be imparted in  $\approx 800$  seconds. During this time the yaw attitude error can build up to 10

degrees, pitch and roll to 5 degrees. At the completion of the burn, the orbit will again be determined via the ground tracking and data system and the effectiveness of the burn determined. Performance of the attitude control system will be assessed and most of the attitude control system errors determined. The orbit determination data would aid in determining thrust vector errors. Actual propellant impulse,  $I_{sp}$ , would also be deduced.

The performance of the second burn can now be predicted to a high degree of accuracy. None of these errors, individually, should exceed 1 percent and the accuracy of the second burn should be predictable to within 1.5 percent. In order to prevent over-correction, the second burn's  $\Delta V$  will be intentionally biased short of the total  $\Delta V$  error by an amount proportional to the expected uncertainty in the burn. The uncertainty in the burn should be no more than 1.5 percent of the total velocity impulse imparted by the burn.

The third burn will remove the bias together with any residuals from the second burn. The resulting altitude errors, expected to be very small, will be superimposed on the altitude decay loss and will eventually be removed by the first drag make-up orbit adjust.

It is proposed that the same engine be used for removing all of the altitude injection error, no attempt will be made to circularize the orbit via burns with both thrusters. Thus, the planned bias should further prevent the need for thrusting in both directions.

#### 4 2 5 3 Orbit Correction Residuals

To gain a complete understanding of the expected extremes on the ground track generation process, it is necessary to include all the possible sources of error that contribute to  $\Delta h$  errors. The errors in  $\Delta h$  are made up of the residuals following an orbit adjust correction. The principle sources of error result from orbit adjust corrections and from orbit determination uncertainties. Orbit adjust errors are in the form of  $\Delta V$  residuals that result in  $\Delta h$  being either too large or too small. Orbit determination uncertainties result in an inaccurate computation of the required change in semi-major axis and consequently a  $\Delta V$  command that is in error. Uncompensated pitch attitude control impulses will be taken into account as part of the uncertainty in altitude decay rate.

#### 4 2 5 3 1 Orbit Adjust Subsystem Correction Residuals

Two separate sets of residuals will be generated, one following corrections to remove launch vehicle injection errors, the other following a drag make-up O/A maneuver.

In Section 4 2 5 2, the technique for removing launch vehicle injection errors was described. Assuming that worst case errors occur, (25 fps  $\Delta V$  correction necessary) the first burn, of 800 seconds duration will have removed 13 fps of velocity error. The performance will then be examined via telemetry observation and from ground tracking orbit determinations. The second burn will require removal of most of the remaining 12 fps. The accuracy of the second burn will now be predictable to within 1.5 percent. The bias will be 1.5 percent of 12 fps or 0.18 fps. The maximum residual is 36 fps, which is twice the bias. This assumes errors in the burn are in the same direction as the bias. The maximum error on the short duration burns are 6.1 percent (Section 4 2 5 1.4). Thus a maximum ( $3\sigma$ ) residual of

$\approx 0.022$  fps can be expected due to the O/A subsystem upon removal of launch vehicle injection errors. From equation (4.2.5-42), the equivalent residual semi-major axis error produced by this velocity residual is 0071 nm.

The drag make-up correction residuals will again be 6.1 percent of the  $\Delta V$  impulse. This impulse magnitude is dependent upon the  $\Delta h$  to be provided which, in turn, is dependent on time lapse between drag make-up corrections. Using 7.5 fps per year as the basic  $\Delta V$  requirement, a correction every 18-day (one coverage cycle) would require 0.375 fps, while 36-day decay time would require, on the average, 0.75 fps. The residual velocity errors are then 0.023 fps and 0.046 fps. The equivalent semi-major axis errors are 0.0074 nm and 0.0148 nm.

#### 4.2.5.3.2 Orbit Determination Uncertainties

Orbit determination uncertainties lead to orbit correction residuals that appear as altitude errors. Again, two sets of numbers will be generated, one for launch vehicle injection error removal, the other for drag make-up corrections. It is assumed that many of the MSFN - 30 foot dish tracking stations will be available for orbit determination purposes following launch vehicle injection and up until the time ERTS is placed into its nominal orbit. This will provide extensive coverage of all operations and should provide a very accurate determination of the orbit.

Subsequent to launch vehicle injection error removal, it has been assumed that only the MSFN tracking station at Corpus Christi, Texas will be dedicated full time to the ERTS mission.

Early in the study, information was provided by GSFC's Tracking and Data Systems Branch that indicated the total ERTS orbit position uncertainty would be on the order of 100m ( $1\sigma$ ) based on one day of tracking with the 30' MSFN stations and about 260m ( $1\sigma$ ) based on one day of tracking data from the Texas station. For preliminary analysis,  $3\sigma$  semi-major axis uncertainties were derived and were used for ground track control analysis presented in Section 4.2.6. Subsequent to this analysis, a complete  $6 \times 6$  covariance matrix of orbit parameter uncertainties were received from GSFC, one for each of the two tracking situations. The semi-major axis errors were computed from the two covariance matrices using standard statistical techniques (as described in Section 4.2.5.3.4). Assuming the matrices as shown in Tables 4.2-4 and 4.2-5 are correct, the  $\delta a$ 's resulting from them appear to be prohibitively large, three times as large as the preliminary  $\delta a$ 's from 260m error from Texas, and six times as large as the preliminary  $\delta a$  error from the 30' MSFN stations. The preliminary  $\delta a$ 's therefore were used for the orbit control studies presented in Section 4.2.6. These studies were begun prior to reception of the covariance matrix. Since the preliminary  $\delta a$ 's were found to provide marginal but adequate performance, it was felt that repeating the studies with the larger  $\delta a$ 's would only confirm the conclusion that orbit determination uncertainties represent the largest single contribution to the problem of maintaining ground track control. It is therefore recommended that the ERTS orbit determination procedure (number of stations, data processing, filter, etc.) for the operational phase of the ERTS mission be reviewed for any reasonable improvements in the estimation of semi-major axis. In Section 4.2.6.2, consideration is given to techniques for prediction of ground track

nodal crossings and decay rates, and for planning orbit adjust maneuvers, which should allow satisfactory performance with the orbit determination capability as presently estimated via the covariance matrices provided by GSFC

The semi-major axis error was obtained from the 100m and 260m position uncertainty designated as  $\delta P$ , in the following manner. It was assumed that only 60 percent of the error was along the in-track direction. The time to traverse this distance is  $0.6\delta P/V$  where the time computation is essentially independent of errors in velocity,  $V$ . The semi-major axis error,  $\delta a$ , is then computed from equation (4 2 4-33) which rearranged yields

$$\delta a = \frac{2}{3} \frac{a \delta \tau}{\tau}$$

During launch vehicle injection error removal, where  $\delta P = 100$  m,  $\delta \tau$  is computed to be 0.024 sec ( $3\sigma$ ) and  $\delta a$  to be 0.0102 nm ( $3\sigma$ ).

During the rest of the ERTS mission,  $\delta P = 260$  m,  $\delta \tau$  is computed to be 0.0624 seconds ( $3\sigma$ ) and  $\delta a$  to be 0.027 nm ( $3\sigma$ ).

#### 4 2 5 3 3 Total Correction Residuals

The total errors in semi-major axis at the conclusion of an orbit adjust velocity impulse maneuver is the root sum square of the two individual sources

$$\delta a_R = \sqrt{(\delta a)_{O/A}^2 + (\delta a)_{O/D}^2} \quad (4 2 5-43)$$

When removing launch vehicle injection errors, the values for  $(\delta a)_{O/A}$  and  $(\delta a)_{O/D}$  ( $\delta a$  from orbit adjust and from orbit determination residuals respectively) were shown to be

$$(\delta a)_{O/A} = 0.0071 \quad (\delta a)_{O/D} = 0.0102 \text{ nm}$$

The total error,  $(\delta a)_R$  is 0.0124 nm

When making up drag losses the values for  $(\delta a)_{O/A}$  and  $(\delta a)_{O/D}$  were shown to be

$$(\delta a)_{O/A} = 0.0074 \text{ (18-day)} \quad (\delta a)_{O/D} = 0.0267$$

$$(\delta a)_{O/A} = 0.0148 \text{ (36-day)}$$

The total RSS errors are 0.0277 nm and 0.0305 nm for the 18 day and 36 day durations between burns, respectively

These  $(\delta a)_R$  errors will be used in Section 4 2 6 to examine the effect of corrections residuals on the subsequent ground track (subsattellite swath) generation

First, though, a discussion of the method used in deriving  $(\delta a)_{O/D}$  from the GSFC provided covariance matrix will be given.

#### 4.2.5.3.4 Covariance Matrix Orbit Determination Uncertainties

The covariance matrices provided by GSFC, Tracking and Data Systems, are as shown in Tables 4.2-4 and 4.2-5. The nominal orbit elements associated with matrices are shown in Table 4.2-6. Also shown are other useful orbit parameters computed from the elements.

The purpose of this section is to show how the standard deviation of the semi-major axis  $\delta a$  was computed from the covariance matrix,  $\sigma^2_{cov}$ . The matrix  $\sigma^2_{cov}$  was computed in an Earth-centered equatorial inertial coordinate system,  $i e$

$$\sigma^2_{cov} = f(X, Y, Z, \dot{X}, \dot{Y}, \dot{Z}) \quad (4.2.5-44)$$

The sensitivity coefficients relating errors in semi-major axis to errors in X, Y, --- Z is required. Designate the resulting matrix as  $[\Delta a]$ . Then  $\sigma^2_{\delta a}$ , the variance, is computed from

$$\sigma^2_{\delta a} = [\Delta a]^{1 \times 6} [\sigma^2_{cov}]^{6 \times 6} [\Delta a]^T{}^{6 \times 1} \quad (4.2.5-45)$$

The matrix  $[\Delta a]$  is a  $1 \times 6$  while  $[\sigma^2_{cov}]$  is a  $6 \times 6$

$[\Delta a]$  is computed as follows, from the vis-viva integral

$$\frac{\mu}{a} = \frac{2\mu}{r} - V^2 \quad (4.2.5-46)$$

Taking partial derivatives we obtain

$$-\frac{\mu}{a^2} \delta a = \frac{-2\mu}{r^2} \delta r - \frac{2V}{V^2} \delta V \quad (4.2.5-47)$$

or

$$\delta a = 2 \delta r + 2 \frac{r}{V} \delta V \quad (4.2.5-48)$$

where  $r = a$ ,  $\mu/a = V^2$  for orbits of very small eccentricity Using

$$r^2 = X^2 + Y^2 + Z^2 \quad (4.2.5-49)$$

and

$$V^2 = X^2 + Y^2 + Z^2 \quad (4.2.5-50)$$

we can obtain the appropriate partials for equation (48) They are

$$\partial r = \frac{X}{r} X + \frac{Y}{r} Y + \frac{Z}{r} \partial Z \quad (4.2.5-51)$$

and

$$\partial V = \frac{X}{V} \partial X + \frac{Y}{V} \partial Y + \frac{Z}{V} \partial Z \quad (4.2.5-52)$$

Substituting these into equation (48) yields for  $[\Delta a]$

$$\Delta a = \left[ 2 \frac{X}{r} \quad 2 \frac{Y}{r} \quad 2 \frac{Z}{r} \quad 2 \frac{\gamma}{V} \frac{X}{V} \quad 2 \frac{\gamma}{V} \frac{Y}{V} \quad 2 \frac{\gamma}{V} \frac{Z}{V} \right] \quad (4.2.5-53)$$

If six orbit parameters were being determined, then  $[\Delta a]$  would be a 6x6 matrix and  $\sigma^2_{\delta a}$  would also be a 6x6 covariance matrix. As is used here, however,  $[\Delta a]$  is a 1x6. After  $[\Delta a]$  multiplied by  $[\sigma^2 \text{ cov}]$ , a 1x6 row matrix results. When this matrix is multiplied by  $[\Delta a]^T$  a single number results, namely the variance of  $\delta a$ ,  $\sigma^2_{\delta a}$ . The square root of a  $\sigma^2_{\delta a}$  is the "1 $\sigma$ " value of  $\delta a$ .

From the MSFN stations' covariance matrix,  $\delta a$  is computed to be 133 feet, or 0.022 nm. The "3 $\sigma$ " value for  $\delta a$  is then 0.066 nm. In section 4.2.5.3.2  $\delta a$ , 3 $\sigma$ , was computed as 0.0102 nm.

Using the Texas station generated covariance matrix,  $\delta a$  was computed to be 148 feet,  $\delta a = 0.0244$  nm, 1 $\sigma$  or 0.073 nm, 3 $\sigma$ .

#### 4.2.6 OPERATIONAL GROUND TRACK CONTROL

In Section 4.2.4, the influence of altitude decay on the ground tracks was shown. The parameter  $\Delta s$  (Equations 4.2.4-37 through 4.2.4-40) was shown to be a measure of a ground tracks deviation for an unperturbed no-drag nominal track. Now the effects of errors in  $\Delta h$ , to be designated as  $\delta a_R$ , on ground track control will be shown. Also shown will be the effects of errors in predicting  $\dot{h}$ . Decay cycles of 18, 27 and 36 days, nominal, will be examined. Nominal decay rates,  $\dot{h}$ , will be .005 nm/day and .0075 nm/day. Only the  $\delta a_R$  residuals after a drag make-up are considered since  $\delta a_R$  is smaller following launch vehicle injection error removal and applies for only one decay cycle. Altitude decay rate uncertainties are



estimated to be 15 percent. This estimation is based on data obtained from the U.S. Standard Atmosphere Supplements, and on the consideration that continued operation of ERTS at nearly constant altitude will produce determinations of  $h$  with sufficient accuracy to allow accurate prediction of  $h$  over the next decay cycle.

The first part of this study concerns the ground track deviations over one decay cycle only. Bounds are then placed on maximum decay time and/or maximum  $\delta a_R$ . The second part discusses control philosophy based on successive decay cycle control.

#### 4.2.6.1 Ground Track Variation Through a Single Decay Cycle

Figures 4.2-8 through 4.2-13 completely summarize the total extremes in ground track variation for the assumed three sigma errors,  $\delta a_R$  and  $\delta h$ . Each figure shows the nominal decay cycle curve and two curves for the  $\pm 15$  percent  $\delta h$  error. Also shown is the decay curve for  $\delta a_T = \Delta h \pm \delta a_R$  for  $\delta h = 0$ , and for  $\delta h = \pm 15$  percent ( $\delta a_T$  is the total semi-major axis deviation from the nominal semi-major axis.) When  $\delta a_R$  is positive, the worst case  $\Delta S$  occurs for  $\delta h$  negative, and vice versa.

Figures 4.2-8 and 4.2-9 show the 18-day decay cycle for  $\dot{h} = 0.005$  nm/day and  $0.0075$  nm/day respectively.  $\delta a_R = \pm 0.277$  nm. Figures 4.2-10 and 4.2-11 show the 27 day decay cycle for  $\dot{h} = 0.005$  nm/day and  $0.0075$  nm/day respectively for  $\delta a_R = \pm 0.291$  nm. Figures 4.2-12 and 4.2-13 show the 36 day decay cycle for  $\dot{h} = 0.005$  nm/day and  $h = 0.0075$  nm/day respectively for  $\delta a_R = \pm 0.305$  nm/day.

Note here that decay cycle is defined as the time to decay from  $\Delta h + \delta a_R$  to  $-(\Delta h + \delta a_R)$ . The time at the start of decay is denoted as "REV No 1 on day 1". The time ticks shown on the curves are for REV No 1 on the day shown. The maximum ground track errors will then occur between the day 1 and day 19 ground track ticks since it is the 18 day coverage cycle duration that governs ground track requirements.

The following observations are made regarding the ground track errors. Figures 4.2-8 and 4.2-9 show the  $\Delta S$  between days 1 and 19 are the same,  $\pm 4.15$  nm regardless of the  $\dot{h}$  and  $\delta a_R$ 's polarity. With the  $\delta h$  errors superimposed on the  $\delta a_R$ 's this statement is no longer quite true, with maximum  $\Delta S$  now being about  $\pm 5$  nm. These two figures indicate that a nominal 18 day decay cycle appears feasible with the orbit determination errors assumed (preliminary numbers, not covariance matrix). In Section 4.2.6.2, the philosophy for determining when in the decay cycle the O/A  $\Delta V$  maneuvers should be performed, is discussed. Figures 4.2-8 and 4.2-9 show two extremes for decay time if the O/A adjusts are to be made when  $\Delta S$  returns to zero, 34 days for  $\delta a_R = +.0277$ ,  $\delta h = -15$  percent,  $\dot{h} = .005$  and 6 days if  $\delta a_R = -.0277$ ,  $\delta h = +15$  percent,  $\dot{h} = 0.005$  nm/day.

Figure 4.2-10 ( $\dot{h} = 0.005$  nm/day, 27 day decay cycle), shows the  $\Delta S$  between days 1 and 19 to nominally be  $3.35$  nm. The same distance also occurs between days 10 and 28, (actually, end of day 10 and end of day 27). When  $\delta a_R$  and  $\delta h$  errors are superimposed,  $\Delta S$  between day 1 and 19 become  $+7.6$  nm for the positive  $\delta a_R$  and  $-7.8$  nm for minus  $\delta a_R$ .

Figure 4.2-11 ( $\dot{h} = 0.0075$  nm/day, 27 day decay cycle) shows nominal  $\Delta S$  to be +5.2 nm and the extremes to be 9.3 nm ( $+\delta a_R$ ) and -9.38 nm ( $-\delta a_R$ ). Note that if careful control of the orbit is not maintained, the total  $\Delta(\Delta S)$  error is greater than 10 nm. That is the net difference in  $\Delta S$  between the 19 day points for the two extremes is  $\approx 15.0$  nm,  $\dot{h} = .005$  nm/day, and  $\approx 18.5$  nm,  $\dot{h} = .0075$  nm/day. From Figures 4.2-10 and 4.2-11, the extremes on decay time are 45 days and 13 days

Figure 4.2-12 ( $\dot{h} = .005$  nm/day, 36 day decay cycle) shows the nominal  $\Delta S$  between days 1 and 19 to be 6.67 nm and increasing to 7.8 nm when  $\delta h = -15$  percent. With  $\delta a_R$  of 0.303 nm added to  $\Delta h$ ,  $\Delta S$  becomes 11.0 nm. Superimposing  $\delta h$  of -15 percent on  $\delta a_R$  results in  $\Delta S$  of 12.2 nm. It is shown therefore, that the ground track requirements of 10 nm maximum distance between the same "REV number ground track" on any coverage cycle cannot be met under the assumed errors  $\delta a_R$  and  $\delta \dot{h}$ . Figure 4.2-13 shows the same conclusions with  $\dot{h} = .0075$ , except that the  $\Delta S$  distances are even larger.

With the -15 percent for  $\delta \dot{h}$ , the maximum  $\delta a$  that gives 10 nm of  $\Delta S$  is 0.105 nm for nominal  $\dot{h}$  of .005 nm/day. Therefore with  $\Delta h$  normally at .09 nm the maximum  $\delta a_R$  is 0.015 nm/day. The orbit adjust system error for a 36 day decay cycle was shown to be 0.0148 nm. This leaves virtually nothing for orbit determination errors. Therefore, in order to use a 36 day decay cycle at  $\dot{h} = .005$ , system errors must be significantly reduced. At  $\dot{h} = .0075$  nm/day, no errors at all are permitted for a 36 day decay cycle.

Figure 4.2-13 ( $\dot{h} = .0075$ , 36 day decay cycle) is shown for completeness of data presentation. With no errors at all, the total  $\Delta S$  allotment of 10 nm is used just for nominal decay cycle control. Any errors at all result in  $\Delta S$  of greater than 10 nm. Thus, it is concluded from Figures 4.2-12 and 4.2-13 that the 36 day decay cycle is not feasible for ground track control.

From Figures 4.2-10 and 4.2-11, a nominal 27 day decay cycle appears feasible with proper control. Depending on  $\dot{h}$ , some duration greater than 27 days may be possible at given times of the year.

This entire section thus far has considered only the 10 nm ground track requirement on successive coverage cycles. The requirement for  $\approx 10$  percent overlap of adjacent swaths on successive days designated  $\Delta \ell$  will now be considered. This effect is essentially independent of  $\dot{h}$ , the maximum distance occurs on the first day of a decay cycle since  $\delta a_T$  is largest at this point. From equation (4.2.4-35) the distance  $\Delta S$  is given as

$$\Delta S_{\Delta \ell} = 8.23 \delta a$$

The nominal  $\Delta \ell$ , at nominal altitude (semi-major axis) is 86.06 nm. This leaves 3.94 nm for  $\Delta S_{\Delta \ell}$  if 90 nm maximum is permitted between adjacent ground tracks. From equation a is computed to 0.478 nm. This is far in excess of any  $\delta a_T$  thus far encountered. Therefore, the requirement for 10 percent overlap on a day to day basis will always be achieved for the assumptions made in this analysis.

#### 4.2.6.2 Ground Track Control

Having determined how the various decay cycle durations, decay rates and systems errors influence ground track position over one decay cycle, it is now necessary to devise a method for establishing and controlling the decay cycles from one cycle to the next.

The ideal situation is one where the nominal cycle, for the  $\dot{h}$  associated with the particular time of the year, would be obtained through the operation of an error free system. Even though this is not realizable, the nominal decay curve can still be used as a reference. All deviations produced in the ground tracks due to system errors could be measured from this reference. Therefore, as an initial ground rule, the orbit adjust maneuvers should be planned to return the ERTS satellite to an altitude that would place it on the nominal decay cycle curve. It is assumed that at no time would correction residuals be so large as to allow the subsequent  $\Delta S$  to exceed 10 nm. This could happen only when the altitude is too high. If this did occur an orbit adjust would be necessary to lower the altitude, a decidedly inefficient maneuver.

Figure 4.2-14 shows functionally the data from Figure 4.2-8, the 18 day decay cycle with  $\dot{h} = .005$  nm and  $\Delta h$  nominally 0.045 nm at the start of decay. This figure will be used for discussing control philosophy. Assume  $\delta a_R = .0277$  nm so that the  $\Delta h + \delta a_R$  solid line curve is being traversed. After 18 days (start of day 19), the actual  $\Delta h$  is only -0.02 nm and the ground track for REV 1 of the "second" coverage cycle is shifted +4.1 nm from the "first" coverage cycle's. (Note that first and second will be used for discussion purposes, this does not imply the first or second coverage cycle after injection into orbit.) An orbit adjust would not be useful at the end of this first coverage cycle since an orbit adjust does not instantly affect  $\Delta S$ , but only the  $\Delta h$  (vertically on the graph). Decay until at least day 27 would be recommended since only then is it possible to return to the nominal curve. If a perfect O/A maneuver were performed on day 27 such that the satellite is now following exactly the nominal decay curve, the satellite altitude would now be nominal, at  $h_H$ . But this is at the middle of decay cycle and another orbit adjust would be required 9 days later. Therefore, it seems prudent to delay the orbit adjust maneuver for three additional days, at which point  $\Delta S$  is zero. Now a perfect return to the nominal curve would allow 18 days of decay prior to the next orbit adjust.

Now, consider the control philosophy if  $\delta a_R$  had been  $-.0277$  nm. The decay cycle curve returns to  $\Delta S = 0$  in only eight days. An orbit adjust at this point might be difficult to make with any degree of accuracy since orbit determination/ground track prediction errors may not be reduced to a sufficiently small uncertainty. Therefore, it is probably better to wait for some longer time, perhaps till start of day 19, then attempt to return to the nominal cycle (dotted line on the  $-\Delta S$  side of plot.) However, another O/A maneuver with  $\delta a_R$  being negative might result in the entire second cycle being spent in the  $-\Delta S$  region. This is not desirable since another O/A may be required a few days later to prevent  $\Delta S$  from becoming too negative and the 10 nm requirement being exceeded.

Two possible solutions to the problem have been considered. One most applicable to the  $-\delta a_R$  case would attempt to optimize the time between day 8 and day 19 for making the maneuver, such that sufficient orbit determination accuracy is obtained while minimizing the possibility of remaining in the  $-\Delta S$  region.

The other solution which pertains to both positive and negative  $\delta a_R$  is to simply box in a 10 nm  $\Delta S$  area (as shown on the figure) and require that at no time will any part of the decay cycle be permitted to exceed these bounds. Note that the  $\Delta S$  limits are not  $\pm 10$  nm from the reference ( $\Delta S = 0$ ) point. If they were, then it is possible that a given rev. number during one coverage cycle, if at +10 nm, might during some other coverage cycle be at -10 nm. In this case there would be a 20 nm separation between the corresponding revs.

The last facet of orbit control to be considered is the determination of the actual decay curve and computation of the next orbit adjust maneuver

A suggested technique for determining the decay cycle curve in the presence of orbit determination errors is to examine the nodal crossing points back in time to the beginning of the decay cycle. This information, being "after the fact", should be very accurate, then the total decay cycle curve can be drawn. As an example, consider Figure 4.2-15, which is effectively a rotation of the decay cycle curves. Note that  $\Delta h$  and time are synonymous when  $\dot{h}$  is constant. All the decay cycle curves of Figures 4.2-7 through 4.2-13 could have had their ordinates labeled as time or the ratio of time to altitude rate,  $h$ , instead of altitude. On Figure 4.2-15, the solid line is the predicted  $\Delta S$  versus time based on data from which the orbit adjust maneuver was computed. The circled points represent the actual nodal positions,  $\Delta S$ . Eventually the curve will be accurately constructed and prediction into the future is obtained by extending the actual curve. On Figure 4.2-15 some  $\Delta S$  violation zones are shown. The cross-hatched regions at the top and bottom represent areas outside of the 10 nm  $\Delta S$  variation permissible. The dashed line regions contain lines of constant  $\dot{h}$  which indicate that if the curve enters this region, the cross-hatched areas will be traversed before  $\Delta h$  gets to zero. Final location of the center of this zone along  $\pm \Delta S$  must be determined from analysis, but there would probably be more of the acceptable region to the  $+\Delta S$  side since the nominal decay cycle extends into this region even when there are no  $\delta a_R$  errors.

The operational system would not use the graphical display, per se, for orbit control. The data on the curve would be mechanized in the operational software. Graphical displays could be included as part of the software's output as a convenient aid for the ground controllers. The actual curve could also be combined with the nodal crossing points predicted by propagating orbit determination data ahead in time, in order to aid in reducing those errors. With data of this form available, it now becomes possible to predict orbit adjust maneuvers well in advance. As a check on the predicted O/A maneuver, all 251 rev number  $\Delta S$ 's from all the previous coverage cycles would be stored. When the orbit adjust maneuver is planned, the new 251 coverage cycle's in nodal positions would be computed assuming worst case errors. Then comparisons are made with all the previous cycles to see that no rev number's ground track will be more than 10 nm from its corresponding rev number on any other coverage cycle.

Analyses of this suggested approach to the orbit control problem should be performed in order to fully evaluate its capabilities. Simulations should be performed which include errors in orbit determination and orbit adjust maneuvers, to determine how the ground track errors accrue over the 20 coverage cycles in a year. Ultimately the total control concept would be evolved.

From this analysis of operational ground track control studies, it is concluded that 18 to 27 day decay cycles are feasible and that all orbit and subsatellite swath requirements can be met. Orbit determination capability should be reviewed for further possible improvement. Although details of the control philosophy remain to be defined, an approach that appears promising has been formulated.

#### 4.2.7 LAUNCH WINDOW ANALYSIS

The ERTS launch window is defined to place the time at the descending node to be between 9 30 and 10 00 hours. The effect of the one-half hour window produces variations to the beta angle, the shadow duration and solar elevation angle at ERTS nadir.

The beta angle is defined as the acute angle between the ERTS orbit plane and the sun-line. It can also be defined as the complement of the angle between the ERTS orbit plane's normal and the sun-line. Figure 4.2-16 shows the beta angle history for both bounds on the launch window. Variations of between 6 to 7.5 degrees is seen.

ERTS will pass through the earth's shadow on every orbit. The time spent in the shadow, nominally (9:30 descending node) varies between 29 and 32.6 minutes. Figure 4.2-17 shows an increase of 1 to 2 minutes if launch is at the end of the launch window (10 00 descending node time).

The beta angle and shadow duration variations affect principally the thermal and power subsystems

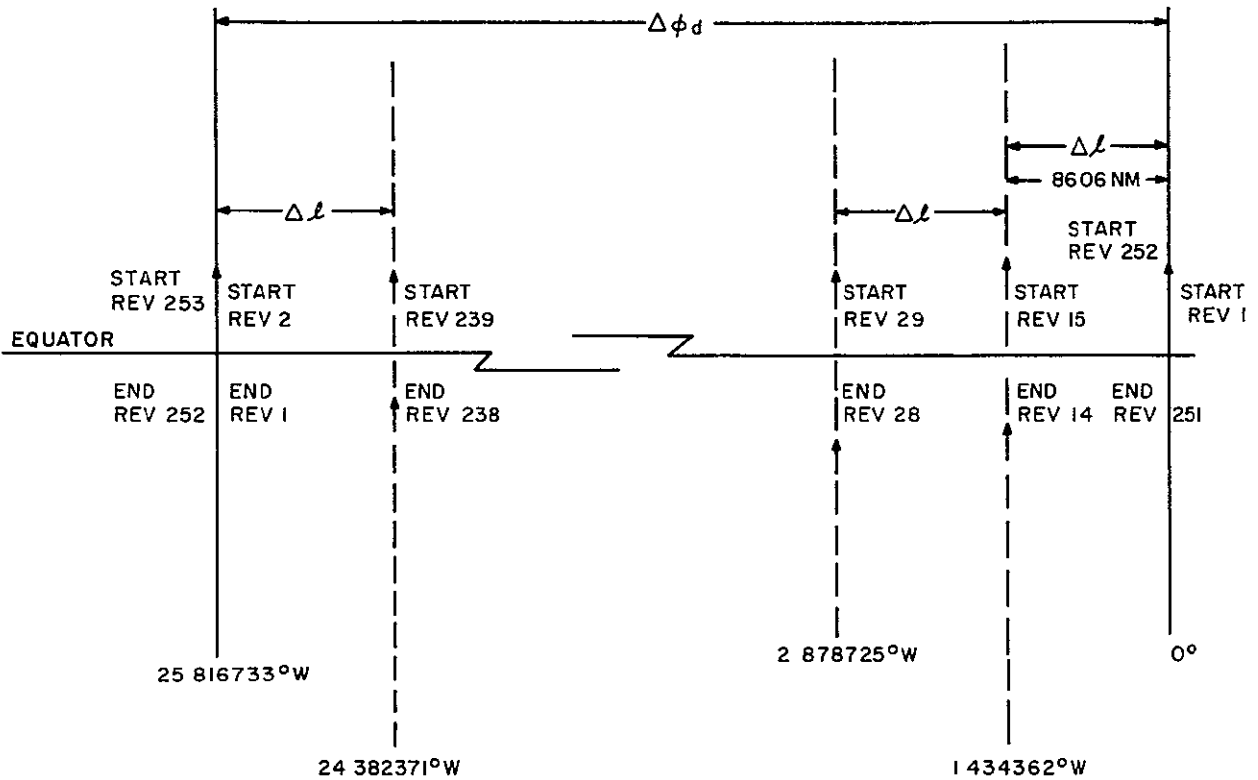
The solar elevation angle is the angle between the sun-line and the local horizon at Satellite Nadir. In Figures 4.2-18 and 4 2-19, the complete yearly history of solar elevation angle variation with latitude is shown for the two ends of the launch window. Of interest is the latitudes  $30^{\circ}$ N and  $50^{\circ}$ N since these encompass most of continental United States. The effect of the launch window on solar elevation angle at these two latitudes is shown in Figure 4.2-20. Variations of at least two degrees but not more than 6 degrees is seen. The effect of the increased angle at the end of the launch window on payload operation is expected to be minor.

$\Delta\phi_d$  LONGITUDE SHIFT FROM ONE ASCENDING NODE TO NEXT

$\Delta l$  LONGITUDE SHIFT FROM ONE DAY TO NEXT (ADJACENT TRACKS)

NOMINAL  $\Delta\phi_d = 25.816733$  DEGREES

$\Delta l = 1.434362$  DEGREES



ORBIT PROVIDES

14% SIDELAP

REPEATING GROUND TRACE-18 DAYS

Figure 4.2-1. Definition of Ground Track Longitude Separation

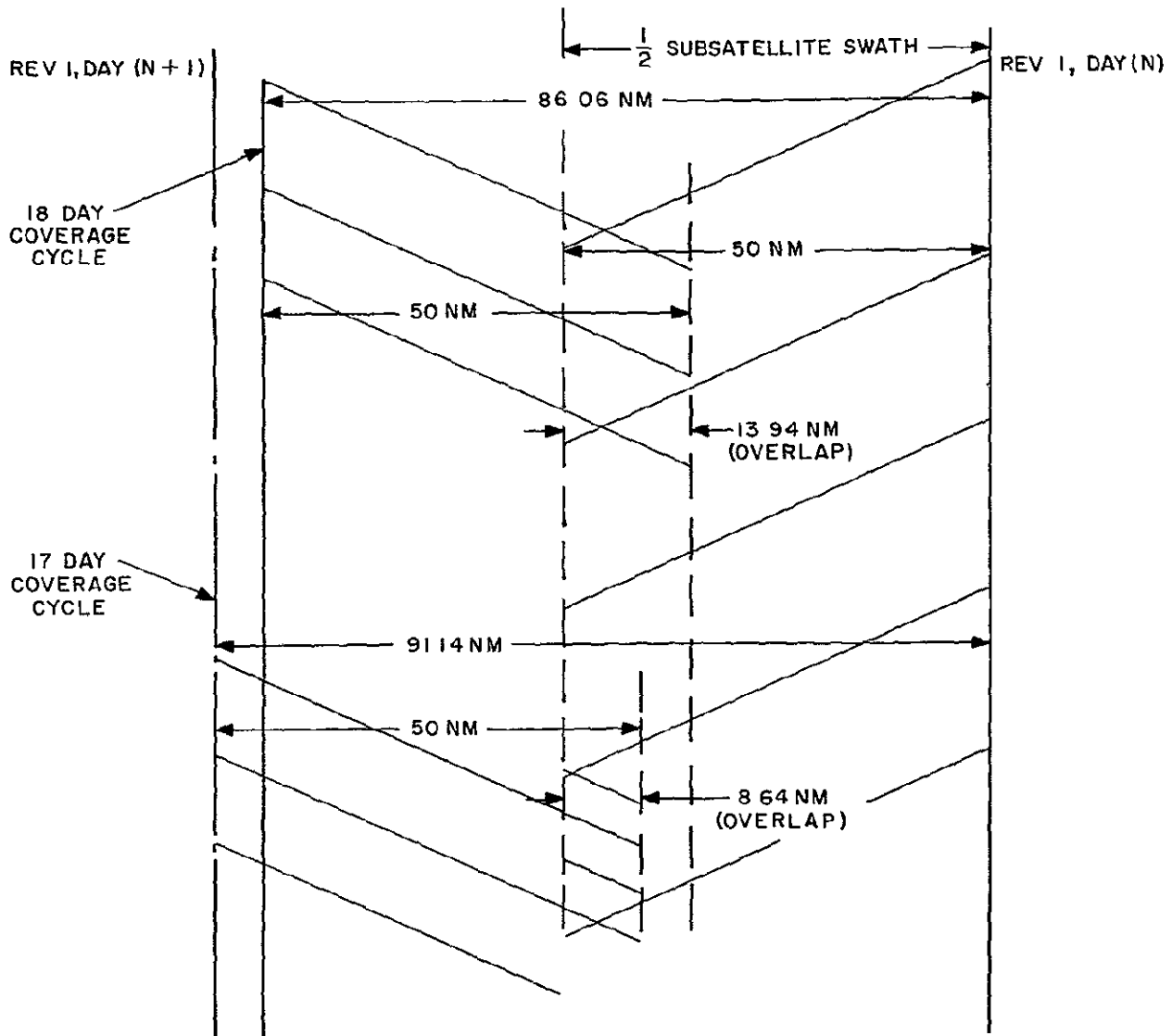


Figure 4.2-2. Definition of Subsatellite Swath Overlap

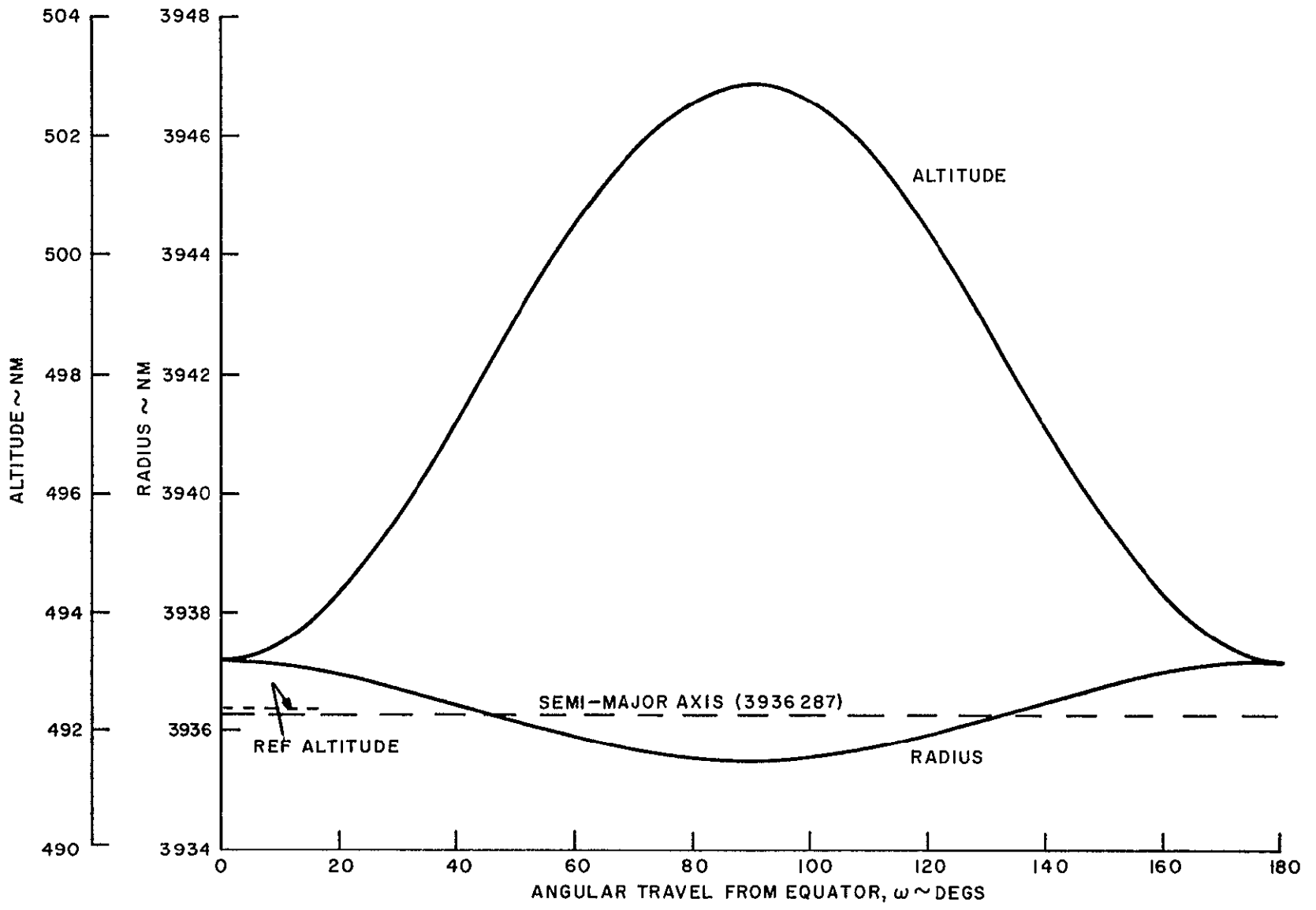


Figure 4 2-3 ERTS Nominal Orbit Altitude and Radius Versus Angular Travel



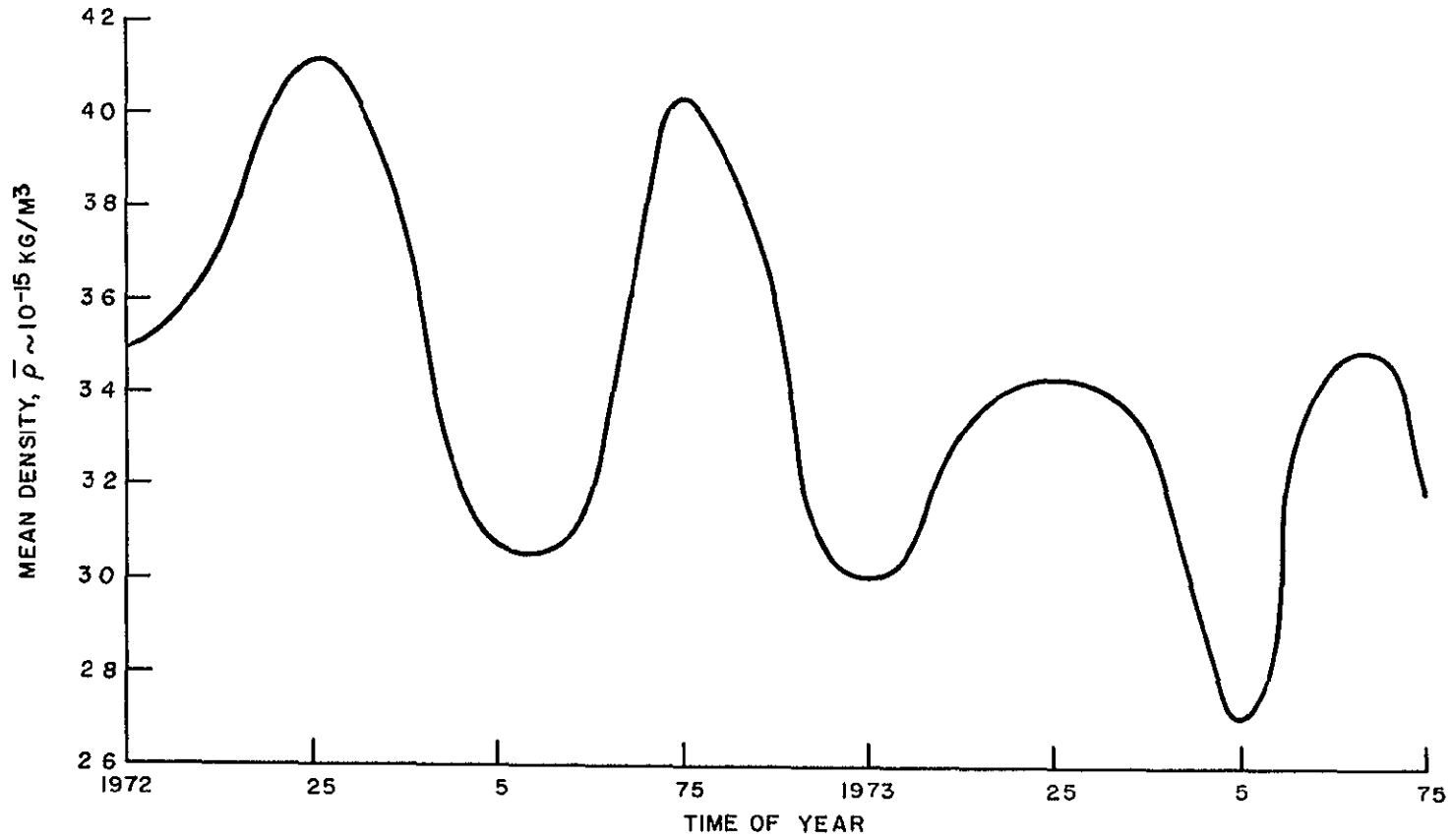


Figure 4 2-4 Variation of ERTS Mean Density During 1972-1973

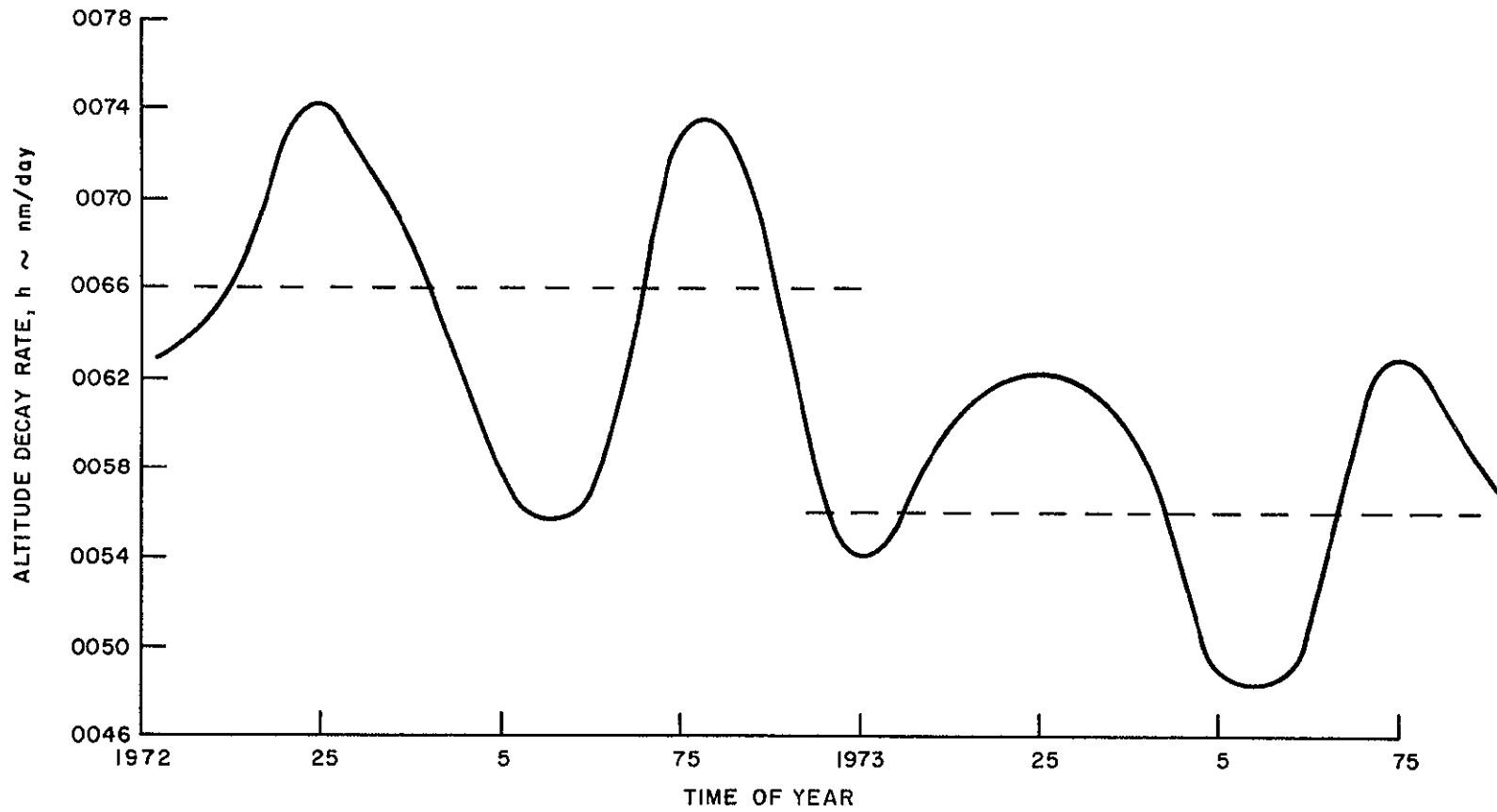


Figure 4.2-5. Variation of Mean Altitude Delay Rate With Time of Year

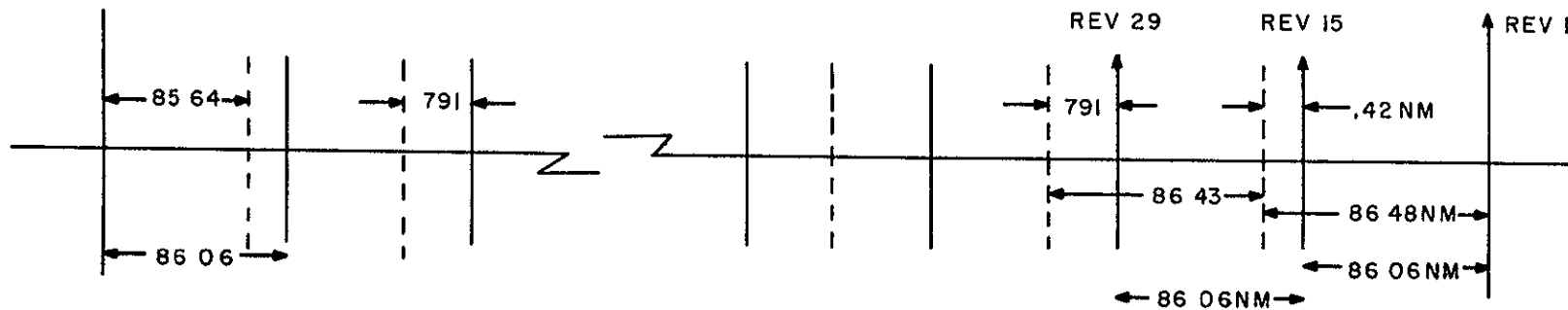
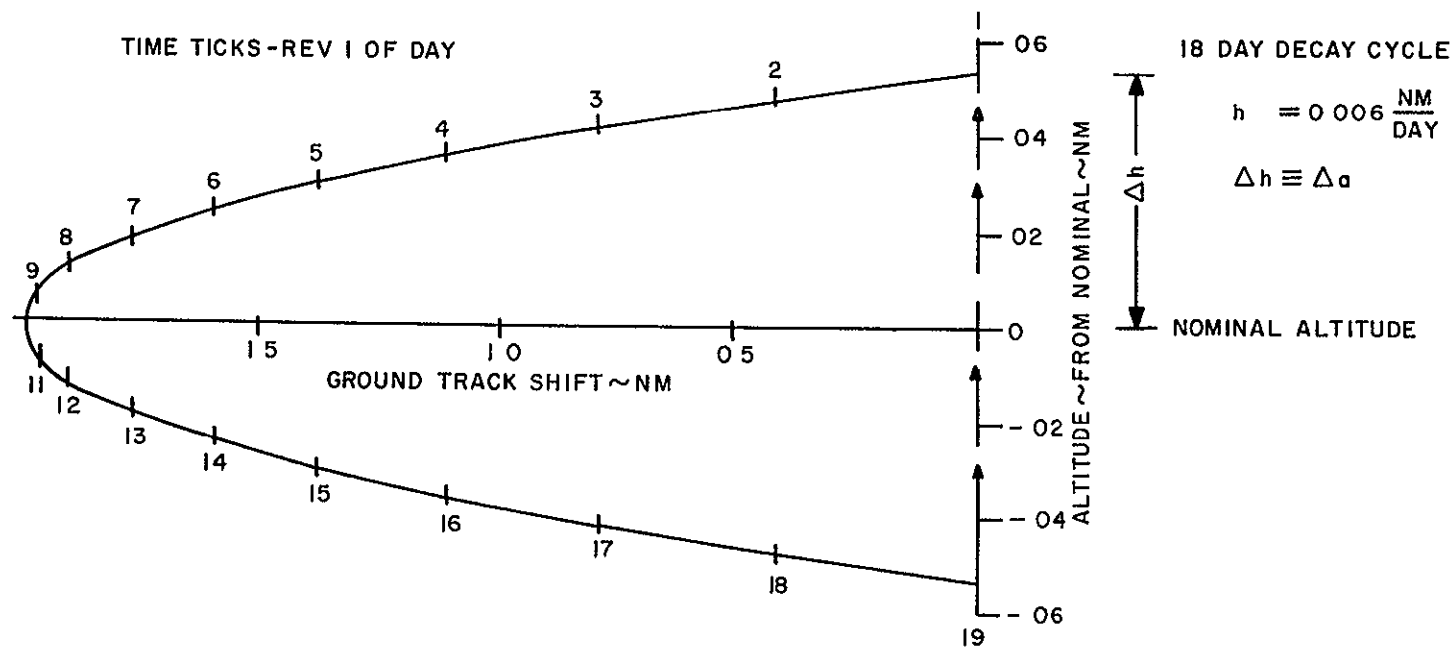


Figure 4.2-6. Description of Ground Track Variation With Altitude Decay

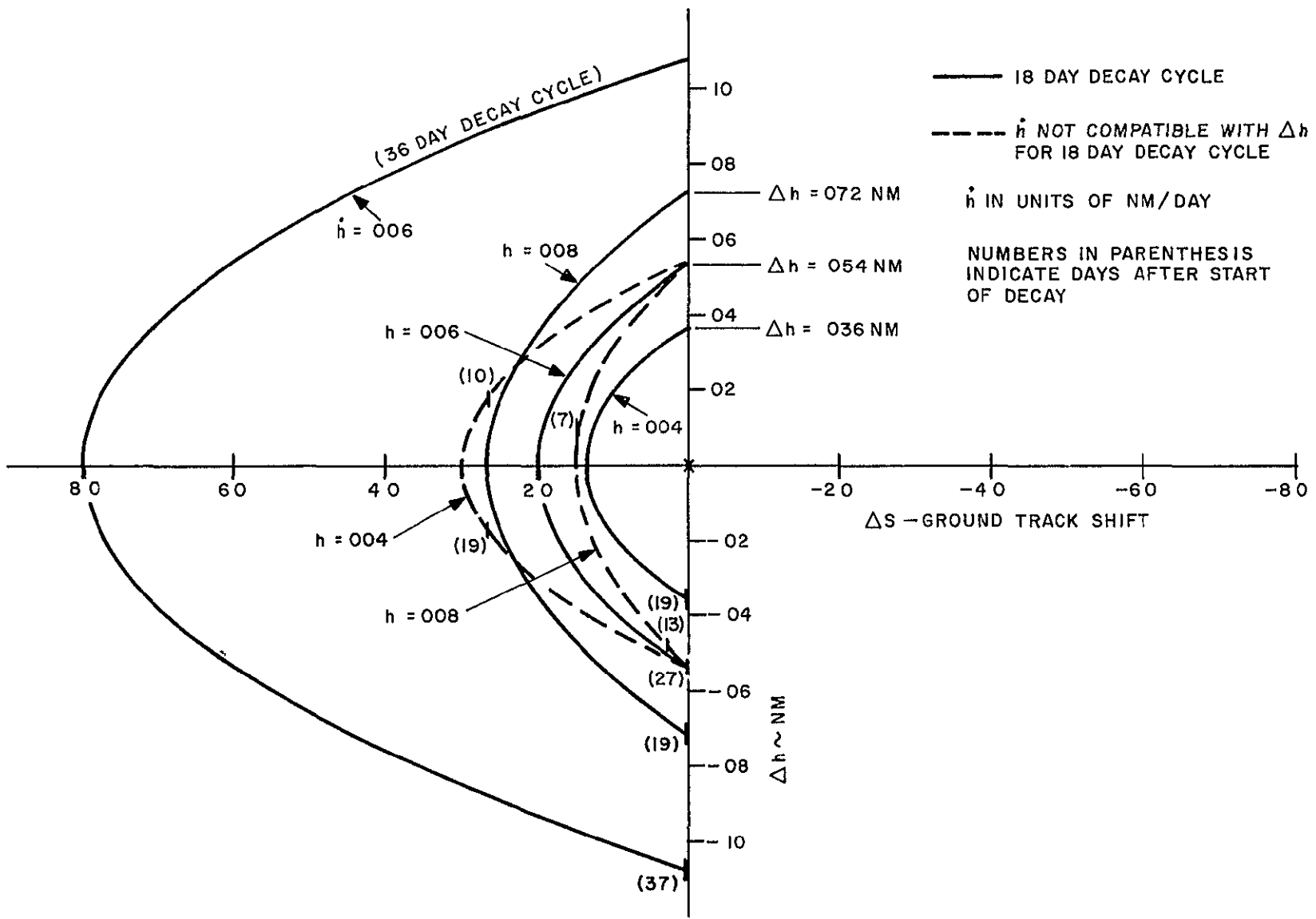


Figure 4.2-7. Variation of Ground Track Node Position With Altitude Decay

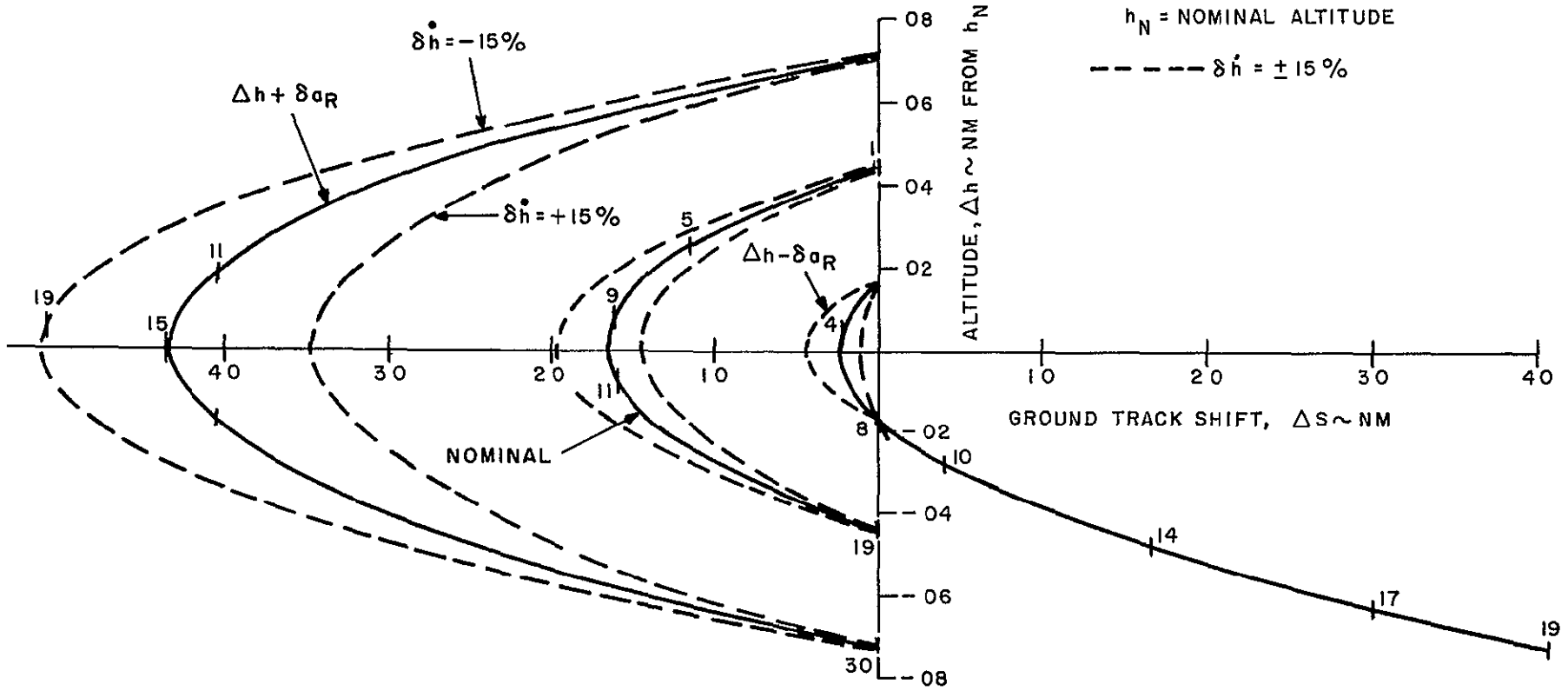


Figure 4.2-8. 18 Day Decay Cycle Curve,  $h = .005 \text{ nm/day}$

11 February 1970

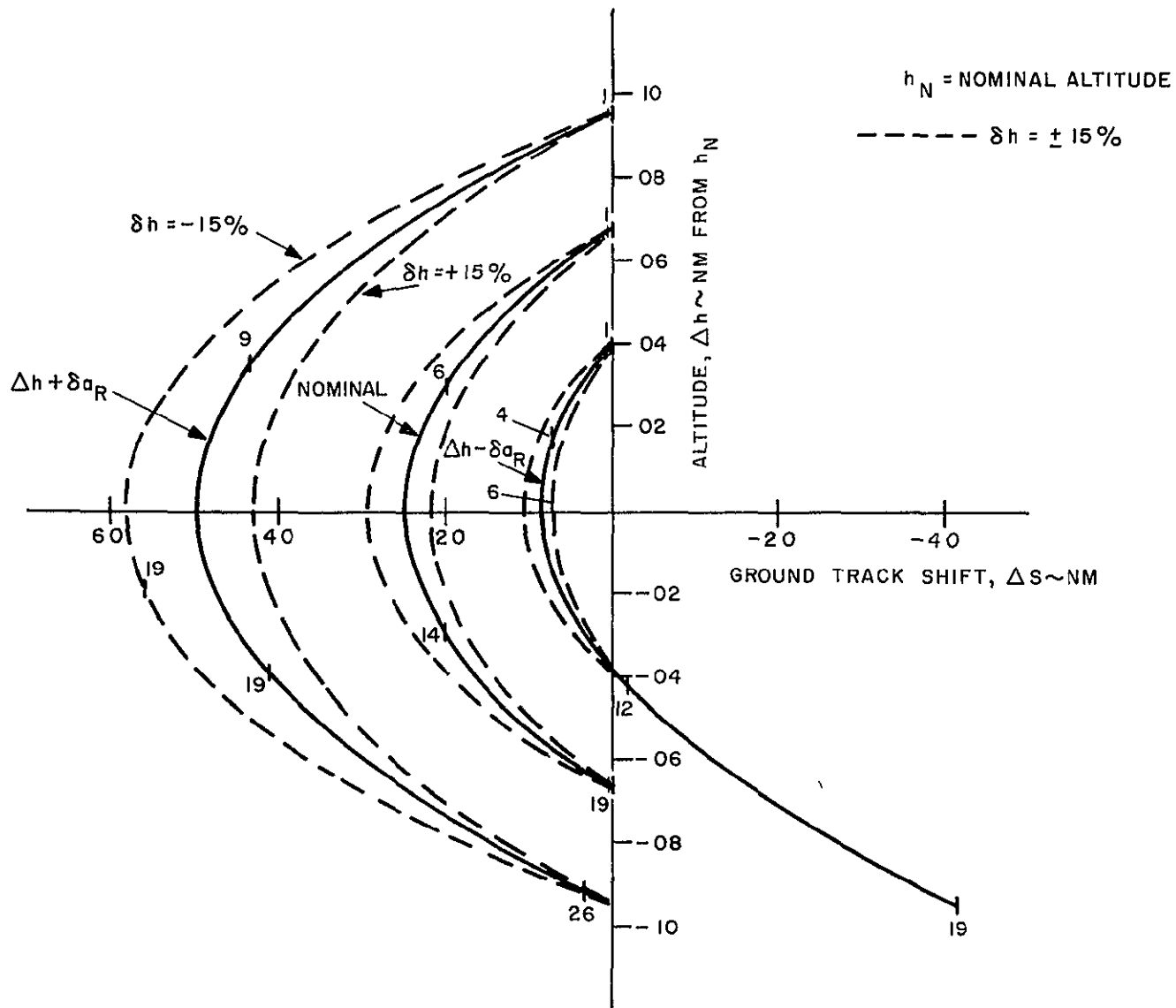


Figure 4.2-9. 18 Day Decay Cycle Curve,  $h = .0075 \text{ nm/day}$

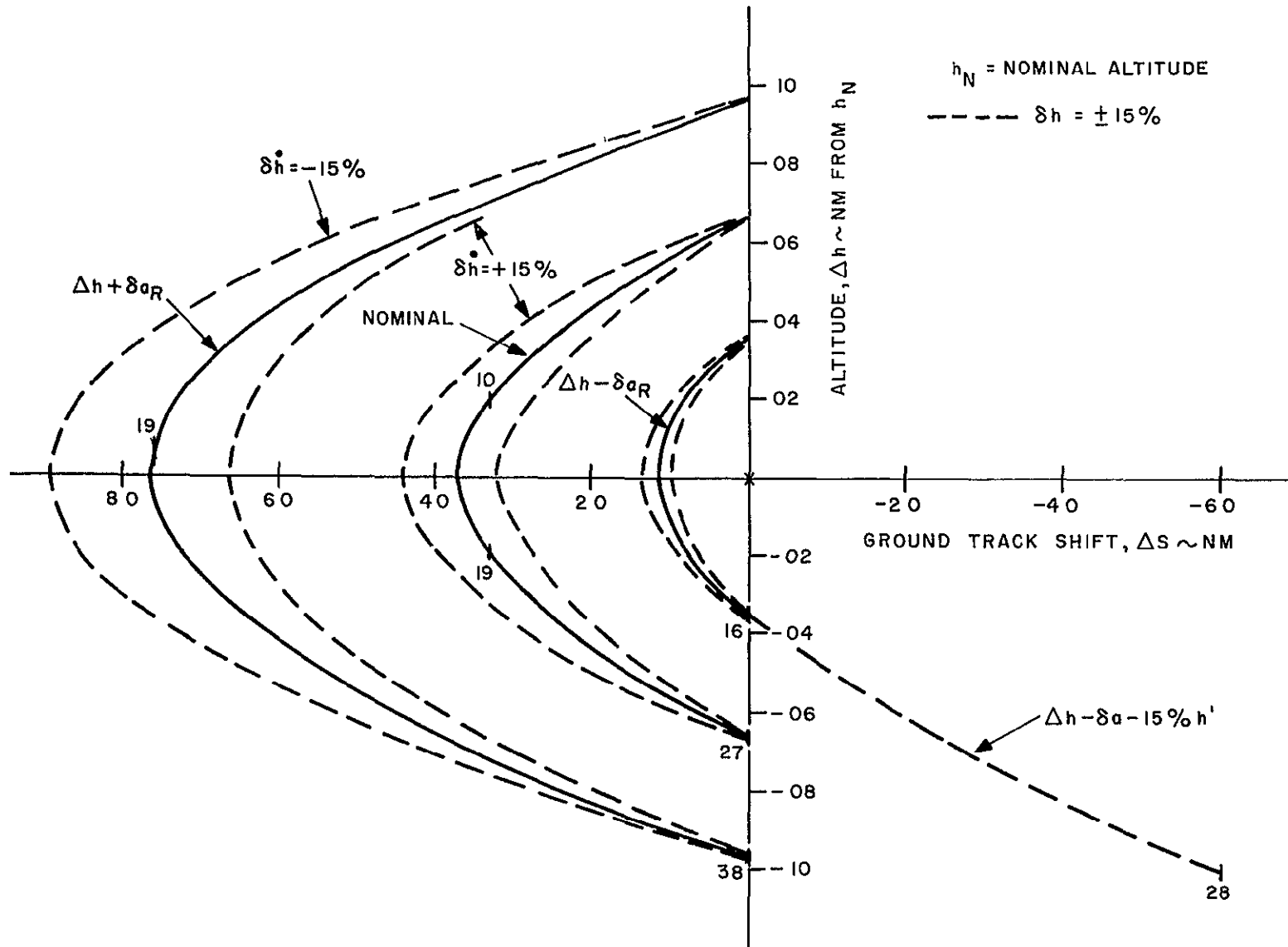
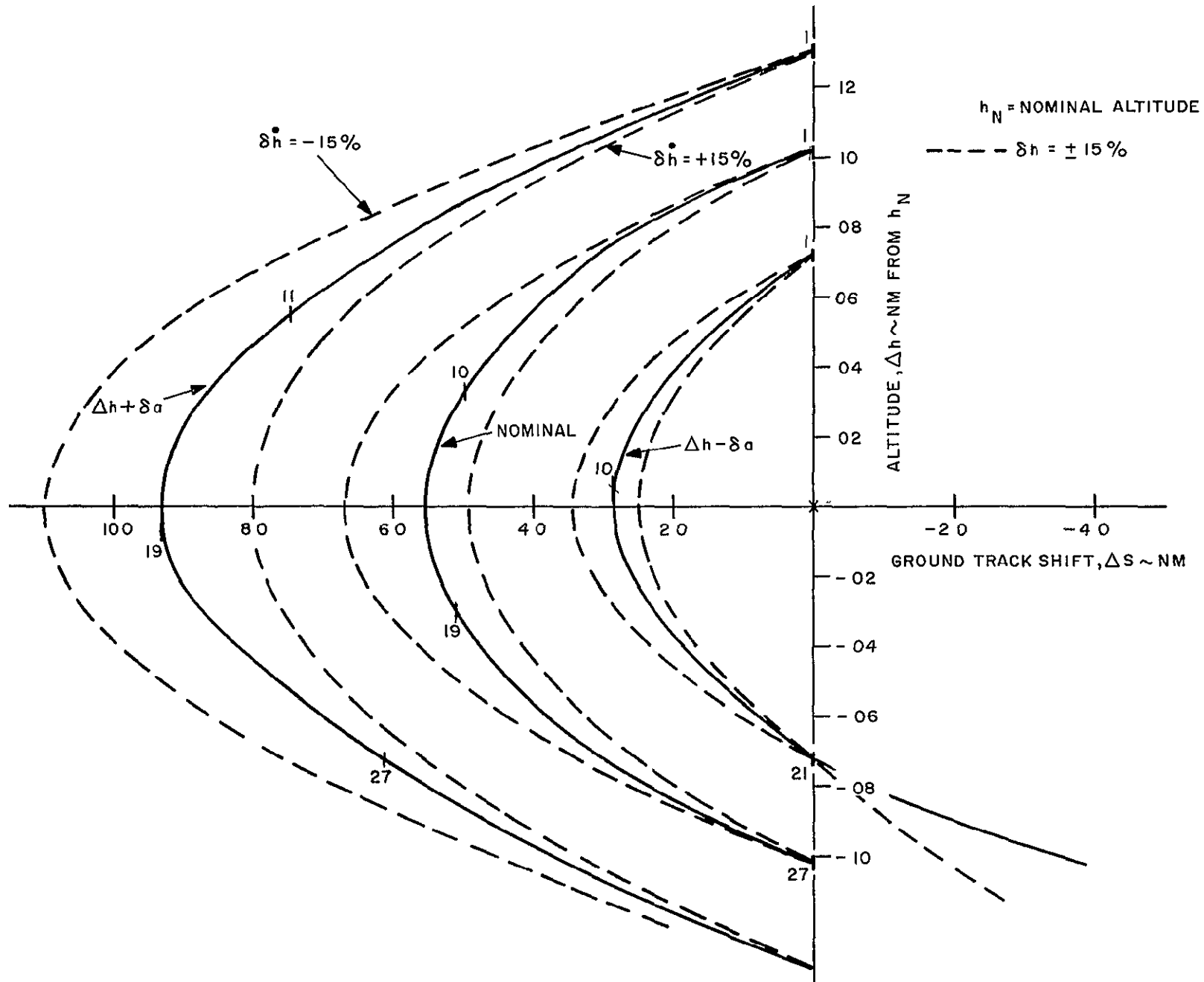


Figure 4.2-10. 27 Day Decay Cycle Curve,  $h = .005 \text{ nm/day}$

Figure 4.2-11. 27 Day Decay Cycle Curve,  $h = .0075 \text{ nm/day}$



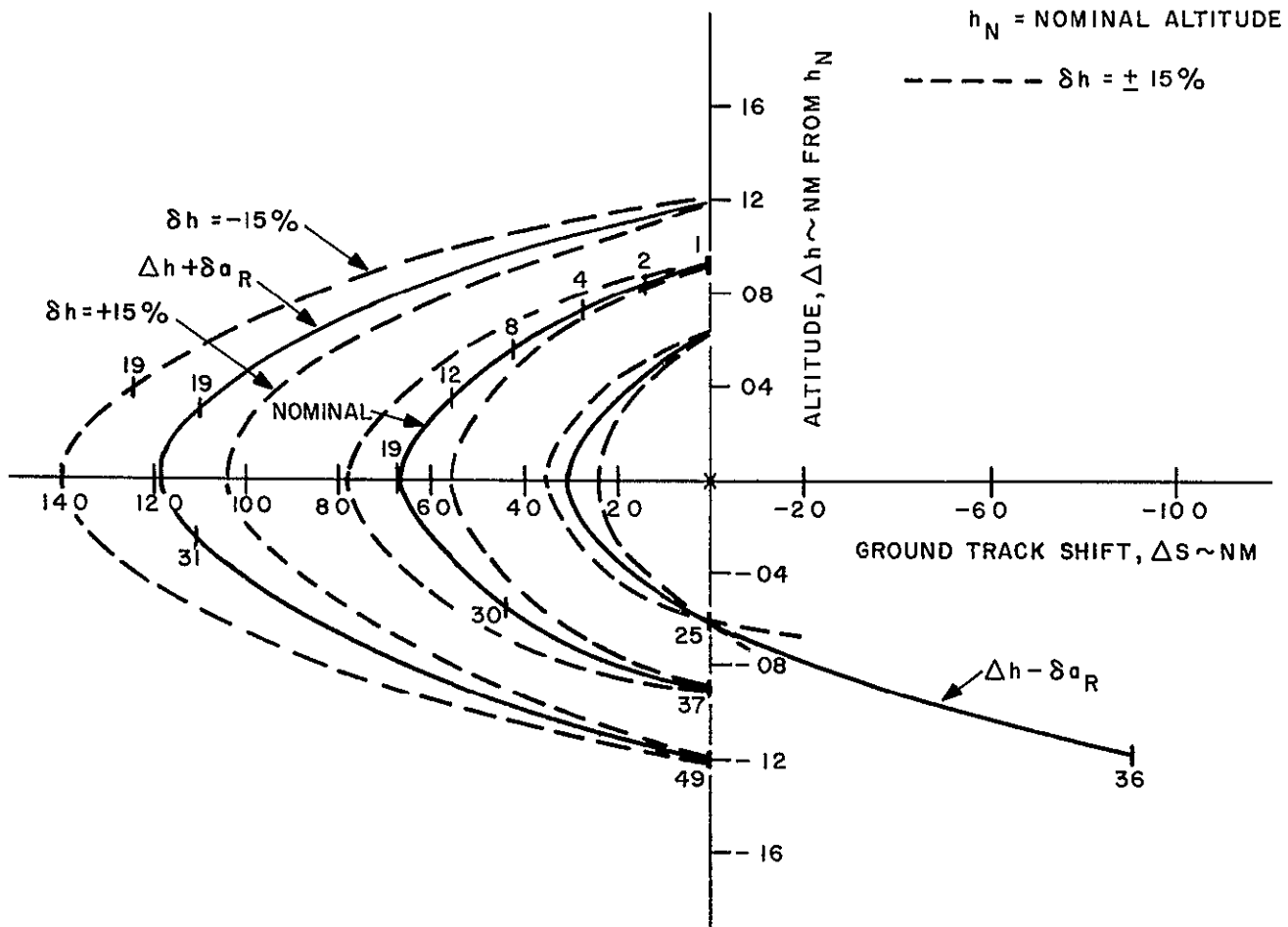
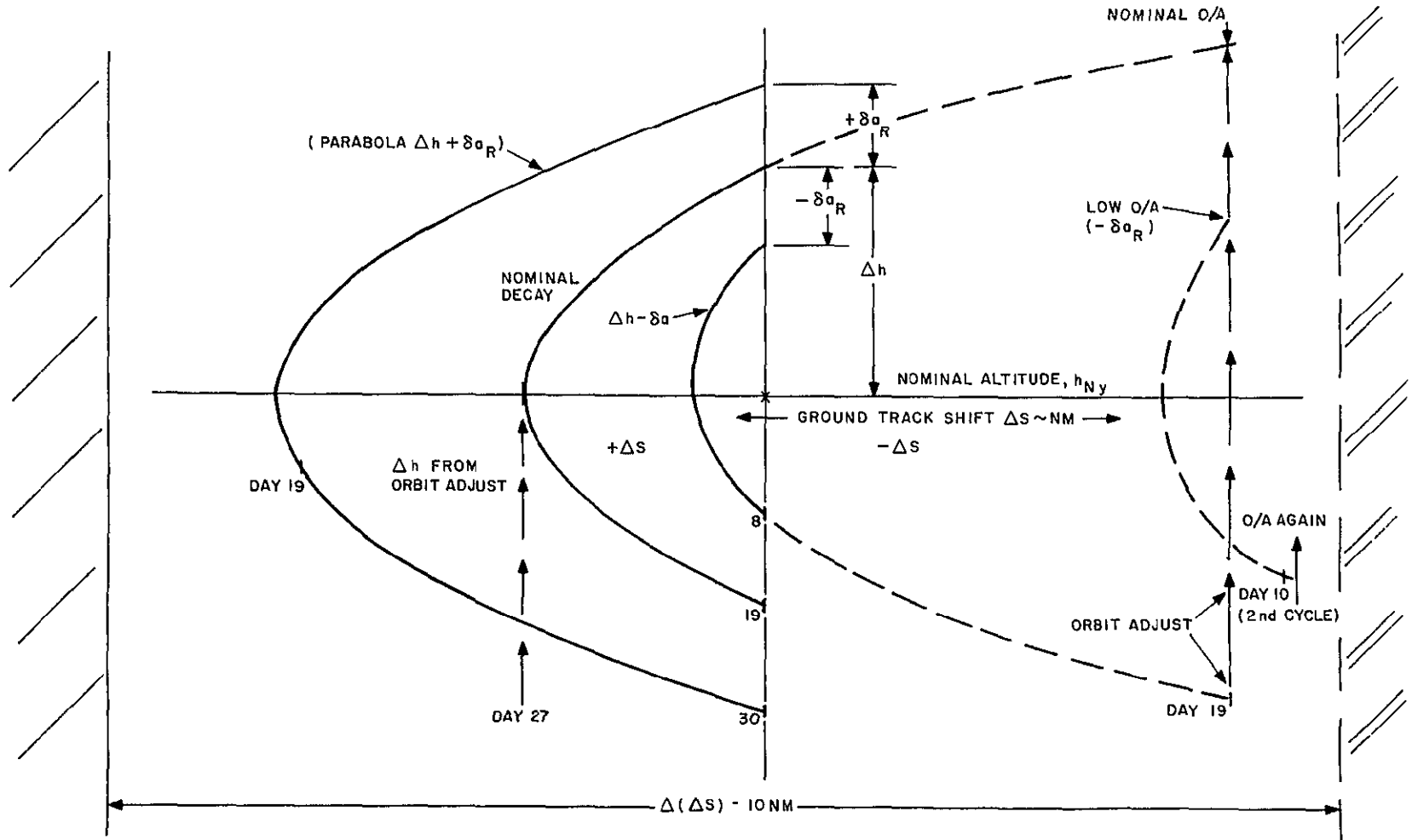


Figure 4.2-12. 36 Day Decay Cycle Curve,  $h = .005 \text{ nm/day}$





11 February 1970

Figure 4.2-14. Orbit Adjust Control of Orbit Decay Cycle

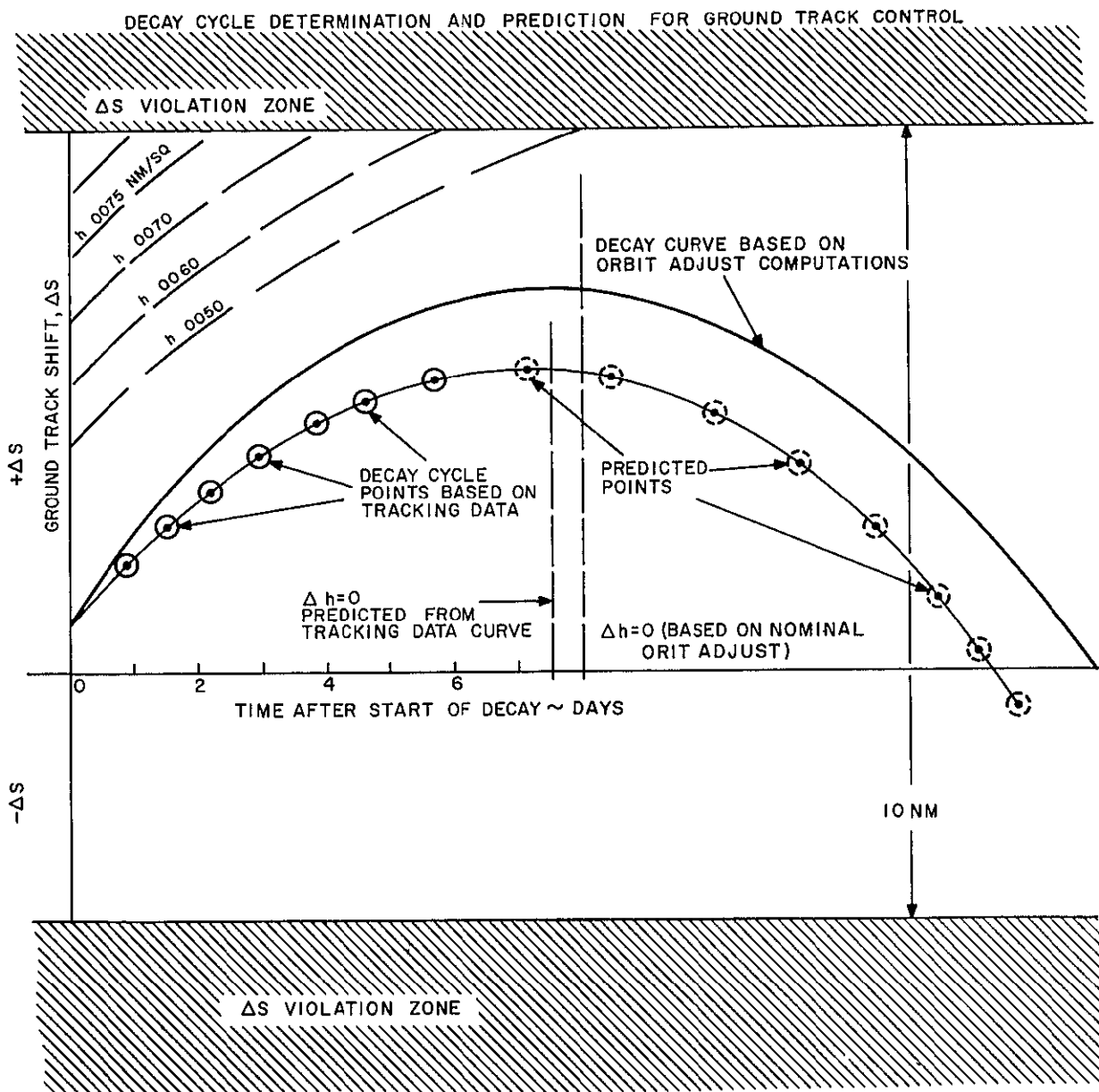


Figure 4.2-15. Decay Cycle Determination and Prediction for Ground Track Control

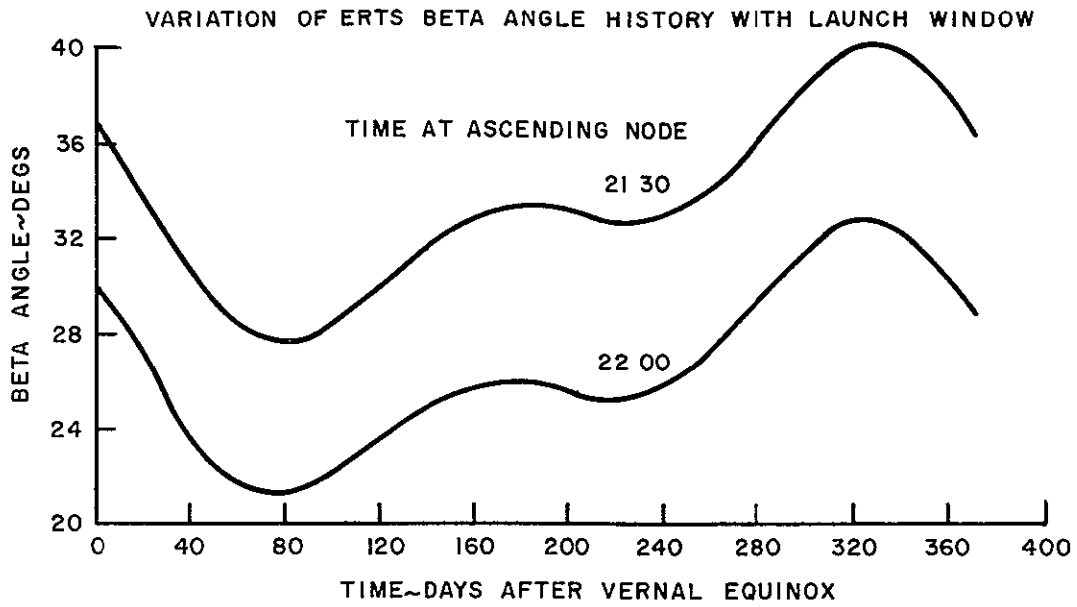


Figure 4.2-16. Variation of ERTS Beta Angle History With Launch Window

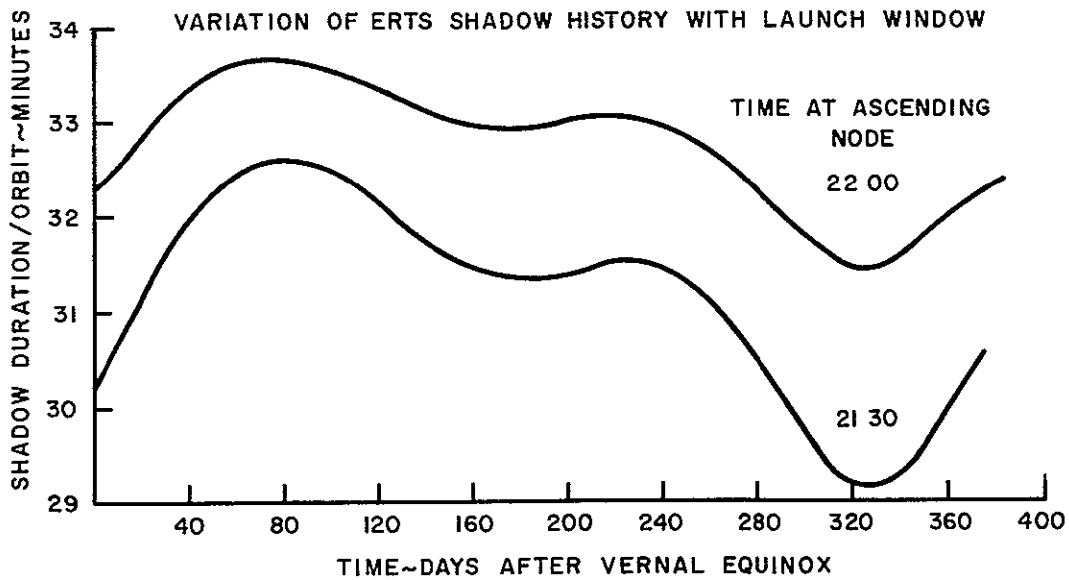


Figure 4.2-17. Variation of ERTS Shadow History With Launch Window

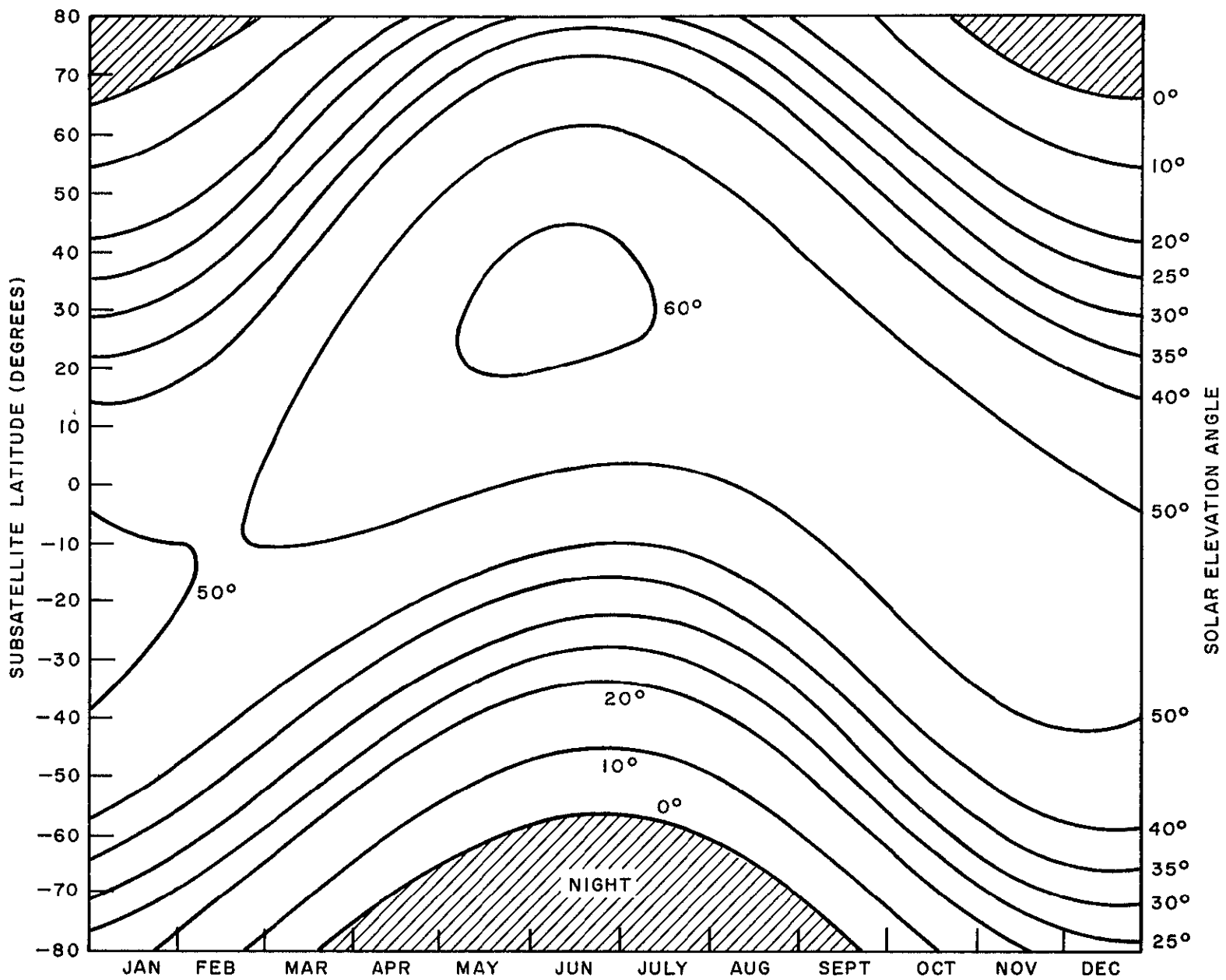
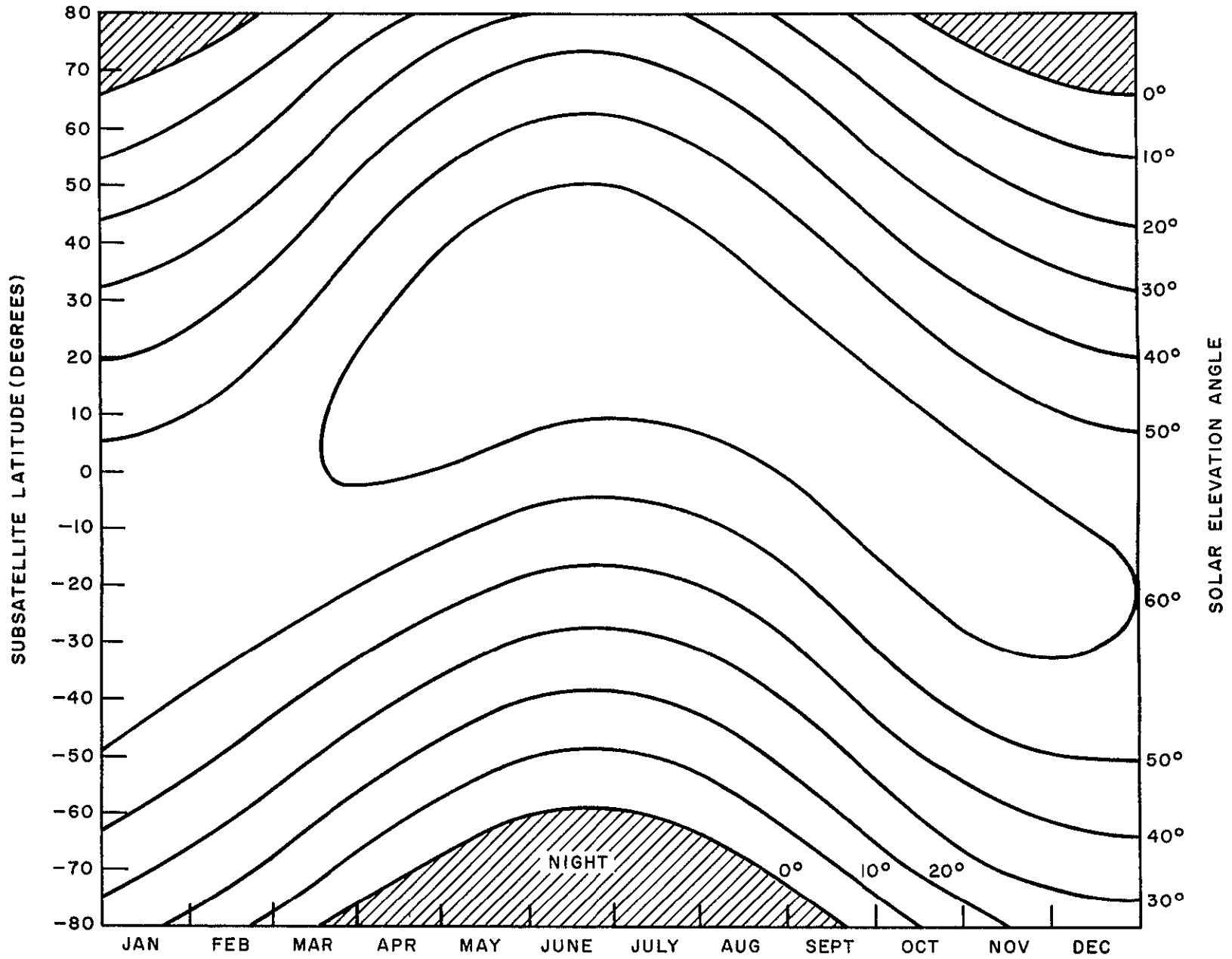


Figure 4.2-18. Solar Elevation Angle History as a Function of Subsatellite Latitude - Ascending Node at 2130 Hours

11 February 1970



11 February 1970

Figure 4.2-19. Solar Elevation Angle History as a Function of Subsatellite Latitude - Ascending Node at 2200 Hours

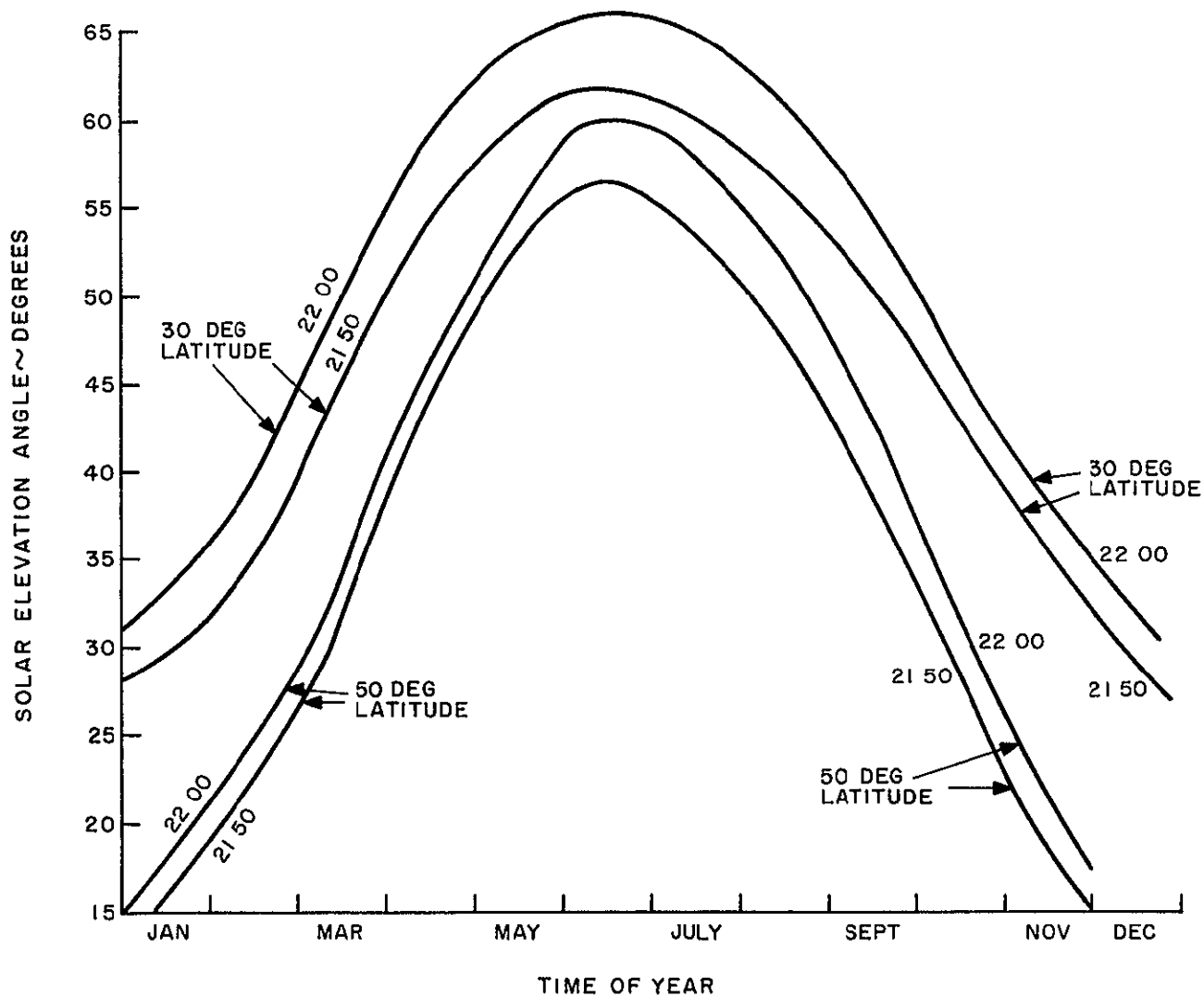


Figure 4.2-20. Effect of 30 Minute Launch Window on Solar Elevation Angle at 30 Degrees and 50 Degrees North Latitude



TABLE 4.2-1. NOMINAL ORBIT

<u>Orbit Parameters</u>	
Altitude*	492.35 nm
Inclination	99.088 degrees
Period	6196.015 seconds
Eccentricity	0
Time at Ascending Node	21 30
Coverage Cycle Duration	18 days (251 revs)
Distance Between Adjacent Ground Tracks = 86.06 nm	

\*Altitude Defined As

Semi-Major Axis Minus Equatorial Radius

TABLE 4.2-2.  $C_D A$  CALCULATIONS

Item	Normal Force			Sheer Force		
	Area (sq ft)	$C_D$	$C_D A$ (sq ft)	Area (sq ft)	$C_D$	$C_D A$ (sq ft)
Ground Plane	0.1	2.2	0.2	0		
Paddles	51.0	$2.8 \left(\frac{2}{\pi}\right)$	90.9	0		
Trans Section	6.2	2.8	17.4	0		
+ Drives	0.43	2.2	0.9			
ACS	4.5	2.8	12.6	8.64 (Sides) 4.1 (top)	0.075	0.6 0.3
Truss Tubes	3.0	2.2	6.6	0		
Aux. Load Panels	0.7	2.8	2.0	0		
ACS I/F Panels	1.2	2.8	3.4			
O/A						
Module	0.19	2.8	0.5	0		
Tank (partially blocked)	0.167	2.0	0.3	0		
Torus Ring	6.1	2.2	13.4			
WBRE'S	2.0	2.8	5.6	35.	0.075	2.6
Sensors, etc.	5.7	2.8	15.9			
			<u>169.7</u>			<u>3.5</u>
Total $C_D A$	173.2 sq ft					

TABLE 4.2-3. ORBIT ADJUST SUBSYSTEM  $\Delta V$  REQUIREMENTS

A. INJECTION ERROR REMOVAL		$\Delta V$ FPS
1.	Nominal - (Remove 14. nm Altitude Error)	21.7
2.	Predictable Losses in Efficiency	
A.	Thruster Cant Angle of $21.5^\circ$ (7% Loss)	1.5
B.	Continuous Thrusting Arc (5% Loss)	1.1
	Subtotal	24.3
3.	Error Sources	
A.	Thrust Alignment	
1.	Thrust Vector $.25^\circ$ } 2. $1.78^\circ$ C.G. Pointing } 1%	
B.	Attitude Control	
	Pitch, Roll $5^\circ$ (added Cant Angle)	2.5%
	Yaw 0 to $10^\circ$ , Avg. of $\approx 5^\circ$	1.0%
	RSS of Error Sources	2.9%
	Total $\Delta V$ Injection Error Removal	<u>25.0</u>
B. DRAG MAKE-UP		
1.	Decay Rate (2.42 nm/Yr.)	7.5
2.	Losses	
A.	Cant Angle - 7%	<u>0.5</u>
	Subtotal	8.0
3.	Error Sources	
A.	Thrust Alignment	1% 0.1
B.	Attitude Control	Neghible
	Total $\Delta V$ for Drag Make-Up	<u>8.1</u>
C. ATTITUDE CONTROL EFFECTS		
1.	Pitch Error Corrections	1.0
D. ADDITIONAL MARGIN ( $\approx 30\%$ )		<u>10.9</u>
	TOTAL $\Delta V$	<u>45.00 FPS</u>

TABLE 4.2-4 COVARIANCE MATRIX - MSFN (METERS AND CENTIMETERS)

$0.461297 \times 10^3$	$0.102584 \times 10^3$	$-0.372790 \times 10^3$	$0.318797 \times 10^2$	$-0.255107 \times 10^2$	$-0.316175 \times 10^2$
	$0.238453 \times 10^3$	$-0.343637 \times 10^3$	$0.123967 \times 10^2$	$-0.310654 \times 10^2$	$0.269304 \times 10^2$
		$0.355040 \times 10^4$	$-0.178066 \times 10^3$	$0.260083 \times 10^3$	$-0.470579 \times 10^2$
	SYMMETRIC		$0.106002 \times 10^2$	$-0.123284 \times 10^2$	$0.208299 \times 10^0$
				$0.199287 \times 10^2$	$-0.487497 \times 10^1$
					$0.101861 \times 10^2$

TABLE 4.2-5. COVARIANCE MATRIX - CORPUS CHRISTI (METERS AND CENTIMETERS)

$0.239313 \times 10^4$	$0.164108 \times 10^4$	$-0.786428 \times 10^4$	$0.402627 \times 10^3$	$-0.594417 \times 10^3$	$0.482858 \times 10^2$
	$0.140231 \times 10^4$	$-0.614073 \times 10^4$	$0.278678 \times 10^3$	$-0.459570 \times 10^3$	$0.888044 \times 10^2$
	SYMMETRIC	$0.633764 \times 10^5$	$-0.336738 \times 10^4$	$0.448782 \times 10^4$	$-0.323752 \times 10^3$
			$0.189397 \times 10^3$	$-0.234938 \times 10^3$	$0.104348 \times 10^2$
				$0.323595 \times 10^3$	$-0.227993 \times 10^2$
					$0.122504 \times 10^2$

TABLE 4.2-6. ORBIT PARAMETERS FOR COVARIANCE MATRICES

Elements	
Semi-Major Axis	= 7296 757 km
Eccentricity	= 0 0001
Inclination	= 99.0 degrees
Right Ascension of Ascending Node	= 300.25 degrees
Argument of Perigee	= 0.0 degrees
Mean Anomaly	= 180. degrees
Calculated Parameters	
Radial Distance $\hat{=}$ Semi-Major Axis	= 23939491. ft
Velocity	= 24249 ft/sec
X	= 12059997. ft
Y	= 20679890. ft
Z	= 0.
$\dot{X}$	= 3275.38 ft/sec
$\dot{Y}$	= 1910 92 ft/sec
$\dot{Z}$	= -23950.4 ft/sec

11 February 1970

#### 4.3 REFERENCES

1. Memorandum for Record - "Proposed Constants and Equations for ERTS-A and ERTS-B Atmospheric Density Model" - Memorandum from Walter D. Bradley to Thomas M Ragland - dated November 24, 1969.
2. "Models of Earth's Atmospheres, 120 KM to 1000 KM", NASA SP-8021 - May 1969.
3. GSFC Operations Control Center - "Satellite Situation Reports" - May 31, 1969 through December 15, 1969.

### 4.3 IMAGE LOCATION AND COVERAGE

The studies in this section relate largely to attitude control and attitude determination requirements. Sections 4.3.1 through 4.3.5 analyze the problem of spatially locating information contained in ERTS imagery to an accuracy of 2 nautical miles. This analysis results in the specification of attitude determination requirements for the spacecraft. Section 4.3.6 investigates the effect of the basic coverage requirements on the control system pointing requirements. Section 4.3.7 summarizes the effects of spacecraft attitude rates on ERTS imagery. Finally, Section 4.3.8 summarizes the attitude control and attitude determination requirements.

#### 4.3.1 GENERAL

Attitude sensors and telemetry provisions to determine attitude to an accuracy sufficient to locate any point on a 100- by 100-nautical mile picture with an accuracy of less than 2 nautical miles is required for ERTS-A and B.

To proceed to a timely solution allowing specification of the accuracy requirement to be met by the attitude determination sensor, an assumption was made in interpreting this requirement. The assumption is that this requirement must be met with a geometrically accurate payload sensor. This requirement then becomes a system/attitude sensor requirement which is not dependent upon the characteristics of any particular payload sensor.

Errors in spatially correlating the imagery obtained to the Earth's surface arise from effects external to the sensor, such as Earth curvature, atmospheric refraction, and terrain relief. Errors in the imagery also arise from effects internal to the sensor, such as lens and scan anomalies. For the purposes of this study, it is assumed that both of these effects will be controlled through an effective sensor implementation and data processing system such that the indeterminate components of these errors will result in picture distortions which are of the order of the ground resolution of the sensor at maximum contrast.

Both the RBV's and the MSS have ground resolutions of 230 to 240 feet from the ERTS altitude. With the assumption that sensor associated random distortions are limited to a ground resolution element (230 feet), it will be shown that position location to an accuracy of 2 nautical miles is essentially independent of the payload sensor.

The total mapping accuracy study to be completed in April 1970 will result in a value for indeterminate sensor distortions based on the analyses performed in that study. When such distortion estimates are available the error analysis will be updated, and the attitude sensor specification and its expected performance will be investigated for margin.

The image location requirement for a 100- by 100-nautical mile picture clearly relates to the RBV's. In consideration of the MSS, where no picture is formed in a conventional sense, the assumption is made that meeting the requirement for an RBV picture results in meeting it for an MSS strip. This is true simply because the MSS is very slightly less sensitive to yaw errors.



### 4.3.2 UNITS

In determining the accuracy requirement for an attitude determination sensor, statistical quantities are involved. Precisely, the accuracy requirement will be in terms of the three-sigma (99.7 percent) value required in three axes (roll, pitch and yaw), where roll and pitch determine the local vertical and yaw determines the heading angle. The 2-nautical mile accuracy is assumed to be a three-sigma value.

As specified in the Design Study Specification, the operational ephemeris location of ERTS will not be known closer than  $\pm 0.16$  statute mile. The precise interpretation is that the in-track position error is 0.16 statute mile, one-sigma, and the cross-track and altitude errors are 50 meters, one-sigma. The three-sigma ephemeris errors are

In-track	Cross-track	Altitude
2534 feet	482 feet	482 feet

The three-sigma accuracy and one-sigma ephemeris assumption is the most pessimistic interpretation.

Timing errors produce location errors due to two types of velocities present in the system. The orbital velocity transferred to the sub-vehicle point produces location errors similar to the effects of ephemeris errors when timing errors exist in the knowledge of shutter time. Angular velocities of the spacecraft frame produce location errors similar to attitude sensor errors when camera shutter operation is not perfectly correlated with the attitude sensor data.

The units employed in this analysis are feet (for ephemeris), minutes of arc (for attitude), and milliseconds (for time errors), and they are three-sigma statistical quantities.

### 4.3.3 GAINS

To set up the error equation, it is necessary to relate ephemeris to surface position, attitude angles to surface position, and time to surface position. These gains then have the units foot per foot, foot per arc-minute, and foot per second, and they allow expression of all error sources in terms of feet on the Earth's surface.

Ephemeris when applied to ERTS would be a table of coordinates with equal time intervals as the argument. To obtain such a table, the ERTS vehicle must be tracked and "fixes" must be obtained. Since the ERTS cannot be tracked continuously, the motion between fixes and tracking times must be modeled. Such modeling requires estimates of the harmonics of the Earth's gravitational field. Once modeled, the series represents the gravitational potential of the Earth so that the Earth's oblateness and its pear shape are represented. (The GSFC Earth model employs 14 to 15 terms.) The effects of drag must also be modeled.

Two types of errors due to ephemeris exist. First, the actual table data can be in error, i.e., at a precise time, the vehicle position as listed in the table has only a finite degree of certainty. Tracking errors usually result in three definable position uncertainties along

11 February 1970

the track, cross-track, and altitude, along the track uncertainties are the largest. Second, the knowledge of time is uncertain, i.e., the table of ephemeris is entered with some basic uncertainty in the argument.

For ephemeris errors when a local vertical sensor is employed, the projection of position from the orbit to the surface is reduced by the ratio of the Earth radius to the orbit radius. For the case of ERTS, this reduction is 7/8. When celestial references are used to determine attitude, the local vertical must be determined from the ERTS position in orbit, and the local vertical thus determined has an error dependent upon the ephemeris error. When this effect is considered, the ephemeris error when projected to the surface has a gain of nearly 1.1.

Attitude when applied to ERTS would be the orientation of the payload sensor with respect to the local vertical and the orbital velocity direction. Attitude errors are small angle perturbations about the references. The gains relate the linear displacement in feet at the Earth's surface to orientation errors about the references.

At ERTS nominal altitude, the length of the arc of 1 minute of central angle is 877 feet. Thus, the first order effect of 1 arc minute of roll or pitch error is 877 feet of surface position error of the sub-vehicle point. At the corner of a picture, a yaw error works through a radius of 70.7 nautical miles. An arc minute of yaw error produces a corner displacement of 125 feet.

Orientation errors are of two types orientation sensor errors and boresight errors. To appreciate these two types of error sources, it is necessary to define the vehicle axes. Let the vehicle control axes be defined as the axes of the orientation sensors. (These axes are not necessarily orthogonal except to first-order effects.) Now let the payload axes be defined as the axes of the sensor/sensors. (These axes are orthogonal since internal sensor anomalies are considered separately.)

Orientation sensor errors are the uncertainties within the sensor (including its data processing) and include non-orthogonalities when more than one sensing head is used.

Boresight errors are the uncertainties which are present between the control axes defined by the orientation sensors and the payload axes defined by the operational sensor or sensors.

Statistically, boresight errors are equal to the mean value of the random process associated with orientation determination and can be estimated statistically. The mean value,  $\bar{X}$ , is  $\int_{-\infty}^{\infty} x f(x) dx$ . Statistically, sensor errors are equal to the square root of the variance where the variance is the mean-squared value of the random process about the mean. The variance,  $\sigma^2$ , is given as  $\int_{-\infty}^{\infty} (x - \bar{X})^2 f(x) dx$ . The mean squared value of the random process,  $\bar{X}^2$ , is given by  $\int_{-\infty}^{\infty} x^2 f(x) dx$  and is equal to the variance plus the square of the mean value.

MEAN SQUARED VALUE = VARIANCE + MEAN VALUE SQUARED

$$\overline{x^2} = \sigma^2 + \overline{x}^2$$

The high gain associated with orientation errors and the a priori knowledge of the cost to improve the attitude determination system suggests that to use the mean squared value of the sensor rather than the variance as the limiting sensor accuracy may be an expensive accuracy criterion, particularly since the mean value (boresight error) will be readily determined from an averaging of a limited number of ground truth operations. This is comparable to sighting in a gun with a few, measurable trial shots

The sub-vehicle point velocity in the orbit plane is 21,195 feet per second. The surface velocity (a function of latitude, earth rate, and earth radius) is zero at the poles and 1,520 feet per second at the equator. The error in surface position due to timing error in milliseconds is

In-track                      21.1 ft/msec

East-West (at equator)    1.5 ft/msec

The vehicle attitude rates will never exceed 0.04 degree per second. This is equivalent to 2.4 arc minutes per second or 2100 feet per second in roll and pitch and 300 feet per second at a picture corner in yaw

Roll/pitch                    2.1 ft/msec

Yaw                            .3 ft/msec

#### 4.3.4 IMPLEMENTATION AND RELATIVE ERROR EFFECTS

The ephemeris errors are considered to be basic system constraints to which a portion of the 2-nautical mile location error must be allocated. The altitude error, to the first order, is assumed to have zero again.

The timing error of interest is the error in determining the shutter operation. Exposure times are 8, 12, and 16 milliseconds. It is reasonable to assume that the system can determine the time of shutter operation to an accuracy commensurate with the exposure time, i.e., the location of the frame center should be as precise as the time of exposure of one part of the picture to any other. The uncertainty in the knowledge of the time of shutter operation is on the order of 10 milliseconds. (Section 4.4 of this volume discusses the approach to achieving this timing information.)

Based upon a 10-millisecond timing error and a picture taken at or near the equator, the position errors of the picture center due to ephemeris and time errors for a local vertical sensor implementation are as follows

In-track	Ephemeris	2216 feet
	Time (velocity)	212 feet
	Time (pitch attitude rate)	21 feet
Cross-track	Ephemeris	422 feet
	Time (velocity)	15 feet
	Time (roll attitude rate)	21 feet

Combining the errors statistically, (both in-track and cross-track) and then geometrically as orthogonal components of an error magnitude results in

$$(\text{Error})^4 = (2216^2 + 212^2 + 21^2)^2 + (422^2 + 15^2 + 21^2)^2$$

$$\text{Error} = 2220 \text{ feet}$$

To make a point, in statistic combination of variances, an order-of-magnitude difference in the standard deviation of two error sources results in the neglecting of that error source with the smaller standard deviation.

With an in-track ephemeris error of 2216 feet, which is non-reducible from an operational system standpoint, a limited number of error sources with an order-of-magnitude lower standard deviation may be ignored.

The assumption in Section 4.3.1 was that if sensor external errors and sensor internal errors are limited to one resolution element (230 feet) on the ground, then these two error sources may be ignored when considering ephemeris and attitude errors. From the above, this assumption is justified.

#### 4.3.5 FIRST-ORDER ERROR EQUATION, ITS SOLUTION, AND ATTITUDE DETERMINATION SENSOR REQUIREMENTS

As indicated in the previous section, there is only one significant error source that must be included in the First-Order Error Equation for attitude errors. This is the in-track ephemeris error, which produces a surface projected error of 2216 feet along the track.

The three attitude errors are the errors in roll, pitch and yaw. Let these errors be  $E_R$ ,  $E_P$  and  $E_Y$ , respectively. In terms of the Allowable Error ( $E_A$ ) these quantities are related by

$$E_A^4 = \left\{ (2216)^2 + (877E_P)^2 + (88E_Y)^2 \right\}^2 + \left\{ (877E_R)^2 + (88E_Y)^2 \right\}$$

The allowable error is at a corner, and the contribution of yaw error has been geometrically projected to in-track and cross-track components. The allowable error is a scalar quantity.

Two approaches to a solution are possible. First, the allowable error can be reduced from 2 nautical miles by the mean value of attitude error, the expected boresight errors between the payload sensor axes, and the attitude determination sensor axes. The solution would be in terms of the standard deviation of the random variables  $E_R$ ,  $E_P$  and  $E_Y$ . Second, the allowable error can remain at 2 nautical miles where it is assumed that the mean values of  $E_R$ ,  $E_P$  and  $E_Y$  are compensated out by a ground command bias. Such an assumption implies that ground truth data is used to determine the boresight error. During early portions of the mission, the attitude data available with the picture data will not be sufficiently accurate to locate any point with an accuracy of 2 nautical miles because the boresight compensation bias will not have been incorporated. Once truth data is produced to allow mean value (boresight) compensation, the attitude data available with picture data will allow location to 2 nautical miles, and all early data can then be post-adjusted to meet the location accuracy specified.

The error allocation for the post-launch boresight error between the payload and the attitude determination sensor will be 3 arc minutes or 0.05 degree in all three axes. This is not the alignment tolerance between the payload and the attitude determination sensor during spacecraft assembly; it is the sum of assembly alignment inaccuracy and any launch induced misalignment. It is felt that such post-launch precision can be achieved by mounting both the orientation and payload sensors to a common support structure, but with difficulty for both payloads (RBV's and MSS). To compensate for the optimism of the 3-arc minutes, a pessimistic rationale will be employed in the allocation of error to boresight sources.

The boresight error is assumed to be 3 arc minutes (optimistic), but the worst case will be used where the 3 arc minutes of boresight error is assumed to exist simultaneously in each axis (pessimistic). The boresight error,  $E_B$ , is

$$E_B = \left[ (3(877))^2 + (3(877))^2 + (3(125))^2 \right]^{1/2} \\ = 3913 \text{ feet}$$

Without in-flight boresight removal, the allowable error is 2 nautical miles less 3913 feet or 8247 feet. With in-flight boresight removal the allowable error is 2 nautical miles or 12160 feet

The object is to solve the error equation

$$E_A^4 = \left\{ (2216)^2 + (877E_P)^2 + (88E_Y)^2 \right\}^2 + \left\{ (877E_R)^2 + (88E_Y)^2 \right\}^2$$

for two values of  $E_A$  to determine how much roll, pitch and yaw error can be tolerated, with and without in-flight ground truth operations. To solve the equation, we must have two additional equations which relate the roll, pitch and yaw errors to each other

The ratio of the errors are dependent upon the implementation employed.

For a celestial sensor,  $E_R$ ,  $E_P$ , and  $E_Y$  should all be equal. The error equation can then be solved for the per axis error in attitude. The in-track error due to ephemeris error must be increased, as previously noted. The value then is 2534 feet.

$$E_A^4 = \left\{ (2534)^2 + (877E)^2 + (88E)^2 \right\}^2 + \left\{ (877E)^2 + (88E)^2 \right\}^2$$

The solution with calibration is 0.2 degree, and without calibration it is 0.126 degree.

For a local vertical sensor,  $E_R$  and  $E_P$  should be equal. Furthermore, a state-of-the-art limit is 0.10 degree in each axis. The solution of the error equation with these conditions results in the yaw attitude precision requirement

	<u>Earth Sensor Implement</u>		
	<u>Allowable Error</u> $E_A$	<u>Axis</u>	<u>Assumption</u> $E_R = E_P = 0.1^\circ$
With Calibration	12,160 feet	Roll/Pitch Yaw	0.10° 1.67°
Without Calibration	8,247 feet	Roll/Pitch Yaw	0.10° 0.80°

11 February 1970

The Yaw axis requirement indicates that with some in-flight ground truth data to determine boresight errors between the attitude determination sensor and the payload sensor, the normal yaw-axis control will provide yaw precision that is more than adequate in conjunction with a local vertical sensor of 0.1 degree accuracy. In summary, the attitude determination sensing system accuracy requirements are

1. For a celestial reference system, the three-sigma accuracy must be 0.2 degree with in-flight calibration and 0.126 degree without. This accuracy must be achievable irrespective of available star density variations due to orbit motion, earth occultation, and solar or lunar interference.
2. For a local vertical system, the three-sigma accuracy must be better than 0.1 degree. This accuracy must be achievable over an off-null range of one degree and independent of solar interference effects.

The selection of a sensor satisfying these requirements is discussed in Section 3.3 5 of Volume II of this design study report.

#### 4.3.6 BASIC COVERAGE

A basic requirement for ERTS is to direct the two primary sensor system FOV's to the local vertical and the velocity vector.

In the case of the RBV camera system, it is required that montage photographs be produced with minimum misalignment between contiguous pictures. To produce such a montage, both image overlaps and sidelaps must be provided. An orbit adjust system is provided to initiate and adjust, if necessary, the satellite track to provide image sidelaps from adjacent orbits.

In the case of the multi-spectral point scanner, it is required that the vehicle orbital pitch rate be regular and provide, in conjunction with a single-degree-of-freedom driven mirror, continuous coverage of the subsatellite swath.

Because coverage connotes pointing and not knowledge of pointing, it is necessary to consider the actual achieved orientation accuracy.

Also, there exists a tradeoff between satellite orientation control and orbit parameter adjustment. To the first order, pitch orientation control and along-track ephemeris are related through RBV overlaps, while roll orientation control and cross-track ephemeris are related through RBV sidelaps. Similar interrelationships exist for the MSS coverage of the subsatellite swath.

The ERTS orbit parameters are adjusted to provide a nominal 10 percent sidelap between contiguous subsatellite swaths in the absence of any attitude error, while the actual subsatellite swaths coincide by  $\pm 10$  miles in any one full coverage period.

The ERTS orbit has a semi-major axis of 3936 nautical miles with an orbit period, ascending node to ascending node, of 6196 seconds. The geographic longitude of ERTS ascending node shifts 25.8167 degrees to the west between each subsequent ascending node.

Contiguous subsatellite swaths occur every 14 revolutions and are separated in longitude by 1.4338 degrees. Since a nautical mile is one minute of longitude, the contiguous subsatellite swaths are separated by 86.028 nautical miles at the equator. Table 4.3-1 shows the ascending node longitude history for an initial ascending node in the prime (Greenwich) meridian plane. At the end of 18 days, or the completion of 251 orbits, the coverage period is completed, and the ascending node is again in the prime meridian plane.

The problem of sidelaps is a question of precision of the ascending node geographic longitude shift in 14 orbits and roll/yaw pointing accuracy to achieve the desired coverage.

The problem of subsatellite track coincidence is a question of precision of the ascending node geographic longitude shift in 251 orbits. Track coincidence and the orbit adjust system are discussed in Section 4.2. However, the  $\pm 10$  miles allowable in 18 days results in an allowable deviation of the center of contiguous subsatellite swaths (tracks separated by 14 revolutions or about one day) of 0.55 mile.

It will be assumed that the orbit adjust system will not be required to operate more often than once in 18 days and that the error in ascending node shift results in the center of contiguous subsatellite swaths being separated by 86.028 nautical miles to within 0.55 nautical mile.

TABLE 4.3-1. ERTS LONGITUDE OF ASCENDING NODE

Orbit	Degrees West Longitude
0	0.0000
1	25.8167
2	51.6334
-	- - -
13	335.6171
14	1.4338
15	27.2505
--	- - -
250	334.1833
251	0.0000



The coverage problem will be investigated for both sensor systems.

For the RBV, the contiguous geometry at the equator is shown in Figure 4.3-1. The interpretation of the sidelaps requirement is that the 10 percent sidelaps must exist to provide for orientation errors and guarantee that for maximum error at least adjacent pictures are butting.

Under "All Nominal" conditions the sidelap at the equator is

$$\begin{aligned} \text{Sidelap} &= \frac{(100\text{nm}) \cos 99^\circ - 86.028 \text{ nm}}{86.028 \text{ nm}} 100\% \\ &= 14.810\% \end{aligned}$$

To investigate off-nominal conditions, it is assumed that orbit errors produce a 10-mile error in 18 days. It is then possible that the 86.028 nautical miles between swath center lines can for example increase to 86.584 nautical miles. The remaining allowable error under these conditions at the equator is

$$\begin{aligned} E_A &= (98.769 - 86.584) \text{ nm} \\ &= 12.185 \text{ nm} \\ &= 74,100 \text{ feet} \end{aligned}$$

To the first order, one arc minute error in roll produces a loss of 877 feet in sidelap, and one minute of error in yaw produces a loss of 88 feet in sidelap. This is shown in Figure 4.3-2.

Considering of course that only part of the total allowable error can be allocated to either of the adjacent orbit passes, and allowing twice the roll error for yaw, the result is

$$877 (E_R) + 88 (E_Y) < \frac{74,100}{\sqrt{2}}$$

$$E_Y = 2E_R$$

$$E_R < 49.6 \text{ arc minutes}$$

$$E_R < 0.83 \text{ degree}$$

$$E_Y < 1.66 \text{ degree}$$

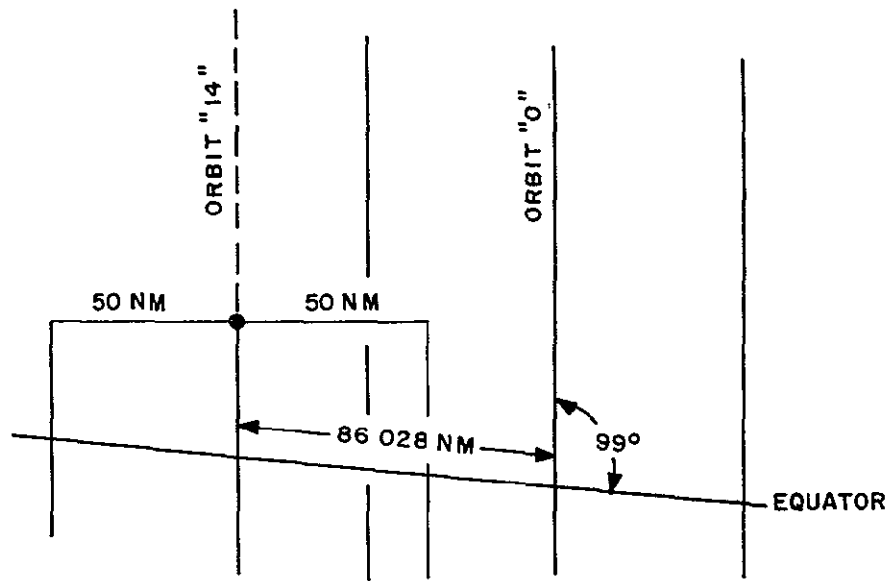


Figure 4.3-1. ERTS Contiguous Geometry

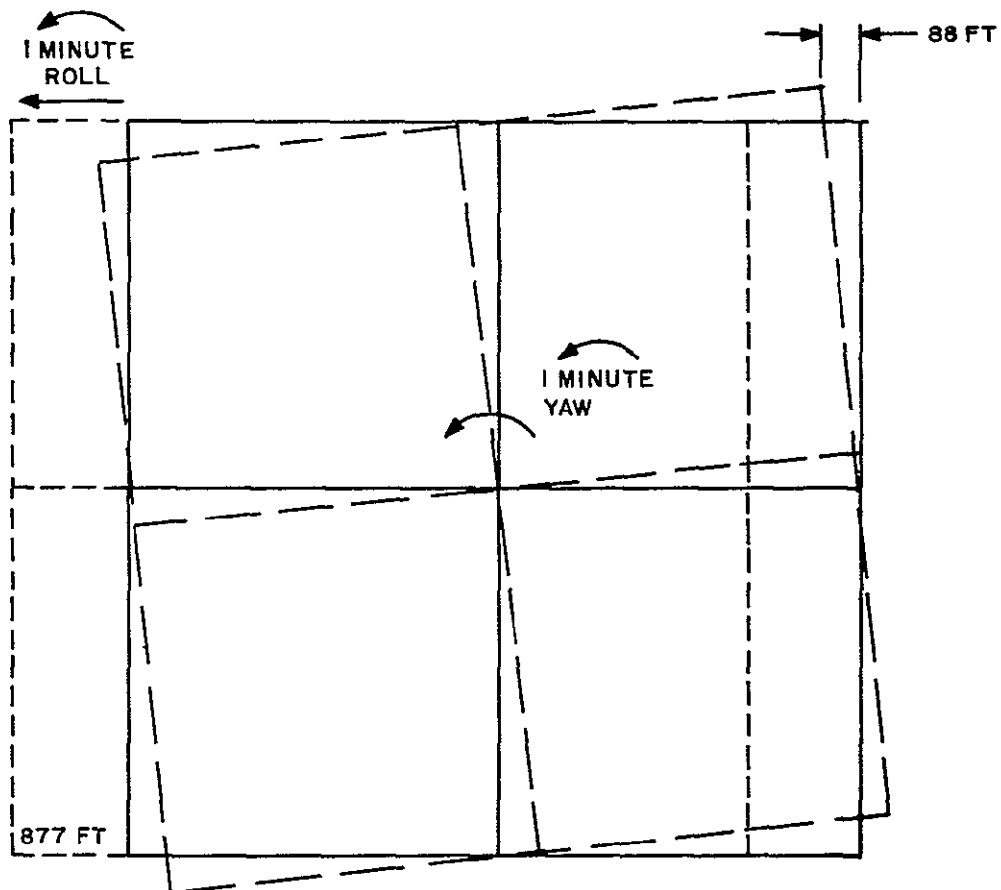


Figure 4.3-2. First-Order Effects of Roll and Yaw Error on Sidelap

11 February 1970

There is no stated overlap requirement. However, if the basic or automatic shutter mode takes a "picture" every 25 seconds, there is a nominal overlap of

$$\begin{aligned}\text{Overlap} &= 100 \text{ nm} - (0.0581^\circ/\text{sec}) (25 \text{ sec}) (60 \text{ nm}/(^\circ)) \\ &= (100 - 87.2) \text{ nm} = 12.8 \text{ nm}\end{aligned}$$

The allowable error is

$$E_A = (12.8 \text{ nm})$$

Picture timing errors between subsequent shutter operations will produce a loss of overlap of 0.3486 nautical mile for every one-tenth second of error. Timing accurate to one part in 250 seems reasonable and will be assumed. (Knowledge of shutter operation time is accurate to 10 milliseconds.)

Yaw error affects overlap as it does sidelap. A pitch orientation error produces 0.144 nautical miles of overlap loss per minute of arc or 8.65 nautical miles per degree.

The allowable overlap loss is  $12.8/\sqrt{2}$  nautical miles. If 0.35 nautical mile is dedicated to shutter timing errors, 8.72 nautical miles is available to pitch attitude error.

$$E_P = \frac{8.72}{8.65} (^\circ) = 1.01 (^\circ)$$

In summary, the most severe pointing requirement to achieve coverage is in roll and yaw, it is 0.83 degree in roll and 1.66 degrees in yaw to achieve butting of adjacent pictures. To ensure  $1-\frac{1}{2}$  nautical mile actual picture sidelap, a roll accuracy of 0.70 degree and a yaw accuracy of 1.40 degrees are required. Pitch accuracy could be relaxed, but with similar implementations, pitch precision of 0.70 degree is implied.

The pointing requirement is 0.70 degree in roll and pitch and 1.40 degrees in yaw and is a requirement on the Attitude Control System. This requirement is in addition to the attitude knowledge discussed in Section 4.3.4.

#### 4.3.7 RATE REQUIREMENTS

A basic requirement for ERTS is to provide rate error of less than 0.04 degree per second, exclusive of orbital rate.

In addition, as a design goal, a rate error of less than 0.015 degree per second is desired for the MSPS.

The rate requirements are due to the finite shutter time of the RBV cameras and the scan implementation of the MSS where the sub-vehicle point velocity is used to provide a "continuous" strip film.

The RBV's have moving slit focal plane shutters that move parallel to the track. The exposure time is 8, 12, or 16 milliseconds. For continuous coverage, a picture is taken every 25 seconds. Picture size is 11.5 degrees by 11.5 degrees.

A total RBV distortion of 1 percent is expected. This corresponds to 1 nautical mile or 6080 feet. If the spacecraft induced distortions are held to 1 percent of the total distortion or less, these distortions will be negligible.

The MSS has a swipe width of 1380 feet. The swipe is accomplished by a cross-track (roll) sweep of 11.5 degrees in 43 milliseconds, with a return sweep in 24 milliseconds. There are 2640 ground elements per sweep. The detector optical resolution is 230 feet in diameter.

The nominal orbital pitch rate is 0.0581 degree per second, with a nominal in-track surface velocity of 21,195 feet per second.

#### 4.3.7.1 Rate Effects on the RBV's

For a roll or pitch rate error of  $\dot{\theta}_E$  degrees per second, the displacement error while the shutter is open is

$$\theta_E = \dot{\theta}_E T_S$$

For the case where  $T_S$  is 20 milliseconds

$$\theta_E = 20 \times 10^{-3} \dot{\theta}_E$$

On the assumption that such error displacement due to rate is to be 10 percent of the total distortion figure

$$\theta_E = \frac{(0.01)(6080 \text{ ft.})}{\sqrt{2}(877 \text{ ft./min})}$$

Then

$$\dot{\theta}_E = \frac{60.8}{(\sqrt{2})(877)(0.02)} \text{ min/sec} = 2.5 \text{ min/sec}$$

$$\dot{\theta}_E < 0.04^\circ/\text{sec.}$$

Or, from the viewpoint of smear, a rate of 0.04 degree per second existing in either roll or pitch will produce a smear of 33.6 feet, which seems quite commensurate with the beam focus resolution of 230 feet.

#### 4.3.7.2 Rate Effects on the MSS

The MSS has four bands for ERTS A. Each band uses six detectors which are scanned simultaneously. Each detector has an instantaneous FOV of 240 feet. (ERTS B has a fifth band with two detectors and instantaneous FOV of 720 feet, which is not as critical.)

The nominal scan is shown in the Figure 4.3-3.

The swipe width is 21,195 feet per second by 0.065 second, or 1380 feet, which is provided by the MSS design of six detectors in a line array. If the maximum constant rate is 0.04 degree per second, the image location error from the start of one swipe to the next is

$$\begin{aligned} \text{Error} &= (.065 \text{ second}) (0.04 \text{ degree/second}) (60 \text{ mm/degree}) (877 \text{ ft/min}) \\ &= 141 \text{ feet} \end{aligned}$$

The width distortion is

$$\text{Distortion} = 43/67 \times 141 \text{ feet} = 90 \text{ feet}$$

It is felt that the 141-foot gap or overlap between swipes is excessive for a basic sensor detector FOV of 240 feet. Overlap should be held to no more than 20 percent, and preferably to about 10 percent. For a 20 percent gap or overlap, the maximum allowable rate is

$$\begin{aligned} \theta_E &= \frac{48}{141} (0.04 \text{ degree/second}) \\ &= 0.0136 \text{ degree/second} \end{aligned}$$

Previous considerations have been of the effects of a constant rate existing in the vehicle frame during an RBV exposure time or during an MSS mirror deflection. Low frequency vehicle frame oscillations about null will have grossly the same worst case effects as a constant rate when the exposure or sweep period is small compared to the period of the oscillation.

In the case of the RBV, shutter a jitter frequency of 786 radians per second would produce a half sine wave position motion during the time of exposure. The jitter rate allowable at this frequency without exceeding the position error of  $2.74 \times 10^{-4}$  degree is 0.338 degree per second.

In the case of the MSS sweep, a jitter frequency of 146 radians per second would produce a half sine wave position motion during the sweep. To keep the position error below 10 percent of a detector instantaneous FOV, the jitter rate allowable at this frequency is 0.105 degree per second.

The allowable jitter rate magnitude as a function of frequency is shown in Figure 4.3-4.

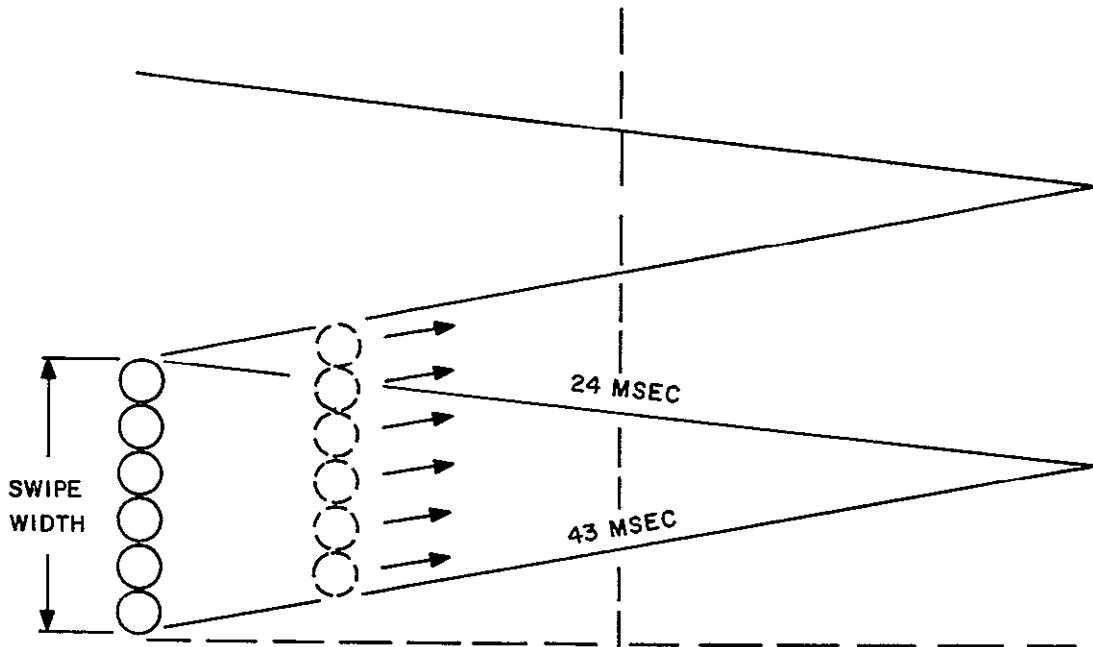


Figure 4.3-3. Nominal Scan

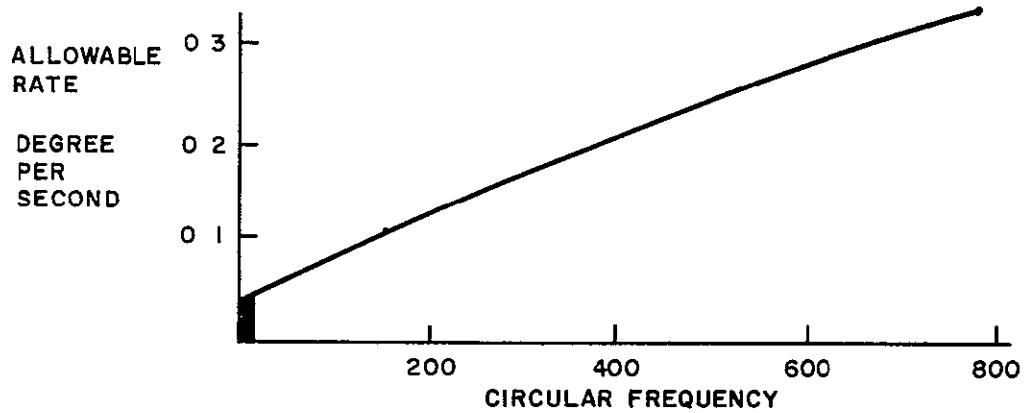


Figure 4.3-4. Allowable Jitter Rate Magnitude as a Function of Frequency

11 February 1970

The approximate controller bandwidth is the dark area. A measurement of the vehicle rates performed by a finite bandwidth instrument or by an infinite bandwidth instrument limited by TM sample rate can ensure that the peak rate is not exceeded for any frequency within its sensitivity.

In the case of high frequency oscillations (those frequencies above the controller bandwidth) instrumentation to measure the instantaneous rate through all these frequencies is very expensive. It is therefore desirable to ascertain the need, i.e., what is the probability that higher frequency oscillations above the controller bandwidth can exist at a sufficient amplitude to produce deleterious effects on the payload sensors.

The source of such oscillations is the structural compliance of the spacecraft, and the higher the frequency the more local the effect. In the present ERTS configuration, high frequency oscillations at the payload would be due to the local structure of the sensor ring. Lower frequency effects would be due to oscillations in the sensor ring/control ring structure or due to bending modes in the articulated solar array.

The cause of such oscillations is not the momentum wheel control actuators because the actuator effects are within the controller bandwidth. Environmental disturbances, also by definition, are within the controller bandwidth. Rather, the oscillations are primarily produced by the RCS. Discrete jet actuation occurring either as a result of orbit control thrusting or momentum wheel unloading are the causes.

At high frequency, the angular acceleration required to maintain a rate amplitude increases linearly with the frequency. This can be seen from the expressions

$$\theta = \frac{A}{\omega} \sin \omega t$$

$$\dot{\theta} = A \cos \omega t$$

$$\ddot{\theta} = A \omega \sin \omega t$$

In order that the displacement be large enough to affect the payload with increasing frequency, the rate amplitude must increase. As a consequence, the acceleration must increase as the square of frequency. For vibrations to shake the massive payload, the large accelerations of high frequency requires large forces, these do not exist in the RCS.

Lower frequency oscillations can produce significant displacement amplitudes with lower accelerations (forces). Primarily, the solar array bending modes when excited by discrete operation of the RCS can be of concern. For ERTS, these frequencies are between one and two cycles per second, and any measure of attitude control subsystem rate performance measurements should include these frequencies.

The instantaneous rate limit should be 0.04 degree per second over a frequency range of zero to 10 cps, with a goal of 0.014 degree per second.

#### 4.3.8 REQUIREMENTS SUMMARY

The ephemeris error for in-track must be less than 0.16 statute mile, one sigma, for cross-track and altitude it must be 50 meters, one sigma. The time of the RBV shutter operations must be known to an accuracy of 10 milliseconds, three-sigma.

The attitude determination sensor should have an accuracy of 0.126 degree, three sigma in all three axes for a celestial type of implementation, for a local vertical type of implementation it should have an accuracy of 0.100 degree in roll and pitch and 0.800 degree in yaw.

Both types of attitude determination systems must retain relative alignment with the payload sensors of 3 arc minutes ( $0.05^\circ$ ). This alignment is the alignment accuracy achieved after the spacecraft has experienced the launch force and vibration environment.

In-flight calibration to remove the mean value of the attitude determination system error (the boresight error) can be performed with ground truth. Such an operation can be looked upon as either improving the image location accuracy to a value less than 2 nautical miles or allowing larger margins for the attitude determination sensor. With in-flight bore-sighting, a celestial type system is required to have an accuracy of 0.200 degree. A local vertical sensor would retain an accuracy requirement of 0.100 degree, but yaw accuracy could be as imprecise as 1.670 degrees.

The Attitude Control System will point the vehicle to the local vertical and in the direction of flight. Such pointing allows the coverage of the Earth's surface by the RBV pictures and the MSS scan. To guarantee that the pictures and the scan do cover the total Earth's surface without gaps, roll pointing must be performed to an accuracy of 0.83 degree, and pitch to 1.01 degrees. To ensure at least  $1-\frac{1}{2}$  nautical mile overlap to facilitate montage construction, the roll/pitch pointing accuracy should be 0.70 degree, and the yaw pointing accuracy should be better than 1.4 degrees.

The allowable rates present on the spacecraft are determined from the RBV exposure time and the MSS active scan time. For a 20-millisecond exposure time and a maximum displacement of 431 feet for the RBV the vehicle rate should be less than 0.0400 degree per second. For a 43-millisecond active scan time and a maximum error in scan start position of one-fifth of one detector instantaneous field of view, the vehicle rate should be less than 0.0136 degree per second.

The attitude determination sensor requirements, along with the precision in the knowledge of time of RBV shutter operations, will meet the image location requirement. The Attitude Control System requirements for pointing precision and allowable instantaneous rates are in substantial agreement with the ERTS specification.



## 4 4 TIME ANNOTATION

### 4 4.1 GENERAL

A basic requirement for the ERTS mission is to provide "attitude sensors and telemetry provisions to determine attitude to an accuracy sufficient to locate any point on a 100 x 100 nautical mile picture with an accuracy of less than two (2) nautical miles. The above concept for determining the location of any point in the imagery is based on a computation of locations, using spacecraft attitude, ephemeris position and universal time as input parameters " Therefore, as part of the overall image location/time/position correlation, the time at which the sensors were operated must be known to some finite accuracy In the image location error study (Section 4.3 of this volume), it was shown that for timing errors on the order of 10 milliseconds, the time error contribution to image position location is negligibly small. This section addresses the problems in achieving this accuracy.

In order to process imagery within the GDHS, it is necessary to construct an Image Annotation Tape (IAT) containing information such as spacecraft latitude and longitude corresponding to the center of each frame of imagery In order to develop this tape and have it available for processing when the video tapes are received at the NDPF, the spacecraft NB telemetry must contain the times at which the RBV shutter operated. (It will be assumed that the strip MSS imagery will be framed to correspond to the RBV images and thus the annotation data for it will be required for the same times as the RBV shutter operation.)

Based on currently available information on the RBV camera system, no entirely suitable telemetry signal has been defined that precisely defines shutter operating time (An ideal signal would be a bi-level, digital B type signal whose transition occurs at the center of shutter travel.) Therefore, the assumption is made that a suitable signal, compatible with the ERTS telemetry system, ultimately will be available. Even with the availability of such a signal, several problems exist in determining its time of occurrence.

The RBV shutter timing is derived from the spacecraft 1 Hz timing signal from the ERTS Command Clock subsystem. However, it may be delayed by some measureable amount from the leading edge of this square due to internal delays in the RBV system Variations in actual shutter operation (motion) will occur because of mechanical delays which change with time or age. This variation in shutter operation has been estimated to be 1 millisecond at the start of life and extending to 10 milliseconds at the end of one year. Depending on how shutter telemetry signal is derived, this variation may not be sensed. If it is not sensed, the possibility exists that it could be calibrated out of the system during normal operation Another source of shutter timing variation exists due to rephasing of the camera system with the WBVTR. A possible 800  $\mu$  second delay per picture cycle can be incurred. The total timing variation due to this could be as much as 38.4 milliseconds for a 20 minute maximum continuous operating cycle This variation will only occur

when the system is operated in the record mode. Thus, the worst case shutter time variation from these two causes could be 48.4 milliseconds. This is shown in Figure 4.4-1.

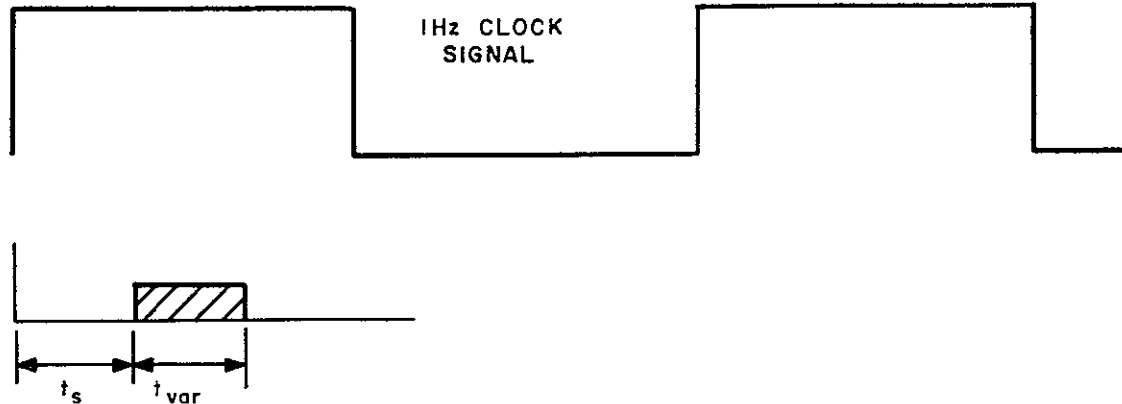


Figure 4.4-1. RBVC Shutter Operating Time Variation

The ERTS telemetry subsystem is also synchronized to the 1 Hz timing signal and if proper attention is taken in assigning the time slot(s) for sampling this RBV shutter signal, reasonable knowledge of its time occurrence can be deduced.

The VIP Telemetry System reads one digital word (10 bits, which could be 10 different bit-level events) into the ITS formatter at a 1 kilobit per second rate. Therefore, it takes 10 milliseconds to read one digital word into the formatter. The 10 bits are clocked in during the last half of the last bit time at the end of a 10 millisecond period. Therefore, the time of occurrence of event is only determinable to this 10 millisecond period. To measure time occurrence of events more accurately than this would require the use of additional equipment which is not now necessary for proper system performance. To be certain the RBVC shutter pulse will be observed and to determine to better than 48 milliseconds when it occurred, even in the 20 minute continuous record mode, will require either multiple sampling of this telemetry output or the selective placement of the three shutter pulses - one from each camera. (It is assumed that the mechanical delays of each are approximately the same, and the build-up of time of shutter operation are identical since the one count down chain controls the entire camera system.) One sampling approach is shown in Figure 4.4-2. The shutter telemetry output would be sampled during one bit of several successive 10 bit digital words. (Five are shown in the example.) The sampling rate for the words shown would be once per second and their time sequence of occurrence would be such that they would be sampled during the interval when the camera shutter could occur. From the resulting telemetry we could determine within one word time (10 milliseconds for a 1 kbps bit rate) when the shutter occurred. Thus, except for errors within the camera between actual shutter travel and the telemetry signal which acknowledges this level, we are able to determine the shutter operating time to  $\pm 5$  milliseconds.

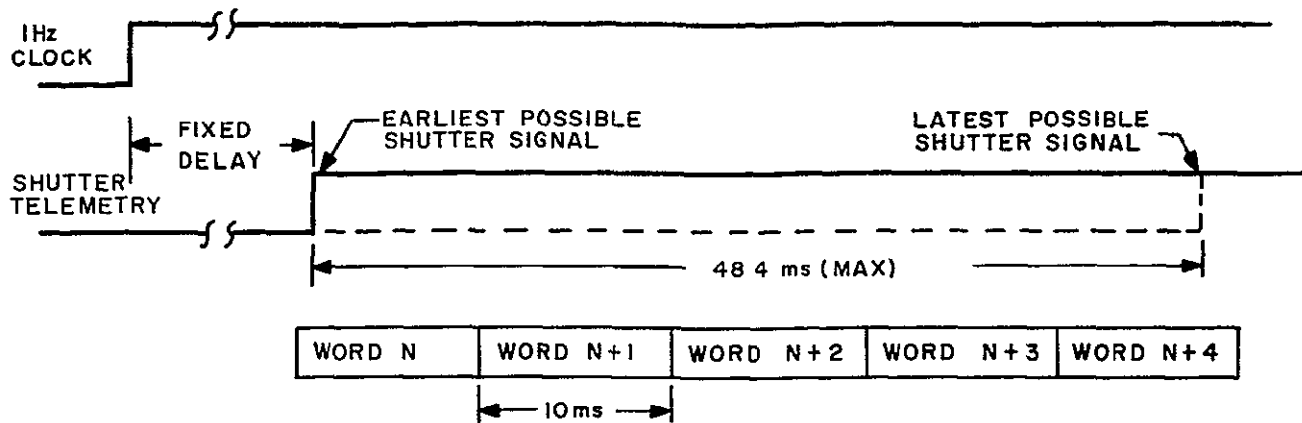


Figure 4.4-2. Shutter Pulse Sampling

Monitoring operation of the MSS involves other considerations. The MSS is not synchronized to the ERTS Command Clock and the sensor can start operation at any time for the real time mode. Therefore, a telemetry output sampled once per second will not have any significant use in determining when the sensor operated any better than within one second. To accurately determine sensor start time requires the knowledge of when the command was received and acted upon. The presence of sensor video output can be an aid here. For stored command operation, the execution time of the command can accurately be determined by knowing where in COMSTOR the command is located. However, this requires a good bit of "bookkeeping" to be done on the ground to keep track of not only when the start commands were sent, but of all the system delays and error sources.

To insure that the sensor video data can be correlated with sensor operate signals (RBVC) or to determine operation time for MSS, time information relating to sensor operation must be stored in some form with the sensor video data. If this is not done, the possibility exists that data will be received without knowing its timing (and therefore, position). To prevent this, several approaches to overall time annotation were evaluated. Common to all approaches is the requirement or assumption that RBV shutter telemetry output is available which relates the initial operation of the sensor to spacecraft time. This is the primary source of information on sensor operation and is used to make up image annotation tapes in advance of receipt of video tapes, as well as time correlating sensor data with NB telemetry support data.

#### 4.4.2 APPROACHES TO TIME ANNOTATION

Four basic approaches were considered for obtaining time information as a function of sensor operation. These approaches are:

1. Record all narrowband (NB) telemetry data on the auxiliary track of the wideband video tape recorder (WBVTR) when recording sensor data.

- a. Real Time - on the ground
  - b. Stored Mode - on the spacecraft (stripped off, sent down via USB, and remerged on the ground with the sensor data)
2. Record the pulse width modulated time code from the ERTS command clock on the auxiliary track of the WBVTR when recording sensor data.
    - a. Real Time - on the ground
    - b. Stored Mode - on the spacecraft (stripped off, sent down via USB, and remerged on the ground with the sensor data).
  3. Record WWV on the auxiliary track of the ground tape recorder in either the real time or stored mode of operation.
  4. Add time code to the sensors.

The fourth approach is the only one requiring an additional modification to the sensors.

#### 4.4.3 DISCUSSION OF APPROACHES

The four approaches considered will be discussed relative to the impact each causes to various sections of the total ERTS System. Each approach offers a feasible concept for the time correlation process. They differ in the amounts of data to be processed or handled and the spacecraft and/or ground equipment required.

1. Record all NB telemetry on the auxiliary track of the WBVTR when recording sensor data.

This approach requires the addition of a buffer amplifier to the spacecraft, so that the single telemetry output channel may be split 3 ways. One to its present path, i.e., the NB link, and the second and third outputs to the auxiliary tracks of the two WBVTR's during the time sensor data is being recorded. During playback the NB telemetry will be stripped off, transmitted to the ground via the USB link and recorded on the same VTR as the sensor data. In the real time mode, the NB telemetry will be recorded on the ground VTR. Two subcarrier oscillators are required in the premodulation processor (PMP) for adding these signals to the USB system. Figure 4.4-3 is a block diagram of this approach

To recover the sensor operation time, the NB telemetry data recorded with the sensor data must be decommutated and processed. This means that the same telemetry data will be processed twice - the first time is the normal processing as the data is received via the NB system, and the second time when the same telemetry data is stripped from the auxiliary track of the ground VTR.

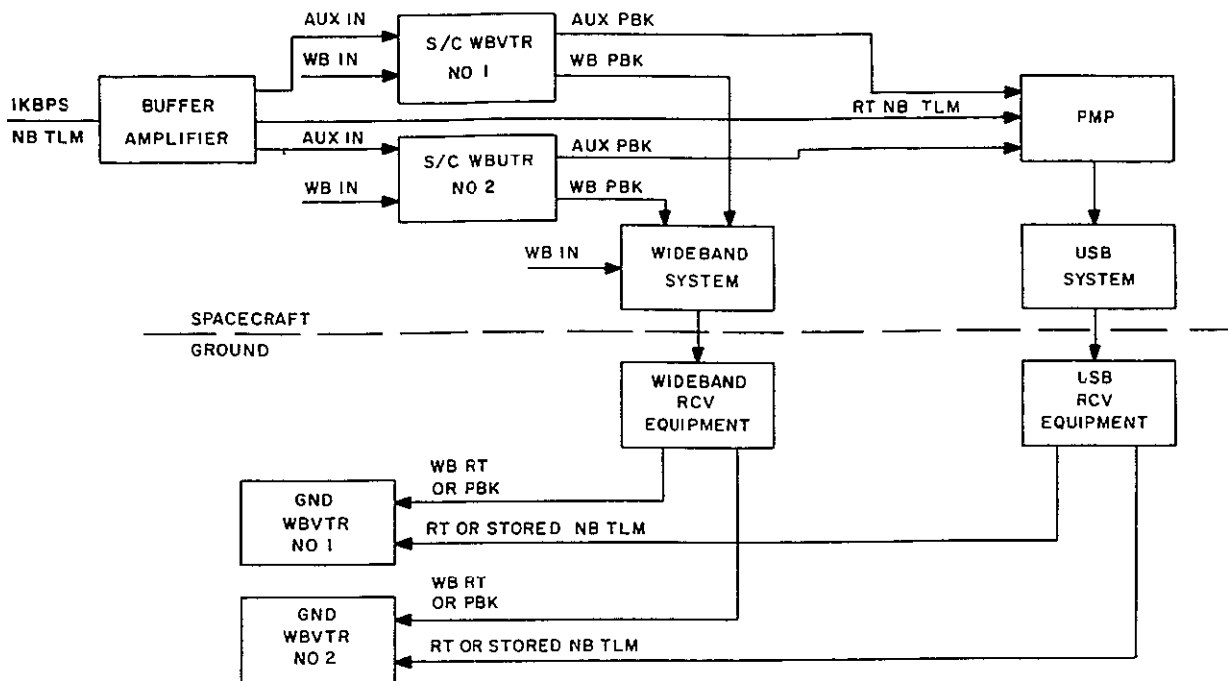


Figure 4.4-3. Time Annotation Approach No.1

2. Record the pulse width modulated time code from the ERTS command clock on the auxiliary track of the WBVTR when recording sensor data.

The comments and discussion for the first approach are pertinent here. The only difference is that the time code from the command clock would be buffered and divided three ways. The time code would be sent down to the ground via the USB link in real-time as well as during playback of stored data. This is shown in Figure 4.4-4.

This approach simplifies time location since only the time code has to be decoded. This is a much simpler operation than processing the entire telemetry matrix. Note that as an alternate for real-time data, time code could be put on at the ground station. It would then be necessary to correlate spacecraft and ground time codes.

3. Record WWV on the auxiliary track of the ground VTR - real time/stored.

This approach eliminates the need for the storing of any type of data on the WBVTR auxiliary tracks. The WWV time of data reception is placed on the auxiliary track of the ground VTR for either real-time or stored data. However, the ground "bookkeeping" becomes quite complex. For recorded data, a complete log of start and stop times of the

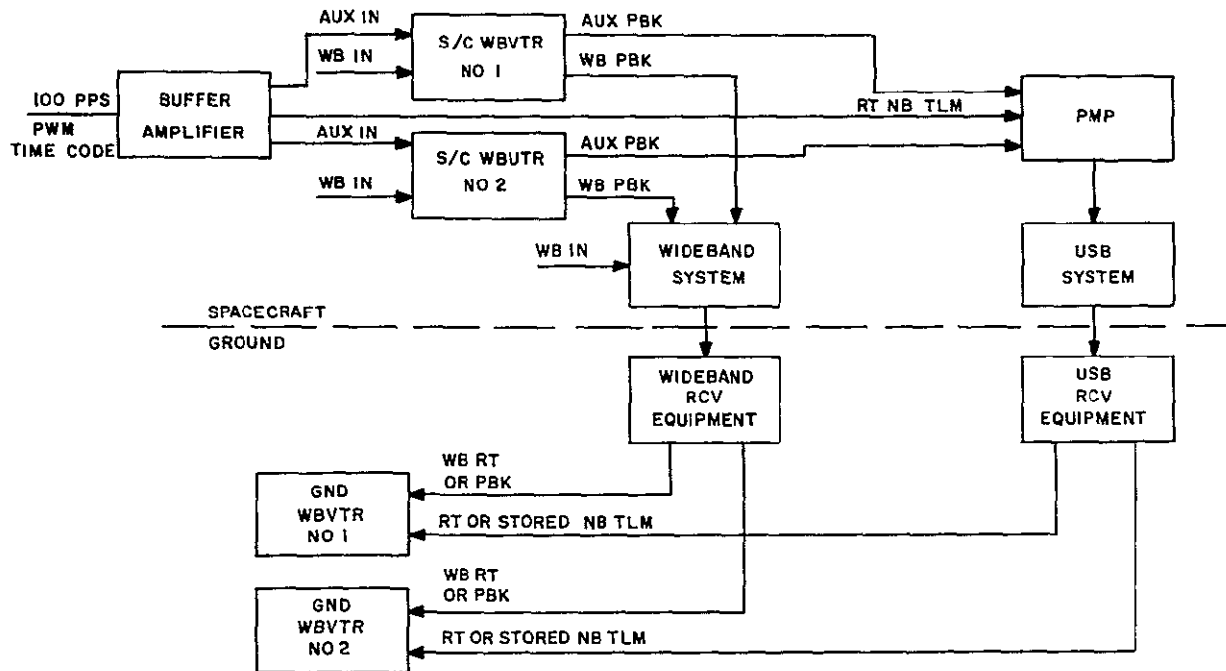


Figure 4.4-4. Time Annotation Approach No. 2

sensors must be maintained for the entire length of the tape. The amount of data played back and at what times must be logged so as to be able to identify where and when the data was taken. Figure 4.4-5 shows the signal flow for this approach

#### 4. Add time code to the sensors.

This approach has the advantage of keeping the video data and the time of its occurrence together. No other auxiliary tracks or data to be stripped and merged are required. It requires the buffering of several ERTS command clock signals so as to make them available to the sensors. Typical signals to be used are time code, 500 Hz and the 1 0 Hz signals. A modification to both the RBV and MSS would be required.

In the case of the RBV, the preferred approach would be to insert the spacecraft time code (modified to give better than one second resolution) just prior to or following the video for each picture. Ideally, the method of implementation should (1) allow for ease in detection and stripping of this time code during video to film conversion, and (2) provide for visual identification in the resulting image. Thus, any and every image would contain an inseparable identifier. The code could also be sampled by the spacecraft telemetry to identify shutter operating time.

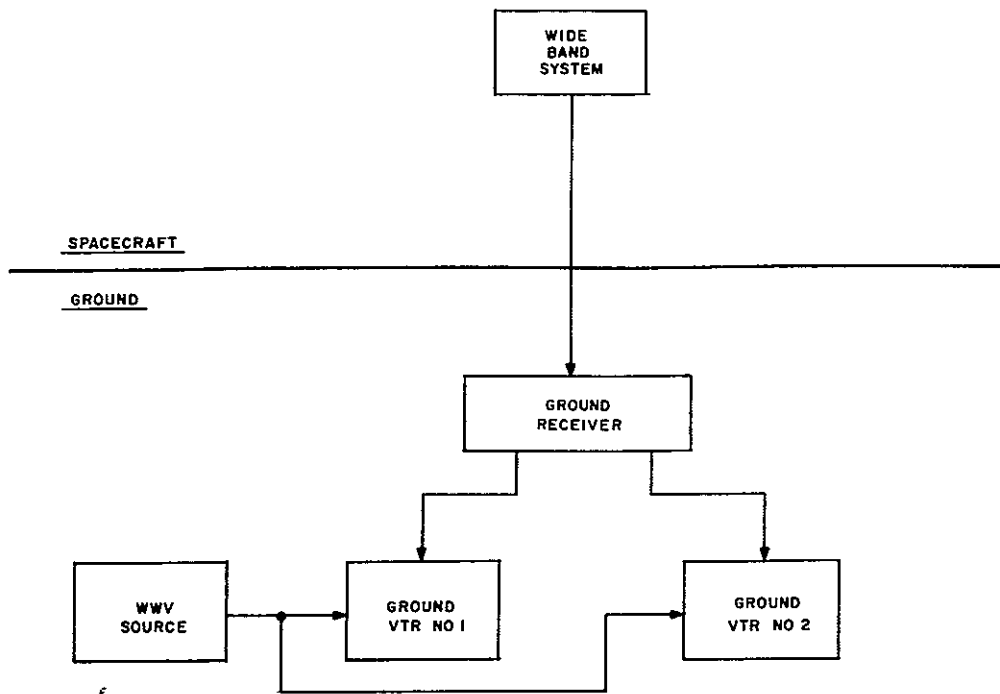


Figure 4.4-5. Time Annotation Approach No.3

For the MSS, time code could be inserted during the retrace time between active scan lines. This could be done during each retrace or periodically every few scan lines. Again, the ideal implementation should be easily detectable electronically or visually.

#### 4.4.4 BASELINE APPROACH

Table 4.4-1 summarizes the advantages and disadvantages for each approach. Approach 4, adding time code to the sensors, is the recommended approach. It simplifies the spacecraft, the ground processing and overall produces a more reliable annotation system. It does, however, depend on sensor modification.

In the case of the RBV camera, an implementation scheme is currently under study by RCA. However, no decision has yet been reached to incorporate this scheme. In accordance with the design study specifications, an alternate approach has been selected as a baseline that is compatible with current sensor definition. On the basis of minimum system complexity, the approach of adding time code to the auxiliary tracks of the WBVTR's is the baseline approach. This approach permits accurate time correlation of sensor video and information contained in the NB telemetry data. The additional spacecraft equipment required is a buffer amplifier and IRIG SCO's for the USB premodulation processor. On the ground, the subcarriers will be stripped from the USB signal and added to another track on the ground VTR which is recording wideband sensor data.

TABLE 4.4-1. TIME ANNOTATION APPROACH EVALUATION

Approach	Advantages	Disadvantages
1. Record all TLM data on auxiliary track of WBVTR	<ol style="list-style-type: none"> <li>1. All support data with video on a one-to-one correspondence</li> <li>2. Enables correlation between time and sensor start</li> </ol>	<ol style="list-style-type: none"> <li>1. Requires duplicate processing of TLM data</li> <li>2. Requires either time on OCC ground station or additional TLM station at NDPF</li> <li>3. Requires 2 NB channels for transmission to ground</li> <li>4. Data must be stripped and transmitted via NB link</li> <li>5. Data must be merged on GNDVTR</li> </ol>
2. Record time code on auxiliary track of WBVTR	<ol style="list-style-type: none"> <li>1. Enables correlation between time and sensor start</li> <li>2. Records only necessary data</li> </ol>	<ol style="list-style-type: none"> <li>1. Requires stripping and merging process as approach 1.</li> <li>2. Requires 2 NB channels</li> <li>3. Time code must be merged on GNDVTR</li> </ol>
3. Record WWV on ground VTR auxiliary track	<ol style="list-style-type: none"> <li>1. Eliminates need for spacecraft auxiliary tracks or additional NB channels</li> <li>2. No merging or stripping required</li> </ol>	<ol style="list-style-type: none"> <li>1. All video and TLM data must be normalized to WWV time prior to any pre- or final processing.</li> <li>2. OCC "bookkeeping" required for every inch of WB tape</li> <li>3. All system errors must be precisely known</li> </ol>
4. Add time code to sensors	<ol style="list-style-type: none"> <li>1. No bookkeeping</li> <li>2. No other data to be processed</li> <li>3. No additional NB channels needed</li> <li>4. Time and data inseparable</li> </ol>	<ol style="list-style-type: none"> <li>1. Modify sensors.</li> </ol>



## 4 5 MISSION SIMULATION

### 4 5 1 SIMULATION PROBLEM

The primary ERTS mission is to gather multispectral data via earth imaging sensors in a manner that will effectively satisfy an overall coverage requirement. Since the system will be capable of acquiring useable data only under certain conditions (i.e., proper scene illumination, availability of desired terrain, etc.), the operation of the sensors will be scheduled accordingly. The schedule against which the system must operate while in orbit then will levy certain requirements on the spacecraft subsystem design, ground support capability, and operational support procedures.

The capability to simulate the on-orbit profile of the ERTS system operations for what is considered to be a typical and realistic set of conditions was developed. The results of these simulations have provided a data base from which design requirements were derived. The adoption of this approach has insured that all subsystem designs are compatible with the overall ERTS mission.

The basic problem simulated was the on-orbit operation of the sensor payloads, the management of the onboard recorder resource, and the management of the acquisition of data by the ground sites. Of primary importance in the design of the simulation capability was to incorporate the ability to consider both the operational capabilities of the system and the constraints and limitations of both the system and the mission. Since much of the overall operational philosophy was not solidified at the time of this design, a need for flexibility in specifying the parameters and conditions of the simulation cases was mandatory. The resulting simulation capability provided a versatile tool that enabled not only a baseline profile to be generated but also provided the capability to investigate the significance of variation in the basic parameters and conditions of the mission/system.

### 4 5 2 SIMULATION MODEL

The simulation capability is a computer aided process. The basic model is designed around four basic types of mission/system descriptors:

1. Prioritized world coverage map
2. Orbital ground trace
3. Data acquisition site coverage
4. Spacecraft and sensor capabilities and constraints

#### 4 5 2 1 Prioritized Coverage Map

To simulate the anticipated preferences for specific geographical coverage by ERTS, the capability was provided to partition the world map into homogeneous regions. The boundary of each region is a variable and each region is assigned to one of eight different categories. Since it is expected that the desire to image certain areas will be greater than for

others, the categories were assigned a relative priority structure. Figure 4.5-1 presents the prioritized map used for this simulation. The finest granularity of region segmenting was at a region level. Although it is expected that finer coverage region definition will be employed operationally, it is felt that the map used here does present a realistic coverage requirement distribution on which to develop design profiles.

#### 4.5.2.2 Orbital Ground Trace

Although the simulation model can handle any specified orbit, the unique features of the ERTS orbit (i.e., 18 day repeat cycle, sun synchronous) allows for some simplifications to be made in the simulation. With this orbit it is necessary to only examine the operations for a single 18 day cycle. The sun synchronous condition simplifies the accounting for variations resulting from effects of time of year. Effectively, different times of year result in a translation of the region of acceptable sun angle within an orbit and can be assumed to be essentially a fixed translation for all orbits within an 18 day cycle. On figure 4.5-1 the descending ground traces for a typical day in an 18 day cycle are shown. The particular case shown is for "day 9" of the cycle. For each successive day, in a cycle the ground trace overlay would shift approximately 1.5 degrees west at the equator and on the 19th day the ground trace pattern will essentially be the same as day 1.

#### 4.5.2.3 Data Acquisition Site Coverage

Three data acquisition sites capable of receiving the wideband sensor video data were used (Alaska, Corpus Christi, and NTTF). It was assumed that data could be transmitted to the ground sites during any pass over the site (day or night). Although the simulation model can handle any station cone angle, it was assumed for these cases that wideband data could be received any time the spacecraft was at an elevation of more than 5 degrees from the site. Figure 4.5-1 shows the ground station cones for 5 degrees elevation angles. In addition to the three wideband acquisition sites, Rosman is also shown.

Where two or more sites can see the spacecraft at the same time, it was assumed that both sites could receive the video data simultaneously.

#### 4.5.2.4 Spacecraft/Sensor Considerations

The operations of the sensors must be scheduled in a manner that will return imagery over the land areas of interest. The ERTS system has been designed to provide the capability to image the ground during the appropriate daylight portion of the orbit and to store this data for future transmission to earth during those times when not in contact with a ground station. During a contact with a data acquisition station, either data from real time operations of the sensors or the dumping of previously recorded data can be scheduled.

The simulation problem is to generate the schedules for the operations of sensors, on board recorders, data transmission cycles, and spacecraft subsystem support requirements in a manner that best satisfies the coverage requirement. The resultant schedules from the simulation must be feasible for the ERTS System to perform. This requires that the simulation process consider the capabilities of the spacecraft/sensor system and any

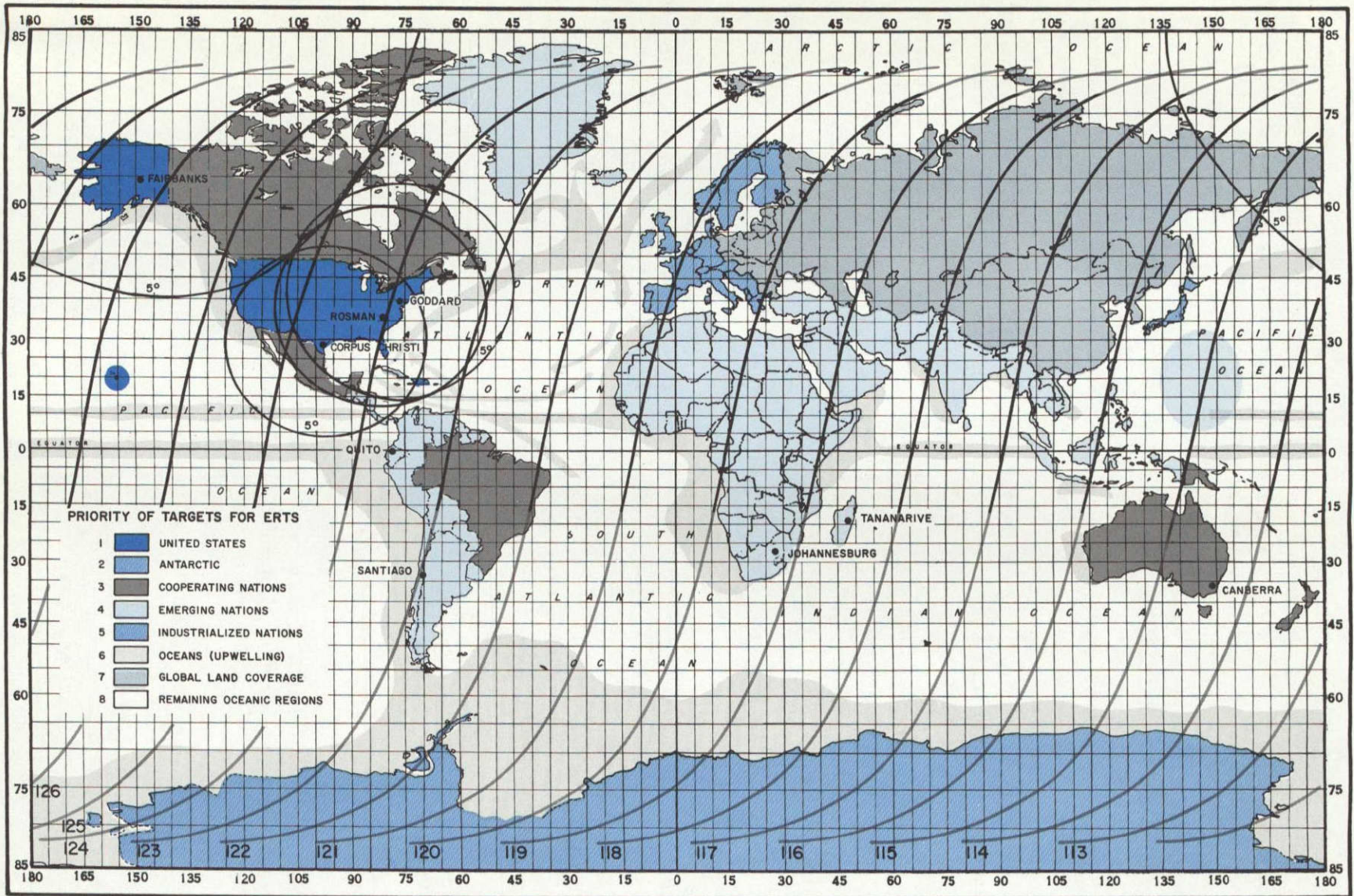


Figure 4.5-1. World Coverage Map

11 February 1970

limitations or constraints imposed on its operations either by the spaceborne system itself, the ground support constraints, or because of operational ground rules. The simulation is capable of handling spacecraft and sensor parameters such as

- 1 On board wideband tape recorder capacity
- 2 Maximum allowable operation time per orbit
- 3 Sensor operating sequences
- 4 Sun angle limits for sensor operations
- 5 Real time or recorded operations
- 6 Selective inhibiting of specific operations or groups of operations

Figure 4 5-2 depicts the simulation tool from a logic flow point of view

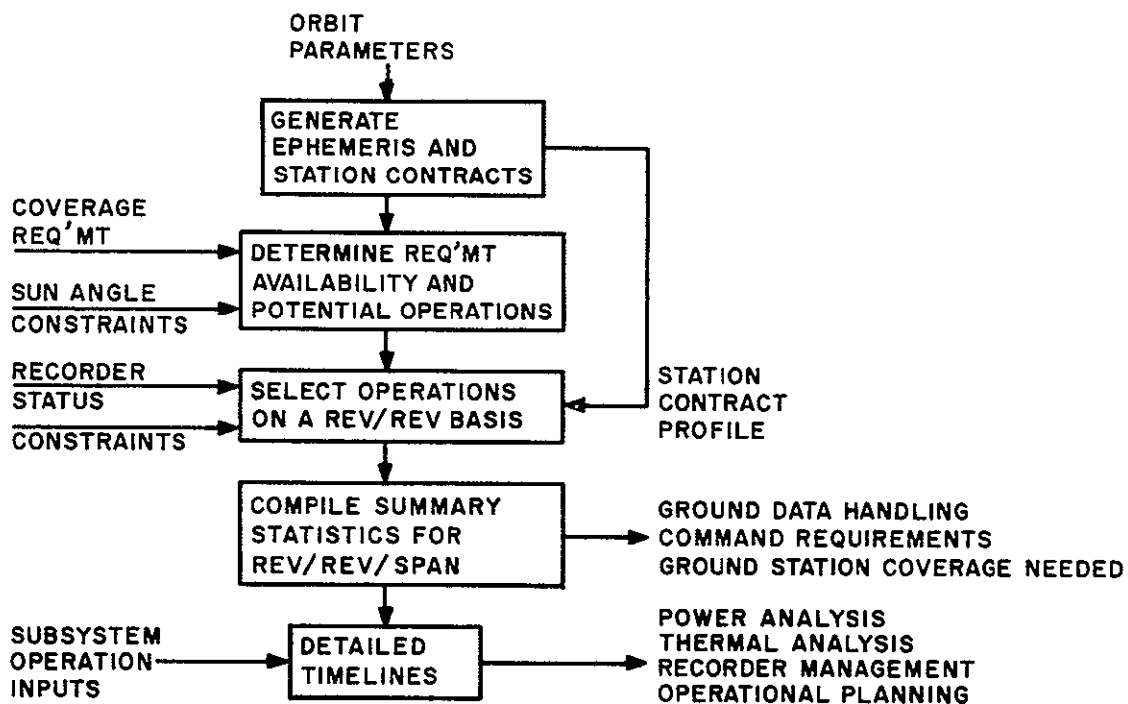


Figure 4 5-2. Simulation Logic Flow

### 4 5 3 SIMULATION CASES

#### 4 5 3 1 Purpose

Simulated mission operations were used to support the spacecraft design and are continuing to establish the ground support requirements. The specific results obtained for use in the spacecraft design include

- 1 Maximum daily payload operations
- 2 Maximum number of stored commands for payload operations between ground station acquisitions
3. Recorder usage

Specific results being obtained for ground data handling system design include

1. Maximum daily payload operations
- 2 Command requirements
- 3 Ground station coverage planned

#### 4 5 3 2 Inputs

The simulated mission operations, that were conducted to establish worst case requirements for the spacecraft design, used the following parameters and operational ground rules

- 1 Orbital parameters (ground traces shown in Figure 4 5-1)

inclination	99 088 °
altitude	492 35 nm
period	6196 0 sec
descending node time	0930

- 2 Land mass coverage

complete global coverage over an 18 day cycle

consider no cloud restrictions

land priority structure used if required (priority structure is shown in Figure 4 5-1)

schedule coverage above 60°N latitude on alternate revs only\*

sensors continue to operate between land masses whenever their off period would be less than 2 minutes

## 2. Payload Operation

Simultaneous MSS and RBV operation are scheduled whenever the following three conditions are met

- (a) sensor operation allowable for sun angle  $\geq 35^\circ$  (Summer solstice case shown in Figure 4.5-1, by darker portion of orbit traces)
- (b) a real time link or WBVTR available
- (c) the subsatellite point is overland, coastal waters or major island groups

## 3 Data Acquisition Stations

Alaska, Corpus and NTTTF/Rosman

unrestricted wideband link operation within 5° elevation cone

Minimum station contact of two minutes required in order to schedule WBVTR playback

unrestricted use of in-cone time (i e , ground station support whenever required)

## 4 Spacecraft recording capability

2 WBVTRS

30 minute capacity each

no operating life restrictions

### 4 5.3 3 Mission Profiles

Simulated mission operations using the above ground rules have been performed for 18 day periods at summer solstice, vernal equinox and winter solstice. The autumnal equinox is nearly identical to the vernal equinox, therefore, changes in payload operation can be projected for a full year of operation.

Mission operations data has been summarized in three tables. Table 4 5-1 contains the information for summer solstice, Table 4 5-2 for fall and spring, and Table 4 5-3 for winter operations.

\*Above 60°N latitude, alternate contiguous subsatellite swaths provide the required coverage including overlap. Therefore, complete coverage can be obtained in 18 days by scheduling alternate rev operation. Elimination of this duplicate coverage permits more effective use of the Alaska ground station and in recovering data from other areas of the world.

Table 4 5-1 Operations Summary 18-Day, Summer Solstice

Day	I Available Land Mass Sun Angle 35°			II Available Land Mass Sun Angle 35° Duplicate Coverage Removed - > 60°			III Actual Scheduled Mission Operations			IV Available Land Mass Missed
	Total	Total Real Time	Total Remote	Total	Total Real Time	Total Remote	Total	Total Real Time	Total Recorded	Total
1	182 4	42 9	139 5	156 9	30 5	126 4	139 3	30 5	108 8	18 6
2	183 3	45 5	139 8	159 4	37 5	121 9	143 4	37 5	105 9	16 0
3	177 6	41 8	135 8	151 7	30 4	121 3	136 9	30 4	106 5	14 7
4	180 4	42 2	138 2	152 1	34 4	117 7	137 1	34 4	102 7	15 0
5	183 0	44 5	138 5	156 2	33 1	123 1	137 1	33 1	104 0	19 1
6	186 5	43 0	143 5	156 3	33 4	123 3	136 2	33 4	101 8	21 5
7	192 0	43 4	148 6	164 9	34 2	130 7	139 3	34 2	105 1	25 6
8	187 9	39 3	148 6	159 1	30 1	129 1	137 0	30 1	106 9	22 2
9	193 6	46 3	147 3	170 7	37 9	132 8	147 1	40 7	106 4	24 5
10	187 9	40 2	147 7	160 8	33.1	127 7	141 2	33 1	108 1	19 0
11	184 7	40 1	144 6	161 4	33 3	128 1	136 2	33 3	101 9	26 2
12	181 3	40 0	141 3	153 6	29 4	124 2	133 3	29 4	103 9	20 3
13	174 8	40 8	134 0	150 2	33 8	116 4	126 9	33 8	93 1	23 3
14	171 9	41 0	130 9	145 6	30 4	115 2	128 0	30 4	97 6	17 6
15	171 7	41 6	130 1	147 2	34 3	113 9	128 8	34 3	94 5	19 4
16	164 9	38 5	126 4	141 3	29 3	112 0	127 0	29 3	97 7	14 3
17	170 0	40 7	129 3	145 1	33 2	111 9	131 8	33 2	98 6	13 3
18	166 9	40 2	126 7	144 1	31 6	112 5	134 4	31 6	102 8	9 7

(TIMES IN MINUTES)

Table 4 5-2 Operations Summary 18-Day, Vernal/Autumnal Equinox

Day	I Available Land Mass Sun Angle 35°			II Available Land Mass Sun Angle 35° & Duplicate Coverage Removed - > 60°			III Actual Scheduled Mission Operations			IV Available Land Mass Missed
	Total	Total Real Time	Total Remote	Total	Total Real Time	Total Remote	Total	Total Real Time	Total Recorded	Total
1	123 6	11 9	111 7	Same as Column I			115 8	11 9	103 9	7 8
2	131 3	17 2	114 1				122 9	17 2	105 7	8 4
3	125 6	15 7	110 0				117 3	15 7	101 6	8 3
4	123 9	15 6	108 3				114 9	15 6	99 3	9 0
5	121 8	16 5	105 3				112 3	16 5	95 8	9 5
6	122 7	15 8	107 0				112 8	15 8	97 0	10 0
7	121 0	14 3	106 7				111 7	14 3	97 4	9 3
8	120 5	13 6	106 9				110 2	13 6	96 6	10 3
9	127 6	20 6	107 0				112 9	20 6	92 3	14 7
10	121 1	16 0	105 1				106 1	16 0	90 1	15 0
11	119 5	14 8	104 7				105 6	14 8	90 8	13 9
12	116 8	14 5	102 3				102 5	14 5	88 0	14 3
13	114 0	16 0	98 0				100 3	16 0	84 3	13 7
14	110 0	14 7	95 3				96 9	14 7	82 2	13 1
15	113 9	15 7	98 2				100 0	15 7	84 3	13 9
16	110 0	13 6	96 4				98 8	13 6	85 2	11 2
17	113 9	14 0	99 9				103 6	14 0	89 6	10 3
18	113 4	14 0	99 4				98 7	14 0	84 7	14 7

(TIMES IN MINUTES)



Table 4 5-3 Operations Summary 18-Day Winter Solstice

Day	I Available Land Mass Sun Angle 35°			II Available Land Mass Sun Angle 35° Duplicate Coverage Removed - >60°			III Actual Scheduled Mission Operations			IV Available Land Mass Missed
	Total	Total Real Time	Total Remote	Total	Total Real Time	Total Remote	Total	Total Real Time	Total Recorded	Total
1	67 9	1 2	66 7	Same as Column I			67 9	1 2	66 7	0
2	77 4	2 6	74 8	NOTE			77 4	2 6	74 8	0
3	75 1	1 7	73 4	Lower latitude limit for a sun elevation angle $\geq 35^\circ$ is $\sim 65.7^\circ$ . All of Antarctica is below this latitude. Sensor operations should be possible for lower sun angles over this region because of the increased reflectivity of the area. These operations are not shown on this table because of the ground rule of sun angle $\geq 35^\circ$ . Alternate rev operation would be scheduled for mission operations over Antarctica.			75 1	1 7	73 4	0
4	72 3	2 5	69 8				72 3	2 5	69 8	0
5	70 3	3 1	67 2				70 3	3 1	67 2	0
6	71 2	2 2	69 0				71 2	2 2	69 0	0
7	68 9	1.9	67 0				68 9	1 9	67 0	0
8	66 3	0 5	65 8				66 3	0 5	65 8	0
9	71 1	3 9	67 2				71 1	3 9	67 2	0
10	64 5	0 5	64 0				64 5	0 5	64 0	0
11	57 9	0 9	57 0				57 9	0 9	57 0	0
12	55.4	0.9	54 5				55 4	0 9	54 5	0
13	54 7	2.4	52 3				54 7	2 4	52 3	0
14	51 1	0.9	50 2				51 1	0 9	50 2	0
15	55 6	2.1	53 5				55 6	2 1	53 5	0
16	56 7	0.5	56 1				56 6	0 5	56 1	0
17	61 8	0.9	60 9				61 8	0 9	60 9	0
18	60 5	1 5	59 0				60 5	1 5	59 0	0

(TIMES IN MINUTES)

These tables show (I), the total land mass covered for a sun angle  $\geq 35^\circ$ , (II), the total land mass covered for a sun angle  $\geq 35^\circ$  less the duplicate coverage that exists in 18 days at latitudes greater than  $60^\circ$ , and (III), scheduled mission operations. Each of these three major columns further shows the breakdown of this coverage by real time, remote coverage and their totals. A fourth major column, (IV), shows the total land mass missed because of combined recorder/ground station limitations.

Examination of the maximum case of payload operations is required as a worst case input to power analysis, thermal analysis, and ground operations. As expected, the maximum payload operations occur during summer solstice. Average daily operations during this season are approximately 135 minutes. Average daily operations for Spring/Fall and Winter seasons are 108 and 64 minutes respectively. Note that summer operations are double those for winter and 25 percent higher than the equinox case. Within summer solstice, day 9 operations (147 minutes), represents the absolute worst case.

Day 9 is examined in detail in the timelines shown in Figure 4 5-3. These timelines show by rev, the latitude and time at which primary ground station coverage is available and the mission operations planned. Subsystem payload operation required to perform the mission operations is shown, including warmup/starting times and recorder operations of rewind, record and playback. Rev summaries of total operating times, frames of data taken, and recorder management are shown.

#### 4 5 3 4 Summary

Maximum payload operations occur during summer solstice due to the fact that most of the world's land mass is in the Northern Hemisphere. Maximum payload operations occur during day 9 of this period, and this day has been examined in detail through the use of a timeline. It should be noted that these represent worst case conditions. Under more realistic conditions cloud coverage restrictions would have been used. Operationally, areas of cloud cover would be inhibited to eliminate useless tape recorder operation. Also, the total world land mass has been attempted during all seasons. It is assumed that preference would likely be given to the Northern Hemisphere during the summer growing season at the expense of Southern Hemispheric coverage. However, the worst case results from the mission simulation studies are the inputs used in the specific studies that follow.

#### 4 5 4 SPECIFIC STUDY RESULTS

##### 4.5 4 1 Power Analysis Input

The power subsystem was evaluated using the maximum daily payload operation. The detailed timeline for this day (Day 9) was used as an input to the power analysis computer program. The mode of operation of all individual payload equipments and the time of day or night these operations occur were inputted to this computer program to develop the detailed load profile.

Power status results, for this simulated worst case day, are discussed in Volume II Section 8.3.

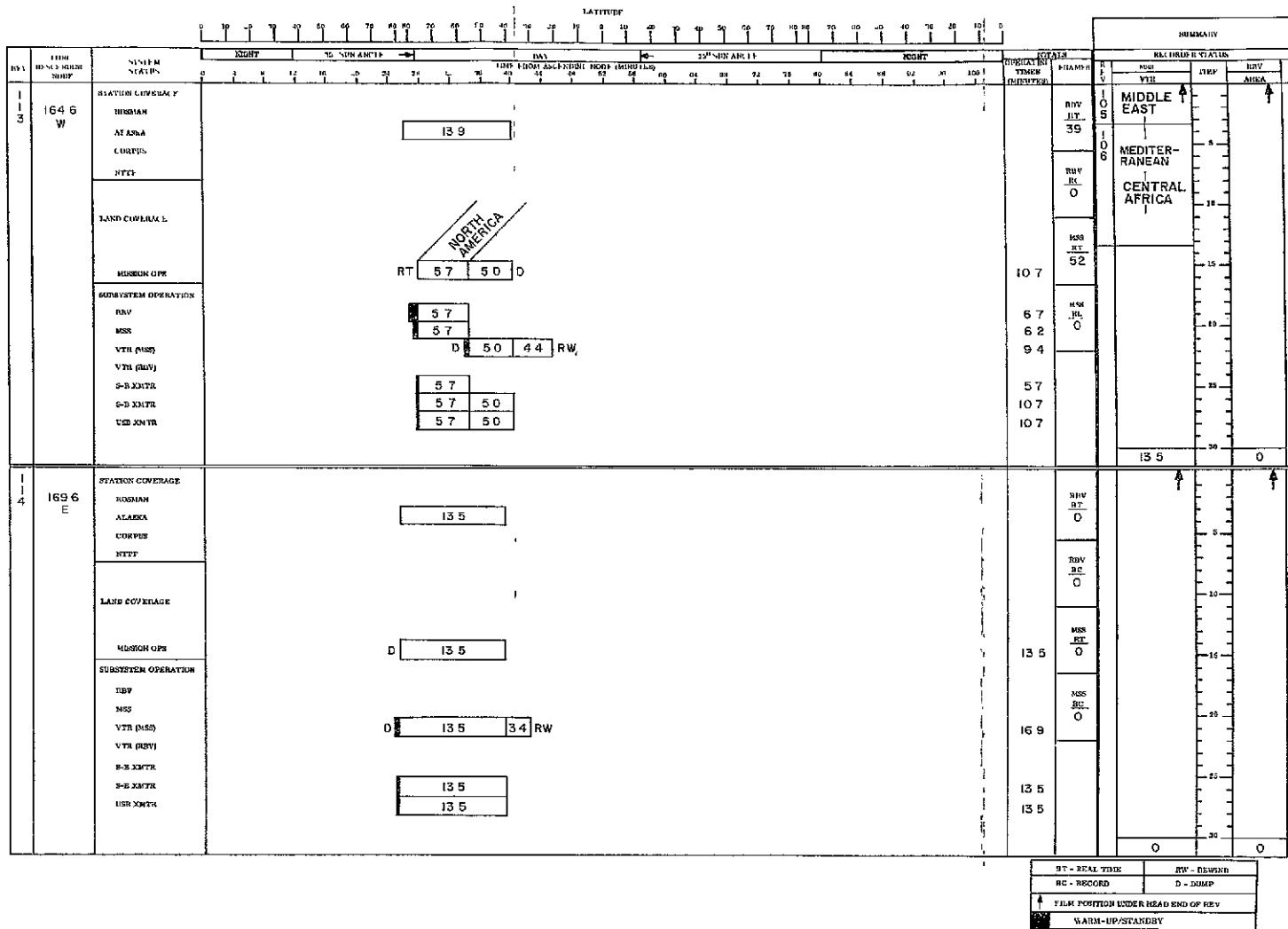


Figure 4 5-3. Mission Timeline-Day 9 (Sheet 1 of 7)

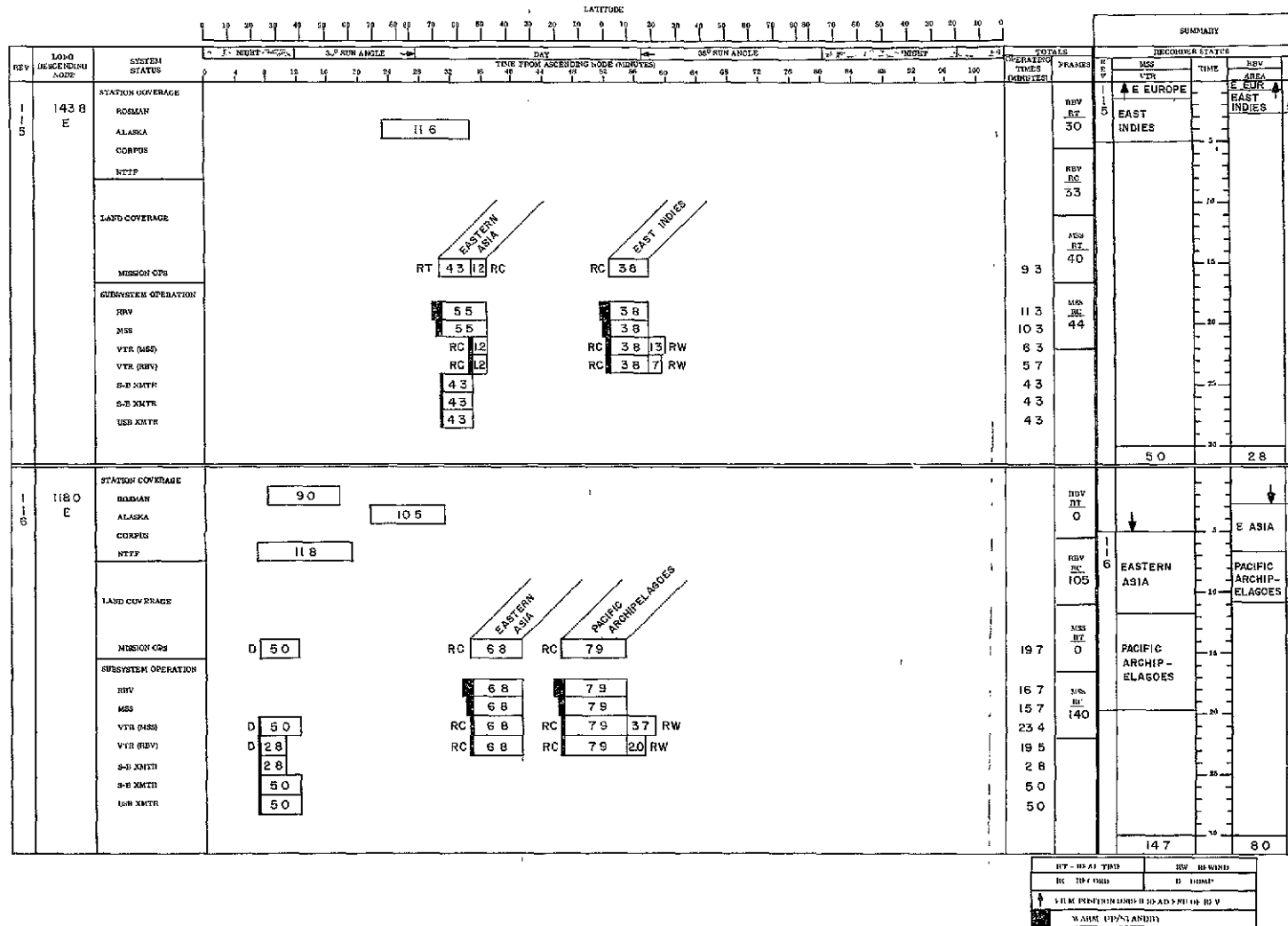


Figure 4 5-3 Mission Timeline-Day 9 (Sheet 2 of 7)

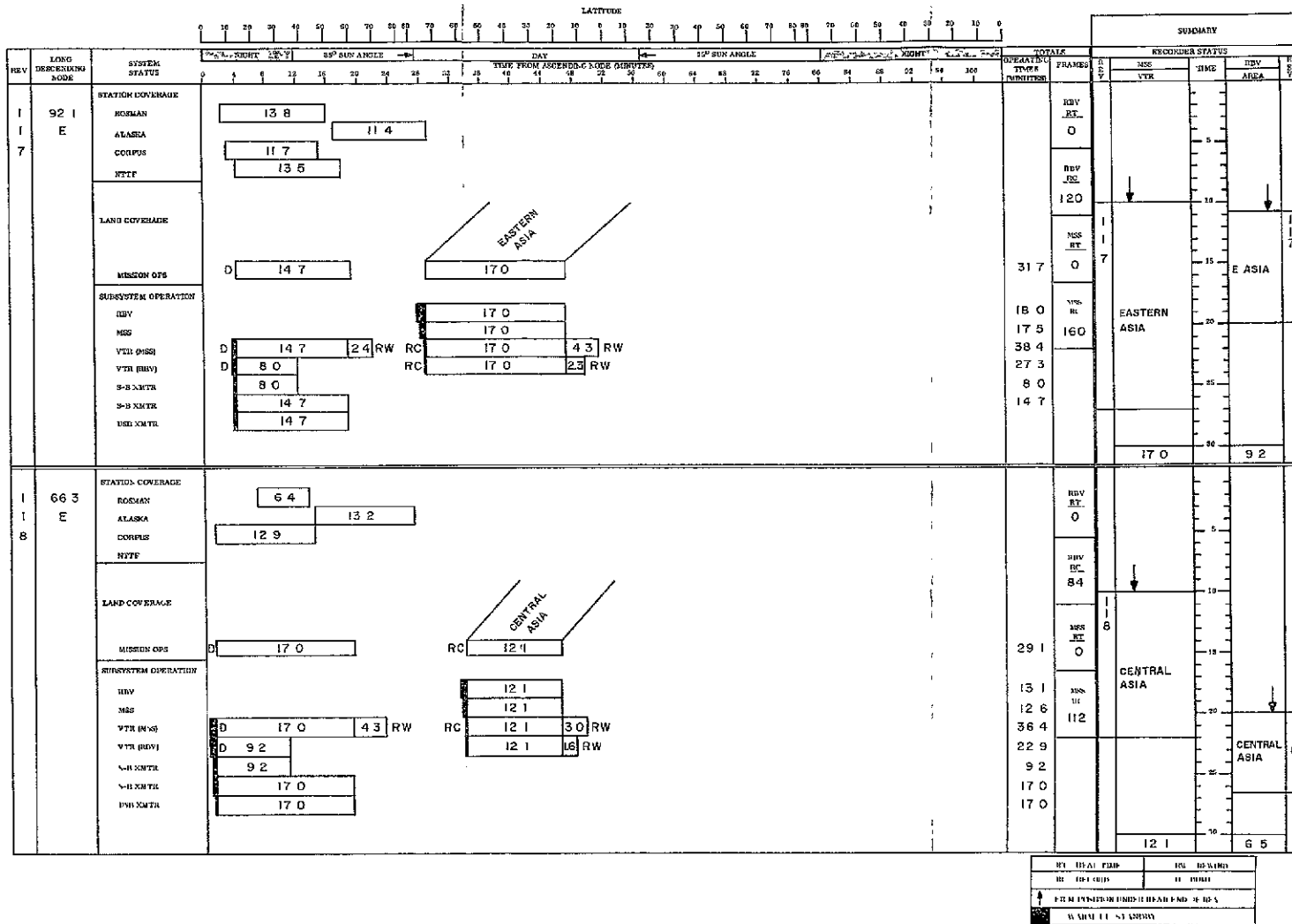


Figure 4.5-8. Mission Timeline-Day 9 (Sheet 3 of 7)

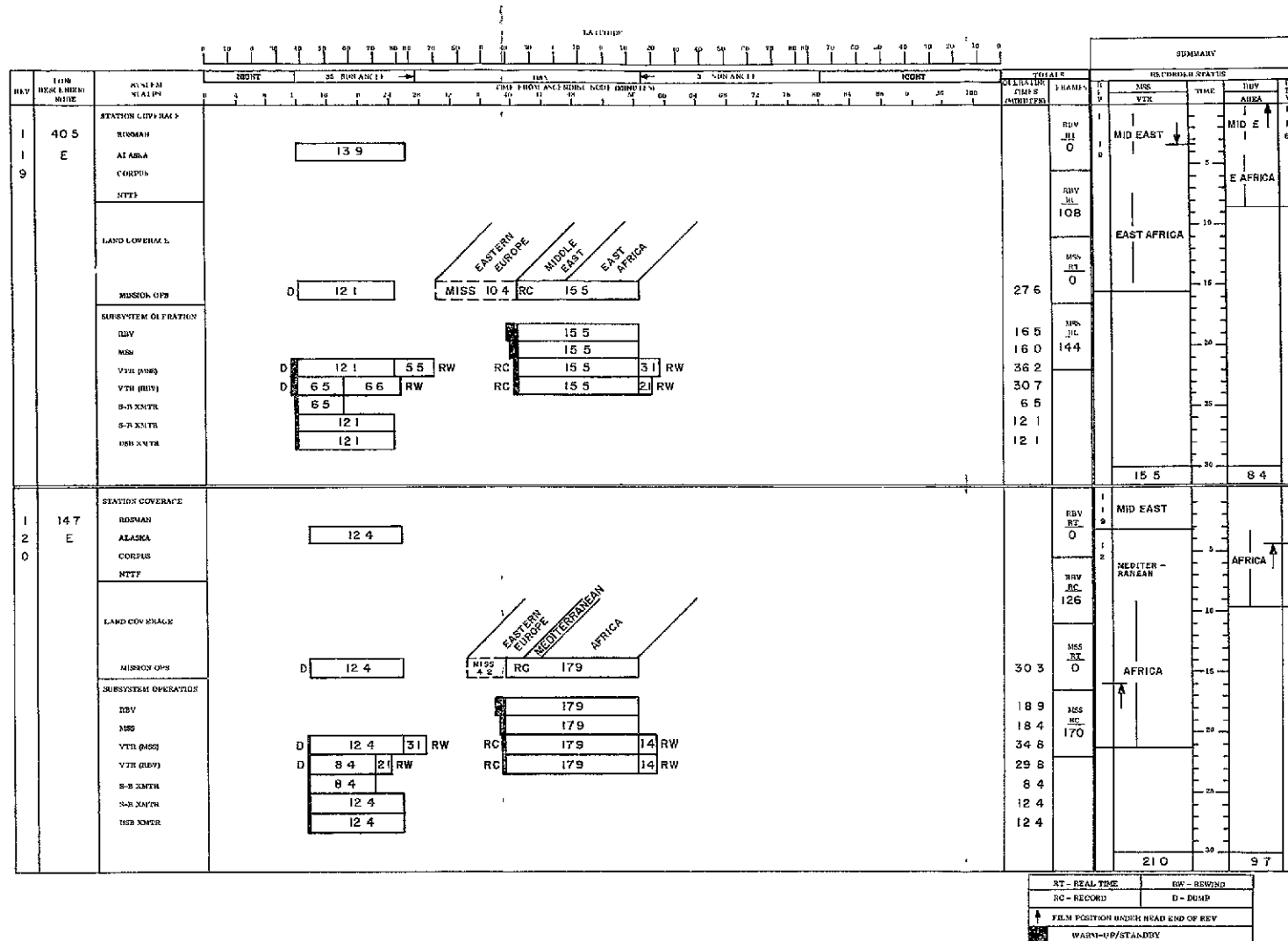


Figure 4 5-3 Mission Timeline-Day 9 (Sheet 4 of 7)



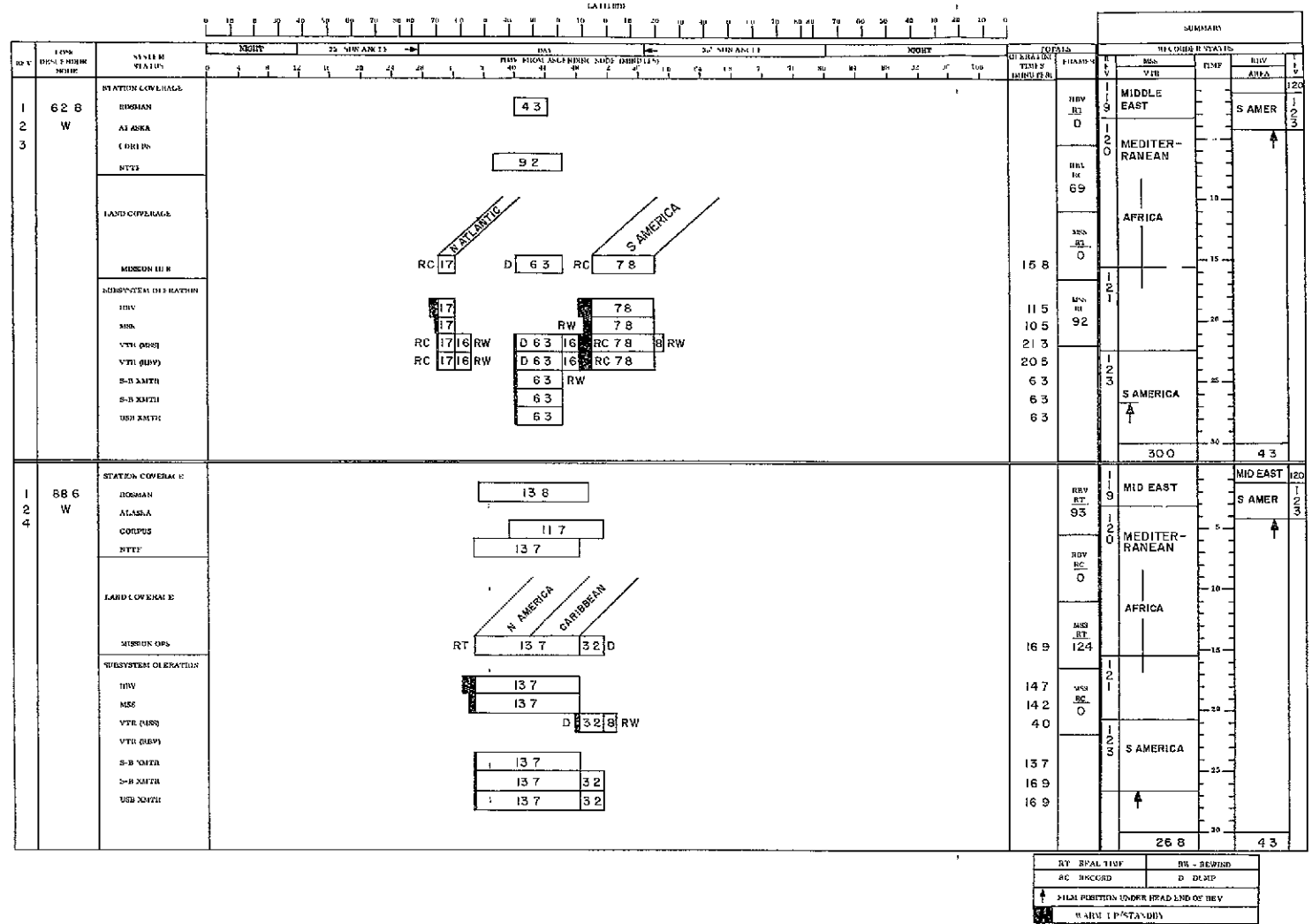


Figure 4 5-3 Mission Timeline-Day 9 (Sheet 6 of 7)



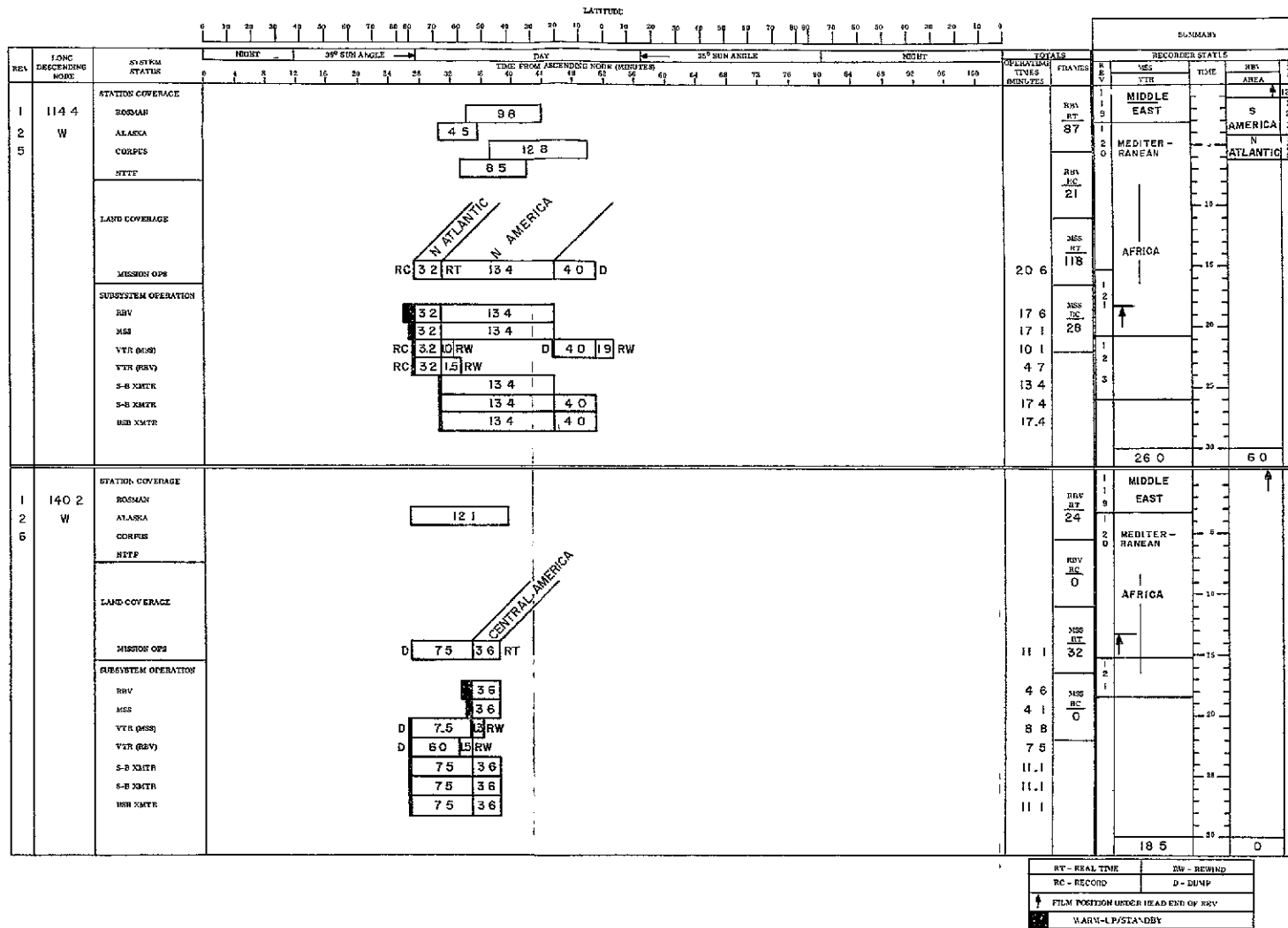


Figure 4 5-3 Mission Timeline-Day 9 (Sheet 7 of 7)

#### 4 5 4 2 Thermal Analysis Input

The worst case system operations for heating occurs not on the longest payload operating rev (27+min) but on a series of successive long operating revs. This is due to the thermal lag in the system in that it cannot return to its starting point in a single rev. Therefore, the input to thermal analysis from the mission simulation studies is to find the greatest accumulation of payload operating time in consecutive revs. This also occurs in Day 9.

Thermal analysis for this mission simulation is contained in Volume II, 7.

#### 4 5 4 3 Command Storage Requirements

##### 4 5 4.3 1 Period Requiring Greatest Number of Stored Commands

The maximum loading on command storage occurs when the greatest number of remote payload sequences are required between station contacts. Mission simulation studies considering station contacts and payload sequences required have shown that this could occur on Days 8, 13, 14, 15, 16 and 17 (of each 18-day series) during spring, summer and fall periods. Table 4 5-4 summarizes the command sequences required, for the "dead" rev station contact period, for summer solstice.

##### 4 5 4 3 2 Sequences required for Maximum Case

Day 13, requiring 5 stored command sequences, is typical of the maximum cases and is illustrated in Figure 4 5-4. The following brief sequence of events occurs for this period.

Mission Operation	Rev	Duration	Event	Place
Station Contact	8	11 5	Comd Loading	Alaska
1st Payload Operational Seq	8	8 6	RBV/MSS Recorded Ops	Eastern Europe
2nd Payload Operational seq	8	9 7	RBV/MSS Recorded Ops	Africa
3rd Payload Operational Seq.	9	12 8	RBV/MSS Recorded Ops	W Europe
4th Payload Operational Seq.	10	0 9	RBV/MSS Recorded Ops	N. Atlantic

TABLE 4 5-4 NUMBER OF PAYLOAD SEQUENCES REQUIRED - "DEAD" REV STATION CONTACT PERIOD

Day	Station Contact Rev	Payload Sequences by Rev					Mission Ops Area	Total Sequences Required
		8	9	10	11	12		
1	9	1					Europe/Africa N Atlantic S America N Atlantic	4
	12		1		1	1		
2	9	1					Europe/Africa N Atlantic S America --	3
	12		1		1	1		
3	9	1					Europe/Africa -- S America N Atlantic	3
	12		0		1	1		
4	9	1					Europe/Africa -- S America --	2
	12		0		1	0		
5	9	1					Europe Africa -- S America N Atlantic	4
	12	1		0		1		
6	9	1					Europe Africa -- N Atlantic S America --	4
	12	1		0		1		
7	9	1					Europe Africa -- S America N Atlantic	4
	12	1		0		1		
8	9	1					Europe Africa S America N Atlantic S America --	5
	12	1		1		1		
9	9	1					Europe/Africa S America --	2
	11		1			0		

Day	Station Contact Rev	Payload Sequences by Rev					Mission Ops Area	Total Sequences Required
		8	9	10	11	12		
10	9		1				Europe/Africa S America N Atlantic	3
	11			1		1		
11	9		1				Europe/Africa S America --	2
	11			1		0		
12	9		1				Scandinavia Europe/Africa S America N Atlantic	4
	11		1		1	1		
13	8	1					Europe Africa Europe/Africa N Atlantic S America --	5
	11	1		1		1		
14	8	1					Europe Africa Europe/Africa S America N Atlantic	5
	11	1		1		1		
15	8	1					Europe Africa Europe/Africa N Atlantic S America --	5
	11	1		1		1		
16	8	1					Europe/Africa W Europe W Africa S America N Atlantic	5
	11	1		1		1		
17	8	1					Europe/Africa W Europe Africa N Atlantic S America --	5
	11	1		1		0		
18	8	1					Europe/Africa W Europe S America N Atlantic	4
	11		1		1	1		

11 February 1970

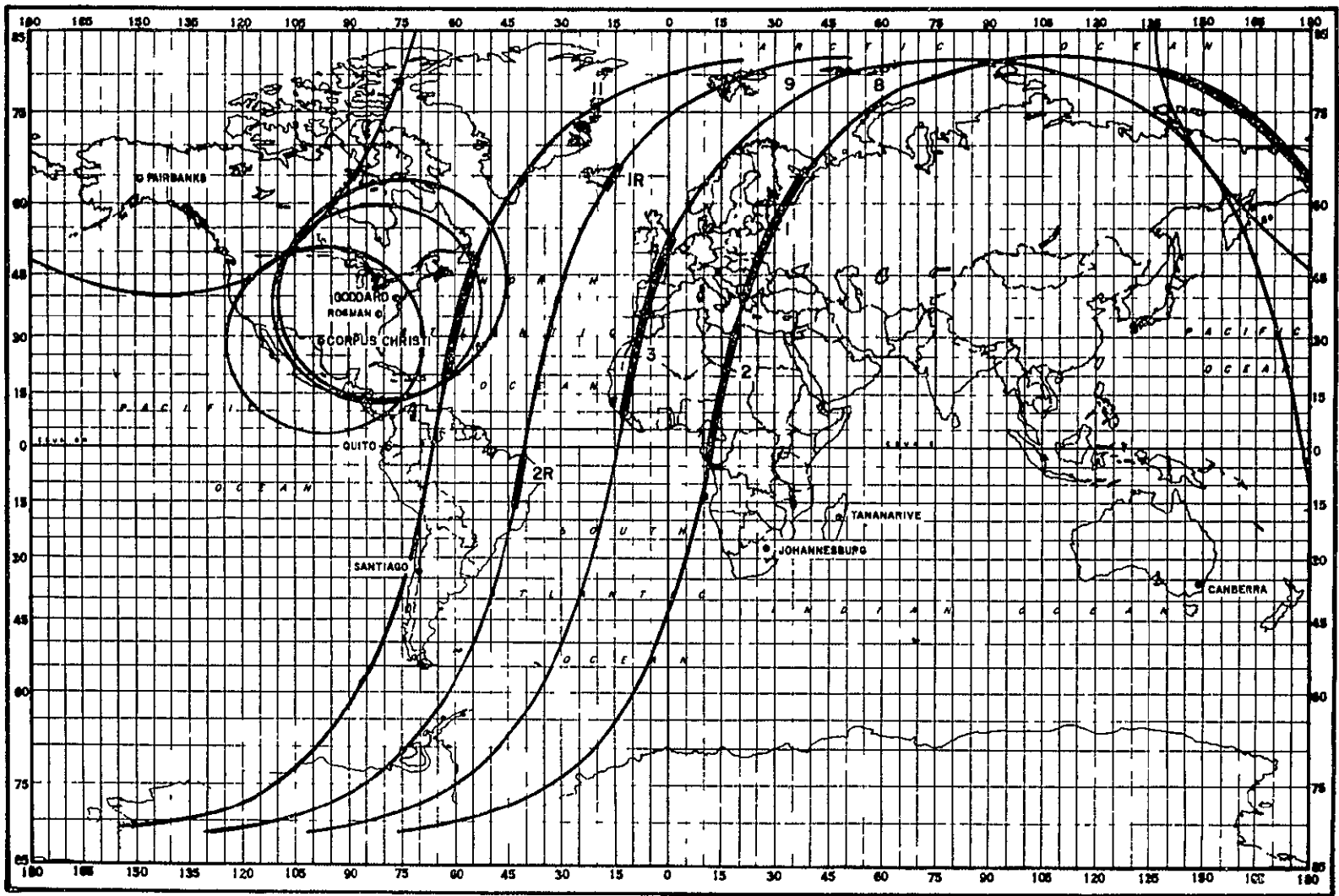


Figure 4 5-4 Operating Profile Requiring Maximum Stored Commands (No Clouds)

Mission Operation	Rev	Duration	Event	Place
5th Payload Operational Seq	10	3 8	RBV/MSS Recorded Ops	S America
Station Contact	11	9 3	Comd Loading	Rosman

Note The small tip of Scandanavia on rev 9, and N Atlantic on rev 11 are not scheduled on Day 13 as they are above 60°N They were scheduled on Day 12 and N Atlantic is scheduled on Day 14 Scandanavia is out of view on Day 14.

Note that the total operations scheduled in Figure 4 5-4 cannot be performed as they exceed the tape recorder capacity by 5 8 minutes even assuming a completely empty recorder at the beginning of the sequence Therefore, some coverage would not be scheduled For worst case sizing of the stored command requirements, it is assumed that this reduction in coverage would not decrease the number of payload sequences scheduled

#### 4 5 4 3 3 Cloud Coverage Consideration

Operational planning will inhibit sensor operations over large cloud masses where it is unlikely that any significant amount of useful data would be collected Such a situation is hypothesized in Figure 4 5-5 Large areas of clouds are considered to be present over the Mediteranean Sea, Southern Europe and Northwestern Asia This cloud pattern segments the operations planned during rev 8 and 9 Thus, the following payload sequences would be required

- Rev 8 one sequence for Central Europe  
one sequence for Central Western Africa
- Rev 9 one sequence for W Europe  
one sequence for West Africa
- Rev 10 one sequence for N. Atlantic  
one sequence for S. America

For this condition, which represents a worst case in terms of the number of operating sequences during dead revs and considers major cloud scheduling, six payload sequences are required

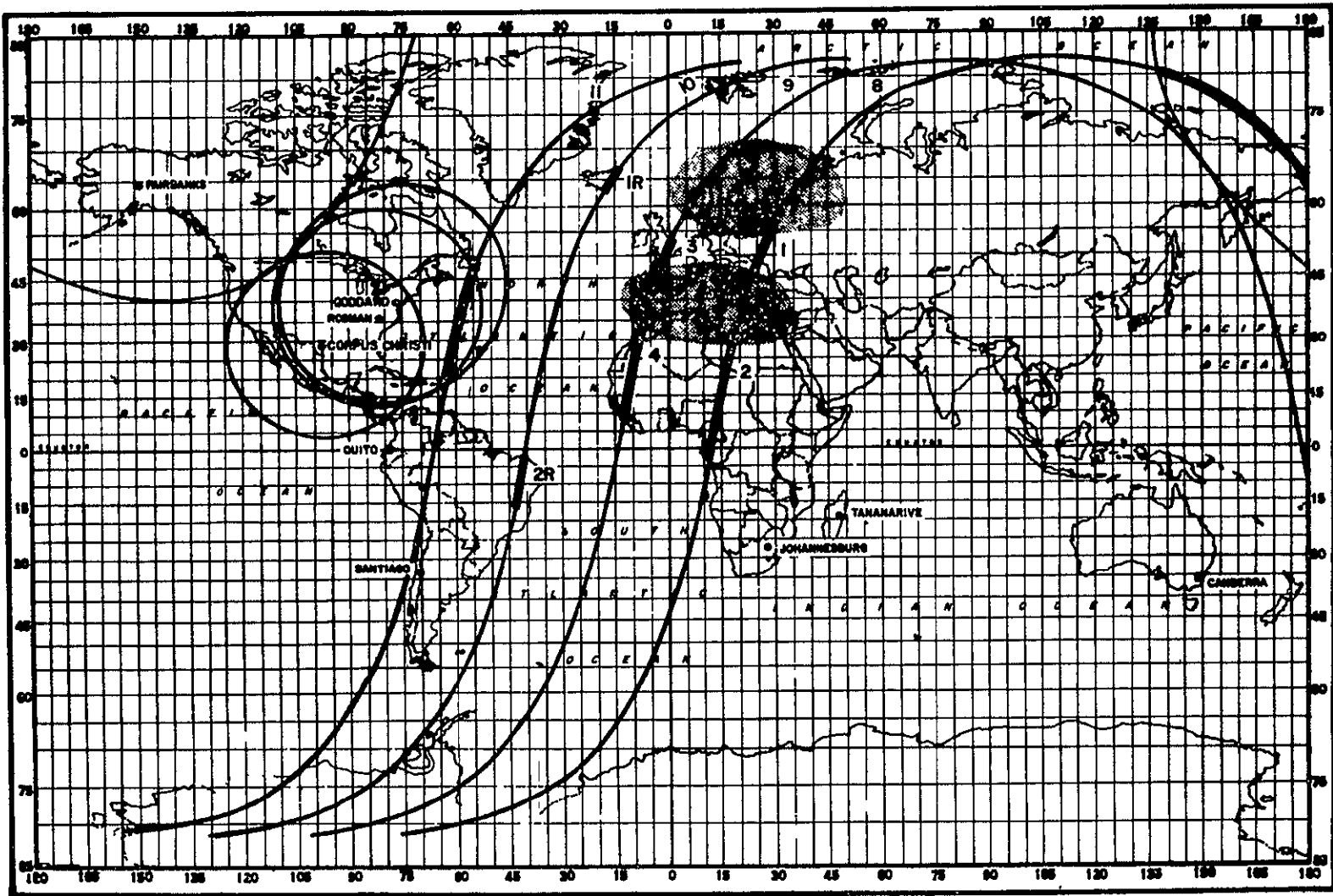


Figure 4. 5-5. Operating Profile Requiring Maximum Stored Commands (With Clouds)

## 4 5 4 3 4 Payload Command Sequence Content

For remote payload operation a command sequence consists of turning both sensors and WBVTR's on and off. A prerequisite is that the RBV, MSS and WBVTR's have been previously set to the desired operating mode (i.e., record mode, continuous operation, etc.) Once this has been accomplished each operates automatically throughout the coverage area and does not require additional commands. A payload command sequence requires the following commands:

<u>Time</u>	<u>Command</u>	<u>Response</u>	<u>Stored Commands</u>
T-50	MSS ON RBV STDBY	MSS turns on RBV in standby	1
T-5	VTR (MSS) RECD	WBVTR (MSS) startup	1
T-0	(AUTO)	RBV begins operating sequence, MSS recording data	0
T+2	VTR (RBV) STDBY	WBVTR (RBV) in standby	1
T+9.5	(AUTO)	WBVTR (RBV) in record	0
T+14.5	(AUTO)	RBV SHUTTER	0
T+25.0	(AUTO)	WBVTR (RBV) in standby	0
≈	(RBV CYCLE REPEATS, MSS RECORDING CONTINUES, UNTIL END OF PASS IS REACHED )		0
T+( <sup>END OF</sup> PASS)	VTR (MSS) OFF	WBVTR (MSS) turns OFF	1
T+( <sup>END OF</sup> PASS)+1	VTR (RBV) OFF	WBVTR (RBV) turns OFF	1
T+( <sup>END OF</sup> PASS)+2	MSS and RBV OFF	MSS and RBV turn OFF	1
		TOTAL	6

## 4 5 4 3 5 Command Recycle

Command recycle capability exists for each stored command \* When the recycle bit is set in the command word, command execution will occur again after the specified recycle time span has elapsed Continued reexecution will occur at this  $\Delta$  recycle time This command feature is used to re-execute sensor and VTR commands This is shown in Figure 4 5-5 where the recycle command indicated by an "R" is used to re-execute the payload sequences 1 and 2 given over Europe and Africa to occur again over the North Atlantic and South America respectively Note that recycle commands are scheduled so that the second re-cycle execution will occur after a station commanding pass For example in Figure 4 5-5, the first recycle is used for the payload sequence for the North Atlantic This payload sequence would be re-executed during rev 12 but it is removed during station passes occurring on either revs 11 or 12

## 4 5.4 3 6 Stored Commands Required - Maximum Case

Combining the number of commands required for a payload sequence, the number of payload sequences required, the command recycle capability and restrictions, plus the stored commands required for vehicle operation, provide the worst case number of command storage spaces filled Since the first command recycle executions should not occur earlier than 2 revs from the initial execution (for this case), then revs 8 and 9 of Day 13 require 2 stored sequences each and rev 10 with two sequences required will be recycle commands from rev 8

Therefore, 4 sequences containing 6 commands are required for payload operation for a total of 24 stored commands One command is required to turn on both S-Band transmitter heater power and one to rewind the MSS recorder, prior to station contact Vehicle operation requires 4 stored commands for scanner turn on/off at sunrise/sunset

Thus adequate command storage exists for the worst case mission operations

## 4 5 4 3 7 Growth

Should the stored command requirements increase beyond the present capacity of 30 stored commands, greater efficiency in the use of commands could be achieved by using a sequencer to program a combined RBV/MSS/WBVTR turn-on operation The sequencer operation would be initiated by a single stored command Turn off would be handled similarly. Thus, a payload sequence after presetting the sensors to the desired operating modes would consist of only two commands Also the segment switches on the solar array drive are being investigated for the ACS scanner on/off commands in place of stored commands This further reduces the stored command requirement.

---

\*The recycle function is described in detail in Volume II Section 4 4 2 2



4 5 4 4 Ground Data System Sizing

Much of the activity required of the ERTS ground support system is very dependent on the way the spacecraft/sensor system will be operated in orbit. The mission simulation capability has been used to develop two sizing studies to date:

- 1 NASA Data Processing Facility Loading Requirements
- 2 Estimation of the number of wide band video tapes to be received from Acquisition sites

At the current time, operational procedure definition and ground system timelines are being studied employing the simulated profiles as a primary input. The following two sections present a brief summary of the results of the two sizing studies. Final results will be included in the final study report in April.

## 4 5 4 4 1 NDPF Loading Requirements

This study examined various loading requirements for the NDPF. The cases selected were based on our orbit studies, the design study specification (S-701-P-3), and conversations with NASA personnel. The results are summarized below:

Operations Mode	Minutes Per Day	Images Per Day	Images Per Week
1 Real-Time, US (incl Alaska)	18	315	2,205
2 Real-Time, All Land with coverage cones	44	740	5,180
3 Real-Time, US plus one hour	78	1,316	9,212
4 30 minute recorder limited, attempt global land coverage	135	2,268	15,876
5 Three ground station contact limit, no recorder limit, attempt global land coverage	208	3,495	24,465
6 Average 20 min/rev operation	280	4,704	32,928

To convert minutes of operation (M) to number of images (I) produced, the following is used:

$$\begin{aligned}
 I &= M \left( \frac{\text{min}}{\text{day}} \right) \times 60 \left( \frac{\text{sec}}{\text{min}} \right) \times \left( \frac{1}{25} \right) \left( \frac{\text{operation}}{\text{sec}} \right) \left( X \right)^7 \left( \frac{\text{images}}{\text{operation}} \right) \\
 &= 16.8 M \left( \frac{\text{images}}{\text{days}} \right)
 \end{aligned}$$

Line 1 is Case A described in section 7.14 of the design study specification and must be throughputed in a 40-hour week at minimum cost. Line 3 is Case B and we must tradeoff throughput rate vs hardware and manpower. No specific time is specified for processing Case B other than the obvious 168 hour/week physical limit.

In performing the trades for Case B design, the following considerations are being included:

1. Equipment cost and amortization
2. Shift bonus costs
3. Growth (say to line 2 plus one hour or line 4)
4. Maintenance of complex equipment

Table 4.5-5 is the conversion of operating times to various product rates.

#### 4.5.4.4.2 Estimation of Number of Wideband Tapes to be Received from Acquisition Sites

Information was generated to estimate the number of wideband data tapes produced daily as a preliminary basis for sizing GDHS design. The estimates are worst case and are based on the day 9 summer solstice operating profile. The following assumptions were made in computing the estimates:

1. A 30-minute record capacity exists on the ground WBVTR's at the acquisition sites.
2. Data received on different passes will be recorded on a single tape if space exists.
3. Data will be received at Alaska, Corpus Christi, and the NTTFF.
4. All acquisition passes (both day and night) were considered available for data receipt.
5. The basic profile considered sensor operations compatible with the compatibility of the S/C system, therefore, the total amount of data gathered exceeds the Case B coverage requirement as stated in the specification.

Table 4.5-6 shows the breakdown of data receiving passes at each of the three acquisition sites as a function of rev. All numbers relating to the amount of data is shown in minutes. For each pass, whether data is real time or dumped recorder is indicated. The status of the WBVTR's at the sites after each pass is also shown.

Table 4.5-7 summarizes the wideband tapes recorded per day as a function of site, tape ID#, amount of data on tape, and the passes (rev) from which data was recorded.

TABLE 4 5-5 PRODUCTION RATES

		Case A	Case B	Recorder Limit
1	Images/day	315	1,316	2,268
2	Images/week	2,205	9,212	15,876
3	Color neg, RBV/week (20% of line 2/3 x 3/7)	63	263	453
4	Color neg, MSS/week (line 3 x 2)	126	526	906
5	Total, line 3 + line 4	189	789	1,359
6	Precision B&W neg/week (5% of line 2)	110 3	460 6	793 8
7	Precision Color net/week (3/7 of line 6)	47 3	197 4	340 2
8	Photogrammetrically Proc Sets/week 5% of line 2)	110 3	460 6	793 8
	B&W Images/hr - 40 hr week	55 1	230 3	396 9
	- 80 hr week	27 6	115 2	198 5
	- 168 hr week	13 4	56 1	96 8
<u>Production Processing</u>				
9.	B&W Bulk/week	22,030	92,120	158,760
10	Color Bulk/week	1,890	7,890	13,590
11	Precision B&W/week	1,103	4,604	7,938
12.	Precision Color/week	473	1,974	3,402
<u>Annual Storage</u>				
13	B&W Masters	114,600	479,000	825,500
14	Color Masters	9,800	41,000	70,700
15	B&W Precision	5,700	24,200	41,300
16	Color Precision	2,460	10,300	17,700
17	Photogrammetrically Proc Sets	5,700	24,200	41,300

TABLE 4 5-6 SENSOR DATA RECORDED BY GROUND STATIONS

Rev	Alaska Pass			Corpus Pass			NTTF Pass		
	Rt	Dump	WBVTR Status	Rt	Dump	WBVTR Status	Rt	Dump	WBVTR Status
1	5 7	5 0	10 7	-	-	-	-	-	-
2	-	12 4	23 1	-	-	-	-	-	-
3	3.3	-	26 4	-	-	-	-	-	-
4	-	-	-	-	-	-	-	6 9	6 9
5	-	2 0	28 4*	-	10 7	10 7	-	13 5	20 4
6	-	5 1	5 1	-	12 9	23 6*	-	-	-
7	-	12 1	17 2	-	-	-	-	-	-
8	-	12 3	29 5*	-	-	-	-	-	-
9	-	5 6	5 6	-	-	-	-	-	-
10	-	-	-	-	-	-	-	-	-
11	-	-	-	-	-	-	-	9 2	29.6*
12	-	-	-	10 0	-	10 0	13 8	-	13 8
13	4 5	-	10 1	8 8	4 0	22 8*	8 5	-	22 3*
14	3.3	8 0	21 4*	-	-	-	-	-	-

\*Indicates that tape cannot accommodate all data from next pass and thus is demounted and ready for shipment to NDPF

TABLE 4 5-7 SUMMARY OF GROUND RECORDED TAPES

Site (Tape ID#)	Amount of Data Min	Passes Recorded (Rev)
Alaska (1)	28 4	1, 2, 3, 5
Alaska (2)	29 5	6, 7, 8
Alaska (3)	21 4	9, 13, 14
Corpus (1)	23 6	5, 6
Corpus (2)	22.8	12, 13
NTTF (1)	29 6	4, 5, 11
NTTF (2)	23 3	12, 13

Based on the above data, a maximum of 14 wideband tapes (7 RBV, 7 MSS) would be required per day. For Case B coverage (a total of approximately 78 min/day as opposed to the approximate 147 min/day as shown), a maximum of 12 tapes would be required per day. This would reduce to a total of 8 tapes per day (4 from Alaska, 2 from Corpus, and 2 from NTTF), if a carry-over of more than a day is permitted for the Corpus and NTTF stations.

The absolute minimum number of tapes based on data volumes and tape capacity would be 6 per day. This assumes a total of 78 minutes of operations per day and would allow approximately 12 minutes for redundant recording by two sites simultaneously. This is not considered practical because of the tape packing density and does not allow adequate room for data segmenting information, headers, etc.

Table 4 5-8 summarizes the various cases vs the tape requirements.

TABLE 4 5-8 MISSION OPERATING CASES VS TAPE REQUIREMENTS

Case	Alaska	Corpus	NTTF	Total
1 Data dumped every pass (20 passes/day) New tape each pass*	22	8	10	40
2 Worst case mission profile (New tape each pass)	20	8	10	38
3 Worst case mission profile (Tape packing)	6	4	4	14
4 Case B profile (Tape packing, contiguous pass)	4	4	4	12
5. Case B profile (Tape packing, day and night passes NTTTF and Corpus packed)	4	2	2	8
6 Absolute minimum number tapes (data volume)	2	2	2	6

\*A total of 20 passes over the acquisition sites occurred on the day considered. Case 1 assumed that data would be received at each of these passes and a new tape would be used each time.

As can be seen from Table 4 5-8, the number of tapes required per day vary significantly depending on assumptions. It appears that (if tape packing is employed) Cases 3, 4, and 5 would most likely occur with Case 3 and 4 being the most probable. Therefore, for design purposes, the Ground Data Handling System should expect approximately 10-12 wideband video tapes per day from acquisition sites.

## 4 6 WIDEBAND VIDEO TAPE RECORDERS MANAGEMENT

### 4 6 1 RECORDER MANAGEMENT

Management of the use of the onboard wideband video tape recorders is necessary for three basic reasons

1. The sensors can produce more data than the recorder is capable of storing.
2. The full contents of the recorder cannot be dumped during the limited time of a station contact.
3. The lifetime of the recorder is limited.

In order to effectively manage the use of the recorder, the Mission Scheduling function in the Operations Control Center (OCC) must maintain an accurate status of the recorder at all times. The primary status information is

- 1 How much, and what data is currently on the tape,
- 2 What is the physical position of the tape at all times,
- 3, What is the current status of the recorder capability (i. e., does a degraded mode exist, what are the actual tape speeds, etc.)
- 4 What operational mode is the recorder currently in

The results of the mission simulations presented in Section 4 5 indicate that typical ERTS operations would include the following types of recorder usage

1. Record data remotely during an orbit and completely dump this data at the next available station pass.
2. Record data remotely during an orbit, or a series of orbits, but be unable to dump all the recorded data during the available station passes on these orbits.

The first of these two cases is obviously the simplest from a recorder management standpoint. The operational sequence would entail the recording of data for some period of time, a rewind of the recorder after recording has ceased by an amount corresponding to the recorded operation, and a dump operation during the pass during which all the previously recorded data is returned to the ground. The tape can either be rewound to the beginning of tape at this time and readied for the next recording operation, or not rewound but readied at its current position for the next recording operation, if sufficient tape still remains on the reel from this point to accept the next anticipated recorded operation. The latter of these two situations could be employed if one wants to wait to verify that the dumped data was received properly since the next record cycle would not erase this data and a retransmission at a later time would still be feasible. The approach might also be employed to limit concentrated usage of a specific section of the tape (the front end) thus possibly reducing potential tape failures attributed to effects resulting from multiple recordings on the tape.

The second operational sequence where all previously recorded data can not be transmitted to the ground during the station pass presents a more complex recorder management problem. It is anticipated that the majority of the remote operations will be between 2 and 10 minutes each. It is possible, however, to have more than one of these operational sequences occur during a single orbit. A typical station pass might be on the order of 10 minutes. Therefore, hopefully, all the data from at least a single operational sequence could be returned during a single station pass. However, it is likely that additional data will be recorded before all the data recorded on the previous orbit is played back. In this type of situation it becomes extremely important to ensure that the new data to be recorded does not in any way interfere with previously recorded data that still needs to be transmitted to the ground. To properly manage the recorder usage under these conditions requires that the OCC maintain an accurate image of the recorder tape situation at all times.

Figure 4 6 1-1 graphically depicts a typical operational sequence for two orbits. It was assumed that the tape was clean at the beginning of the pass in rev N. Two remote operational sequences (A&B) were scheduled on rev N. The available dump time during the station pass on rev N however was only sufficient to transmit the recorded data from operation A. Therefore at the beginning of the remote operations planned for rev N+1 (operational sequences C&D), the recorder tape still contains untransmitted data from operation B. The recording of data from operations C and D must then be recorded on the tape exclusive of where operation B is contained. As is shown it was elected to record operation C behind operation B and to record operation D over the area where the already transmitted operation A was contained.

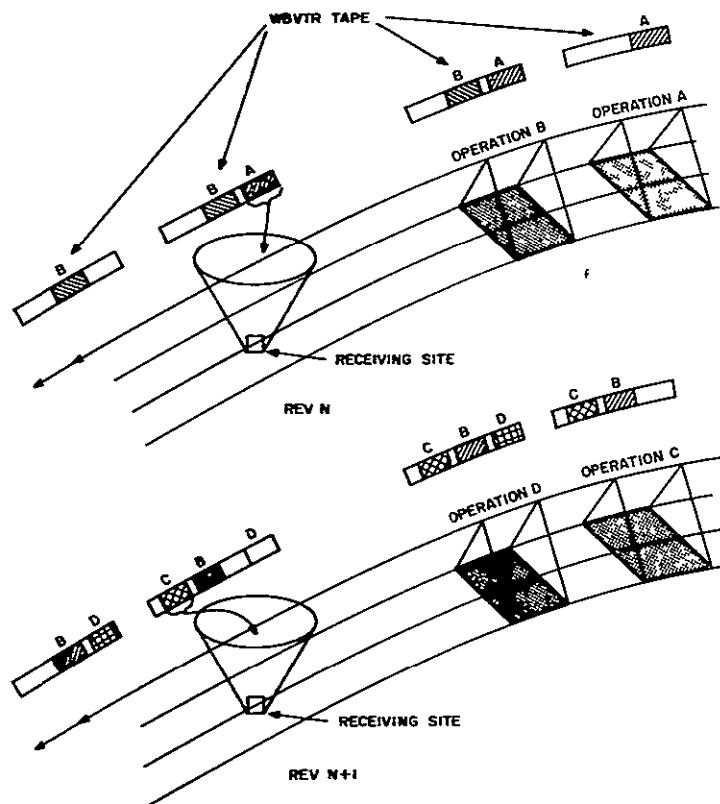


Figure 4 6 1-1 Typical Operational Sequence for Two Orbits

11 February 1970

The station pass on rev N+1 is such that only operation C can be transmitted to the ground. This, therefore, was scheduled and at the beginning of rev N+2, the tape contains recorded, but still untransmitted data from operations B and D.

This type of sequence will generally continue to occur for a period of a few orbits (see Section 4.5) until sufficient dump time becomes available to allow all the recorded data to be transmitted to the ground. At this point the situation as described in case 1 will prevail again for a series of orbits until a case 2 condition arises again. Typically one finds a single case 1 series of orbits and a single case 2 series of orbits in any given day. The case 2 condition arises generally around those orbits that contain no or very short station passes.

In the previous discussion the recorder management problem was examined from the standpoint of mission operations and recorder usage requirements. At this point some key considerations can be noted.

1. Since the recorder has a limited storage capacity, certain potential remote sensor operations over available coverage requirement must be inhibited (see Section 4.5). This implies that at times the full capacity of the recorder will be used and all the data on the resulting fully loaded tape will not as yet have been transmitted to the ground.
2. Generally, the data on the tape will be in segments related to specific operational sequences and these segments will generally be on the order of 2 to 10 minutes of data each.
3. The order of the individual segments on the tape may not necessarily be time-sequenced since, to maximize the efficiency of the use of the tape, data will be recorded on a space available basis (i.e., if a 3-minute recorded operation is planned, the current tape content status will be examined to determine the best area on the tape to record the operation).
4. Since ground site contact time and the availability of station passes relative to desired recording cycles constrains what can be recorded, the efficient use of the available ground contact time is mandatory. The current content of the tape must be examined to determine which specific recorded data segment(s) are best scheduled for transmission during the anticipated pass. The transmission of partial segments is not desirable and therefore should not be scheduled if possible.

The key to effective tape recorder management is the capability to have accurate knowledge of and control over the tape content. The system must have

1. The ability to move the tape to a predetermined position prior to an operational record sequence, and,
2. The ability to move the tape to a predetermined position prior to a recorder dump sequence over a data acquisition site.



In order to position the tape to satisfy the above two conditions, the OCC will require knowledge of a tape position vs sensor operation history. This profile will allow for correlation of the video with tape position. The OCC must also maintain an accurate history of tape position vs video data dumped. Finally, the OCC must have accurate knowledge of the actual position of the tape at any point in time.

#### 4.6.2 TAPE HANDLING REQUIREMENTS

Accurate knowledge of the status of the onboard wideband tape recorder is necessary. The questions which need to be examined are:

1. How accurately must the knowledge of tape position be for both monitoring and controlling, and
2. How can this information be obtained on the ground.

##### 4.6.2.1 Accuracy of Tape Position

Tape-positioning accuracy requirements are directly related to how the video data is recorded on the tape. The tape must be positioned properly (1) to allow recording of additional data without destroying previous records, and (2) to allow for readout of a total previously recorded operational sequence. Improper tape positioning in either the record or dump mode can result in the loss of data.

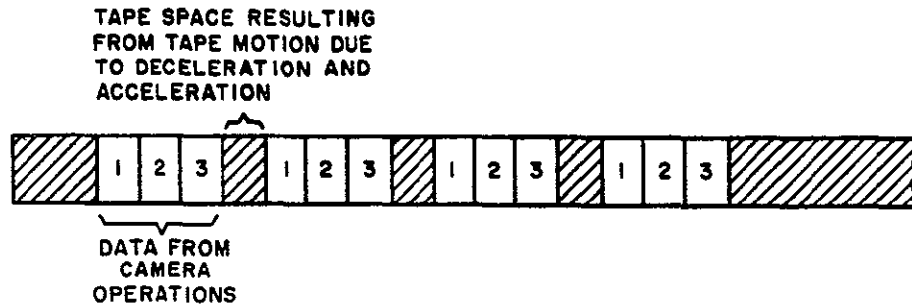
The configuration of data on the tape will be different depending on whether the data is from the RBV or the MSS. During RBV operations in the recorded mode, the camera controls the motion of the tape. The cameras are readout during part of the camera operating sequence. During the readout phase the tape is set into motion and the data recorded. At the completion of the readout, the tape is stopped and not moved again until the next camera readout cycle. Figure 4.6.2-1 graphically depicts the configuration of the tape resulting from an RBV operating sequence.

The operation of the MSS in the recording mode is such that data is continuously being outputted from the sensor. This data is continuously recorded for the duration of the operating cycle. The configuration of the resulting MSS tape is also shown in Figure 4.6.2-1.

The tape is moving at 12 ips during all recording operations. The amount of tape required to record the readouts of the 3 RBV cameras is 126 inches. The space between camera readout data due to tape movement during deceleration and start up is 36 inches. For the MSS data, the data recorded from two operating sequences will contain a buffer area between them on tape. This can be assumed to be at least 36 inches also due to normal tape movement due to deceleration and acceleration of the tape.

The recorder management function will require that the tape be capable of being positioned to a point within a buffer area between recorded data such that the first data following the buffer area can be readout when the tape is up to speed. The characteristics of the recorder are such that it takes 0.4 seconds from receipt of "record" command until the tape is up to speed and an additional 2.8 seconds to synchronize the recorder so data can be recorded. A total of 33.6 inches of tape is moved during this time period.

RBV



MSS

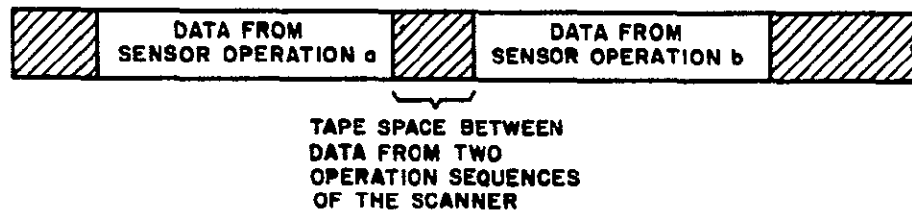


Figure 4 6 2-1 Wideband Tape Content Configurations

The amount of tape moved from the time the command to stop is received until the tape has stopped depends whether the tape was moving at the low or high rate. If it was moving at the 12 ips rate, then 2.4 inches of tape is moved, if at the 48 ips, then 9.6 inches is moved.

The total amount of tape moved during a record to standby to record cycle is 36 inches. It can therefore be expected that a buffer area of at least 36 inches will occur between any recorded two segments of recorded data.

The positioning of the tape in anticipation of a data dump cycle requires that the tape be up to speed at the point data is encountered. To allow for normal start up movement, the tape position must be positioned to at least 2.4 inches ahead of the data (Figure 4.6.2-2). This results in a tape positioning procedure capable of positioning the tape within a pre-determined 36 inch segment. Given that the midpoint of this segment will be nominally sought, the accuracy must be such that the tape can be positioned to within  $\pm 16.8$  inches of the nominal.

#### 4 6 2 2 Monitoring Tape Position

Two means are currently available for monitoring tape position. Position data is available as a normal telemetry point in form of the tape footage indicator. This data point however will not be sufficient to position within the required  $\pm 16.8$  inches because it is accurate to approximately 5% of the total tape length (1440 inches of tape).

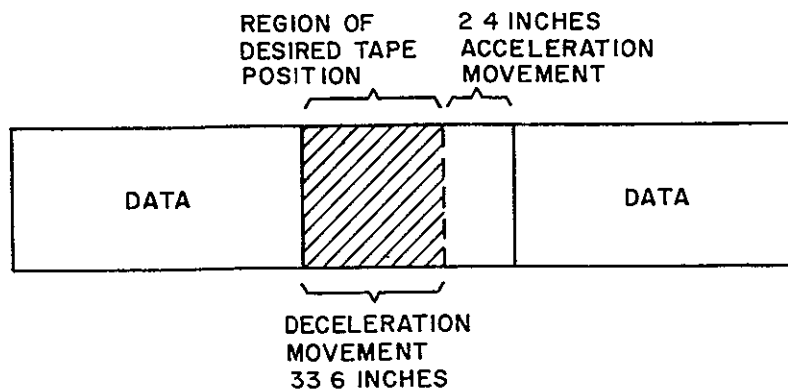


Figure 4.6.2-2. Tape Position Regions

The tape also contains a search track with a prerecorded code of tape position data. This track contains prerecorded unique 12 bit words every 6 inches along the tape. The monitoring of this information will allow for a measurement of tape position to within an accuracy of 6 inches. This accuracy falls well within the required  $\pm 16.8$  inches and thus is an acceptable monitor for tape position location.

#### 4.6.3 DESIGN APPROACHES

##### 4.6.3.1 Tape Position Monitoring

Two primary approaches were evaluated to transfer this data from the spacecraft to the OCC where it is ultimately needed.

1. Dump the search track on a separate subcarrier during the normal tape dump operation, and
2. Monitor the search track and merge the position data into the normal PCM telemetry data.

The first of these approaches although the simplest to implement from the spacecraft point of view was eliminated for the following reasons:

1. The only-time tape-position data would be available is during a dump operation.
2. The complexity of the problem of handling the signal at the remote site and transmitting it back to the OCC in real time during the dump operation.
3. The inability to effectively apply corrective measures (fine-tune tape repositioning) if it was found that the tape was not positioned properly prior to start of the dump operation.
4. Inability to accurately determine the location of recorded but yet untransmitted data since accurate tape position data is only available for data that has been dumped.

The approach of merging into the PCM telemetry provides several desirable features although it does require the addition of some specific circuitry to the spacecraft. The features that prompted the selection of this approach are as follows:

1. Tape position data available for all tape recorder modes.
2. Inclusion of this data in the normal PCM telemetry requires no special ground data handling procedures.
3. Actual tape position can be viewed from real time telemetry prior to a planned tape dump and fine repositioning can be effected if required prior to dumping.
4. Since tape position data is monitored during remote recorded sensor operations, an evaluation of the playback PCM telemetry will provide an accurate knowledge of recorder content status.

#### 4.6.3.2 Search Track Telemetry Processor

The implementation of this design approach is described in Volume IIE, Section 5.11 of the Phase D Technical proposal. A summary bilevel output signal from each Wideband Video Tape Recorder auxiliary track is inputted to a processor which performs the necessary storage and synchronization to permit the telemetry system (VIP) to read the twelve-search track data bits serially. The VIP will read the processor 10 bits at a time using two channels separated in time by ten milliseconds. The processor inhibits any new data transfers into the output for 30 ms  $\pm$  5 ms after the VIP starts to read the data. After the VIP reads the data it is retained in the processor unless updated with new search track data.

A Forward/Reverse signal is provided so that the processor correctly formats the data when the tape is operating in either direction. The format is such that the search track data is always read out to the VIP as if the tape were in forward motion.

A stop/start signal will be provided so that the processor will be able to store the last search-track data output and inhibit subsequent data during the tape deceleration. The first search-track data output after a tape start, however, will not necessarily be valid.

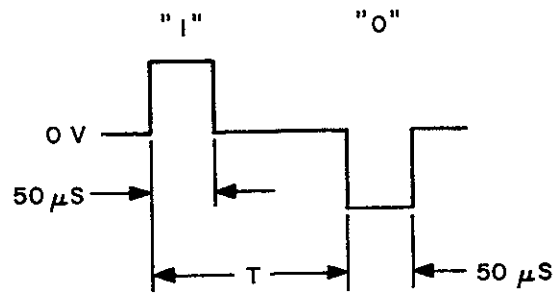
Search-track data will be presented to the processor at two speeds which correspond to tape speeds of 12 IPS and 48 IPS. The 12-bit data repetition time is shown in Figure 4.6.3-1.

#### 4.6.3.3 Positioning of the Tape

In addition to obtaining an accurate knowledge of the tape position at any time, effective recorder management requires the capability to accurately reposition the tape to a predetermined position. The tape must be positioned in two situations:

1. To move the tape to appropriate position in order to dump the desired video data to the data acquisition site, and,
2. To move the tape to the appropriate position that allows data to be recorded on the allocated space.

The first situation requires that the tape be positioned far enough in advance of the data scheduled to be dumped such that, with the normal tape start up movement, the tape will be moving at the dump speed when the first data is encountered. It is desirable to position to tape relatively close to this limit position to eliminate the unnecessary waste of station contact time. In addition, the positioning of the tape too far in advance of the limit position could result in video data from the previous segment on the tape being dumped to the site. Although this is not expected to be catastrophic, it is not a desirable condition.



TAPE SPEED	
12 IPS	48 IPS
T = 400 μS	T = 100 μS

Figure 4 6 3-1 12-Bit Data Repetition Time

The second tape movement situation requires that the tape be positioned such that when the record operation is initiated, it occurs in an area of the tape that doesn't contain data that still must be transmitted. This means that the planned recorded operation must be evaluated and the required tape space allocated within the space available.

In both of the tape movement situations, the desired position, which can be expressed in terms of a search track word, will be known in advance in the OCC. The OCC will also have an accurate knowledge of the current tape position or the estimated tape position prior to the expected tape repositioning. As pointed out earlier, there will exist a minimum of 36 inches of buffer area between any two segments of video. Actual tape movement during start up motion is approximately 2.4 inches. Thus, positioning the tape in either of the two tape positioning situations to a point within the 36-inch buffer, not closer than 3 inches of the video on either side, should satisfy all conditions. It is anticipated, however, that an additional amount of tape will be moved to provide a larger buffer region between separate operational sequence segments.

Since dump operations will generally be scheduled to accommodate data from a complete operational sequence, it can be expected that the region within which the tape must be positioned will be larger than the minimum 30 inches as previously defined.

Two basic approaches to commanding position were considered.

1. Using an on command to start tape motion (either fast or normal, forward or rewind) followed by an off command scheduled to occur a specific time later.

2. Providing the capability to command the recorder to move the tape directly to the predetermined position and automatically return to the standby condition.

The first of these approaches requires the use of two discrete commands. If the movement was implemented by use of stored program commands, the desired position can be achieved to within  $\pm 24$  inches. This results from the fact that the granularity with which two commands can be specified is one second. Movement initiated by real time commands can achieve a granularity of  $\sim 0.4$  seconds from a STADAN site and  $\sim 0.25$  seconds from a MSFN site. The positioning accuracy in these cases are  $\pm 9.6$  and  $\pm 6$  inches respectively.

The utilization of this approach for large tape movements via stored command and allowing for fine repositioning with real time commands if required as a result of the real time TLM evaluation will then provide tape position capability within the desired accuracy. This approach can be implemented without modification or additional hardware for either the WBVTR or spacecraft.

The second approach provides the capability for positioning of the tape to approximately the accuracy of the word displacement on the search track. This approach, however, requires that additional capability be added to the spacecraft. Conceptually, a quantitative command would be sent which defines the desired tape position (search track word). A comparison would be made between this word and the search-track word as monitored during tape movement. The recorder would be stopped when coincidence occurs. Since the capability to monitor the search track for position data is required, some of the circuitry required to implement this approach can be considered to exist. Nevertheless, the former approach provides the desired positioning capability with no additional equipment and therefore is selected.

**GENERAL  ELECTRIC**  
**SPACE DIVISION**  
**SPACE SYSTEMS ORGANIZATION**

N70-34454

EARTH RESOURCES TECHNOLOGY SATELLITE SPACE-  
CRAFT SYSTEM DESIGN STUDIES - VOLUME I-  
SYSTEMS STUDIES

General Electric  
Valley Forge Space Center  
Philadelphia, Pennsylvania

11 February 1970

